S. SUWANNAPINIJ.

"The Mechanical and Cutting Properties of Rocks related to the Application of Tunnel Boring Machines."

The testing procedures used to determine the mechanical and physical properties of rock materials covering a broad spectrum of strength and abrasivity are described and critically examined in the first part of the work. Statistical analysis is used to determine the inter-relationship between these properties, in order to establish the validity and interpretation of the test methods employed.

Laboratory based tests are described, which were developed to assess the cutability and abrasivity of rock materials, which are used in conjunction with the physical and mechanical properties of these rocks to determine their suitability for the application of tunnelling mechines.

The majority of the samples studied were obtained from strata to be excavated during the construction of the proposed Tyne-Tees Aqueduct Tunnels and for drivages in connection with the Tyneside Metro System.

The data obtained is used to provide information on the suitability of application for a range of tunnel boring mechines.

To

Dr.F.F. Roxborough

and

Dr.R.J. Fowell

UNIVERSITY OF NEWCASTLE UPON TYNE

DEPARTMENT OF MINING ENGINEERING

THE MECHANICAL AND CUTTING PROPERTIES OF ROCKS RELATED TO THE APPLICATION OF TUNNEL BORING MACHINES

A THESIS SUBMITTED FOR THE DEGREE OF

DOCTOR OF PHILOSOPHY

BY

SOMPOP SUWANNAPINIJ

(B.ENG. CHULA, M.SC. NEWCASTLE)

SEPTEMBER, 1975.

Acknowledgement

The author would like to express his sincere appreciation to the following people without whose help much of the research work would have been impossible.

Professor E.L.J. Potts, Milburn Professor of Mining Engineering at the University of Newcastle upon Tyne for the facilities and opportunity he provided.

Dr. F.F.Roxborough, Reader in Mining Engineering for his excellent supervision, his kindness and generousity.

Dr. R.J.Fowell for his valuable help and supervision.

The Greenside Machine Co.Ltd. for their sponsoring and financial support throughout the investigation.

Mr. W.B.Bell for his kindly guidances during the first year.

Mr. A.Szeki for his helpful discussions.

Mr. A.Crozier for taking part in the site investigation.

Mr. T.Pollock and his staff for their help in the design and construction of the equipment.

The staff and colleages in the Department whose helpful is highly appreciated.

Contents

Tables

Tables (continued)

Appendices

Illustrations

Illustration Number	
1	Rock Cutting Mechanics
2,3	K.M. Tunnelling Machine
4	Robbins Soft Ground Tunnelling Machine
5	Robbins Medium-hard and Hard Rock Tunnelling Machine
6	Robbins 3.30 m Diameter Machine Used by Foundation Co. of Canada to Bore Interbedded Sandstone, Limestone, and Shale with up to 190 MN/m^2
7	Demag Machine
8	Hardrock Tunnelling Machine Developed by Lawrence Manufacturing Co.
9	How the Lawrence Tunnelling Machine Works
10	Jarva Tunnelling Machine
11	How the Jarva Tunnelling Machine Works
12	Caldweld's Oscillating Cutterhead Machine
13	Caldweld Hardrock Tunnel Boring Machine with Rotating Cutters
14	Wirth Tunnelling Machine
15	Atlas Copco Tunnelling Machine
16A	Anderson Mavor Heading Machine
16B,C	Eickhoff Heading Machine
17	Greenside Tunnelling Machine
18	Exotic Drills
19	The Effects of Cobalt on Hardness & Strength
20A	Position of Strain Gauges on Measuring Bars
20B	Arrangement of Strain Gauge Bridges
21A	The Linear Rock Cutting Rig
21B	Recording Apparatus
22	Pycnometer
23A	Influence of Length/Diameter Ratio on Uniaxial Compressive Strength
23B	Contours of the McClintock - Walsh Parameter
23C	Relationship between Uniaxial Compressive Strength of Springwell Sandstone and Height/Diameter Ratio, Using Different Platens
24A	Static Tensile Strength Tests
24B	Direct Tension Test

Illustrations (continued)

Illustrations (continued)

Illustration Number	
53	Geology of Airy Holm-Derwent Tunnel
54	Geology of Derwent-Wear Tunnel
55	Geology of Wear-Tees Tunnel
56	Graph of Shore Hardness V Specific Energy
57	Graph of Cone Indenter Hardness V Specific Energy
58	Graph of Rebound Number V Specific Energy
59	Graph of Compressive Strength V Specific Energy
60	Graph of Tensile Strength V Specific Energy
61	Graph of Young's Modulus V Specific Energy
62	Graph of Specific Energy V Coarseness Index
63	Graph of Abrasive Wear V Cutting Wear
64	Graph of Abrasive Wear V Machineability Index
65-70	Graphs of Distance Cut V Weigth Loss

Chapter 1

Introduction

Tunnelling for what ever purpose, has occupied mankind since the beginning of time. Tunnels for protection, tunnels for secret access to forbidden places, tunnels for the extraction of minerals and tunnels for speedier transportation have been gouged through every form of strata.

For centuries the task of boring below ground was performed by rudimentary tools, and it was not until a scant 110 years ago that the first successful attempt was made at mechanising the process (1).

It is recognised (2) that machine tunnelling has several advantages over the conventional drilling and blasting method as :-

1. Greater safety
2. Less overbreak
3. Less labour required
4. Continuous excavation and muck removal
5. No blasting damage to nearby structures
6. Potentially faster rate of excavation.

However, much more research and development work is needed to make the tunnelling machine more versatile, reliable, and economical than they are today. The research should concentrate on the following problems:-

1. Capital cost is high
2. Boring in harder rocks
3. Dust control
4. Cutter wear
5. Muck removal
6. Tunnelling in zones of high water flow
7. Tunnelling in zones of defective rock
8. Prediction of machine performance in advance of construction
9. Bearing wear
10. Alignment of bore
11. Change of diameter.

In this work the prediction of machine performance in advance of construction was carried out, using the standard rock cutting test as a primary factor and the other rock properties as the relevant factors. These tests were conducted using the core samples obtained from the preliminary boreholes along the two proposed tunnelling projects, namely the Tyne-Tees aqueduct tunnel and the Tyneside Rapid Transit tunnels.

Chapter 2

Review of Tunnelling Machine and Application

2.1 Introduction

Some of the major contributions towards improving tunnelling technology were black powder for blasting in the second quarter of the 17 th century; mechanical drills, dynamite, and long-distance ventilation (from one opening) in the third quarter of the 19 th century; mechanical rock loaders in the first quarter of this century; and continuous full-face boring machines in the present quarter of this century. To illustrate the impact of improved technology, the estimated linear advance rate of tunnels was less than 0.5 m per week (*) in the first century; about 1 m per week up to the 17 th century before black powder was used for blasting; between 2 and 5 m per week up to the middle of the 19 th century while using black powder but prior to the introduction of mechanical drilling and high explosives; between 10 and 40 m per week in the second half of the 19 th century after the introduction of mechanical drilling and high explosives; and between 25 and 190 m per week by drilling-and-blasting methods and between 60 and 320 m per week by boring machines in this century (1).

Since their introduction, performance of boring machines has steadily improved in soft to medium hard rock. There is widespread confidence that it is only a matter of time and effort before their applicability is extended to harder rocks. It is possible that exotic or novel methods of breaking rock, now being investigated, may be incorporated into a continuous boring machine.

2.2 Rock cutting mechanics

It is recognised that there are four established techniques for rock excavation by machine, all of them having the common feature of wedge penetration. These are:-

2.2.1 Drag picks (fig. 1A)

Tools which are commonly of simple chisel form (although more complex shapes are known) and which are assembled in array on the peripheral surface of a rotating cylindrical drum or face plate of a boring machine. This tool is widely used in coal mining industry.

2.2.2 Disc cutters (Fig. 1B)

A solid steel disc with a pointed circumferential edge. The disc operates as a free rolling wheel, in which a high thrust forces the sharpened circumference to penetrate the rock face. A superimposed translatory motion causes the disc to roll, gouging a furrow in the rock in much the same way as a heavily loaded wheel rolling over yielding ground.

(*) All linear advance rates refer to the rate in one heading only.

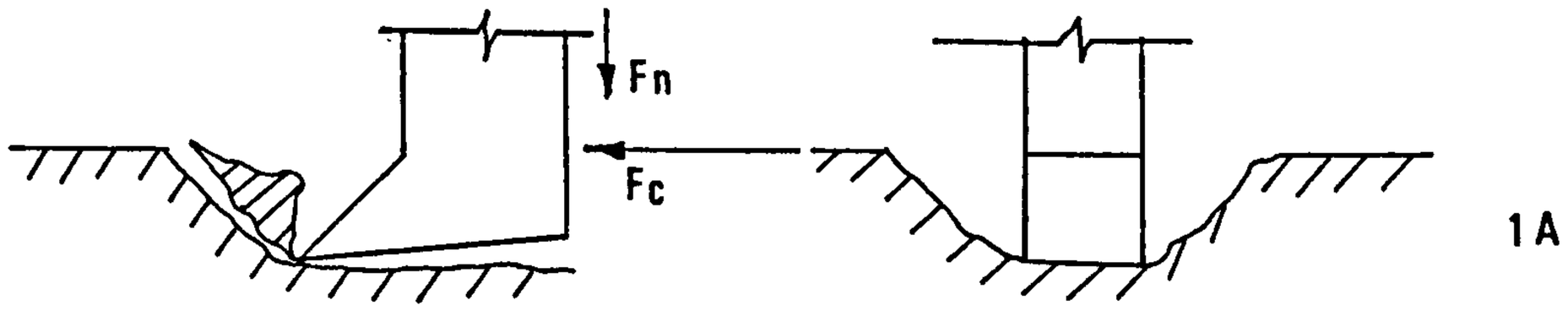

1A

Drag pick

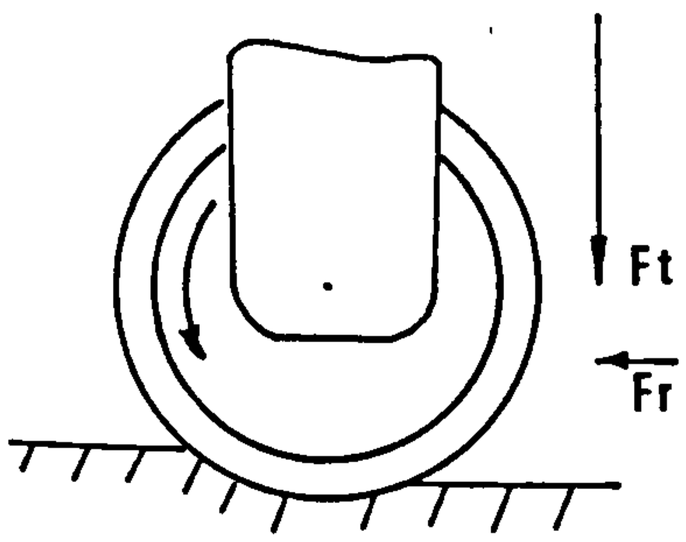

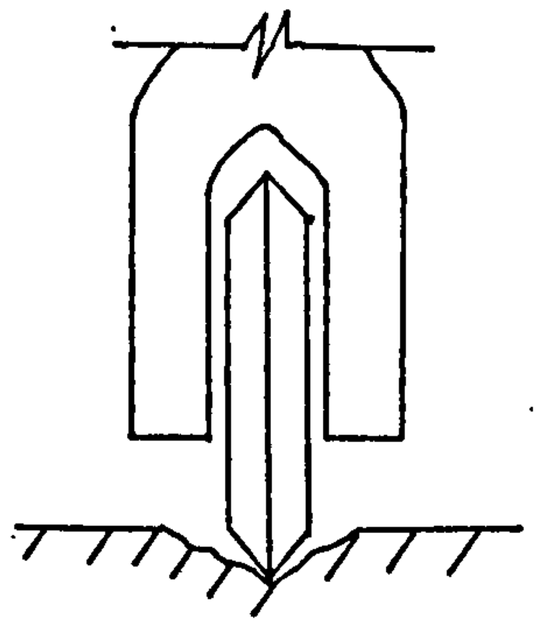

1B

Disc cutter

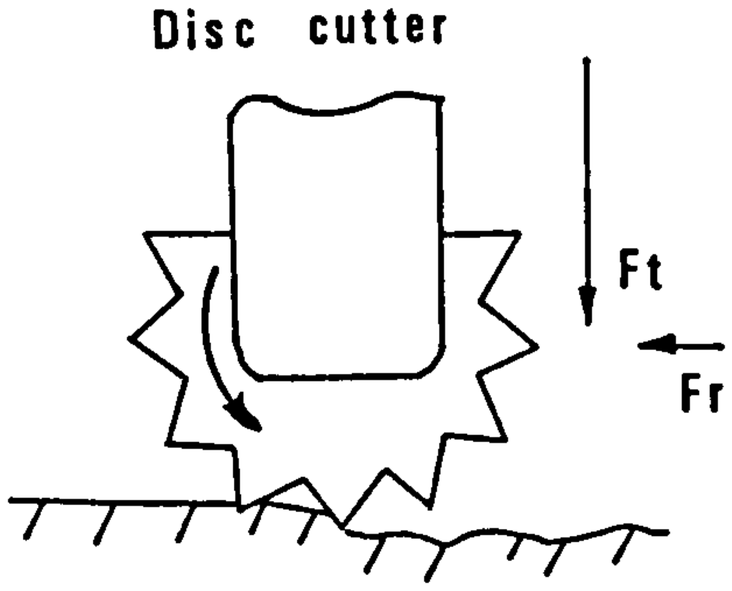

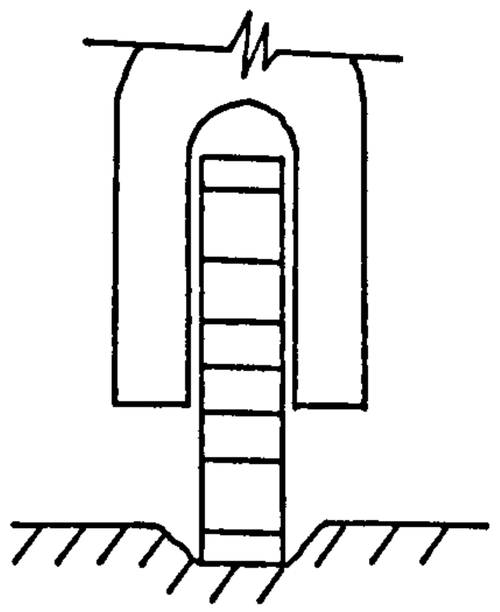

1C

Roller cutter

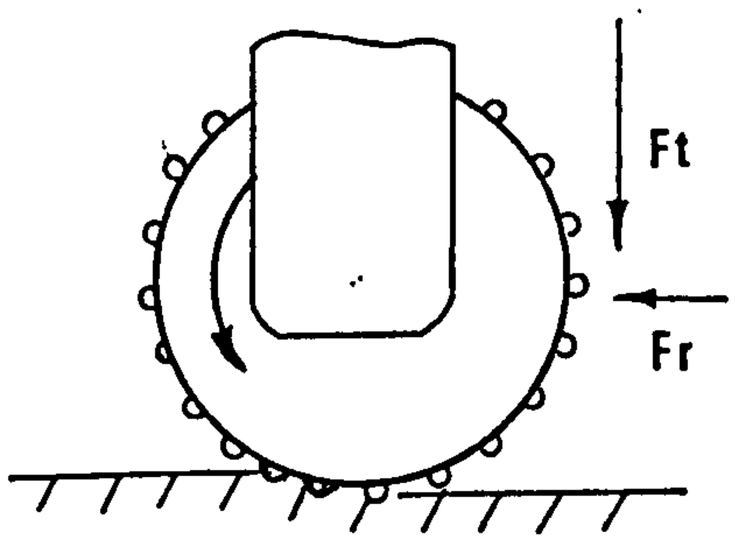

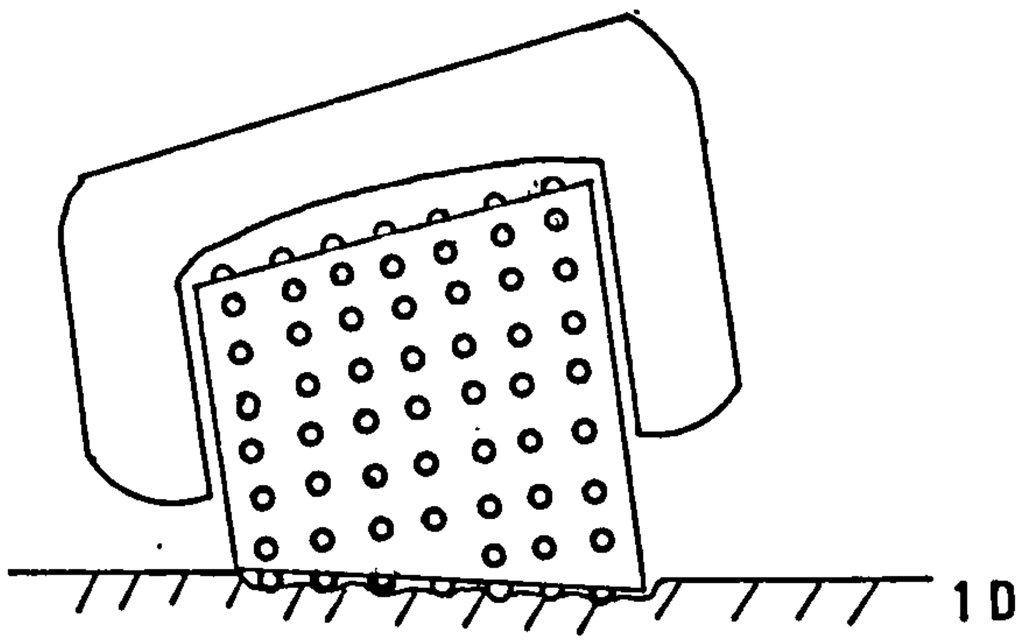

1D

Button cutter

Rock cutting mechanics

Figure 1

2.2.3 Roller cutters (Fig.1C)

Similar in concept and design to the disc cutter. In this case, however, the circumference of the cutter is equipped with teeth, thus having an appearance very similar to that of a simple gear wheel. As each tooth engages the rock during rotation of the wheel, a rock fragment is chipped away. The tool is commonly used in the oil industry for cutting large diameter boreholes to great depth.

2.2.4 Button cutters (Fig.1D)

This is very much a grinding tool. It usually takes the form of a free rolling cylinder or frustrum of a cone, the surface of which is studded with tungsten carbide buttons. It is operated in similar fashion to the disc and roller cutter. A high penetrating force into the rock surface, supplemented by a translatory motion to the tool, causes rock degradation by grinding and pulverisation.

2.2.5 Limit of application

It is well accepted that there is a limit of application of the cutters with the type of rock materials. The table below, after Muirhead and Glossop (3), illustrates the general area of application of each type of tool.

Cutters	Hardness	Rock CS (MN/m^2)	Typical Rocks
Picks, Discs, Gear Rollers	Soft	40 (max.)	Shale, Clay
Picks, Discs, Gear Rollers	Medium	40 - 80	Dolomite, Sandstone, Marble
Buttons, Discs	Medium Hard	80 - 170	Limestone, Gneiss, Granite
Button Cutters	Hard	170 +	Diorite, Quartzite, Hornblende

From this it is seen that Picks, Discs and Gear cutters might be suitable for soft rock materials and Button cutters for hard rock materials.

2.3 Types of tunnelling and heading machines

The type of tunnelling machine being used depends on the geological conditions of rock it is encountered. The design of each machine is suitable for a limit range of conditions, and it is usual for a machine to be built specifically for a particular tunnelling project. The machine, however, can be divided into two categories:-

1) the shield machines, which are used for driving through soil and loose rock, and

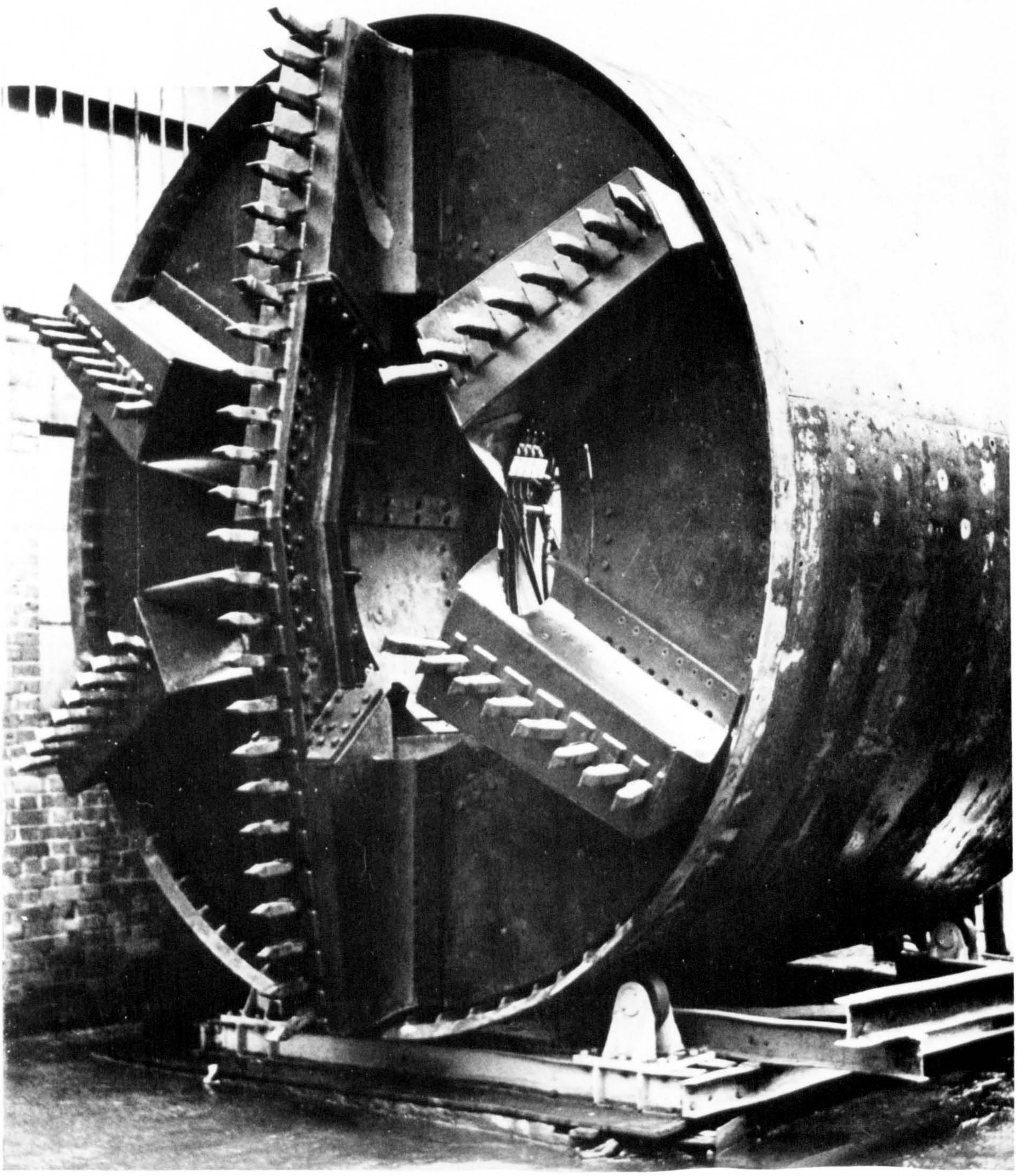

K.M. Tunnelling Machine

Figure 2

2) the hard rock machines, which are used for driving through rock which has self supporting tendencies.

2.3.1 Shield machines

Shield-type tunnelling machines consist of a more or less conventional shield with thrust rams and an erector system. The cutterhead and cutterhead support are contained within the shield in place of the work platforms and breast-board supports.

Shield machines are usually used in soil formations and soft ground where the compressive strength is less than 20 MN/m^2(4). This may be a competent, cohesive, relatively self-supporting soil like the clays in Chicago, Detroit, and London, or it may be cohesionless running material like the sand and gravel found in Milan.

More than 25 different companies around the world are building this type of tunnelling machine.

2.3.2 Hard rock machines

It is considered that hard rock is the rock which would normally required drilling and blasting methods for removal. Hard rock machines can themselves be divided into two groups according to the types of cutters used:-

1) machines using roller cutters, called full-face borers, and,
2) machines using drag picks usually with carbide cutting edges.

2.3.2.A Full-face borers (5-12 incl.)

The principal type of hard rock tunnelling machines is the full-face borer. This method of boring the tunnel has been developed from techniques used in oil-well drilling.

The full-face borers use either one or a combination of basically three different types of cutters or rollers (gears-discs-, and button-) attached to the cutters by the machine either anchoring itself to the sides of the tunnel and pushing the cutterhead forward from this anchorage, or by drilling a hole ahead of itself and then using the hole as an anchorage to pull itself forward. The thrust applied to the cutters causes them to penetrate the rock by a small amount, setting up high and complex stresses in the rock, resulting in rock chipping and spalling from the face. Sharp teeth or cutting edges can be used for the softer formations, whereas semispherical tungsten carbide inserts are required for the very hard formations.

During early trials with these machines in the 1950's, it was found that simple single drag bits were unsuccessful for cutting the hard rock due to high abrasion, which causes excessive wear. and impact shock, resulting in tool breakage. The next development was the tricone type bit which pulverises the rock rather than cuts it. Although these showed a marked improvement in cutting on the single bit, cutter costs and power consumption were high. A significant improvement came with the development

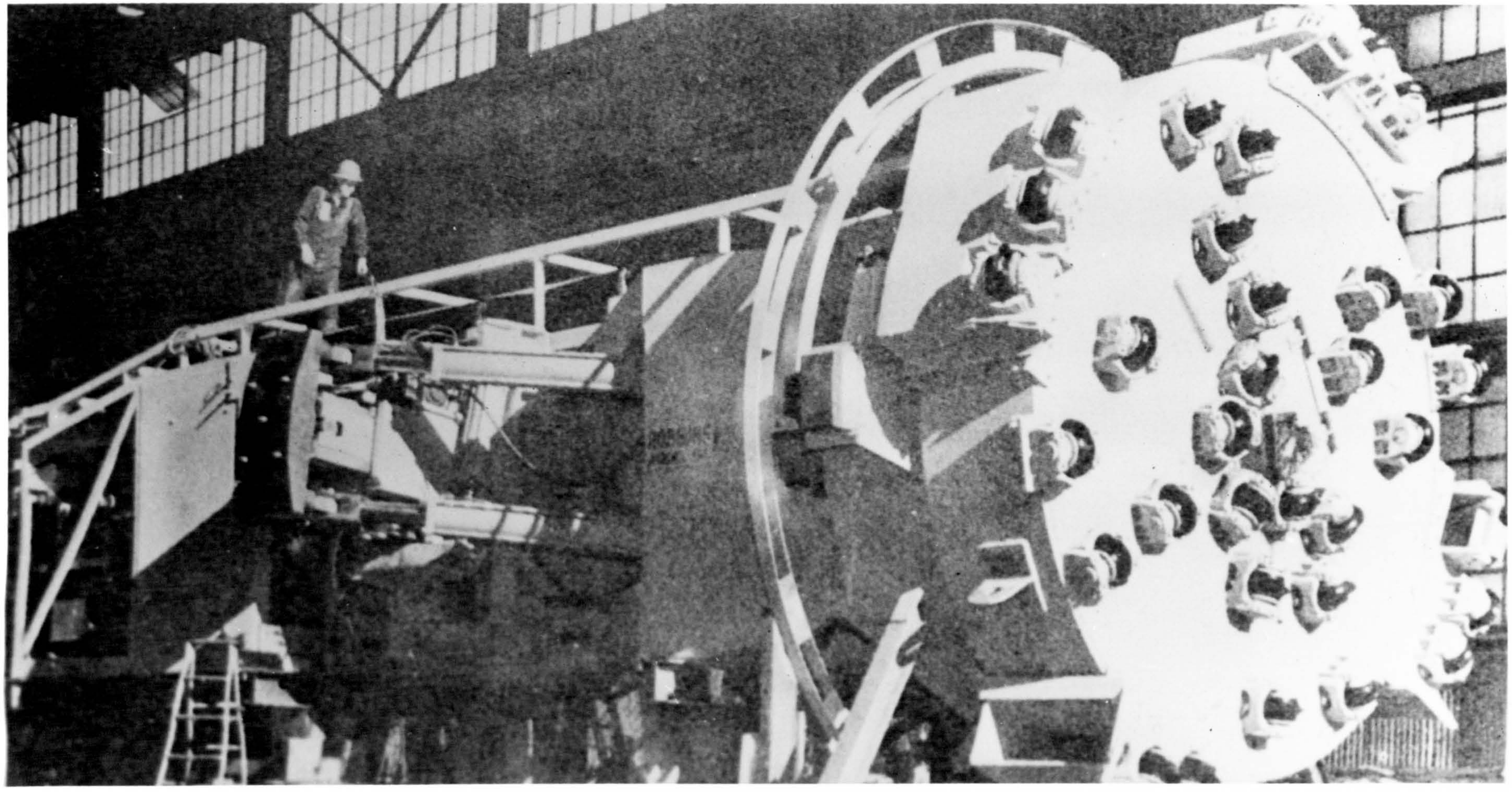

Robbins Medium-hard and Hard Rock Tunnelling Machine

Figure 5

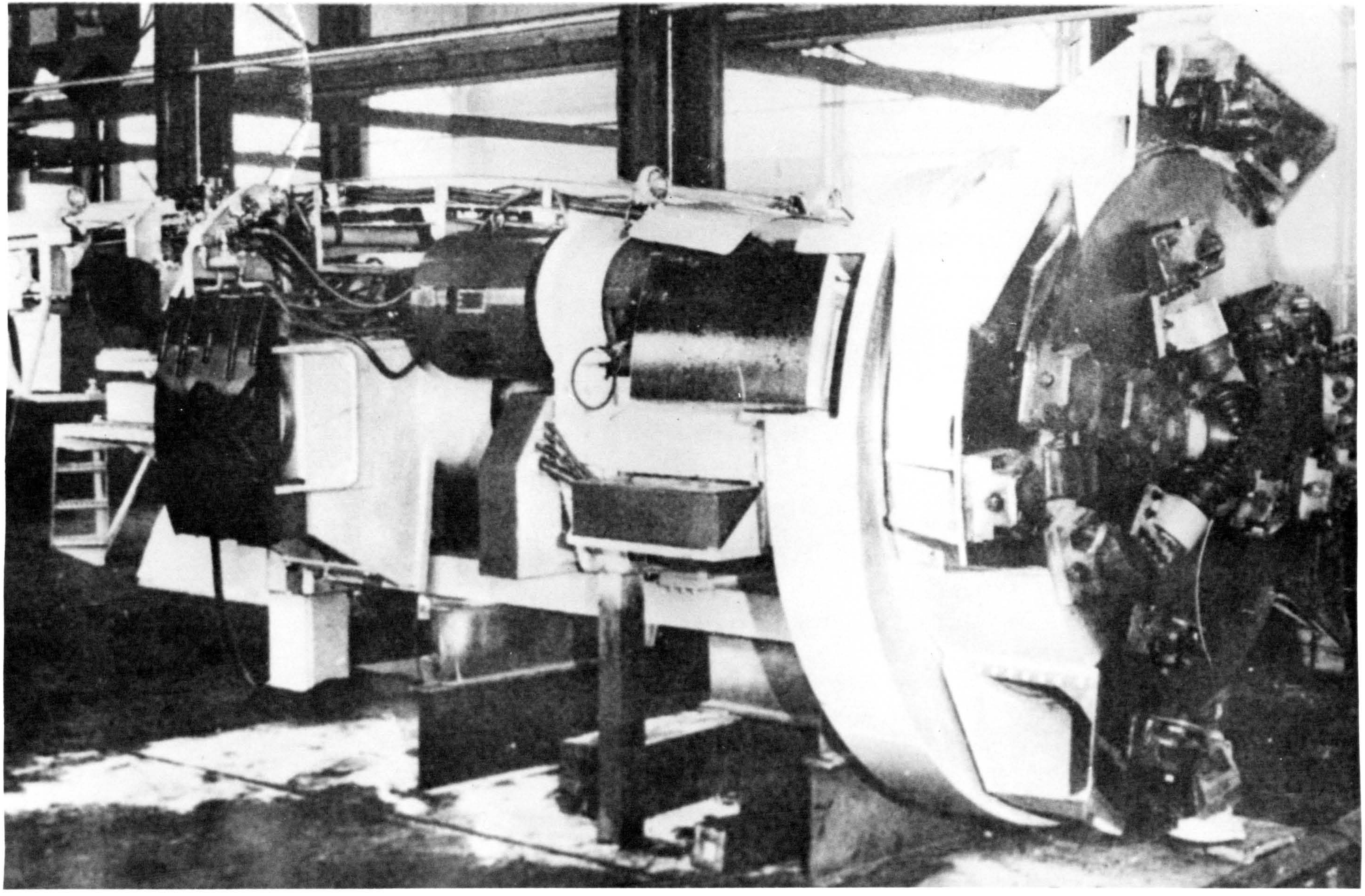

Robbins 3.30 m Diameter Machine Used by Foundation Co. of Canada to Bore Interbedded Sandstone, Limestone, and Shale with up to 190 MN/m^2 Compressive Strength

Figure 6

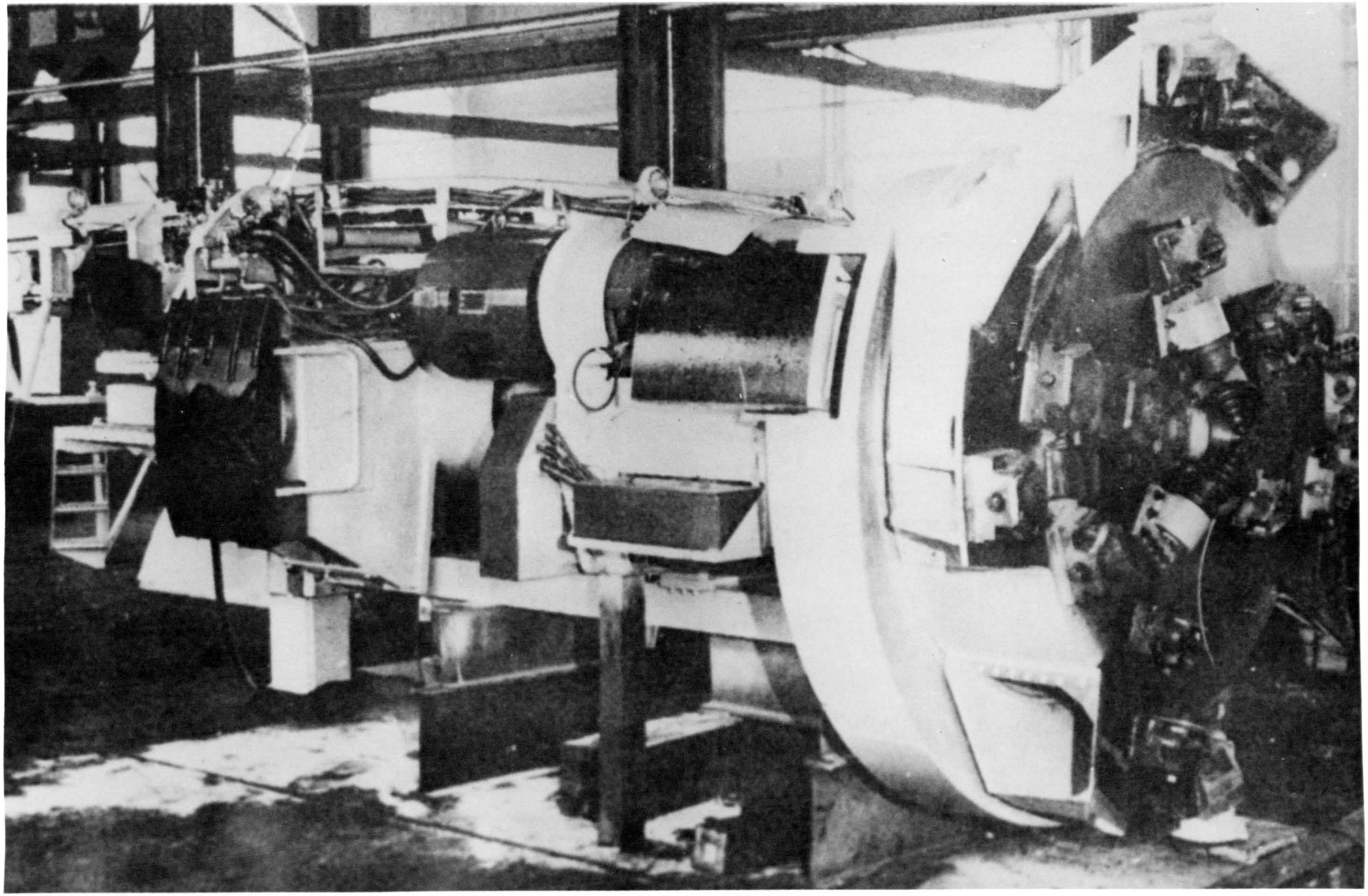

Robbins 3.30 m Diameter Machine Used by Foundation Co. of Canada to Bore Interbedded Sandstone, Limestone, and Shale with up to 190 MN/m^2 Compressive Strength

Figure 6

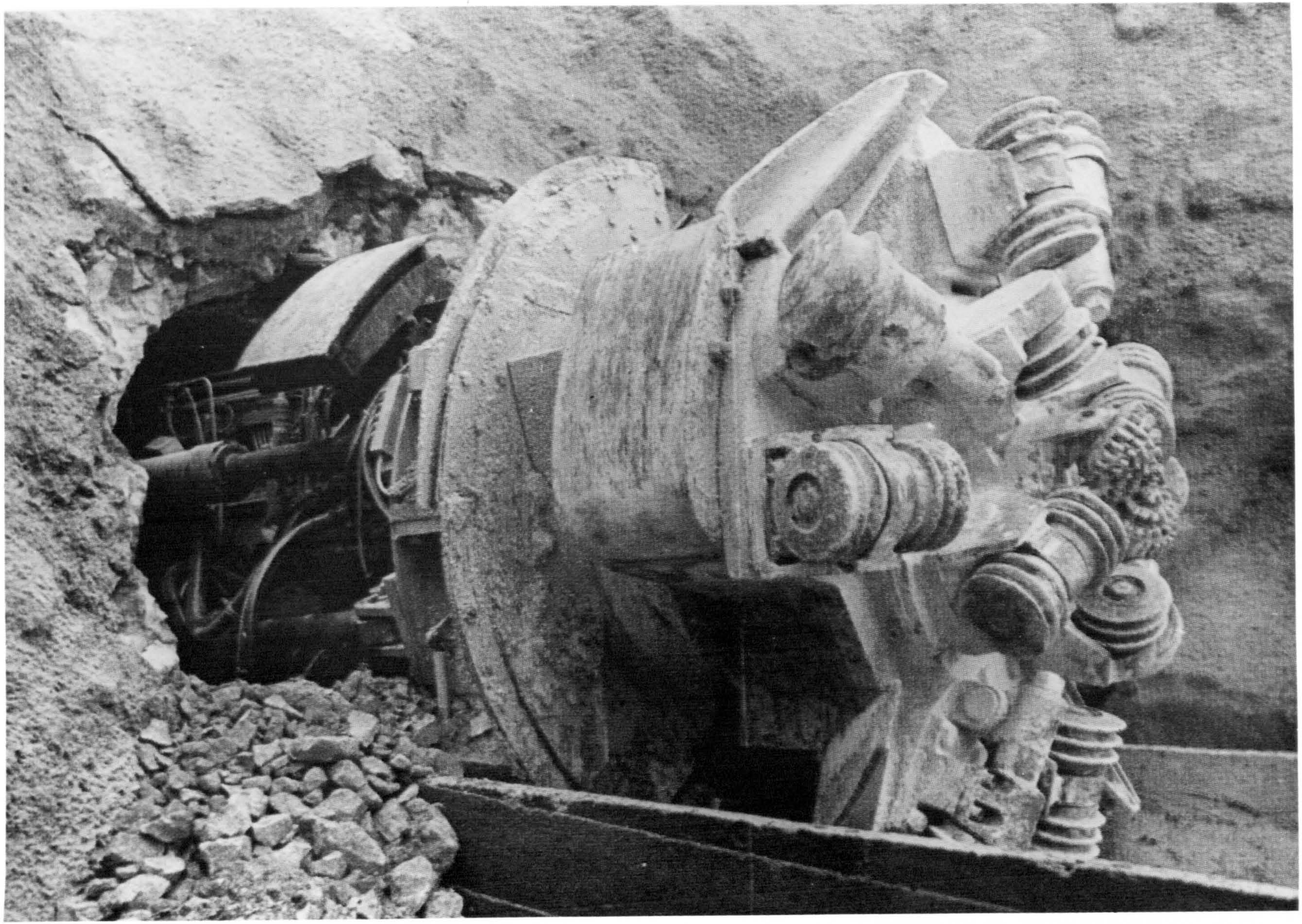

Demag Machine

Figure 7

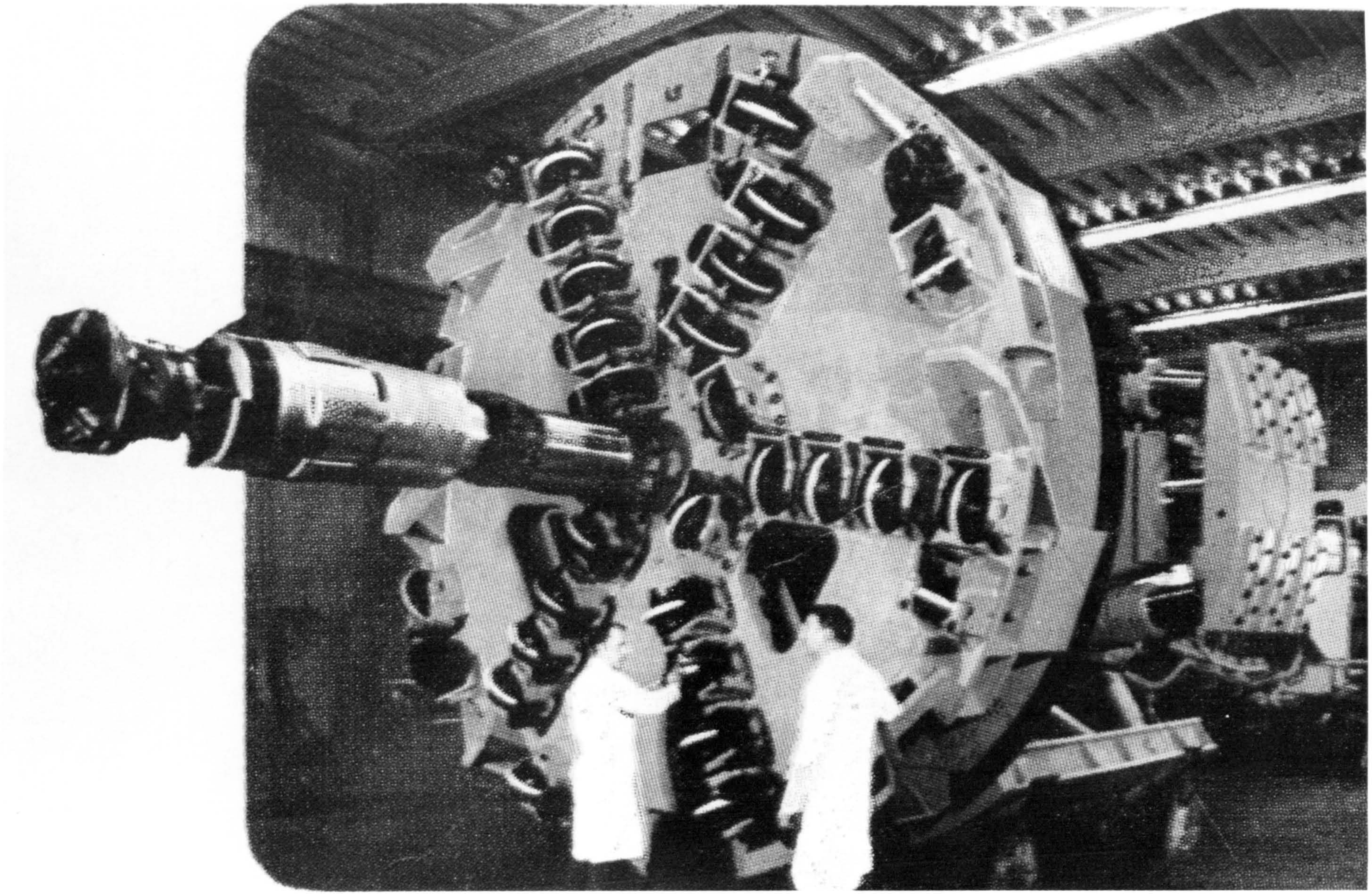

Hardrock Tunnelling Machine Developed by Lawrence Manufacturing Co.

Figure 8

HOW THE LAWRENCE TUNNELLING MACHINE WORKS.

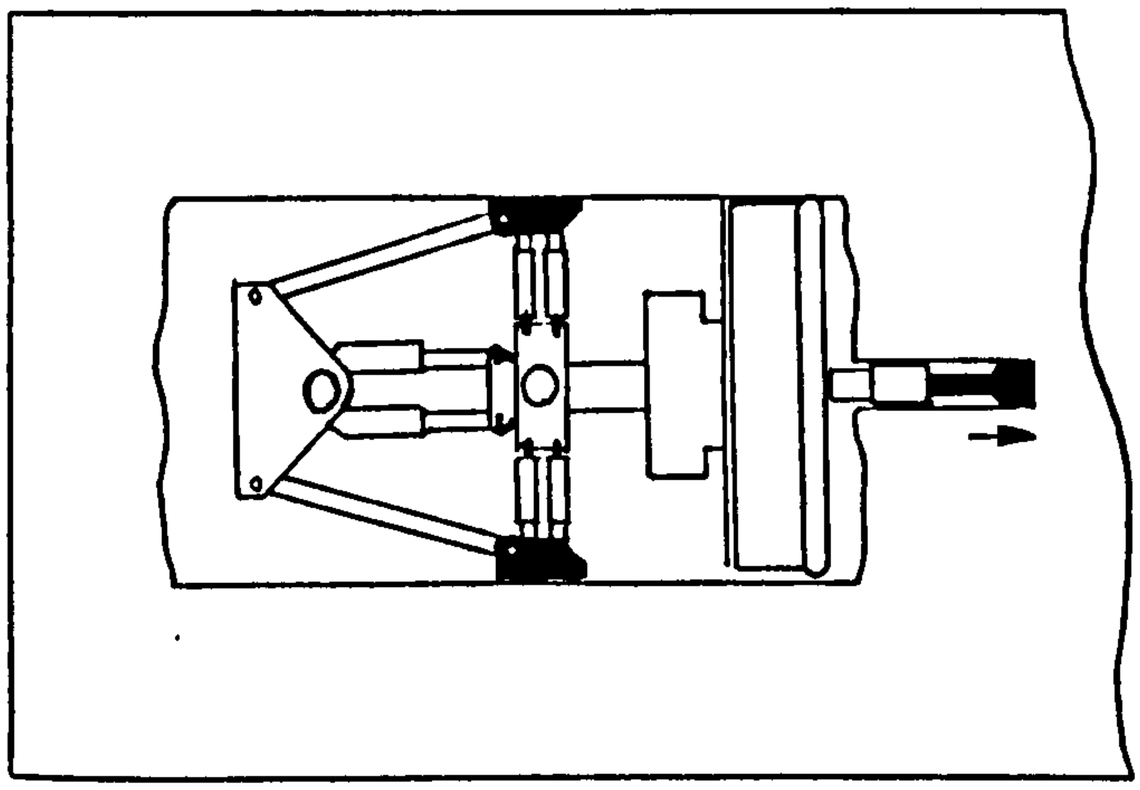

1. Pilot bit drills into tunnel face as rib jacks support tunneller.

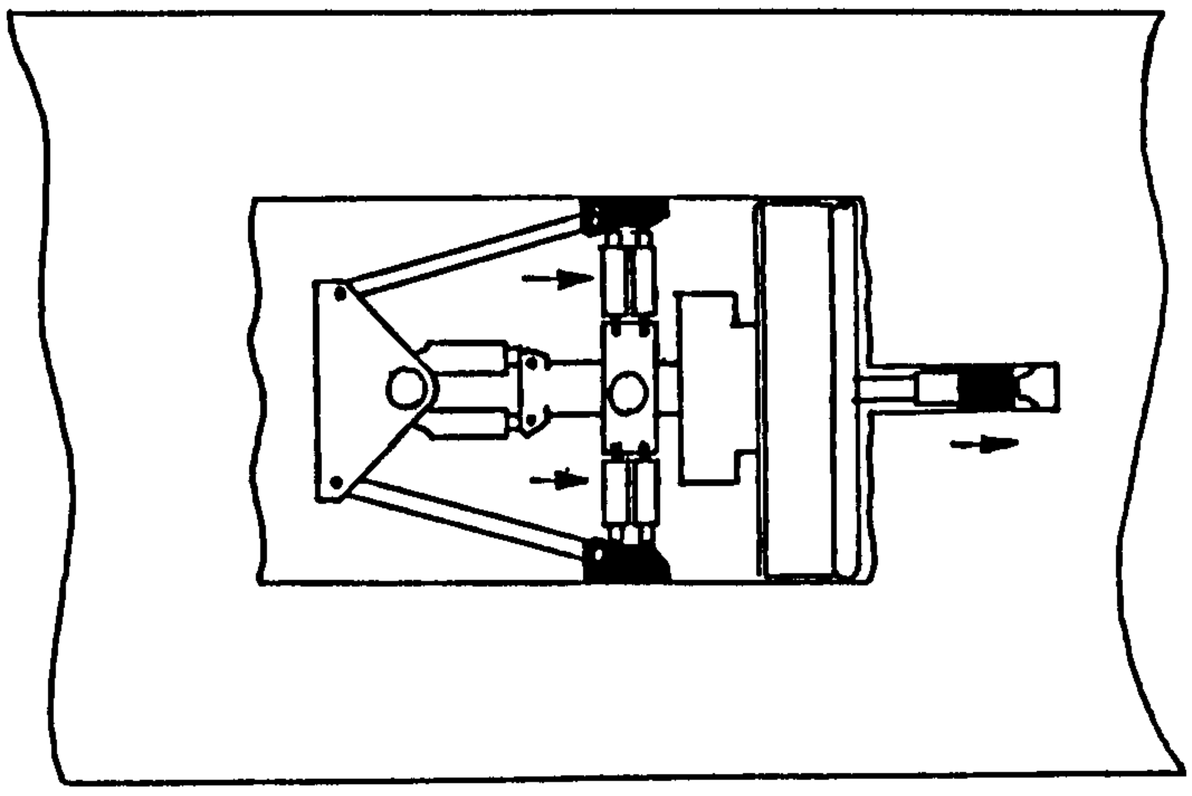

2. Pilot anchor and rib jacks advance.

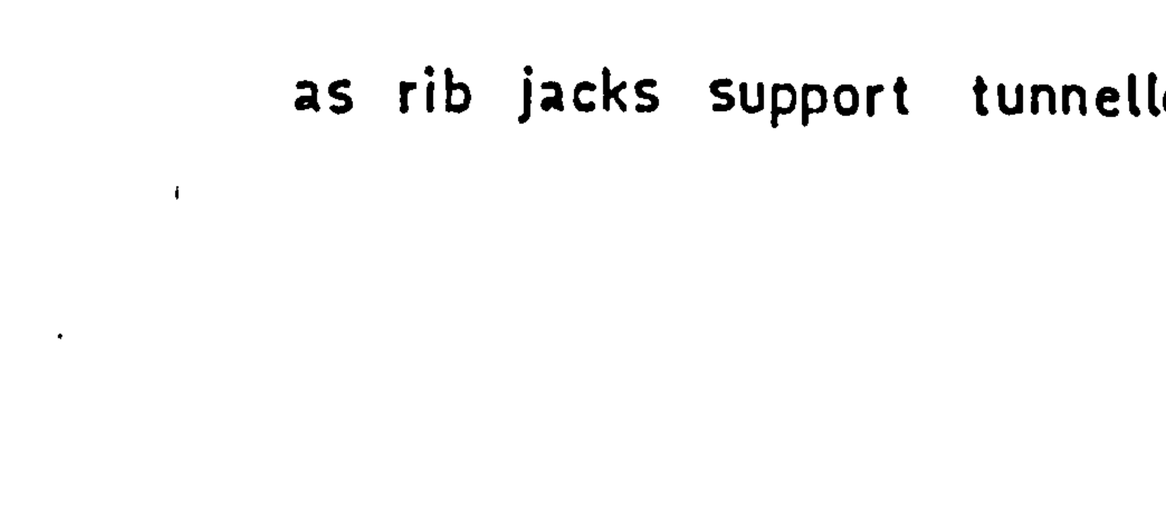

3. Pilot anchor locks into pilot hole and rib jacks support cutterhead shaft. Pilot bit and cutterhead bore simultaneously.

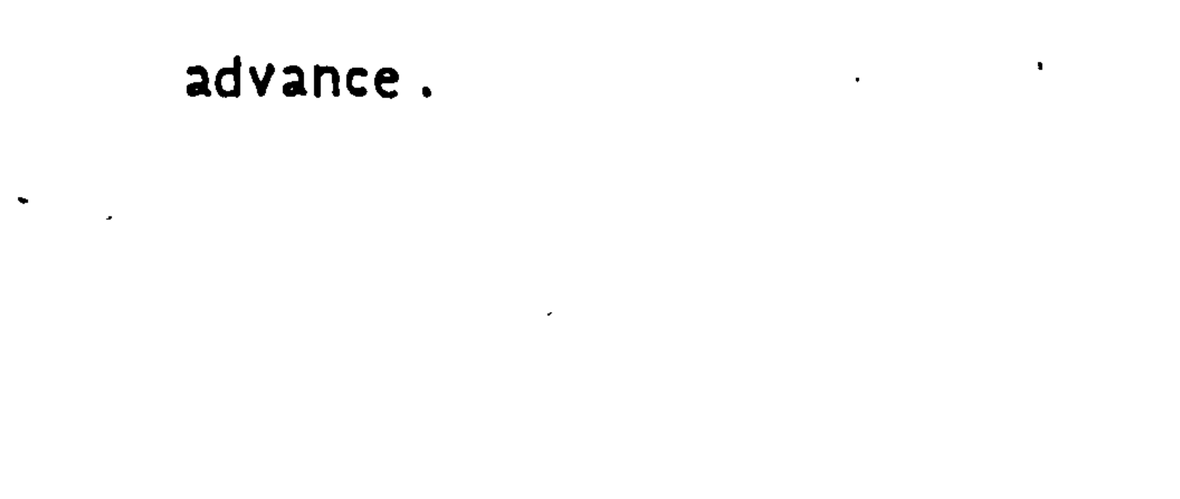

4. Pilot anchor and rib jacks advance again, cycle ready to repeat.

FIG. 9

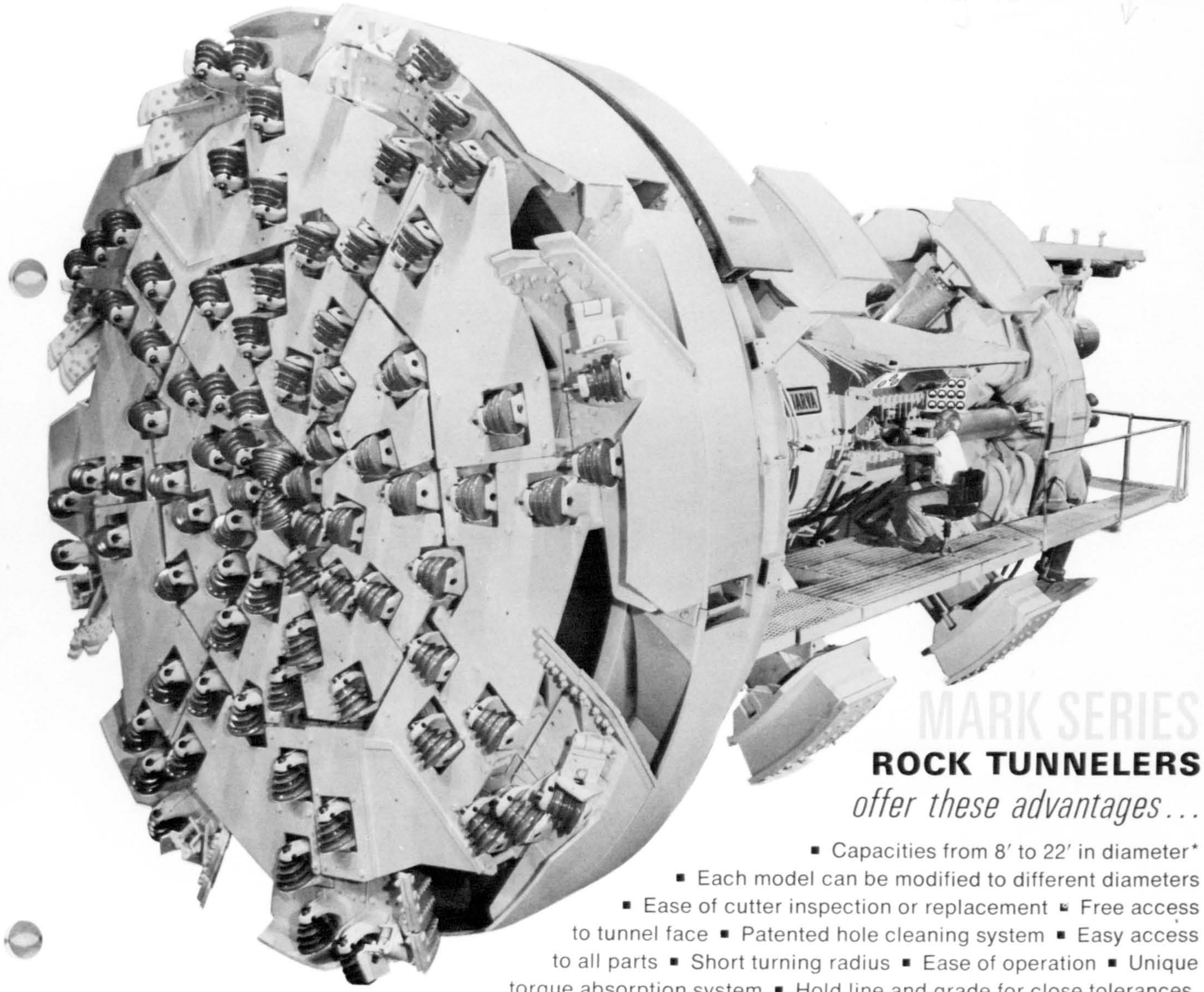

MARK SERIES

ROCK TUNNELERS

offer these advantages...

- Capacities from 8′ to 22′ in diameter*
- Each model can be modified to different diameters
- Ease of cutter inspection or replacement
- Free access to tunnel face
- Patented hole cleaning system
- Easy access to all parts
- Short turning radius
- Ease of operation
- Unique torque absorption system
- Hold line and grade for close tolerances.

Jarva Tunnelling Machine

Figure 10

HOW THE JARVA TUNNELLING MACHINE WORKS

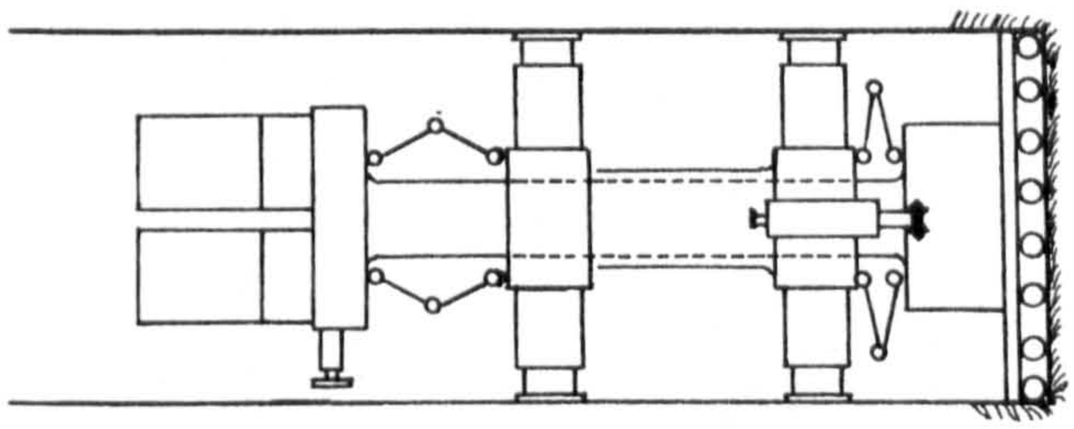

Step 1: Start of boring cycle. Machine clamped, rear support legs retracted.

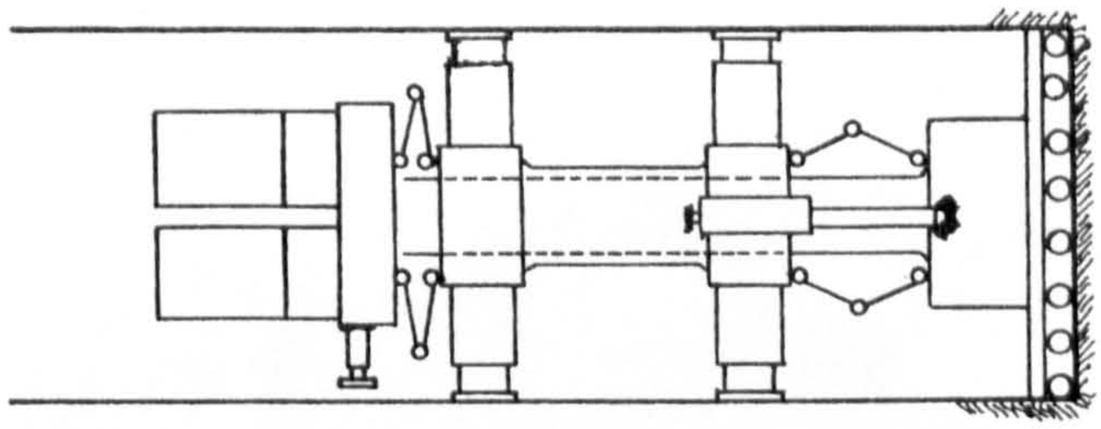

Step 2: End of boring cycle. Machine clamped, head extended, rear support legs retracted.

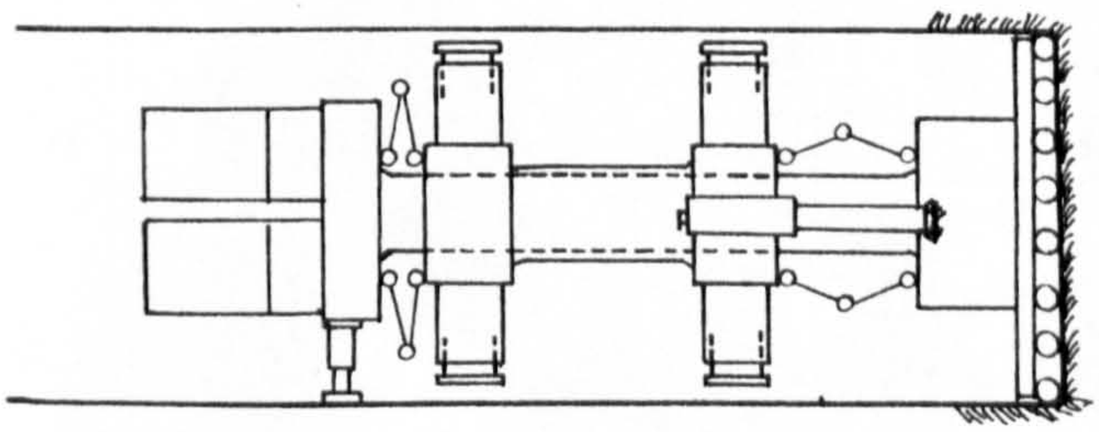

Step 3: Start of reset cycle. Machine unclamped, rear support legs extended.

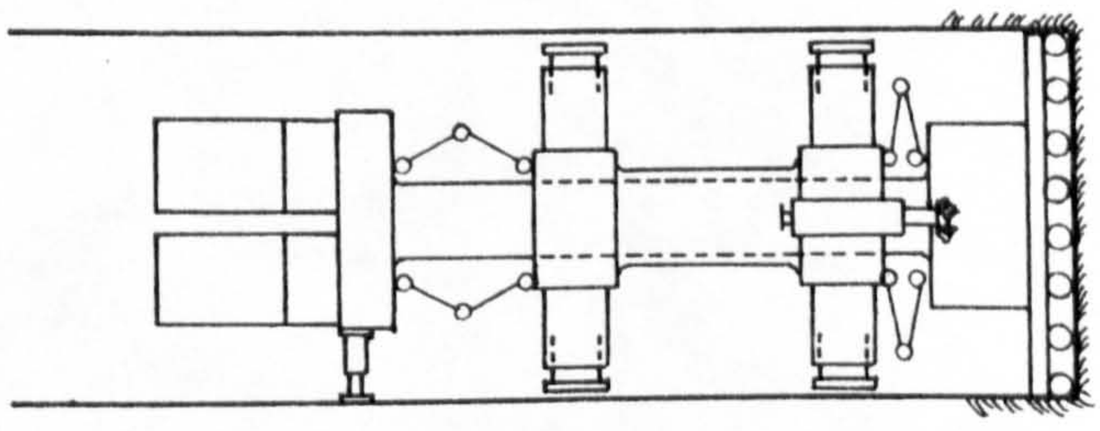

Step 4: End of reset cycle. Machine unclamped, head retracted. Machine now ready for clamping beginning another boring cycle.

FIG 11

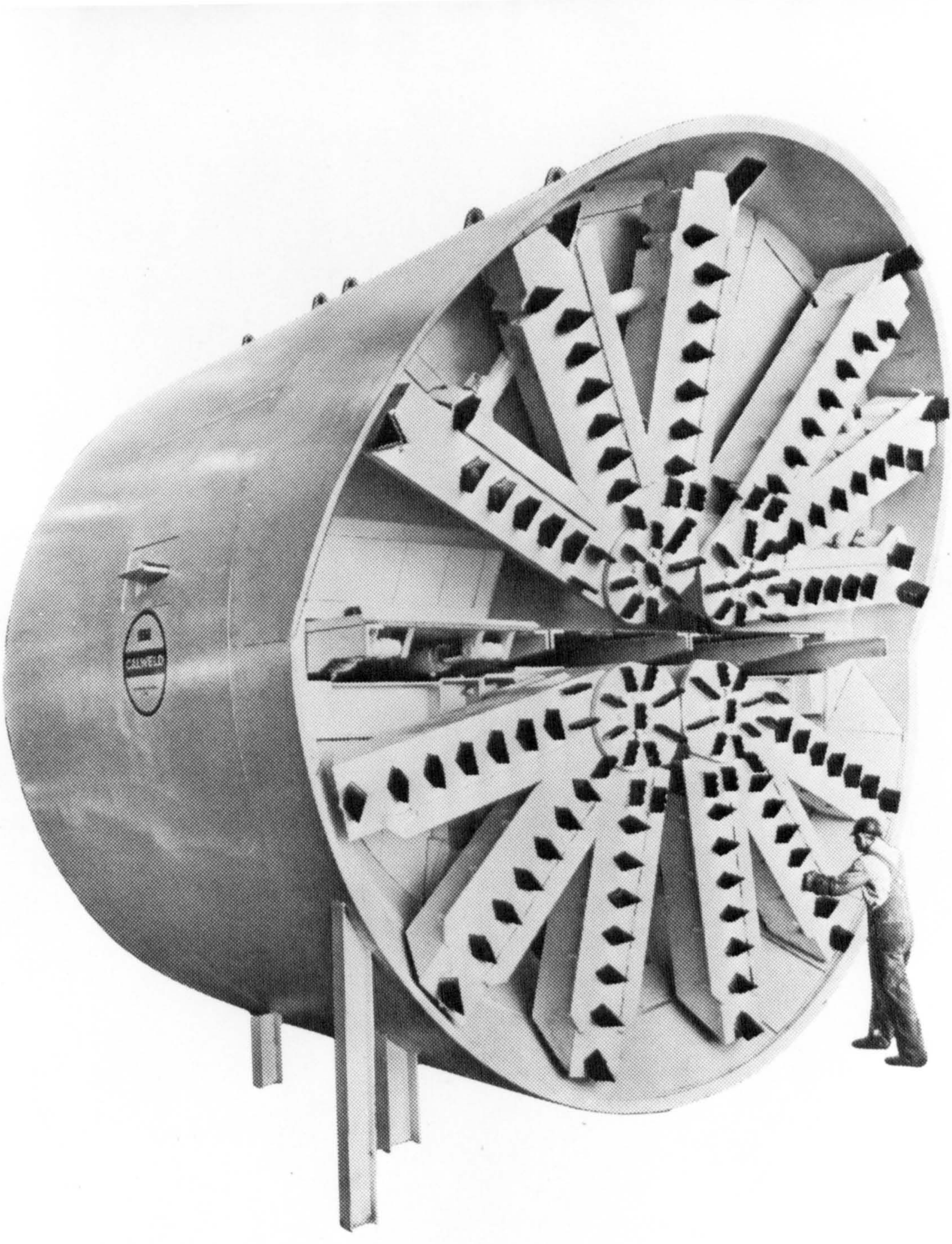

Caldweld's Oscillating Cutterhead Machine

Figure 12

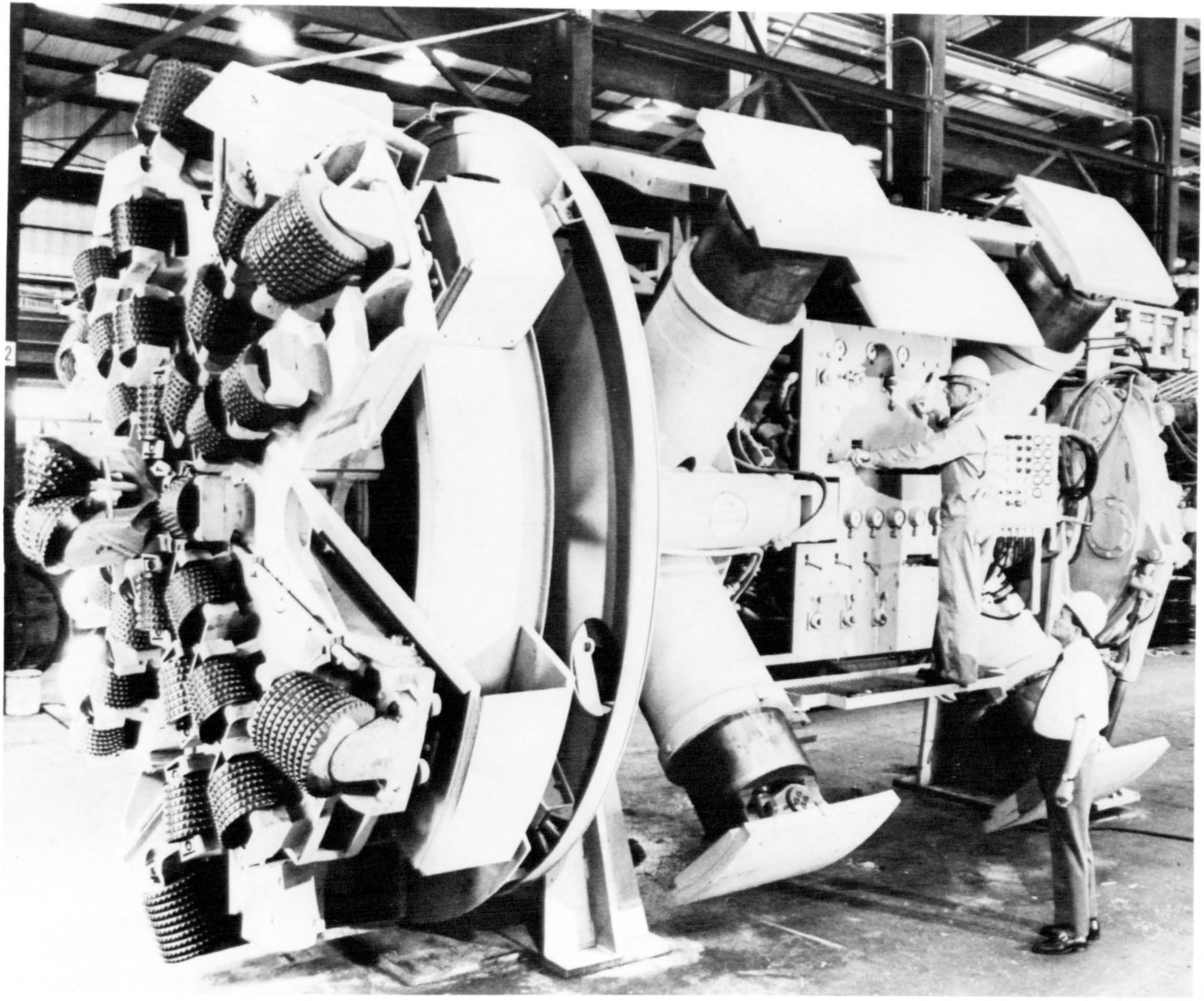

Caldweld Hardrock Tunnel Boring Machine with Rotating Cutters

Figure 13

of the disc cutter, materially reducing the cutter costs per cubic metre of material mined. The disc cutters tended to burst the rock from the face and the material broke away in pieces about the size of one's hand. Machines fitted with disc cutters usually have a single tricone bit mounted on the axis of the head. One advantage of the tricone type bit is that it will cut very much harder rock than the disc cutter so far developed, but the economics of the tricone are debatable when applied to tunnel boring machines used in competitive contracting. Button cutters are also suitable for cutting very hard rock, having been used on raise borers, to cut chloritoid shale with a compressive strength of 370 MN/m^2. These button cutters are, however, expensive being two or three times the price of the disc cutters.

The full-face borers compare very favourably with the conventional methods of tunnelling since some impressive rates of advance have been achieved under ideal conditions. However machines are now being employed in tunnels where the conditions are less favourable and the rock is much stronger. With this wider experience the opportunities for the use of tunnelling machines with their inherent advantages over conventional methods can only increase.

With most innovations, however, disadvantages soon make themselves apparent and handicap progress. There appear to be five main areas where research and development must be applied to improve design and thus increase opportunities for tunnel borers.

1. Capital cost - the initial cost of a tunnelling machine is high, being about £700/kW. As there is no standardization on the size of tunnels each machine is usually written off for each tunnel. It is obvious that such a large investment would need to be amortized over several thousand metres of tunnel to be an economical investment. This minimum length varies with diameter being approximately 4,500 metres for a 2.1 metre diameter tunnel down to 1,500 metres for a 10 metre diameter tunnel (3).

2. Inability to bore hard rock - a few machines are capable of drilling hard rock above 170 MN/m^2, but the cost of such project have been prohibitive. The key to progress in this area lies in increased cutter life.

3. Lack of experience with difficult conditions.

4. Assembly and disassembly time - a borer normally requires one to two weeks for assembly and disassembly underground. This is a significant disadvantage on short tunnels.

8. Curved tunnel bottom - machines produce a circular tunnel, and, especially in mining, operations become more complicated.

For tunnelling machines to be economically justifiable in shorter length of tunnel and in hard and abrasive rocks, capital

and cutter costs will have to be considerably reduced. Cutters for boring machines of 6-10 metre diameter cost around £250 each and a machine requires between six and ten cutters for each metre of tunnel bored. These have to be replaced periodically and cutter cost account for a high proportion of running costs. A more efficient and much cheaper type of rock cutter is the drag pick.

2.3.2.B Machines using picks

According to the method of attacking the tunnel face, tunnelling machines using picks can be further subdivided into two groups:-

1. Machines that work the full-face at any one moment, while being continuously advanced.

2. Machines with a cutterhead that is substantially smaller than the tunnel cross-section and which can only work the face in sweeping movements. Feed in longitudinal direction is discontinuous.

2.3.2.B.1 Full-face pick machines

The main feature of the full-face pick machine is the undercutting method, for which Atlas Copco holds all patents and manufacturing rights. This method was first invented by the Austrian engineer Wohlmeyer and further developed by the Swiss firm Habegger Ltd., Thun. The method is unique in its applications on a tunnelling machine and can be explained as follows:-

A number of cutterheads equipped with tungsten carbide tipped cutter shanks are mounted on a revolving drum in such a way that axis is off angled slightly from the drum axis. This permits the face to be worked in multiple helical planes, with the cutters acting laterally, not frontally.

As the cutterheads operate at high speed in one direction and the drum revolves in the opposite direction at low rpm, the machine actually cuts a multistart, internal thread in the rock, destroying the thread profile as it is being formed. By this arrangement a number of advantages are gained:-

1. The rock can be undercut so that only one-third to one-fourth of the total rock volume is actually cut by the tungsten carbide tips, leaving the intermediate ridges to be sheared off. This means reduced tool costs.

2. By the same corkscrew action, the machine more or less pulls itself into the face. This means that less thrust values are required.

3. The undercutting technique also results in a comparatively coarse fragmentation of the rock which poses less problems

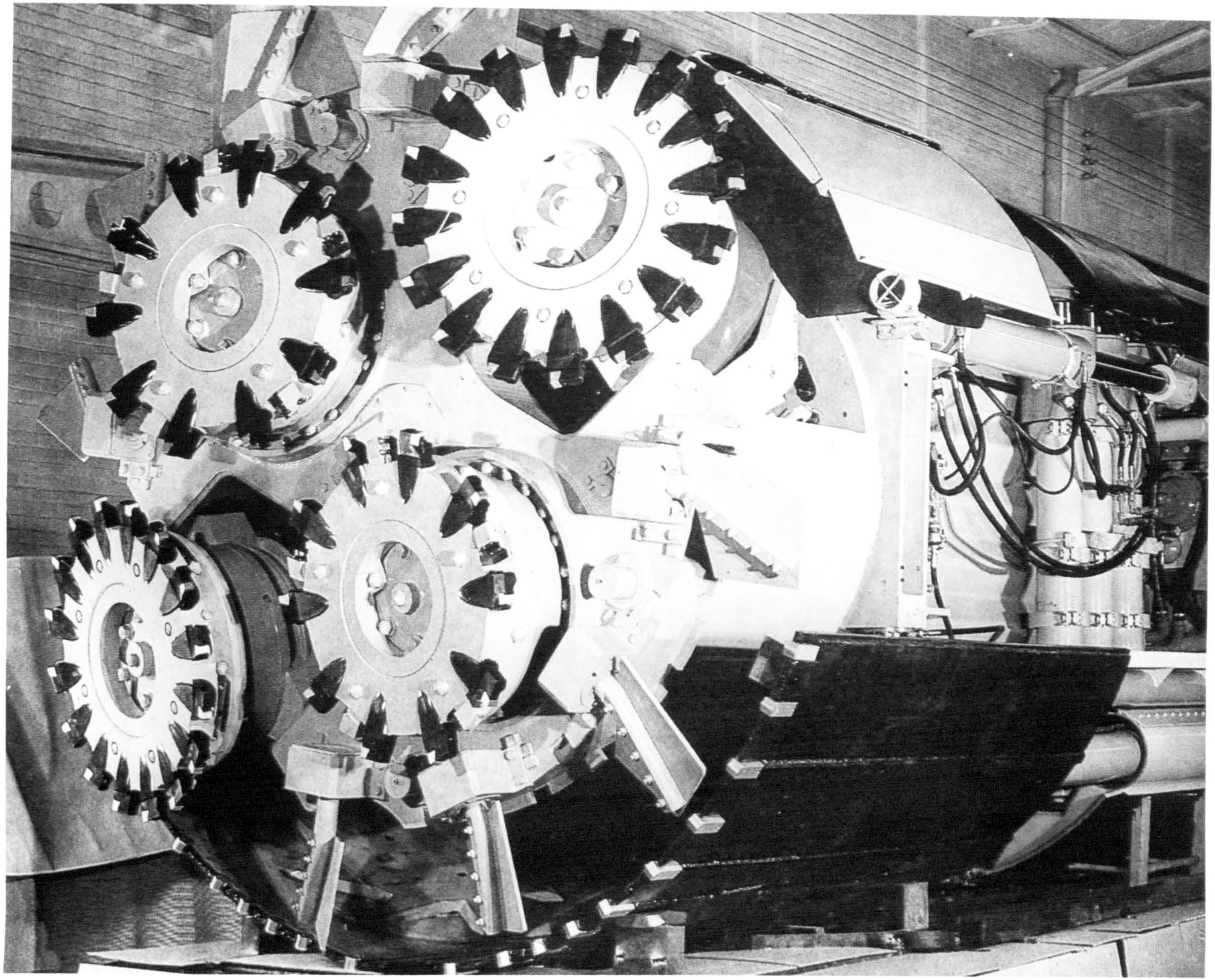

Atlas Copco Tunnelling Machine

Figure 15

for transport, especially when operating in tunnels with large inflows of water.

2.3.2.B.2 Shearer and selective heading type machines

In this type the cutterhead of tunnelling machine is substantially smaller than the tunnel cross section and can be subdivided into three sub-groups:-

1) Ripping machines (13-15 incl.)

The ripping machine was designed, in 1958, to mechanised the ripping lip in coal mines in Great Britain. The Mark 1 machine was the test rig while the Mark 2-4 were the production versions, built by Joy Sullivan Ltd., Meco, and Richard Sutcliffe Ltd. respectively. The Mark 2 consisted of three shearer type drums which mounted on the traversing arm and can take a minimum web of 0.3 metres and a 0.6 metres advance obtained before the machine is advanced. The Mark 3 used the vertical drum which fitted to the traversing arm and different roadway size can be cut by fitting extension drums. The heavy-duty picks were used in order to reduce the number of picks on the cutting drum. The Mark 4 machine consisted of a cutting arm fitted with four milling discs, which can arc through 196°. Each disc was fitted with 2-4 heavy-duty picks to build more power into each pick and so cut the harder strata.

However, the ripping machine is, at present, little used in mining industry.

2) Selective heading machines (16,17)

The selective heading machines, the socalled roadheaders, incorporate a moving telescopic boom terminating in a conical cutting head to make the sumping operation independent of the movement of the crawler tracks. The advantages of the selective heading machine are that power can be concentrated in the single cutting head and optimum cutting efficiency can be achieved. The machine can cut a roadway in any shape or size within a certain limits. Where strong inclusions are incorporated in the face, the softer material can be selectively removed before the heading profile is completed. The limitations with the heading machine is that the reaction thrust is normally taken up solely by the machine so there is definite limitation to the cutting pressure possible. This had resulted in the use of this type of machine being restricted to medium soft and soft strata, and coal seams.

3) Shearer type drum machines (18-16 incl.)

One machine that overcomes a number of disadvantages associated with a full-face tunnelling machine is the Greenside tunneller (18-25 incl.) . Its cutterhead consists of one or two cutting drums, laced with a battery of tungsten carbide-

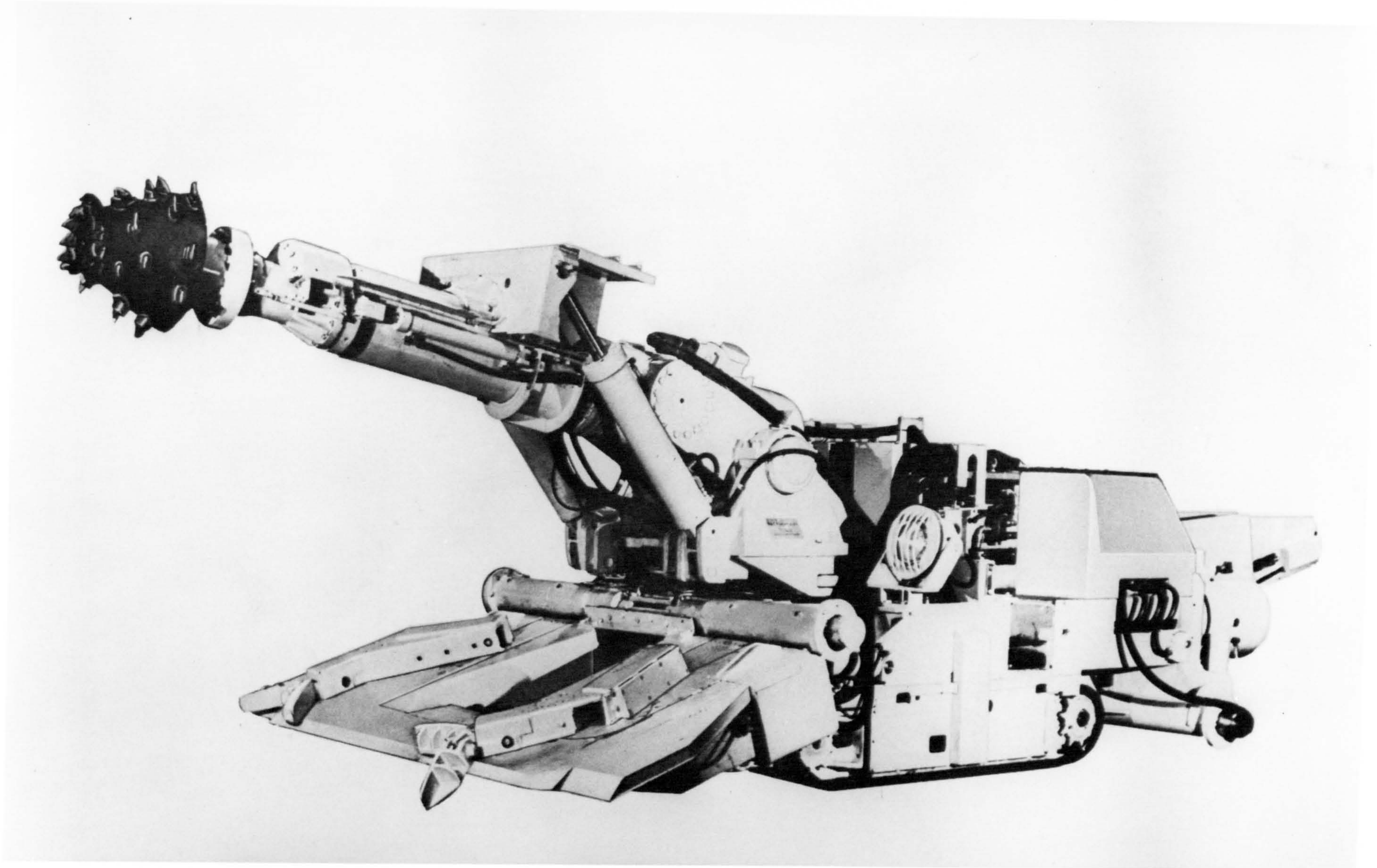

Anderson Mavor Heading Machine

Figure 16/A

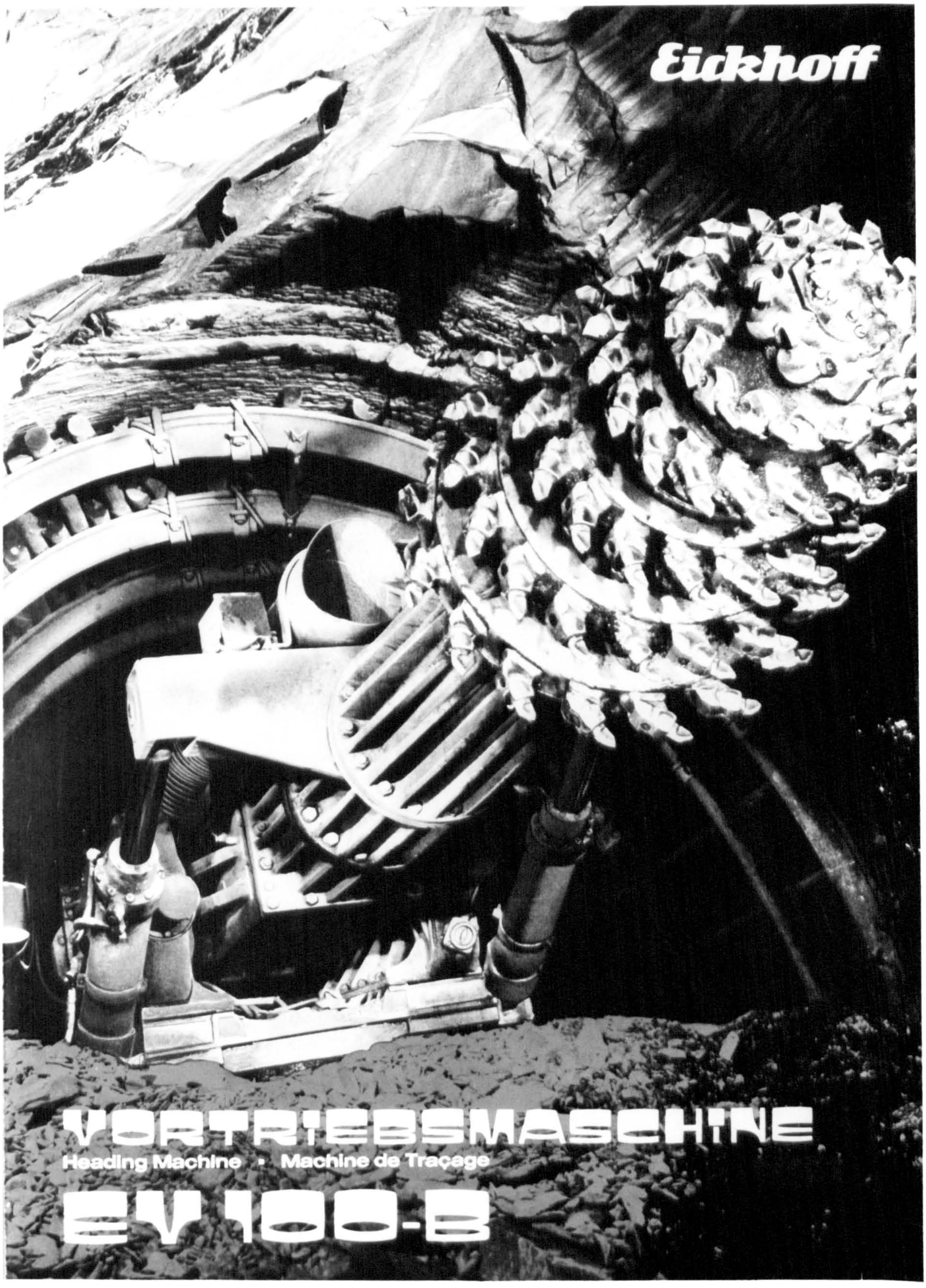

Eickhoff Heading Machine

Figure 16/B

tipped picks, which can traverse along an arm rotating about the central axis of the machine. It has been designed to cut a circular shape or horseshoe shape tunnel profile. The machine was successfully cutting a 4 metre diameter in limestone having the compressive strength of about 225 MN/m^2 (26).

The full-face tunnelling machine requires very high thrust on the cutterhead and when working in variable strata, the problems of providing anchorage are obvious. As the Greenside tunneller is not a full-face machine, it needs only exert a thrust of 10 tonnes to sump the cutting drum into the face, then all subsequent breakout of the rock is radially from the axis, thus utilizing the second free face. The tunneller can machine rock selectively and can sump in where the strata is softest. Other advantages this machine has over tunnel borers are:-

1. a third of time is required for assembly and disassembly,

2. with this unique method of cutting it is possible to have a basic machine able to cut a range of sizes of tunnel with 85 per cent of basic equipment remaining the same,

3. access to the cutting head is easy for inspection and changing of the drag picks, and,

4. principally, the low capital cost of the machine, being less than half that of a full-face borer of equivalent wattage, makes the drivage of tunnels of shorter length than previously thought economically possible.

2.4 Tunnelling machine manufacturers

There are more than 20 companies manufacture tunnelling machine. The following table describes the name of some manufacturers and tunnelling machine types they built.

Manufacturer	Machine Type	Tunnel Diameter (m)	Cutters	Total Power (kW),	Special Feature
Alpine, Germany	Selective heading	Variable	Picks	Variable	Radially cutting point-attack.
Anderson Mavor, UK.	Selective heading	Variable	Picks	Variable (approx.100)	Bore successfully through homogeneous rock up to 55 MN/m^2, and laminated sedimentary rock up to 90 MN/m^2.
Atlas Copco, Sweden.	Fullfacer (mini-fullfacer)	Rectangular Variable (2.10-5.50)	Picks	Variable (220-1000)	Undercutting method. Good for small size tunnelling project. Suitable for soft rock up to 120 MN/m^2.
Calweld, USA.	1. Shield	Variable	Picks	Variable	Oscillating tunnelling machine available apart from the conventional rotary one.
	2. Fullfacer	Variable	Discs or button cutters with tricone bits	Variable	Successfully bore through hard sandstone and compact sedimentary rock up to 220 MN/m^2.
Demag Industrial Equipment, Ltd., Germany.	1. Selective heading	Rectangular, circular and arched of variable size	Picks	Variable	Continuous operation suitable for soft rock up to 100 MN/m^2.
	2. Fullfacer	Variable	Discs, buttons or roller cutters	Variable	Can bore a certain diameter range without the main units or drives having to be changed. Suitable for rock up to 150 MN/m^2.
Dosco Overseas Eng., UK.	Selective heading	Variable	Picks	120	Suitable for soft rock up to 100 MN/m^2.

Manufacturer	Machine Type	Tunnel Diameter (m)	Cutters	Total Power (kW)	Special Feature
Dresser Industries, USA.	Fullfacer	Variable	Discs	Variable (547 up)	Infinitively variable control of rotation speed and thrust pressures. A large opening in the cutterhead assembly permits easy inspection of the face or cutters.
Eickhoff,	Selective heading	Variable	Picks	Variable (300 up)	Available with radially cutting point-attack or axially point-attack.
Jarva Inc., USA.	Fullfacer	Variable	Discs,buttons or roller cutters	Variable (285 up)	Cutters are designed for complete and easy interchangeability. The mixed face machine can bore through rocks, soil, or mixed conditions, cutterhead can overcut or undercut shield diameter.
Kinnear Moodie,UK.	Shield	Variable	Picks	Variable	
Lawrence Manufacturing, USA.	Fullfacer	Variable	Discs,buttons or roller cutters		Use the patented technique of drilling the hole ahead of itself to use as anchorage to pull the main element forward. Able to bore rock up to 350 MN/m^2.
McAlpine,UK.	Shearer type drum machine	Circular and horseshoe shape of variable size			Available with 1,2 or 4 cutting heads. Radial cut requires less force. Able to bore limestone up to 200 MN/m^2.
Robbins, USA.	Fullfacer	Variable	Discs,buttons or rollers	Variable	Bore through limestone up to 240 MN/m^2.

2.5 Application of tunnelling machines

In machine tunnelling the major factor that affects the choice of the type of machine is the strength of rock formation, however the abrasivity is also vital.

In soft formation two types of machine can be chosen, either shield machine or selective heading machine. The project in this type of formation which is worthy to mention, at present, is the Channel tunnel where the tunnel will be bored by a shield machine through the lower chalk formation. At the University of Newcastle an investigation into the mechanical cutting characteristics of the lower chalk was undertaken to provide information on the type of cutter, the cutting array on the cutterhead and the power supply to the cutterhead. The cutter recommended is the disc cutter.

The selective heading machine is able to bore a tunnel to any shape within the range of size, however the machine is restricted to soft formations. There are more than ten companies manufacturing this type of machine. In British coal mines it is very common to see the Dosco road-header in operation.

Tunnelling in unstable ground or very poor conditions is a problem, Nuttal and Priestley have designed the "Bentonite tunnelling machine" to be used in this condition. This machine did well in a trial and is convertible. The same machine could be converted to digging rock by changing to the right sort of cutting head. This machine is now under development.

In hard formation the button cutterhead machines are used but when the strength of rock is too high and also the abrasivity the project might be uneconomical. The pilot hole, using the conventional drill-and-blast method, has to be bored ahead of the machine and using the machine as a reamer to make the tunnel to the full tunnel diameter. One company, the Lawrence Manufacturing Co. has invented a fullfacer which employs a pilot hole principal. This machine has successfully bored through rock with compressive strength up to about 350 MN/m^2.

Tunnelling in mixed face is a difficult job, Jarva Inc. has announced a new type of tunnelling machine that has the capabilities of boring through either hard rock or soils in either supported or unsupported conditions. The cutterhead has the ability to undercut or overcut the shield diameter depending on the type of formations. The cutterhead is designed to use drag picks, disc cutters, or carbide insert cutters as condition require.

Chapter 3.

Previous Research in Rock Cutting

Research into rock cutting, that has been undertaken to improve the performance of machine tunnelling techniques will be reviewed under the following headings:

1. Exotic and novel methods of rock cutting.
2. Metallurgical considerations in cutting tool design.
3. Instrumented cutting experiments.
4. Rock property testing.

3.1 Exotic or novel methods of rock cutting

The "exotic" methods of rock cutting are those which do not use conventional picks or cutters to attack rock. They remove rock by four basic mechanisms:

1. Mechanically induced stresses
2. Thermally induced stresses
3. Fusion and vaporization and
4. Chemical action.

3.1.1 Mechanically induced stresses (27 - 36 incl.)

There are five principle mechanical methods namely: a) erosion by water jets, b) erosion by steel pellets, c) implosion, d) shock wave produced breakage, and e) ultrasonic drilling methods. These methods are considered as being unlikely to attain commercial importance in the foreseeable future, except in the case of specialised application. However, high speed water jets are under investigation to be used together with tunnelling machine cutters (34 - 36).

3.1.2 Thermally induced stresses. (37)

The drills in this type destroy rock by thermal action heat the surface of the rock to 400°- 600°C, producing stresses which break the rock by causing the surface layer to spall.

The drills of this type of mechanism are a) Jet-piercing drill, and b) Forced flame drill.

However the application of thermal spalling drills is limited because many rocks will not spall and more energy is required to heat rocks to a spalling temperature of 400°- 600°C than is required to remove them by rotary bits and also of high operating cost.

3.1.3 Fusion and vaporisation (38 - 40 incl.)

This method of rock breakage is based on the concept of heating the rocks above their melting or vaporising temperatures.

Examples of such drills are: a) nuclear drill, b) fusion drill, c)electric arc drill, e) plasma drill, f) electron beam drill, and g) laser drill. These drills, however, are used for drilling rocks on a small scale and only the latter two have any present commercial application.

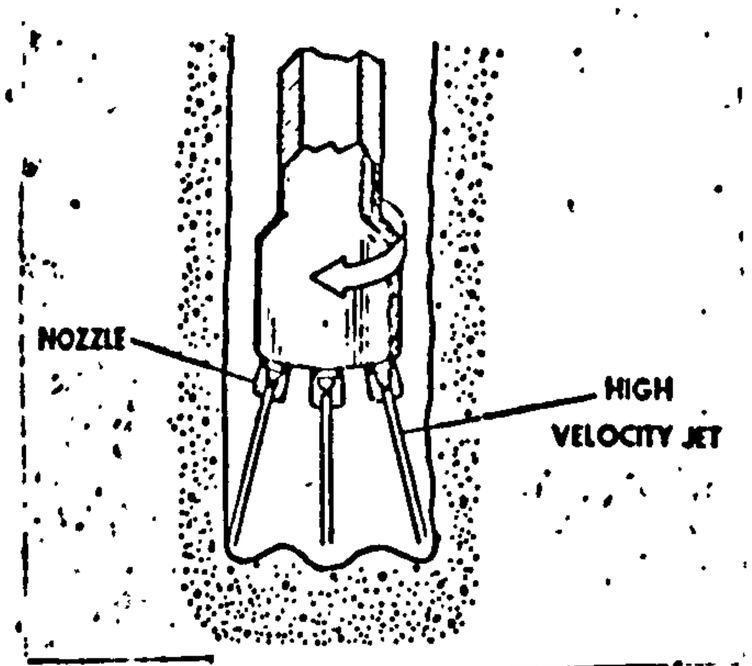

Erosion drill

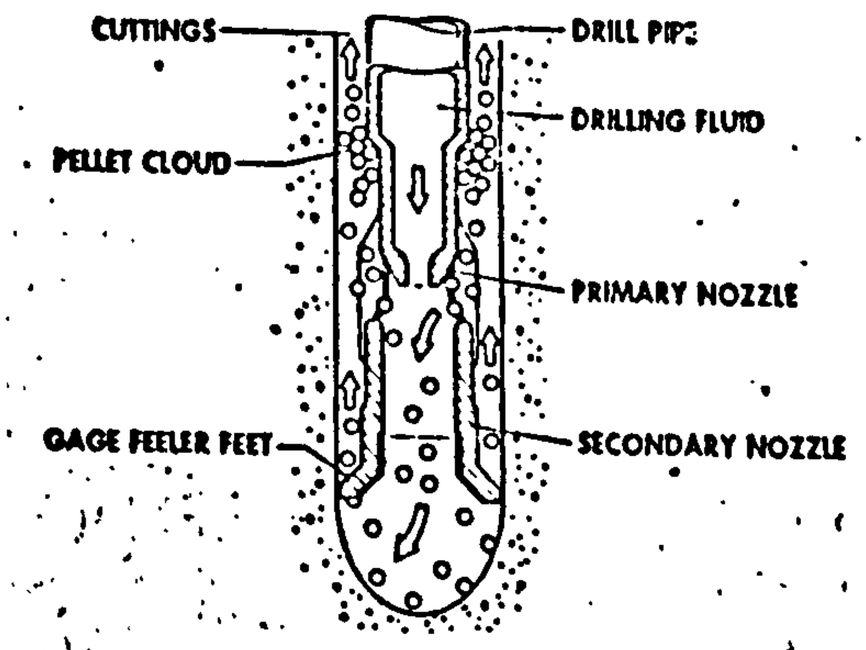

Pellet drill

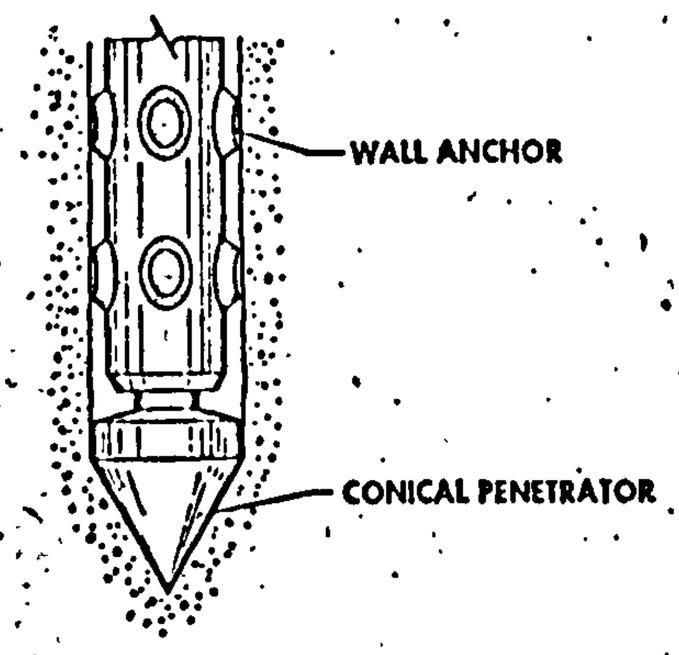

Continuous penetrator

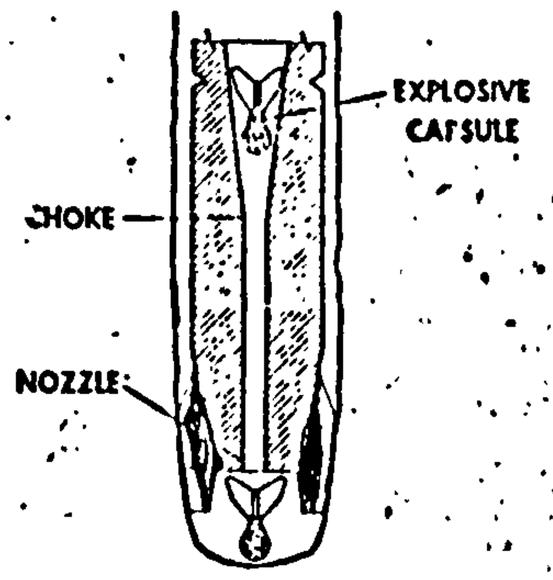

Soviet explosive capsule drill

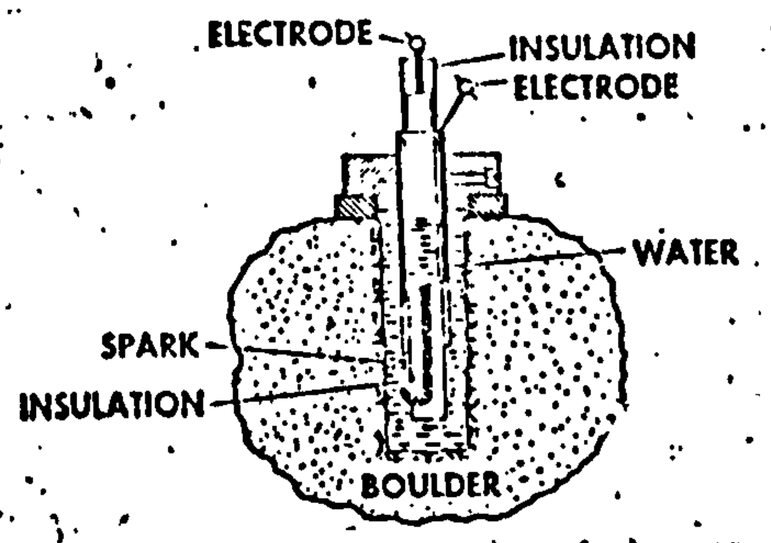

Electrohydraulic rock splitter

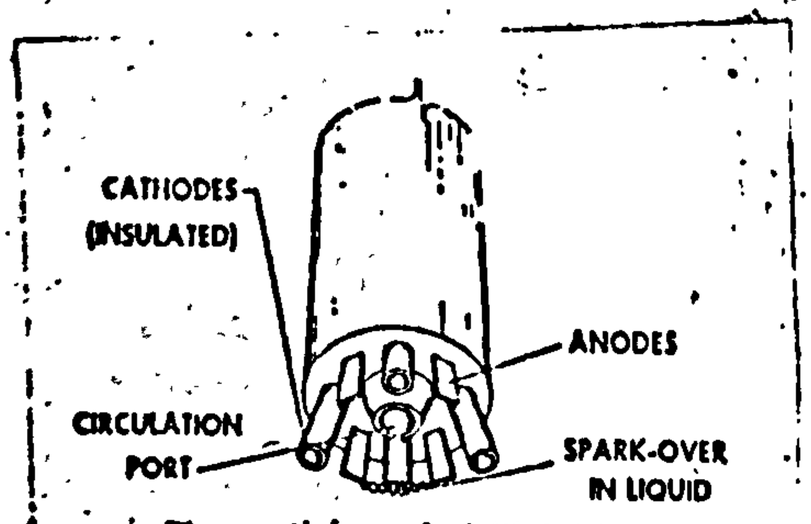

Tangential spark drill (Titkov *et al.*).

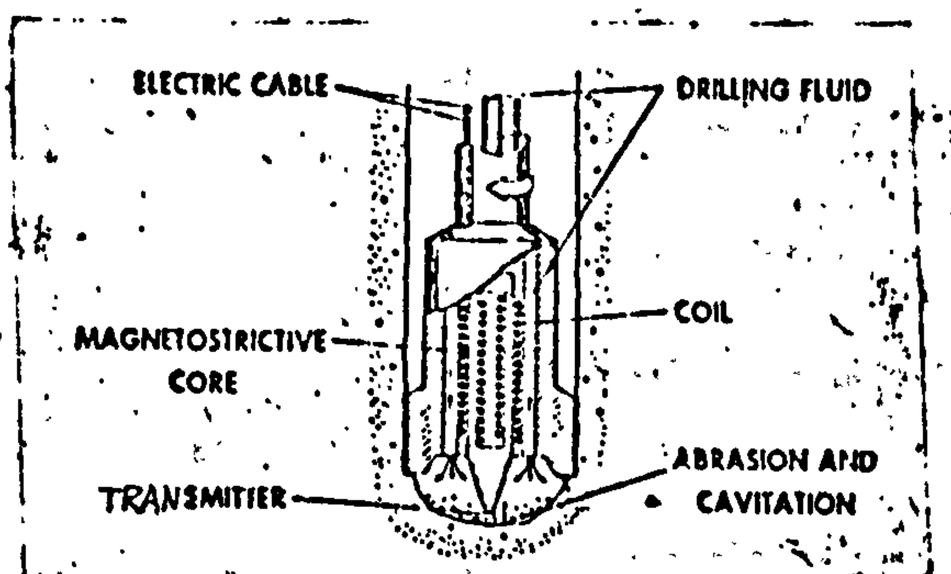

Ultrasonic drill

Mechanically induced stress

Fig.18 Exotic drills

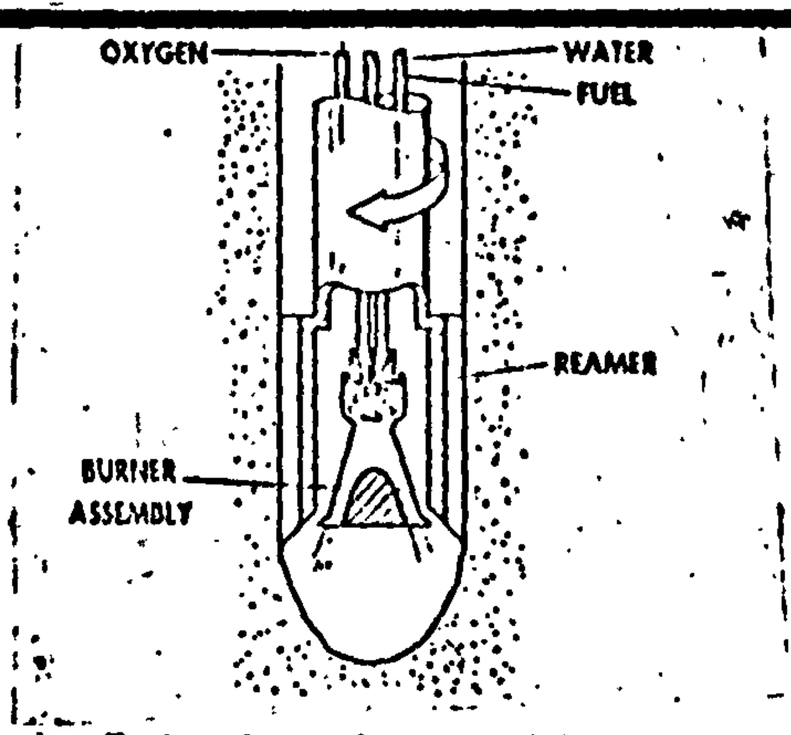

Jet-piercing drill

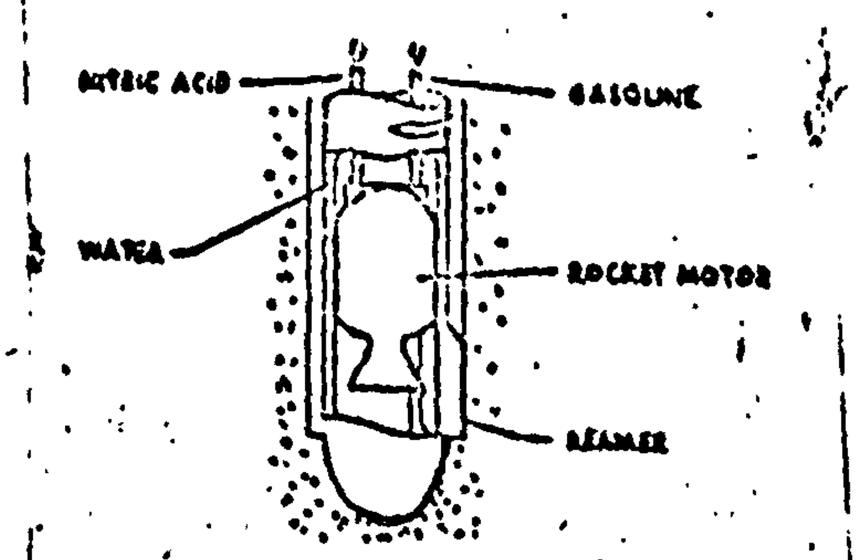

Forced flame

Thermally induced stress

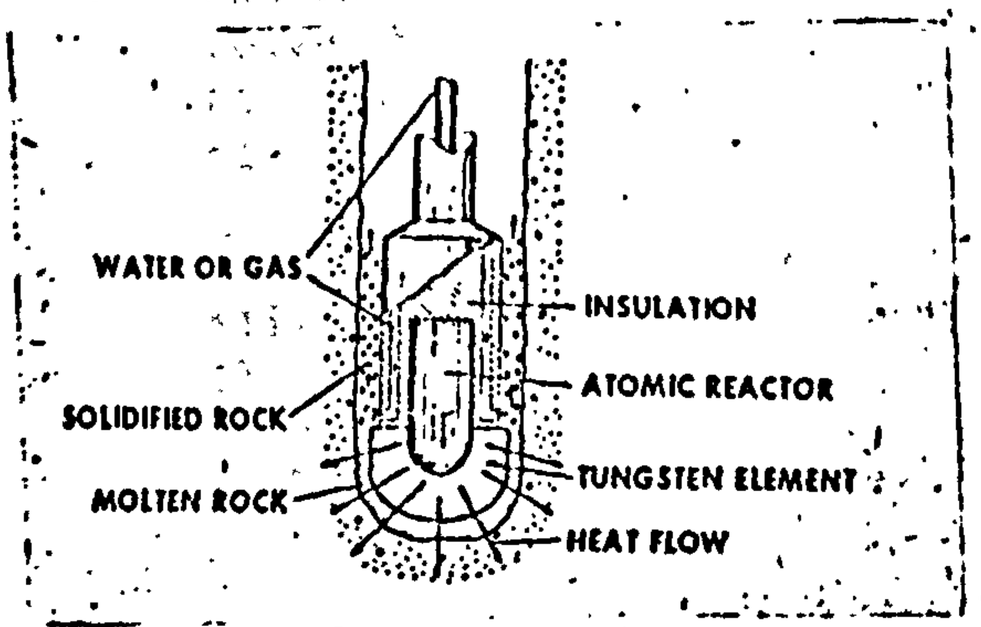

Nuclear drill

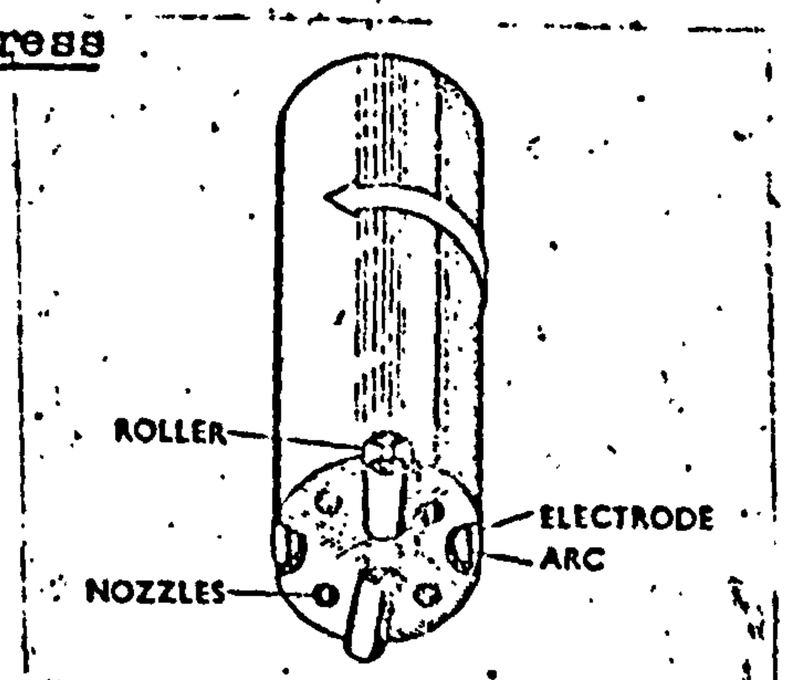

Electric arc drill

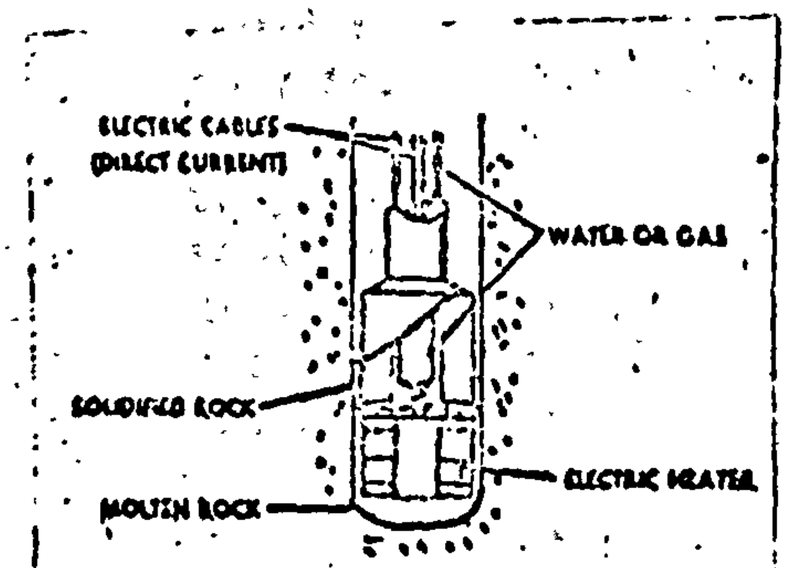

Fusion

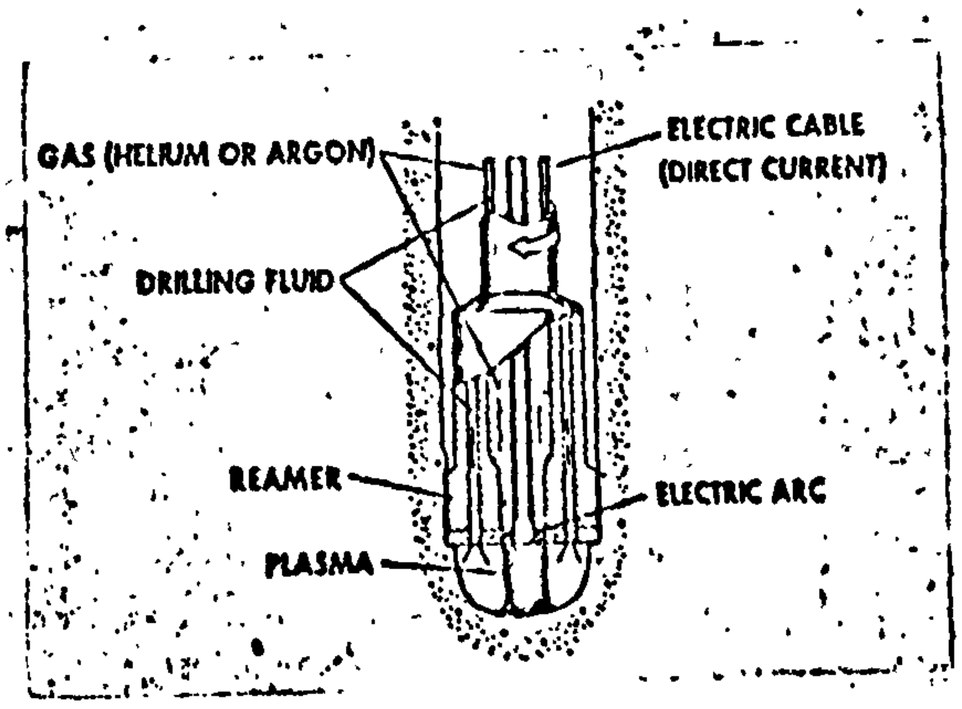

Plasma drill

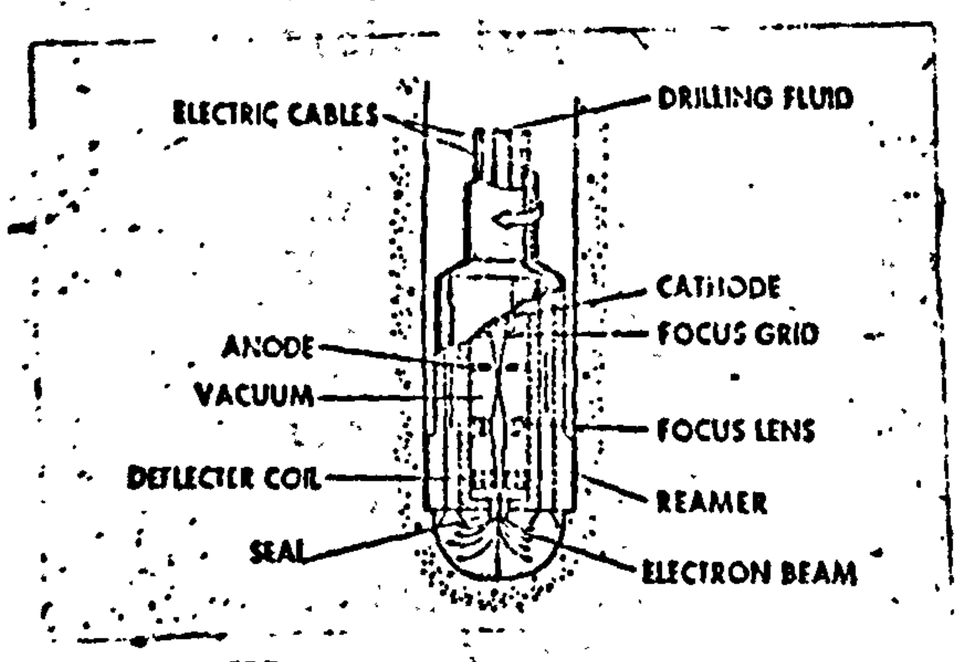

Electron beam drill

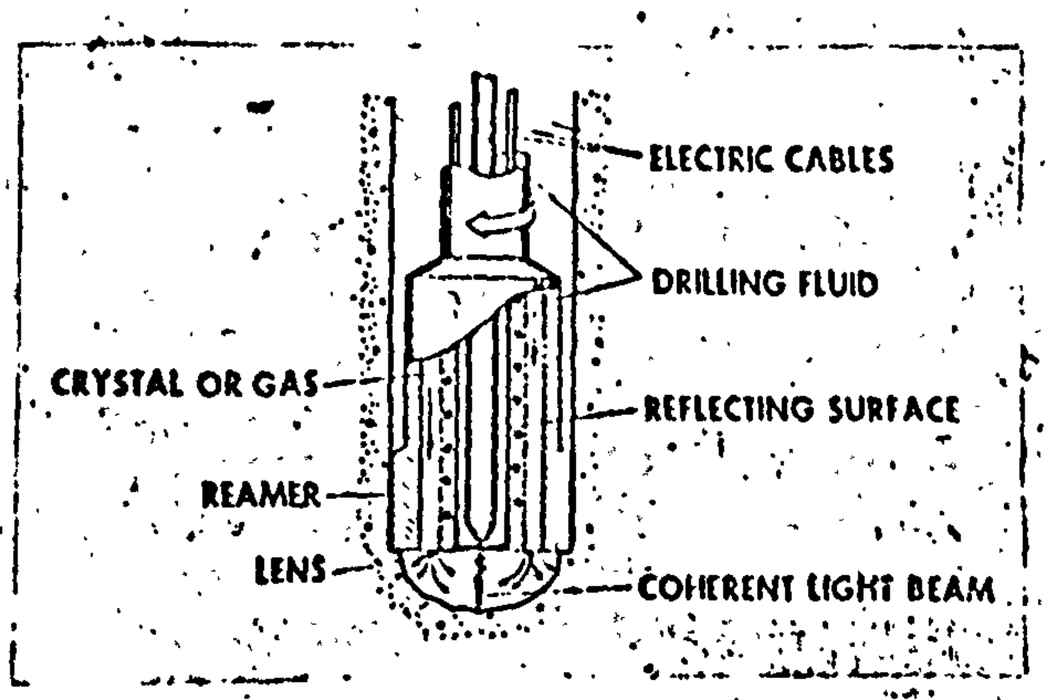

Laser drill

Fusion and Vapourization

Fig.18 Exotic drills

In USA, engineers at the United Aircraft Research Laboratories have published (40) a design concept for a laser-powered heat assisted tunnelling machine, which is basically feasible, though the design of such a machine obviously presents some problems.

3.1.4 Chemical drills(41,42)

The drill uses a high reactive chemical, such as fluorine, to remove the rock. On application the fluorine would be blown against the rock by compressed gas in the form of high velocity jets to dissolve the rock. Obvious difficutties are the frequent recharging necessary, high chemical costs and the problem in handling large volumes of highly reactive chemicals.

In conclusion, the exotic methods of rock cutting, at present, is still under the developing stage in order to use it in conjunction with the machine tunnelling cutters. The most promising method might be the erosion by water jets, however much research and development remains to be done before suitable applications can be found.

3.2 Metallurgical considerations in cutting tool design

With respect to the cost involved in a tunnelling project, it is invariably found that cutter cost are the largest single variable factor. With proprietary cutters (drag picks, disc or button cutters) it is found that tool life is affected by the conditions under which they operate. It is reported (43) that one of the main factors influencing the wear rate of the cutters is the abrasivity of the rock in which they operate. The effect of bluntness is to increase the forces on the tool for a given depth of cut. Thus for a machine of given axial thrust, as wear progresses, penetration will become less, and therefore the cutting process less efficient. It is, therefore, necessary to study the mechanisms of wear.

3.2.1 Mechanisms of wear

Wear has been defined (44) as the gradual deterioration of at least one of two contacting surfaces by mechanical dislocation of particles from the surface or surfaces.

The majority of work considered for the mechanisms of wear is for WC/Co alloys, but the mechanisms may be considered to be equally applicable to other tool materials, since they basically consist of a hard and a soft phase. Doeg (45) suggested that the wear is dependent on the form of the WC crystal, the α_1 WC being more wear resistant than the α_2 (secondary) WC, and the cobalt content. This view is partially disputed by Lardner (46) who stated that grain anisotropy is responsible for the differing wear rates. Doeg does, however, suggest a simple mechanisms for wear which is split into three distinct phases:

a) Erosion of the binder phase
b) Abrasion of the WC which is exposed
c) Fracture and subsequent removal of the WC.

Furthermore, he recommends that by decreasing the cobalt content to a minimum, maximum wear resistance could be obtained, However other works (47) decided against this mechanism, and concluded that the wear of the soft and hard phases takes place simultaneously. Cook et al (47) whilst

cutting quartzite, come to the conclusions that with speeds up to 125 mm/sec the wear rate increased greatly. They also showed that initally there is a very high wear rate, but this decreases once a slightly worn state has been reached. **Osburn** (48) reviews in great detail the possible mechanisms of wear that could occur when cutting rock with tungsten carbide tools. His work can be summarised as follows:-

a) Frictional wear and attrition:

When two surfaces make contact, there are extremely high localised pressures and this leads to welding at the point of contact. In this type of wear shearing can take place in either of the metals or in the weld, depending upon which is the weaker. Work hardening may take place in the softer material and cause wear on the harder surface. A mechanism of solid film lubrication is also postulated where a hard material is overlain with a thin film of soft material and rubbed against another hard material. Here the area of contact is low, but shearing takes place in the soft film where the effective shear strength is low. The result is solid film lubrication where the frictional force is lower than might have been expected. If this mechanism work for WC/Co, there should be a cutting speed at which the rate of wear suddenly increases (47) when the rate of diffusion of the cobalt from the matrix is insufficient to provide this solid film effect. If cobalt is removed from the rock tool interface, attrition will occur with a resulting weakening of the matrix and the subsequent removal of the WC grains. This is now similar to the mechanism as proposed by Doeg.

There is some practical evidence in support of this mechanism, Pearson (49) observed that whilst cutting quartzite, a black streak of metal was fused to fine silica particles in the cut groove and that a deposit of fine quartz remained on the underside of the tip. Pearson speculates that this could have been caused by either pressure welding or fusion during the cutting process. A similar occurence was reported by **Rae** (50) when sandstone was found fused to a mild steel slider. It is possible that the formation of a layer of work hardened material on the back face of the tool changes the mechanism of wear, since it would offer some measure of protection to the tool material this could explain Cook's results that, after an initial high rate of wear, the rate decreases as cutting continues.

b) Abrasion wear and erosion:

When the condition of rubbing are more severe than those above, deeper penetration of the surface will result. The wear can be likened to a process of micromachining of the surface and is termed abrasive wear, although frictional wear still occur. One material will scratch another, provided that there is a difference of approximately 20% in their relative hardnesses. The depth to which a quartz grain will penetrate is dependent on the relative hardness of the tool. The greater the initial penetration the greater the wear. Once the grain has penetrated the tool, in order for it to scratch, its transverse rupture strength must be high enough to stop its fracturing under the forward force of the tool. Where loose grains impact against the tool, erosion wear takes place. Under the repeated impact of slow moving particles, brittle materials will fail by a slow propagation of fractures from a surface flow at stress levels much lower than those needed to propagate macroscopic cracks.

c) Microfracturing of surface layers and fatigue.

This mechanism includes the process of microchipping or flaking of the surface. When impacting at a higher rate, the surface cannot deform as easily and there is a tendency to brittle fracture, this occurs as microchipping and it may be difficult to distinguish from abrasive wear.

Thermal fatigue does occur from repeated thermal cycling and surface cracking of the carbide occur. Microscopically, the cracking seems to be of haphazard shape. However both the thermal shock and thermal fatigue resistance of WC/Co is good.

d) Impact damage

The effect of a branched crack is more harmful than of a single crack. Branching from the main crack to form a network of cracks is caused by the reflection of shock waves from the back and edges of the material. The initial compressive shock wave is reflected back as a more destructive tensile wave. This leads to the possibility of gross failure of the material.

e) Chemical aspects of wear

Although Osburn does consider this mechanism, there is no empirical evidence in rock cutting.

3.2.2 Wear research

Early work conducted in 1955 by Latin (51) at the M.R.E. established fundamental relationships between wear rates (for both abrasive and impact conditions), carbide composition, the material being cut and lubrication effects.Further work carried out after Latin's inital investigation at M.R.E. is reported by Evans and Pomeroy (52). More recently in 1969, Johnson & Morgans (53) reached the following conclusions whilst studying abrasive wear in different tool materials (stellite, tool steel and carbide):-

a) General pattern of abrasive wear is similar for the three types of materials examined.
b) The width of the wear flat obtained for a given length of cut appears to be related to the V.P.N.
c) The wear angle is greater for carbides than tool steels.
d) The general relationship $W = KD^N$ holds for all materials tested, where
   W = width of wear flat
   K = constant dependent upon shape of tool and depth of cut
   D = distance cut
   N = constant which is dependent of the shape of tool and depth of cut.
e) For a given width of wear flat, a stellite tool needs to cut approximately five times as much as a tool steel, the average carbide forty times as much.
f) For carbides of differing grain sizes but the same hardness, larger grain sizes produce more wear.

Full scale wear research was submitted by Brodbeck (54) and Lauber (55) that experiments to provide valuable information can only be

carried out with a real heading machine. Furthermore, they state at best, small scale laboratory results can provide fundamental points of departure, but are hardly capable of giving results which can be transferred, since the forces occurring in the machine, speed, shock, vibration and, most of all, long term performance cannot to any great extent be intiated expermentally. Two developments resulted from field trials with an operating machine:-

1) A resilient mounting for the carbide tools.

2) Cooling of the tool by compresses air/water sprays was found necessary due to excessive tool wear.

Lauber (55) also reports that a machine operating on the undercut principal reduced tool wear by these means in addition to the machine being of very rigid construction.

The method of testing a new type of carbide was to replace half the used cutters with new ones, and then see how far they would cut. Altogether, ten makes of carbide from six countries were tried, and a Japanese make of Pryhard was found to be best, it greatly exceeding the 90 hours cutter life needed for an economic operation.

3.2.3. Factor relating to improvements in wear-resistant properties

In present applications, whether for heading machines or in rotary drilling, the prime consideration in reducing wear is to improve the fracture-resistant properties of the tool material-at an appropriate level of hardness to combat the effect of frictional and abrasive wear. The primary factors are:-

a) Cobalt content
b) Carbon content
c) Porosity
d) Grain size

a) Cobalt content:-

The effect of cobalt on the physical properties of the carbide are shown diagrammatically in Schwartzkopf & Kieffer(44) and is shown in Figure 19. As the cobalt content increases, the hardness decreases. Gurland (56) reports that for a particle size of 2 microns the hardness falls from 1650 V.P.N. to 1150 V.P.N.when the cobalt is increased from 5% to 30% by weight. The transverse rupture strength increases to a maximum at 20% cobalt with increasing cobalt content.

The function of the cobalt, as stated by Osburn (57) is to act a "crack stopper". That is, to dissipate the fracture energy of the crack reaches the binder phase layer. Therefore, the binder material should be as pure as possible so that its ductility is not impaired. Schwartzkopf & Kieffer state that cobalt is the best binder for tungsten carbide when used for fracture resistant applications. The ductility of the matrix can be impaired by dispersion strengthening or by solid solutions being formed. Rigid control of the carbon content can prevent dispersion hardening effects. The more uniformly the cobalt is distributed, the better its action as a crack stopper. The formation of cobalt lakes is indicative of poor milling or sintering practice.

THE EFFECTS OF COBALT ON HARDNESS & STRENGTH

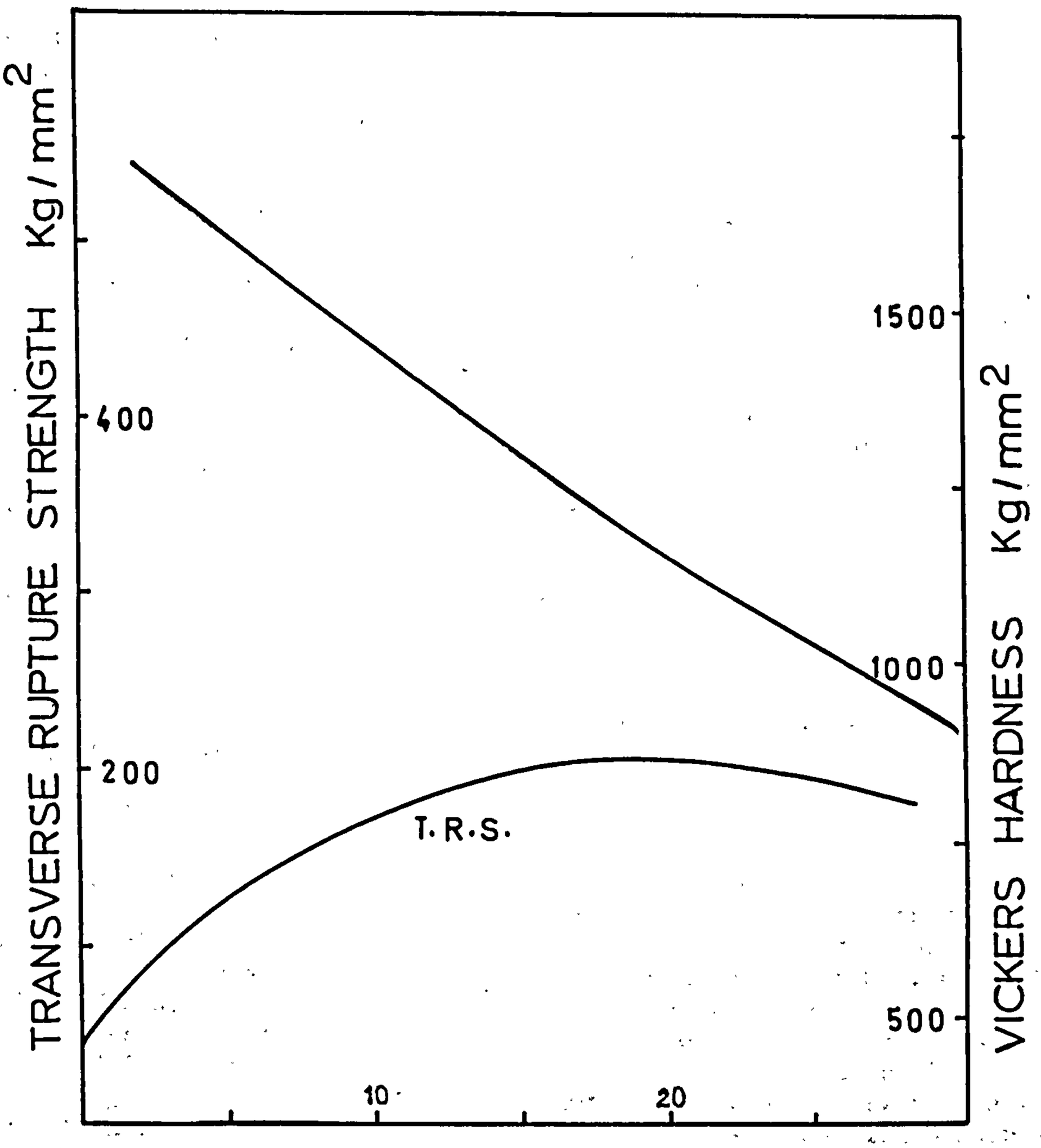

FIG. 19

b) Carbon content:-

Tungsten monocarbide should theoretically have a 6.12 % carbon content. If this value is exceeded, free carbon in the form of graphite is introduced into the tip, decreasing the transverse rupture strength.

If, however, there is a deficiency of carbon, a very brittle compound of the form $Co_3W_3C_4$ is produced. Lardner reports that the carbon content should be controlled to ± 0.04 % and suggests that this value could still be improved upon.

c) Porosity:-

Porosity is an important consideration in improving the performance of tools made from WC/Co. It is reported (51) that for an alloy containing 6 % cobalt the transverse rupture strength decreases by 57 % for an increase in voids from 0.9 % to 2.6 %. Lardner reports that by normal powder metallurgy standards, WC/Co is essentially free from porosity. The porosity that occurs is randomly distributed voids of varying size and shape. The main cause is grossly contaminated powder or very bad lubricant distribution. Carbides are usaully assessed for porosity by comparing polished surfaces examined at x 200 with the standard charts presented in ASTM B406-64. The effect of porosity on bending strength of the material has been reported by Knudsen (58) as:-

$$S = So \exp(-bp)$$

where So = strength of a fully dense material
b = empirical constant
p = porosity.

The effect of porosity is that of stress raisers and attainment of a carbide free from porosity should be sought.

d) Grain size:-

The effect of grain size on the physical properties of the alloy are such that at a constant cobalt content, the finer the particle size, the harder the material becomes. Gurland reports that decreasing the grain size from 6 microns to 1 micron increases the hardness from 1200 V.P.N. to 1450 V.P.N. for an alloy containing 20 % Co by weight. He also states that the strength of the alloy at 20 % Co increases as the grain size increased from 1 micron to 3.5 microns, and thereafter decreasing with increasing size, Thus, there is a maximum strength for a given cobalt content which depends upon the grain size. This conforms with Osburn's view that there should be an optimum grain size for a given cobalt content. Osburn also advocates grain size blending showing that the theoretical packing density can be increased. This is not, however, carried out in practice, since grain size as supplied is only nominal, there being considerable over and under-size particles present.

3.2.4 New tool materials

There are many compounds which are harder than tungsten carbide which should be considered as the basis for a new tool material. Some of these compound are listed below:-

Material	Microhardness Kg/mm^2
WC	2400
Al_2O_3	2800
TiC	3200
$Ti\ B_2$	3400
SiC	3500
B_4C	3700
Diamond	8000

Most of these materials cannot be bonded to form solids of satisfactory strength and toughness. Only aluminium oxide Al_2O_3 and the boride material have found some application in metal cutting.

The proving ground for most new tool materials is in the workshop, and if they should prove successful, further applications can be sought. Aluminium oxide tools have found usage for taking finishing cuts, but they are not strong enough to withstand the intermittent shock loading which occurs during roughing cuts. This would apparently preclude the use of this hard material for rock cutting, since it would be subjected to highly fluctuating forces as the cutting is a discontinuous process.

An attempt has been made (59) to increase the life of standard cemented carbide tools by the addition of 10 % large grain size boron nitride to the tool. The results showed conclusively that the material was inferior in performance to straight WC/Co alloys because it chipped and cracked easily.

Thus it would seem unlikely that with the present state of knowledge that any form of rock cutting material will become available from these harder compounds.

3.3 Single tool rock cutting experiment

In this country, research into the performance characteristics of rock cutting picks has been concentrated at the Mining Research & Development Establishment of the National Coal Board, and in the Department of Mining Engineering at the University of Newcastle upon Tyne.

Evans and Pomeroy (52) have published a monograph, summarising the work of the National Coal Board applied to coal cutting machinery.

A theoretical model describing wedge penetration into coal has been proposed, and its development is seen from the work of Dalziel and Davies (62) and Evans (63,64). Important laboratory studies have been made by the National Coal Board in order to define the influence of various operational parameters on the coal cutting process. O'Dogherty (65) has shown the variation in tool forces, due to changes in rake angle. The effects of different tool profiles (66,67) and spacings (68) on forces and efficiency when cutting coal and some rocks have also been studied.

When applying laboratory results to the real situation, it was found that tool wear in abrasive rocks could be a dominant factor in any excavation system design.

Accordingly, research at the University of Newcastle upon Tyne has been directed, in part, towards an understanding of abrasive wear mechanisms (57,69). Studies of the effect of tool shape and material on cutting performance in highly abrasive quartzites have optimised these parameters for a particular mining application (60).

Research into the effect of some design parameters on rotary cutter performance have been carried out by the National Coal Board, but published only in confidential internal reports (70-72), and in America by the U.S.B.M. (73).

The experiment conducted by the National Coal Board were carried out in Darly Dale and Pennant sandstones. Both materials are abrasive. Darley Dale sandstone has a compressive strength of 57 MN/m^2(8,300 psi), while that for Pennant sandstone is 145 MN/m^2 (21,100 psi). Some cutting work on concrete was also carried out (74).

The experiments undertaken at the U.S.B.M. were five rock types, ranging from 62 MN/m^2(9,000 psi) to 186 MN/m^2(27,000 psi) compressive strength.

Prediction equations for penetration in terms of the physical properties of the rock were obtained for one particular set of experiment conditions.

From these previous studies, a valuable insight can be gained into the techniques of experimenting with rotary cutters, and many of the problems involved in such work.

The experiments conducted by the Department of Mining Engineering at the University of Newcastle upon Tyne were carried out by Allington(4), Rispin (60), and Humphries (61) mostly based on the linear cutting apparatus using various types of cutter. It has been successfully studied for several rock materials.

3.3.1 The linear cutting apparatus

The experiment is based on a 9 kW Butler 660 mm "Super Shaper" machine, which has a modified head to support a triaxial force dynamometer. The maximum stroke of the arm is 660 mm, and like the speed, is adjustable over a wide range. The speed of the arm is constant over the middle 75 % of the stroke. The depth of the cut can be varied by raising or lowering the tool holder, which is attached to the cross slide by means of a lead screw. The machine table can be traversed vertically and horizontally.

The dynamometer was designed by Allington (4), based on work done at M.R.E.. It consists of a central plate, held to a rigid framework by four rectangular measuring bars which support the tool. Each bar is instrumented with etched foil strain gauges, which are connected to three Wheatstone bridge circuits, 24 gauges being used for the complete dynamometer (Figure 20).

For bridge 1 - output is proportional to sideways force.
For bridge 2 - output is proportional to normal force
For bridge 3 - output is proportional to cutting force.

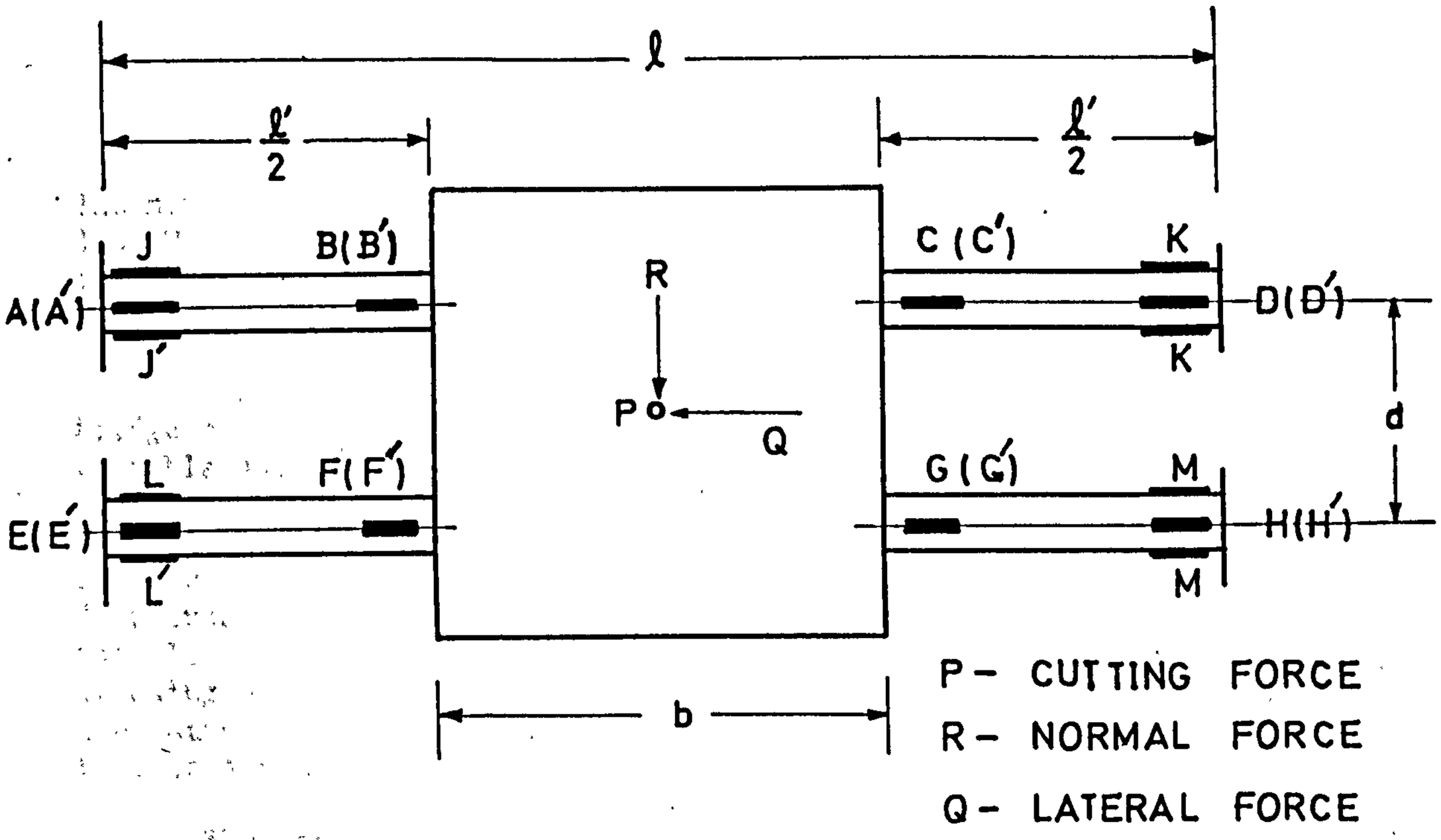

(a) POSITION OF STRAIN GAUGES ON MEASURING BARS

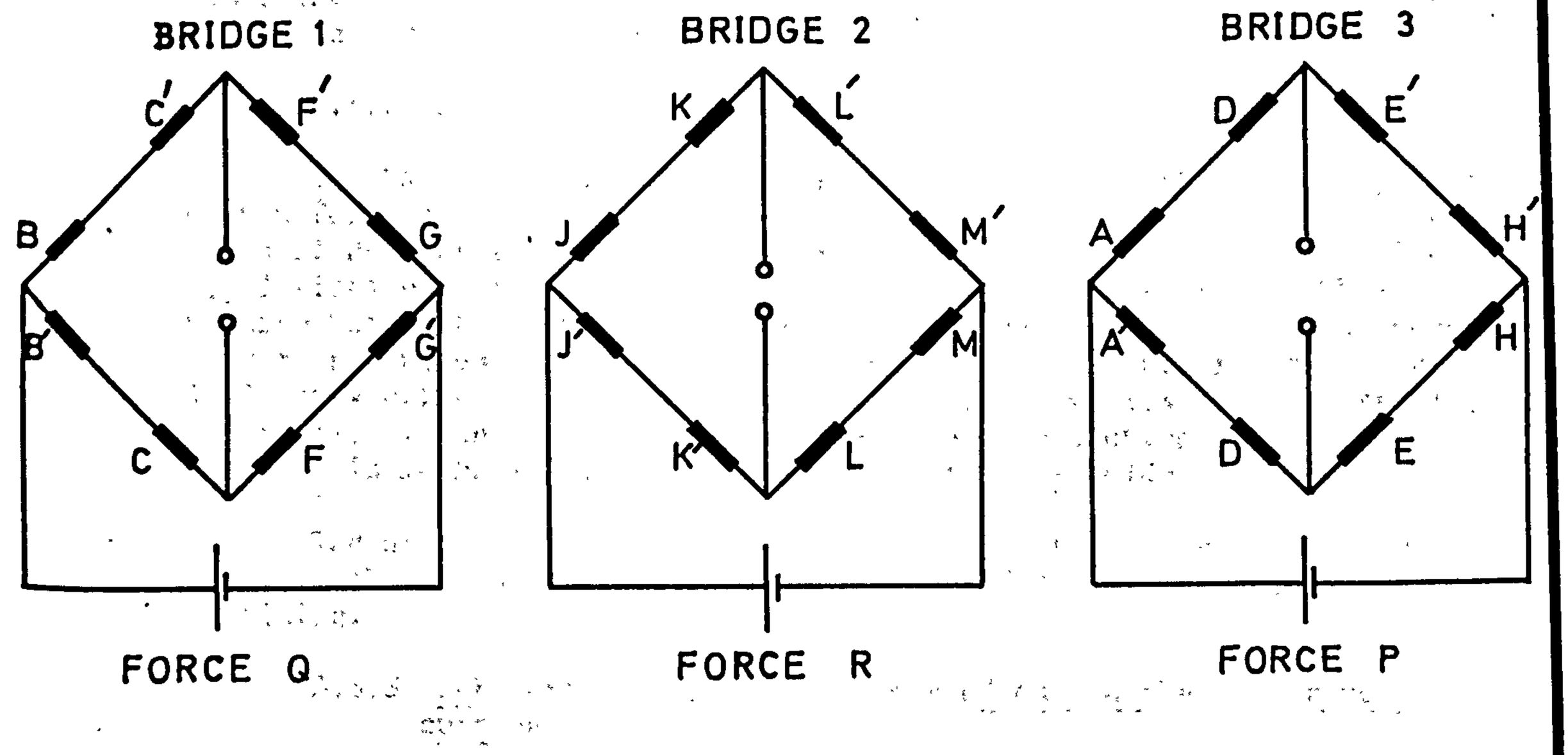

(b) ARRANGEMENT OF STRAIN GAUGE BRIDGES

FIG. 20

The maximum force that can be measured by the dynamometer are cutting 100 kN; normal 50 kN; sideways 20 kN. For symmetrical cutting, the sideways force is usually small and oscillatory about zero, and is therefore usually neglected.

Each bridge is supplied with a 12 volt supply and the fluctuating bridge responses during the cutting are amplified through a Southern variable gain (10-500) amplifier.

An SE 3006, 12 channel ultraviolet recorder is used to record these responses during cutting and they are displayed as three independent traces on ultraviolet sensitive paper (Figure 21). The circuitry has also been adapted so that mean forces during cutting can be measured by using electronic integration (resistor and condenser in parallel). As the output varies with cutting speed, the instrumentation has a variable time constant device.

The tool is clamped by means of a tool holder to the central plate of the dynamometer.

The rock sample is usually cut from a larger block to a rectangular shape, using a diamond cutting wheel. It is important that at least one face of the specimen is flat, so that it can be attached to a base plate. The specimen is glued to the mild steel plate with araldite AY 103 and the plate tightened to the table before setting is completed. This is to ensure that the stresses induced in the plate during tightening do not cause the araldite to crack. The block is then left for 24 hours to set and is then ready for cutting.

3.3.2 The rotary cutting apparatus

The basis of this is a Richards (model 1466) vertical borer, fitted with a four foot diameter table and twin saddles operating on a single cross slide. The table speed is variable in 12 stages from 2.3 to 48.4 revolutions per minute, and it is powered by an 11.2 kW motor. The machine has both automatic vertical and horizontal cross feeds, although they cannot be used simultaneously. The feed is mechanical working on a lead screw arrangement. The feed range available varies for each saddle, but it lies in the range 0.2 mm to 0.9 mm per revolution of the table. The tool is mechanically clamped into the machine holder.

The specimen was secured to the table by four screw-type clamps after which a standard cylindrical diameter of 480 mm was obtained by machining.

3.3.3 Rock cutting experiments carried out on the linear rock cutting rig

The instrumented rock cutting machine was firstly designed to determine the relationship between the variables involved in simple linear rock cutting, i.e. depth of cut, line spacing, pick geometry, etc., and secondly to investigate the comparative effects of using different types of picks cutting in different rock materials.

ROCK READY FOR CUTTING ON THE LINEAR RIG

Figure 21/A

Rock investigated were selected to represent the following types of materials:-

very high strength, abrasive	- South African quartzite
high strength, non-abrasive	- Hinkley Point limestone, Anhydrite
medium strength, abrasive	- Dunhouse sandstone, Springwell sandstone
low strength, abrasive	- Scotswood sandstone
low strength, non-abrasive	- Chalk.

Several quantities are used to indicate the performance of a rock cutting tool under different operational conditions.

a) Mean cutting force	- the average force on the tool in the direction of cutting. Multiplying this by the distance cut gives the amount of work done.
b) Mean peak cutting force	- the average of the peak forces acting on the tool in the direction of cutting. This is relevant to the mechanical strength of the tool design and its holder.
c) Mean normal force	- the average force acting normal to the direction of cutting, tending to push the tool into or out of the rock face. This value is the thrust required to maintain the tool at its required depth of cut.
d) Mean peak normal force	- the average of the peak forces acting as above
e) Yield	- the quantity of rock produced in either mass or volume per unit distance cut.
f) Specific energy	- the work done per unit mass (or volume) of rock cut.
g) Coarseness index	- a comparative measure of the size distribution of the cut rock.

3.3.4 Rock cutting experiment carried out on the rotary cutting rig

The experiment was designed to give an insight into the manner in which tools made from different materials wear under abrasive conditions for various lengths of cut. In previous wear research carried out at Newcastle (69) the length of cut has been restricted to 600 mm, the maximum useful stroke of the linear rig. The effect of temperature build up and subsequent softening of the tool could therefore only received limited attention, because at the end of each cut, the table has to be transversed, the shaper arm returned and then the table reposition for the next cut. During this time, the tip has ample opportunity to air cool and thus the heating effects are not so pronounced.

To overcome this limitation, it was suggested that the workshop vertical borer could be used to take shallow depths of cut in an abrasive rock under constant cutting conditions. Thus the effects of length of cut could more easily be studied, there being no real limitation on the distance cut, except tool life.

In this experiment the same parameters used for the drag pick analysis were used, except that the terminology was modified in some cases to conform with common usage.

a) Cutting forces are referred to as rolling forces.
b) Normal forces are referred to as thrusts.
c) Depth of cut is referred to as penetration.

3.4 Rock properties testing

Generally rocks are classified by their geological names, and the property they are normally given is their uniaxial compressive strength. When mechanizing the process of rock excavation the above information is totally inadequate to determine its machineability or cutability. Since compressive strength bears no relationship to rock cutting processes. Although a vague correlation can be found to exist between rock strength and the machine performances, there are many significant departures from it. Some rocks of comparatively high strength are easier to cut than others of low strength. A known machine has successfully cut limestone, having a uniaxial compressive strength of the order of 120 - 150 MN/m^2 at a regular rate of 5 m/shift. The same machine operating in a coarse grained sandstone of about 40 - 50 MN/m^2 was completely ineffective and had to be withdrawn. Other properties have to be known.

Previous investigations in rock properties testing, too numerous to be listed entirely. However there are few standardized rock-testing techniques with universal acceptance (75-77 incl.). Accepted techniques are fairly widespread and may be divided into laboratory tests and in-situ tests. All of them may be classified into the following principal groups:-

1. Strength of rocks or their resistance to destruction by elementary stresses (compression, tension, shear).
2. Deformability of rocks or their resistance to change their shape or volume.
3. Hardness of rocks or their resistance to local destruction (indentation or scratch hardness).
4. Grindability of rocks, or their resistance to breakage.
5. Extractability of rocks or their resistance to destruction during various mining processes (cutting, breaking-off, drilling, blasting properties, etc.).
6. Resistance of rocks to destruction during various mining processes (planing, boring) effected by tools or special instruments simulating actual mining processes under certain idealized standard conditions.
7. Abrasive properties of rocks or their wearing effect on the working tools of mining equipment.

These tests will be detailed in the following chapters.

Chapter 4

Objectives of Research

This research programme is divided into two parts. The objective of the first part is to select a wide range of rock materials covering a broad spectrum of strength and abrasivity. Specimens of the selected rock are studied in detail to provide a full mineralogical description highlighting those features which are likely to influence the machineability of the rock. In this connection primary mineralisation, quartz content, grain size, cementing material and porosity are of prime importance.

The mechanical and physical properties of each rock are also measured. Several parameters are used to fully define the mechanical strength of a rock type. Other empirical test procedures are employed, abrasivity is believed to be due mainly to the presence of quartz, although it is recognised that other hard minerals can create problems in this connection.

The machineability of a rock material is defined in terms of specific energy using a standardised cutting test procedure. Also abrasivity is reflected in tool material lost per unit volume of rock cut during the same test. This involve using a standardised tungsten carbide tool and recording the carbide loss for a given volume of rock cut.

The inter-relation of the mineralogical and mechanical properties will be exercised by using statistical techniques. Furthermore these properties will be related to the known machineability data in order to expose those rock properties which are of relevance to the cutting process.

Along a tunnel line the many different rock types which are likely to be encountered are rarely homogeneous and therefore it is desirable to assess in-situ rock. The ideal situation is to assess rocks obtained from a horizontal borehole which follows the line of the proposed tunnel. This however, is seldom possible owing to the economic commitment of such a scheme. A more practical solution is to use a series of vertical boreholes which intersect the proposed tunnel line at predetermined points. The second part of this research contains the information on the machineability and abrasivity of strata obtained from experiment carried out on cored rock samples recovered from a drilling programme along the line of the proposed Tyne-Tees aqueduct tunnel and Tyneside Rapid Transit tunnel. This information will provide a basis for the choice of a tunnelling procedure, especially if the use of a tunnel boring machine is considered.

Chapter 5

Experimental Procedures and Equipment

In the first part of the research programme the investigations into rock properties will concentrate on the laboratory investigations which are simple, economical and describe independent rock properties as accurately as possible. The range of tests selected cover as full a range of properties as time and facilities allowed. The tests are classified into 3 major groups viz:

1. Mineralogical and Physical Properties
2. Mechanical strength
3. Empirical strength.

Table 1 shows the details of the tests in these groups.

Table 1 Proposed Test Matrix

Property tested	Available tests	Units
1. Mineralogical and Mechanical properties.		
1.1 Quartz grain size	Petrographic examination	μm
1.2 Quartz content	" "	per cent (Volume)
1.3 Density and porosity	Specific gravity and porosity test	Mg/m^3;per cent
2. Mechanical strength		
2.1 Uniaxial compressive strength	Core testing	MN/m^2
2.2 Tensile strength	Direct pull and Disc test	MN/m^2
2.3 Static modulus and Poisson's ratio	Cycle loading	MN/m^2
2.4 Dynamic modulus	Wave velocity test	MN/m^2
2.5 Biaxial compressive strength	Biaxial rig	MN/m^2
3. Empirical strength.		
3.1 Indentation hardness	Cone indenter test Brinell hardness test	
3.2 Rebound hardness	Shore Scleroscope test Schmidt hammer test	
3.3 Abrasivity	Blade abrasivity test Intrinsic abrasivity test	
3.4 Impact strength	Impact strength index test	

5.1 Selection of rock Samples.

Rock samples which were readily available in the Department were selected to cover the full range of strength and abrasivity. Rocks with compressive strength up to 100 MN/m^2 are classified as having low strength. High strength rocks are ones with a compressive strength greater than 100 MN/m^2. Abrasivity is classified by quartz content, at this stage. For example quartzites, granites and sandstones, the rocks with high content of quartz are classified as highly abrasive. Limestone are non-abrasive rocks. Table 2 shows the classification of rock samples according to their strength and abrasivity.

Table 2 Rock Samples Classification

		Abrasivity	
		High	Low
Strength	High	Post sandstone Creetown granite (white) Creetown granite (blue) Stilfontein quartzite Auriferous quartzite Scottish quartzite	Frosterly limestone Stanhope limestone Hinkley Point limestone Beachley limestone Whinstone Anhydrite Honister slate
	Low	Scotswood sandstone Bunter sandstone Springwell sandstone Dunhouse sandstone Hunterston sandstone Mansfield whitestone	Bulwell limestone Gypsum Rocksalt Lower chalk Aust mudstone

The majority of the rock samples were supplied by the Greenside Machine Co.Ltd.. Generally, standard diameter cores were taken from block samples perpendicular to the bedding, except as noted otherwise, and were cut to the required length with a diamond saw. When the test specimens required any preparation other than coring and sawing, the details are given with the description of each procedure.

5.2 Testing description

5.2.1 Petrographic analysis

During the course of a rock cutting operation, the tools employed become subject to extreme heating and the hardness of quartz may be greater than the reduced hardness of tungsten carbide(78,79).It is for this reason that quartz-bearing rocks are thought to be so highly abrasive and responsible for a major part of tool wear and grain size, texture and manner of distribution of the quartz agrains. To this end, studies of the rock in thin section were undertaken to assess the abrasive mineral content and the grain size of the abrasive mineral within the rock.

Normally five thin sections of each rock type which were prepared from the cylindrical rock specimens were studied. The modal composition of each of the five specimens was then determined on the basis of point counting, using a mechanical stage, in combination with a polarising microscope and a 1 cm graticule eyepiece which is divided into 100 equal division. The section is moved through the field of vision along a straight line at equal intervals, dependent on the grain size of rock in question. The random index points are noted. After traversing several lines across the full length of the section so that a total of between 700-1000 points have been counted, the counts of individual components

are summed and re-calculated to percentage values. The volume percentages can be re-calculated to weigh percentages if required by using the density values of the individual components.

If as a result of this modal analysis, significant quantities of quartz have been found to be present in the rock, a grain size analysis was undertaken on each section. Grains were selected for measurement in a similar fashion to that used for modal analysis and the length of the longest axis of the grain section noted.

Method of making thin sections of rocks and minerals as well as the method of impregnation of specimen of friable rocks are described in appendix 1.

5.2.2 Specific gravity and porosity test

Apparent specific gravity is defined as the ratio of the weight of a specimen of given exterior volume to the weight of an equal volume of water. Thus apparent specific gravity does not take into account voids within the specimen. For specimens of regular shape (prisms or cylinders), the exterior volume can be calculated from linear measurements. The apparent specific gravity is calculated as follows:

$$\text{Apparent specific gravity (Sa)} = \frac{Mo}{V.dw}$$

Where

Mo = weight of oven - dried specimen,
V = external volume,
dw = density of water (1 Mg/m^3)
D = Bulk density (Mg/m^3) = Sa X dw

For specimens of irregular shape the exterior volume can be determined from the saturated weight of the specimen, and the weight of the saturated specimen when it is immersed in water, by

$$V = \frac{Mw - Ms}{dw}$$

Where

Mw = Weight of saturated specimen,
Ms = Weight of saturated specimen suspended in water.

Hence

$$\text{Apparent specific gravity} = \frac{Mo}{Mw - Ms}$$

Apparent porosity is defined as the ratio of the volume of open pore space to the exterior volume of the specimen. This quantity can be calculated from the dry and saturated specimen weights by

$$P = \frac{Mw - Mo}{dw.V} \times 100$$

Where

P = apparent porosity, per cent.

In this research Mo is the desiccator dry weight of specimen rather than the oven dry weight.

Saturated specimen can be achieved by immersed the specimen in water in a vacuum desiccator and the air pumped out. The effect of this is to draw air out of the specimen and replace it with water.

Because some of the voids in rock may not be interconnected, the true porosity generally will be greater than the apparent porosity. The specific gravity method is the technique use to obtain the true porosity. This is briefly outlined as follows:

Specific gravity has to be determined first by dividing the weight by the calculated volume.

Grain density of the specimen is then obtained. This can be done by reduce a small section of rock specimen (about 100 g) to grain size by crushing the rock to a powder and retaining it in the appropriate sieves, i.e., between B.S. sieves 30 and 120 for sandstones. From this, three 20 g. samples are taken.

The density of the grains is found by using the pycnometer method. The procedure is described briefly as follows:

The pycnometer (Fig. 22) is filled with water at the temperature of between 15 and 25°C until the water is level with the hole in the top. The outside of the pycnometer is then wiped dry and its weight (b) recorded. A 20 g. sample of the rock is then weighed, the bottle half emptied, the top removed and the sample placed inside. The grain-water mixture is thoroughly stirred with the glass rod to remove air entrapped in the grains, the top replaced and bottle again filled with water. Any remaining air is removed by shaking the bottle, holding one finger over the hole at the top. This may tend to form a froth which collects under the top; if so, it should be carefully removed and the bottle topped up with water. The outside is then dried and the weight (w) recorded.

$$\text{Volume of grains} = 20 + b - w$$

Hence

$$\text{Grain density} = \frac{20}{20 + b - w}$$

and

$$\text{True porosity} = \frac{\text{Grain density} - \text{Bilk density}}{\text{Grain density}} \times 100 \text{ per cent}$$

It should be noted that the soluble rocks cannot be tested by this method.

Figure 22

Pycnometer

Table 3. Specific Gravity and Apparent Porosity of Typical Rocks (After Obert & Duvall (80)).

Rock type	Average specific gravity	Apparent porosity (Per cent)
Marble	2.87	0.6
Limestone	2.37	11.0
Granite	2.66	0.9
Sandstone	2.06	16.0
Slate	2.74	1.0
Greenstone	3.02	0.7

5.2.3 Uniaxial conpressive strength.

This is the most commonly quoted parameter of machineability though it is not reliable as it fails to take into account the abrasive properties of the rcck and seems to have little relationship to cutting process involving wedge penetration into a rock surface (81). Compressive strength is normally defined as the stress required to crush a cylindrical rock sample unconfined at its sides. True compressive failure in rock can only occur through internal collapse of the rock structure due to compression of pore space resulting in grain fracture and movement along grain and crystal boundaries. The true compressive strength of a rock is therefore influenced by its internal structure, and sedimentary rocks with a relatively large amount of pore space will tend to be weaker in compression than fine-grained metamorphic or igneous rocks.

Since true compressive failure would require hydrostatic loading conditions, and would in any case be difficult to detect, the compressive strength of a rock specimen is, in many ways, a reflection of its shear strength.

In concept the compressive strength test is deceptively simple but in reality there are a number of factors that can affect the test results significantly, such as the flatness of the bearing surfaces, the specimen size and shape, the moisture content in the specimen, the effect of friction between the bearing platens and the specimen, the alignment of the swivel head, and the rate of loading.

The flatness of the specimen ends (bearing surfaces) is critical. In general the deviation from flatness should be small compared to the deformation produced by the axial load at failure. This degree of flatness is difficult to achieve by lapping even if jigs are used to hold the specimens, but uniformly flat surfaces can be obtained by surface grinding. Parallelness between and surfaces should be within $\pm$ 1° , a specification that is not difficult to realize.

The alignment of the spherical bearing head used to accommodate for the lack of parallelism between the ends of the specimen is one of

the more critical factors in compression testing. If the diameter of a spherical head is too large in relation to the specimen diameter or if the spherical surfaces are not properly ground or lubricated, or if the specimen is not accurately centered, the measured compressive strength values may be substantially less (as much as 50 %) than those obtained using the correct technique. For testing drill core specimens with diameter between 28 mm and 54 mm a 75 mm diameter spherical headed lubricated with oil and graphite when used on the lower platen of the testing machine is relatively easy to align.

When a specimen is loaded in compression, the specimen and bearing plates expand laterally. If the specimen is rock and the bearing plates steel, the difference in expansion creates lateral stresses in the ends of the specimen. The magnitude of these stresses depends on the coefficient of friction between rock and steel on their elastic constants. To improve the situation steel platens were used throughout the investigation.

The compressive strength of rock increases with the rate of loading. For high rates of loading as, for example, that produces by stress waves from blasting, this increase in strength may be appreciable. Also, for very long loading periods a substantially reduced strength may be obtained. It has been observed (75) that, for rates of loading of 0.69, 1.38, 200, and 2.76 MN/m^2/sec the difference in the measured compressive strength of rock was found to be negligible. However, the rate of loading of 0.69 MN/m^2/sec was employed in all subsequent tests.

Standardization of sample geometry for routine testing is desirable, as it facilitates comparison of strength (82) have shown the superiority of cylindrical specimens. In rock testing, cylindrical samples are easy to prepare by core drilling, whereas cubes must be formed by precise sawing and grinding. The simplest type of axially symmetric specimen is the right circular cylinder, which is load across the end surfaces.

Since the test is usually intended to measure bulk properties of the rock, the sample must obviously be big enough to be representative of the bulk material, which suggests a lower limit of D/d approximately equal to 20 where D and d are sample diameter and maximum grain diameter respectively (83). Practical considerations, such as expense of sample preparation, usually determine the upper limit of size for test samples; for most rocks, sample diameter rarely exceeds 54 mm (NX core size).

Once the diameter of a specimen has been chosen and found adequate in terms of grain size, the length of the specimen can be expressed as a multiple of the diameter.

The A.S.T.M. standard for uniaxial compressive tests on natural building stone (c 170-50) specifies that the samples, which may be cubes, square prisms, or cylinders, should be at least 50 mm high with a height to width ratio L/D = 1.0. Results from tests in which L/D≠1.0 are adjusted by means of the formula:

$$\frac{Sc}{Sc1} = 0.778 + \frac{0.222}{(L/D)}$$

where Sc and Sc1 are measured strength at a certain L/D and L/D = 1.0 respectively. A value of L/D = 1.0 was also suggested by Hardy (84).

However, on the basis of both theoretical studies and experimental findings, most investigators in rock mechanics would agree that a height to width ratio of unity is too small, since the entire sample is influenced by end effects.

An acceptable lower limit for L/D is debatable, but it should probably be taken at the point where the (negative) slope of the strength versus L/D = 2.0 - 2.5.Theoretical studies (Fig 23 A) indicate that rough and rigid platens cause significant perturbation of the field to a distance of D/2 from each end.

Coates and Gyenge (85) recommend L/D = 2.0, but consider 1.0 < L/D<2.0 acceptable. Therefore L/D = 2.0 was employed in all subsequent tests.

Test results with the L/D ratio differ from 2.0 can be computed to standard compressive strength by using Hobbs' (86) formula:

$$\frac{Sc}{Sc2} = 0.848 + \frac{0.304}{(L/D)}$$

where Sc and Sc2 are measured strength at a certain L/D and L/D = 2.0 respectively.

In brief the standard procedure used for the uniaxial compressive strength in this analyses is

1. cylindrical air-dried specimen of L/D = 2 and of 35 - 50 mm diameter
2. loading rate of 0.69 MN/m^2/sec (100 psi/sec)
3. steel platens.

5.2.4 Tensile strength

Rock,usually a brittle material, is relatively weak in tension and this weakness can be very significant in determining its behaviour in structures and excavations. Consequently, accurate knowledge of the tensile strength of rock has long recognized as important.

Tensile strength of rock is determined statically in a hydraulic testing machine, and dynamically, by various methods.

Static tensile strength can be determined by 3 methods. These are:
1. The direct pull test
2. The indirect "disc" test
3. The bending test

Due to the difficulty in preparation of the specimens, the third method , the bending test has been discarded from the test matrix.

The method of determining the dynamic tensile strength of rock will be described later.

5.2.4.A The direct pull test (Fig. 24)

In this test the cylindrical rock specimen, of L/D ratio of

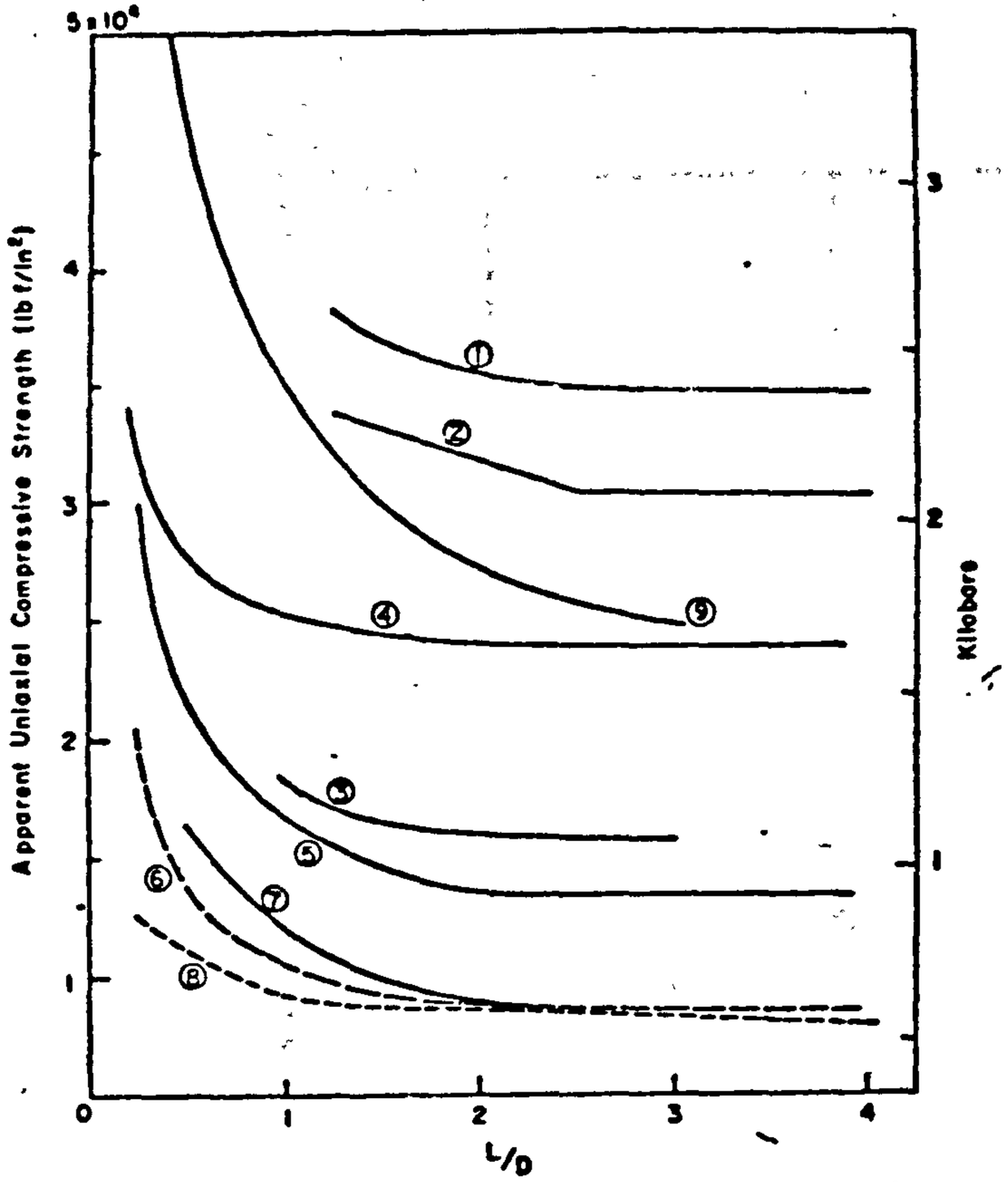

Figure 23a

Influence of length/diameter ratio on uniaxial compressive strength. 1,2,3: Mogi (87); 4,5,6: Hobbs (86); Chakvarty (88); 8,9: Mellor (unplublished).

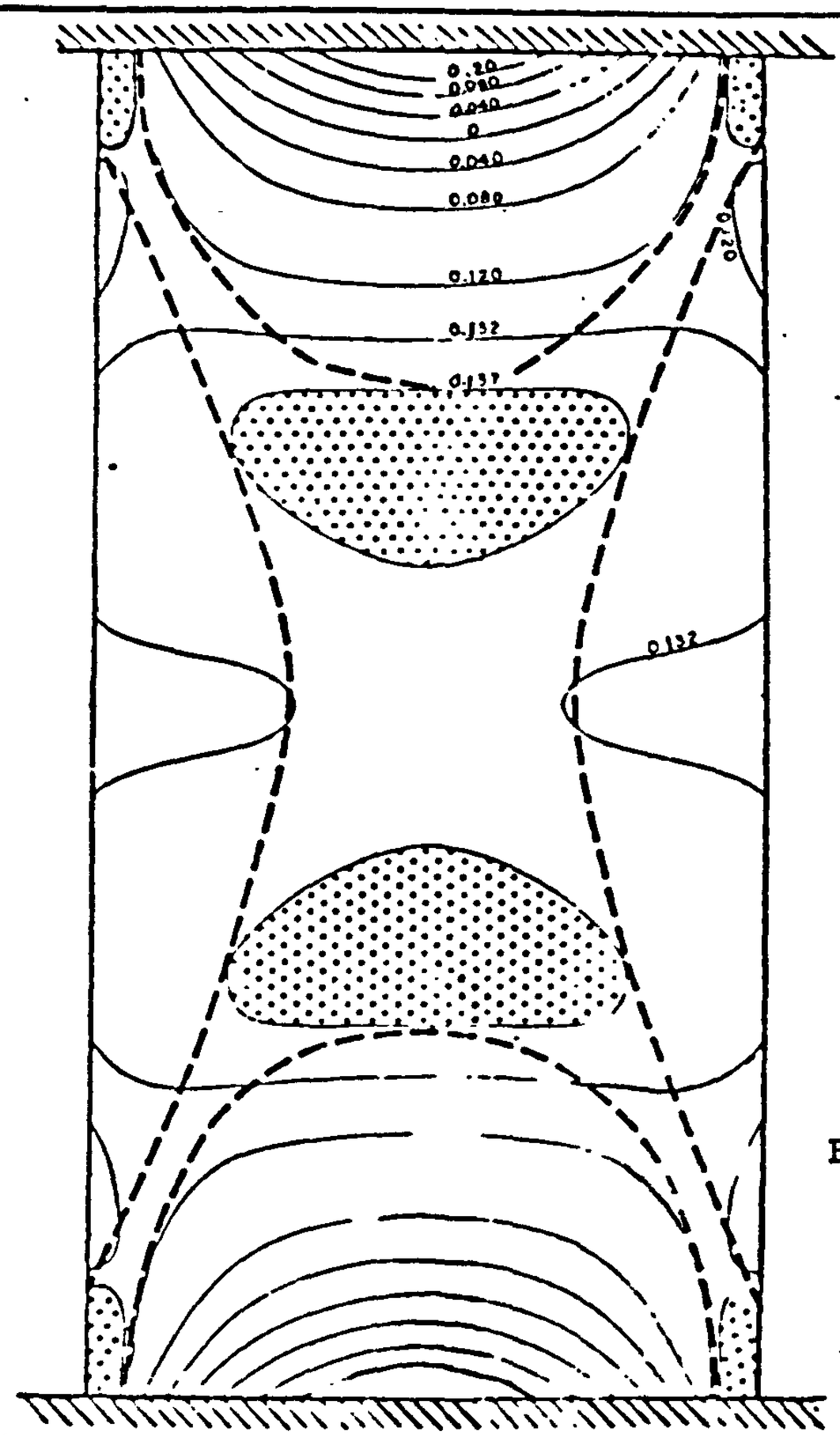

Figure 23b

Contours of the McClintock-Walsh parameter, C, for uniaxial compression with radial restraint at the sample ends. The numbers give the magnitude of C as a multiple of the mean axial stress.

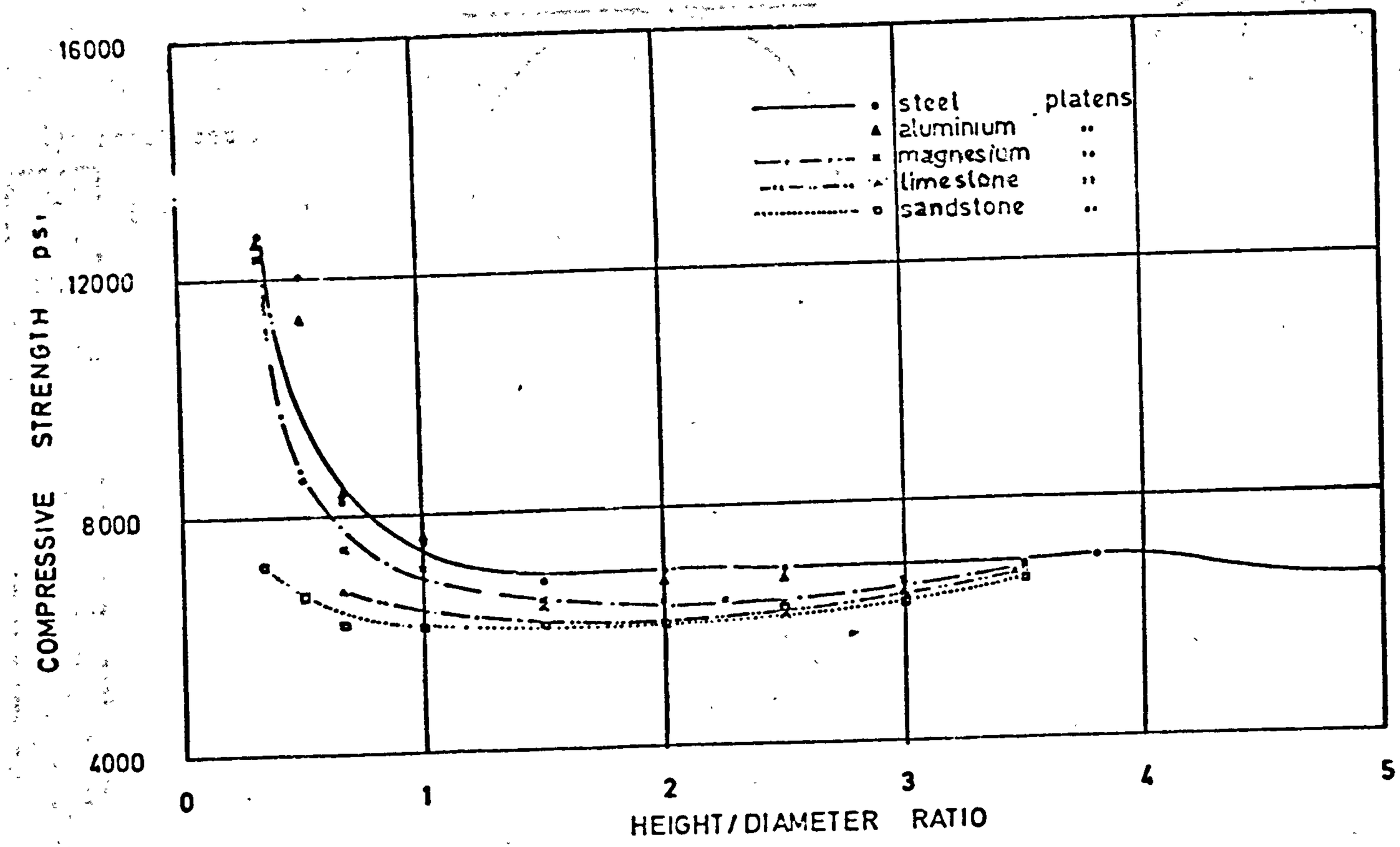

Relationship between uniaxial compressive strength of Springwell sandstone and heigth / diameter ratio, using different platens

Figure 23c

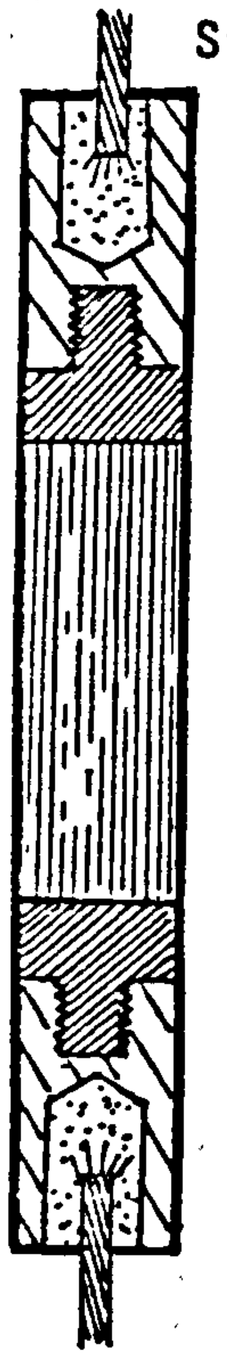

Direct tensile strength test

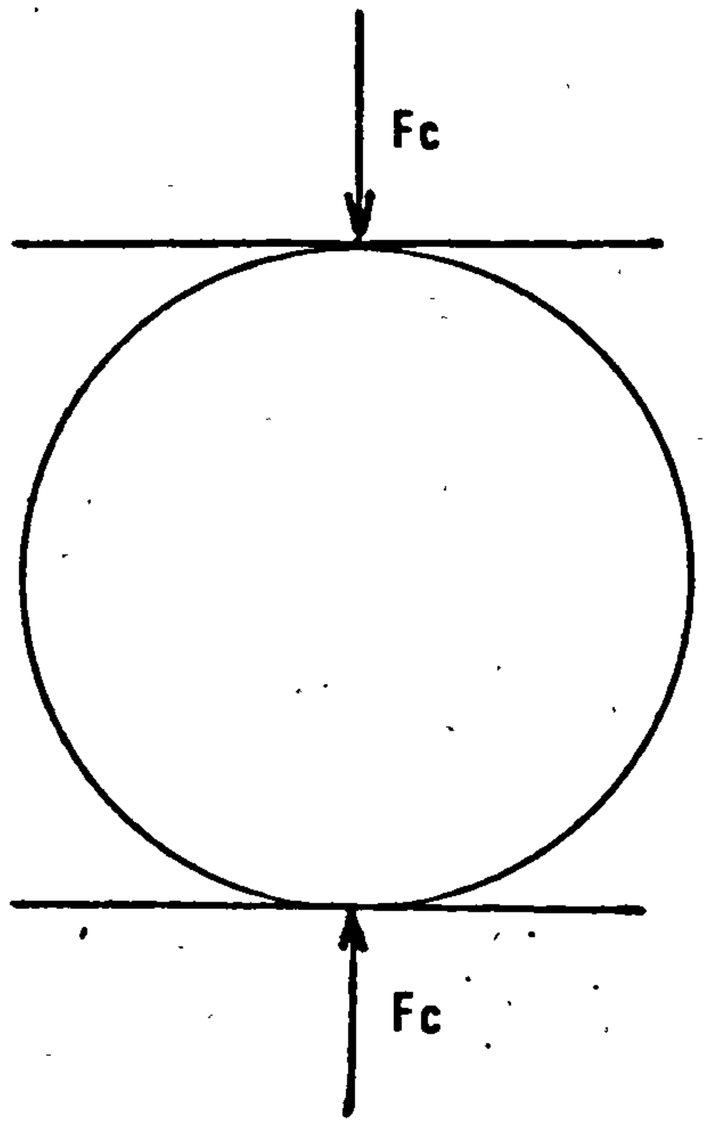

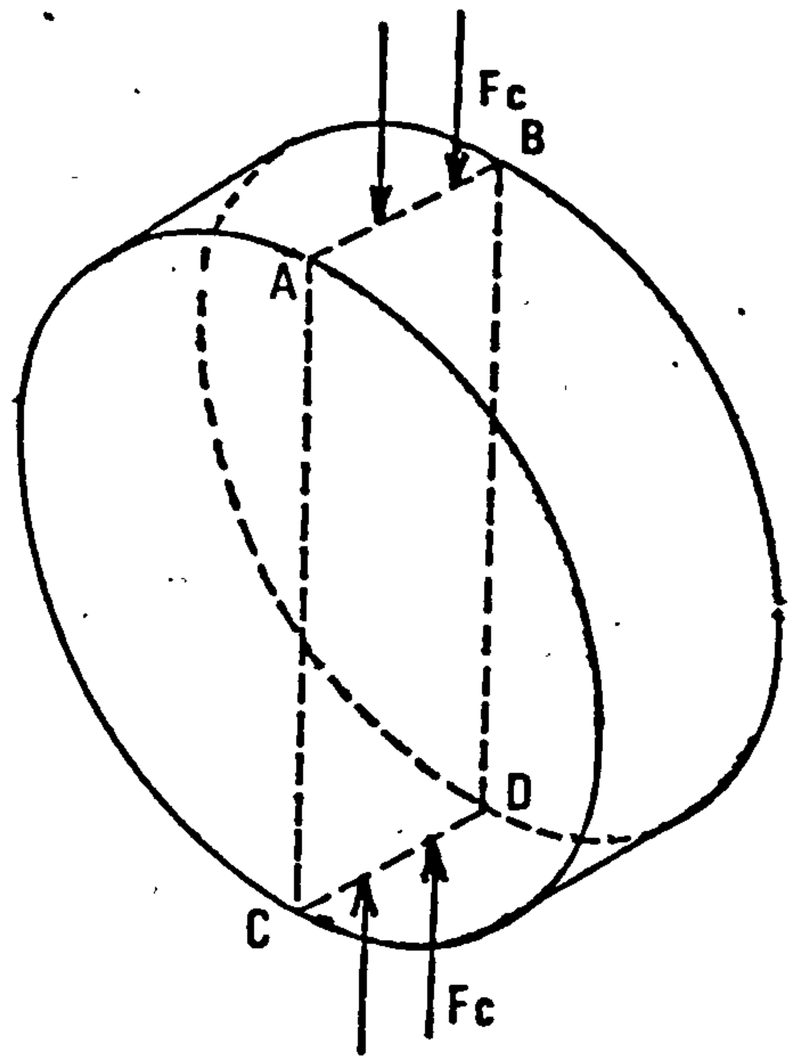

Disc test

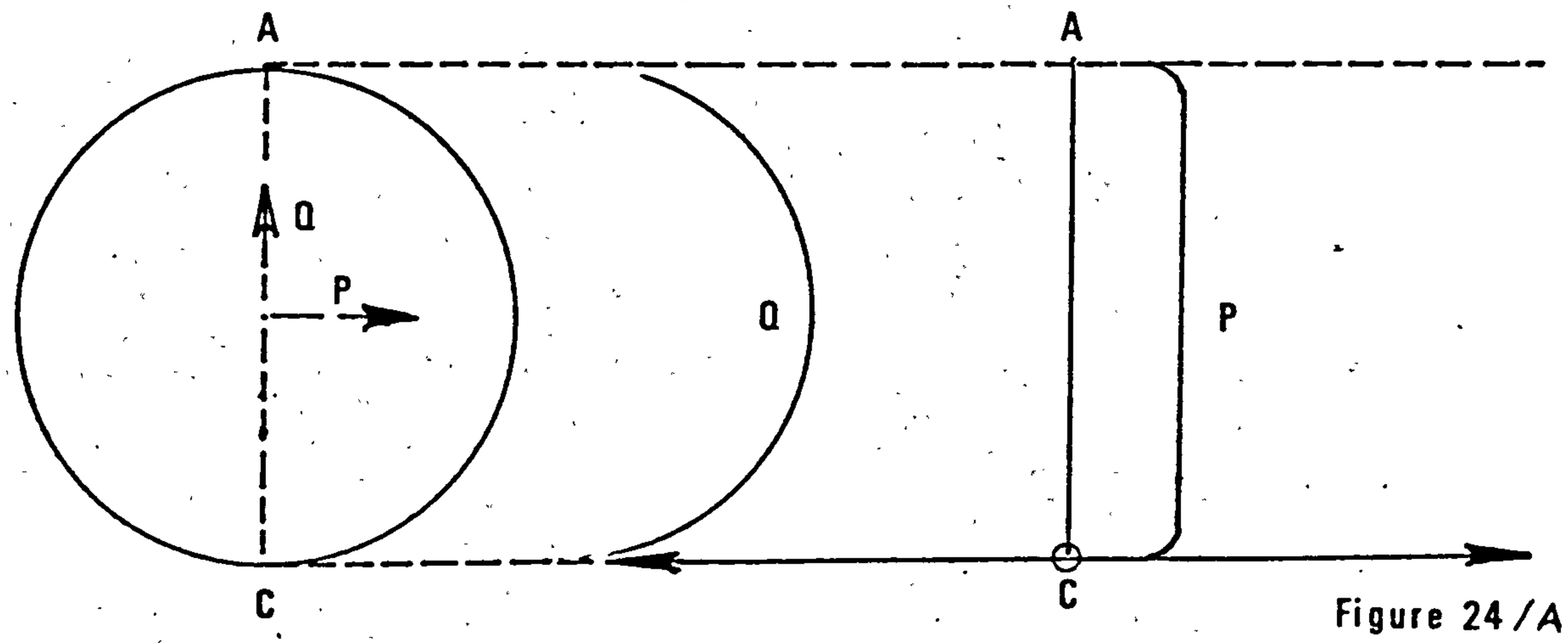

STATIC TENSILE STRENGTH TESTS

Figure 24/A

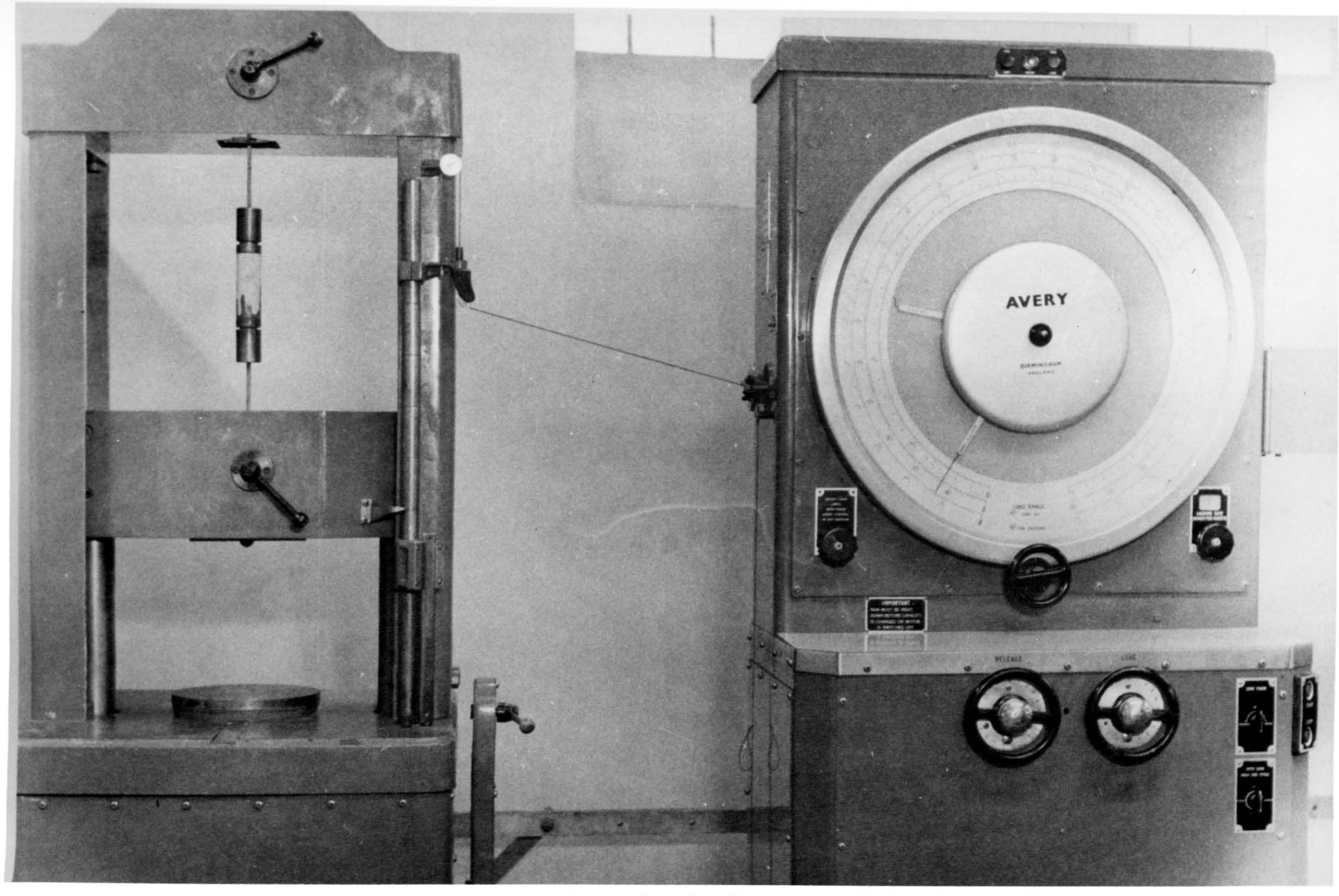

Direct Tension Test

Figure 24 /B

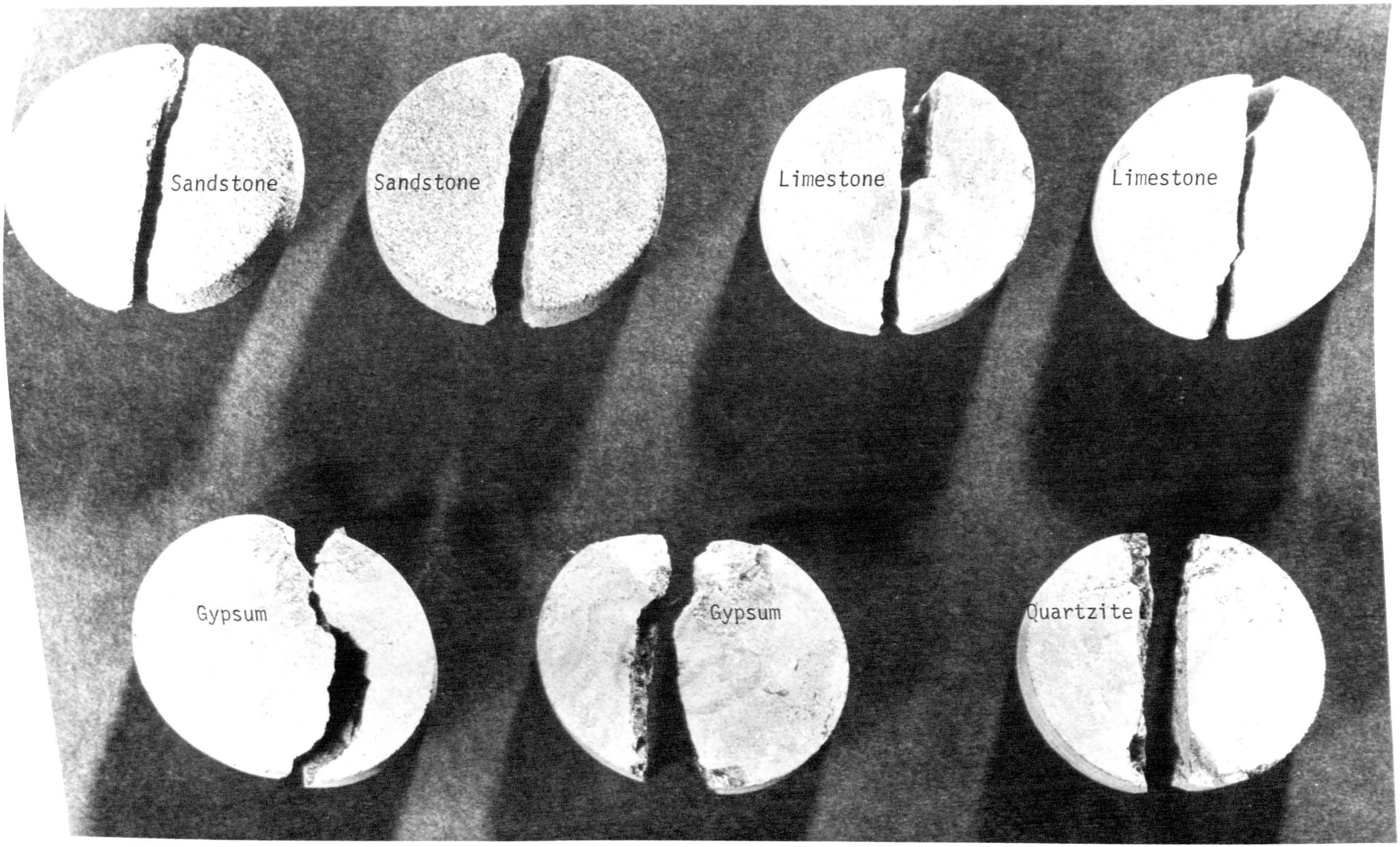

Fracture of Rock Type using the Disc Test

Figure 25

more than 2.5 is cemented to a metal cap by direct butt-jointing. Modern high-strength adhesives, such as Araldite, permit high tensile stresses to be transmitted across a plane cemented joint. Thus the squared ends of rock cylinders can be butted directly against the end faces of connector plugs, cemented in place, and pulled.

In the pulling action, the specimen is pulled by stranded steel cables screwed into the end caps; one of the cables is attached to the loading device through a thrust bearing to eliminate torque from cable twisting.

This method is quite satisfactory for tests on sandstones. For tests on high strength rocks, the bonds developed by cold-setting epoxies tend to be inadequate. However high temperature curing is inadvisable, as it may affect the properties of the test specimen.

The standard procedure is simple, the rock specimen with accessories was placed vertically and loaded axially in tension in a 250 KN Avery machine. Initially the weakest flaws failed, but as the test was repeated after progressively recementing the fracture surfaces the load gradually increased.

If W = Breakage load, N
D = diameter of specimen, mm

Tensile strength (Ts) = $\frac{4W}{\pi D^2}$ MN/m^2

5.2.4.B The indirect "disc" test

In the indirect tensile strength test a cylindrical test specimen in the form of disc is placed horizontally between the bearing plates of a testing machine and loaded to failure in compression.

If the diameter of the specimen is D(mm), and the width t (mm), and the line load Fc (N) is applied along the width of the specimen, a uniform tensile stress

$$P = \frac{2Fc}{\pi Dt} \quad MN/m^2$$

should develop across the plane ABCD. If Fc is the load at failure, the tensile strength Ts is

$$Ts = \frac{2Fc}{\pi Dt} \quad MN/m^2$$

in addition to the tensile strength that develops across the diametral plane, a vertical compressive stress occurs in the plane, which varies in magnitude from point to point. This stress is given by:

$$Q = \frac{-2\,Fc}{\pi t}\left(\frac{2}{D-2y} + \frac{2}{D+2y} - \frac{1}{D}\right) \quad MN/m^2$$

where y is the distance along the diameter measured from the centre. This compressive strength causes high shear stresses and local crushing along the loading line as shown in Fig 25.

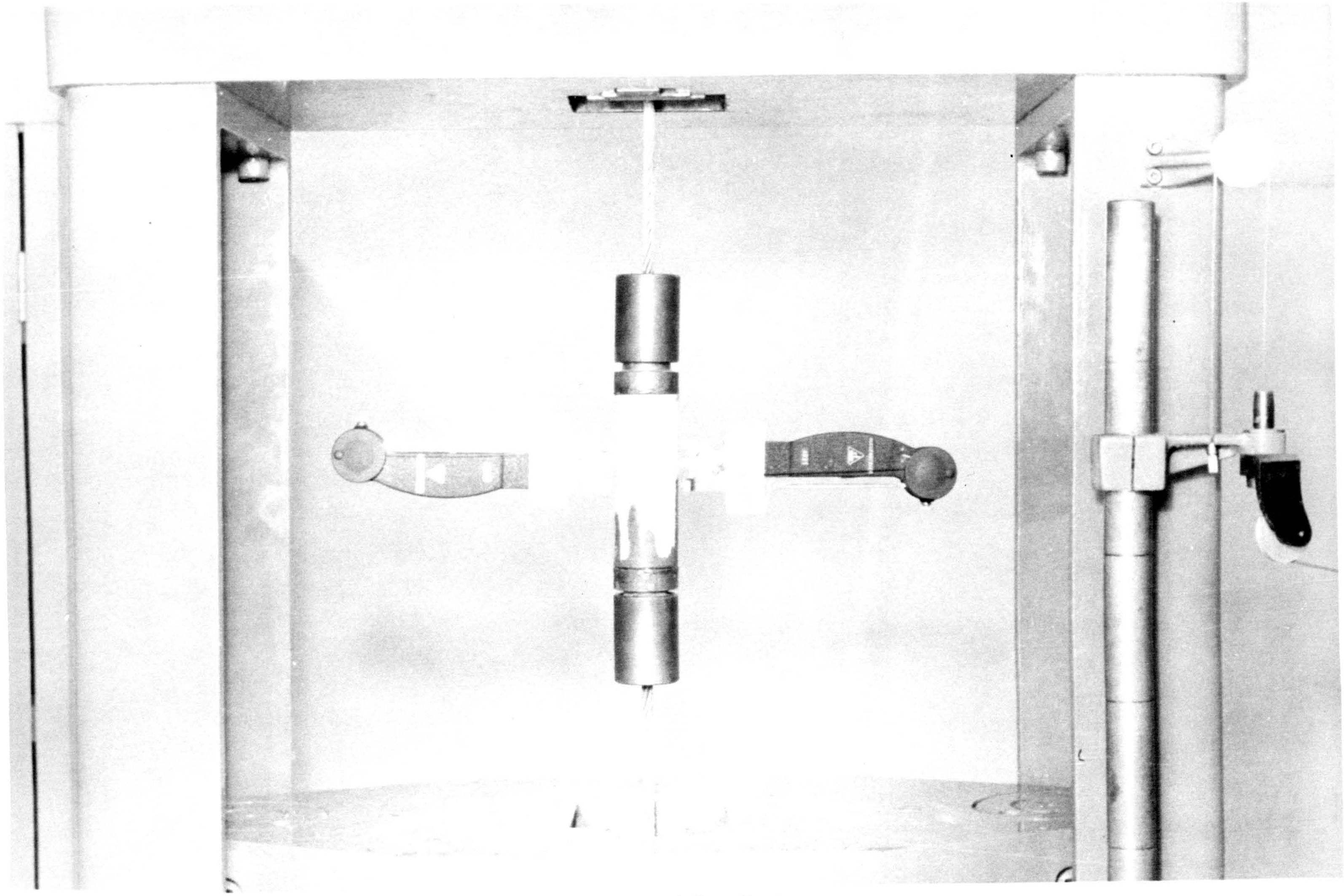

Tension Modulus Test

Figure 26

results and the measurement technique was less involved. For this reason only the wave velocity tester will be used.

The test to standardised the size of specimen were conducted as follows:-

Thirty nine cores of Bunter sandstone, ranging from 560 to 15 mm long were used. The cores had previously been cut parallel to the bedding. The length, bulk density, and wave velocity was measured in each case and the results plotted on Figure 27A. The graph illustrates that the wave velocity is approximately constant for cores greater than 50 mm long but with length shorter than this the velocity drops rapidly. Unfortunately this logical trend is partly obscured by the scatter of results.

The test was repeated using one 600 mm core each time shortening the core by 25 mm. This was repeated until the core was 50 mm long. Below this the core was shortened by decreasing lengths until it was 1.3 mm. Figure 27B shows the relationship between core size and wave velocity. The plot illustrates that a maximum velocity is reached with cores between 50 and 200 mm long. Below this the minor fractures produced by machining of contact faces causes a rapid drop in the velocity values. With cores of length greater than 200 mm the velocity falls slightly as the number of minor fractures and laminations become increasingly important. The size of wave velocity test specimen will then be standardised between 50 and 200 mm.

The test requirements for measurement of wave velocity is as follows:-

a. The bulk density of rock must be measured. This is most conveniently done using a regularly shaped specimen.

b. The length of the specimen should be between 50 and 200 mm.

In the test the time of travel of the wave through the specimen cores was measured four times, each time reversing the direction of travel. The results calculated using the following equations:-

$$V = \frac{L}{T} \times 10^6 \quad ; \quad Ed = XV^2$$

where

V = wave velocity in m/s, Ed = dynamic Young's modulus in MN/m^2,
L = length of specimen in m, X = bulk density of specimen in Kg/m^3,
T = time of travel in microseconds.

5.2.7 Biaxial compressive strength

There are two simple methods to measure the biaxial strength of rock. In one, hollow cylinders of rock were fractured under external pressure, and failure occurred under localised stresses at the internal surface; in the other, cubes of rock were fractured by simultaneous compression between two pairs of their faces, and failure occurred under distributed stresses.

After careful consideration the method of fracturing cubes of rock under biaxial compression was used in this work, In this method the

Wave velocity measurements to determine a suitable size of test specimen

A. Different cores of Bunter sandstone

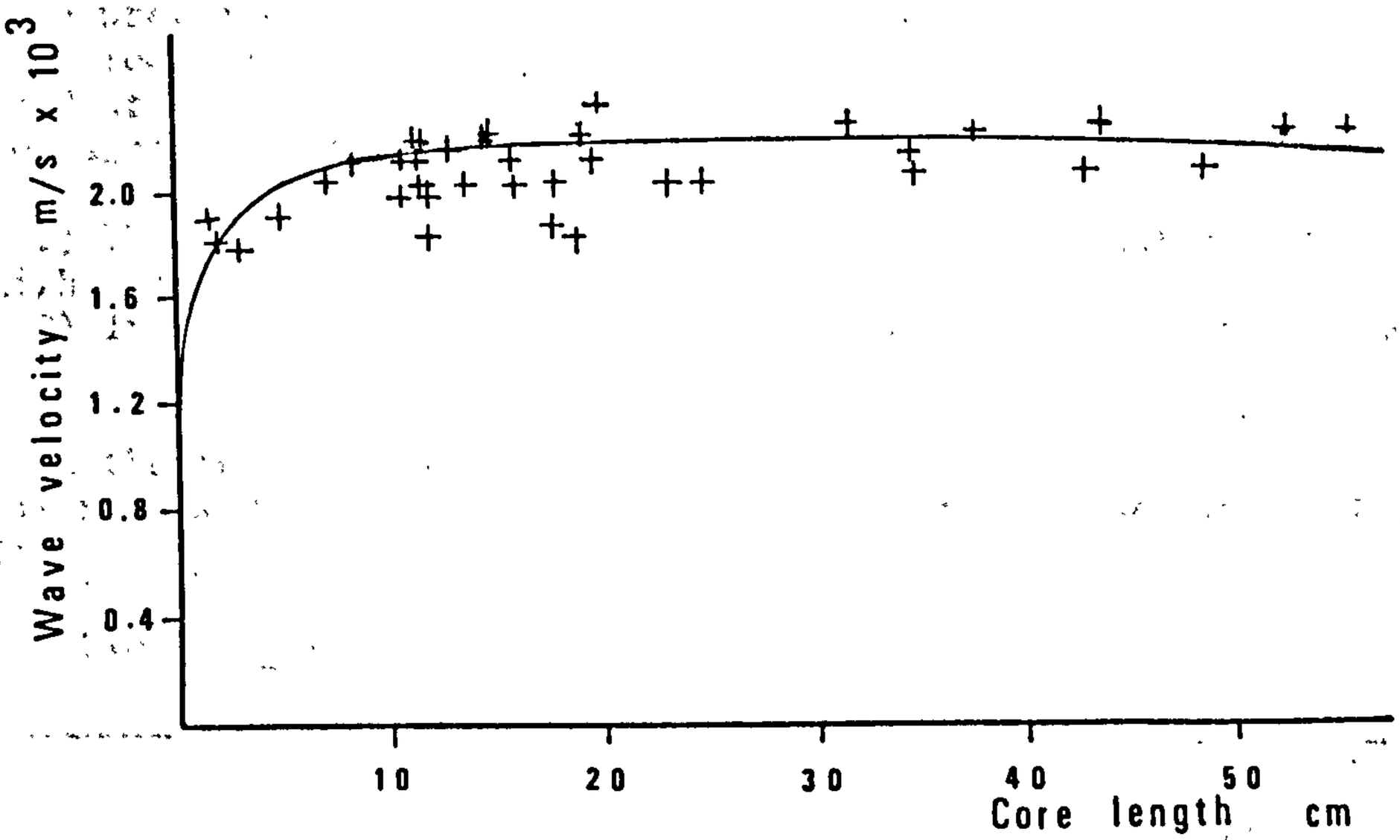

B. One core of Bunter sandstone

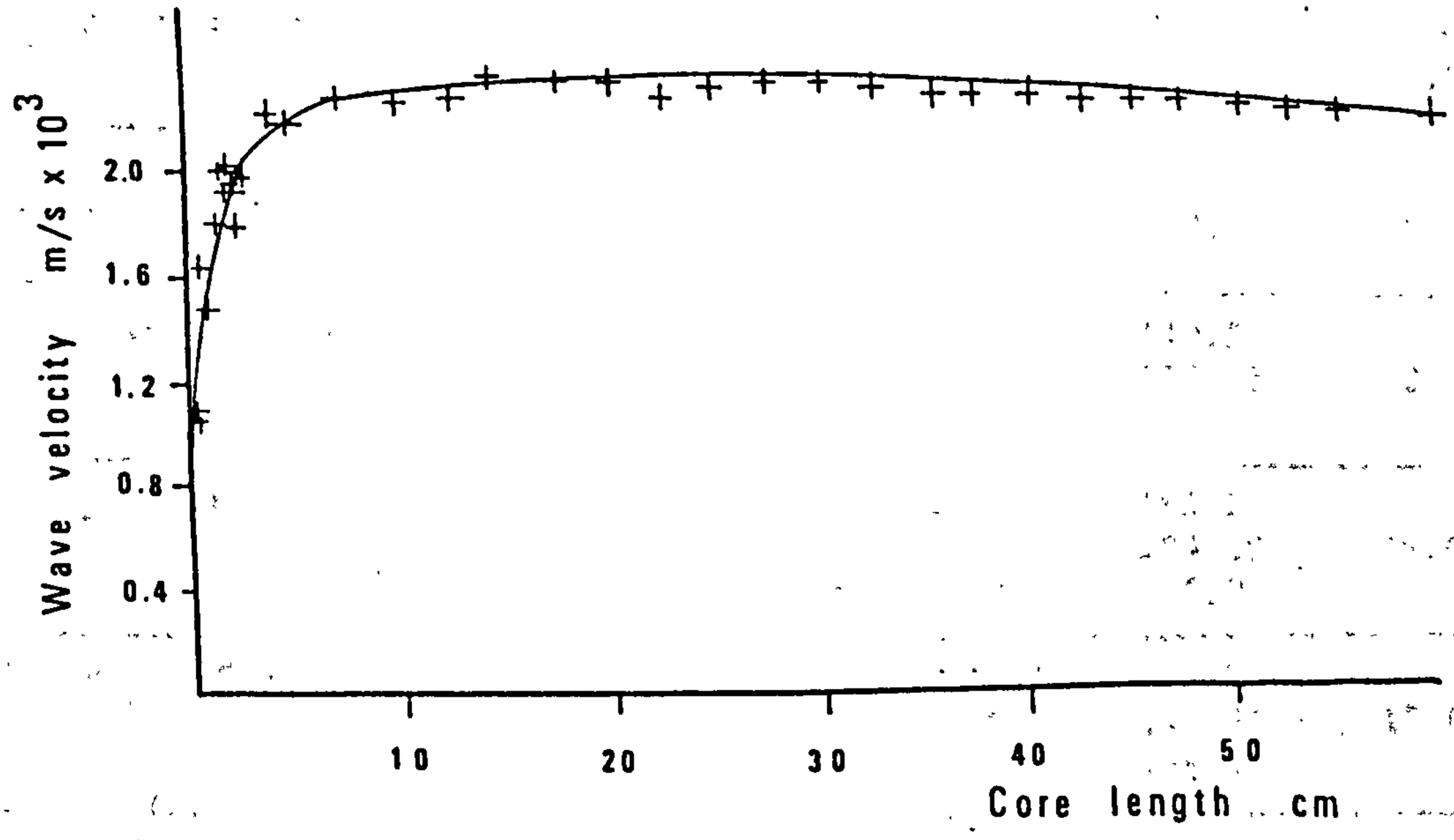

Figure 27

unequal compressive stresses applied being much uniform than hollow cylinders.

The biaxial rig was designed, as shown in Figure 28, to test a 76 mm cube of rock. The intermediate or constraining load was applied using a hydraulic jack and the cubes were loaded on an 5000 KN Avery loading machine until failure (Figure 29).

The intermediate and fractured stress was calculated (Table 4). As the tensile strength (Disc) and compressive strength of each specimen had been previously calculated for each rock type the Mohr envelopes for each rock tested. The plot illustrates that in many cases failure occurred at stresses much lower than was expected and the Mohr envelope did not agree with the Mohr's theory. This is explained by the following:

1) The intermediate stresses applied by the hydraulic jack were too high and
2) Incipient cracks were present in the specimens partly because of 1).

As the test is time consuming and elaborate preparation of specimens is necessary the test will not be repeated, nor used in the test matrix.

Table 4 Bi-axial Test Results

Rock	Ts* MN/m2	Cs* MN/m2	Intermediate Gauge psi	Intermediate Actual MN/m2	Fractured Applied KN	Fractured Stress MN/m2	Shear Stress MN/m2
Springwell Sandstone	10.40	50.61	400	6.67	386	66.83	
			750	16.26	450	77.91	16.0
			1100	23.84	380	65.79	
Scotswood Sandstone	1.69	45.77	500	10.84	422	73.06	10.0
			700	15.17	438	75.83	
Bunter Sandstone	1.78	40.48	250	5.41	362	62.67	8.0
Hinkley Point Limestone	9.45	116.60	600	13.00	864	149.58	
			1000	21.66	1000	173.13	22.0
			1500	32.50	950	164.47	
Frosterly Limestone	10.14	172.74	650	14.08	1070	185.25	
			1300	28.16	1180	204.29	35.0
			1900	42.16	1080	186.98	
Anhydrite	5.47	112.94	650	14.08	1050	181.79	
			1300	28.16	845	146.30	15.0
			1900	41.16	1075	186.11	

*Ts Brazilian Disc Tensile Strength MN/m2

Cs Compressive Strength MN/m2

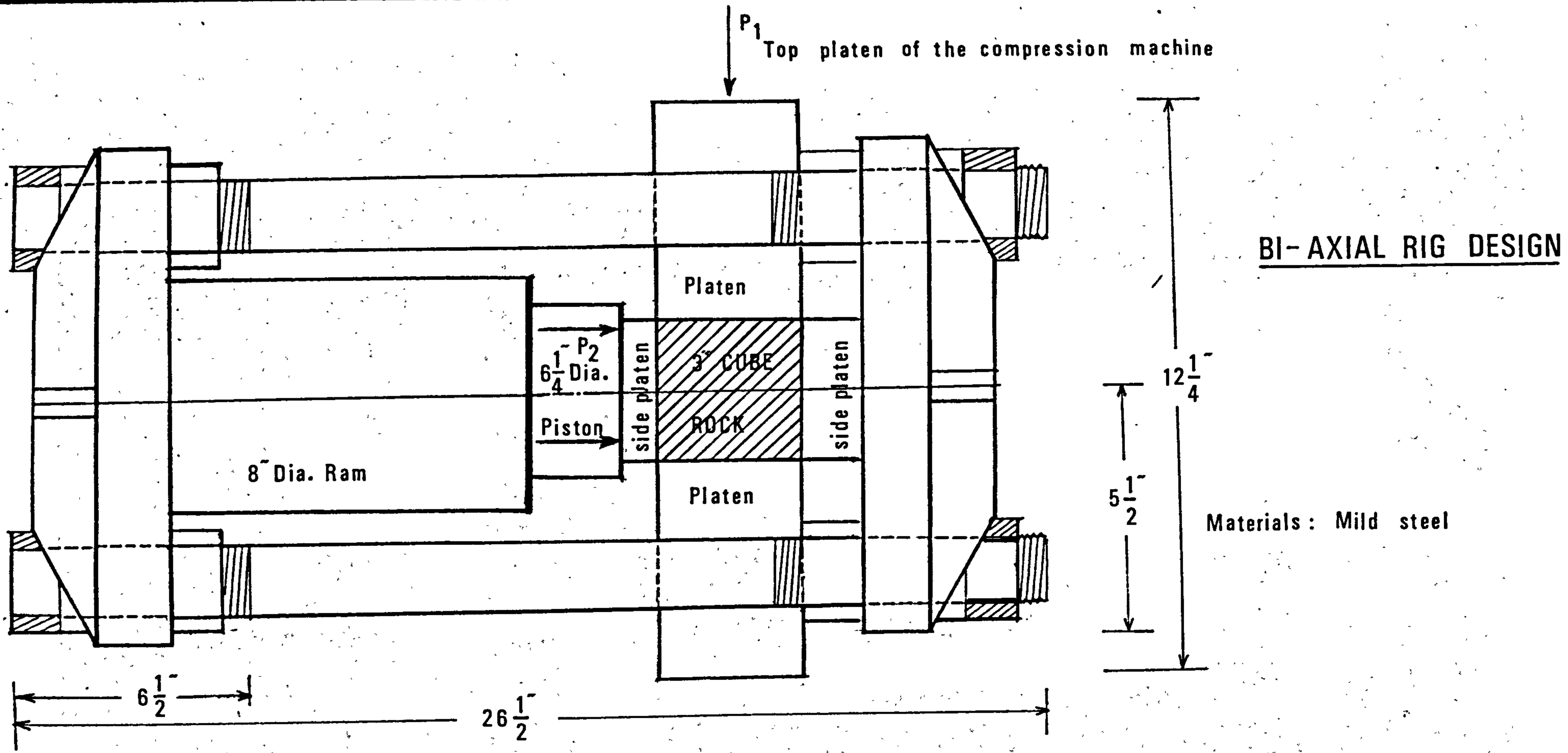

BI-AXIAL RIG DESIGN

Materials : Mild steel

Not to scale

Figure 28

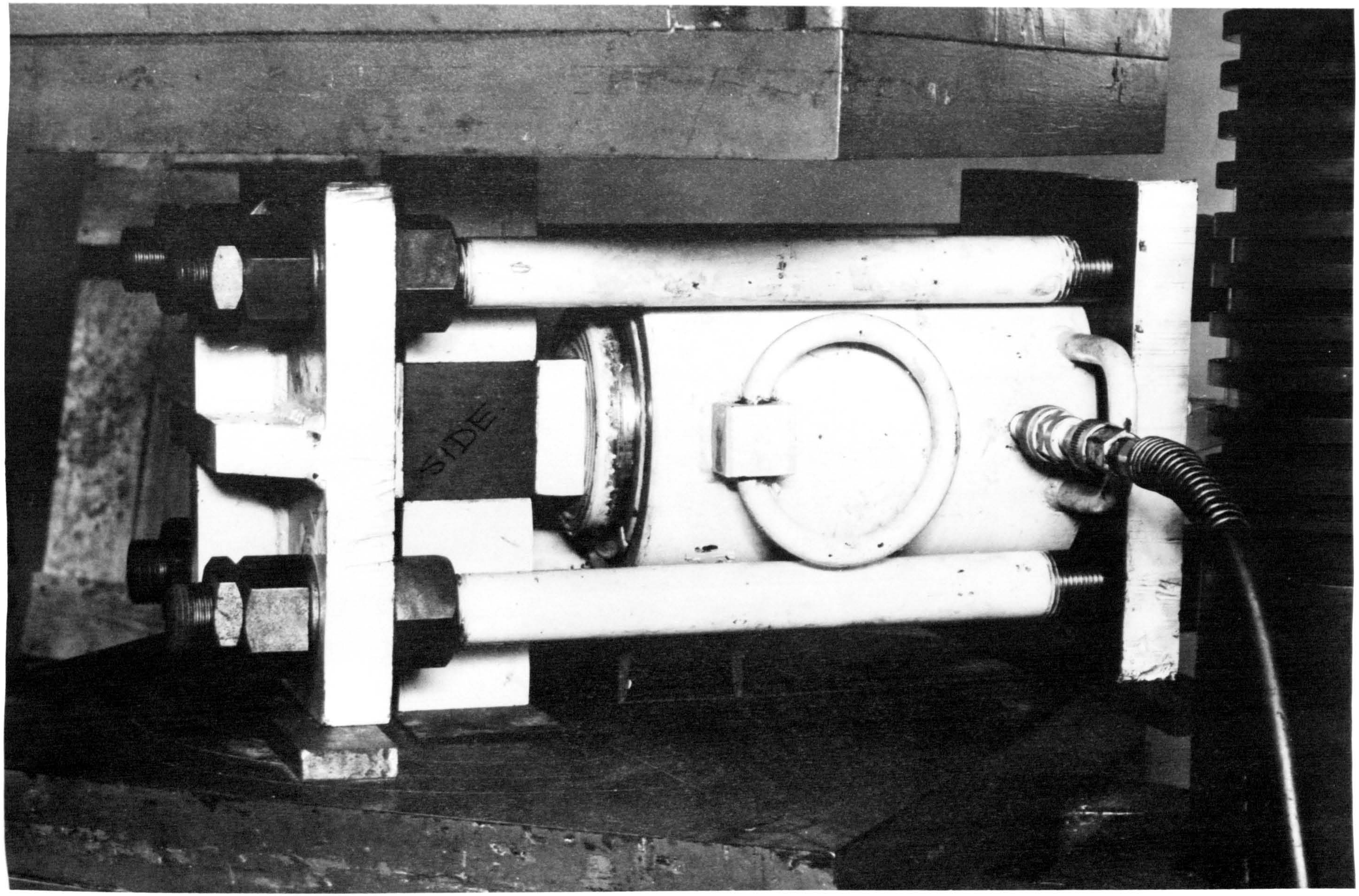

Rock under Bi-axial Rig

Figure 29

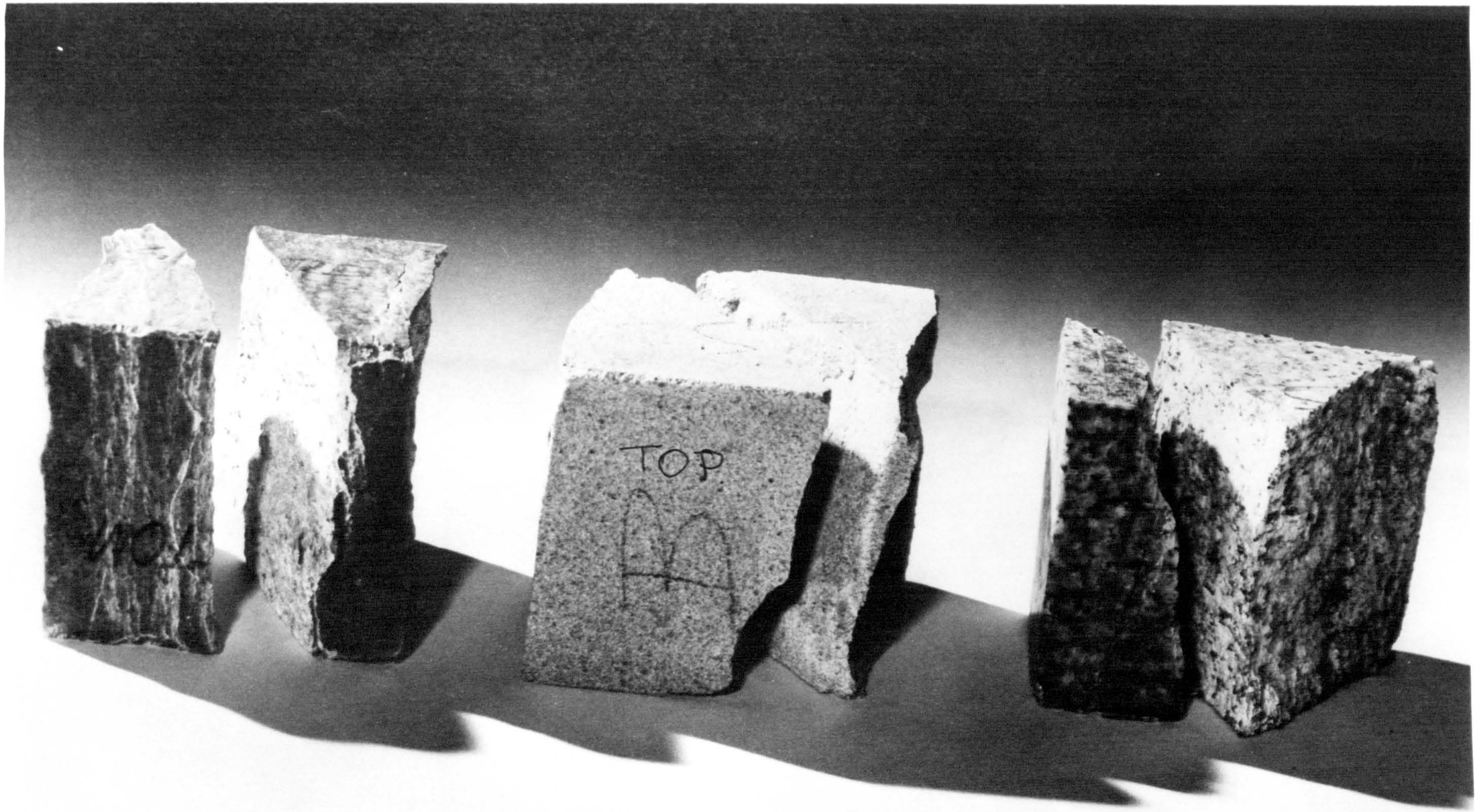

Type of Failure of Rock under Bi-axial Test

Figure 30

Biaxial test results and estimated Mohr envelope.

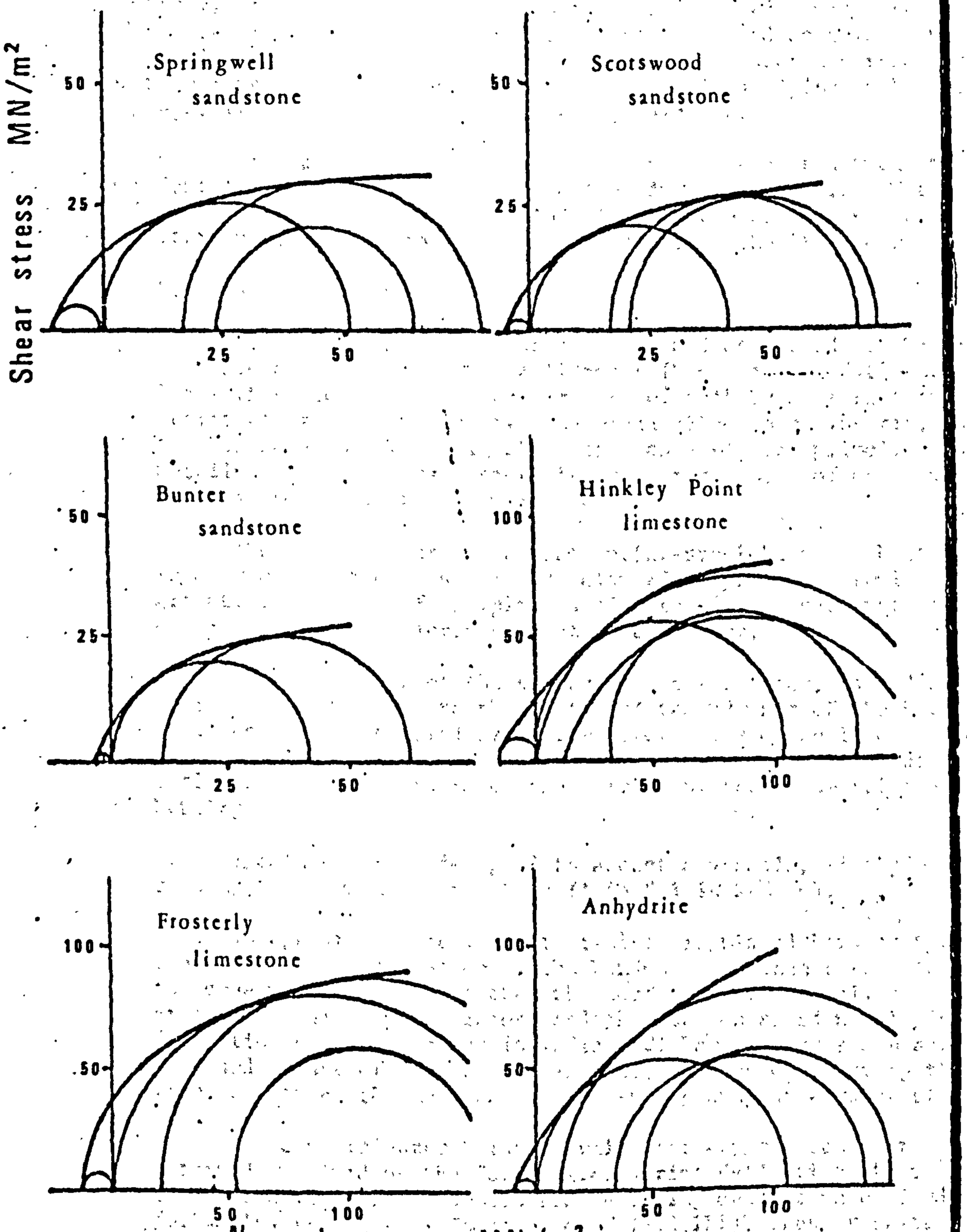

Figure 31

5.2.8 Indentation hardness

In machine tunnelling, it is recognized that the hardness of rock is an important factor in determining the ease with which a tunnelling machine can bore a tunnel. The rate of advance is influenced as well as the cutter cost. Various types of hardness may be designated in accordance with the type of test performed. Thus, these are an indentation hardness, rebound hardness, scratch hardness, or abrasion hardness, and undoubtedly, there are other types that could be named. Much work on hardness testing has been carried out by the metal and ceramic industries and certain standard tests have been established. Research workers in rock have used some of these standardized procedures in studying rock hardness or have modified them or invented some of their own.

Due to the availability of the equipments in the Department only the indentation hardness and the rebound hardness are studied. The first one is exercised by using the Cone Indenter and the Firthbrown Hardometer. The latter by using the Shore Scleroscope and the Schmidt Hammer.

5.2.8.A Cone Indenter test

A special instrument was designed and developed at the Mining Research and Development Establishment (MRDE) at the National Coal Board (NCB) to determine the hardness of rock by measuring its resistance to indentation by a Tungsten carbide cone. The rig, called the NCB Cone Indenter (Fig 31), works on a similar principle to metallurgical hardness testers in which the amount of penetration is measured for a known applied force.

The unit consists of a flat spring-steel beam which is mounted in a frame in which its ends are clamped to produce a semi-encastre' effect. The degree of clamping is adjusted during calibration to ensure a 'standard' force-deflection characteristic.

The deflection of the spring, hence the force, is indicated by a dial gauge attached to the frame and the advance of the hardened steel cone is controlled by a micrometer screw which is operated by a handwheel. The movement of the cone is measured by a vernier-type scales which are engraved on the barrels of the handwheel and screw housing.

The indenter is designed to accept any small, flat piece of rock up to 25 mm X 25 mm X 6 mm (1 in X 1 in X ¼ in).

To operate the device a test-piece is placed between the anvil, i.e. the spring and the cone. The handwheel is then turned to advance the cone until it just touches the surface of the specimen. At this stage the dial gauge is zeroed and the cone advanced until a spring deflection of 25 divisions is indicated. The vernier scale are then read and amount of penetration is determined by calculating the difference between the movement of the spring and the advance of the cone.

The cone indenter hardness value for any particular test is obtained by dividing the force, i.e. spring deflection, by the amount of penetration which has occurred. A spring deflection of 25 divisions (0.025 in) represent a force of 40 N (8.8 lbf). These results are referred to as NCB Cone Indenter (Standard) values.

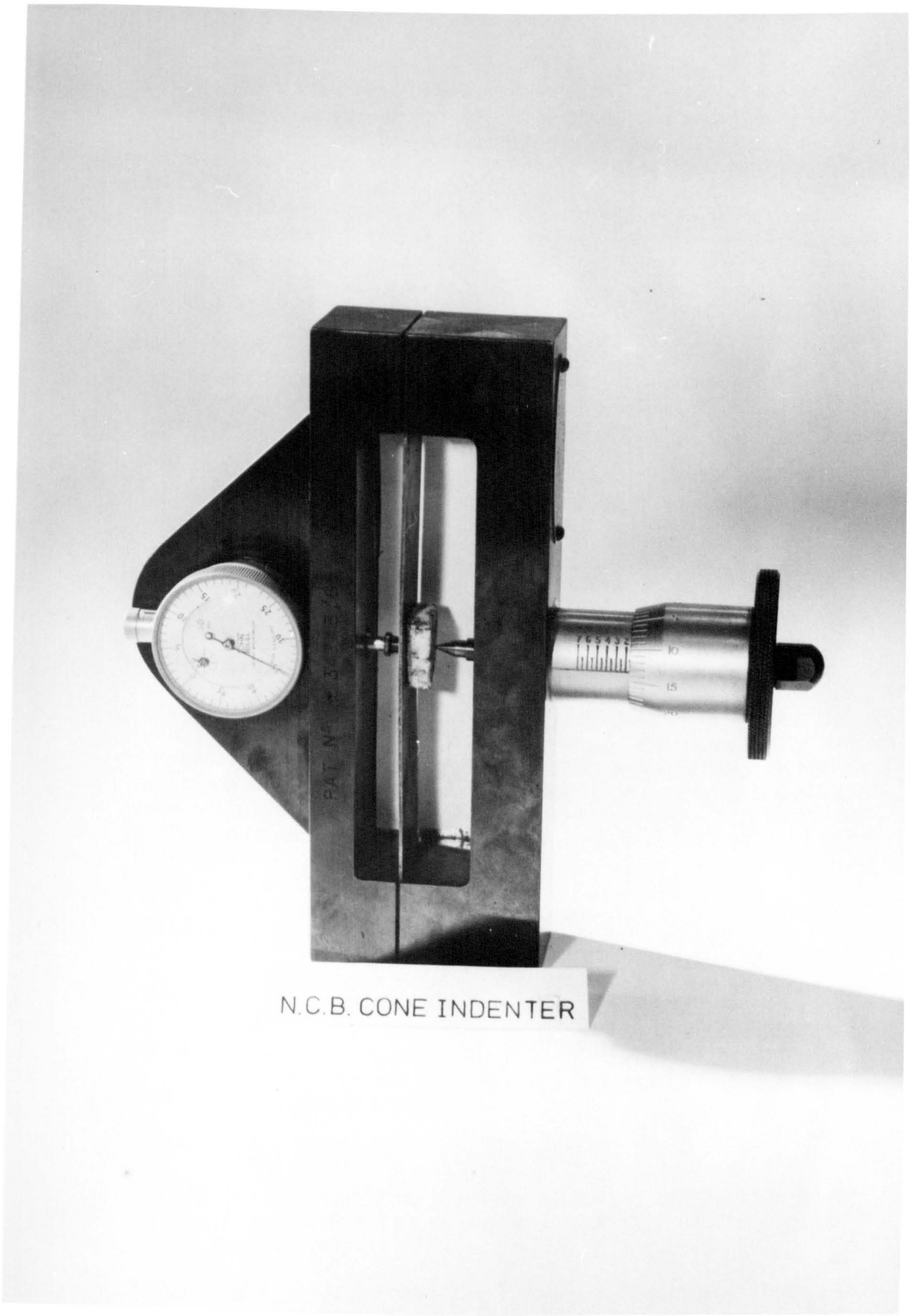

N.C.B. CONE INDENTER

Figure 32

A limitation was found when testing sample of hard rock (compressive strength of more than 100 MN/m^2) using the standard technique where the amount of penetration was relatively small A modified test was devised in which the force on the cone was increased to 110 N (24 lbf); this was represented by a spring deflection of 50 divisions (0.050 in). The result obtained by this method are classified as NCB Cone Indenter (Modified) values.

A minimum of twenty Cone Indenter was obtained from each test-piece of rock type.

5.2.8.B Brinell hardness (BHN)

In this method, a hardened steel ball with a diameter D is forced into test surface under a known load P and the hardness of the test specimen is then determined in terms of the ball imprint diameter d.

The average pressure on spherical surface of the indentation is the Brinell Hardness Number, or BHN, or by formula

$$BHN = \frac{P}{\frac{\pi D}{2}\left(D - \sqrt{D^2 - d^2}\right)}$$

A Firthbrown Hardometer was used to provide an alternative method frequently. It has previously been used to test metals and tests were made to determine its suitability for use in rocks.

By this rig a small steel ball (1 or 2 mm diameter) is applied by a known load to the surface of a rock. The diameter of the indentation figure produce on the rock is measured with a Micrometer Eye-piece and the BHN found by making an average of a number of successful indentations and noting the corresponding hardness values from calibration table for the appropriate ball diameter and load.

For rocks, however, there are special test requirements, these are:-

1. The specimen thickness should be greater than 1.5 cm.
2. As the indentation figure is not always clear, particularly in sandstones, it is necessary to grind the test surface to a flat finish and coat it with a thin film of Aluminium paint.
3. A large number of tests are required to give a representative average hardness for the rock.

5.2.9 Rebound hardness

The explanation for this hardness method is simply that hard meterials have high elastic limits and absorb little of the kinetic energy of the dropped weight.

Softer materials will have lower elastic limits and thus deform plastically, absorbing more energy.

5.2.9.A Shore hardness test

The rebound hardness as measured by the Shore Scleroscope is another method frequently used to compare rock characteristics. It is easy to prepare the samples since they need to be made flat and smooth on one surface only. This can be simply effected with a carborundum stone over the small area necessary for test purposes.

Some attempts have been made to correlate Shore hardness to the compressive strength of the rock (89,90). These are reasonable satisfactory, but where samples have a high quartzitic content, the relationship is unreliable. The Shore Scleroscope (Fig. 33) consists of a diamond-tipped or tungsten carbide-tipped, mass which is fitted into a vertical guide tube and set at a predetermined height. Practically, the mass is raised by suction about 300 mm. The specimen is mounted on the anvil situated below the tube and the mass is allowed to fall freely onto the surface of the specimen by squeezing the rubber bulb of the equipment. After striking the surface the mass rebounds and the height, at the top of the hammer, of the rebound, which is indicated on a graduate tube, is a measure of the sample's resilience. It is necessary to take a large number of readings and to treat the results statistically. It is evident that the test measures the hardness of a minute area of the surface and in consequence the presence of a large number of hard crystals, such as free quartz, contributes to high individual and average rebound values which are unrelated to the cohesive strength of the test specimen.

At M.R.E. the relationship between Shore hardness and compressive strength, as found by Fish (89), approximate to be:

$$H = 3\ fc$$

where: H is the rebound hardness
fc is the compressive strength measured in 1,000 lb/in²

Another correlation between Shore hardness and compressive stress has been found by Greenland (90) who mades the point that apart from being used for the solution of strata control problems, strain-energy theory has been applied to explain the failure on an elastic material in comminution.

The theory states that the condition of yielding can be expressed by the equation:-

$$M = \frac{fc^2}{2E} \times \text{volume}$$

where: M is the modulus of resilience, $\frac{\text{in lb}}{\text{in}^3}$
fc is the tensile or compressive stress at yield, $\frac{\text{lb}}{\text{in}^2}$
E is the modulus of elasticity, $\frac{\text{lb}}{\text{in}^2}$

It has to be noted here that the diamond-tipped mass, the so-called Universal hammer, is used when testing hard rock. The tungsten carbide tipped mass, the Magnifier hammer, is used on softer rock to enable the hammer to rebound higher for the ease of reading.

Shore Scleroscope

Figure 33

The following table provides a conversion for the two hammer scales.

Universal Hammer	Magnifier Hammer	Universal Hammer	Magnifier Hammer
1	3	21	37
2	4	22	38
3	6	23	40
4	7	24	41
5	8	25	43
6	11	26	45
7	12	27	47
8	14	28	49
9	16	29	51
10	17	30	52
11	20	31	55
12	21	32	57
13	22	33	58
14	25	34	60
15	26	35	61
16	28	36	64
17	30	37	65
18	32	38	66
19	34	39	68
20	35	40	70

The figures quoted in this work are taken from the magnifier scale.

5.2.9.B Schmidt hammer test

The Schmidt hammer (Fig 34), one type of rebound hammer, is used primarily in concrete work for determining when the forms may by removed or how much the compressive strength of concrete is. The instrument was developed in Germany to be a field instrument. A type used to measure rock hardness, the Schmidt Betonpruf-hammer type N, is about the size of a flashlight and the striking energy, the kinetic one, is lower than that of the larger hammer used for concrete. This is necessary because the concrete hammer fractures many of the lower strength rocks. The basic parts of the hammer are shown in Fig 35.

The working principle of this manually-operated rebound tester depends on a steel mass which, after the release of a catch, travels a fixed distance under spring pressure, The mass will develop a kinetic energy on striking an anvil held against the rock under test. Unlike the scleroscope, this anvil has a flattened nose-piece to produce the blow. The measurement is recorded by means of the rebounding mass and a pointer on a linear scale of 1 to 100. The instrument may be pointed at the rock in any direction normal to its surface, but the gravitational effect due to inclination of the tool must be accounted for the results are corrected for inclination from the graph (Fig 36.) supplied with the instrument.

It has been found (77) that the rebound values obtained from this instrument do not relate linearly to the compressive strength of the rock.

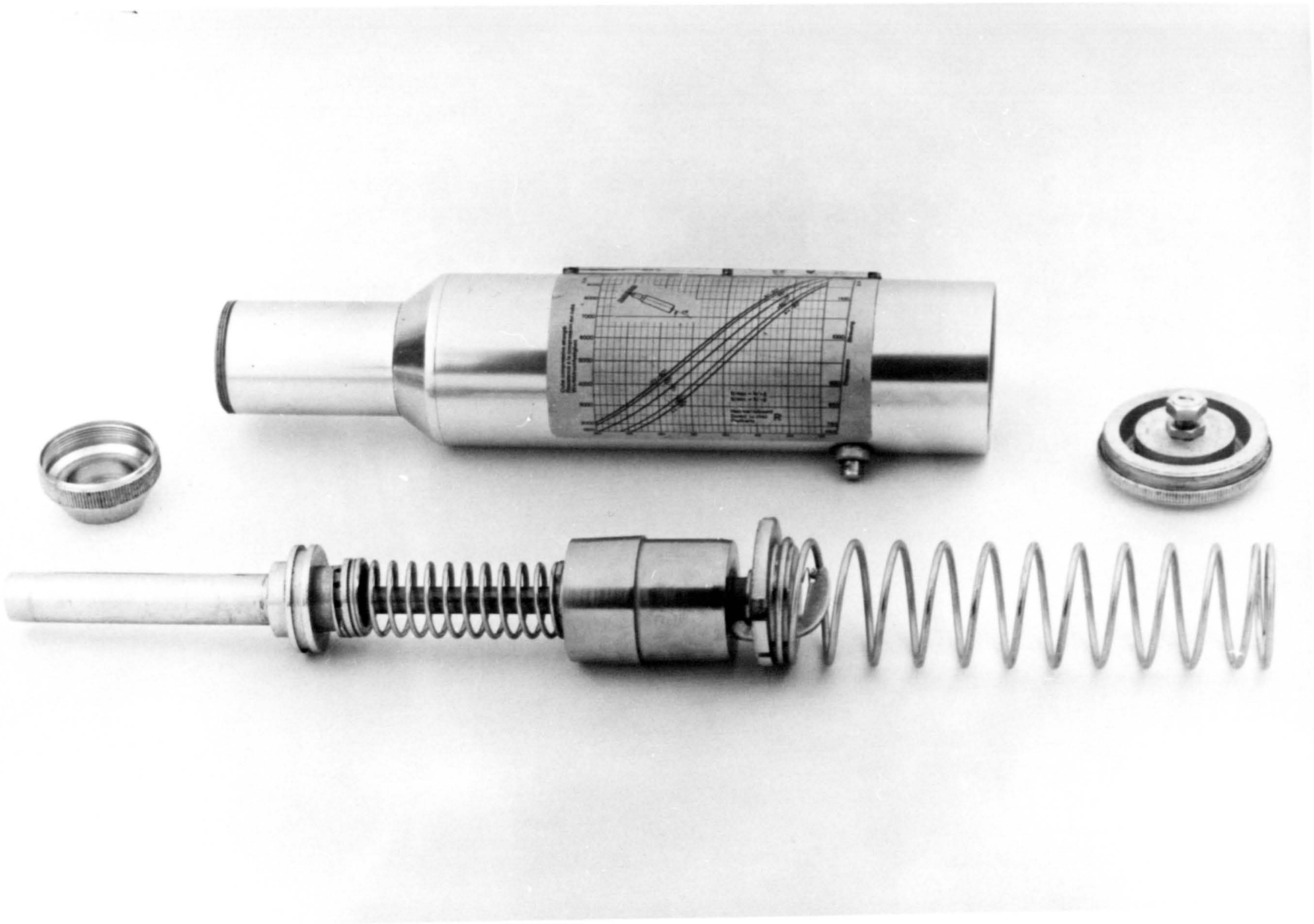

Schmidt Hammer

Figure 34

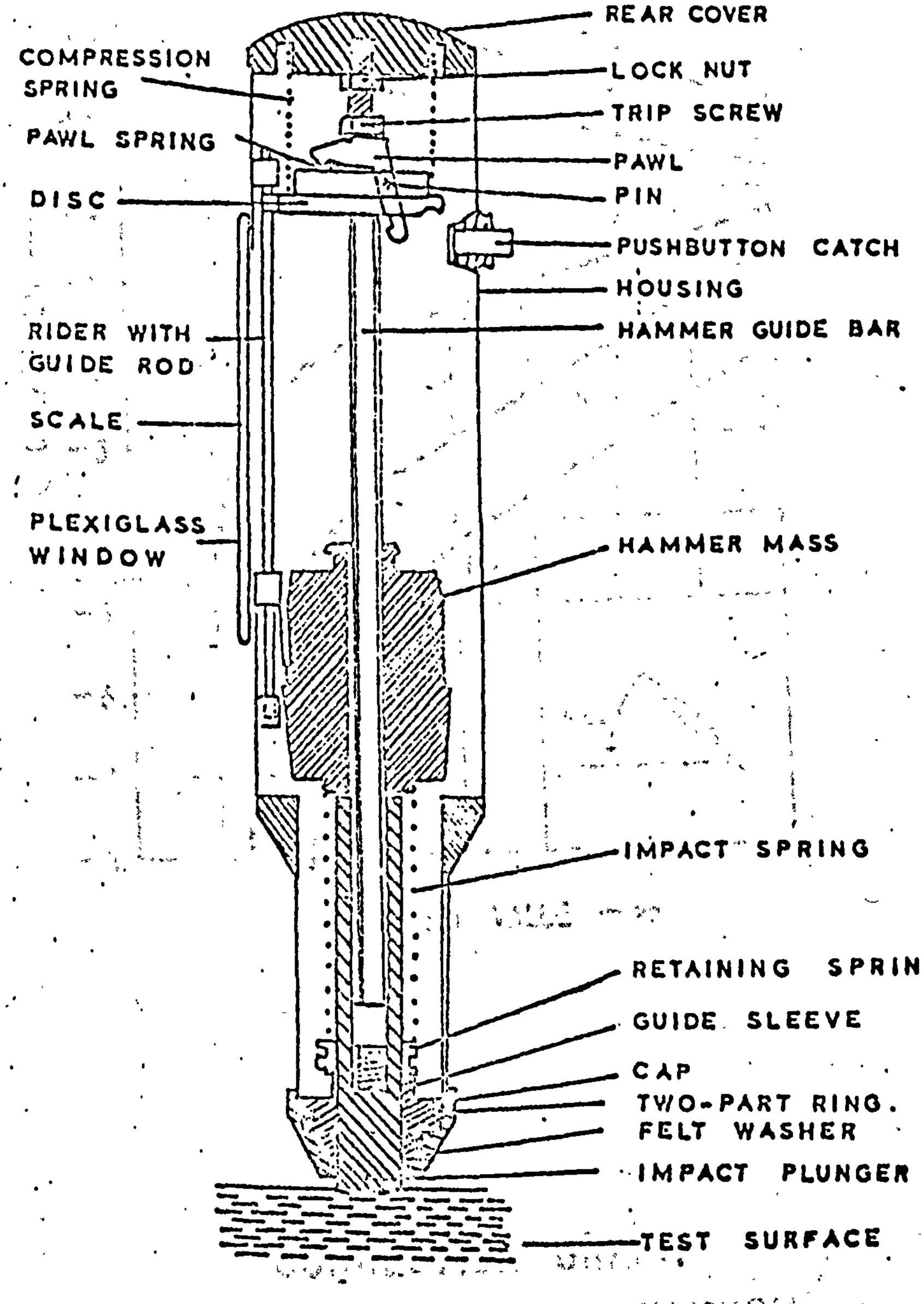

FIG. 35. LONGITUDINAL SECTION OF SCHMIDT REBOUND HAMMER TYPE N

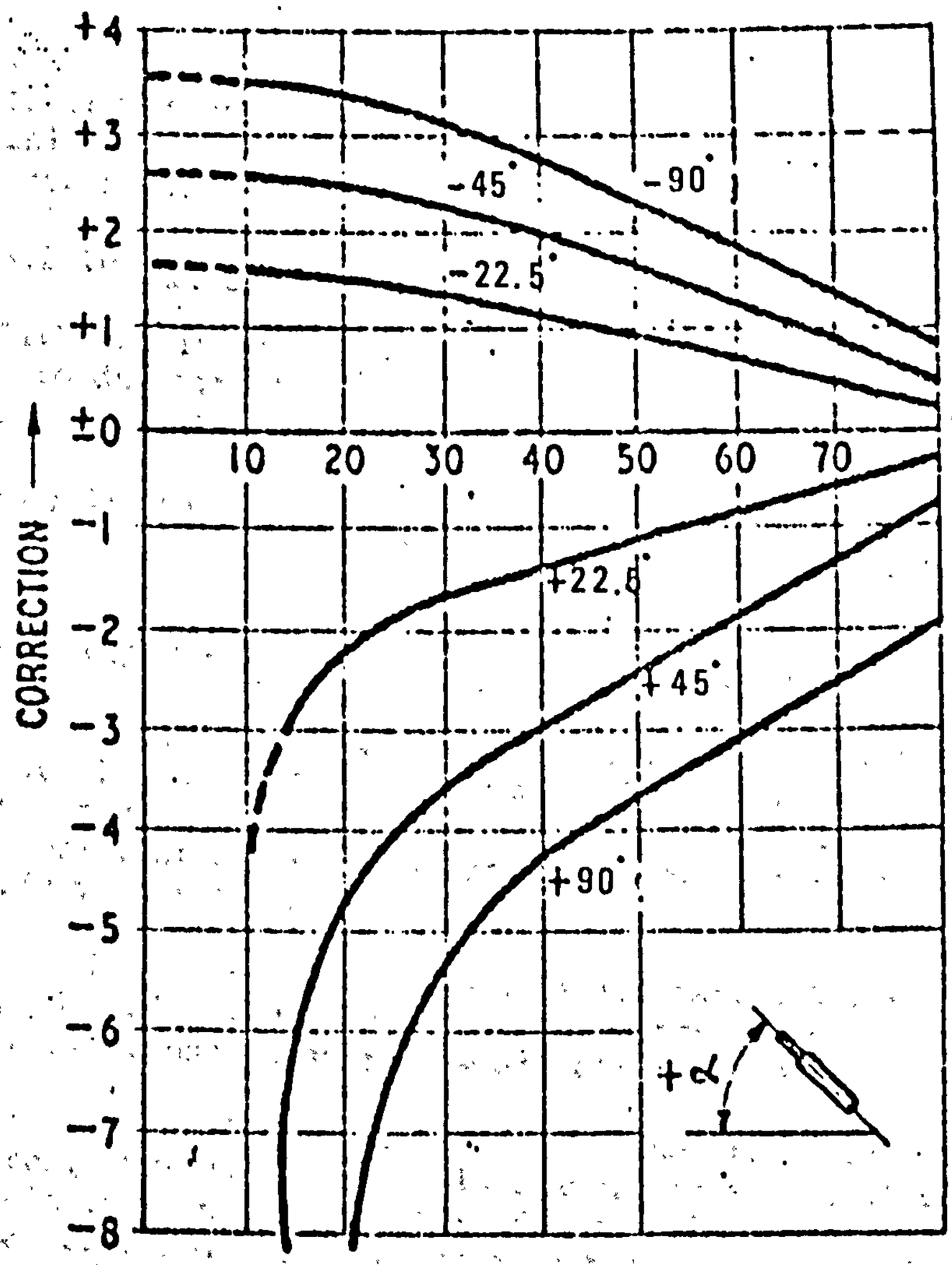

CORRECTION GRAPH
FOR INSTRUMENT INCLINATION
(SCHMIDT BETONPRÜFHAMMER – TYPE N)

Figure 36

The success of the Schmidt hammer as a field instrument led to investigation of its suitability as a laboratory instrument. In this test, the investigation into specimen size for laboratory testing is undertaken.

5.2.10 Abrasivity test

Although it is not possible to give a rigid definition, it is convenient to describe the abrasivity of a rock as its ability to destroy the tools attacking it.

Many methods to assess the abrasivity of rock have been invented, due to the availability of the equipment, only two methods are investigated.

5.2.10.A Blade abrasivity and machineability

In this test a Rapidor reciprocating arm hacksaw machine which has a stroke of 117 mm has been used to determine the machineability and the abrasivity of rock. This machine cuts the material at a 100 strokes/min. giving an average cutting speed of 0.39 m per second.

High speed steel blades which have a Vickers hardness value of 800, with four teeth per centimetre are used as the cutting tool. The blade has an average width of 1.329 mm.

Generally this test, the hacksaw test, is carried out on drill cores. The rock specimen is clamped in a vice at right angles to the blade and ten full strokes of the reciprocating arm are counted for each test and the test repeated between ten and fifteen times depending on the rock type. After each test, the blade teeth are thoroughly cleaned with a stiff brush, to remove any adhering rock particles. A new blade is used for each rock specimen.

As the width of the slot cut by these blades is constant, the area cut is directly proportional to the volume removed and this is used to determine the machineability.

The abrasive properties of the rock are assessed by weighing the blades accurately before and after each cutting test. Prior to each test, the diameter of each specimen is measured along the whole length at selected sections in order to determine the initial volume of rock. The area cut in each test is determined by measurement of the chord length of the groove with a micrometer and calculation using previously measured diameter.

The area cut is then plotted against the test number. The shapes of the curves vary with the type of rock cut, and these are assumed to characterise their machining properties. The area of the curve for the first ten cuts is taken as the measure of the machineability of the rock.

If the machineability of the rock is related to the machineability of a typical non-abrasive rock, such as gypsum, a non-dimensional parameter which can be defined as the machineability

Hacksaw Machine

Figure 37/A

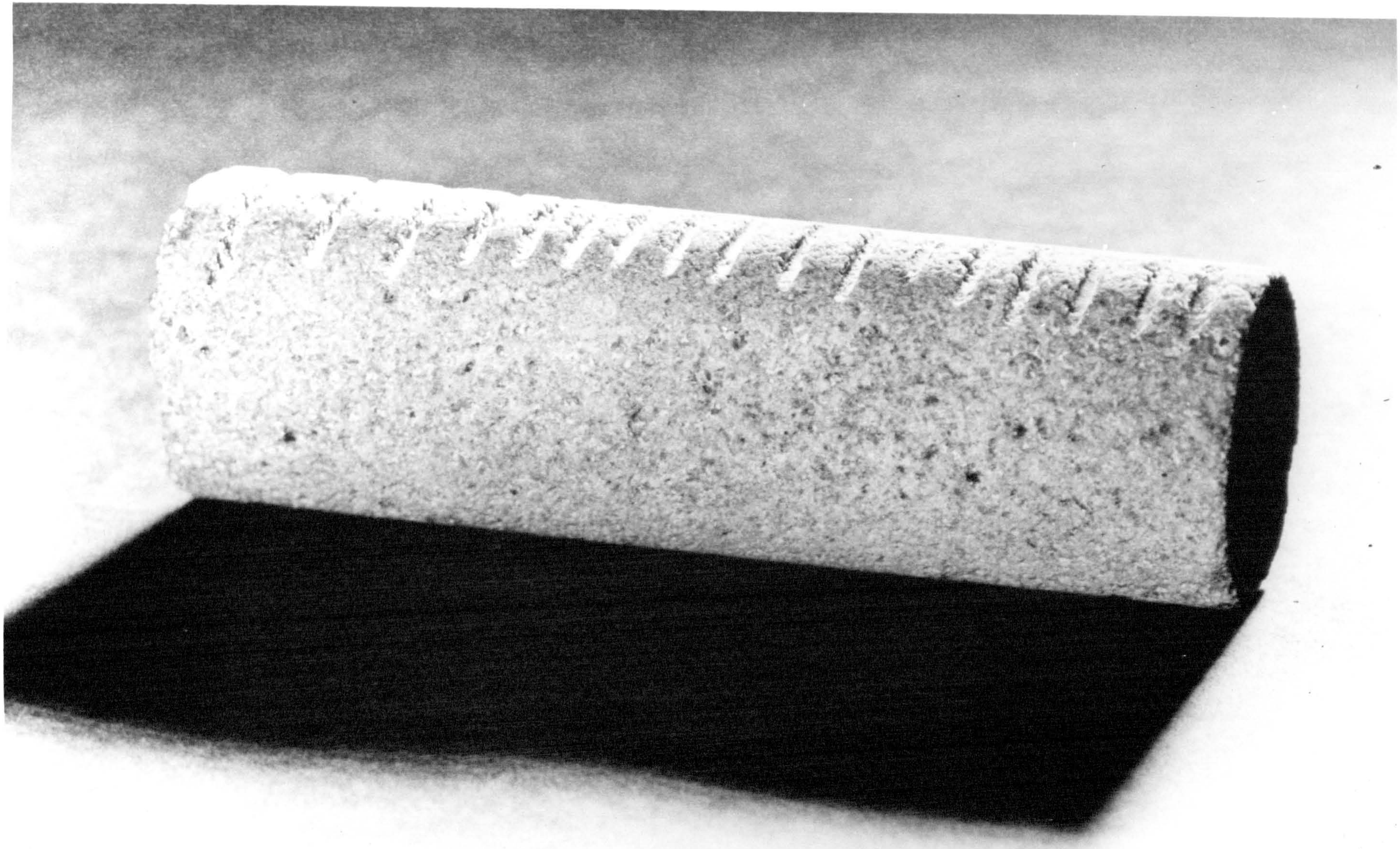

Sandstone Specimen after Hacksaw Test

Figure 37/B

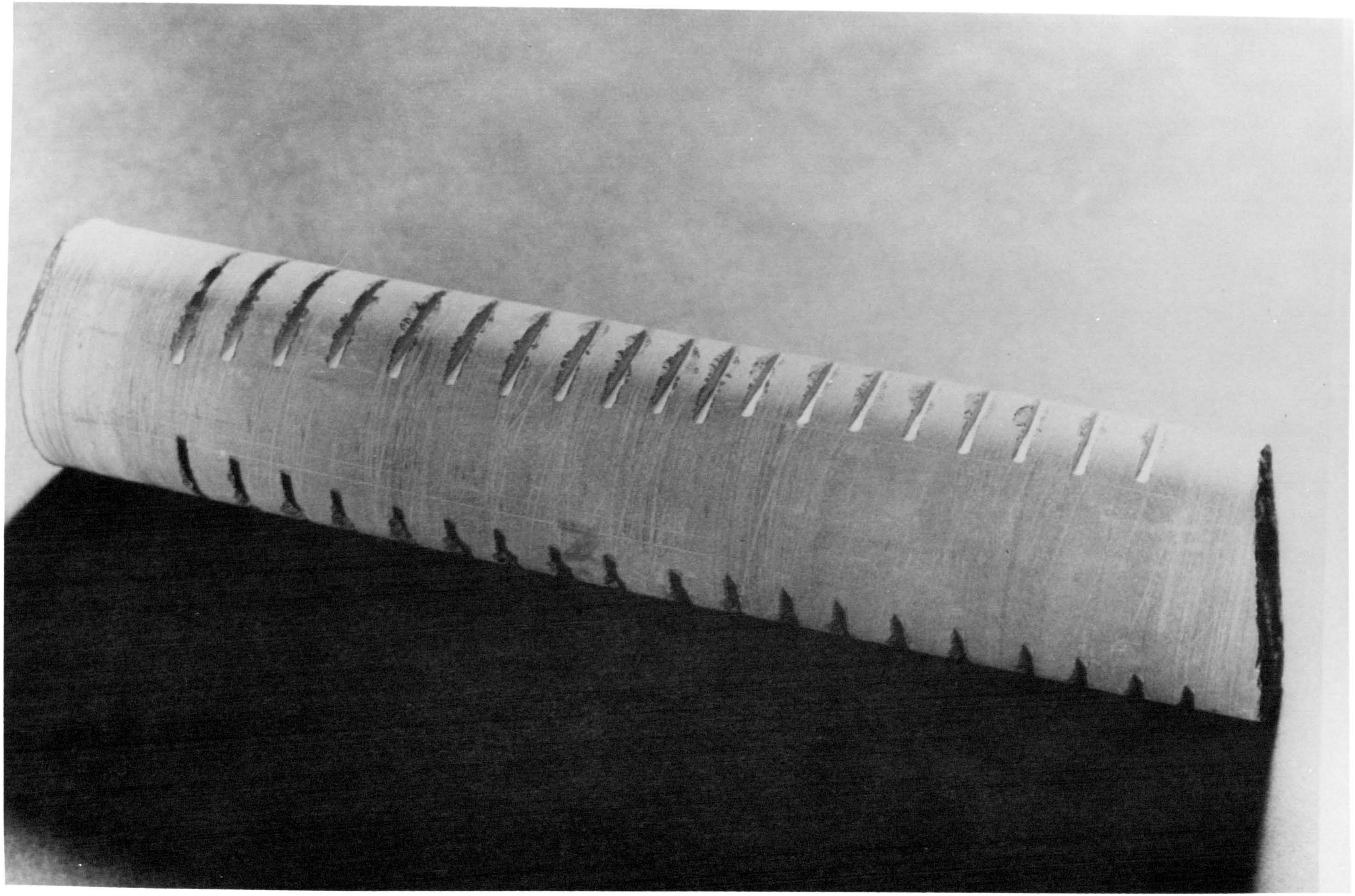

Limestone Specimen after Hacksaw Test

Figure 37/C

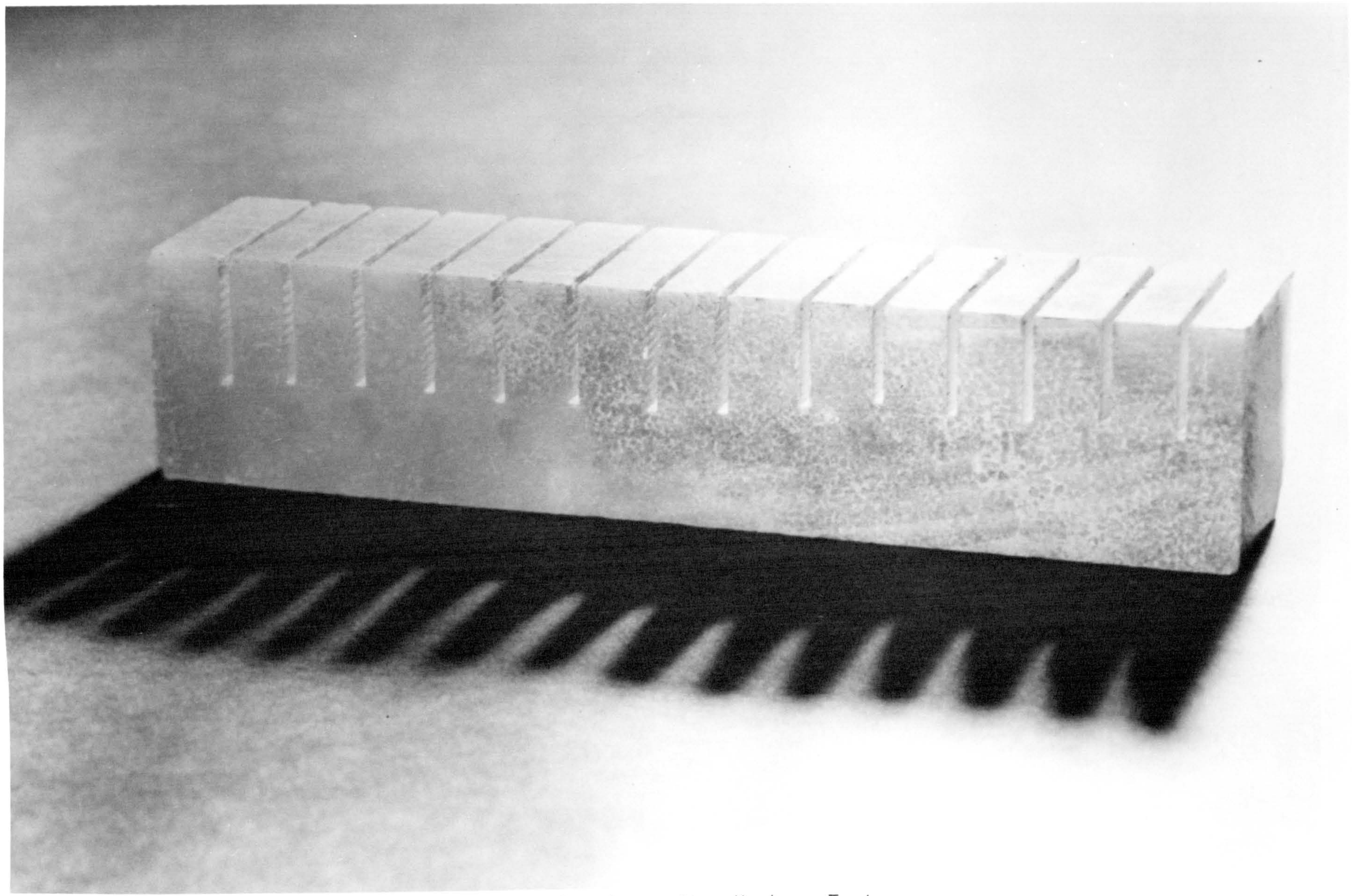

Gypsum Specimen after Hacksaw Test

Figure 37/D

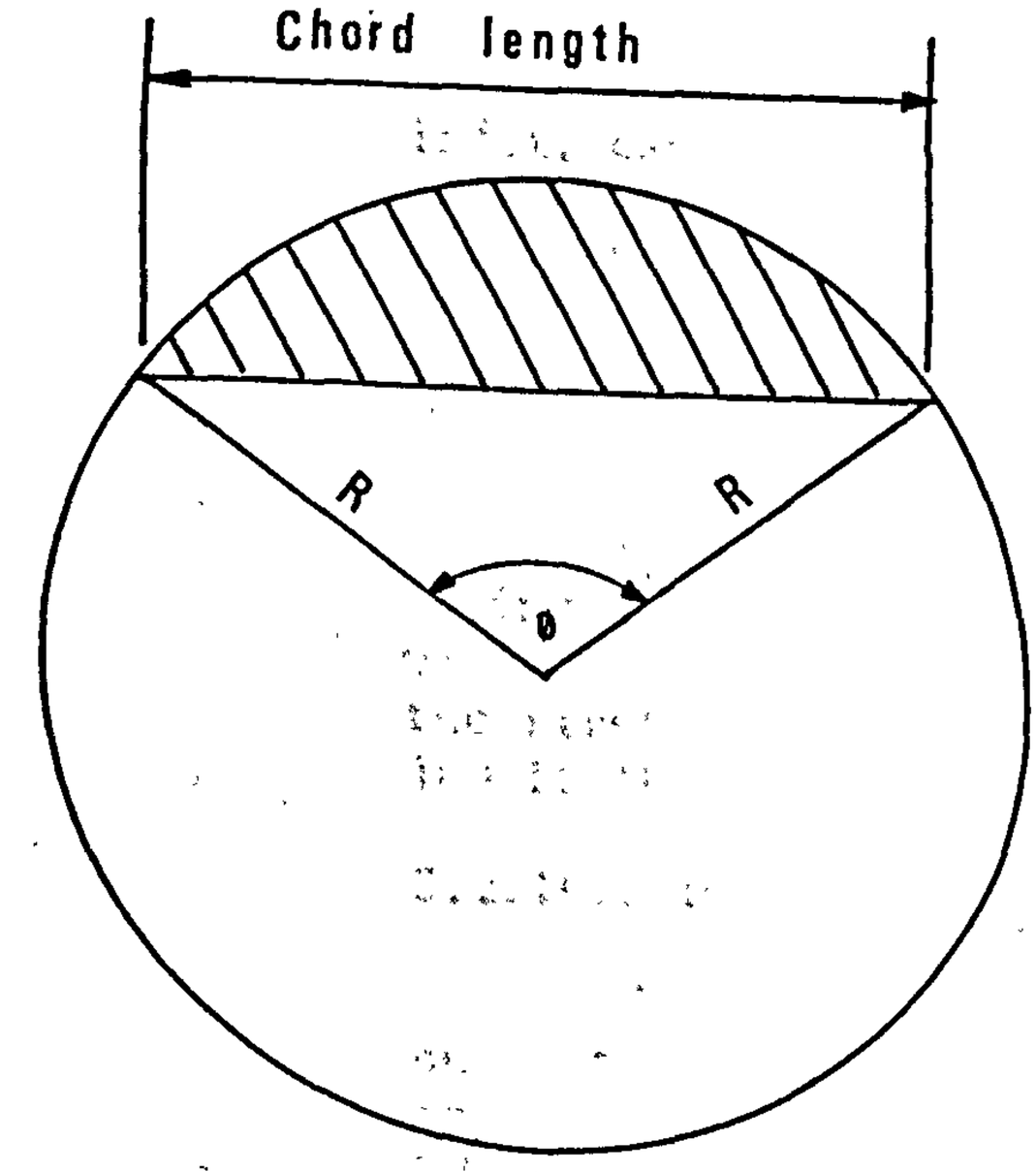

$$\text{Area cut} = \frac{1}{2} R^2 (\phi - \sin \phi)$$

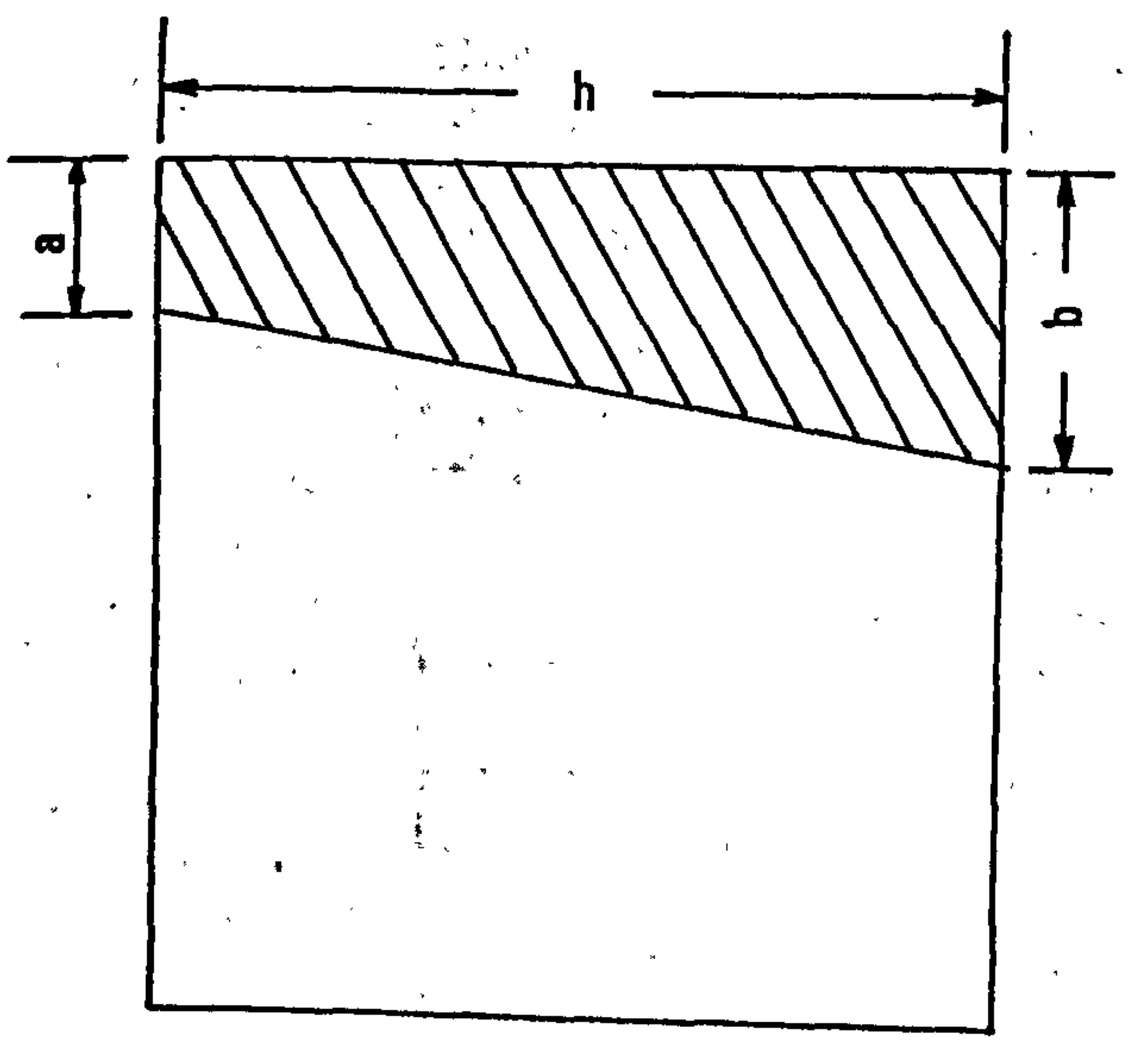

$$\text{Area cut} = \frac{a + b}{2} \cdot h$$

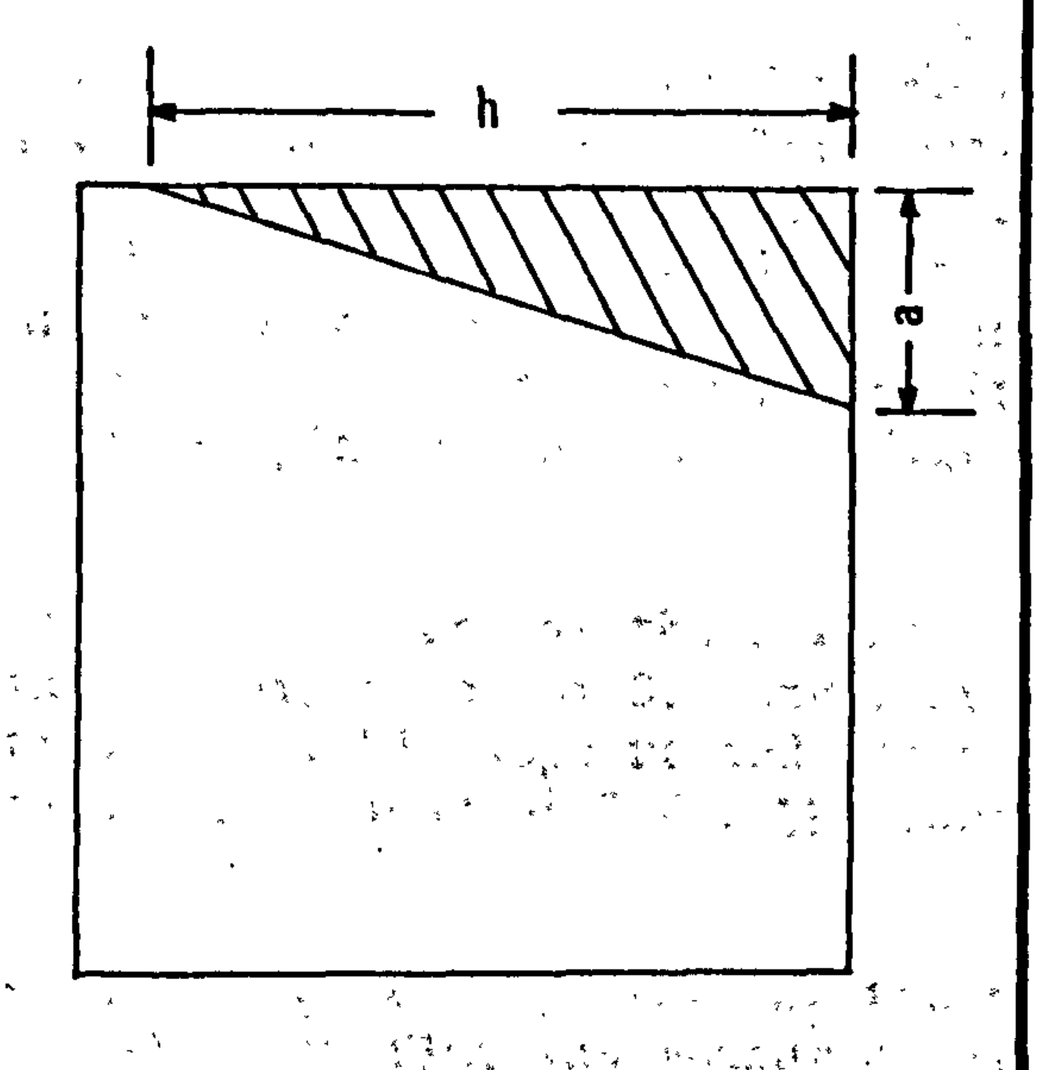

$$\text{Area cut} = \frac{a \cdot h}{2}$$

Base for determination of area cut

Figure 38

index, can be obtained.

The index is assumed to be the ratio

$$\frac{\text{Machineability of test rock}}{\text{Machineability of gypsum}} \times 100.$$

In the hacksaw test maximum wear of blade teeth occurred during the first test cut and when the results of area cut are plotted against test number, the steepest slope was obtained between the first and second cut. The tangent of this slope multiplied by 100 is the abrasivity of a particular rock.

5.2.10.B Intrinsic abrasivity test

The intrinsic abrasivity test is carried out similar to that suggested in the Cerchar abrasivity (91) and based on a steadily-applied constant force of 7 Kg. on a rod having a sharp point of 90° cone angle applied against the rock sample. The rock is then displaced by dragging it a distance of 1 cm at a slow speed. The abrasivity is a function of the diameter of wear flat created on the point of the tool.

In this test the rock specimen under investigation was clamped on the movable steel table which was designed to move the specimen 1 cm by pulling a lever between end stops. The specimen used was 100 X 75 X 50 mm having two ground parallel surfaces. The samples were first cut roughly to the size required on a Clipper masonry saw, and the test surfaces were then ground smooth and parallel on an Excel surface grinder to any size providing it was greater than that necessary for clamping and allowing a free path of 1 cm for the indenter.

A conical high speed steel tip which has the hardness of 720 VPN of 6.35 mm diameter having a sharp point of 90° angle at the end was inserted into a vertically movable support and was applied against the rock surface with a normal load of 7 Kg. The equipment is shown in Fig. 39.

The rock specimen was then displaced by dragging the tip a distance of 1 cm at low speed. The wear flat was measured, using a microscope furnished with a micrometer eyepiece, having the total magnification of 100 times, and then the test repeated with the same tip for five consecutive 1 cm displacements. Furthermore five steel tips were used for each rock specimen, thus providing five test replications.

The depth of penetration for each scratch was also measured by using a dial gauge giving an accuracy of 1/1000 in (1/2540 cm).

An attempt was made to measure the loss of weight of the tip, but this was found impossible over such a small distance of travel.

The tip loss in each test was determined by its volume calculated from the wear flat.

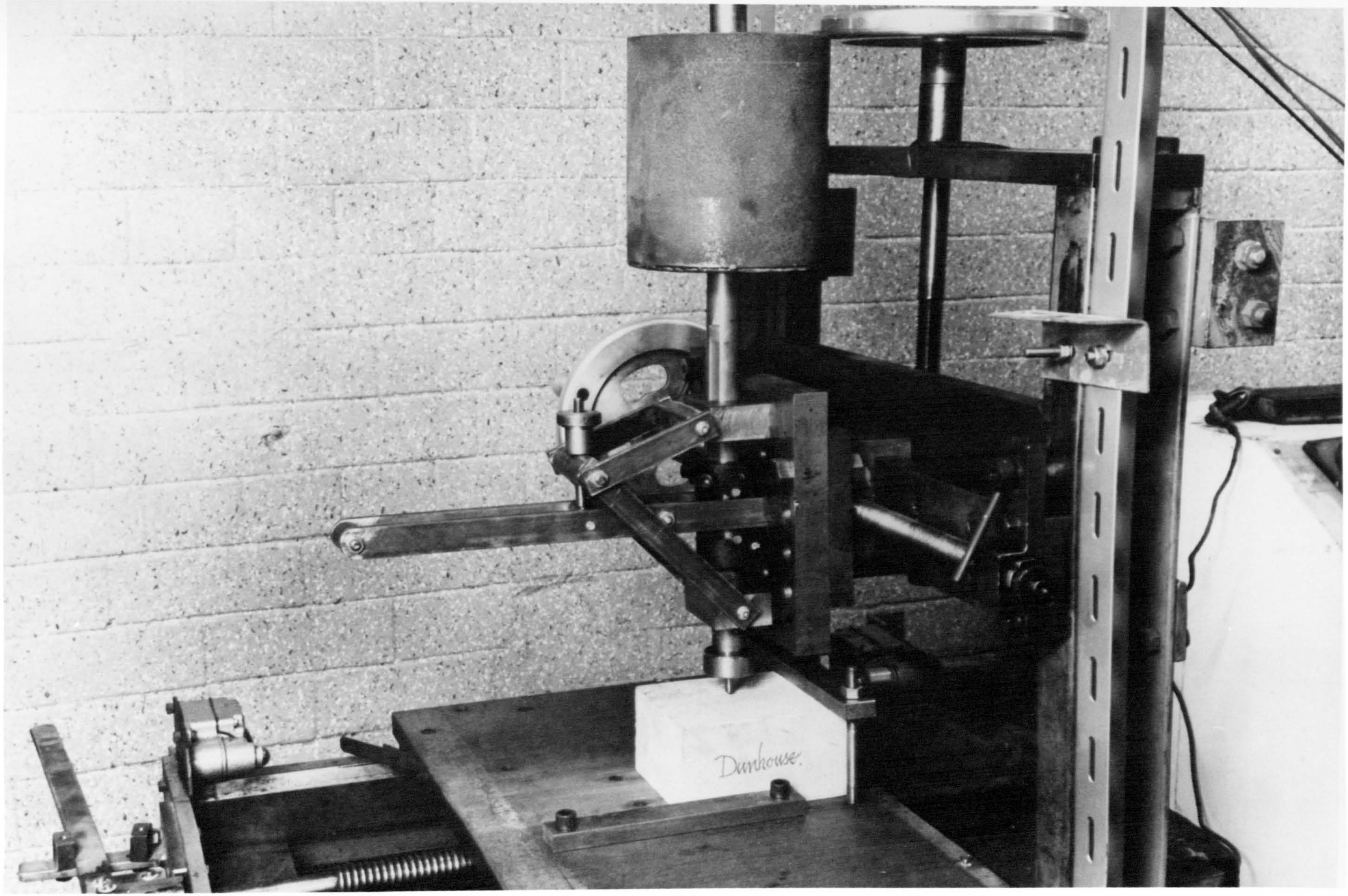

Abrasivity Test Machine

Figure 39

Abrasion factor of rock could be found by the equation:-

$$\text{Abrasion factor} = \frac{\text{Wear flat}}{100} \times \text{Compressive strength} \quad \text{MN/m}$$

By using high speed steel tips it was impossible to obtain a visible wear flat with the non-abrasive low strength rocks for the small distance travelled. The abrasion factor of these rocks therefore cannot be determined.

Other type of tool materials such as silver steel which has the hardness of 240 VPN, mild steel of 170 VPN and brass of 145 VPN were tried to find the possible type of tool materials in order that a classification on the basis of abrasivity of rock under the same test conditions can be made. After completion of the investigation it appears to be that none of them were successfully applicable for the whole range of rock samples and silver steel is the most suitable.

In all "abrasion Index" of the rock samples test are constructed based on abrasion factor of rocks using silver steel tool.

$$\text{Abrasion index} = \frac{\text{Abrasion factor of rock} \times 100}{\text{Abrasion factor of Scottish quartzite}}$$

5.2.11 Impact strength index

This is a laboratory test which was developed by the National Coal Board and based on a test originally proposed by Protodyakonov (92). It consists of taking exactly 100 g of rock fragments within the size range 9.5 - 3 mm and enclosing this in a vertical steel cylinder of 44 mm internal diameter, which is sealed at the base. A 1.8 kg. weight in the form of a piston is dropped freely 20 times a distance of 304.8 mm onto the enclosed fragments. After testing, the 100 g of material is sieved on the 3 mm screen and the amount in grammes retained on the screen is taken as the Impact Strength Index.

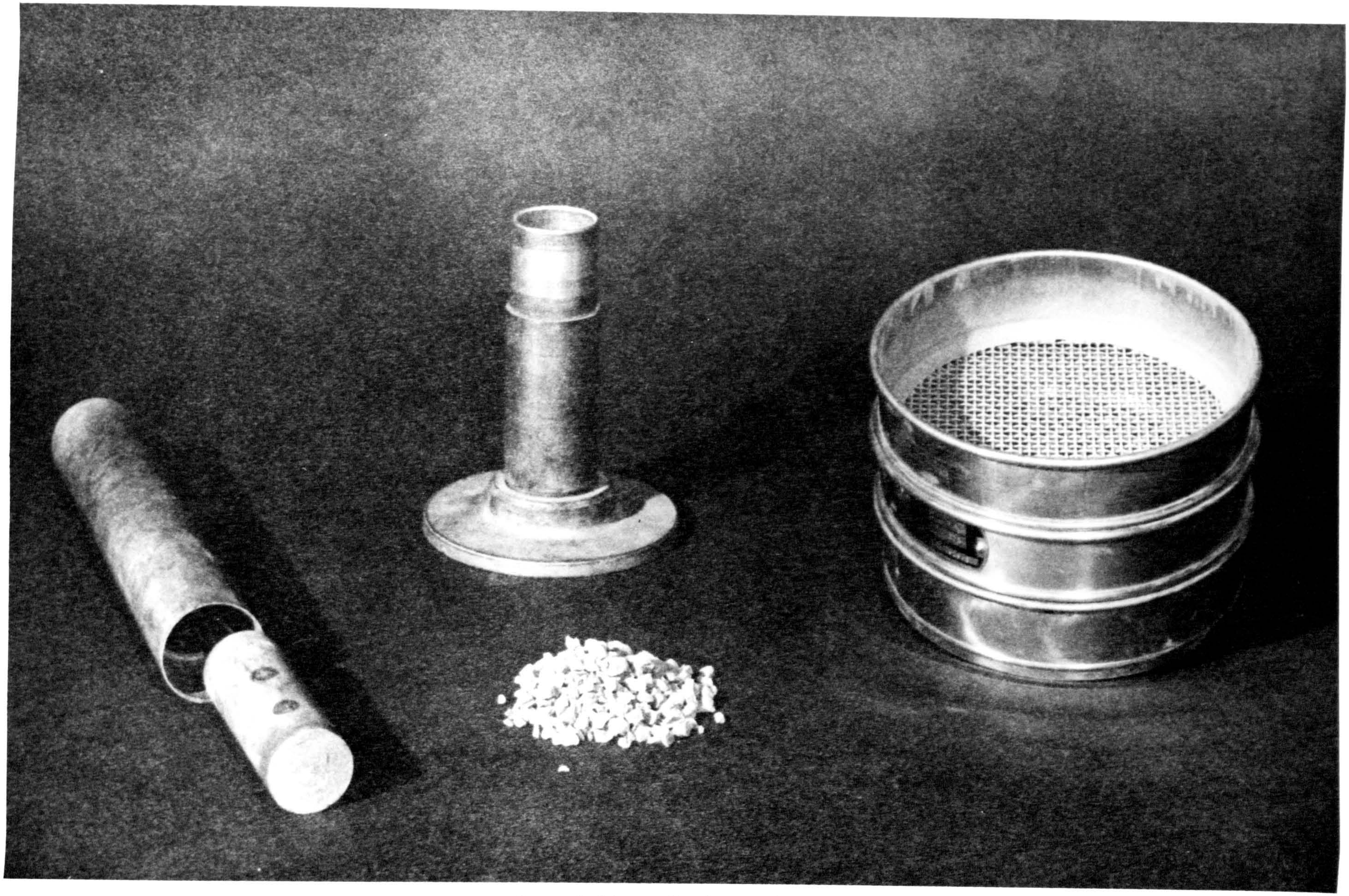

Impact Strength Apparatus

Figure 40

Chapter 6

Experimental Results

6.1 Petrographic analysis

Thin sections of the selected rocks were carefully studied and the petrographic descriptions of these rocks together with the major mineral constituents, quartz grain size distribution and quartz content are shown in Table 5.

Table 5 Petrographic Analysis

Rock	Description	Major mineral constituents	quartz grain size μm	quartz content per cent
Scotswood sandstone	subround grains with very variable grain size, silica matrix, high porosity	quartz, mica	max.1600 min. 120 Av. 480	90
Bunter sandstone	subangular to subround grains with very variable grain size, iron oxide matrix	quartz, iron oxide	max. 420 min. 30 Av. 210	73
Springwell sandstone	subangular to subround grains in silica and iron oxide matrix, high porosity	quartz, iron oxide	max. 430 min. 40 Av. 190	82
Dunhouse sandstone	almost evenly subangular to subround grains, high porosity	quartz, mica	max. 300 min. 50 Av. 160	88
Post sandstone	subangular to subround grains with silica matrix low porosity	quartz, mica	max. 380 min. 20 Av. 150	85
Hunterston sandstone	subangular to subround grains with very fine quartz grains filled some of interstices, mica and iron oxides matrix	quartz, mica, iron oxides	max. 470 min 40 Av. 180	78
Lazenby sandstone	subround grains with iron oxides matrix	quartz, mica. iron oxides	max. 680 min. 110 Av. 380	93
Mansfield whitestone	subangular grains with silica and clay minerals matrix	quartz, clay minerals	max. 400 min. 25 Av. 270	91
Frosterly limestone	very fine grains of calcite of about 95% consisted in the sections	calcite		

Rock	Description	Major mineral constituents	quartz grain size μm	quartz content per cent
Stanhope limestone	very fine texture, consists of about 100% calcite	calcite		
Hinkley limestone	this dark limestone consists of nearly 100% of very fine calcite	calcite		
Bulwell limestone	the rock consists of 90% angular medium grains calcite	calcite quartz		
Beachley limestones	the compact, well cemented rock consists of irregular fine to medium grains calcite	calcite		
Whinstone	the dark colour igneous rock consists mainly of pyroxene and plagioclase feldspar with no quartz	pyroxene, feldspar		
Creetown granite (white)	the rock consists of about 30% quartz, feldspar and mica	quartz, feldspar, mica	max.3700 min. 170 Av. 780	30
Creetown granite (blue)	about 40% quartz, feldspar mica and other minerals contain in the section	quartz, feldspar,	max.1000 min. 85 Av. 480	40
Anhydrite	this evaporitic rock consists of various patterns of mineral anhydrite, about 20% of calcite and iron oxides inclusion in the section, no quartz	anhydrite, iron oxides, calcite		
Gypsum	a fine grained evaporitic rock, no quartz	gypsum, undefined		
Stilfontein quartzite	a metamarphosed rock consists of subround medium to coarse grains of quartz in the matrix of mica	quartz, mica	max.1440 min. 120 Av. 410	53
Auriferous quartzite	this highly metamorphosed rock consists of coarse grains of quartz which is the results of the original granins, the smaller ones, were silicified. Silica matrix	quartz mica, iron oxides	max.3200 min. 210 Av. 610	60

Rock	Description	Major mineral constituents	quartz grain size μm	quartz content per cent
Scottish quartzite	a subround medium grains metamorphosed rock consists of quartz, mica, iron oxides	quartz, mica, iron oxides	max.400 min.100 Av. 250	63
Honister slate	a dark green colour metamorphic rock consists mainly of calcite small amount of quartz were observed	calcite		
Aust mudstone	a fine grained, well cement mudstone, no quartz was observed.	calcite		
Shale	this sedimentary rock consists of very fine clay minerals and some fine subangular quartz grains	clay minerals quartz, calcite	Av.70	32

It has to be noted that rocksalt and lower chalk can not be thin sectioned.

6.2 Specific gravity and porosity

Bulk density, grain density, apparent porosity and true porosity of rock samples were achieved by using the methods described in section 5.2.2. Samples of Hunterston sandstone, Mansfield whitestone, Stanhope limestone, Bulwell limestone, Beachley limestone and Aust mudstone were not available at the time of testing. The results are shown in Table 6.

It is very typical to see that the grain density of rock is always greater than the bulk density and the true porosity greater than the apparent one.

The results obtained in this work can be compared to published one (80) as follows:

Rock type	Average apparent SG.		Average apparent porosity	
	published	This work	Published	This work
sandstone	2.06	2.25	16.0	6.81
limestone	2.37	2.70	11.0	0.15
granite	2.66	2.65	0.9	0.11
slate	2.74	2.74	1.0	0.05

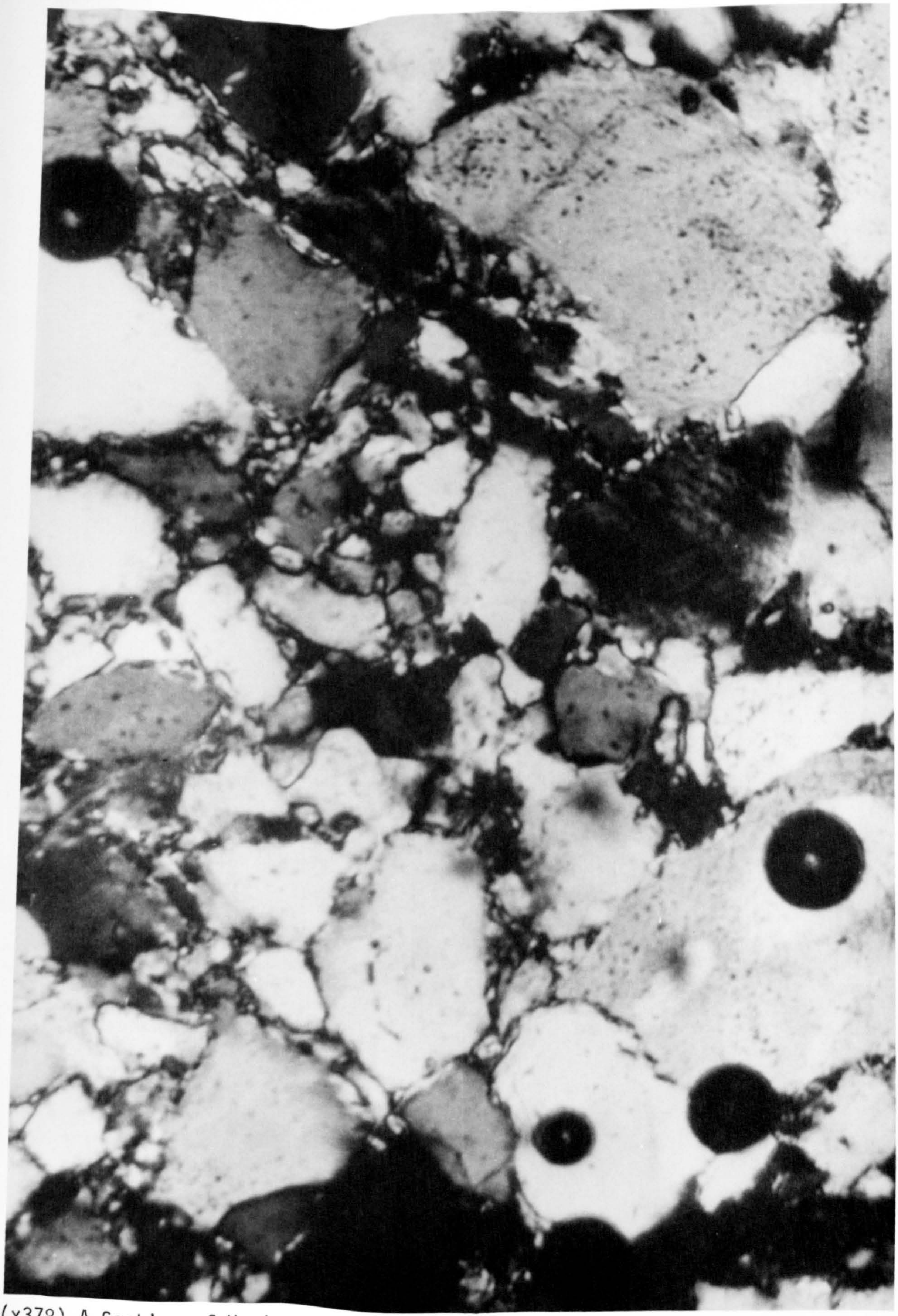

(x378) A Section of Hunterston Sandstone Showing Great Variation in Size of Quartz Grains in Iron Oxide Matrix (x nicols)

Figure 41/1

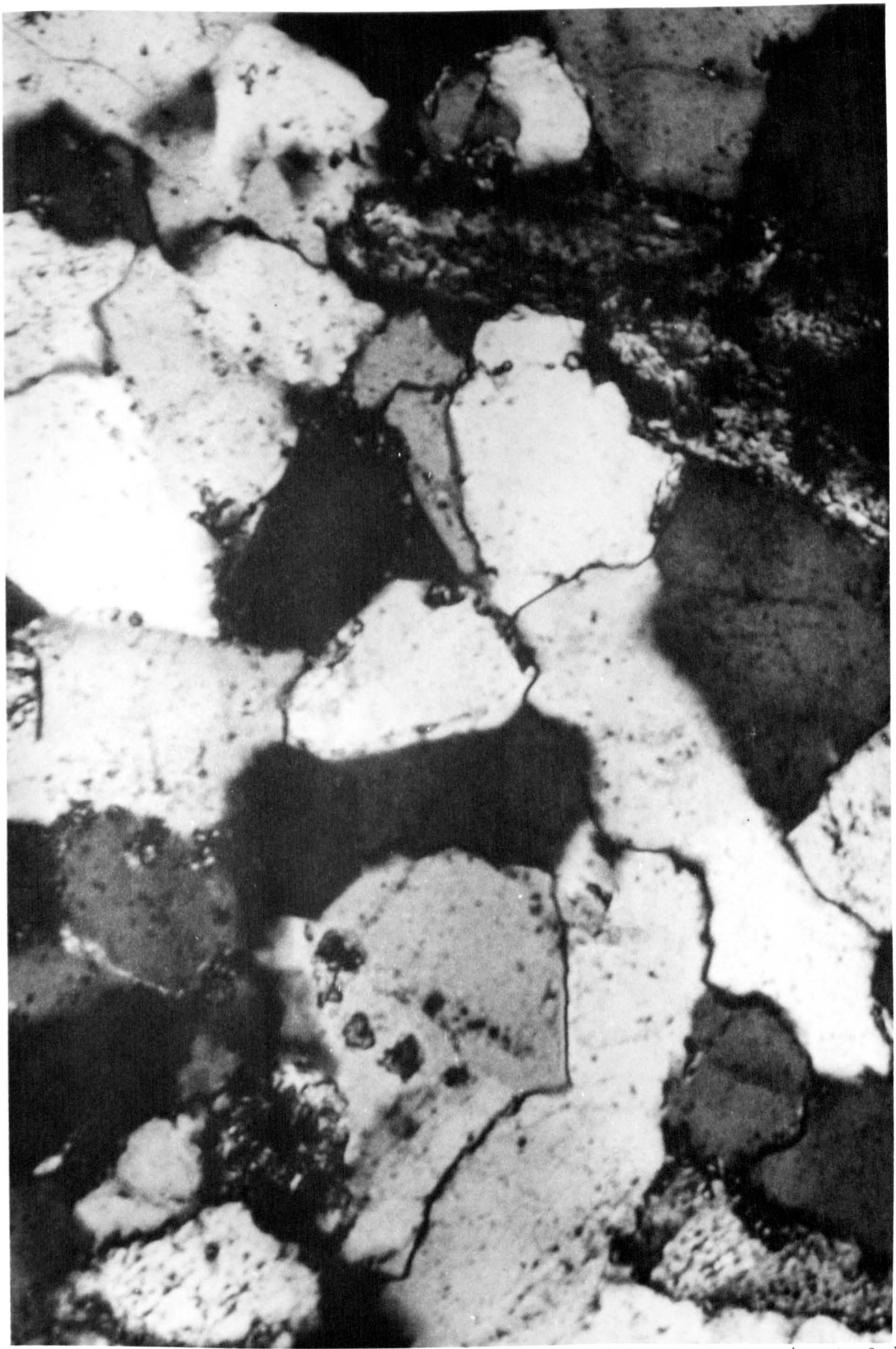

(x378) A Section of Post Sandstone Showing Compacted Quartz Grains (x nicols)
Figure 41/2

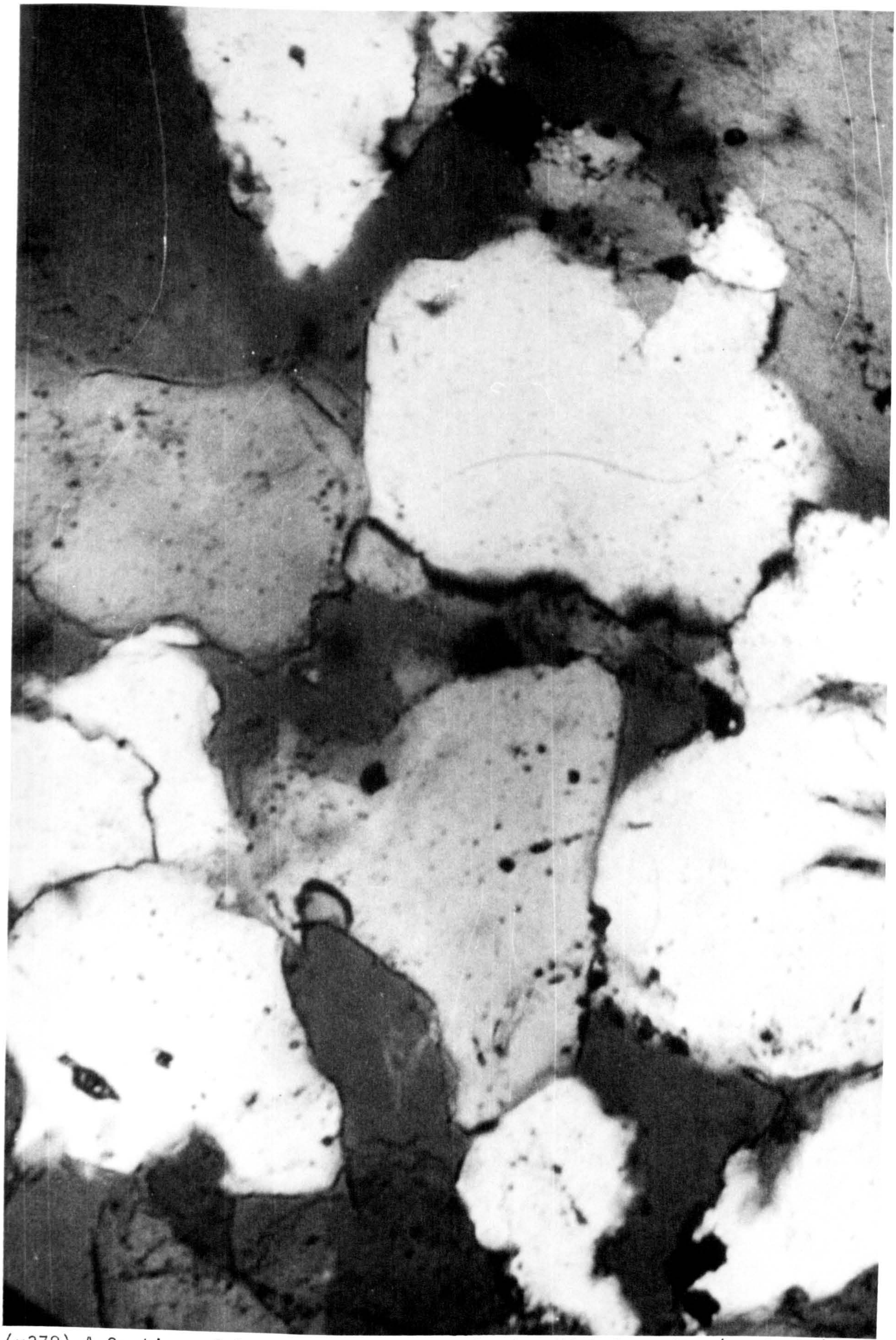

(x378) A Section of Scotswood Sandstone Showing High Porosity (x nicols)

Figure 41/3

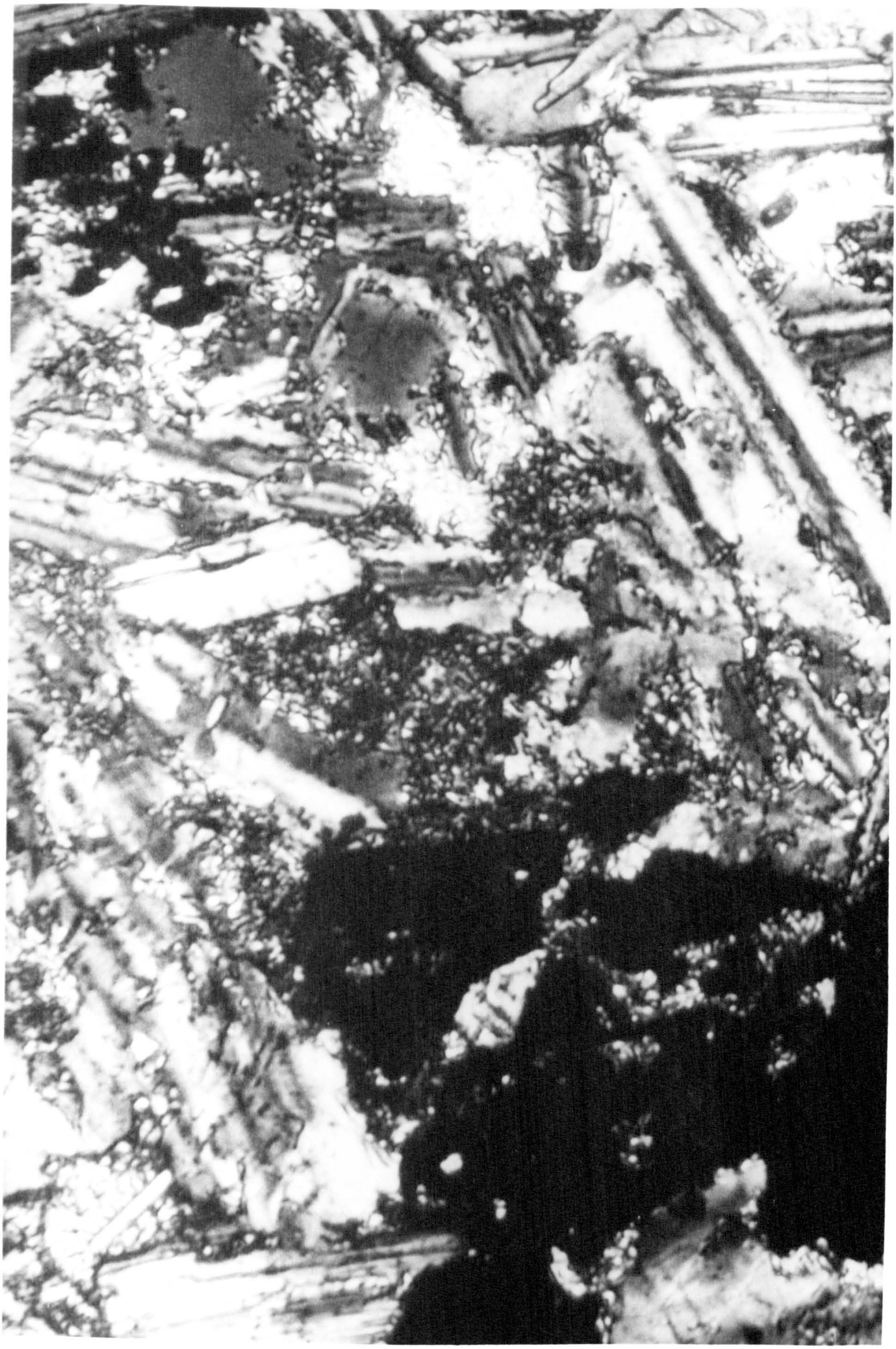

(x378) A Section of Whinstone

Figure 41/4

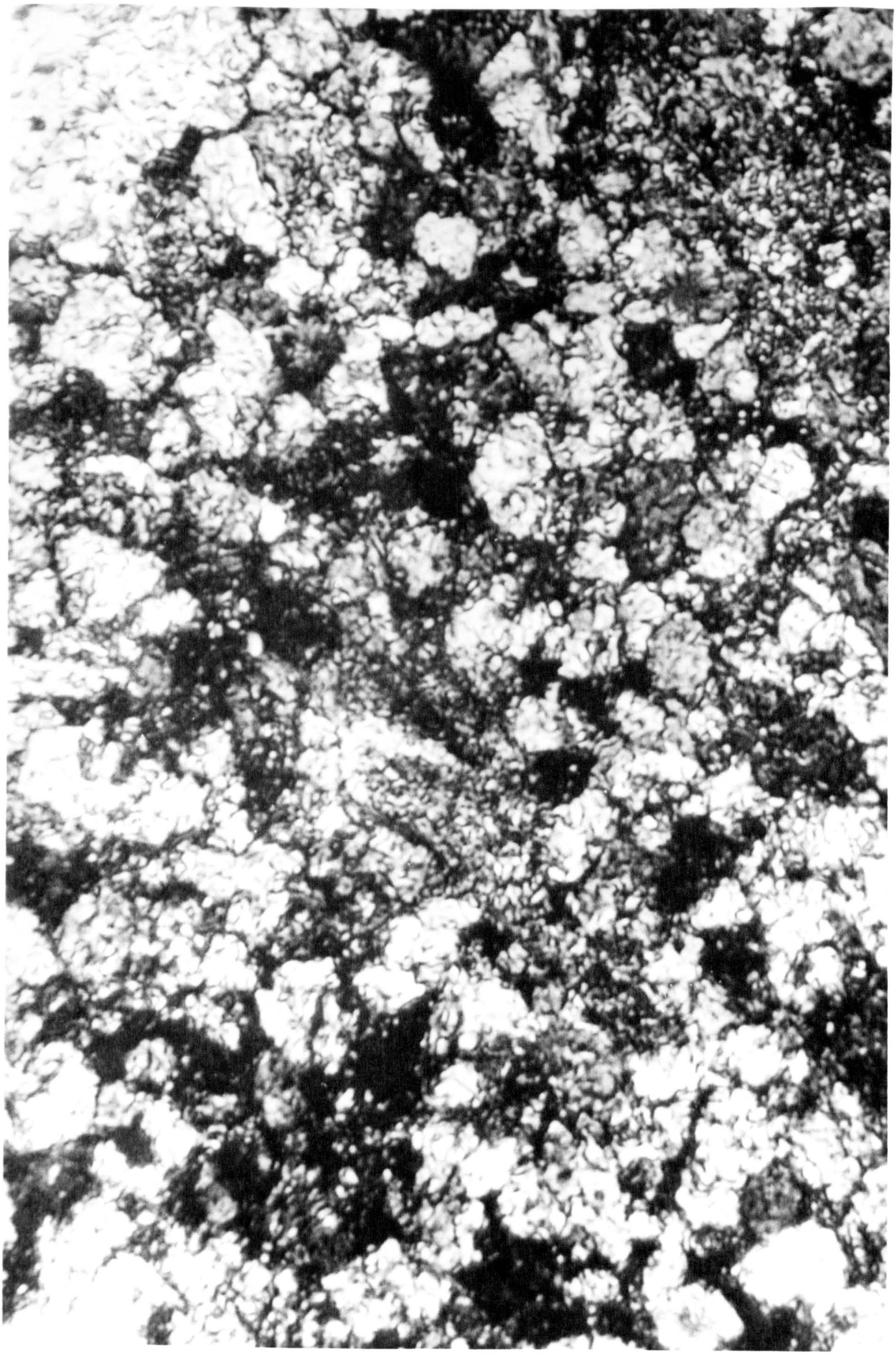

(x378) A Section of Stanhope Limestone

Figure 41/5

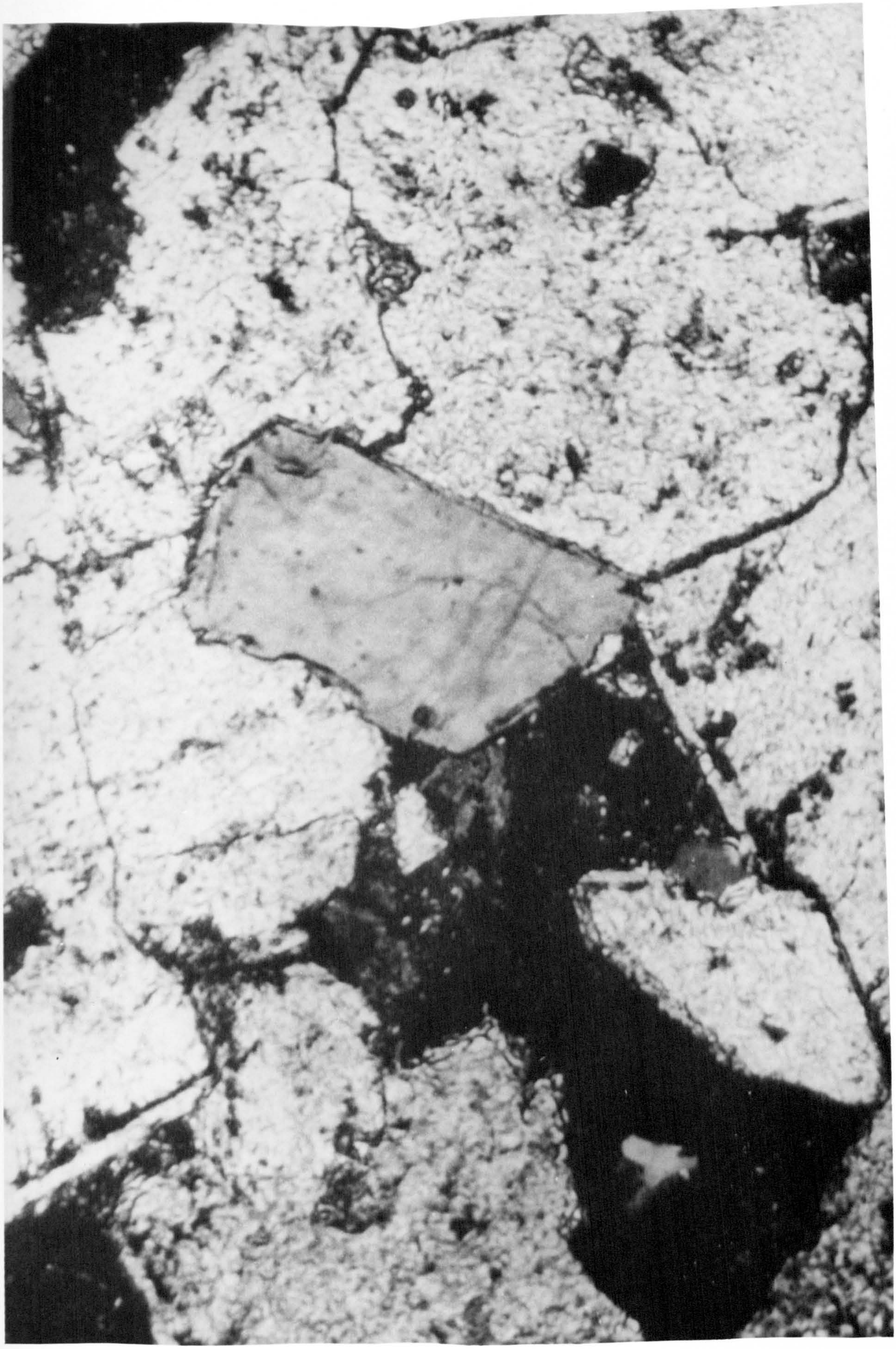

(x378) A Section of Bulwell Limestone Showing a Quartz Inclusion
Figure 41/6

(x378) A Section of Anhydrite Showing the Various Patterns Displayed by the Minerals

Figure 41/7

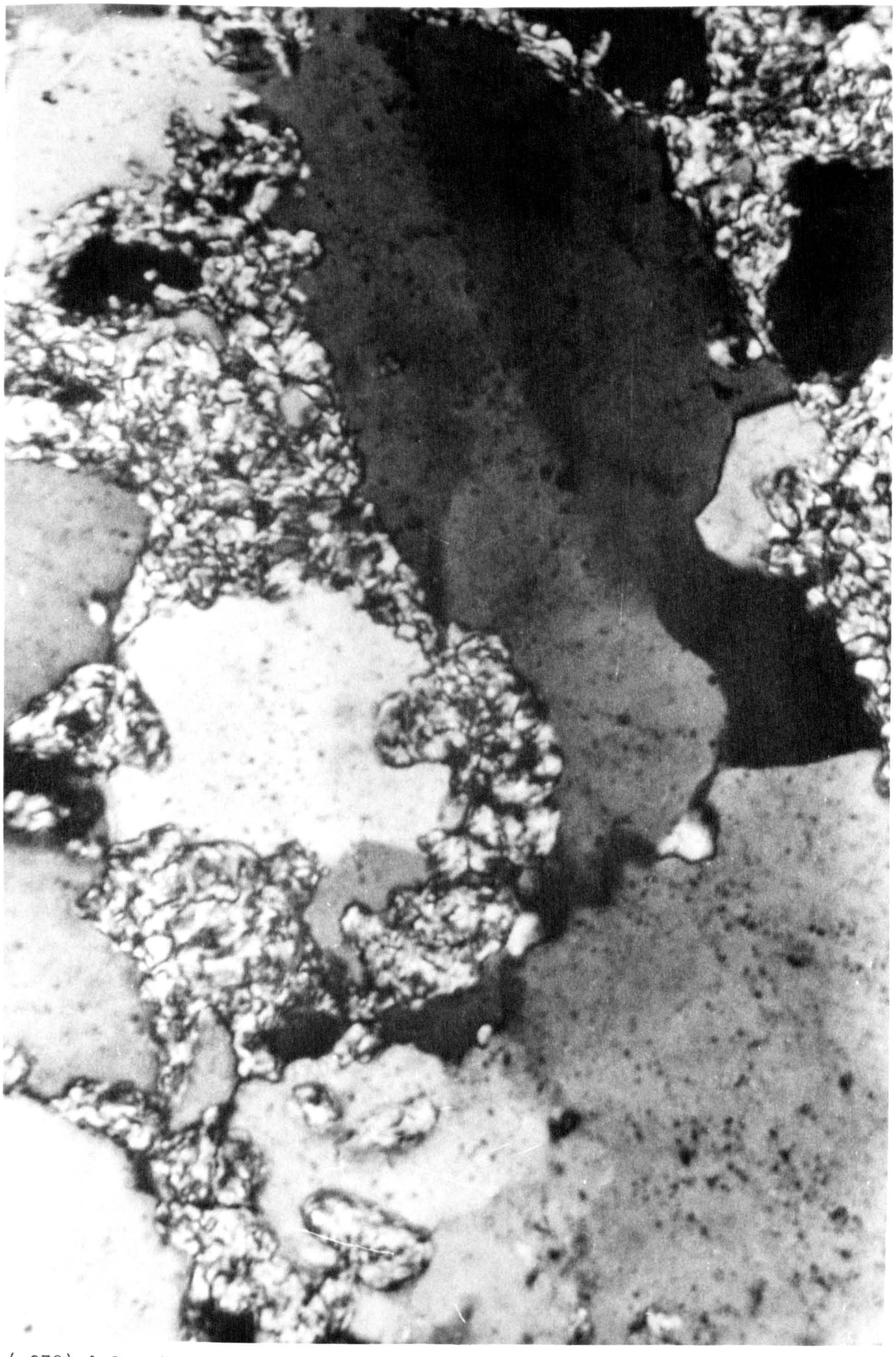

(x378) A Section of Stilfontein Quartzite Showing Quartz Grains in Micaceous Matrix (x nicols)

Figure 41/8

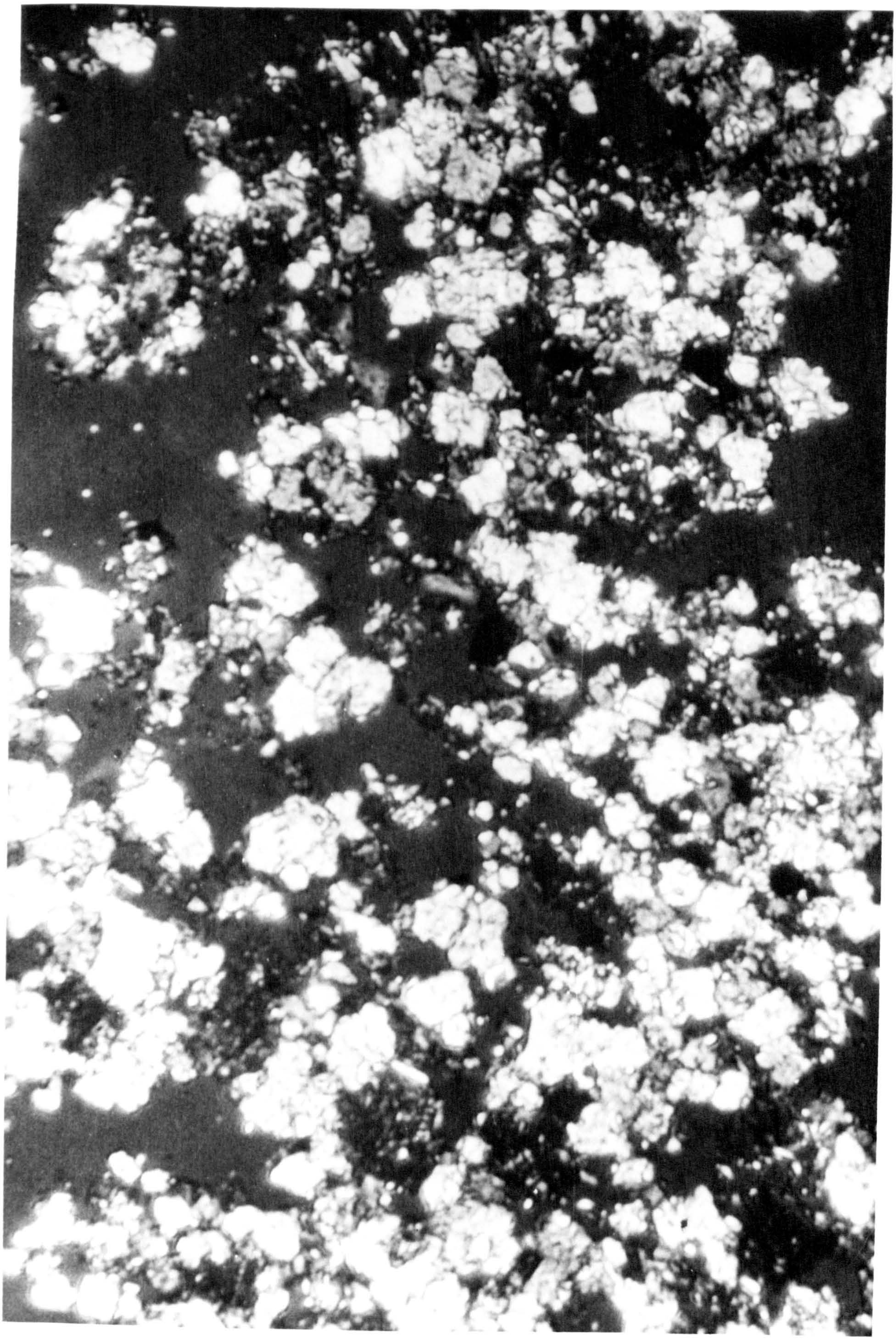

(x378) A Section of Aust Mudstone Showing High Porosity

Figure 41/9

Table 6 Density and Porosity

Rock type	Density (Mg/m^3)		Porosity (Per cent)	
	Bulk	grain	Apparent	True
Scotswood sandstone	2.19	2.59	15.60	15.80
Bunter sandstone	2.10	2.58	10.93	17.10
Springwell sandstone	2.21	2.64	15.00	14.60
Dunhouse sandstone	2.23	2.60	13.60	14.20
Post sandstone	2,48	2,60	1.20	16.50
Lazenby sandstone	2,26	2.61	12,10	13.40
Frosterly limestone	2,70	2.71	0.10	0.23
Stanhope limestone	2.76			
Hinkley point limestone	2.63	2.70	0.20	2.51
Whinstone	2.89	2.91	0.15	2.47
Creetown granite (white)	2.65	2.67	0.02	0.75
Creetown granite (blue)	2.65	2.67	0.20	0.89
Anhydrite	2.91	2.92	0.20	0.48
Gypsum	2.26	2.33	0.00	3.05
Stilfontein quartzite	2.70	2.73	0.30	1.00
Auriferous quartzite	2.67	2.69	0.30	0.53
Scottish quartzite	2.63	2.66	0.42	0.98
Rocksalt	2.19	2.42	soluble	
Lower chalk	1.88	2.46	23.00	24.10
Honister slate	2.74	2.77	0.05	0.77
Aust mudstone	2.66			
Shale	2.83		3.70	

6.3 Uniaxial compressive strength

Rocks are classified into 5 classes according to their uniaxial compressive strength obtained under the standard procedure as :

1. very high	220 <	MN/m^2
2. high	110 — 220	MN/m^2
3. medium	55 — 110	MN/m^2
4. low	28 — 55	MN/m^2
5. very low	< 28	MN/m^2

Therefore rocks tested in this work can be classified according to their compressive strength as in Table 7.

The compressive strength of the typical types of rocks obtained in the work are as follows:

sandstone	40.48 - 119.96	MN/m^2
limestone	116.60 - 172.74	MN/m^2
granite	174.75 - 262.00	MN/m^2
quartzite	141.20 - 218.16	MN/m^2
chalk	35.45 -	MN/m^2
slate	135.00	MN/m^2
shale	92.07	MN/m^2
mudstone	75.84	MN/m^2

Table 7 Rocks Classification

Rock type	Class of strength	Mean MN/m^2	S.D. MN/m^2	Number of observations
Whinstone	very high	318.90	9.44	9
Creetown granite (blue)		262.00	15.16	8
Post	sandstone	119.96	21.84	5
Frosterly	limestone	172.74	15.67	8
Stanhope	limestone	169.65	21.97	5
Hinkley Point	limestone	116.60	19.73	5
Creetown granite (white)		174.75	10.66	8
Anhydrite		112.94	7.16	6
Stilfontein	quartzite	141.20	20.51	6
Auriferous	quartzite	164.16	15.14	5
Scottish	quartzite	218.16	27.58	5
Honister	slate	135.00	11.20	6
Dunhouse	sandstone	72.53	5.68	6
Hunterston	sandstone	67.29	1.62	5
Aust	mudstone	75.84		1
Shale		92.07		1
Scotswood	sandstone	45.77	3.02	6
Bunter	sandstone	40.48	4.27	5
Springwell	sandstone	50.61	5.35	6
Lazenby	sandstone	54.51	2.03	8
Gypsum		45.02	6.23	10
Lower	chalk	35.45	0.73	7
Rocksalt	very low	27.57		

6.4 Tensile strength

Six medium strength and one high strength rocks were direct pull tested. Higher strength rocks could not be tested by this method since the cold setting adhesive joining the metal caps and the rock specimen failed before the test was accomplished .

The rocks tested were placed vertically and loaded axially in tension in a 250 KN Avery machine. The test was repeated 5 successive times after recementing the fracture and the tensile strength gradually increased as shown in Table 8, and were plotted in Figure 42.

However this method of testing was discarded from the test matrix since it was a time consuming one.

Indirect "disc" tensile strength test was carried out under the standard procedure, as described in section 5.2.4.b, on 21 rock types. All cores were drilled at right angles to the bedding planes.

Results obtained were listed in Table 9.

Table 8. "Direct" Tensile Strength of Rocks

Rock type		Tensile strength (MN/m^2)				
		Test Number				
		1	2	3	4	5
Dunhouse	sandstone	1.78	1.58	1.76	1.91	2.18
Bunter	sandstone	0.31	0.39	0.44	0.46	0.66
Scotswood	sandstone	1.74	1.75	1.91	1.98	2.09
Springwell	sandstone	3.23	3.06	3.08	3.14	3.15
Shale		1.41	1.67	1.96	2.08	2.16
Gypsum		1.67	1.82	2.12	2.16	2.24
Anhydrite		4.80	4.79	5.63	5.77	6.46

Table 9 "Indirect" Tensile Strength of Rocks

Rock type		Mean tensile strength MN/m^2	Standard deviation	Number of observations
Scotswood	sandstone	1.69	0.28	8
Bunter	sandstone	1.78	0.43	9
Springwell	sandstone	10.40	0.95	12
Dunhouse	sandstone	3.84	0.35	11
Post	sandstone	7.72	1.46	7
Lazenby	sandstone	3.03	0.27	5
Frosterly	limestone	10.14	1.37	9
Stanhope	limestone	9.19	2.18	5
Hinkley Point	limestone	9.45	2.17	9
Whinstone		21.65	0.95	8
Creetown granite	(white)	14.68	1.91	10
Creetown granite	(blue)	10.56	0.82	10
Anhydrite		5.47	0.99	9
Gypsum		2.75	0.47	9
Stilfontein	quartzite	13.88	1.23	4
Auriferous	quartzite	13.27	3.09	10
Scottish	quartzite	16.23	3.22	5
Rocksalt		1.42	0.31	18
Lower	chalk	1.58	0.47	6
Honister	slate	8.89	1.92	5
Shale		10.14	2.97	8

Comparing the results of the indirect tensile strength and the direct tensile strength, it might be seen that the latter always gives lower strength for the corresponding rock.

6.5 Static and Dynamic Modulus of Elasticity

Sixteen rock types were strain gauged with electrical resistance gauges and subjected to cycle loading, in compression. They were loaded up to 60 per cent of their compressive strength for 3 cycles, strains at the pre-determined level of stresses were recorded and plotted. Secant modulus (Es), tangent modulus (Et), and Poisson's ratio (u) were calculated at the stress level of 50 per cent of the compressive strength of the third cycle.

Direct pull test

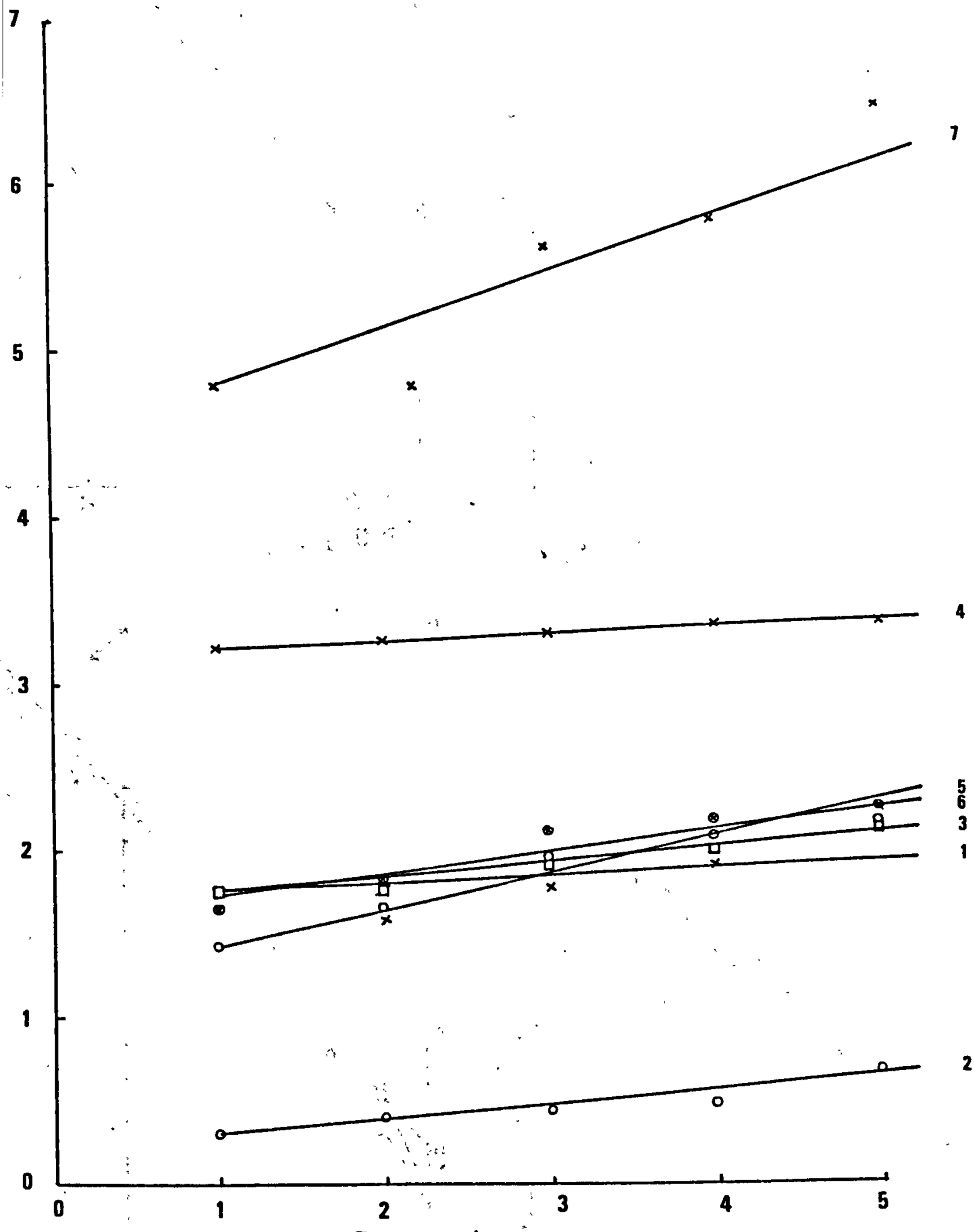

1 Dunhouse sandstone
2 Bunter sandstone
3 Scotswood sandstone
4 Springwell sandstone
5 Shale
6 Gypsum
7 Anhydrite

Figure 42

SCOTSWOOD SANDSTONE

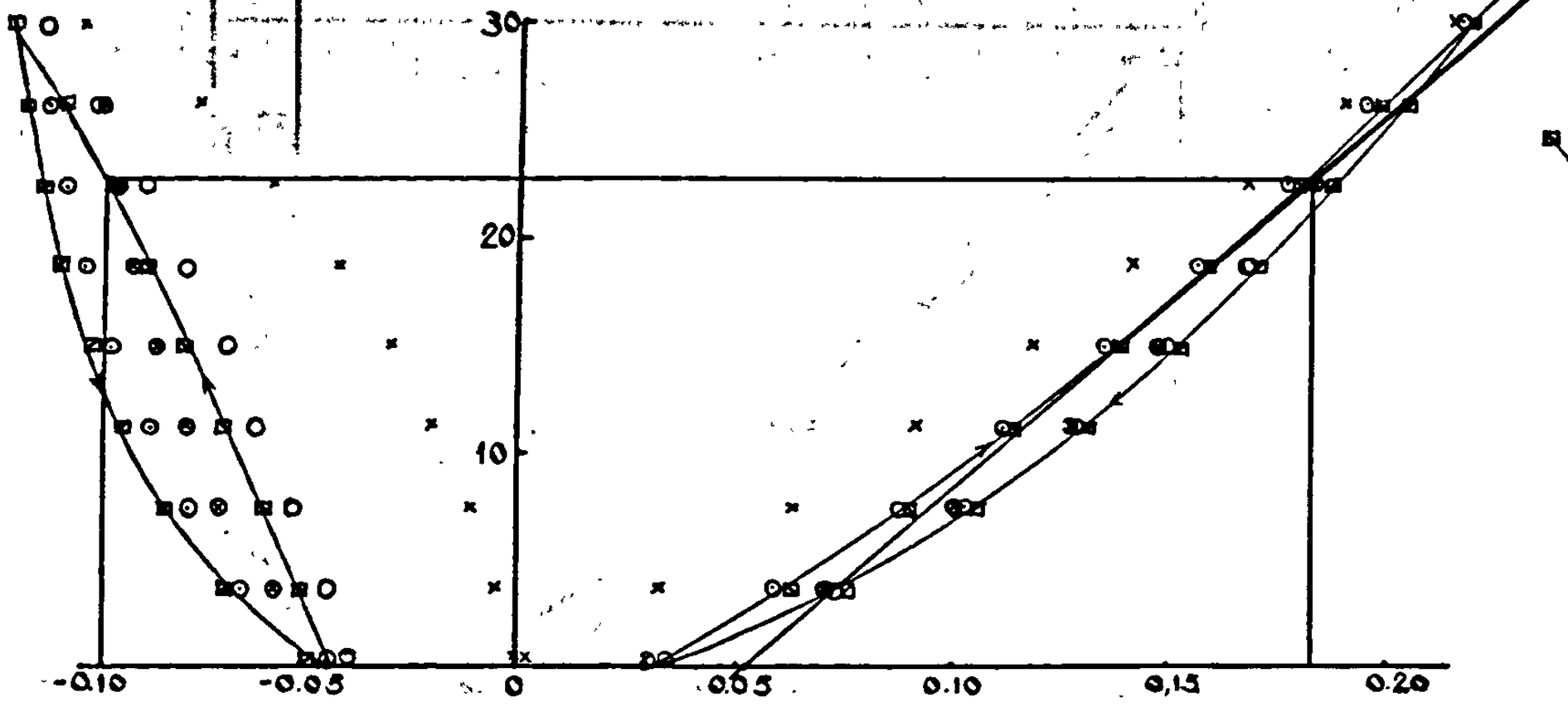

BUNTER SANDSTONE

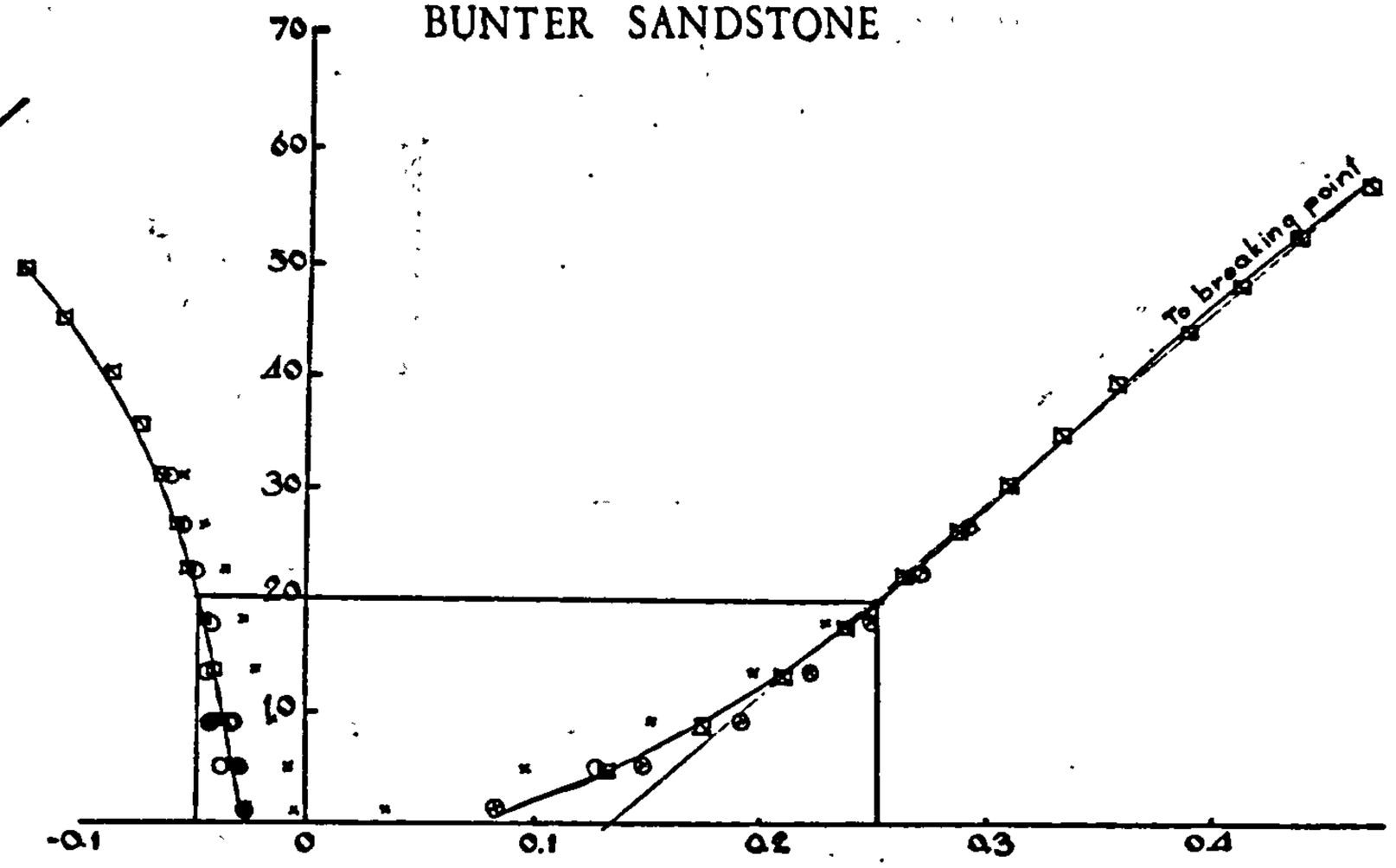

SPRINGWELL SANDSTONE

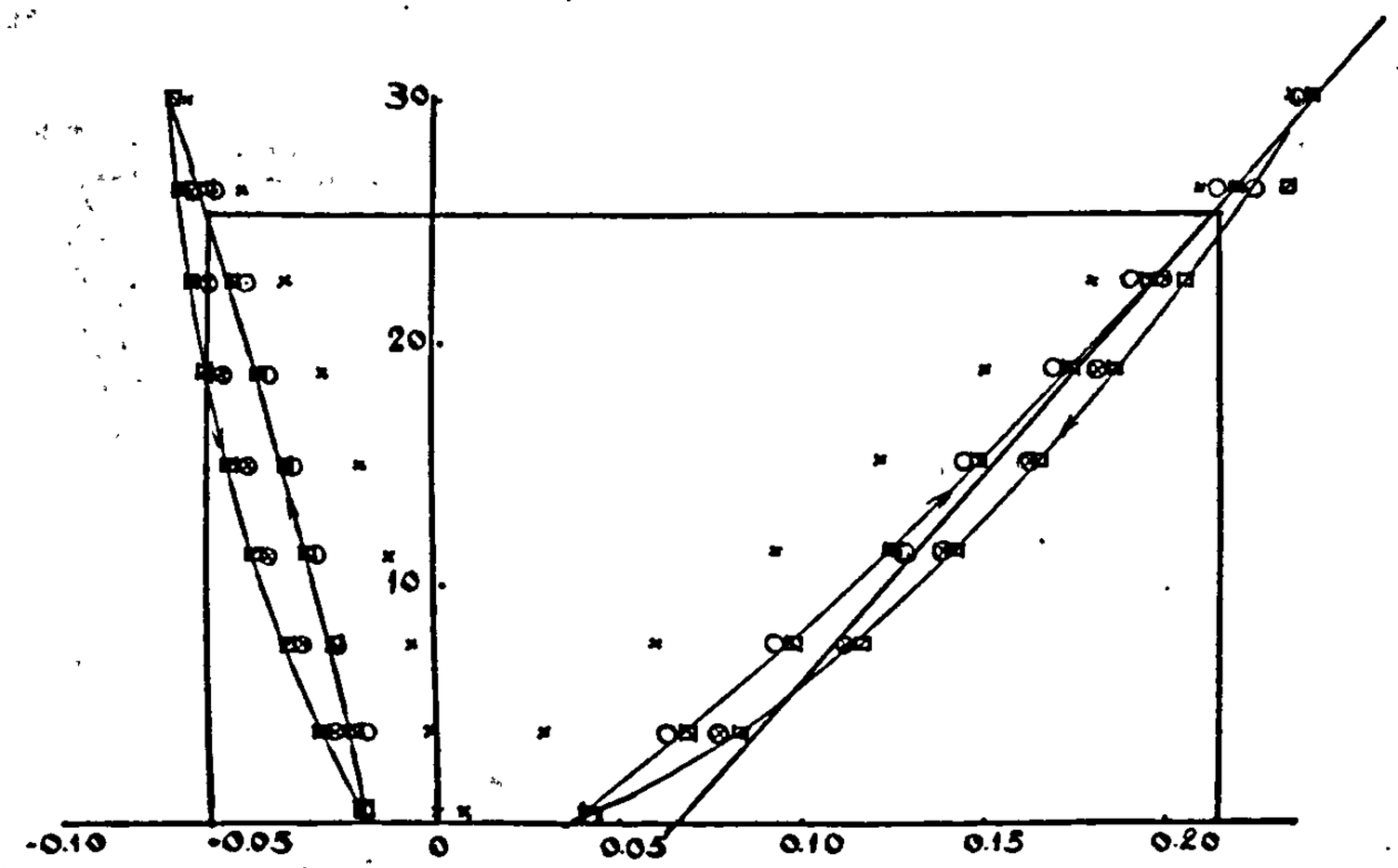

DUNHOUSE SANDSTONE

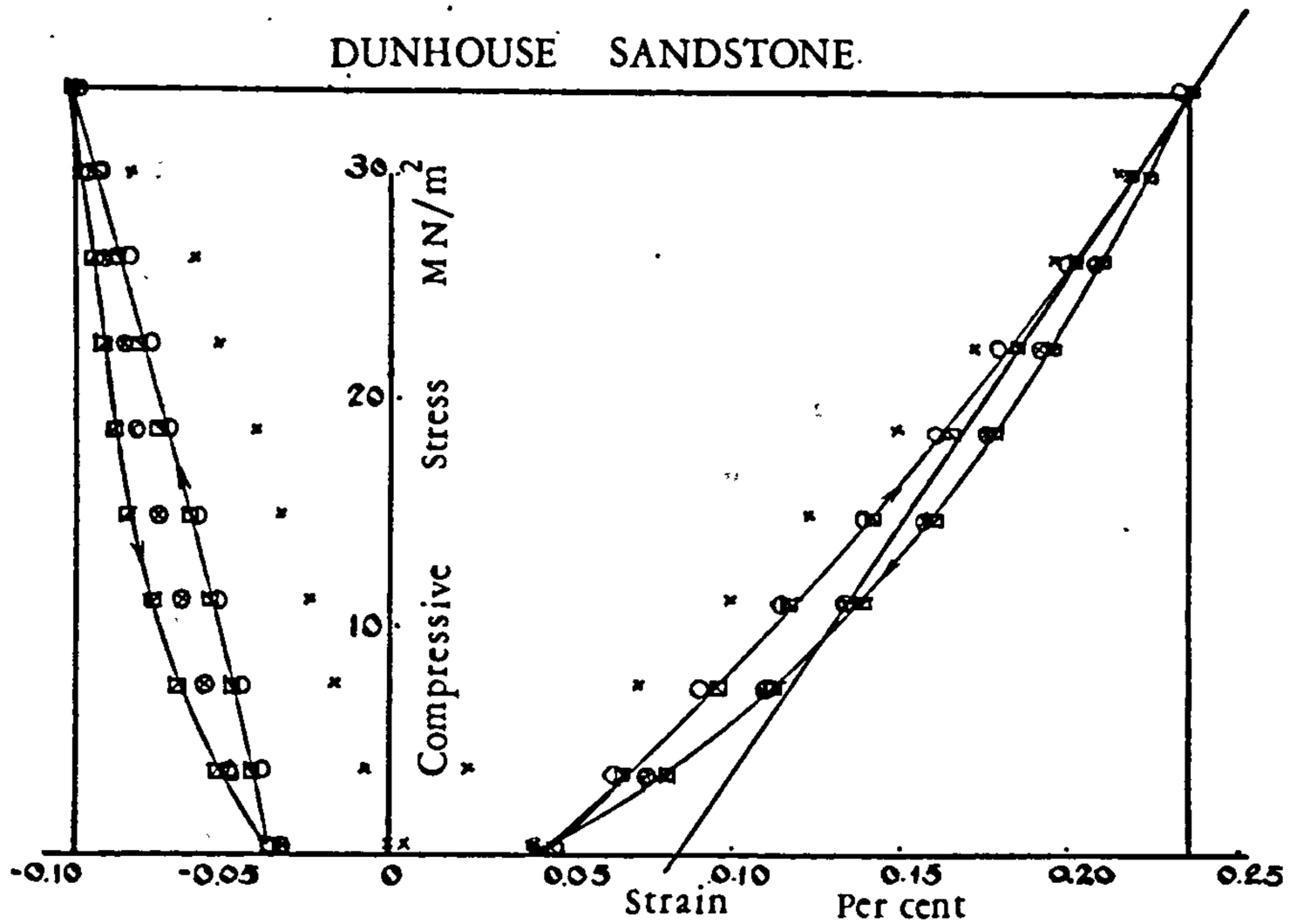

Figure 43-1

POST SANDSTONE

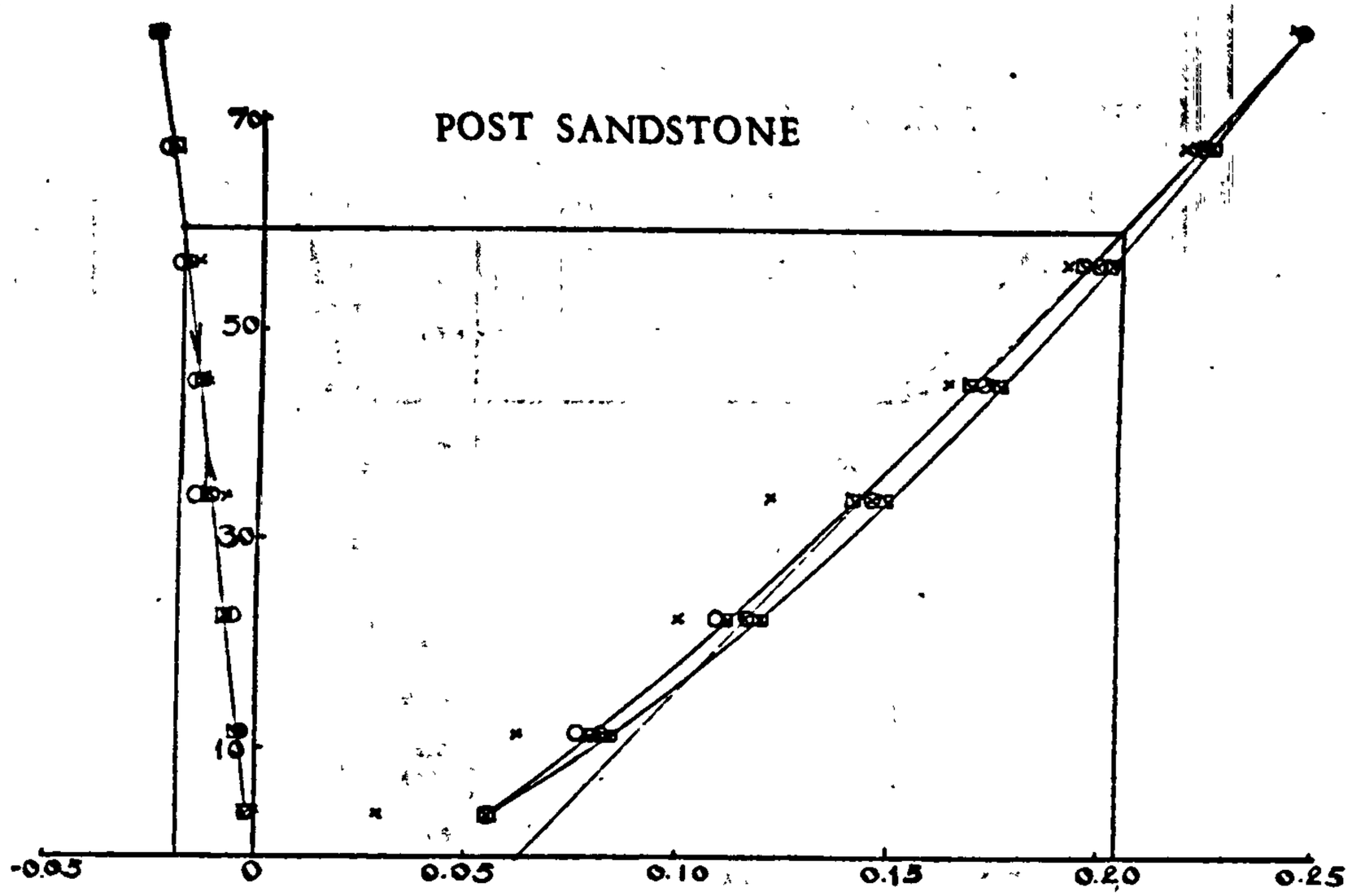

STANHOPE LIMESTONE

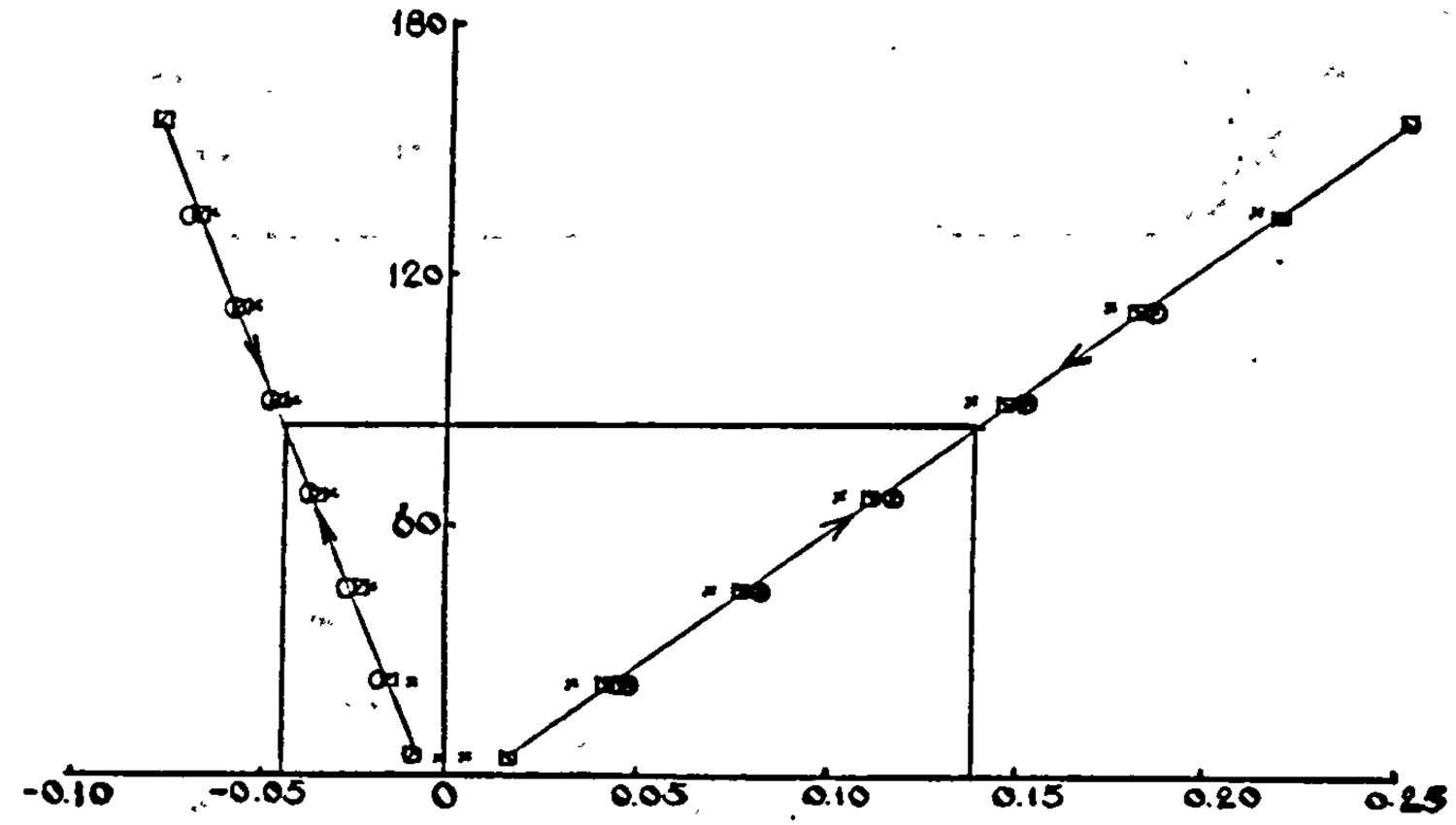

HINKLEY POINT LIMESTONE

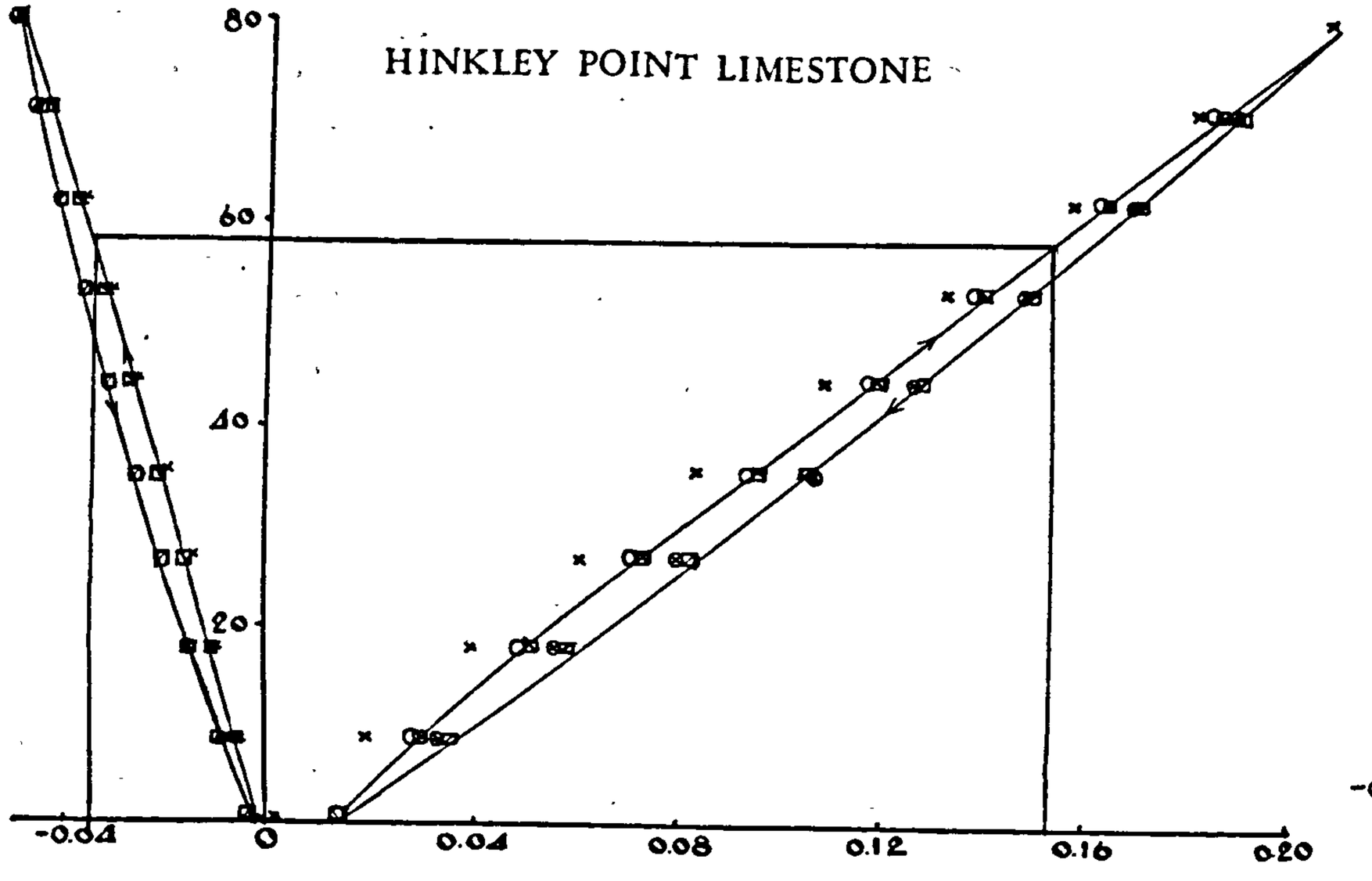

WHINSTONE

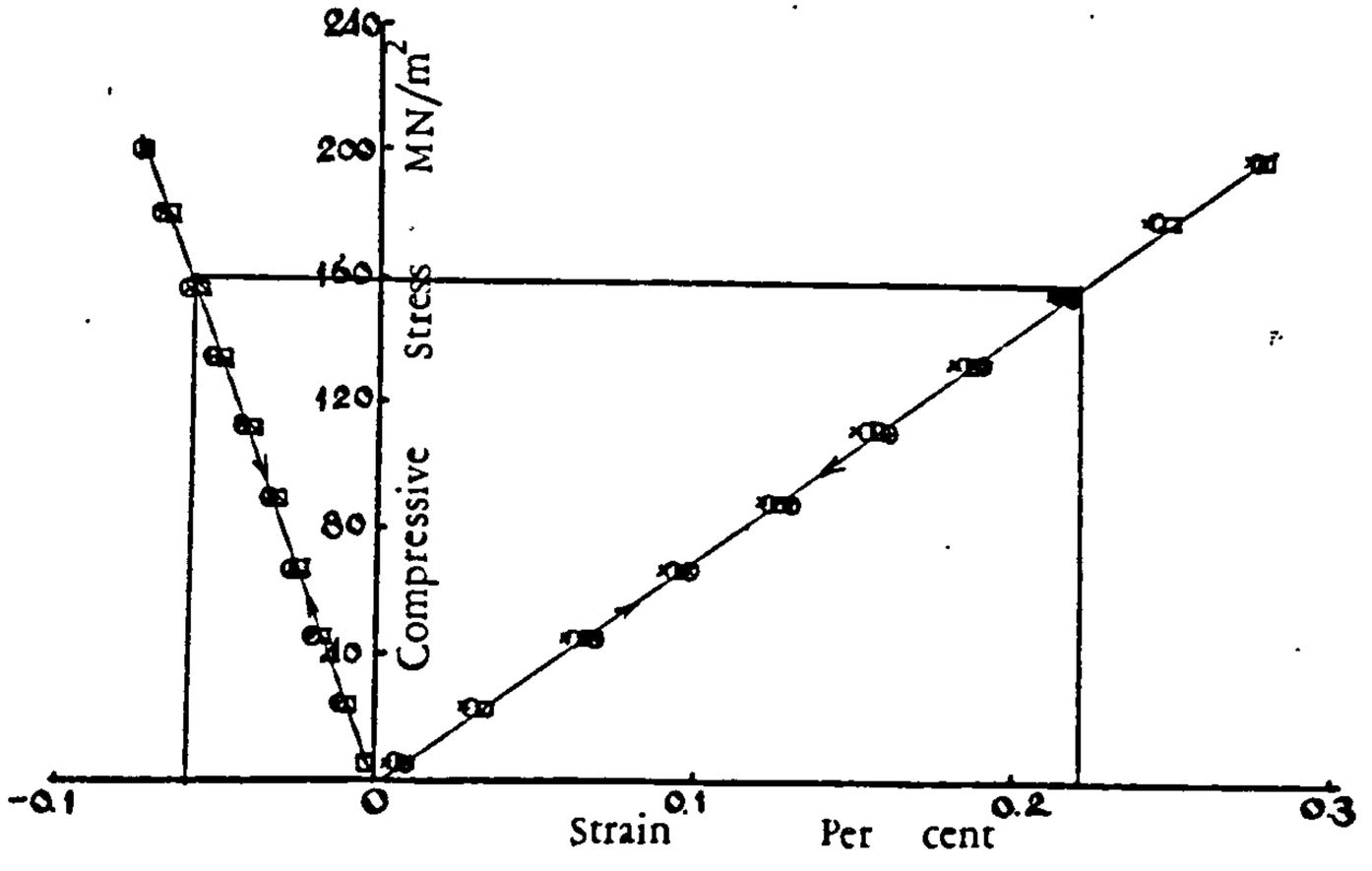

Figure 43–2

CREETOWN GRANITE (WHITE)

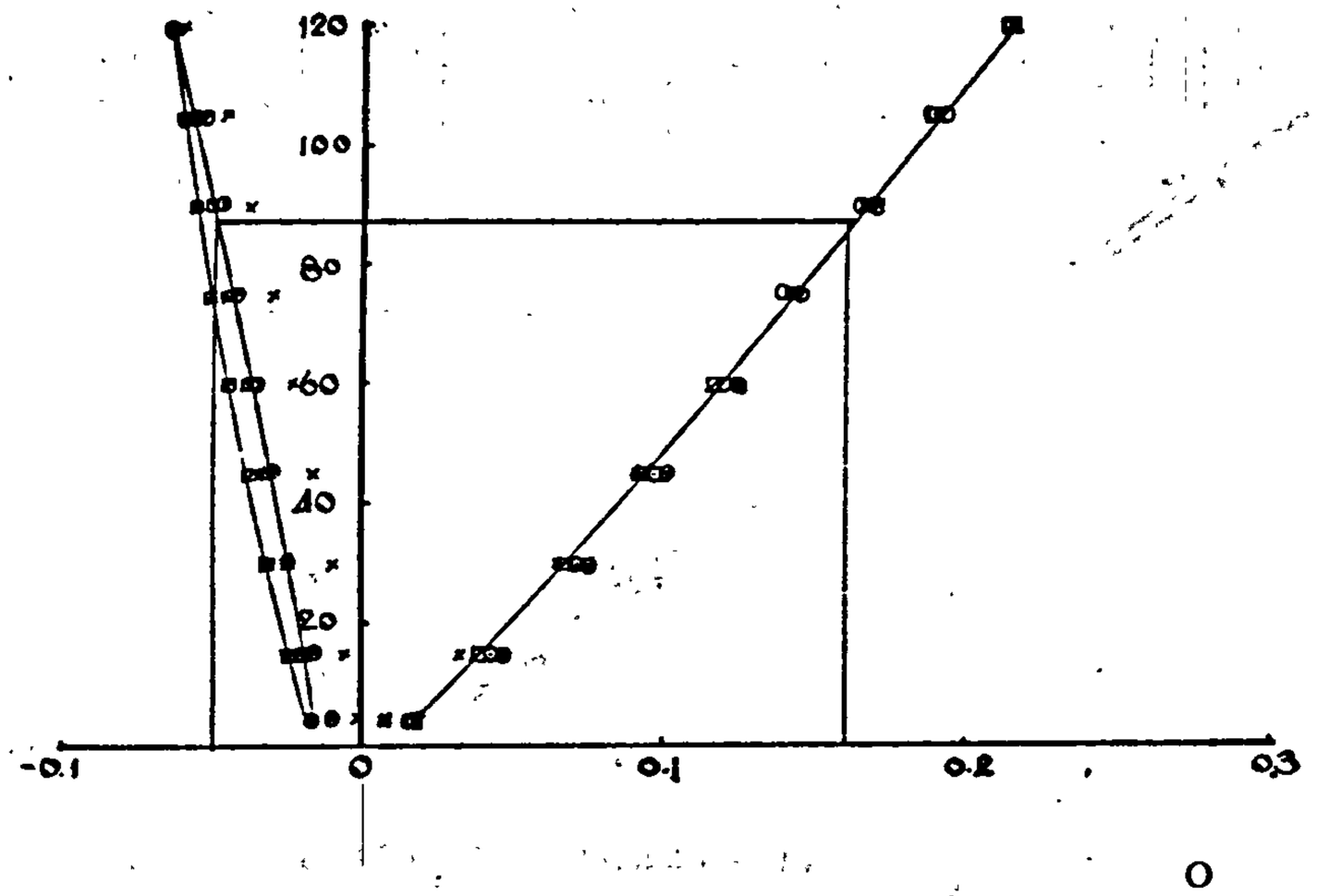

CREETOWN GRANITE (BLUE)

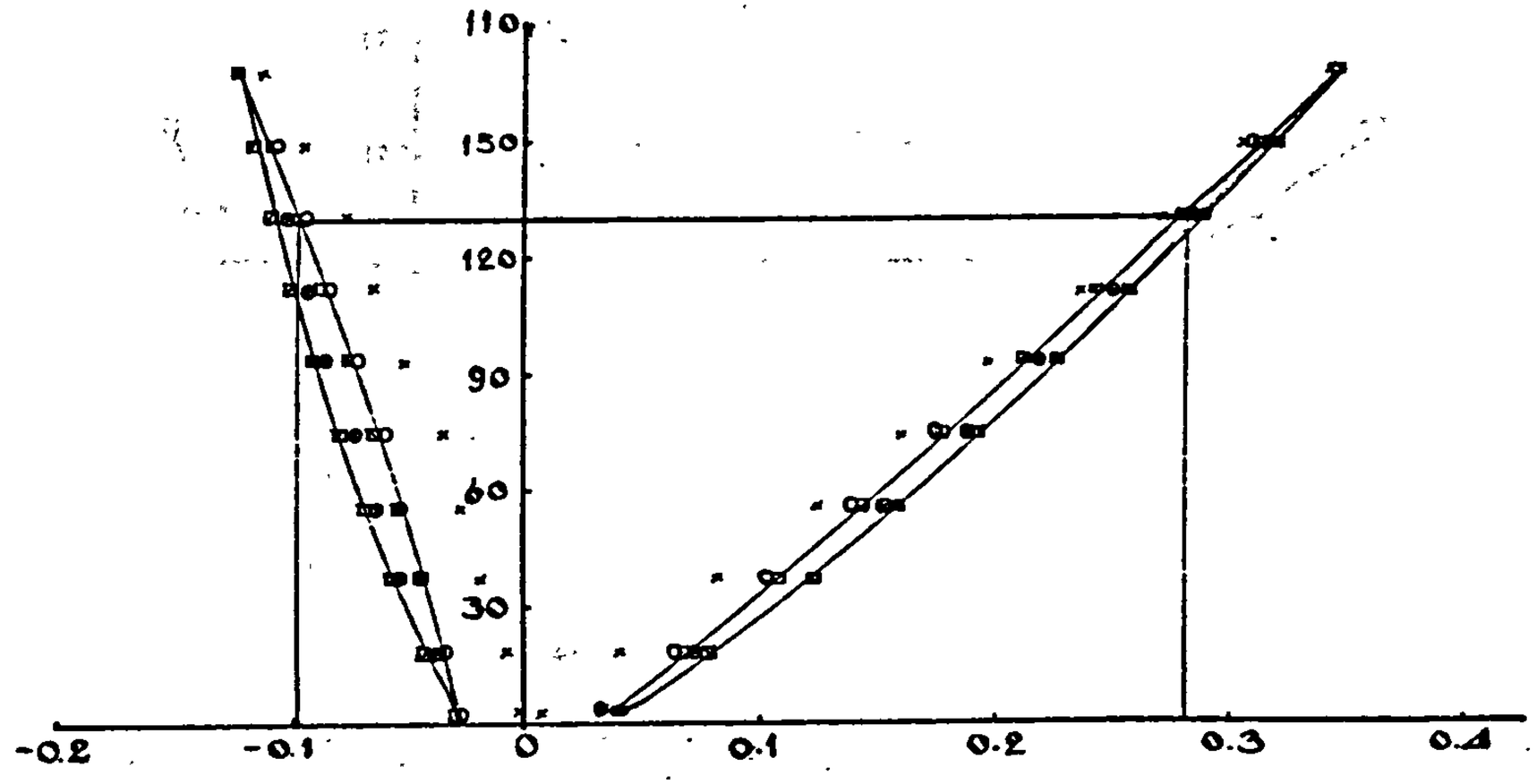

ANHYDRITE

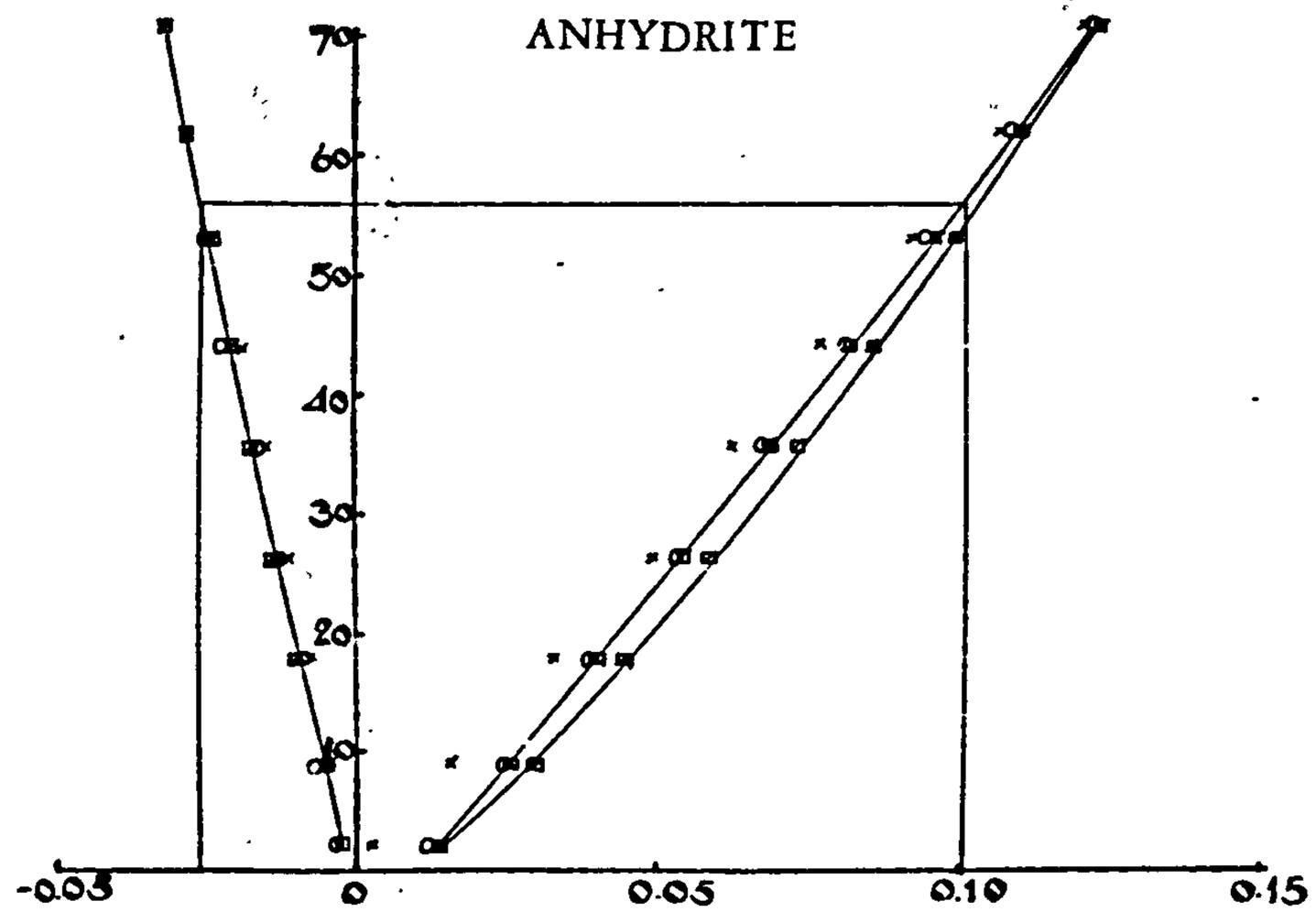

GYPSUM

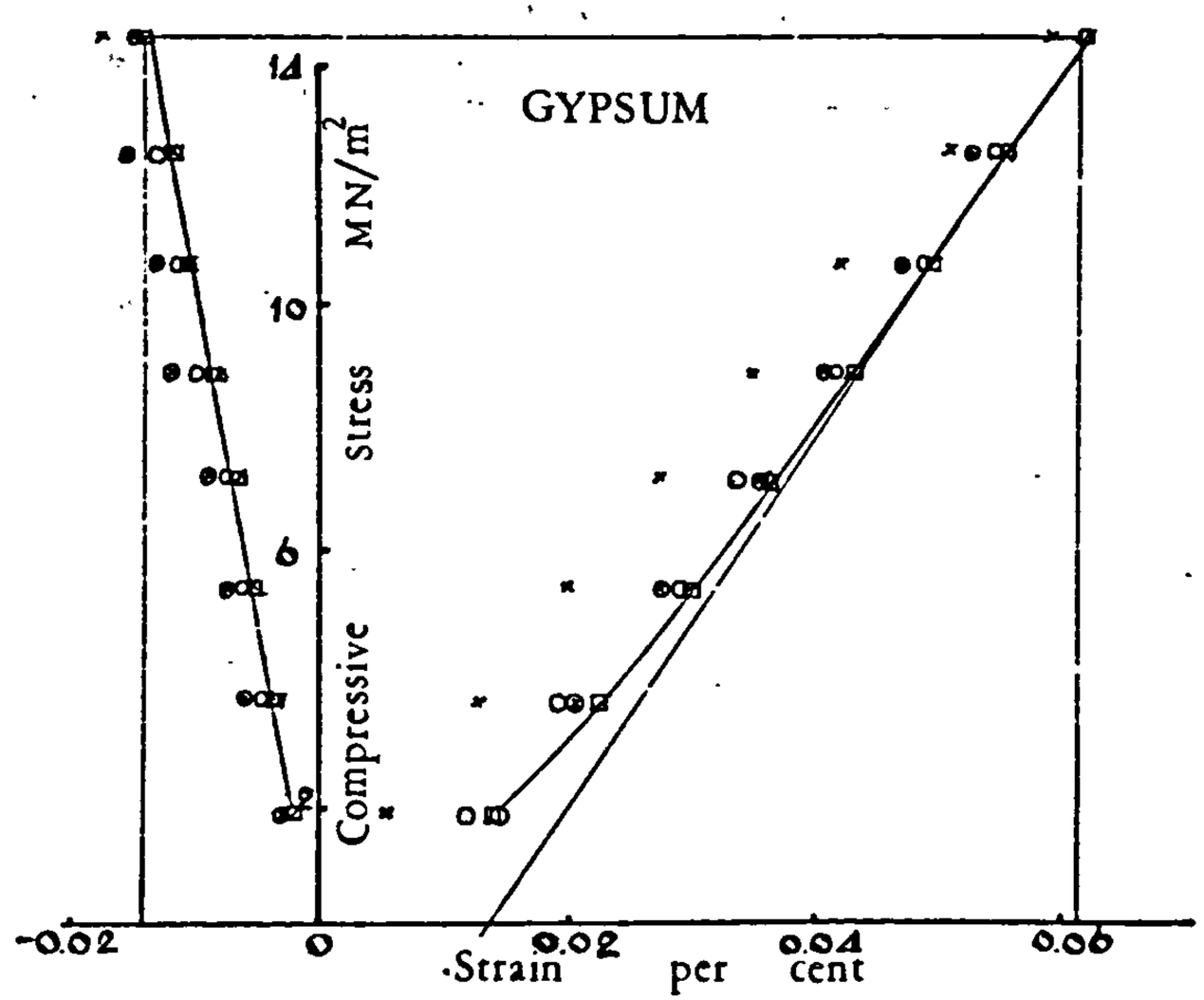

Figure 43–3

STILFONTEIN QUARTZITE

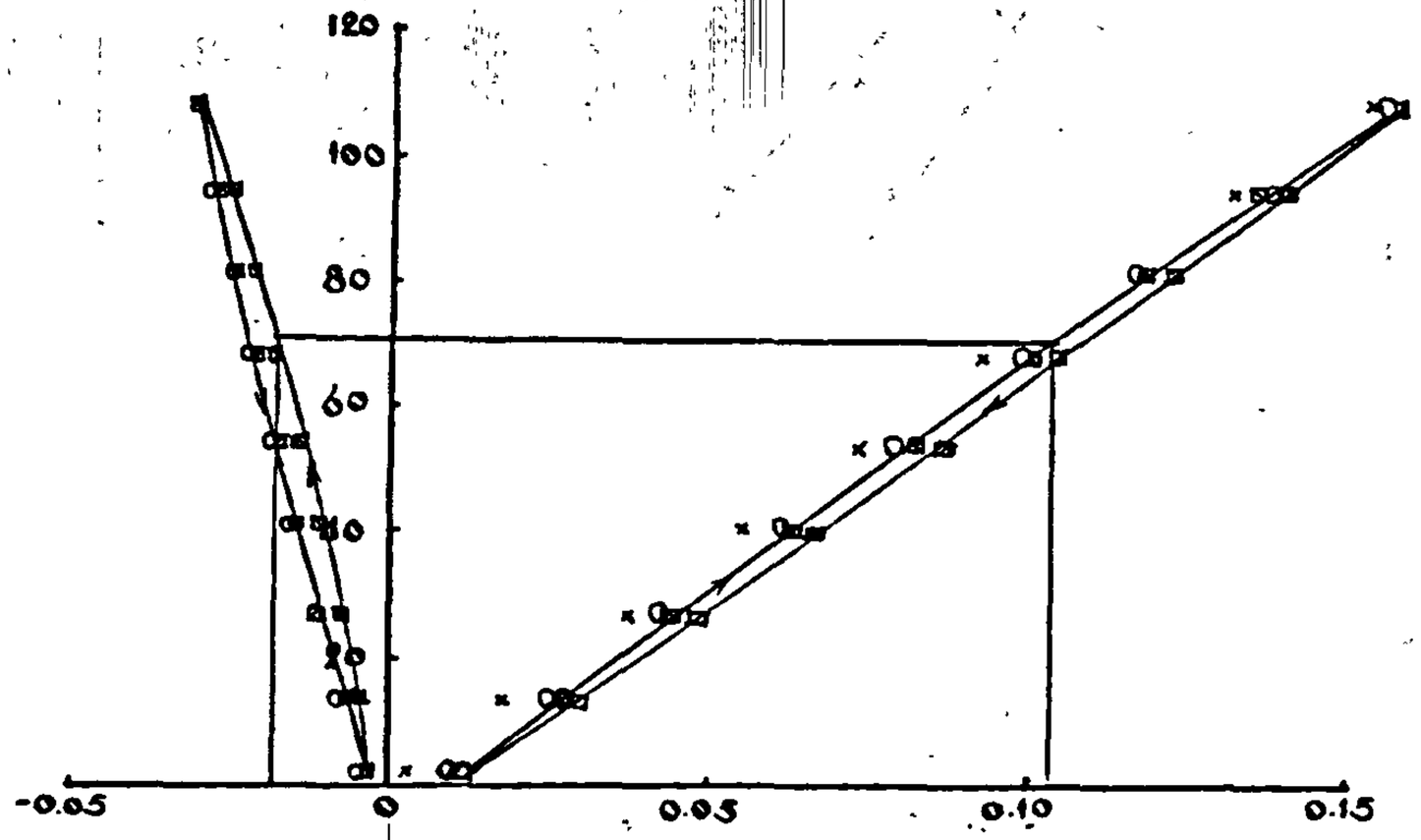

AURIFEROUS QUARTZITE

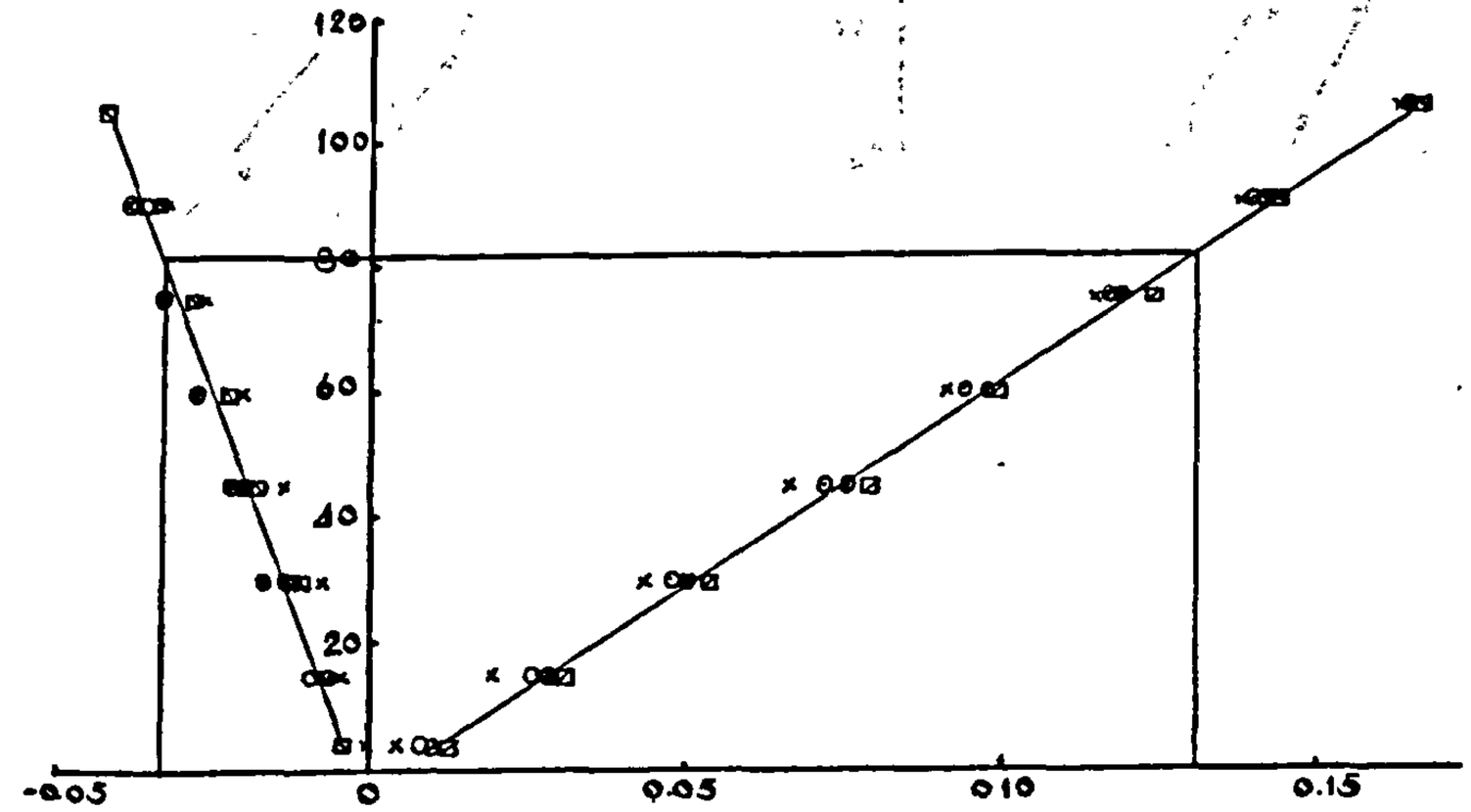

SCOTTISH QUARTZITE

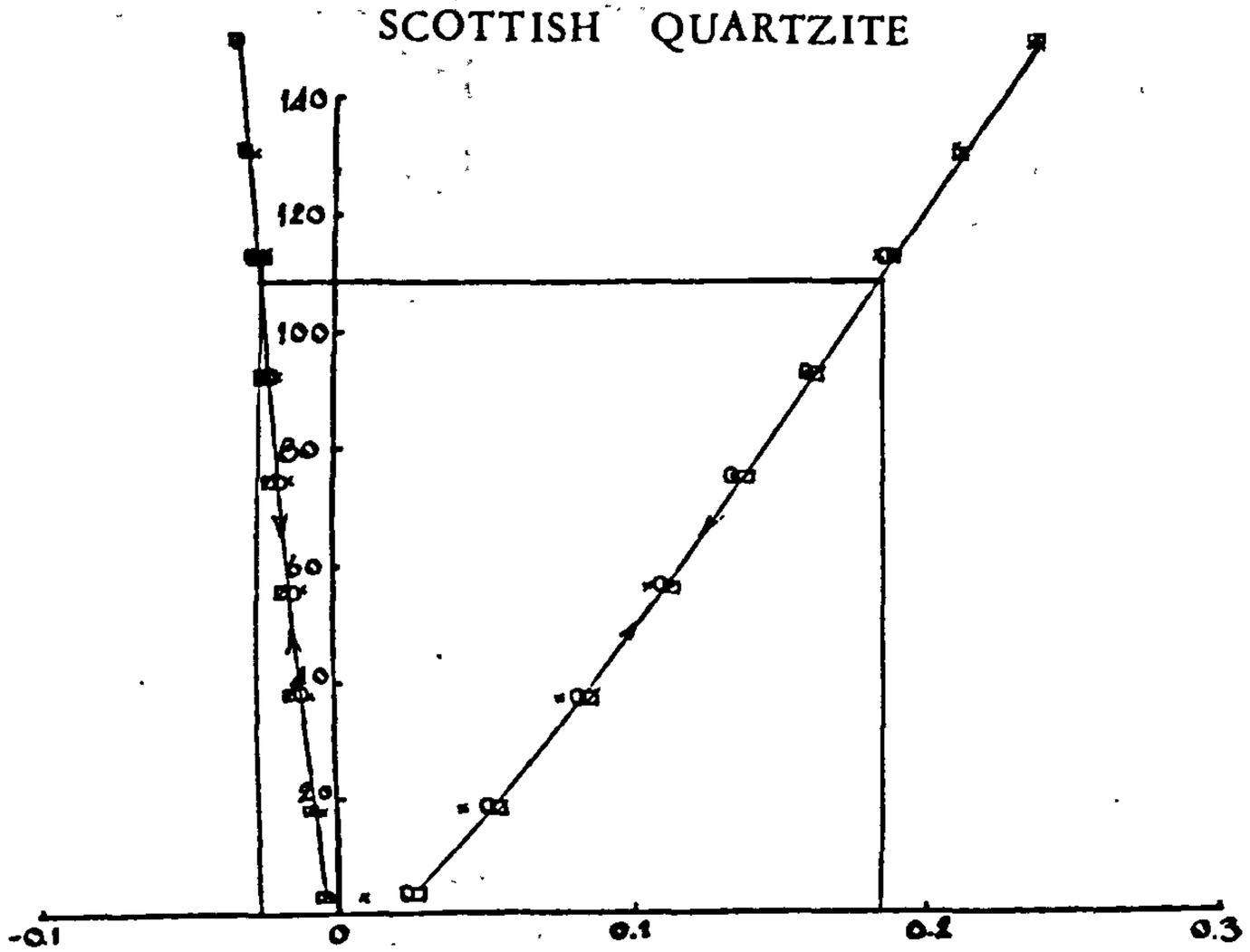

HONISTER SLATE

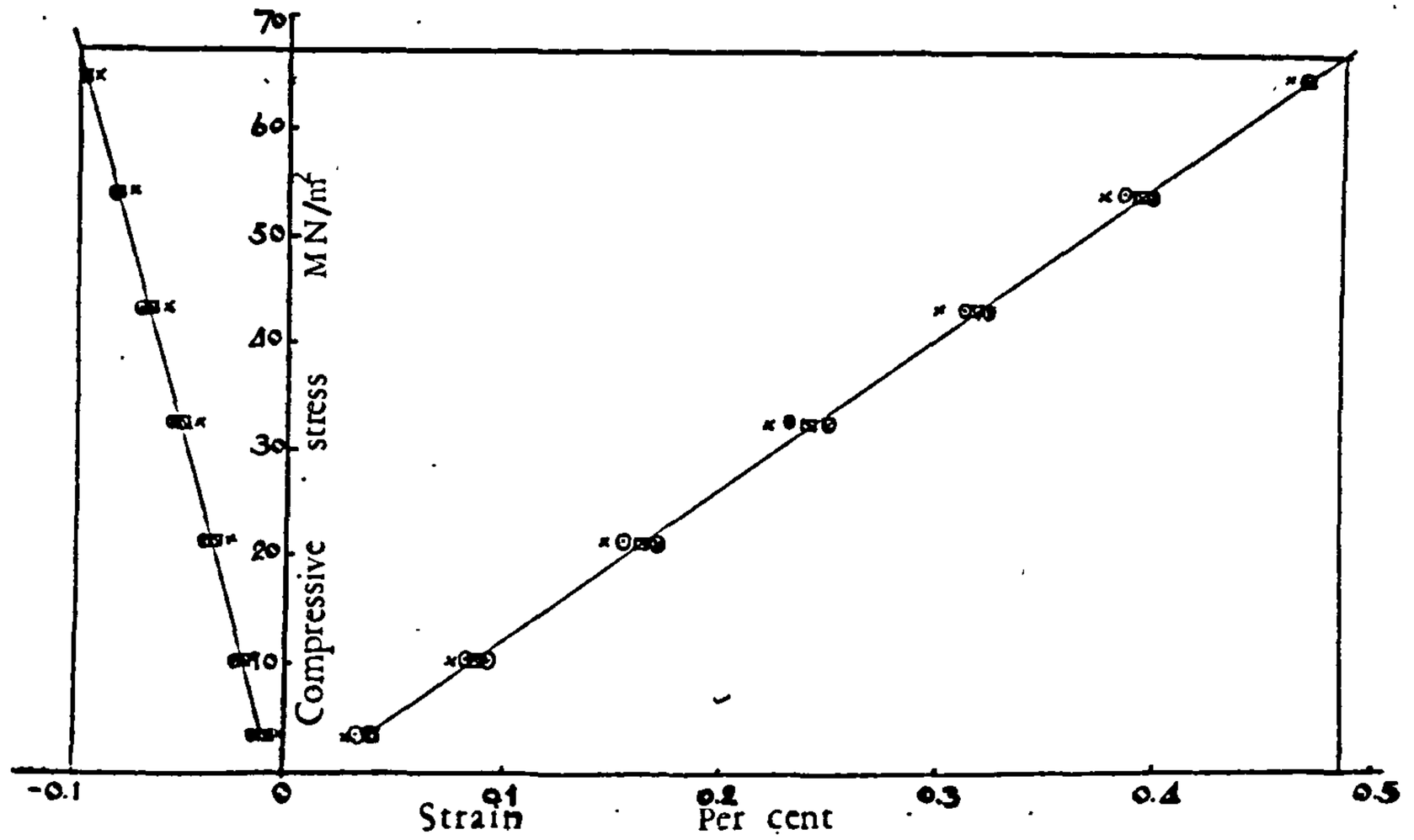

Figure 43–4

TENSILE STRESS STRAIN CURVES

TENSILE STRESS MN/m^2 x 10^{-2}

STRAIN mm/mm x 10^{-6}

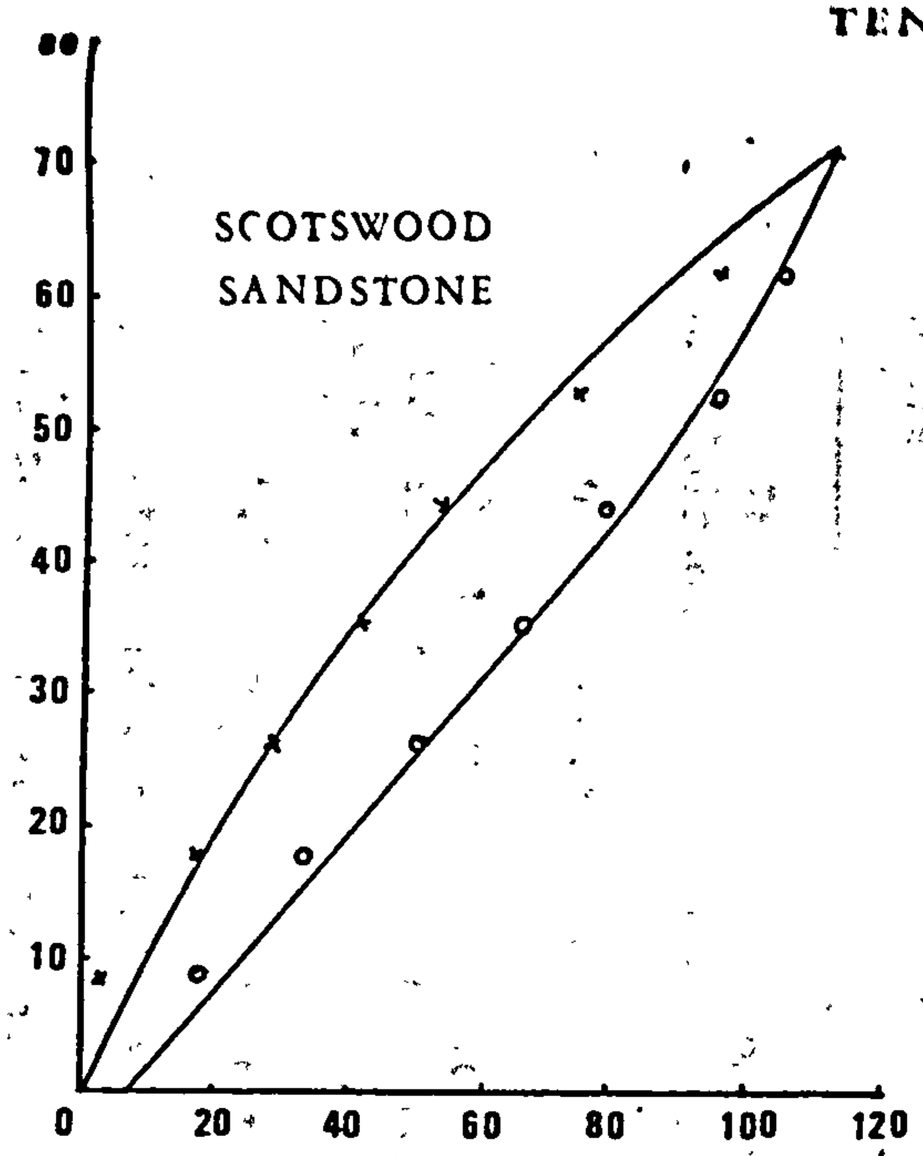

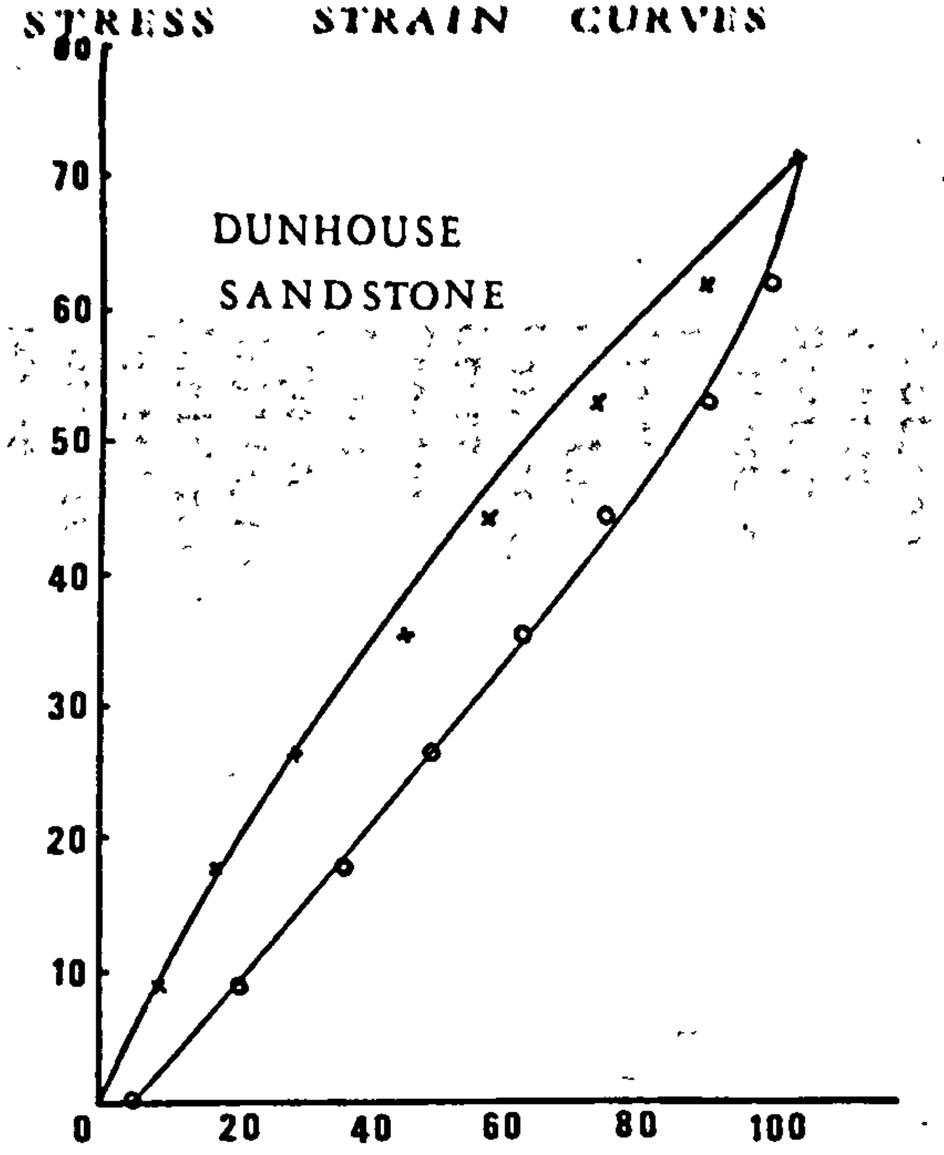

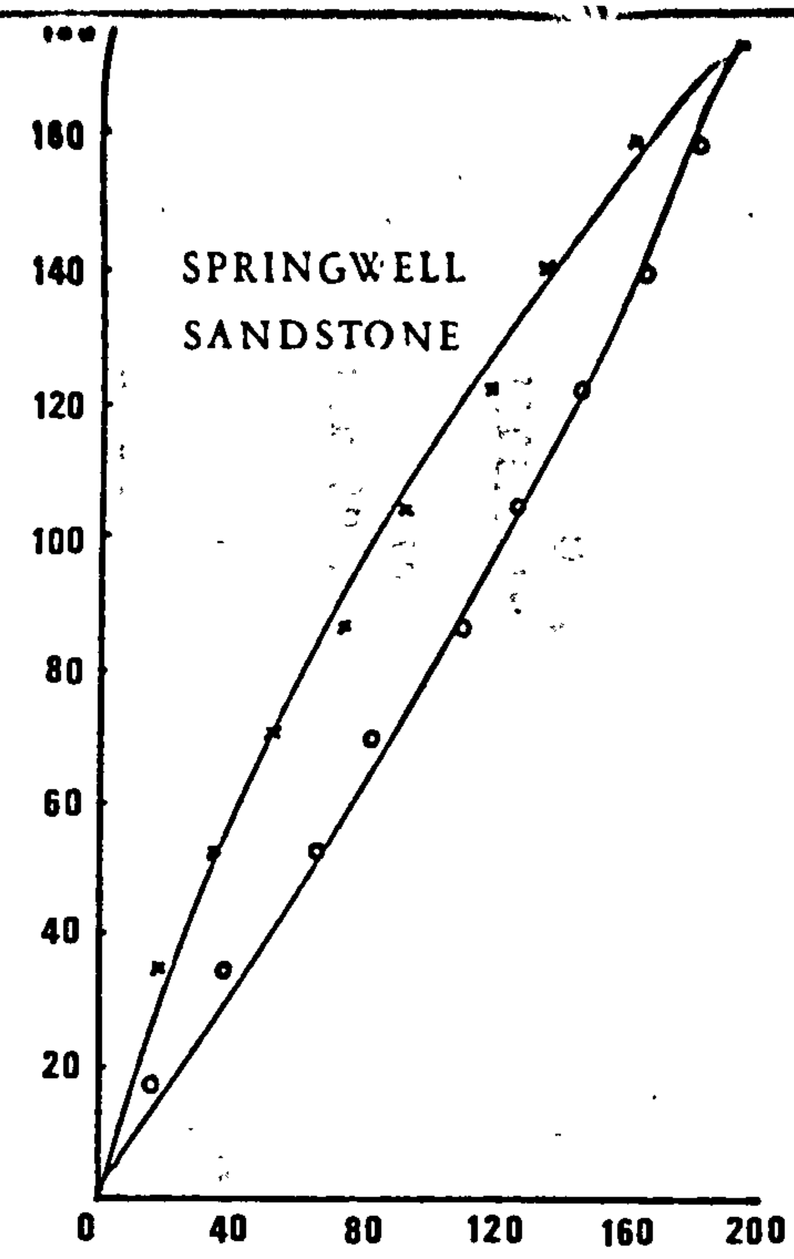

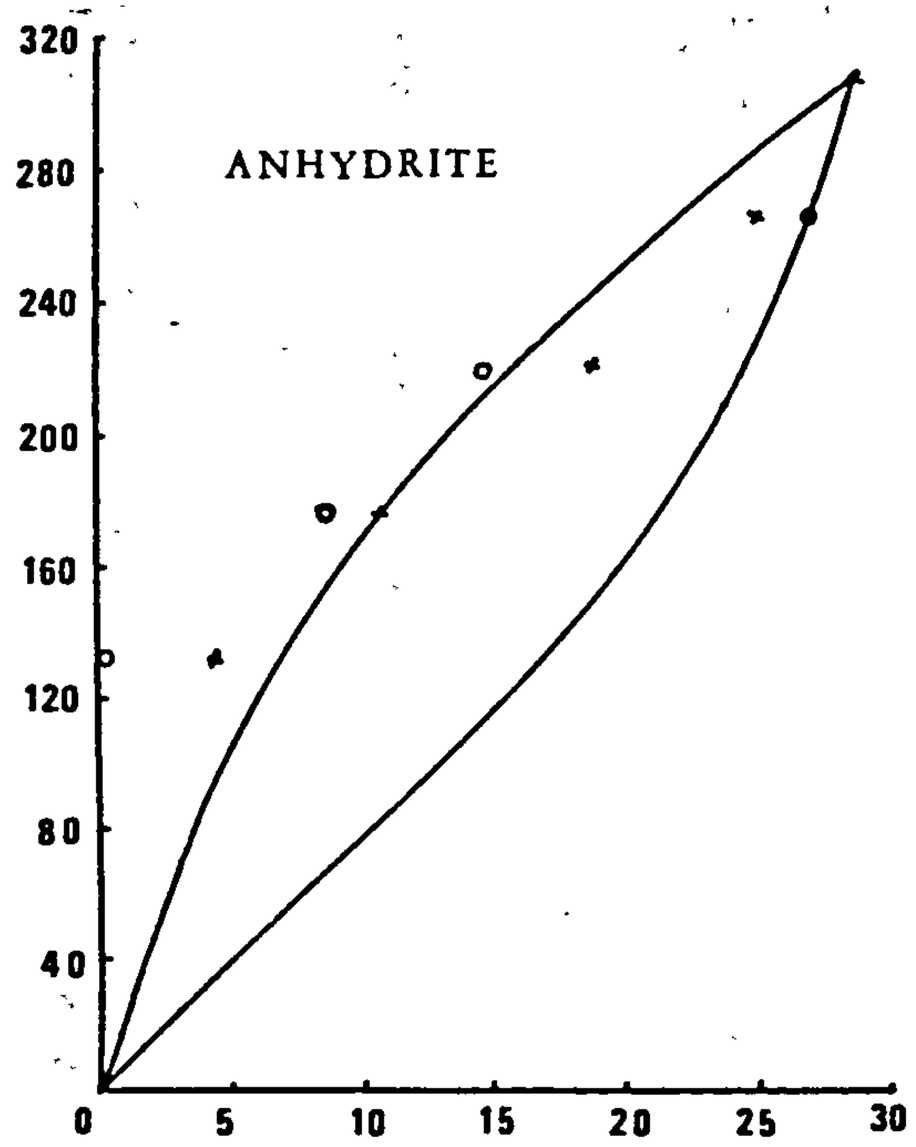

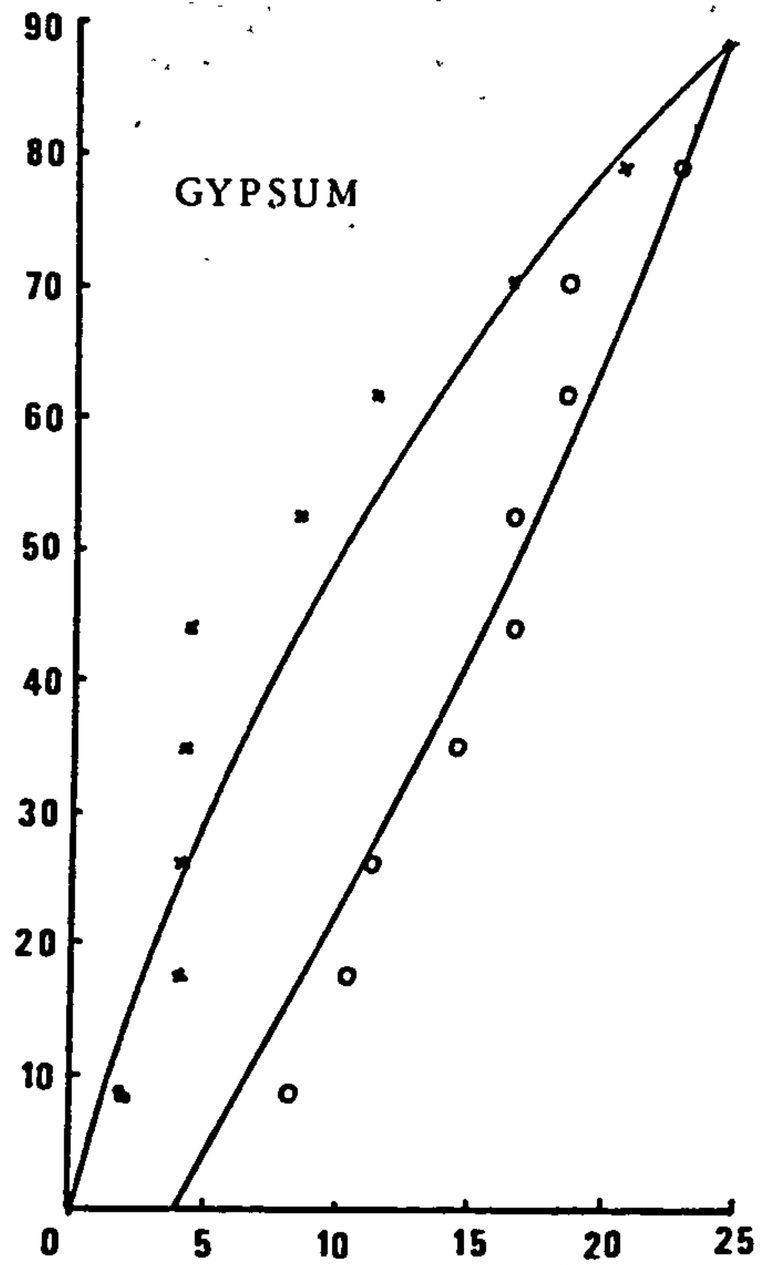

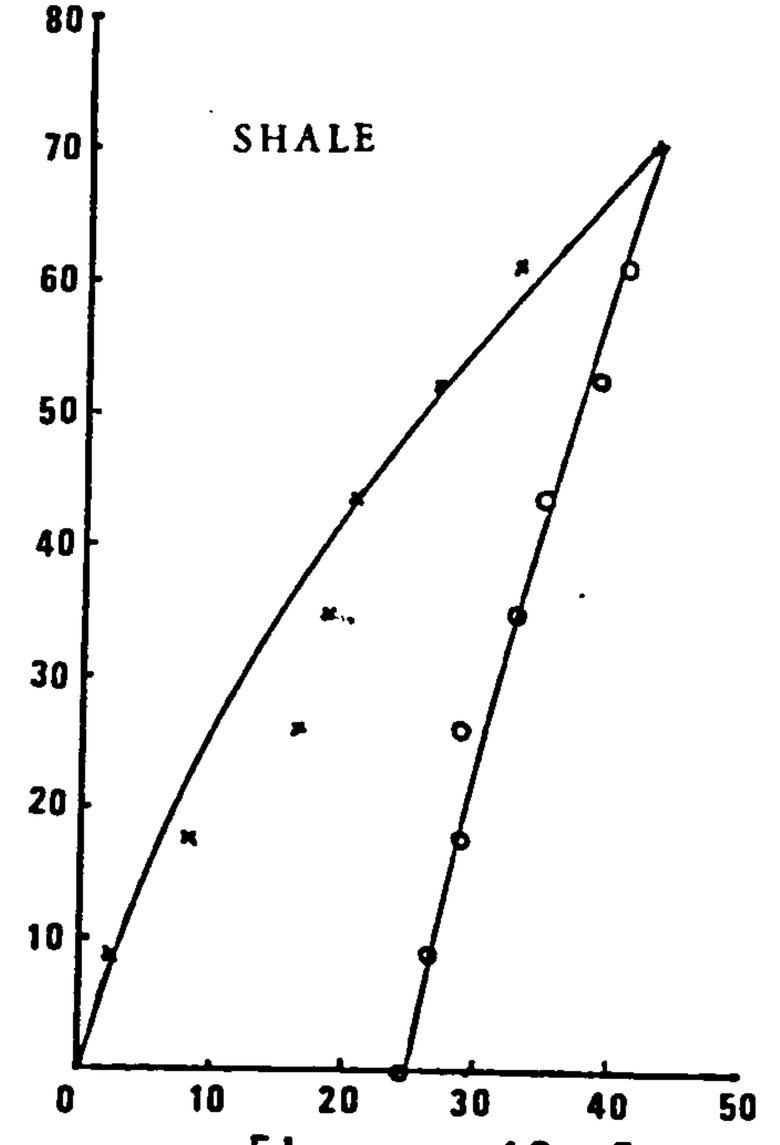

Figure 43–5

Only 6 rock types were subjected to tension modulus test due to the difficulties in testing. Secant modulii were calculated.

The dynamic modulus was obtained from longitudinal wave velocity for 20 rock types. These result are shown in Table 10.

Table 10 Modulus of Elasticity of Rocks

Rock type	Static modulus $MN/m^2 \times 10^4$				Ed $MN/m^2 \times 10^4$
	Et	Es	Poisson's ratio	Es (tension)	
Scotswood sandstone	1.97	1.27	0.55	0.64	1.57
Bunter sandstone	1.72	0.81	0.19		1.16
Springwell sandstone	1.76	1.20	0.29	0.93	2.18
Dunhouse sandstone	2.26	1.44	0.39	0.70	1.10
Post sandstone	4.29	2.96	0.09		
Stanhope sandstone	6.64	6.20	0.32		8.67
Hinkley limestone	4.00	3.83	0.23		6.57
Whinstone	7.25	7.25	0.26		10.13
Creetown granite(white)	6.34	5.47	0.30		6.51
Creetown granite(blue)	6.24	4.68	0.34		6.63
Anhydrite	6.35	5.65	0.26	10.76	9.53
Gypsum	3.08	2.37	0.23	3.58	4.96
Stilfontein quartzite	7.22	6.85	0.17		8.62
Auriferous quartzite	6.62	6.31	0.25		8.53
Scottish quartzite	7.47	5.93	0.14		7.68
Rocksalt					3.73
Lower chalk					1.36
Honister slate	1.44	1.41	0.20		11.6
Aust mudstone					3.15
Shale				1.64	3.36

It can be noticed from the table that Et is always greater than Es, and Poisson's ratio varies from 0.09 to 0.55.

6.6 Indentation hardness

Two testing methods were investigated to determine the indentation hardness of rock, i.e. the cone indenter test and the Brinell hardness test.

6.6.1 Cone indenter test

Standard cone indenter test was performed on the rocks having the compressive strength of less than 100 MN/m^2. The rocks of higher strength were tested by the "modified" method.

6.6.2 Brinell hardness test

In this test rock specimen was indented at a predetermined load by a hardened steel ball of small diameter or a diamond tip on the Firth-brown Hardometer. Load level and the indenter type used were chosen depending on rock strength. Method of testing was described in section 5.2.8. b and the results shown in Table 12.

Table 11 Dynamic Modulus Test Data.

Rock		Length cm	Density Mg/m3	Av.Time 4 readings Microseconds	Velocity $m/s \times 10^3$	E_d $MN/m^2 \times 10^4$	
Scotswood	sandstone	8.25	2.19	30.80	2.63	1.57	
Bunter	sandstone	1. 7.6	2.10	30.40	2.52	1.33	1.16
		2. 8.8		40.50	2.17	0.99	
Springwell	sandstone	17.4	2.21	55.40	3.14	2.18	
Dunhouse	sandstone	15.0	2.23	67.50	2.22	1.10	
Post	sandstone	1.11.5	2.48	36.90	3.12	2.41	2.41
		2. 6.05		19.40	3.11	2.41	
Shanhope	limestone	12.5	2.76	22.30	5.61	8.67	
Hinkley Point	limestone	5.1	2.63	10.20	5.00	6.57	
Whinstone		14.0	2.89	23.65	5.92	10.23	
Creetown granite(white)		16.9	2.65	34.10	4.96	6.51	
Creetown granite(blue)		10.0	2.65	20.00	5.00	6.63	
Anhydrite		9.9	2.91	17.30	5.72	9.53	
Gypsum		1. 8.35	2.26	17.50	4.77	5.15	4.96
		2. 9.8		21.30	4.60	4.78	
Stilfontein	quartzite	7.6	2.70	13.45	5.65	8.62	
Auriferous	quartzite	7.8	2.67	13.80	5.65	8.23	
Scottish	quartzite	7.7	2.63	14.25	5.40	7.68	
Rocksalt		1. 6.65	2.19	15.25	4.36	4,16	
		2. 7.55		19.48	3.88	3.29	
Lower	chalk	5.95	1.88	22.10	2.69	1.36	
Honister	slate	11.45	2.74	17.60	6.06	11.60	
Aust	mudstone	10.05	2.66	29.20	3.44	3.15	
Shale		7.55	2.83	21.90	3.45	3.36	

6.7 Rebound hardness

Shore hardness represents the rebound hardness in the test matrix because of the ease of testing procedure and the reliability of results. The results follow the theory that hard materials have high elastic limits and absorb little of the kinetic energy of the dropped weight.

At least 20 readings on each rock specimen is necessary to obtain a reliable mean result. The results along with the cone indenter hardness and the Brinell hardness are shown in Table 12.

Table 12 Rock Hardness

Rock type		Compressive strength, MN/m^2	Cone indenter hardness	Brinell hardness	Shore hardness
Scotswood	sandstone	45.77	5.43	77.25	36.40
Bunter	sandstone	40.48	2.78	97.00	36.26
Springwell	sandstone	50.61	3.03	83.30	41.08
Dunhouse	sandstone	72.53	8.85	113.30	46.95
Post	sandstone	119.96	6.85	131.35	26.63
Hunterstone	sandstone	67.29	11.54	90.19	34.30
Lazenby	sandstone	54.51	7.20	88.69	37.60
Frosterly	limestone	172.74		88.90	
Stanhope	limestone	169.60	25.00	135.65	40.70
Hinkley	limestone	116.60	6.10	125.70	50.72
Bulwell	limestone				7.25
Whinstone		318.90	11.84(M)	170.80	81.89
Creetown granite (white)		174.75	14.29(M)	220.00	90.45
Creetown granite (blue)		262.00	15.63(M)	238.90	102.21
Anhydrite		112.94	4.09	99.60	36.24
Gypsum		45.02	4.50	70.70	26.03
Stilfontein	quartzite	141.20	9.55(M)	268.67	46.05
Auriferous	quartzite	164.16	14.66(M)	281.00	96.74
Scottish	quartzite	218.16	14.17(M)	225.00	
Rocksalt		27.57		21.60	
Lower	chalk	35.45	1.32	10.05	14.89
Honister	slate	135.00	7.03	88.65	43.62
Aust	mudstone	75.84		58.00	38.70
Shale		92.07		30.10	

In the Schmidt hammer test, an investigation into specimen size for laboratory testing was undertaken.

A series of 256 evenly distributed rebound values were made on the vertical face of a large block of Mansfield whitestone. The hammer was held perpendicular to the face. The contoured results are shown in Fig.44 A. The Figure illustrates that, while the rebound values are lowest around the edges of the block i.e. near free faces, they did not vary to any great extent. Thus to reduce error, readings should not be made less than 50 mm from any free face.

Furthermore, a block 60 mm x 100 mm x 300 mm was used. The hammer was held perpendicular to the smallest face which was vertical, and 20 tests were made on the small face. This was repeated 10 times, each time shortenting the length by 30 mm and testing the new face. The results were averaged each time, and a plot of block thickness versus rebound value is shown Figure 44 B.

The plot shows that, as the block becomes thinner, the rebound value falls slowly until, at 80 mm. thickness, it suddenly rises. This is due to the effect of the base. When the block was thinner than 50 mm,

Schmidt hammer test

on Mansfield whitestone

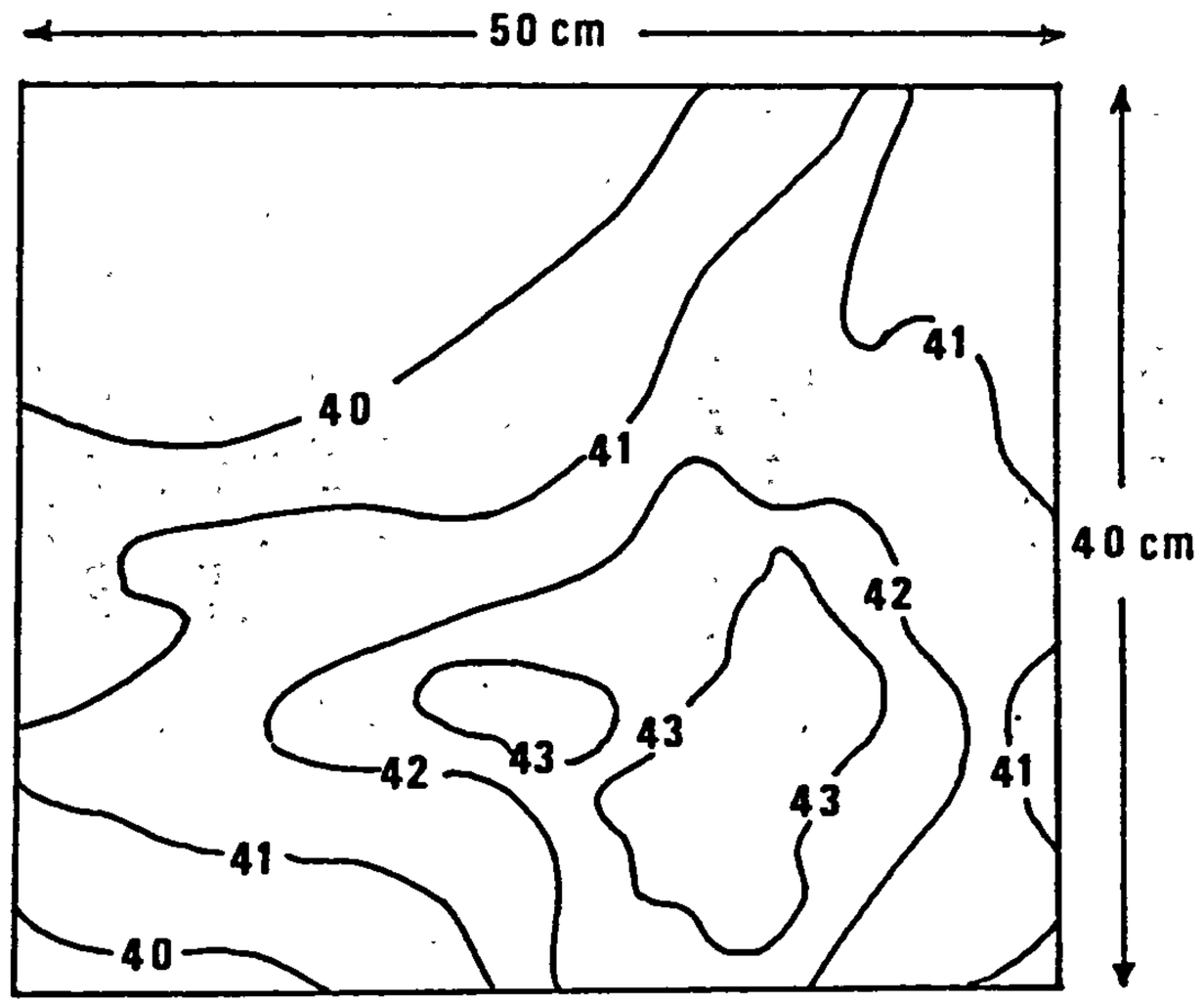

A. Distribution of Shmidt rebound values

not to scale

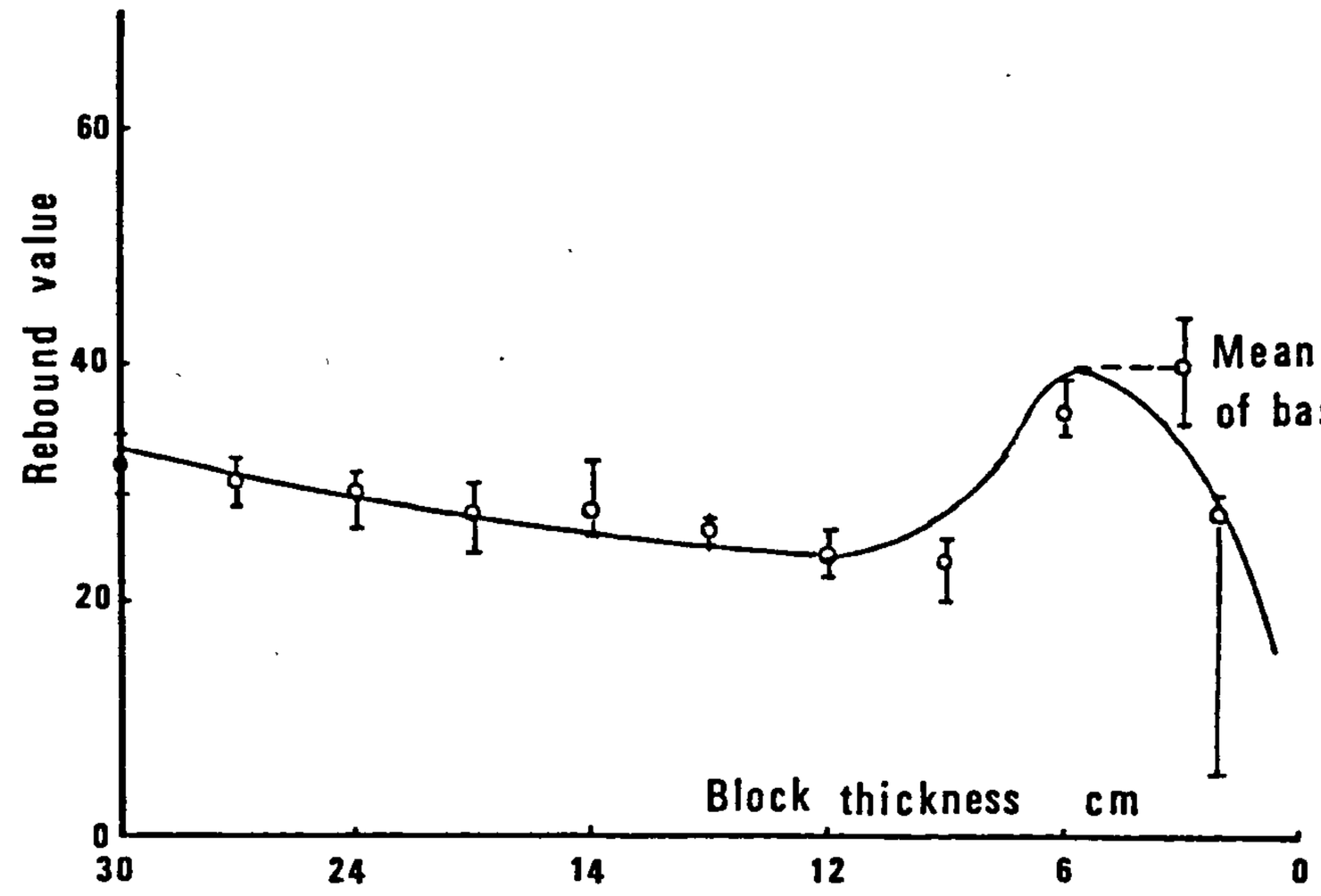

B. Rebound hardness value versus block thickness

Figure 44

it began to fail under the impact of the hammer and failure planes were obseved.

Thus, to avoid any effect from the base, it is necessary to use a block no thinner than 200 mm. The most suitable size of block which should be used in this test is one about 200-250 mm square.

6.8 Abrasivity

Two methods for assessing the abrasivity of rocks have been investigated. The results obtained are as follow:

6.8.1 Blade abrasivity and machineability

Experience has been gained on a number of different rocks, using drill cores and rectangular prisms as test specimens. It was observed that in abrasive rocks, the area cut under standard conditions decreases as the blade wears. Very little wear took place when cutting non-abrasive rocks and the area cut remained almost constant. However cutting in non-abrasive hard rocks produced very low area cut thus gave low machineability.

Abrasivity of rock is the tangent of the curve between the first and second cut multiplied by 100. However the abrasivity obtained by this method appears to be unreliable.

Results are shown in Table 13.

6.8.2 Intrinsic abrasivity test

In this test the abrasivity of a rock is taken as a function of the diameter of the wear flat created under identical test conditions. Standard procedure was described in section 5.2.10.B.

After each test had been done, the depth of penetration on rock specimen and wear flat of the tip wear measured. The average of the two measurements were calculated from five test replications.

Abrasion factor of rock can be calculated from the equation:-

$$\text{Abrasion factor} = \frac{\text{Wear flat}}{100} \times \text{Compressive Strength} \qquad \text{MN/m}$$

Abrasion factor of rocks can be compared if one type of tool materials could be applicable to the whole range materials. This was found to be impossible, for example high speed steel tips could not be used with low strength and/or rocks of little or no quartz content, silver steel was found to be too soft for high strength and/or abrasive rocks. Due to this reason two types of tool materials, i.e. high speed steel and silver steel were used and the abrasion factor of rocks for each type of tool material were set up. Some rocks were tested with both silver steel and high speed steel, allowing a correlation between the two materials to be obtained. The regression equation was computed, taking silver steel as the standard material, and found to be

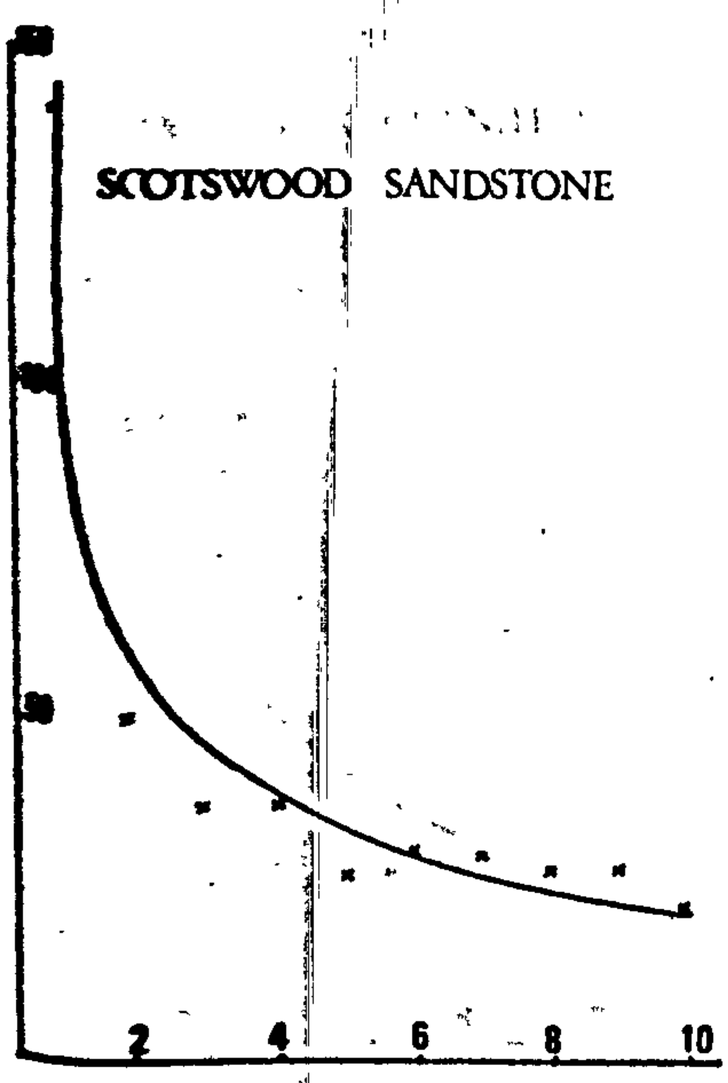

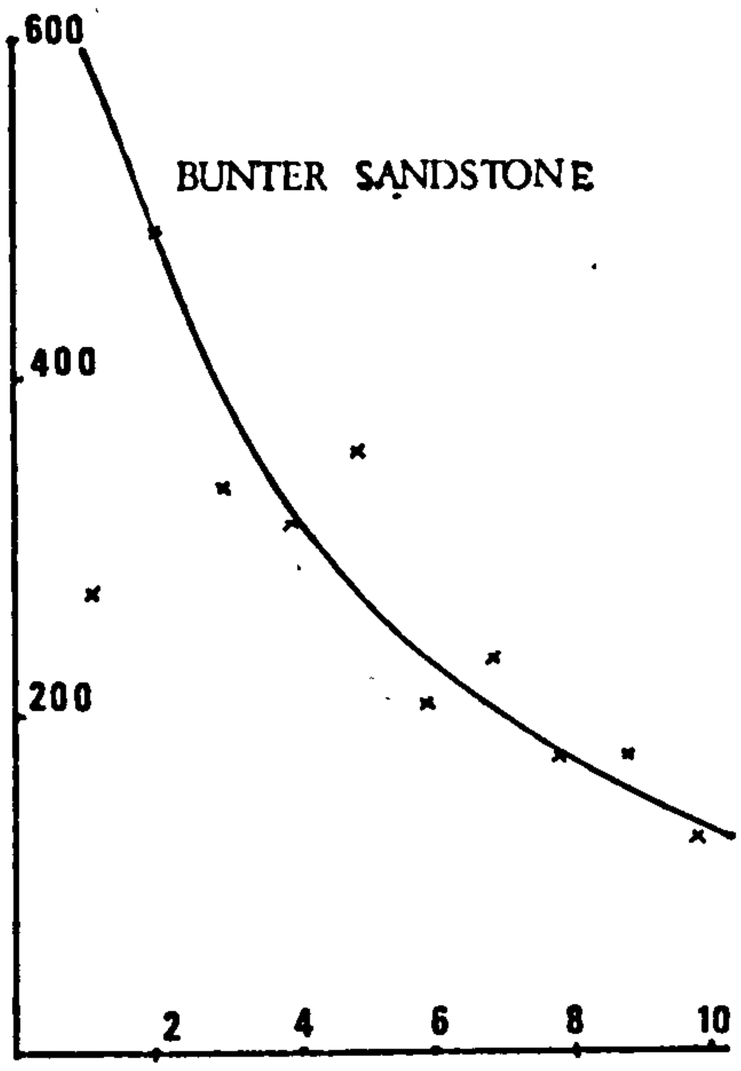

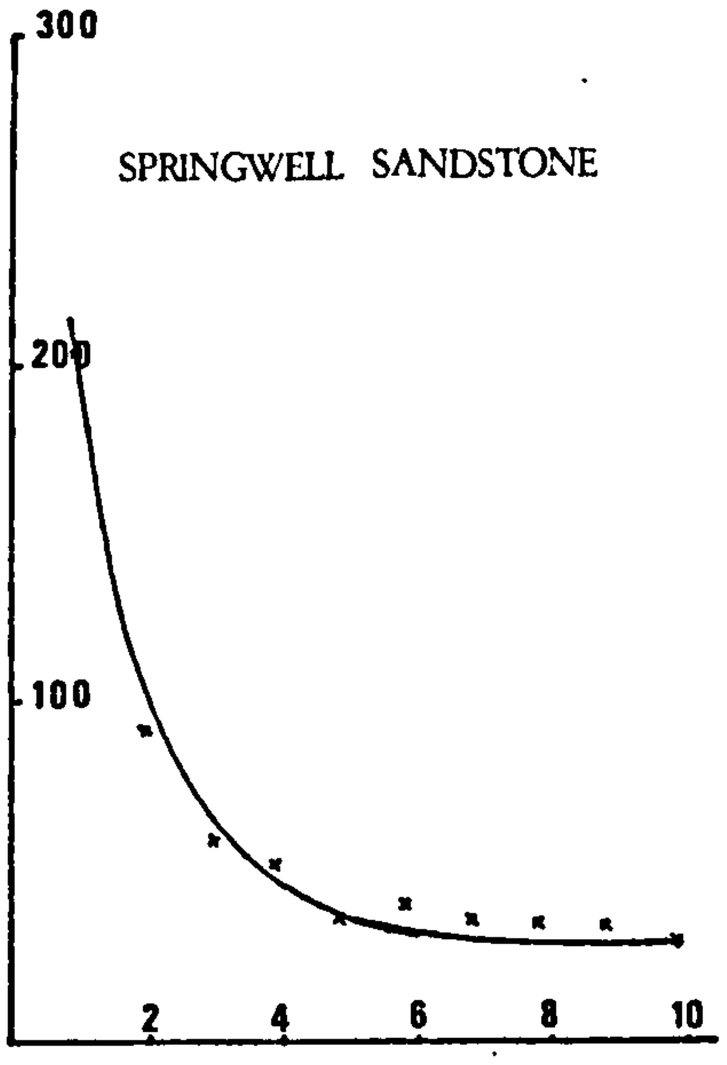

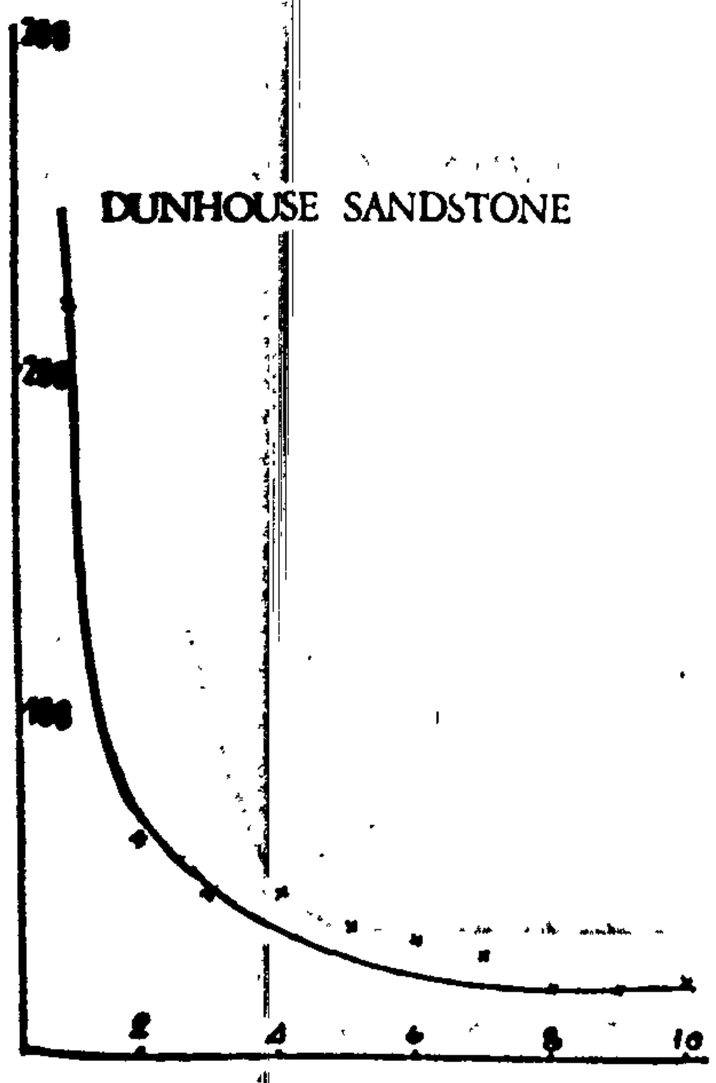

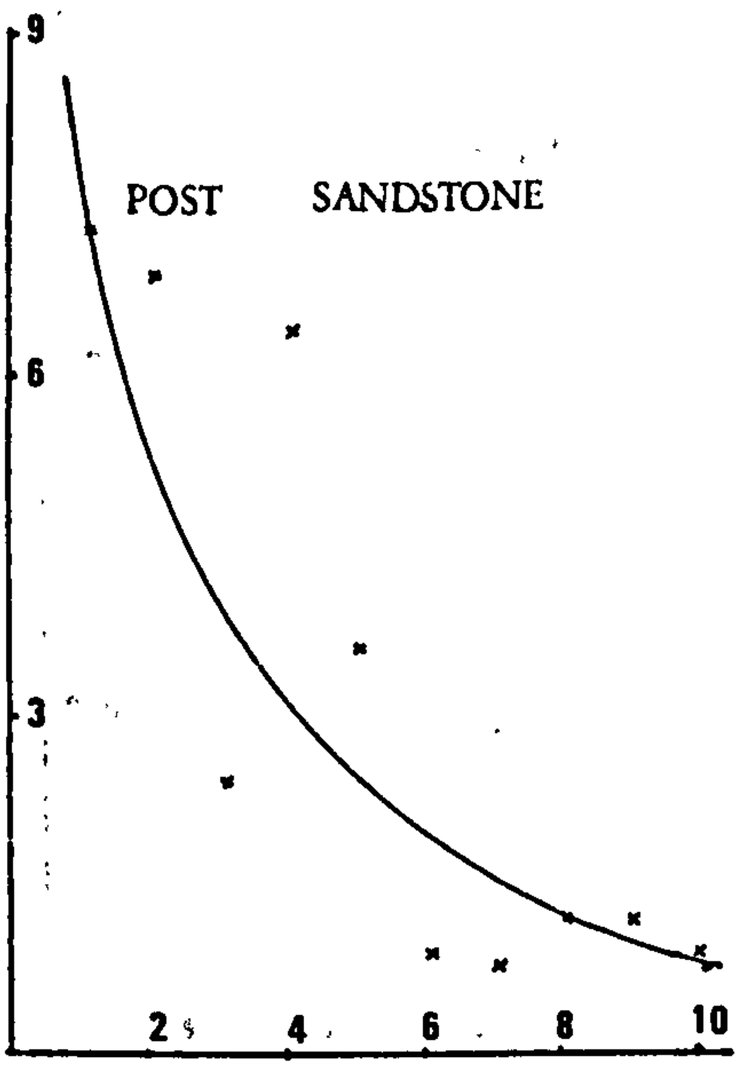

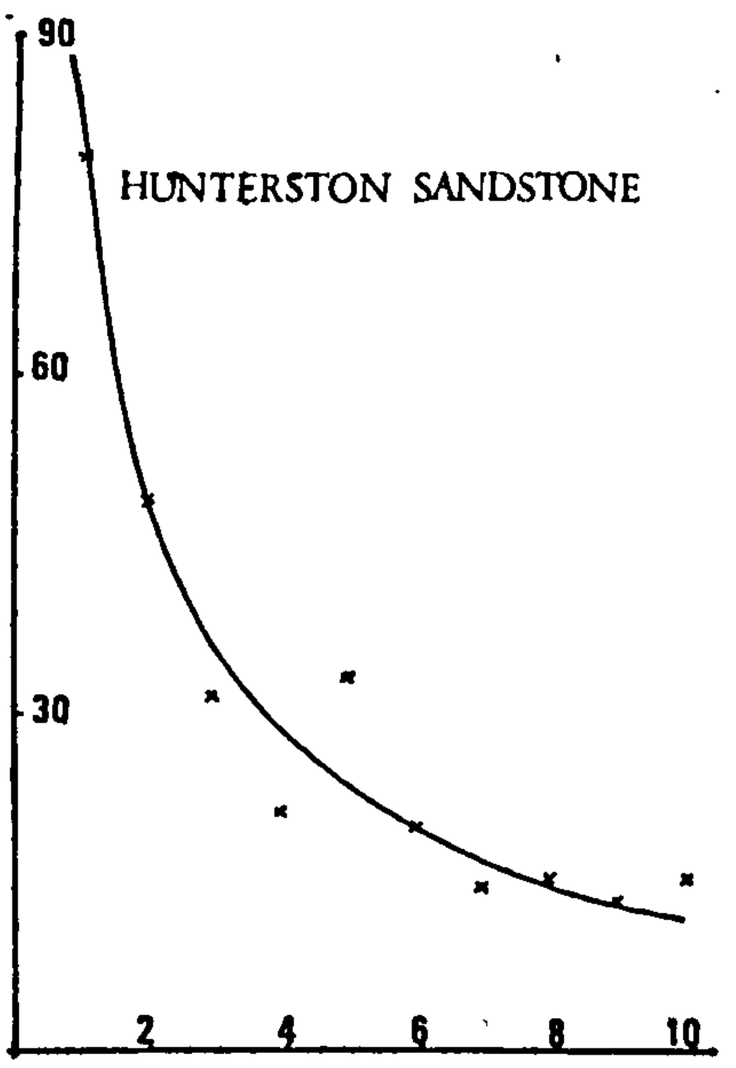

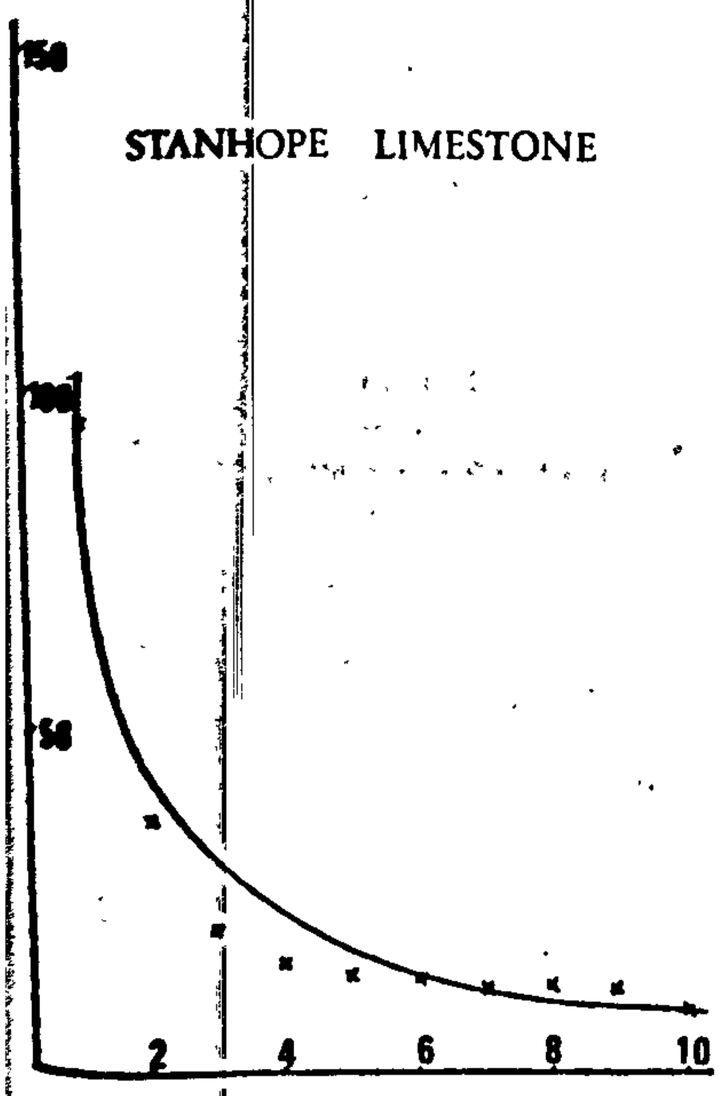

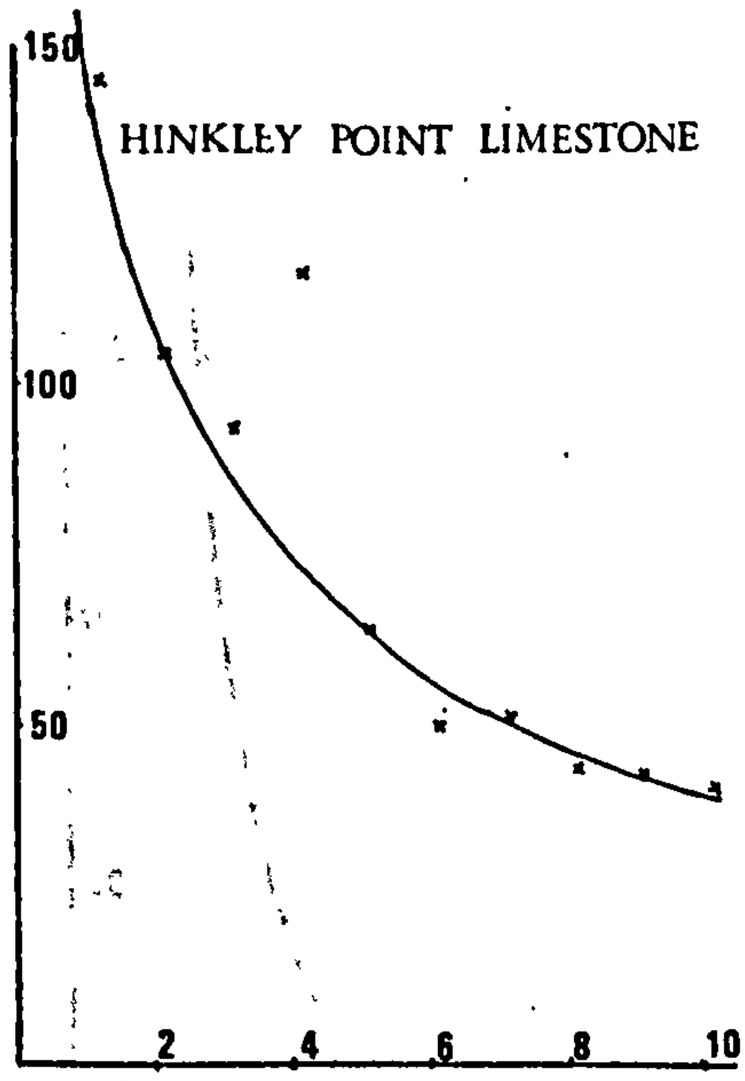

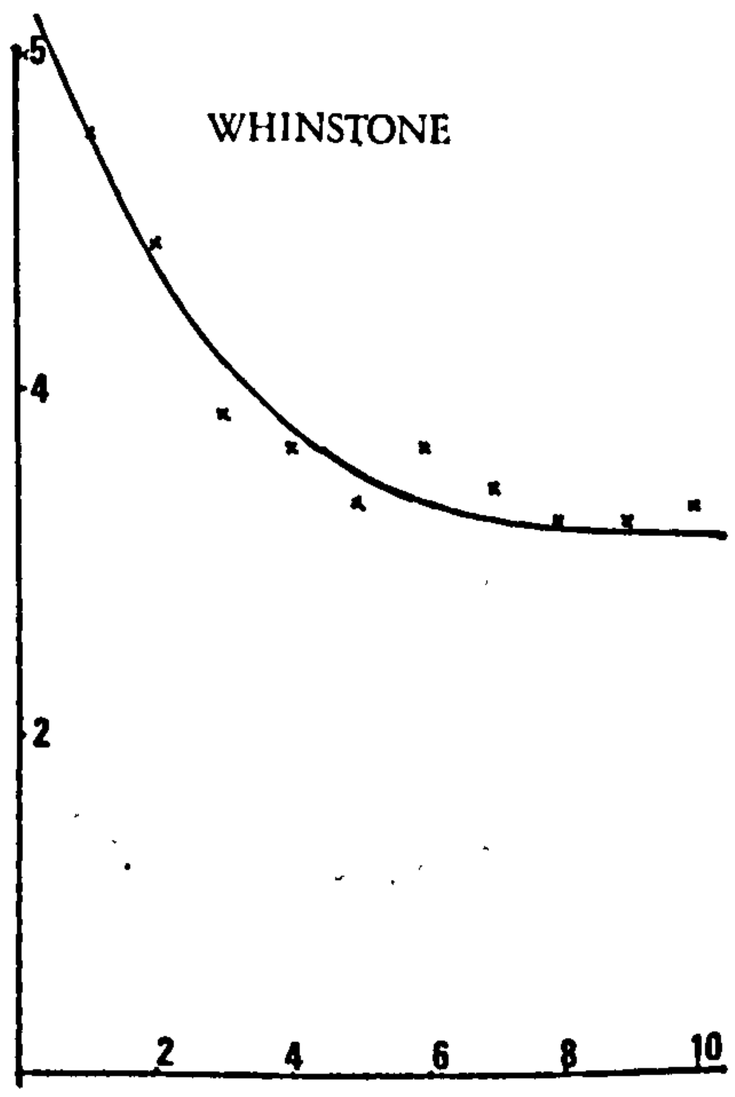

Blade abrasivity test

Figure 45-1

CREETOWN GRANITE (WHITE)

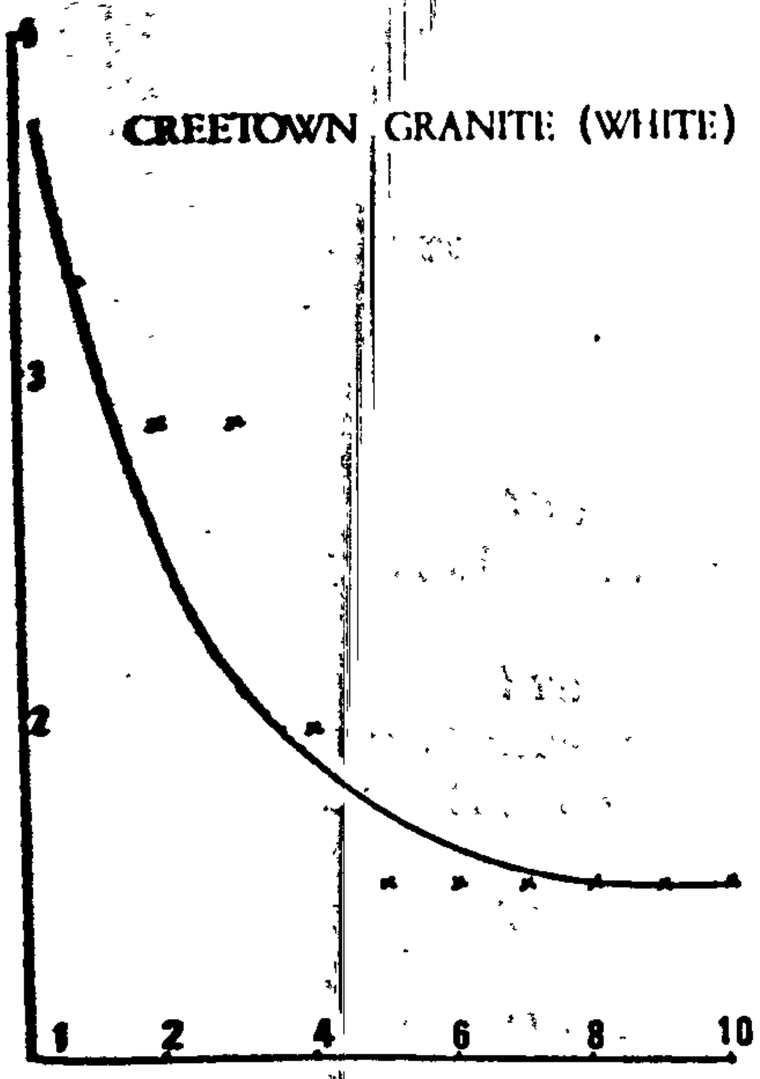

ANHYDRITE

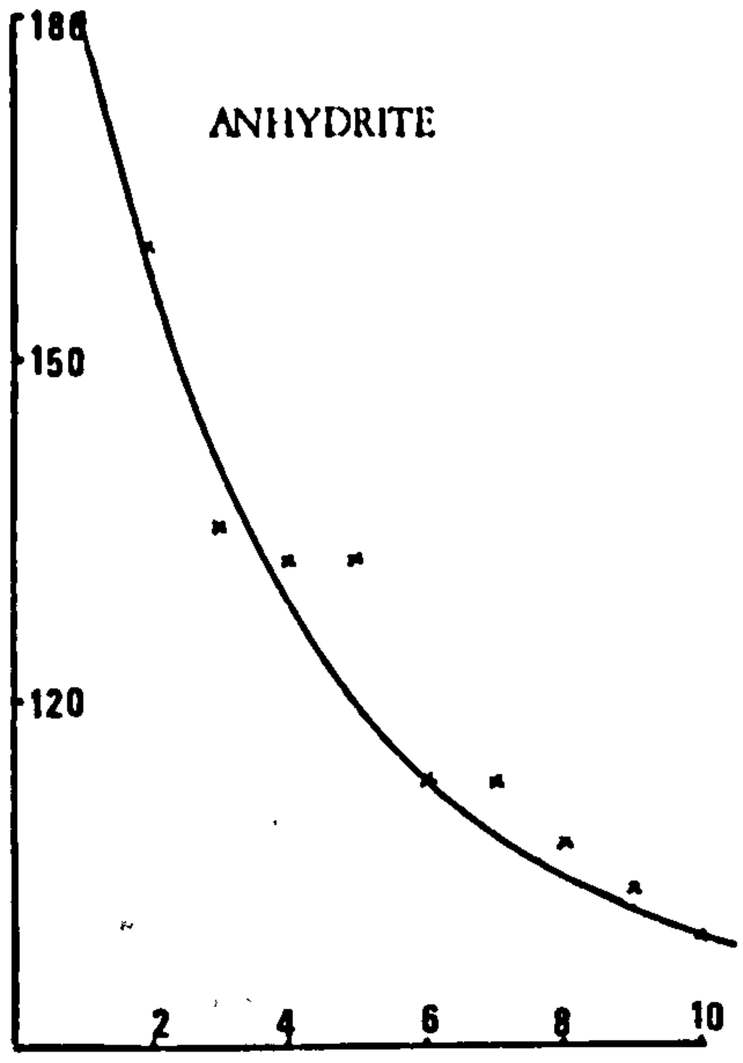

STILFONTEIN QUARTZITE

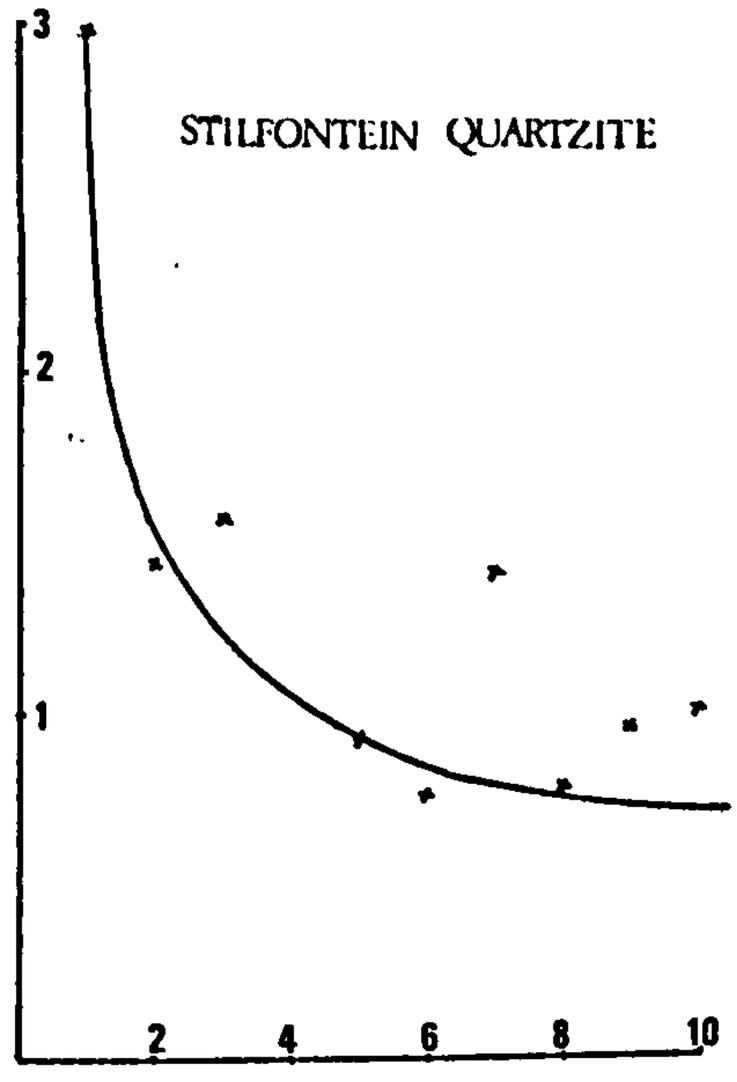

AURIFEROUS QUARTZITE

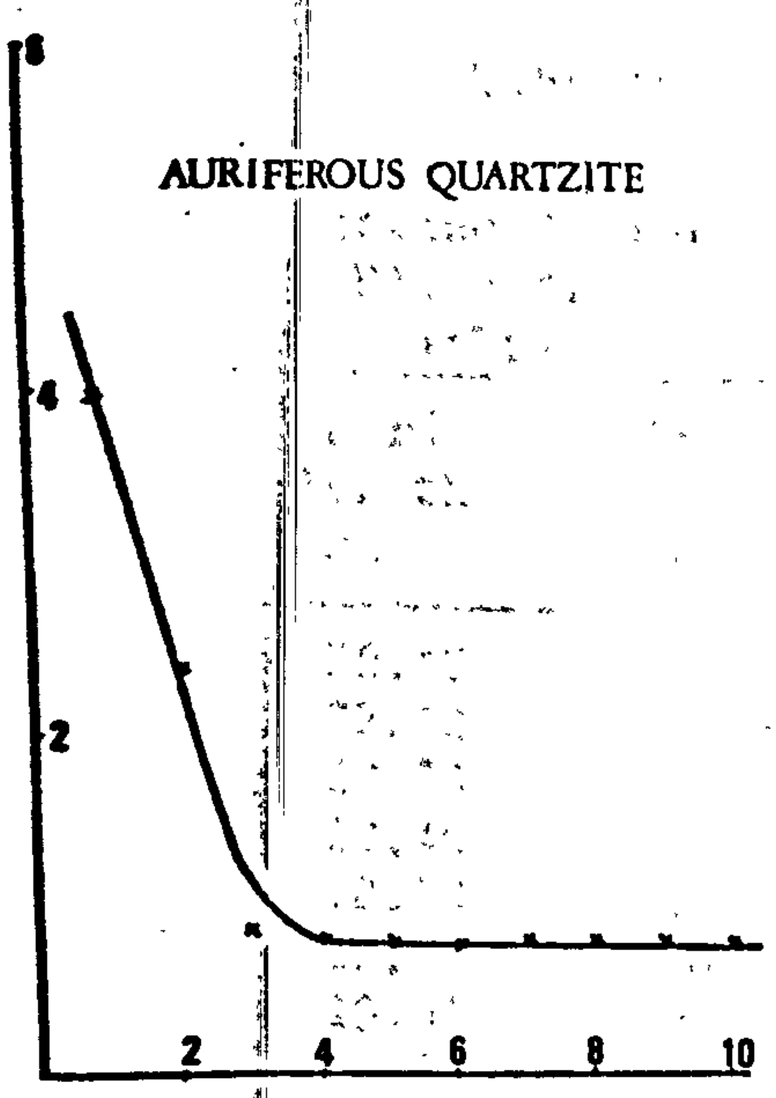

SCOTTISH QUARTZITE

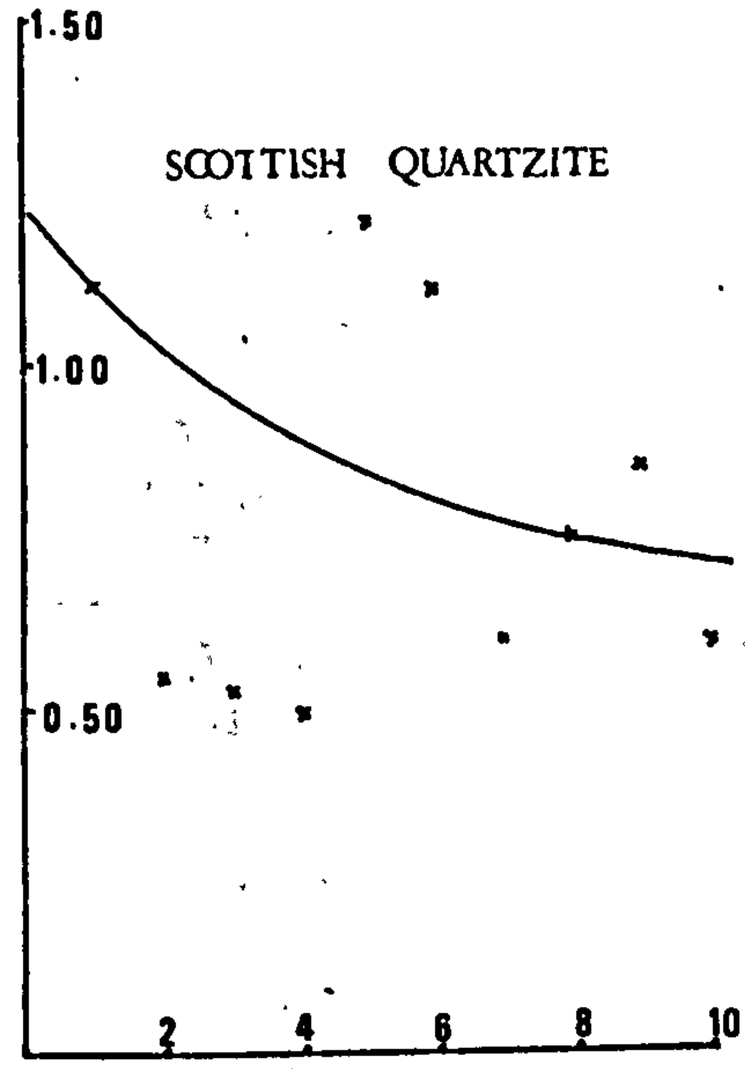

HONISTER SLATE

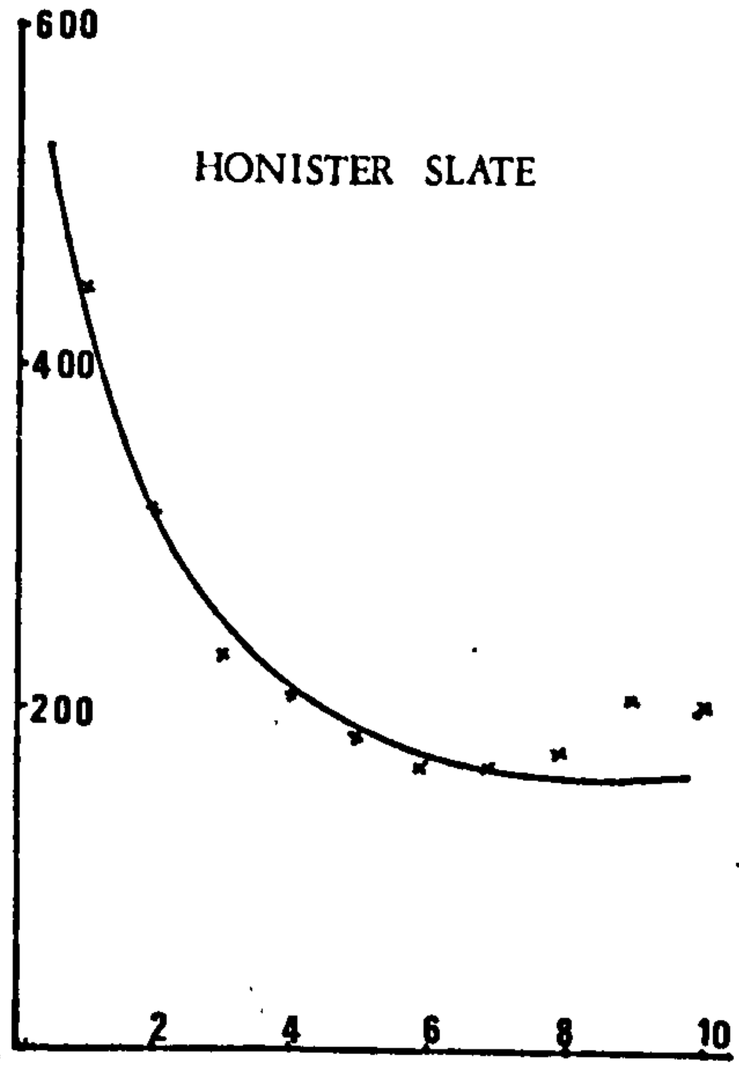

GYPSUM

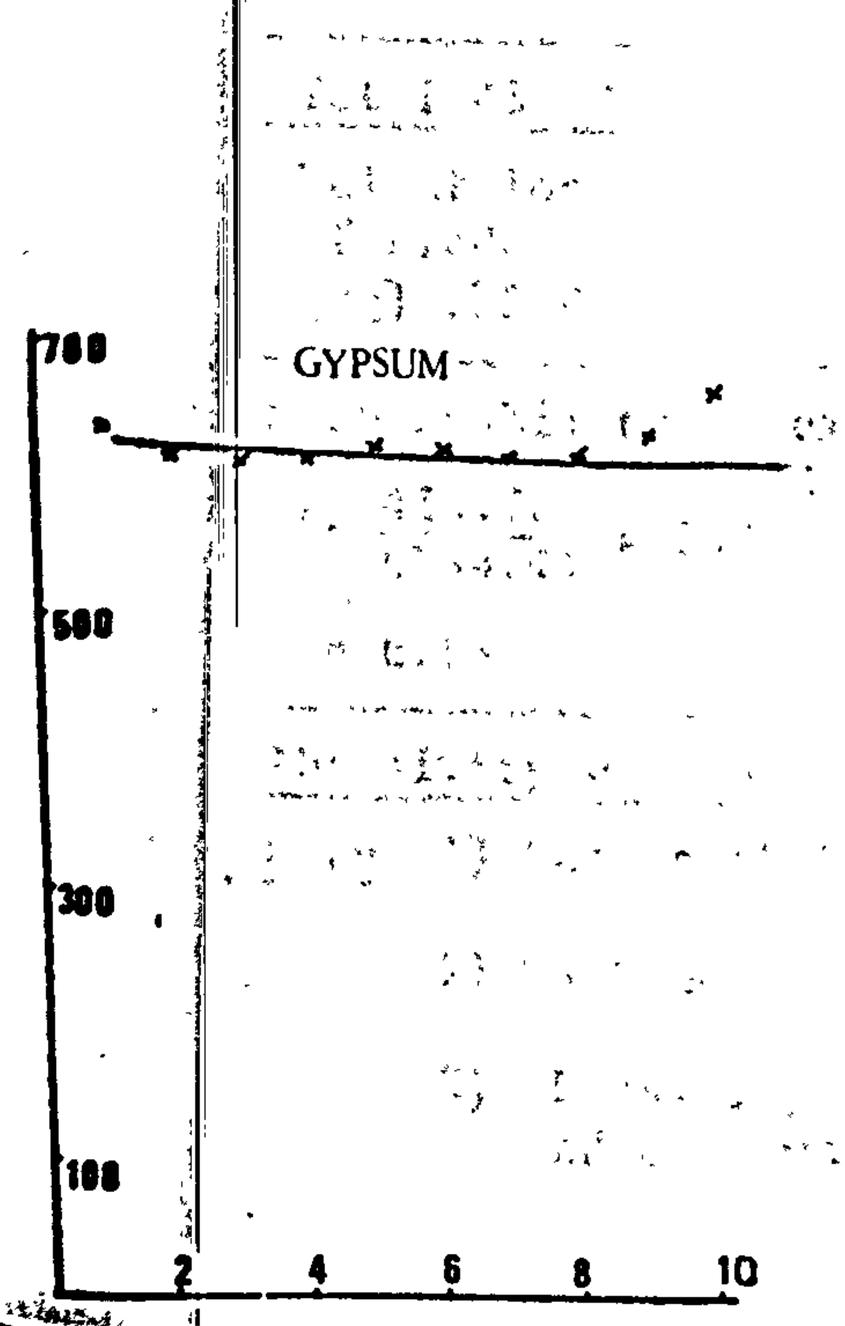

SHALE

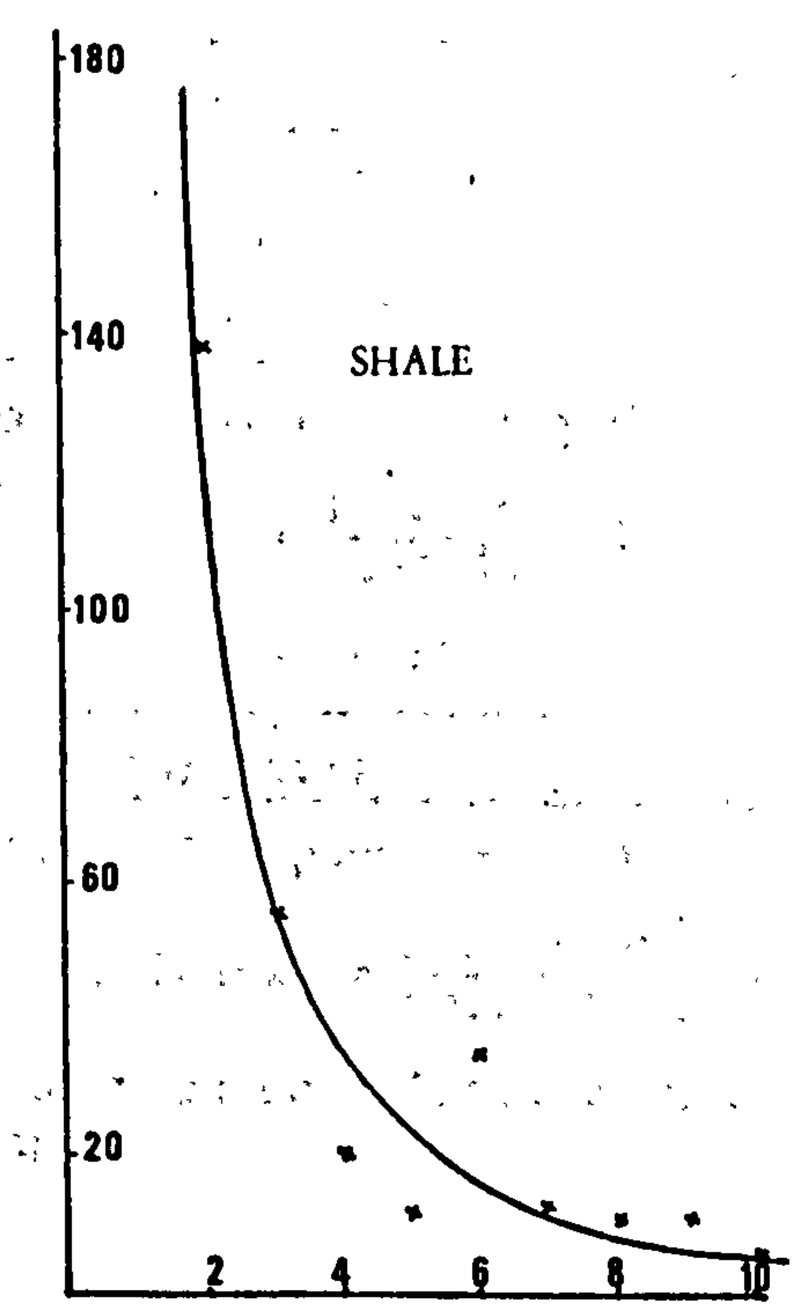

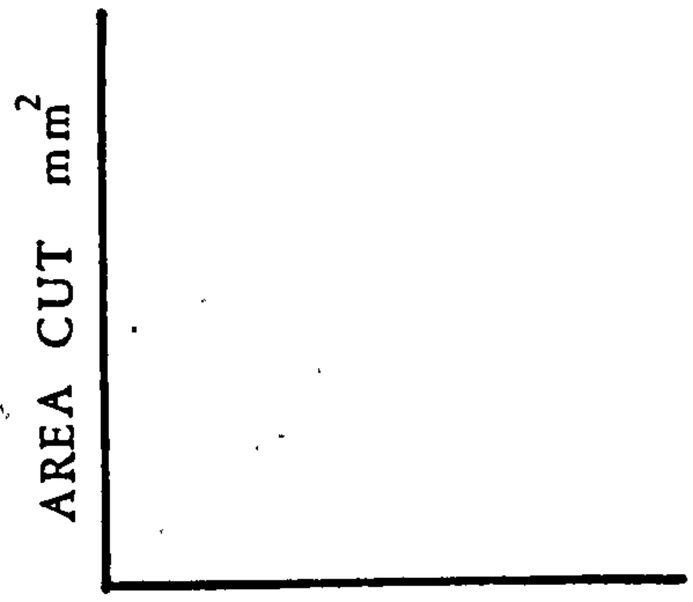

Blade abrasivity test

Figure 45-2

$$Y = 0.350957\ X - 0.006786$$

where

Y = abrasion factor using high speed steel tip

X = abrasion factor using silver steel tip.

The fitted curve was good, as shown in Figure 46, and has correlation coefficient of 0.916 which is statistically highly significant.

From the regression equation, it was possible to construct an arbitrary scale's wear flat scale based on silver steel tip, and this enables one to calculate a "standard abrasion factor".

The abrasion index of rock assumed to be

$$\text{Abrasion index} = \frac{\text{Standard abrasion factor of rock X 100}}{\text{Standard abrasion factor of Scottish quartzite}}$$

Full results are shown in Table 14.

Table 13 Blade Abrasivity Test Results

Scotswood sandstone Dia = 41.1 mm (abrasive)		Anhydrite Dia = 41.1 mm (non-abrasive)		Whinstone Dia = 41.1 mm (hard rock)	
Chord length mm	Area mm^2	Chord length mm	Area mm^2	Chord length mm	Area mm^2
30.42	141.72	32.47	180.05	11.03	5.56
22.42	50.59	31.57	162.14	10.55	4.86
20.38	37.26	30.07	135.91	9.80	3.88
20.46	37.72	29.87	132.72	9.60	3.65
18.50	27.43	29.83	132.19	9.33	3.34
19.40	31.86	28.53	113.04	9.60	3.65
19.04	30.03	28.60	113.97	9.40	3.42
18.62	28.00	28.13	107.65	9.23	3.23
18.82	28.95	27.80	103.33	9.23	3.23
17.34	22.39	27.47	99.15	9.33	3.34
Total 435.96		Total 1280.14		Total 38.17	
Weight loss of blade (mg) 175.00		Weight loss of blade (mg) 0.00		Weight loss of blade (mg) 15.05	
Machineability index $= \frac{435.96}{6244.44} \times 100$		Machineability index $= \frac{1280.14}{6244.44} \times 100$		Machineability index $= \frac{28.17}{6244.44} \times 100$	
= 6.98		= 20.50		= 0.61	
Abrasivity = 1.10		Abrasivity = 5.58		Abrasivity = 182.86	

Note 1) Machineability of Gypsum = 6244.44 mm^2

2) $\text{Machineability index} = \frac{\text{Machineability of particular rock x 100}}{\text{Machineability of gypsum}}$

3) Abrasivity of rock calculated from curve plotted between area cut and cut number.

RELATIONSHIP BETWEEN SILVER STEEL AND HIGH SPEED STEEL WEAR FLAT

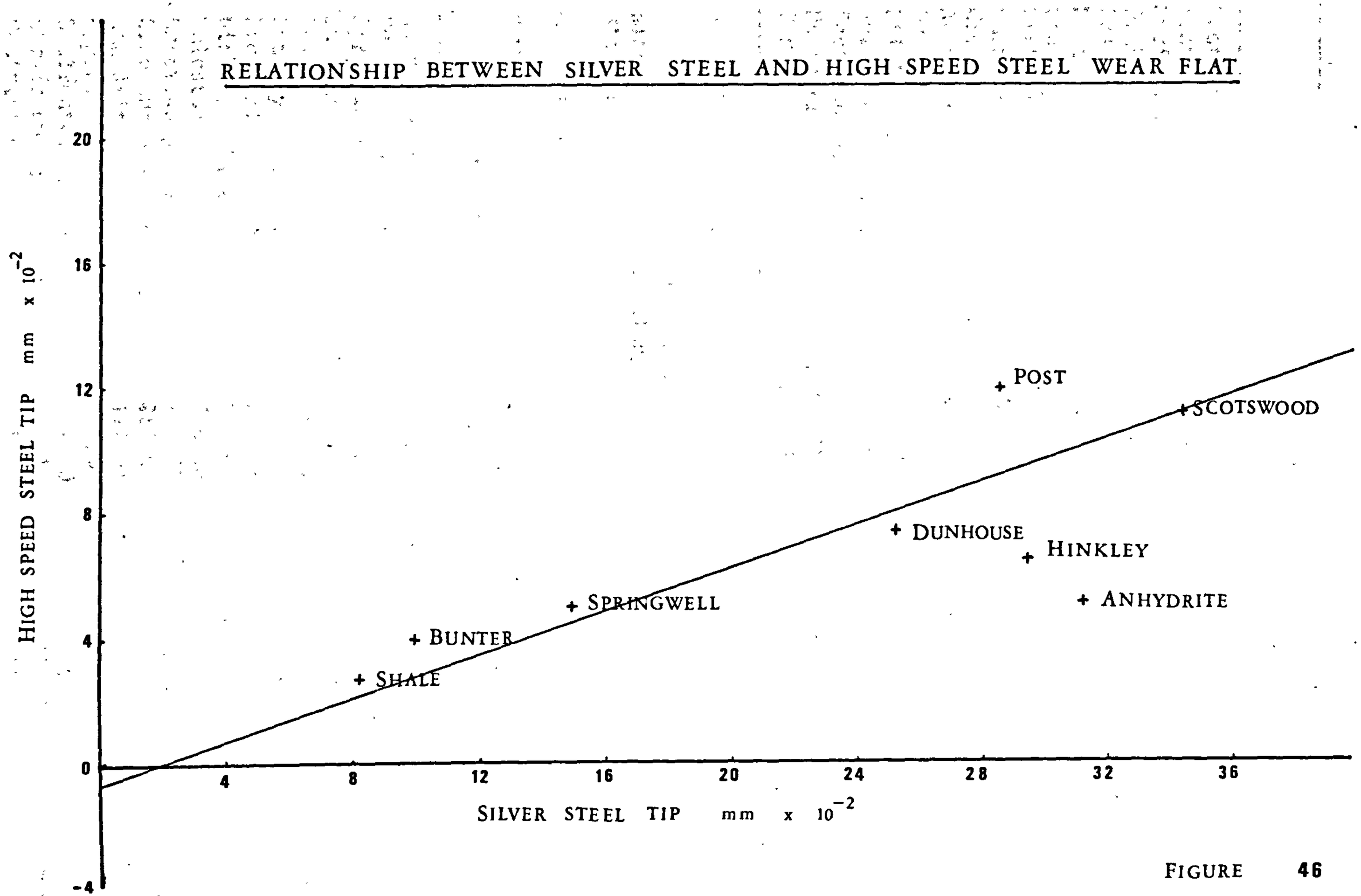

FIGURE 46

Table 13 (continued).

Rock	Machineability mm^2	Machineability index	Abrasivity
Scotswood sandswood	435. 96	6.98	1.10
Bunter sandswood	2680.38	42.92	0.68
Springwell sandswood	643.46	10.30	0.66
Dunhouse sandswood	555.84	8.90	0.62
Post sandswood	31.36	0.05	250.00
Hunterston sandswood	294.23	4.71	3.39
Stanhope limestone	248.12	3.97	1.73
Hinkley limestone	748.88	11.99	2.52
Whinstone	38.17	0.61	182.86
Creetown granite (white)	19.96	0.32	238.10
Anhydrite	1280.14	20.50	5.58
Gypsum	6244.44	100.00	5.49
Stilfontein quartzite	12.94	0.21	64.94
Auriferous quartzite	12.65	0.20	62.11
Scottish quartzite	8.09	0.13	172.41
Honister slate	2282.21	36.55	0.79
Shale	507.64	8.13	1.24

6.9 Impact Strength Index. (ISI)

Standard procedure was described in section 5.2.11.Results of this simple test are shown along with compressive strength and "disc" tensile strength in Table 15.

Table 15. Impact Strength Index Test.

Rock type	CS MN/m^2	TS MN/m^2	ISI
Scotswood sandstone	45.77	1.69	40.09
Bunter sandstone	40.58	1.78	42.07
Springwell sandstone	50.61	10.40	58.82
Dunhouse sandstone	72.53	3.84	51.99
Post sandstone	119.96	7.72	40.55
Lazenby sandstone	54.51	3.03	39.29
Frosterly limestone	172.74	10.14	89.34
Hinkley limestone	116.60	9.45	87.30
Whinstone	318.90	21.65	89.74
Creetown granite (white)	174.75	14.68	81.50
Creetown granite (blue)	262.00	10.56	86.89
Anhydrite	112.94	5.47	76.36
Gypsum	45.02	2.75	76.36
Stilfontein quartzite	141.20	13.88	87.15
Auriferous quartzite	164.16	13.27	86.09
Scottish quartzite	218.16	16.23	83.49
Rocksalt	27.57	1.42	58.84
Lower chalk	35.45	1.58	68.44
Honister slate	135.00	8.89	82.94
Shale	92.07	10.14	84.63

Table 14. Intrinsic Abrasivity Test Results.

Rock	CS MN/m^2	High speed steel				Silver steel				Standard abrasion factor MN/m	Abrasion index
		Wear flat mm	Vol. removed $x10^{-5}$ mm^3	Depth of pen. mm	Abrasion factor MN/m	Wear flat mm	Vol. removed $x10^{-5}$ mm^3	Depth of pen. mm	Abrasion factor MN/m		
Scotswood sandstone	48.77	0.250	204	0.633	0.114	0.778	6166	2.202	0.356	0.356	14.95
Bunter sandstone	40.48	0.100	13	0.781	0.040	0.265	243	2.521	0.107	0.107	4.49
Springwell sandstone	50.61	0.120	22	0.543	0.061	0.321	433	1.934	0.162	0.162	6.80
Dunhouse Sandstone	72.53	0.110	17	0.529	0.080	0.380	718	1.592	0.276	0.276	11.59
Post sandstone	119.96	0.100	13	0.931	0.120	0.240	181	2.806	0.288	0.288	12.09
Hunterston sandstone	67.29	0.110	17	0.495	0.074	no test				0.230	9.66
Stanhope limestone	169.65	no test				0.360	610	0.673	0.610	0.610	25.61
Hinkley Point limestone	116.60	0.055	2	0.236	0.064	0.254	214	0.589	0.296	0.296	12.43
Whinstone	318.90	0.220	139	0.110	0.702	no test				2.019	84.76
Creetown granite(white)	174.75	0.260	230	0.00	0.454	0.500	1636	0.00	0.879	0.879	36.90
Creetown granite(blue)	262.00	0.280	287	0.00	0.734	no test				2.111	88.62
Anhydrite	112.94	0.044	1	0.501	0.050	0.279	284	0.752	0.315	0.315	13.22
Gypsum	45.02	0.00	0.00	0.497	0.00	no test				0.00	0.00
Stilfontein quartzite	141.20	0.360	610	0.009	0.508	no test				1.467	61.59

Table 14. (continued)

Rock	Cs MN/m^2	High speed steel				Silver steel				Standard abrasion factor	Abrasion index
		Wear flat mm	Vol. removed x10^{-5}mm^3	Depth of pen. mm	Abrasion factor MN/m	Wear flat mm	Vol. removed x10^{-5}mm^3	Depth of pen. mm	Abrasion factor MN/m	MN/m	
Scottish quartzite	218.16	0.380	718	0.036	0.829	no test				2.382	100.00
Rocksalt	27.57	0.00	0.00	0.527	0.00	0.055	2	1.710	0.150	0.150	0.63
Honister slate	135.00	no test				0.302	360	0.747	0.408	0.408	17.13
Aust mudstone	75.84	no test				0.171	65	1.945	0.130	0.130	5.46
Shale	92.07	0.030	0.3	0.610	0.028	0.089	9	1.738	0.082	0.082	3.44

Note

1. Abrasion factor $= \frac{\text{Wear flat x CS}}{100}$ MN/m
2. Standard abrasion factor
   = Abrasion factor using silver steel
3. Abrasion index $= \frac{\text{Standard abrasion factor of rock x 100}}{\text{Standard abrasion factor of Scottish qtz}}$
4. Volume lost $= \frac{1}{3}\pi r^2 h = \frac{11}{84} D^3$

   when D = wear flat diameter

Chapter 7

Interpretation of results

The results of the standard rock property tests have led to the construction of the test matrix and the statistical techniques were used to provide an insight into the relationships that exist between rock properties and to determine whether there are statistically significant correlations between the properties of rocks which would enable estimates to be made of one property from another property easier to determine.

The first step in determining relationships was to prepare scatter diagrams, of the pairs of variables. This permitted a visual comparison of the data. Thus enable one to approximate a relationship between two variables. In this work the relationship was assumed to be of a "straight line" form.

A computer program and data were then fed into the computer and the relationships between the variables were obtained in terms of regression equations, correlation coefficient and significant level. These were clearly shown in Appendix 2, Table 16 and Table 17. The scattergrams with the best straight line were illustrated in Figure 47.

The results printed out, in Appendix 2, are:-

1. the linear regression equation in the form of

$$Y = a + bX$$

where

a = Y - intercept
b = the slope of the regression line

2. number of pairs of properties (n of X and Y)

3. the correlation coefficient (r_{xy}), which is explained as (94):-
   r from .00 to ±.20 denotes indifferent or negligible relationship;
   r from ±.20 to ± .40 denotes low correlation; present but slight;
   r from ±.40 to ±.70 denotes substantial or marked relationship;
   r from ±.70 to ±1.00 denotes high to very high relationship.

4. the significant level of r_{xy} at 95 per cent, and 99 per cent confidencelevel.

5. the significance level of b at 95, 99, and 99.5 per cent confidence level.

6. T value for testing the hypothesis.

7. the standard error of estimate ($S.E._{yx}$) which means that at $\pm S.E._{yx}$ we may expect to find about 2/3 of the items to fall within the band.

8. the coefficient of determination (R^2xy), which is the square of the correlation coefficient, is the proportion of the variance accounted for by the linear regression.

Table 16. Test Matrix

Rock Types	Y_1	Y_2	Y_3	Y_4	Y_5	Y_6	Y_7
Scotswood sst.	480	90	2.19	2.59	15.60	15.80	45.77
Bunter sst.	210	73	2.10	2.58	10.93	17.10	40.48
Springwell sst.	190	82	2.21	2.64	15.00	14.60	50.61
Dunhouse sst.	160	88	2.23	2.60	13.60	14.20	72.53
Post sst.	150	85	2.48	2.60	1.20	16.50	119.96
Hunterston sst.	180	78					67.29
Lazenby sst.	380	93	2.26	2.61	12.10	13.40	54.51
Mansfield whitest.	270	91	2.70				
Frosterly 1st.	0	0	2.76	2.71	0.10	0.23	172.74
Stanhope 1st.	0	0					169.65
Hinkley Point 1st.	0	0	2.63	2.70	0.20	2.51	116.60
Bulwell 1st.	230	5					
Beachley 1st.	0	0					
Whinstone	0	0	2.89	2.91	0.15	0.47	318.90
Creetown granite (white)	780	30	2.65	2.67	0.02	0.75	174.75
Creetown granite (blue)	480	40	2.65	2.67	0.20	0.89	262.00
Anhydrite	0	0	2.91	2.92	0.20	0.48	112.94
Gypsum	0	0	2.26	2.33	0.00	3.05	45.02
Stilfontein quz.	410	53	2.70	2.73	0.30	1.00	141.20
Auriferous qtz.	610	60	2.67	2.69	0.30	0.53	164.16
Scottish qtz.	250	63	2.63	2.66	0.42	0.98	218.16
Rocksalt	0	0	2.19	2.42			27.57
Lower chalk			1.88	2.46	23.00	24.10	35.45
Honister slate	0	0	2.74	2.77	0.05	0.77	135.00
Aust mudstone	0	0	2.66				75.84
Shale	70	32	2.83		3.70		92.07

Table 16. (continued)

Rock Types	Y_8	Y_9	Y_{10}	Y_{11}	Y_{12}	Y_{13}	Y_{14}
Scotswood sst.	1.69	1.97	1.27	0.64	0.55	1.57	5.43
Bunter sst.	1.78	1.72	0.81		0.91	1.16	2.78
Springwell sst.	10.40	1.76	1.20	0.93	0.29	2.18	3.03
Dunhouse sst.	3.84	2.26	1.44	0.70	0.39	1.10	8.85
Post sst.	7.72	4.29	2.96		0.09	2.41	
Hunterston sst.							11.64
Lazenby sst.	3.03						7.20
Mansfield whitest.							
Frosterly 1st.							
Stanhope 1st.	9.19	6.64	6.20		0.32	8.67	
Hinkley Point 1st.	9.45	4.00	3.83		0.23	6.57	6.10
Bulwell 1st.							
Beachley 1st.							
Whinstone	21.65	7.25	7.25		0.26	10.13	
Creetown granite (white)	10.56	6.34	5.47		0.30	6.51	
Creetown granite (blue)	14.68	6.24	4.68		0.34	6.63	
Anhydrite	5.47	6.35	5.65	10.76	0.26	9.53	4.09
Gypsum	2.75	3.08	2.37	3.58	0.23	4.96	4.50
Stilfontein qtz.	13.88	7.22	6.85		0.17	8.62	
Auriferous qtz.	13.27	6.62	6.31		0.25	8.53	
Scottish qtz.	16.23	7.47	5.93		0.14	7.68	
Rocksalt	1.42					3.73	
Lower chalk	1.58					1.36	1.32
Honister slate	8.89	1.44	1.41		0.20	11.60	7.03
Aust mudstone						3.15	
Shale	10.14			1.64		3.36	

Table 16. (continued)

Rock Types	Y_{15}	Y_{16}	Y_{17}	Y_{18}	Y_{19}	Y_{20}	Y_{21}
Scotswood sst.		77.25	36.40	435.96	1.10	0.356	40.09
Bunter sst.		97.00	36.26	2680.38	0.68	0.107	42.07
Springwell sst.		83.30	41.08	643.46	0.66	0.162	58.82
Dunhouse sst.		113.10	46.95	555.84	0.62	0.276	51.99
Post sst.	6.85	131.35	26.63	31.36	250.00	0.288	40.55
Hunterston sst.		90.19	34.30	294.23	3.39	0.230	
Lazenby sst.		88.69	37.60				39.29
Mansfield whitest.							
Frosterly lst		88.90					89.34
Stanhope lst.		135.65	40.70	248.12	1.73	0.610	
Hinkley Point lst.		125.70	50.72	748.88	2.52	0.296	87.50
Bulwell lst.			7.25				
Beachley lst.							
Whinstone	11.84	170.80	81.89	38.17	182.86	2.019	89.74
Creetown granite (white)	14.29	220.00	90.45	19.96	238.10	0.879	81.50
Creetown granite (blue)	15.63	238.90	102.21			2.111	86.89
Anhydrite		99.60	36.24	1280.14	5.58	0.315	76.36
Gypsum		70.70	26.08	6244.44	5.49	0.000	79.61
Stilfontein qtz.	9.55	268.70	46.05	12.94	64.94	1.467	87.15
Auriferous qtz.	14.66	281.00	96.74	12.6			
Scottish qtz.	14.17	225.00		8.09	172.41	2.382	83.49
Rocksalt		21.60				0.015	58.84
Lower chalk		10.05	14.89				68.44
Honister slate		88.65	43.62	2282.21	0.79	0.408	82.94
Aust mudstone		58.00	38.70			0.130	
Shale		30.10		507.64	1.24	0.082	84.63

Nomenclature:-

Y_1 = Quartz grain size, μm
Y_2 = Quartz content, %
Y_3 = Bulk density, Mg/m^3
Y_4 = Grain density, Mg/m^3
Y_5 = Apparent porosity, %
Y_6 = True porosity, %
Y_7 = Compressive strength, MN/m^2
Y_8 = "Disc" Tensile strength, MN/m^2
Y_9 = Tangent modulus, $MN/m^2 \times 10^4$
Y_{10} = Secant modulus, $MN/m^2 \times 10^4$
Y_{11} = Tension modulus, $MN/m^2 \times 10^4$
Y_{12} = Poisson's ratio
Y_{13} = Dynamic modulus, $MN/m^2 \times 10^4$
Y_{14} = "Standard" Cone indenter hardness
Y_{15} = "Modified" Cone indenter hardness.
Y_{16} = Brinell hardness
Y_{17} = Shore hardness
Y_{18} = Blade " Hacksaw " machineability, mm^2
Y_{19} = Blade abrasivity
Y_{20} = "Intrinsic abrasivity" Abrasion factor, MN/m
Y_{21} = Impact strength index

Table 17A Correlation Matrix

Column	01	02	03	04	05	06	07	08	09	10	11
Row 1	1.000	0.477**	-0.131	-0.024	0.129	0.032	0.146	0.143	0.241	0.178	-0.572
Row 2	-0.477	1.000	-0.574**	-0.209	0.746**	0.803**	-0.396*	-0.237	-0.343	-0.415	-0.751*
Row 3	0.151	0.574	1.000	0.818**	-0.851**	-0.887**	0.718**	0.727**	0.760**	0.818**	0.689*
Row 4	0.024	0.209	-0.818	1.000	-0.454*	-0.544**	0.653**	0.639**	0.472*	0.554*	0.617
Row 5	-0.129	-0.745	0.851	0.454	1.000	0.892**	-0.657**	-0.612**	-0.684**	-0.701**	-0.708
Row 6	-0.022	-0.803	0.887	0.544	-0.892	1.000	-0.697**	-0.671**	-0.693**	-0.752**	-0.875*
Row 7	-0.146	0.369	-0.718	-0.653	0.657	0.697	1.000	0.902**	0.768**	0.762**	0.689*
Row 8	-0.143	0.237	-0.727	-0.639	0.612	0.671	-0.902	1.000	0.715**	0.737**	-0.074
Row 9	-0.241	0.343	-0.760	-0.472	0.684	0.693	-0.758	-0.715	1.000	0.978**	0.993**
Row 10	-0.178	0.415	-0.818	-0.554	0.701	-0.752	-0.762	-0.737	-0.978	1.000	0.997**
Row 11	0.572	0.751	-0.689	-0.617	0.708	0.875	-0.689	0.075	-0.993	-0.997	1.000
Row 12	-0.273	-0.114	0.276	0.074	-0.591	-0.235	0.162	0.295	0.246	0.230	0.532
Row 13	0.032	0.573	-0.785	-0.683	0.766	0.895	-0.697	-0.637	-0.611	-0.701	-0.980
Row 14	-0.074	-0.221	-0.373	-0.236	0.319	0.381	0.3222	-0.172	0.119	0.058	0.348
Row 15	-0.534	0.513	-0.280	-0.055	0.748	0.711	-0.477	-0.343	-0.512	-0.326	0.000
Row 16	-0.643	-0.086	-0.456	-0.443	0.544	0.609	-0.697	-0.715	-0.779	-0.745	-0.246
Row 17	-0.529	0.143	-0.513	-0.430	0.504	0.636	-0.780	-0.730	-0.560	-0.538	0.321
Row 18	0.367	0.335	0.377	0.580	0.055	0.007	0.441	0.526	0.464	0.452	-0.196
Row 19	-0.374	-0.076	-0.251	-0.156	0.437	0.168	-0.631	-0.521	-0.526	-0.445	-0.820
Row 20	-0.366	0.092	-0.435	-0.438	0.418	0.553	-0.879	-0.829	-0.746	-0.696	-0.171
Row 21	0.808	0.724	-0.705	-0.410	0.662	0.832	-0.643	-0.686	-0.669	-0.721	-0.493

* Significant at the 5 % level
** Significant at the 1 % level

Table 17A (continued)

Column	12	13	14	15	16	17	18	19	20	21
Row 1	0.273	-0.032	0.074	0.534	0.643**	0.529**	-0.367	0.374	0.366	-0.080
Row 2	0.114	-0.573**	0.221	-0.513	0.086	-0.143	-0.335	0.076	-0.092	-0.724**
Row 3	-0.276	0.785**	0.373	0.290	0.456*	0.513*	-0.377	0.251	0.435*	0.705
Row 4	-0.074	0.683**	0.236	0.055	0.443*	0.430*	-0.580*	0.156	0.437*	0.410*
Row 5	0.591**	-0.766**	-0.319	-0.748*	-0.554*	-0.504*	-0.055	-0.437*	-0.418	-0.662**
Row 6	0.235	-0.895**	-0.381	-0.771*	-0.609**	-0.636**	-0.007	-0.168	-0.553*	-0.832**
Row 7	-0.162	0.697**	0.322	0.477	0.697**	0.780**	-0.441*	0.631	0.829**	0.686**
Row 8	-0.295	0.637**	0.172	0.343	0.715**	0.730**	-0.526	0.521*	0.829**	0.686**
Row 9	-0.246	0.611**	-0.119	0.512	0.779**	0.560*	-0.464*	0.526	0.746**	0.649**
Row 10	-0.230	0.701**	-0.058	0.326	0.745**	0.538*	-0.452*	0.445*	0.696*	0.721*
Row 11	-0,532	0.980**	-0.348	0.000	0.246	-0.321	0.196	0.820*	0.171	0.493
Row 12	1.000	-0.293	0.297	0.752*	-0.225	0.155	-0.108	-0.399	-0.135	-0.253
Row 13	0.295	1.000	0.283	0.457	0.538**	-0.448*	-0.093	0.141	0.519*	0.779**
Row 14	-0,297	-0.283	1.000	0.000	0.504*	0.459	-0.365	-0.012	0.351	-0.059
Row 15	-0.752	-0.457	0.000	1.000	0.580	0.984**	-0.478	-0.224	0.662	0.717*
Row 16	0.225	-0.538	-0.504	-0.580	1.000	0.808**	-0.439*	0.543**	0.836**	0.418*
Row 17	-0.155	-0.448	-0.459	-0.984	-0.808	1.000	-0.424*	0.451*	0.813**	0.549*
Row 18	0.108	0.093	0.365	0.478	0.439	0.424	1.000	-0.377*	-0.419	-0.022
Row 19	0.399	-0.141	0.012	0.224	-0.543	-0.451	0.377	1.000	0.582**	0.081
Row 20	0.135	-0.519	-0.351	-0.662	-0.836	-0.813	0.419	-0.582	1.000	0.521*
Row 21	0.253	-0.779	0.059	0.059	-0.717	-0.418	-0.549	0.022	0.521	1.000

* Significant at the 5% level
** Significant at the 1% level

Table 17B Significant Level of b

Column	1	2	3	4	5	6	7	8	9	10	11	12	13	14	15	16	17	18	19	20	21
Row 1		**														***	**				
Row 2			***		***	***	*				*		**								***
Row 3				***	***	***	***	***	***	***			***			*	*			*	***
Row 4					*	**	***	***	*	*			***			*	*	*			*
Row 5						***	***	***	***	***		**	***		*	**	*				***
Row 6							***	***	***	***	*		***		*	***	***			*	***
Row 7								***	***	***			***			***	***		***	***	***
Row 8									***	***			***			***	***	*	*	***	***
Row 9										***	***		**			***	*	*	*	***	***
Row 10											***		***			***	*	*	*	***	***
Row 11													***						*		
Row 12														*							
Row 13															**	*				*	***
Row 14																					
Row 15																	***				*
Row 16																	***	*	*	***	*
Row 17																			*	***	*
Row 18																					
Row 19																				**	
Row 20																					*
Row 21																					

* Significant at the 5% level
** Significant at the 1% level
*** Significant at the 0.5 % level

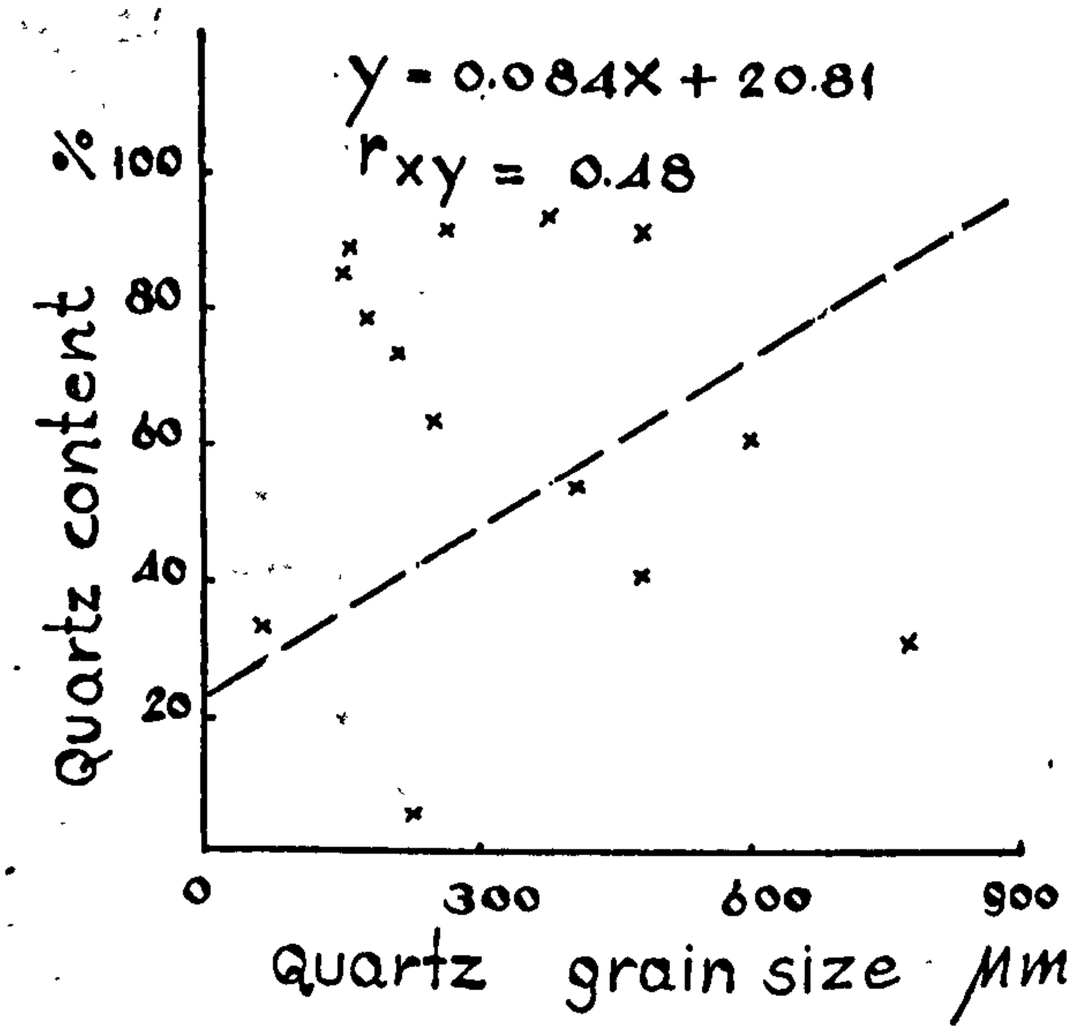
y = 0.084X + 20.81
r_{xy} = 0.48
Quartz content %
100
80
60
40
20
0
300
600
900
Quartz grain size μm

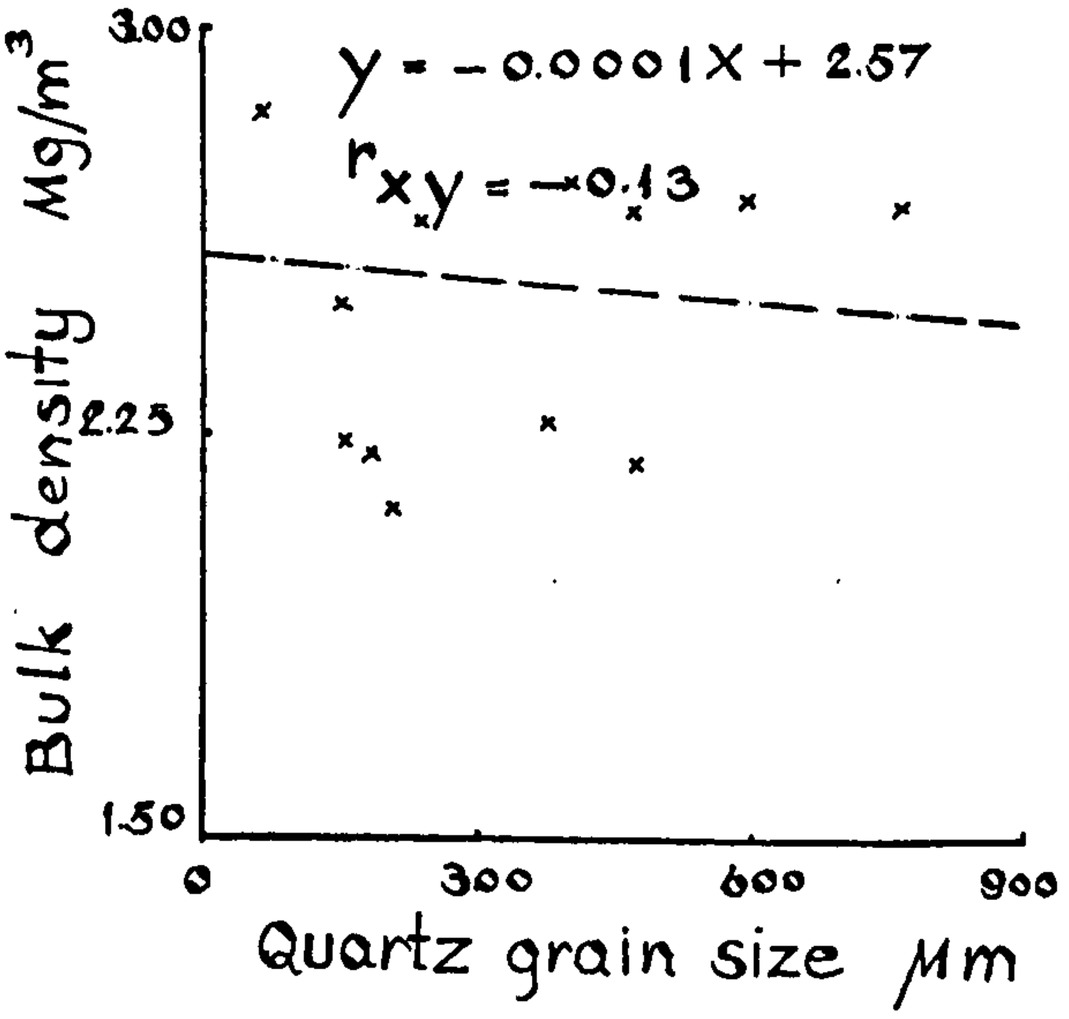
y = −0.0001X + 2.57
r_{xy} = −0.13
Bulk density Mg/m³
3.00
2.25
1.50
0
300
600
900
Quartz grain size μm

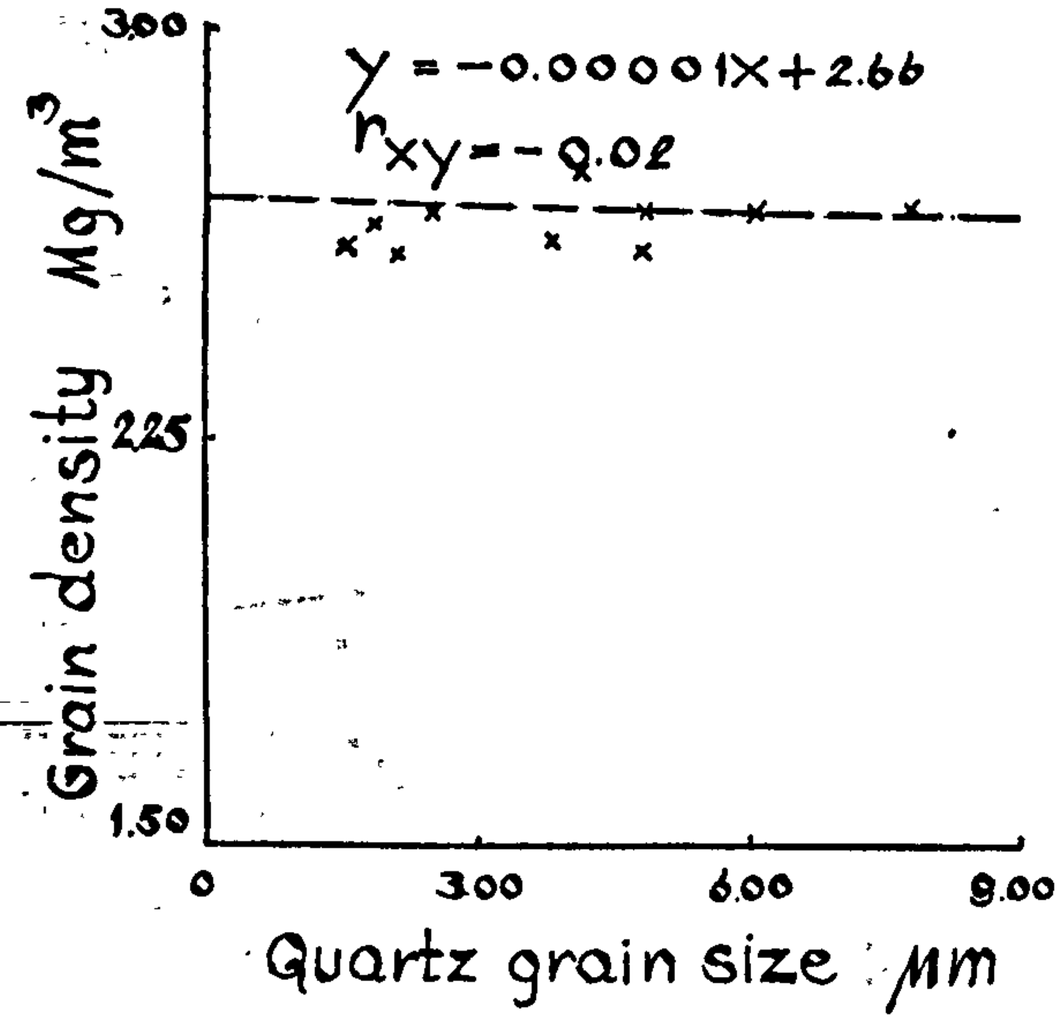
y = −0.00001X + 2.66
r_{xy} = −0.02
Grain density Mg/m³
3.00
2.25
1.50
0
300
600
900
Quartz grain size μm

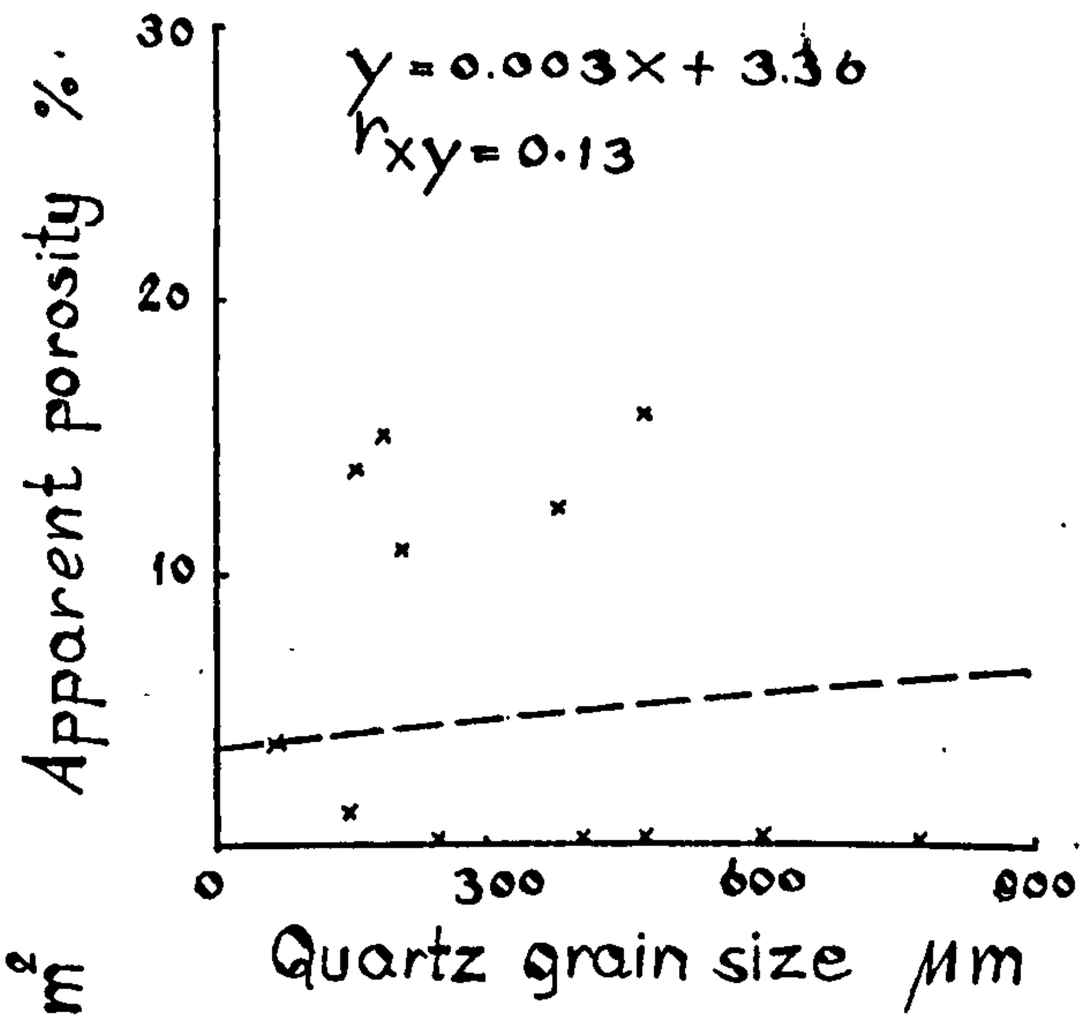
y = 0.003X + 3.36
r_{xy} = 0.13
Apparent porosity %
30
20
10
0
300
600
900
Quartz grain size μm

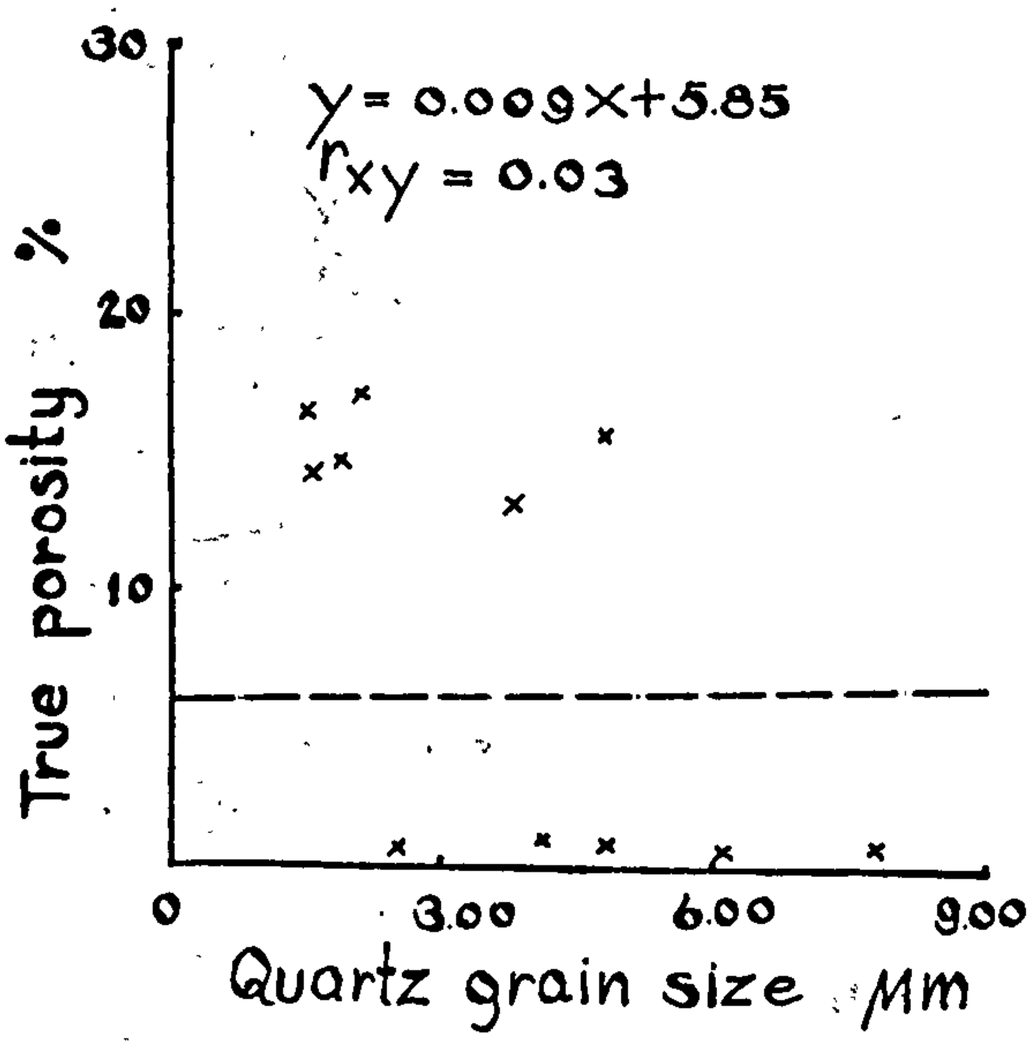
y = 0.009X + 5.85
r_{xy} = 0.03
True porosity %
30
20
10
0
3.00
6.00
9.00
Quartz grain size μm

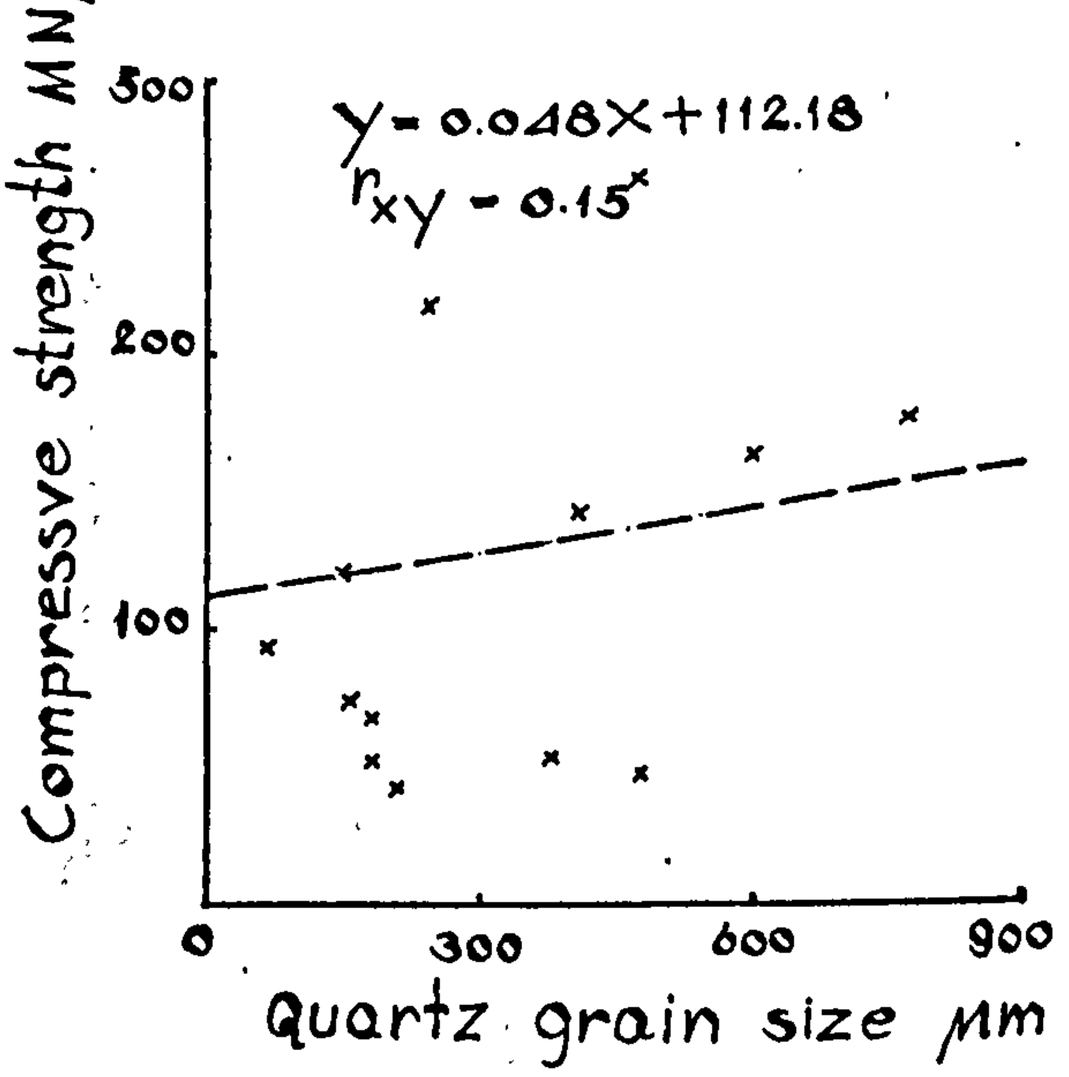
y = 0.048X + 112.18
r_{xy} = 0.15
Compressve strength MN/m²
300
200
100
0
300
600
900
Quartz grain size μm

Figure 47 (1)

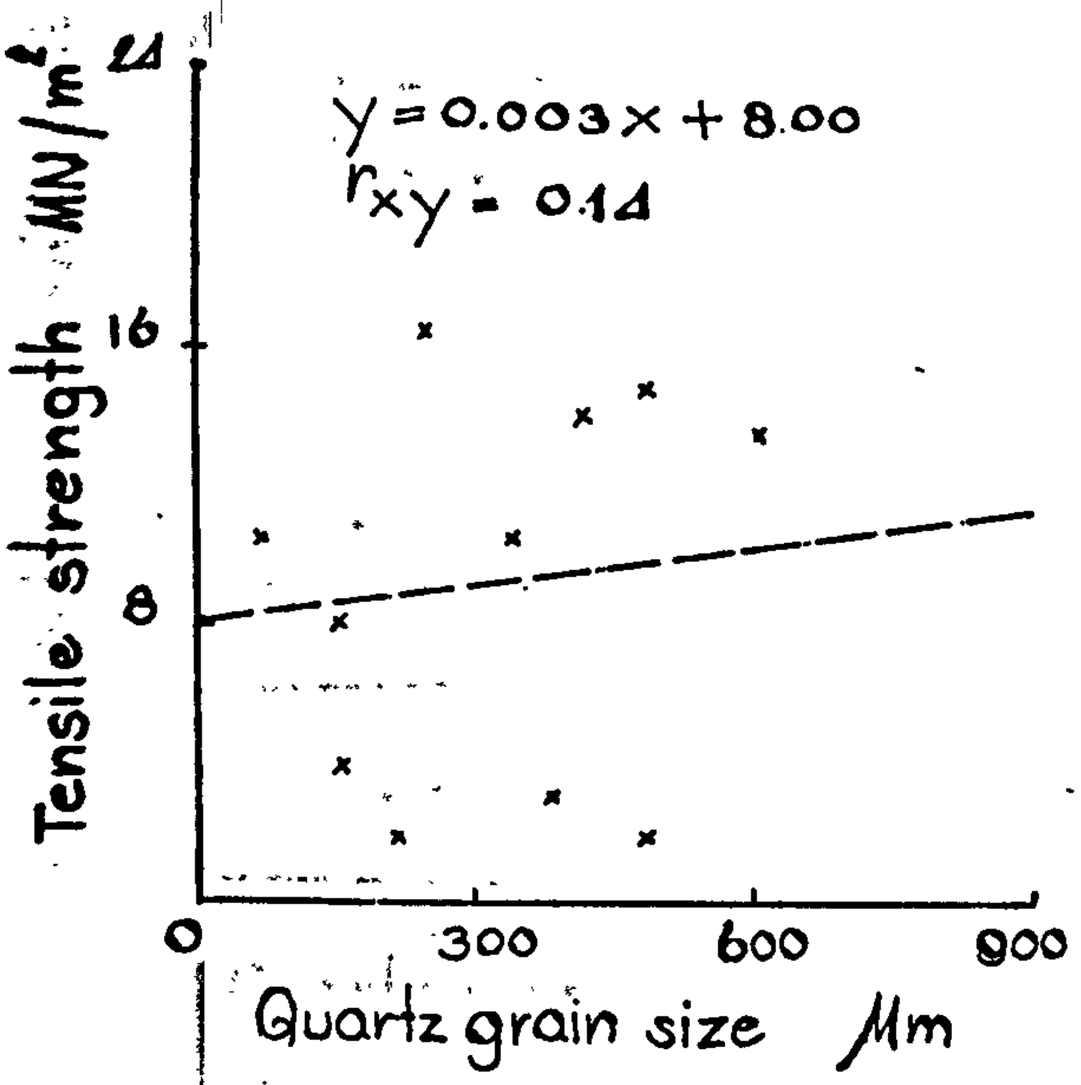
Tensile strength MN/m²
y = 0.003x + 8.00
r_xy = 0.14
16
8
0
300
600
900
Quartz grain size /Mm

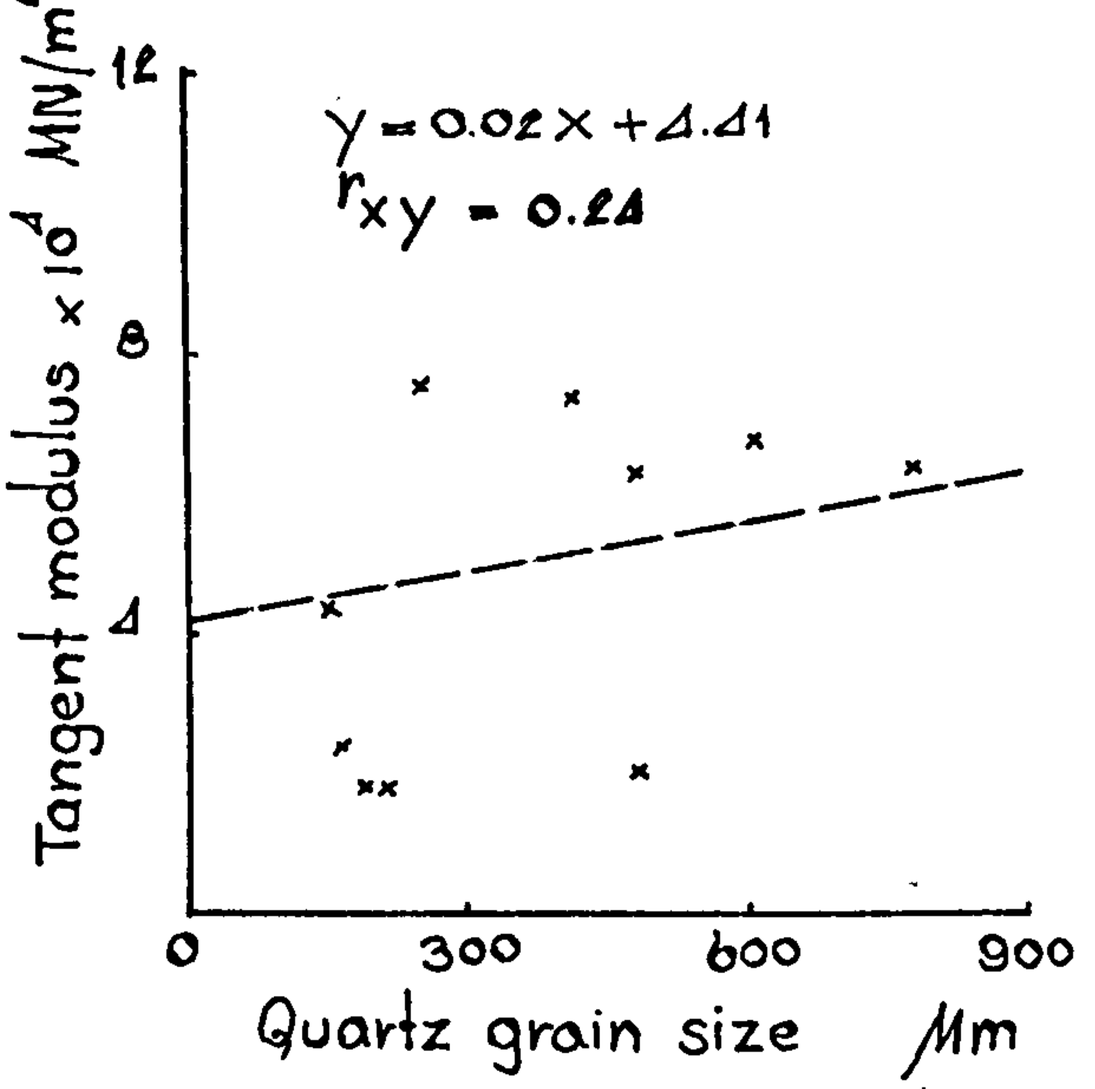
Tangent modulus ×10⁴ MN/m²
y = 0.02x + 4.41
r_xy = 0.24
12
8
4
0
300
600
900
Quartz grain size /Mm

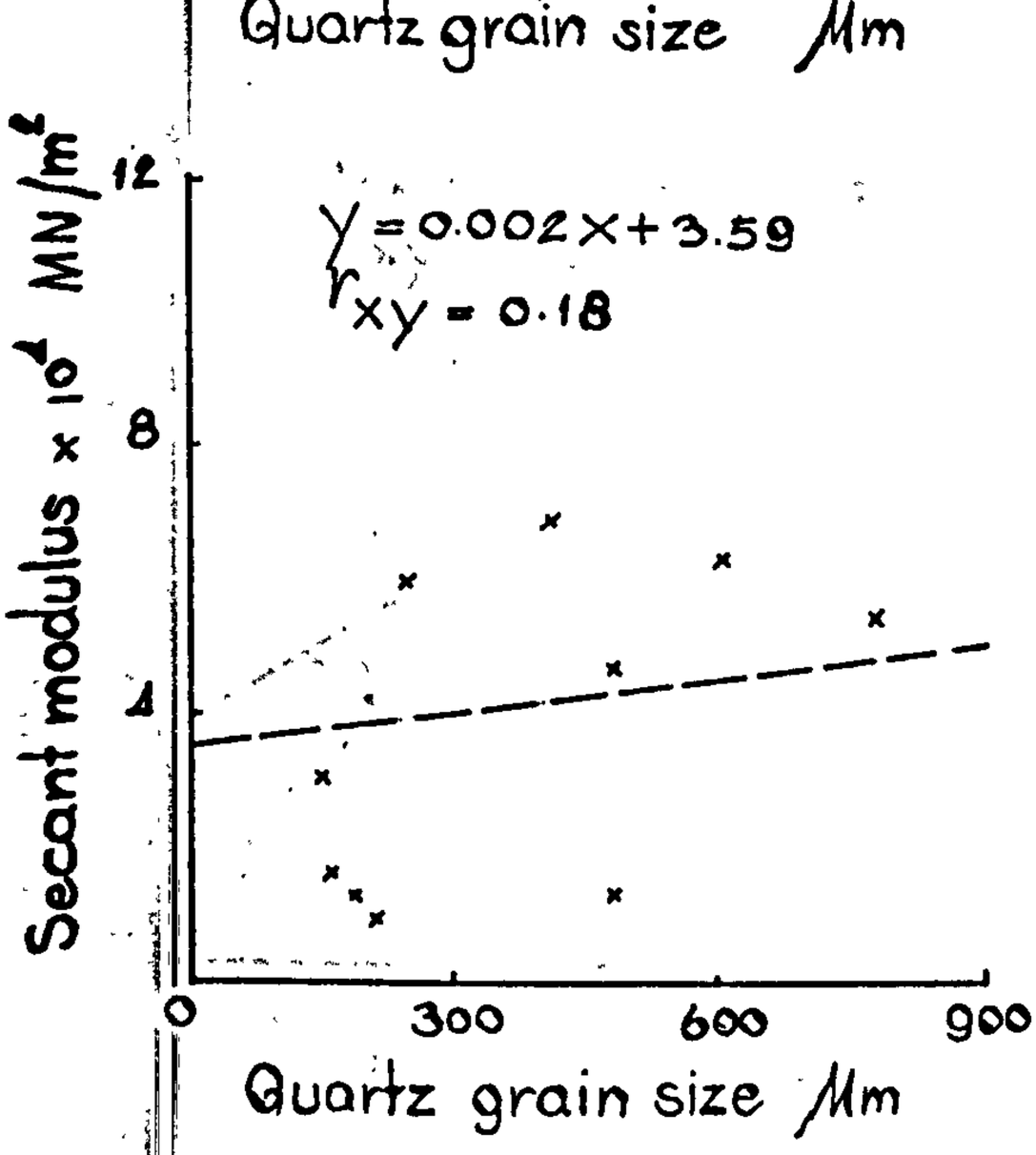
Secant modulus ×10⁴ MN/m²
y = 0.002x + 3.59
r_xy = 0.18
12
8
4
0
300
600
900
Quartz grain size /Mm

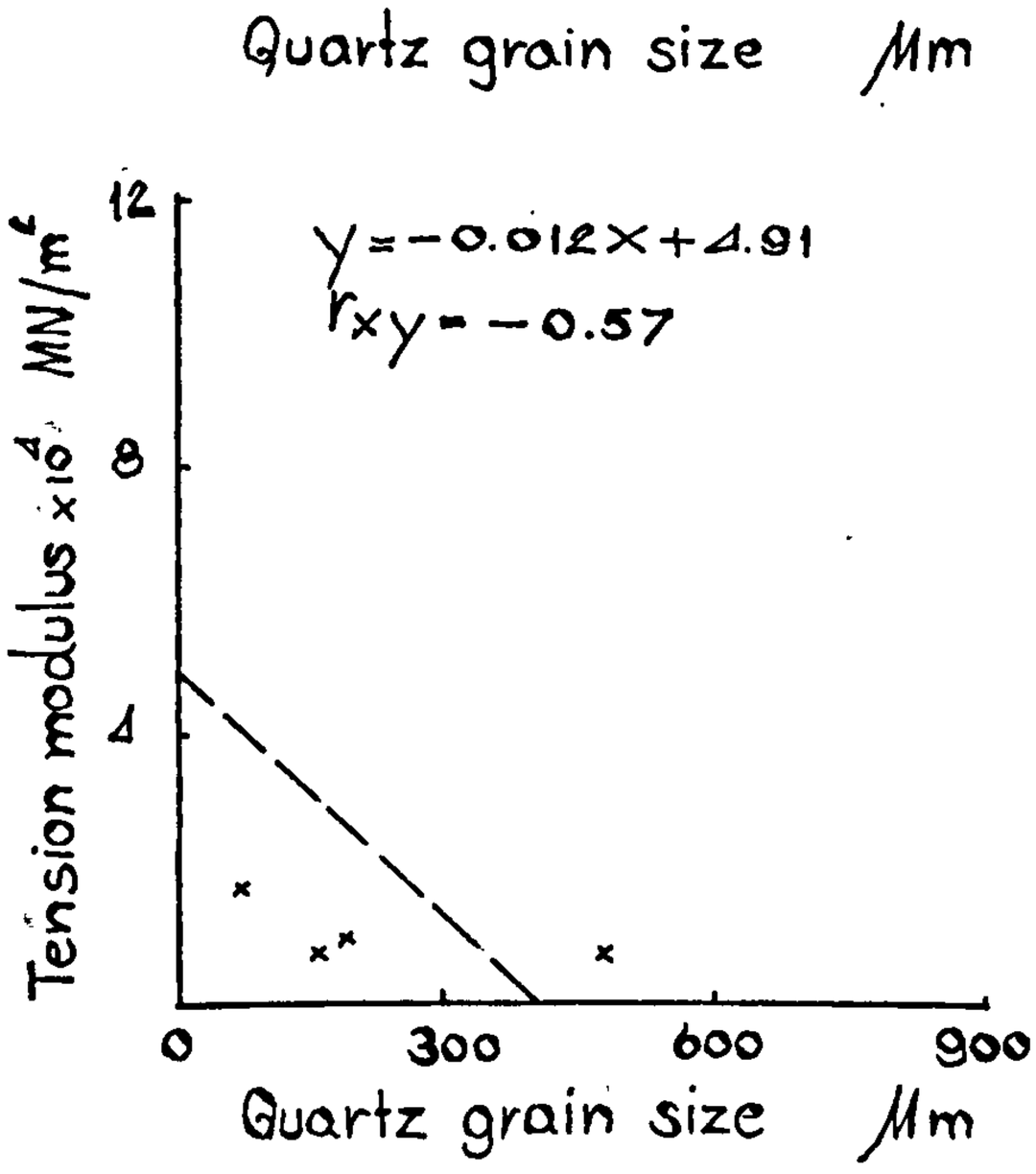
Tension modulus ×10⁴ MN/m²
y = −0.012x + 4.91
r_xy = −0.57
12
8
4
0
300
600
900
Quartz grain size /Mm

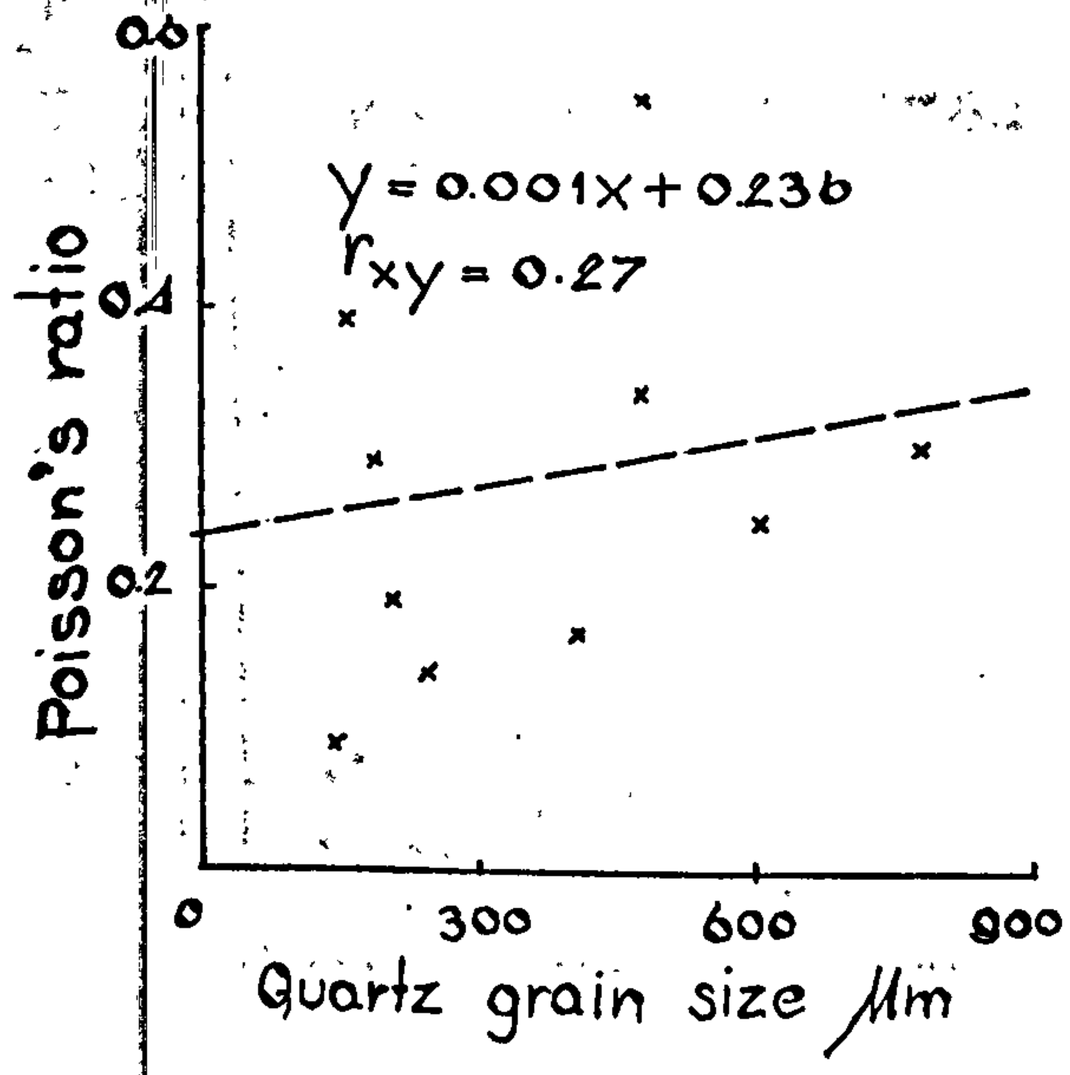
Poisson's ratio
y = 0.001x + 0.236
r_xy = 0.27
0.6
0.4
0.2
0
300
600
900
Quartz grain size /Mm

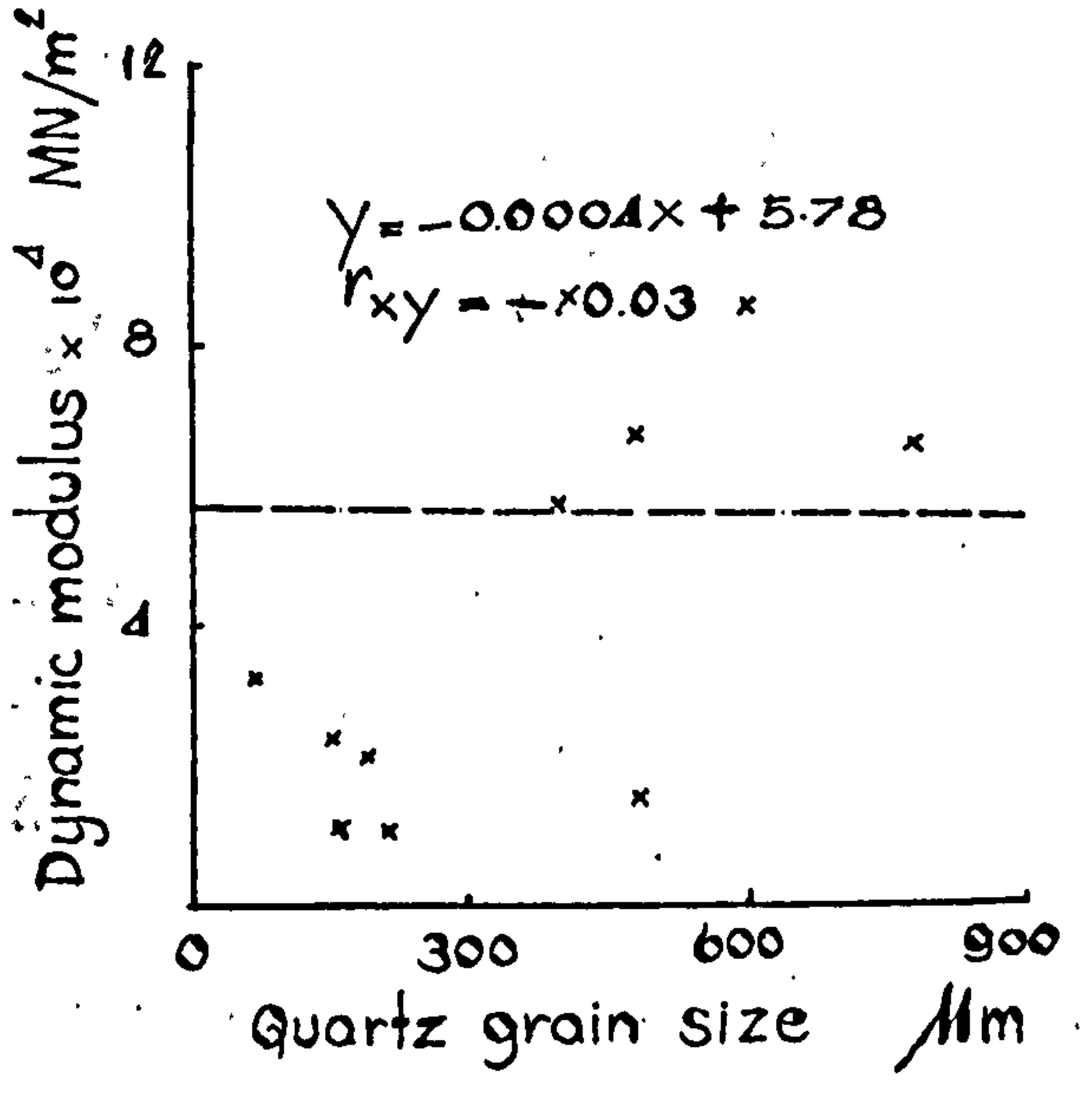
Dynamic modulus ×10⁴ MN/m²
y = −0.0004x + 5.78
r_xy = −0.03
12
8
4
0
300
600
900
Quartz grain size /Mm

Figure 47 (2)

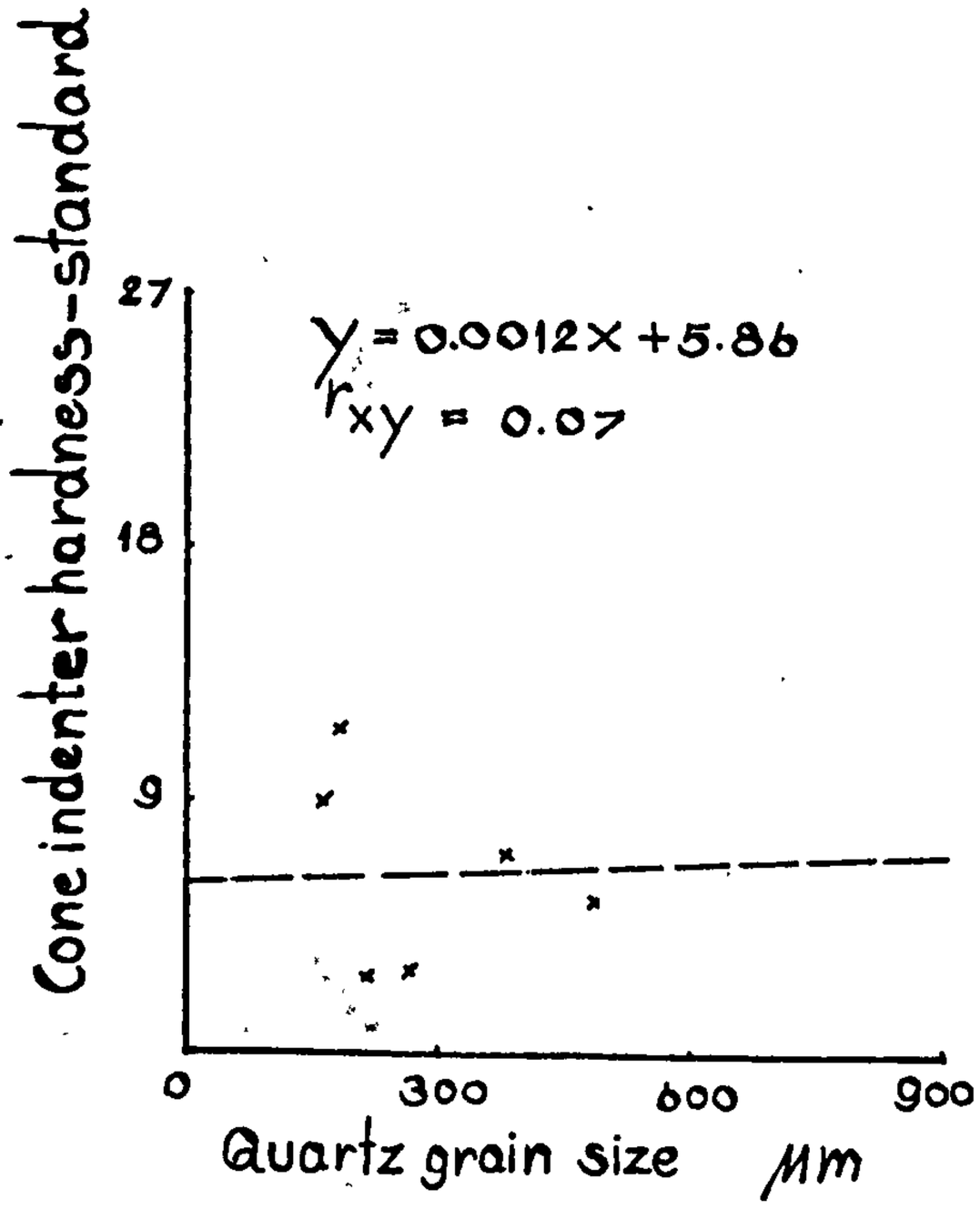
Y = 0.0012X + 5.86
r_{xy} = 0.07
Cone indenter hardness-standard
27
18
9
0
300
600
900
Quartz grain size μm

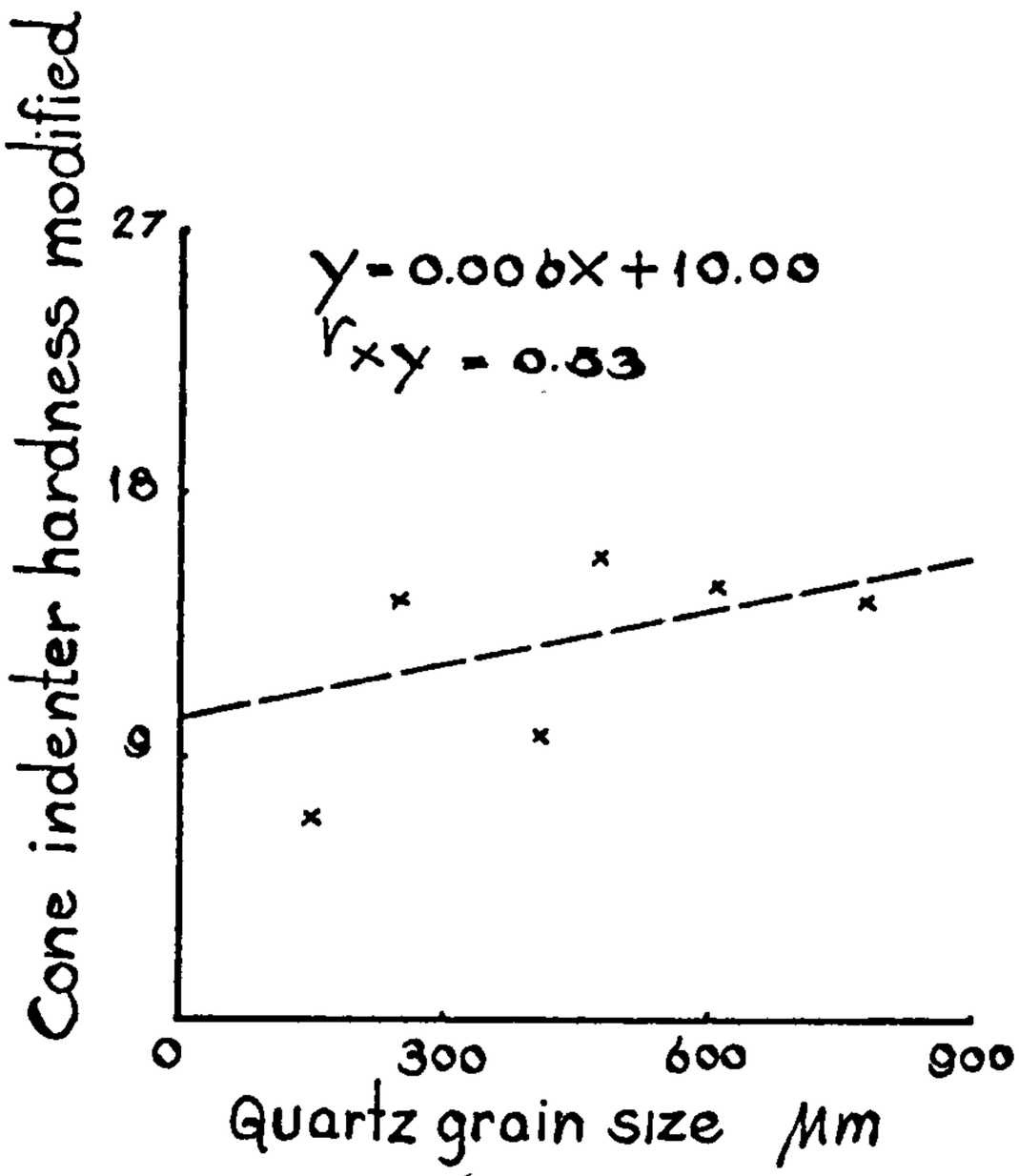
Y = 0.006X + 10.00
r_{xy} = 0.83
Cone indenter hardness modified
27
18
9
0
300
600
900
Quartz grain size μm

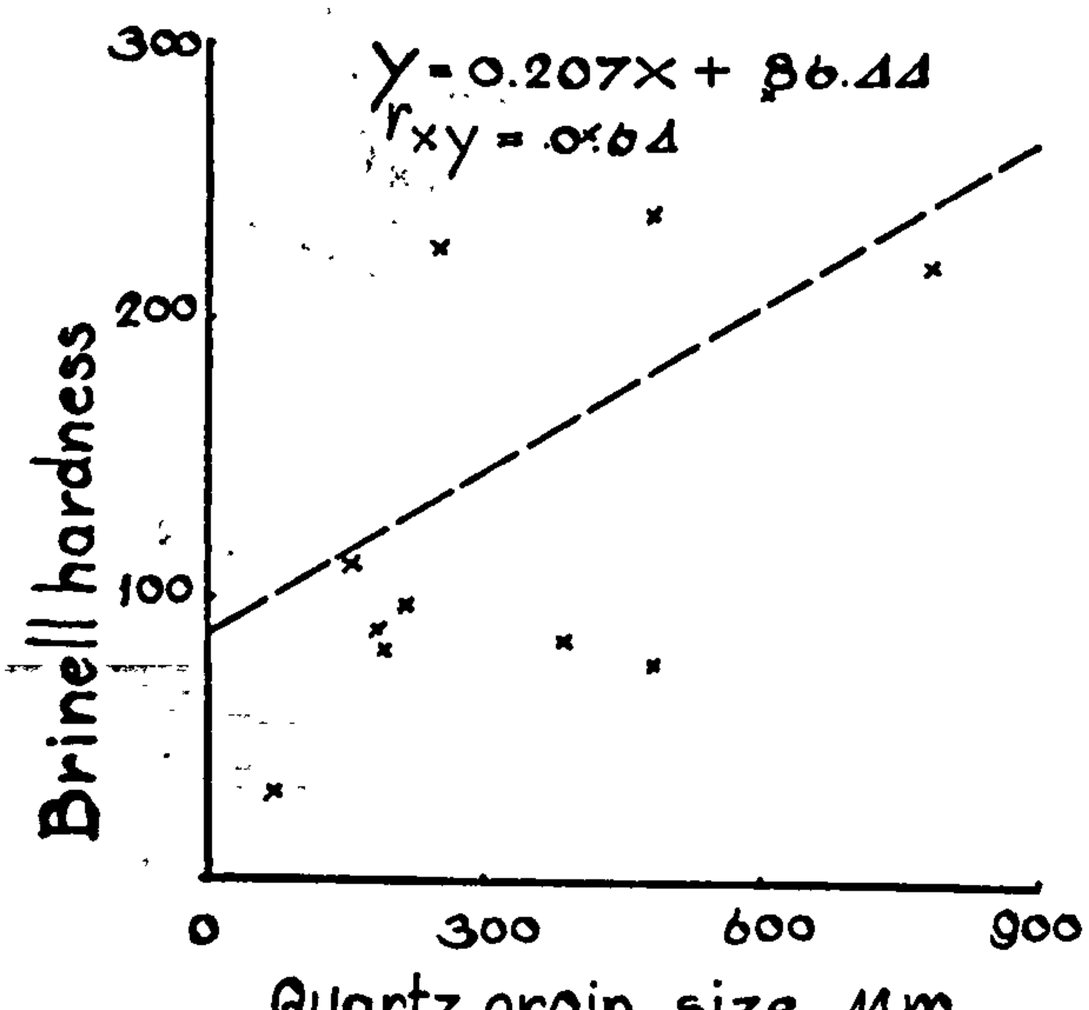
Y = 0.207X + 86.44
r_{xy} = 0.64
Brinell hardness
300
200
100
0
300
600
900
Quartz grain size μm

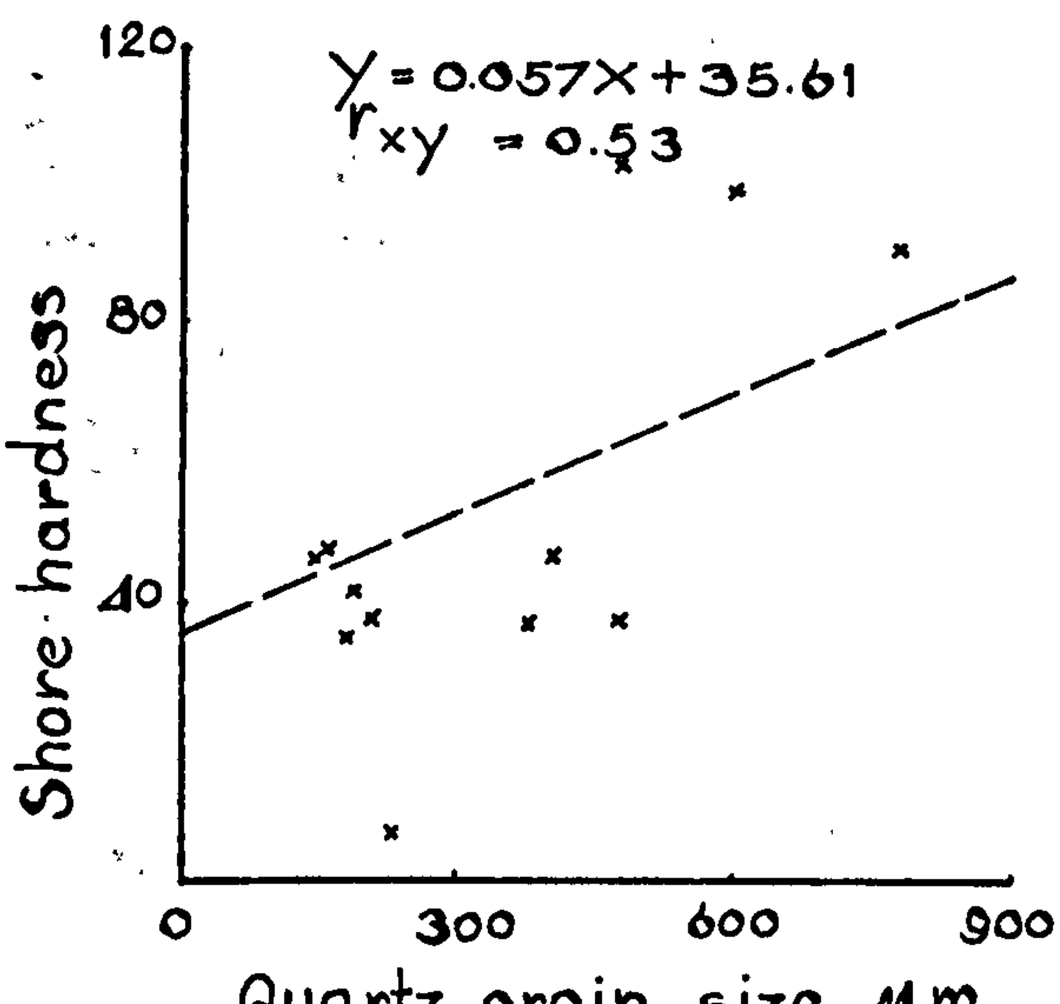
Y = 0.057X + 35.61
r_{xy} = 0.53
Shore hardness
120
80
40
0
300
600
900
Quartz grain size μm

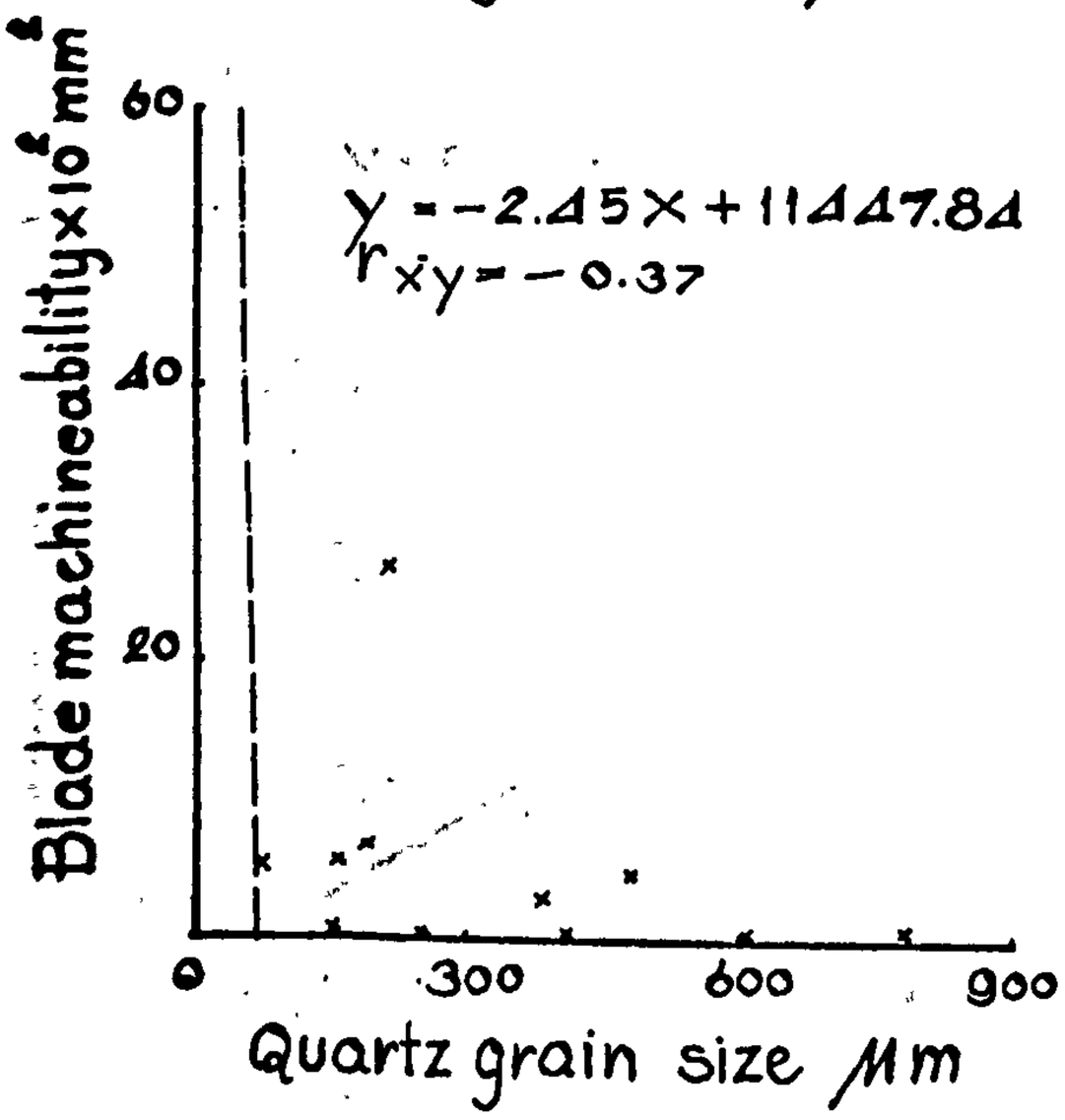
Y = −2.45X + 1147.84
r_{xy} = −0.37
Blade machineability x 10^4 mm
60
40
20
0
300
600
900
Quartz grain size μm

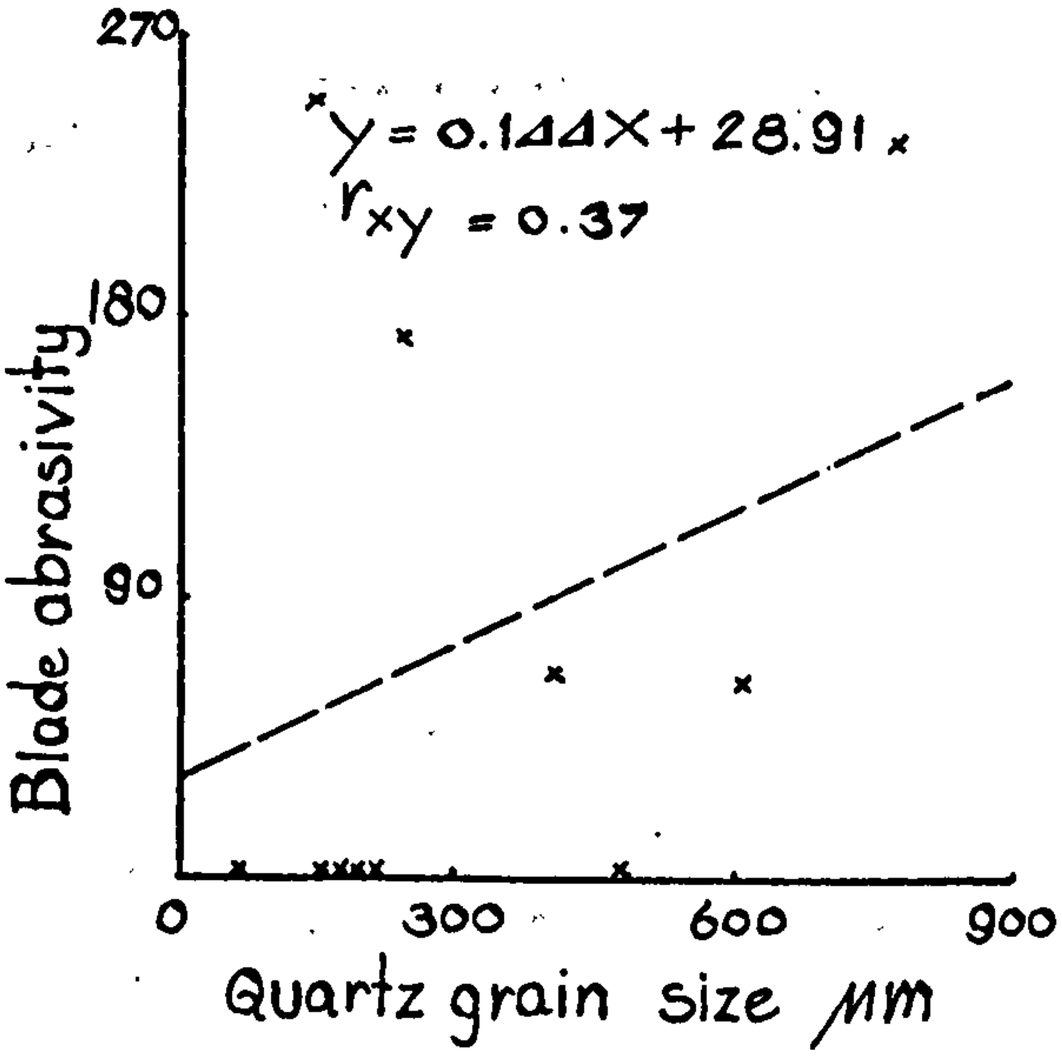
Y = 0.144X + 28.91
r_{xy} = 0.37
Blade abrasivity
270
180
90
0
300
600
900
Quartz grain size μm

Figure 47 (3)

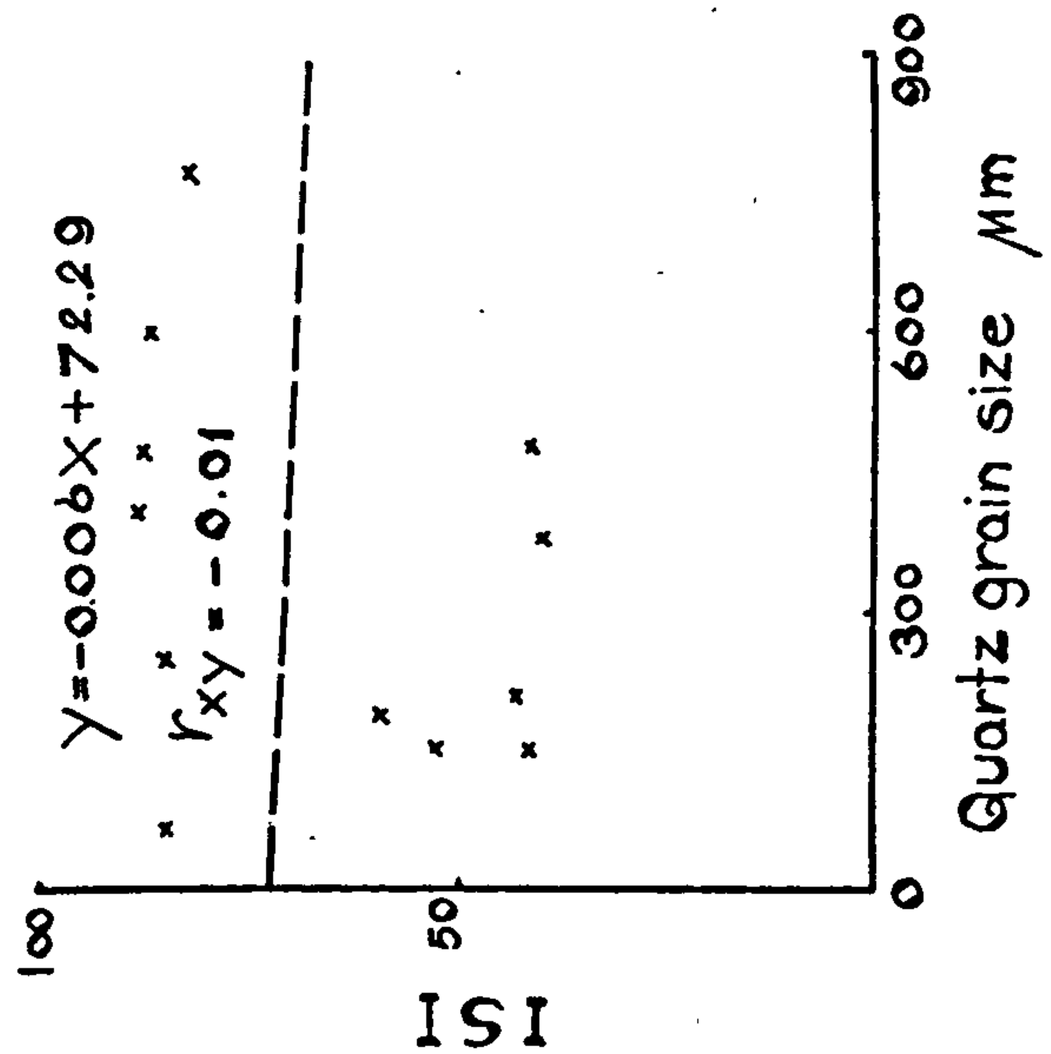
ISI
100
50
0
Y=-0.006X+72.29
r_{xy} = -0.01
0
300
600
900
Quartz grain size /Mm

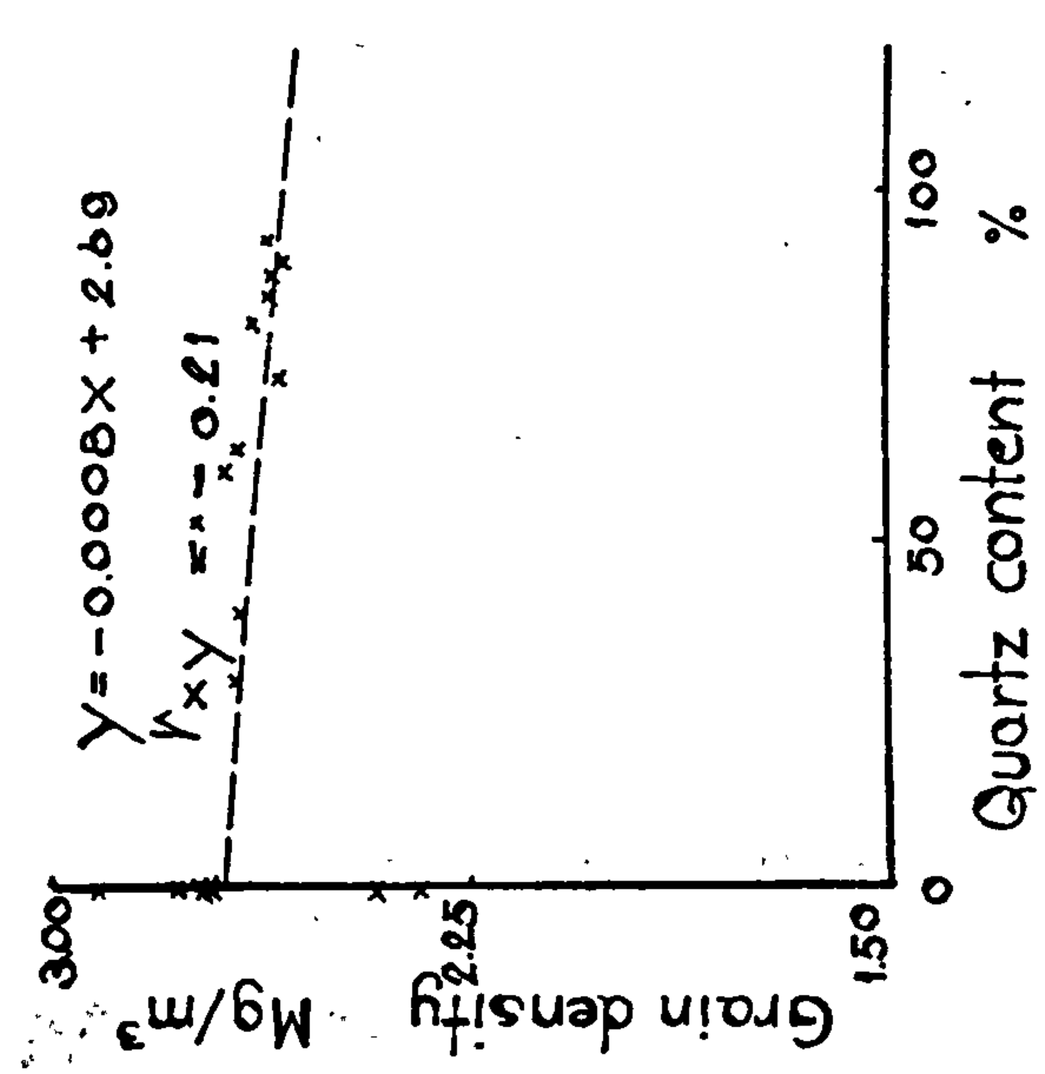
Grain density Mg/m³
300
2.25
150
Y=-0.0008X+2.69
r_{xy} = -0.21
0
50
100
Quartz content %

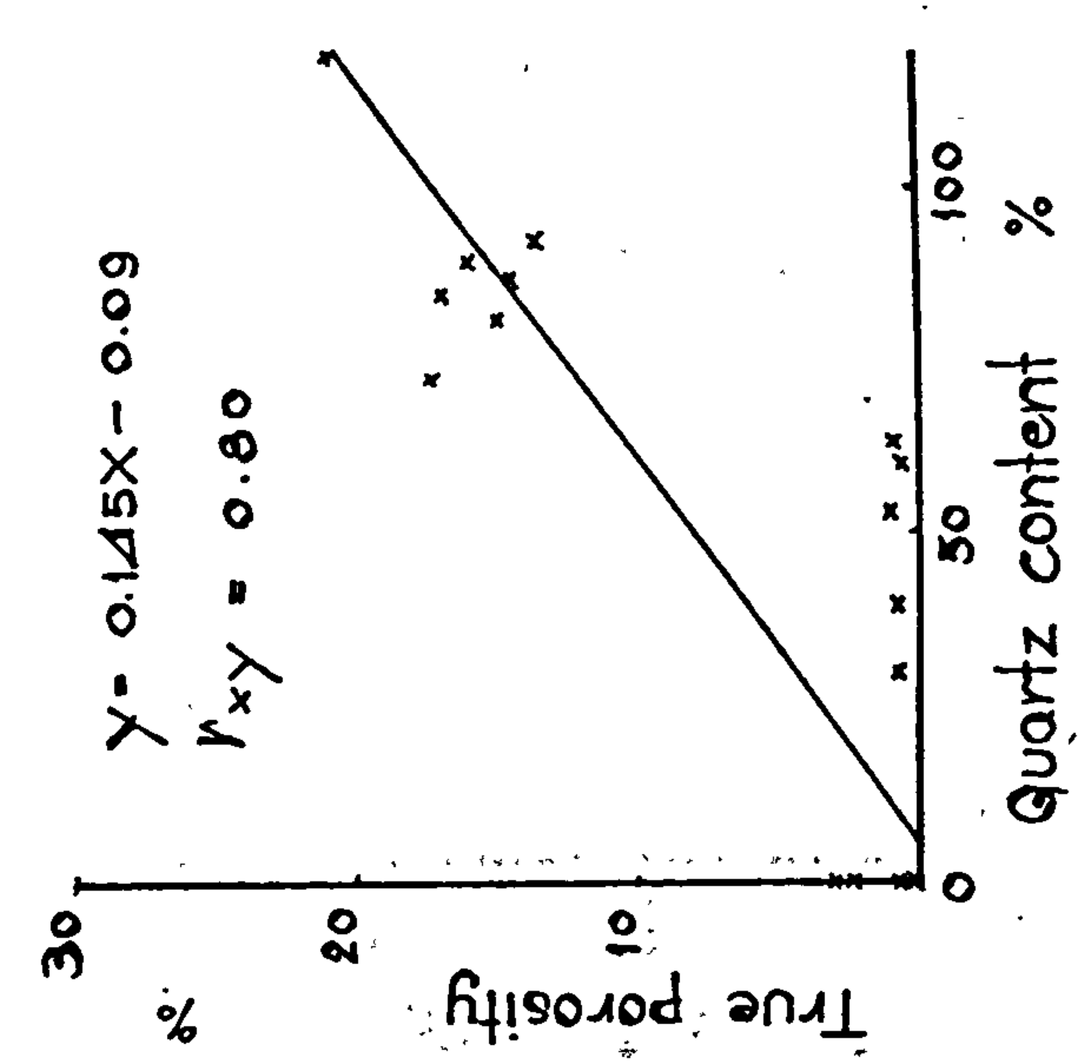
True porosity %
30
20
10
Y= 0.145X-0.09
r_{xy} = 0.80
0
50
100
Quartz content %

Figure 47 (A)

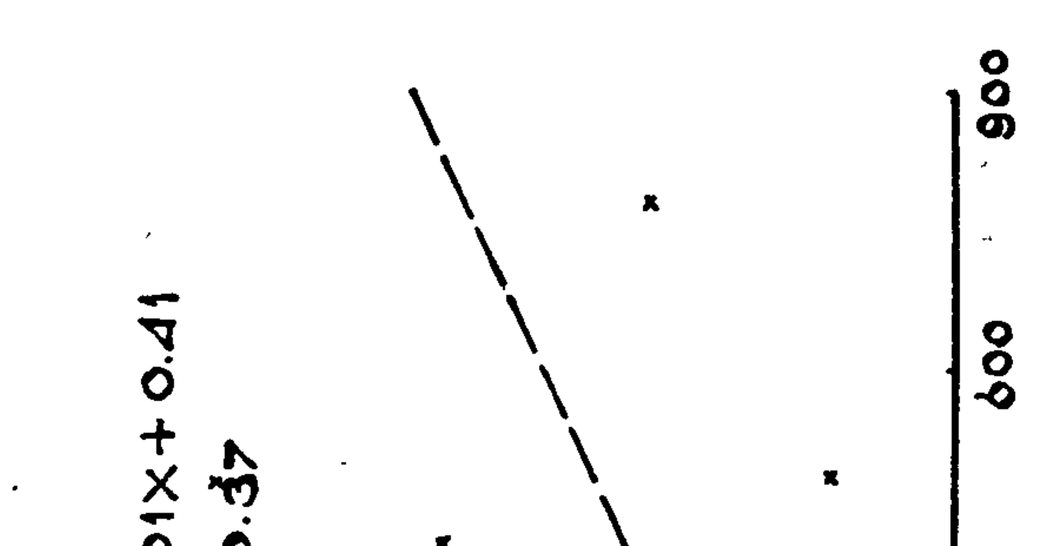
Abrasion factor MN/m
2.4
1.6
0.8
Y= 0.001X+0.41
r_{xy} = 0.37
0
300
600
900
Quartz grain size /Mm

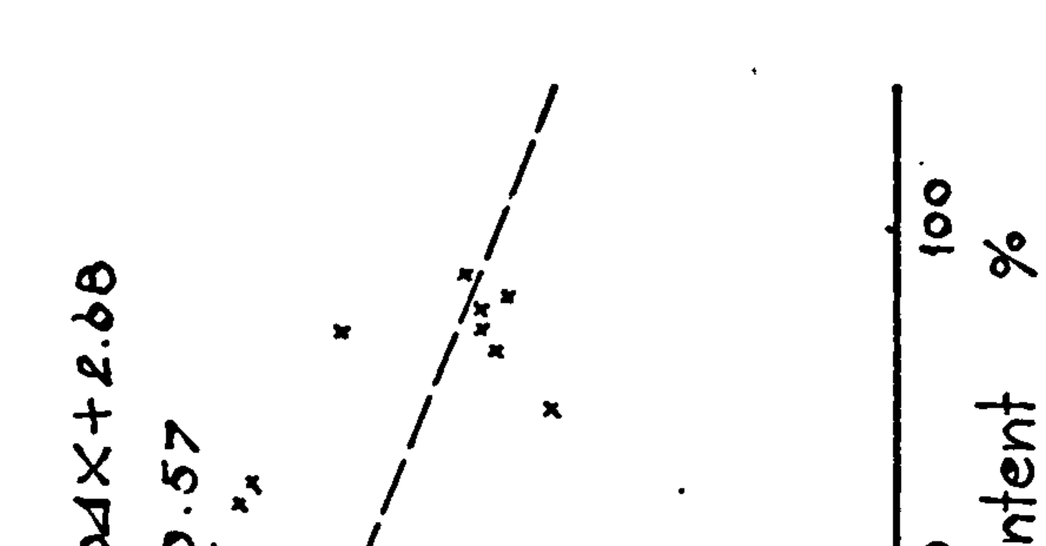
Bulk density Mg/m³
3.00
2.25
1.50
Y=-0.0024X+2.68
r_{xy} =-0.57
0
50
100
Quartz content %

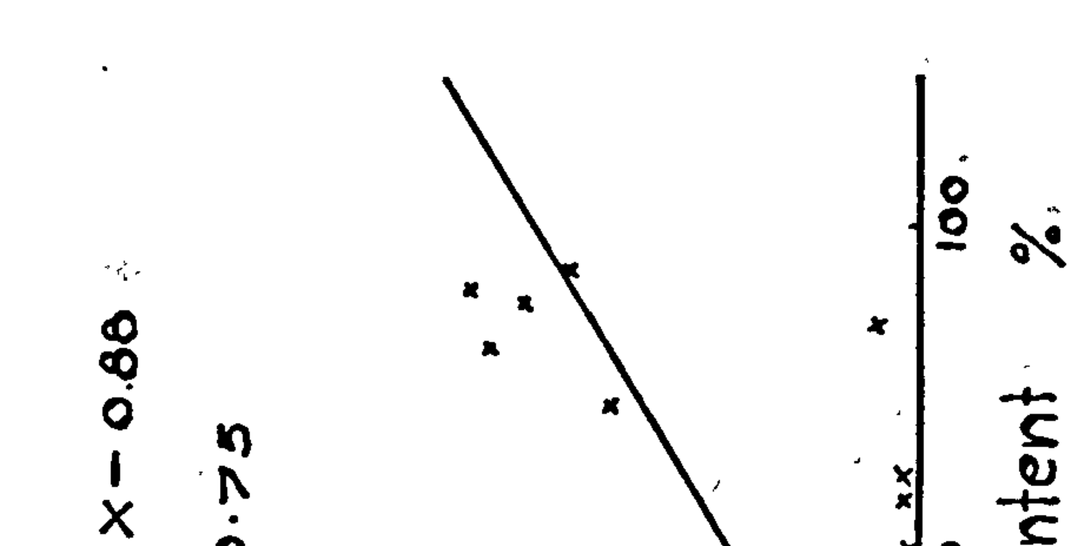
Apparent porosity %
30
20
10
Y= 0.119X-0.88
r_{xy} = 0.75
0
50
100
Quartz content %

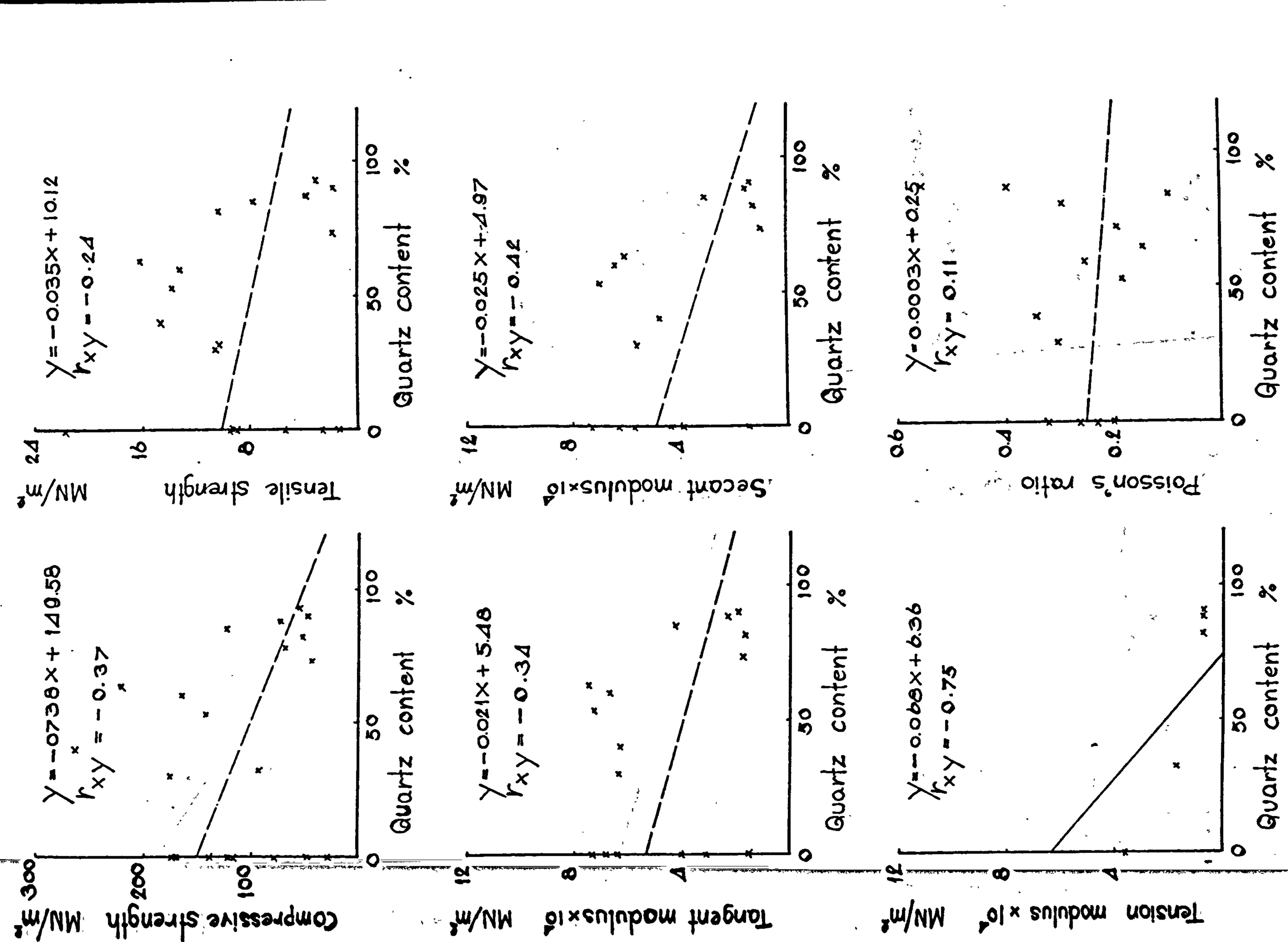
Tensile strength MN/m²
Y=-0.035X+10.12
r_xy=-0.24
Quartz content %
Secant modulus×10⁴ MN/m²
Y=-0.025X+4.97
r_xy=-0.42
Quartz content %
Poisson's ratio
Y=-0.0003X+0.25
r_xy=-0.11
Quartz content %
Compressive strength MN/m²
Y=-0.738X+140.58
r_xy=-0.37
Quartz content %
Tangent modulus×10⁴ MN/m²
Y=-0.021X+5.48
r_xy=-0.34
Quartz content %
Tension modulus ×10⁴ MN/m²
Y=-0.069X+6.36
r_xy=-0.75
Quartz content %

Figure 47 (5)

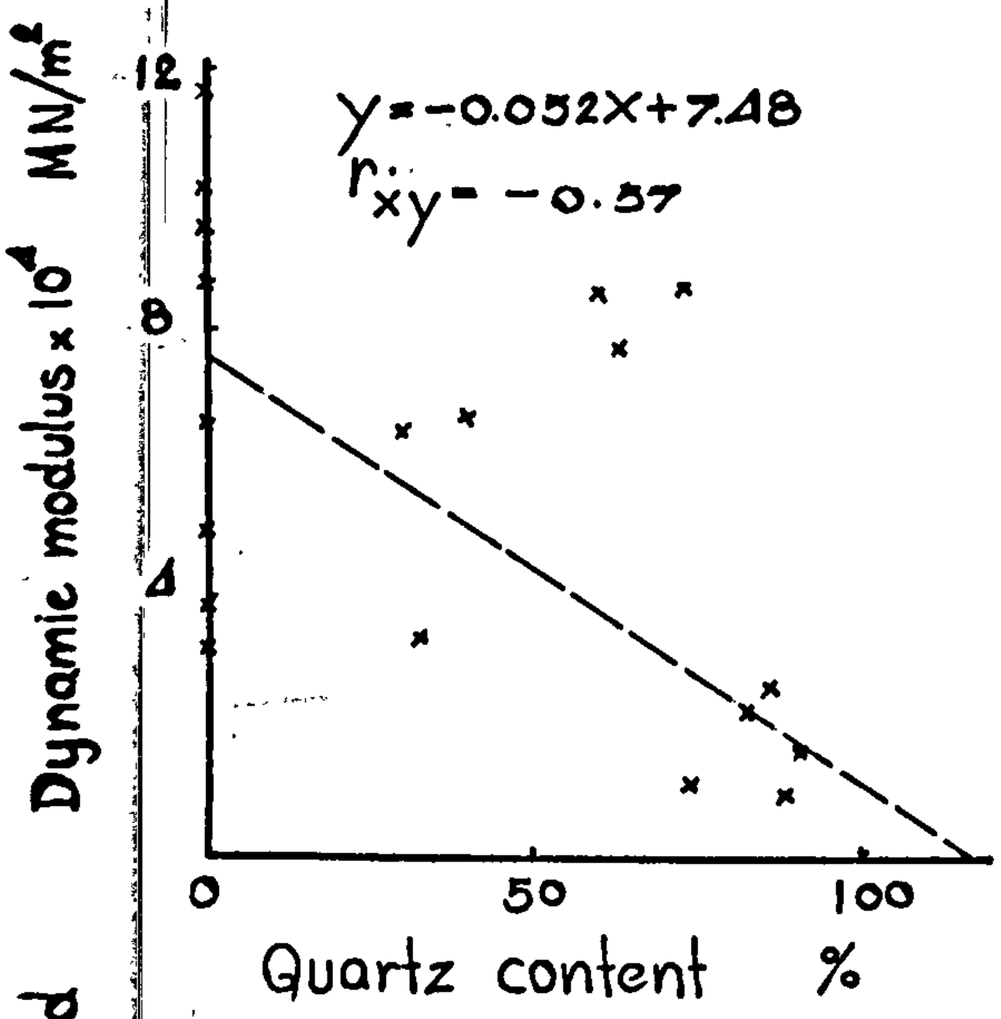
Dynamic modulus x 10⁴ MN/m²
12
8
4
0
50
100
Quartz content %
y=-0.052X+7.48
r_xy = -0.57

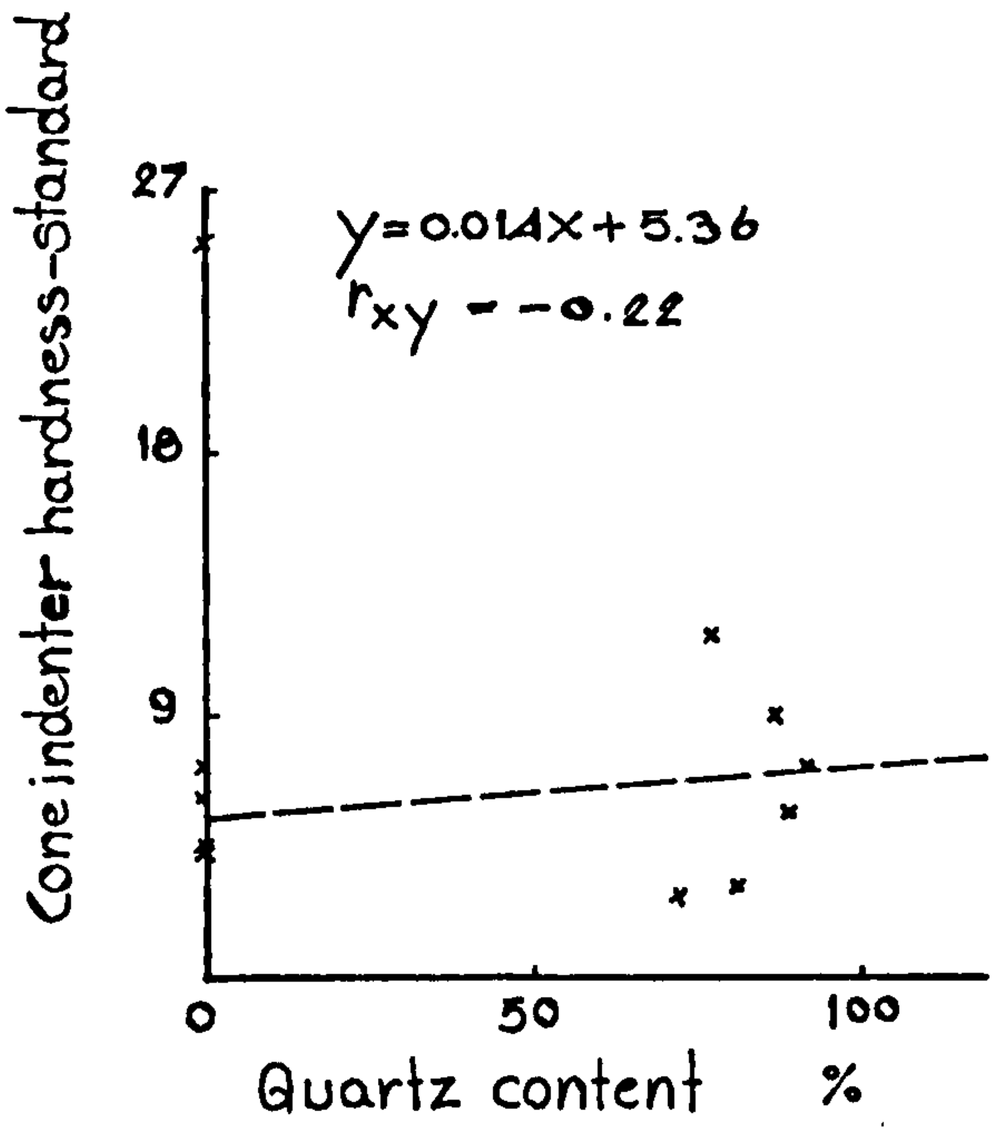
Cone indenter hardness-standard
27
18
9
0
50
100
Quartz content %
y=0.014X+5.36
r_xy = -0.22

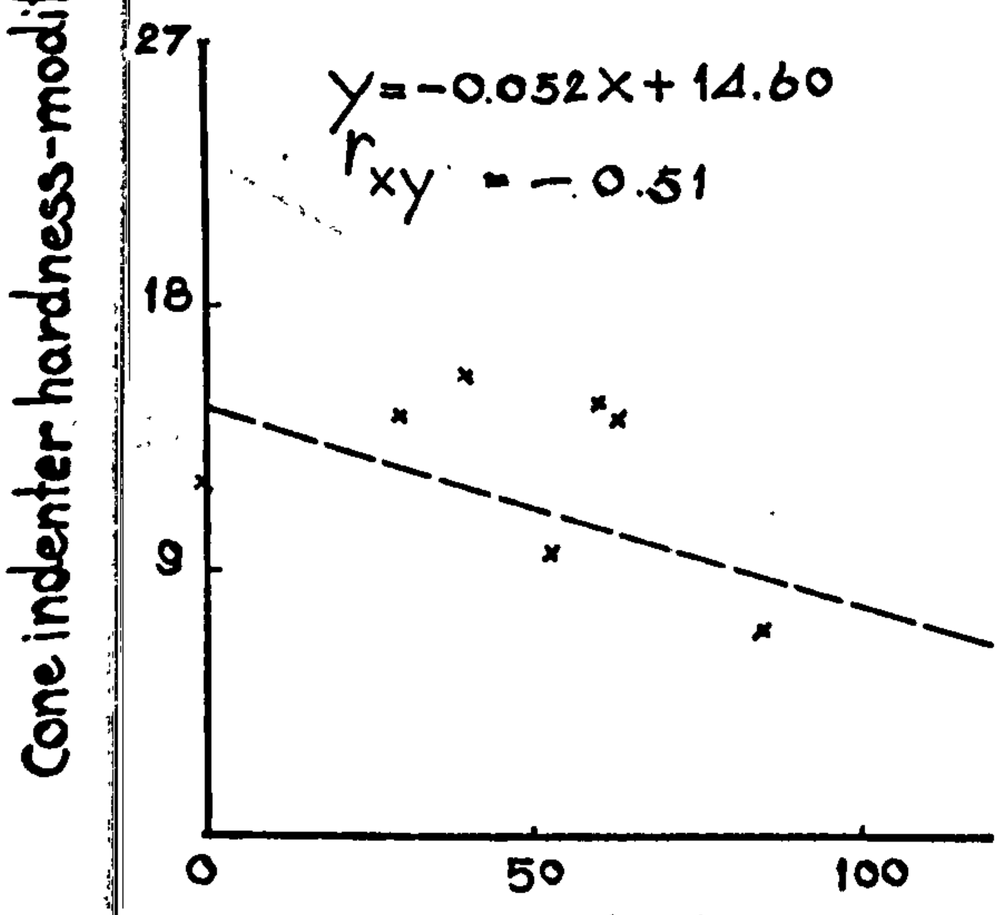
Cone indenter hardness-modified
27
18
9
0
50
100
Quartz content %
y=-0.052X+14.60
r_xy = -0.51

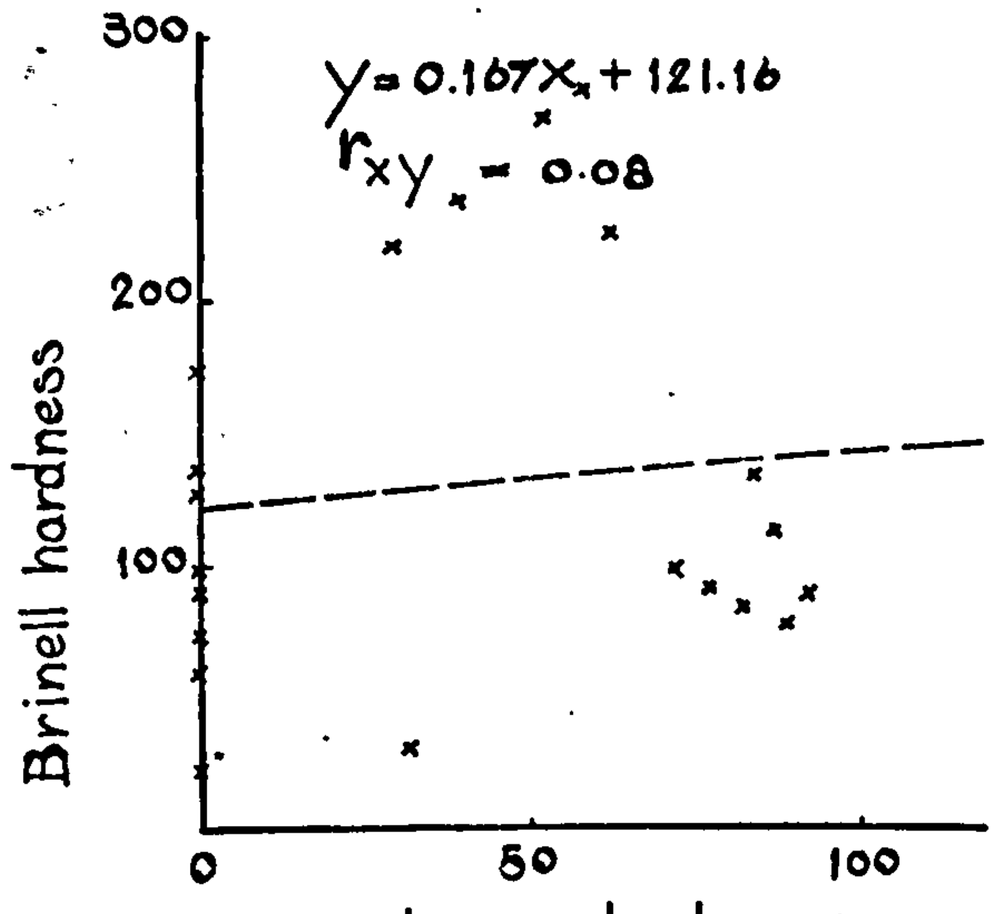
Brinell hardness
300
200
100
0
50
100
Quartz content %
y=0.167X+121.16
r_xy = 0.08

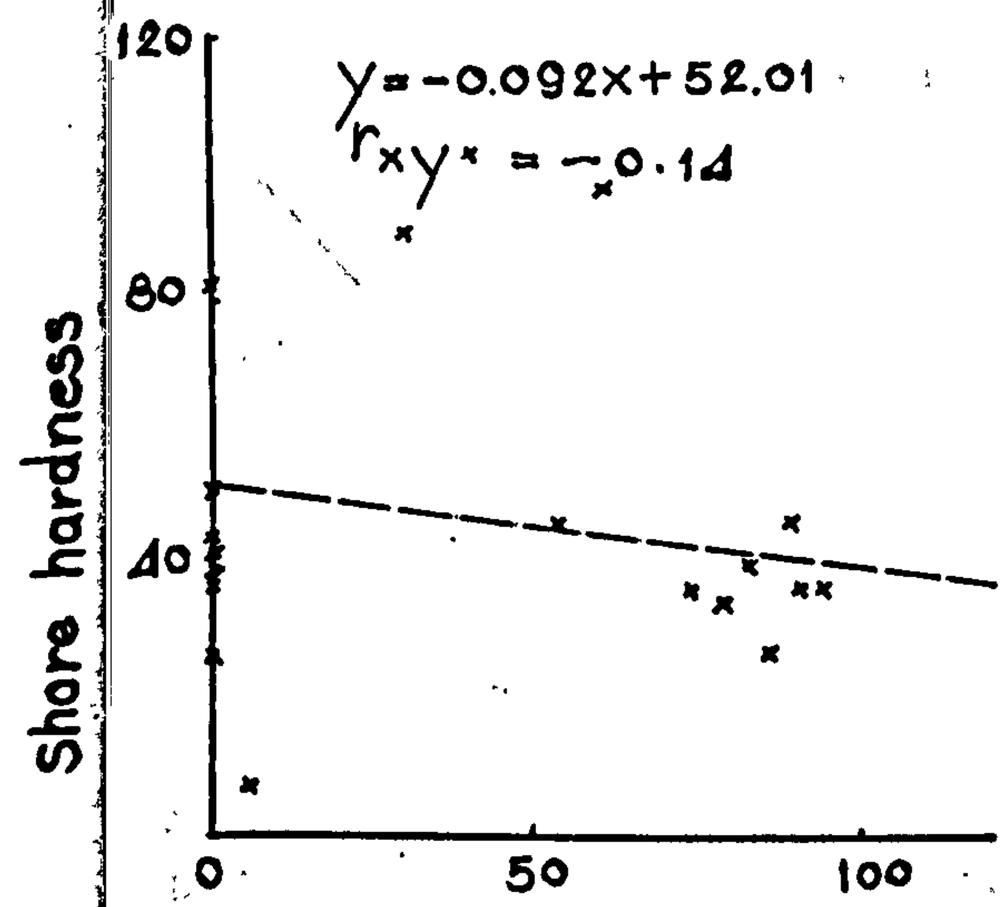
Shore hardness
120
80
40
0
50
100
Quartz content %
y=-0.092X+52.01
r_xy = -0.14

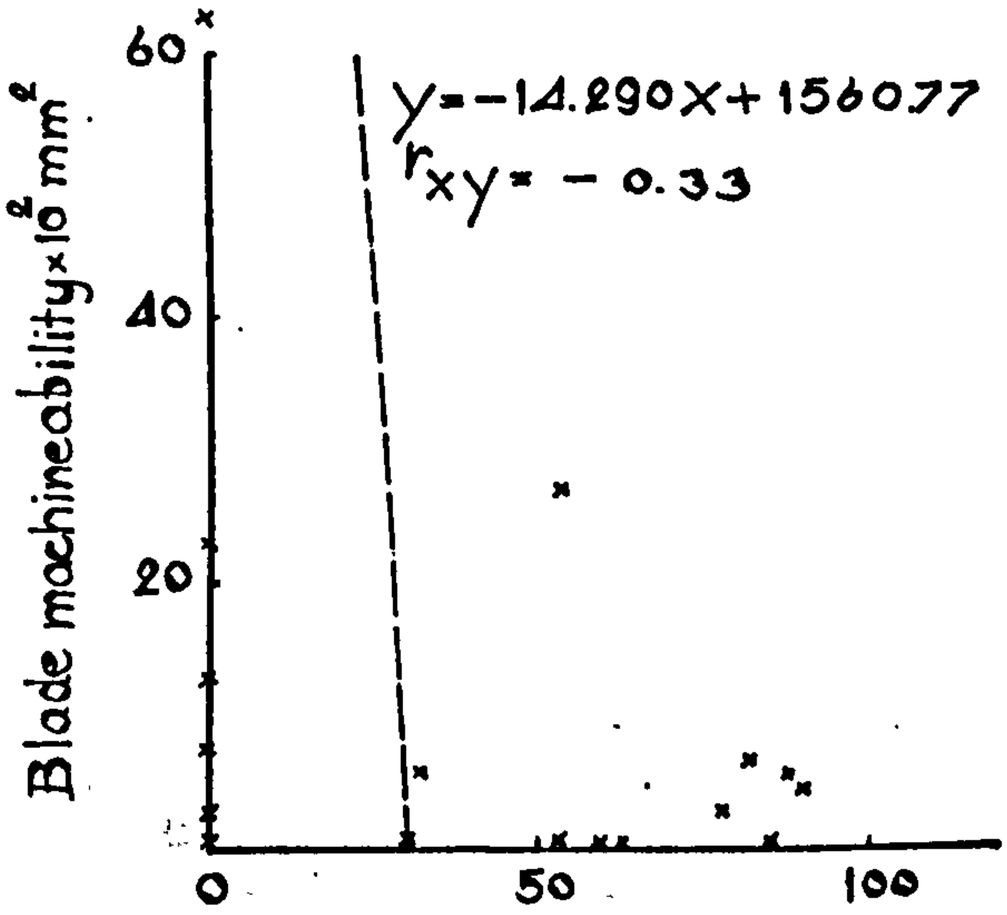
Blade machineability x 10² mm²
60
40
20
0
50
100
Quartz content %
y=-14.290X+156077
r_xy = -0.33

Figure 47 (6)

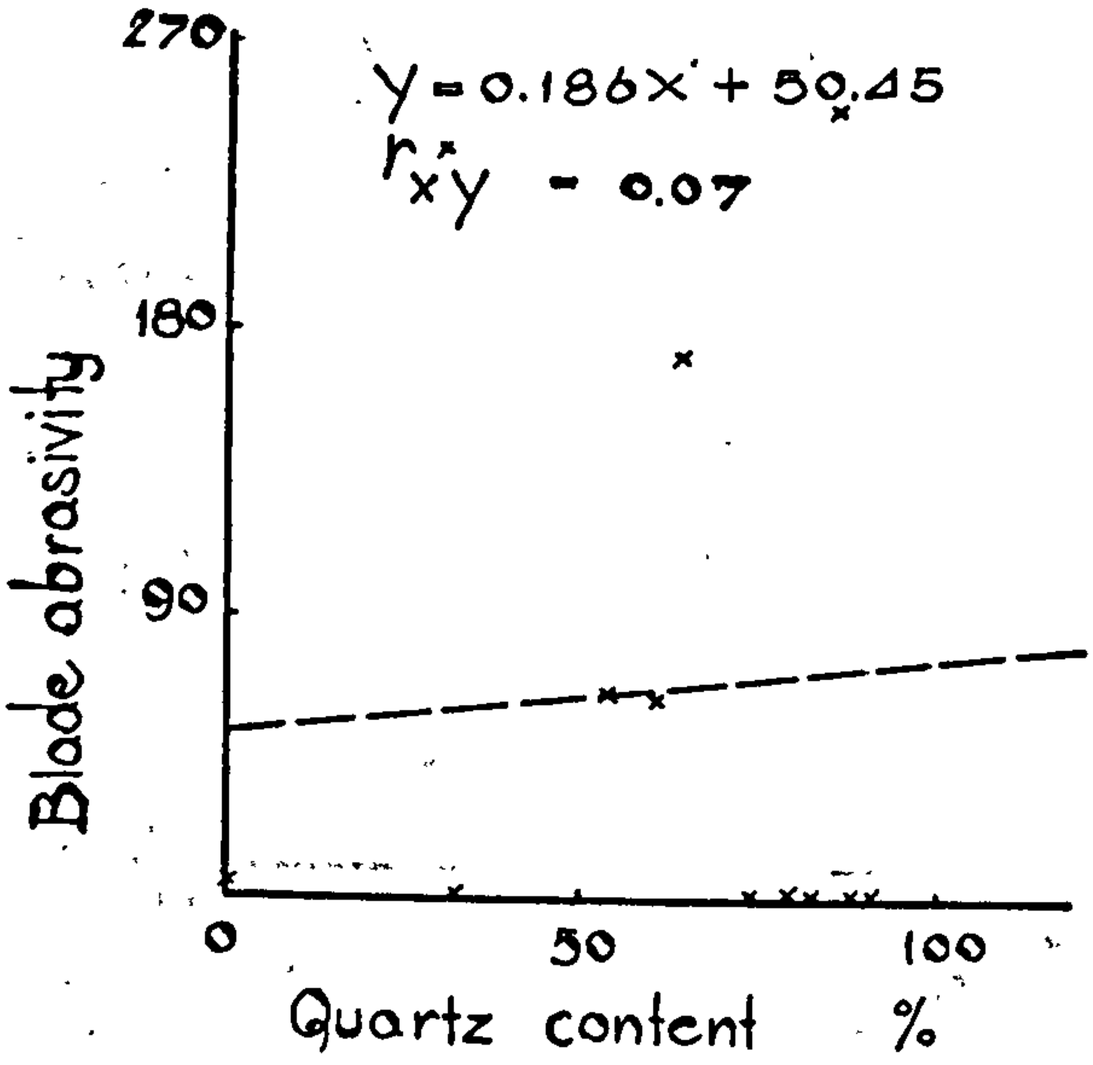
Y = 0.186X + 50.45
r_{xy} = 0.07
Blade abrasivity
270
180
90
0
50
100
Quartz content %

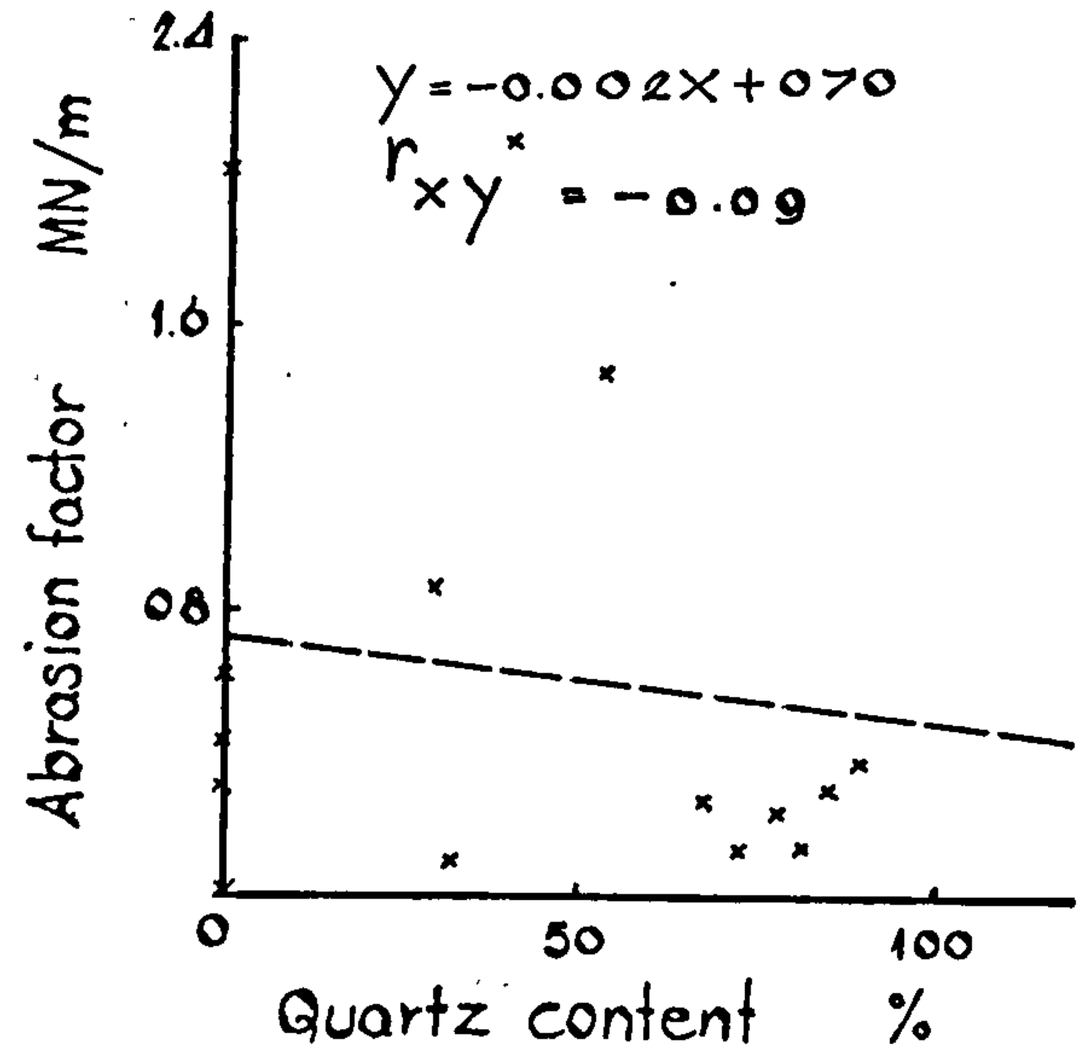
Y = -0.002X + 070
r_{xy} = -0.09
Abrasion factor MN/m
2.4
1.6
08
0
50
100
Quartz content %

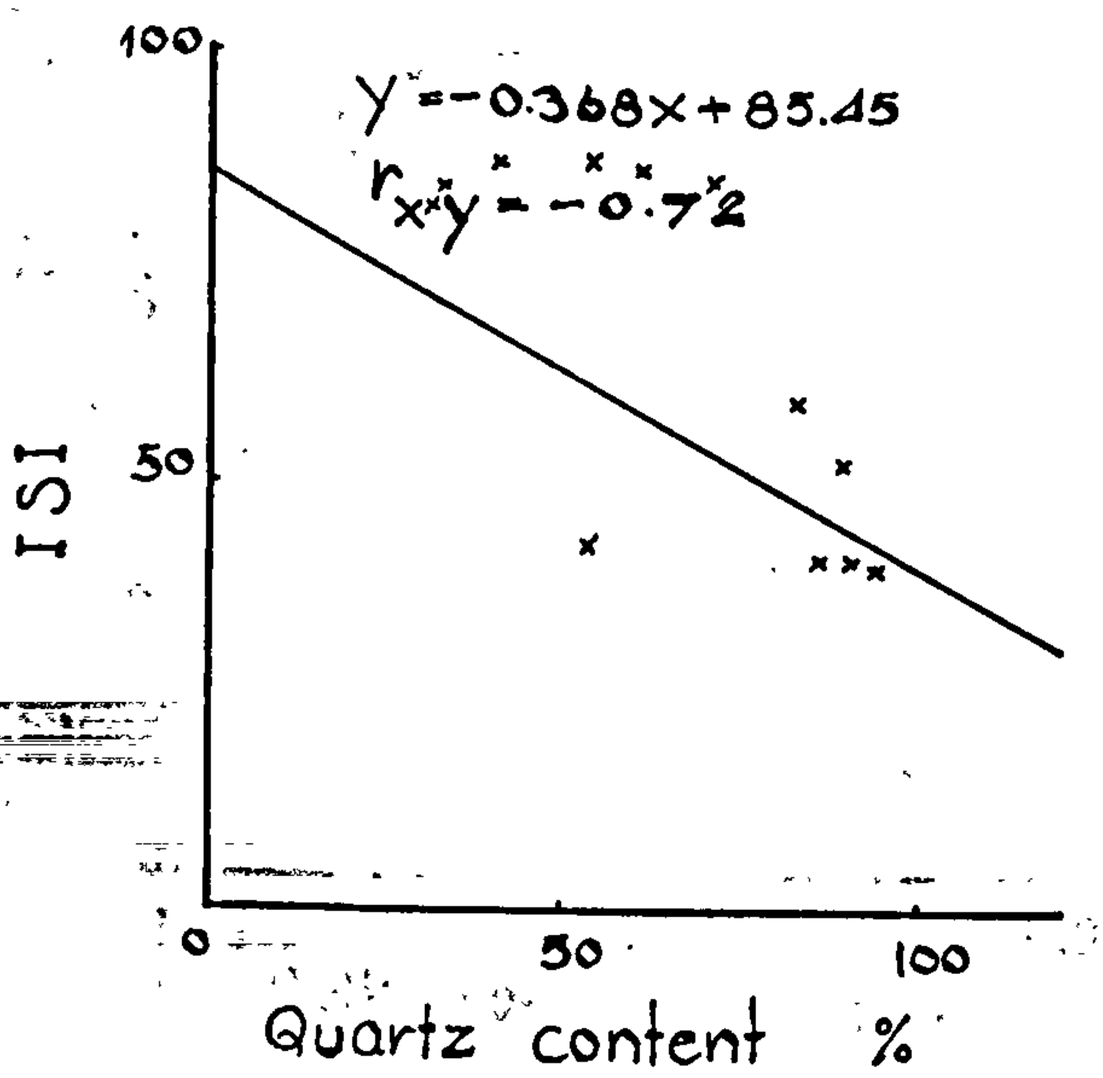
Y = -0.368X + 85.45
r_{xy} = -0.72
ISI
100
50
0
50
100
Quartz content %

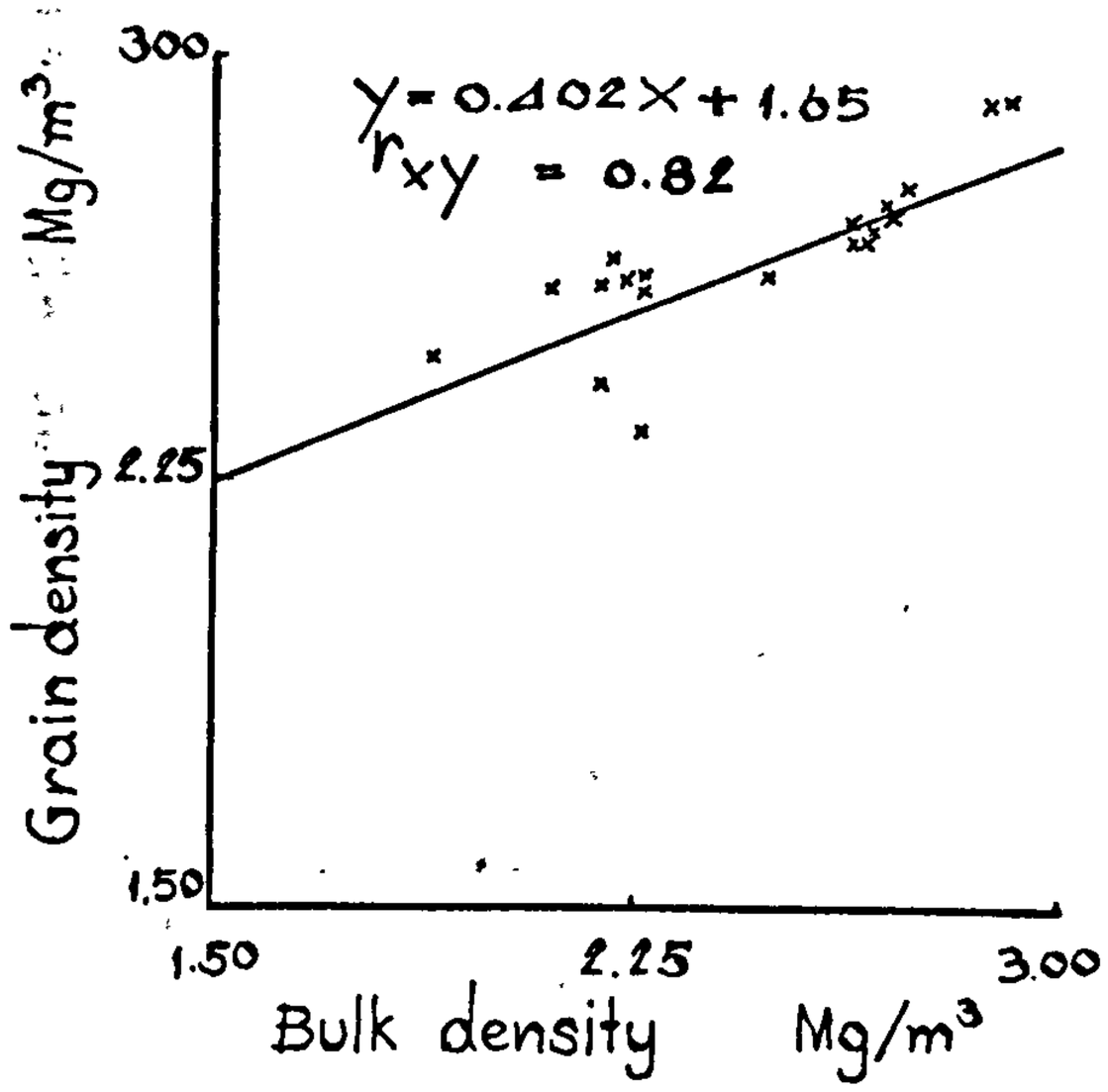
Y = 0.402X + 1.65
r_{xy} = 0.82
Grain density Mg/m³
300
2.25
1.50
1.50
2.25
3.00
Bulk density Mg/m³

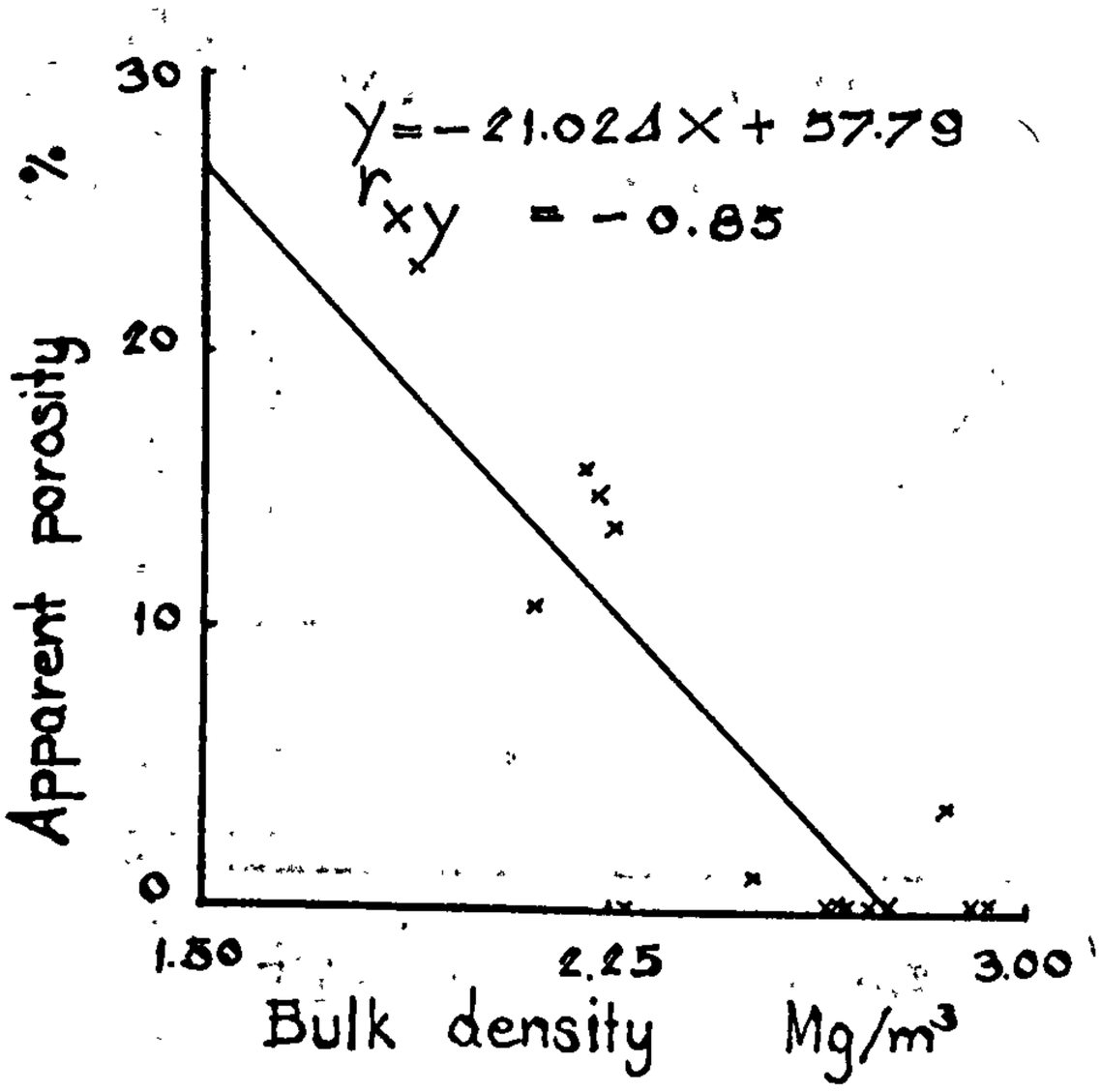
Y = -21.024X + 57.79
r_{xy} = -0.85
Apparent porosity %
30
20
10
0
1.50
2.25
3.00
Bulk density Mg/m³

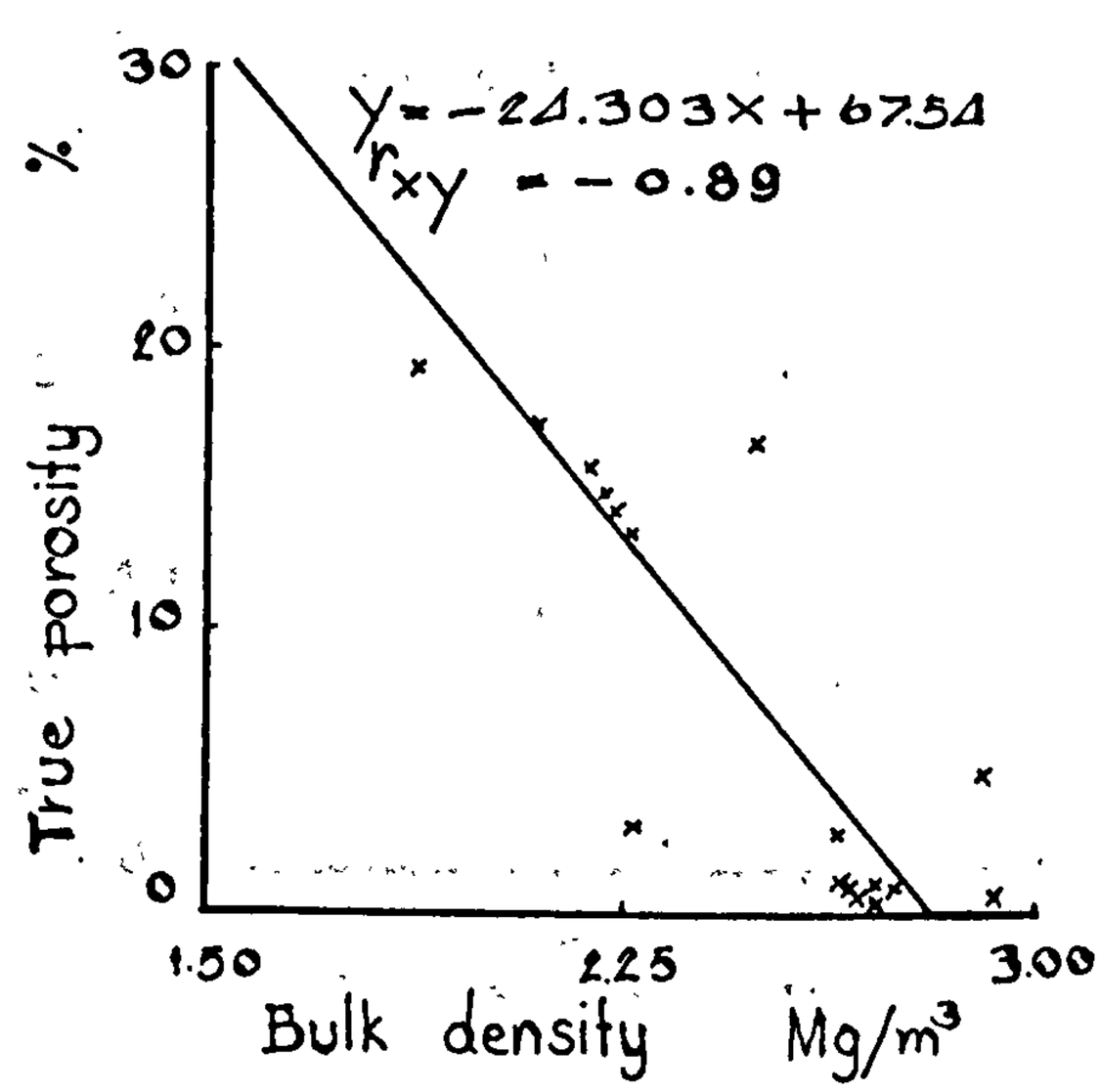
Y = -24.303X + 67.54
r_{xy} = -0.89
True porosity %
30
20
10
0
1.50
2.25
3.00
Bulk density Mg/m³

Figure 47 (7)

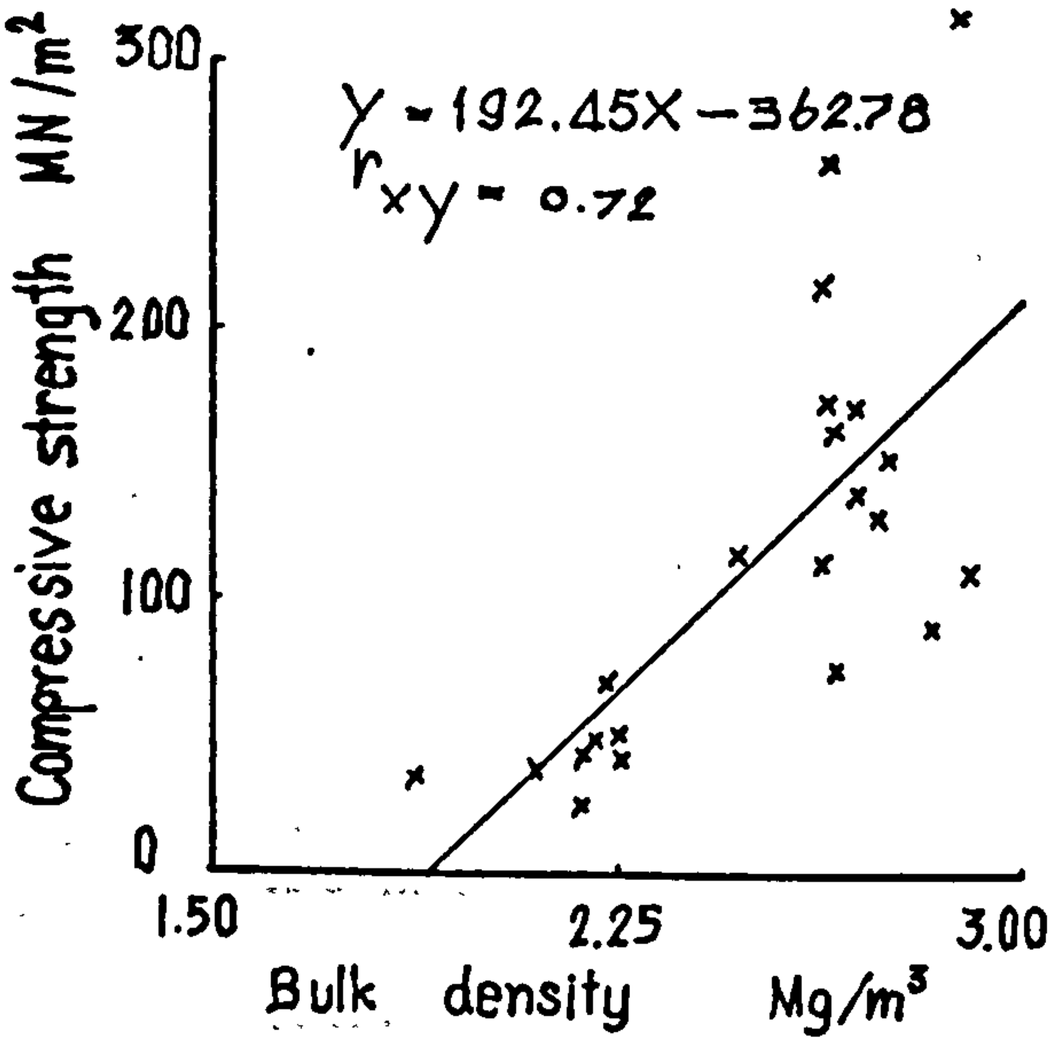
Y = 192.45X − 362.78
r_{xy} = 0.72
Compressive strength MN/m²
300
200
100
0
1.50
2.25
3.00
Bulk density Mg/m³

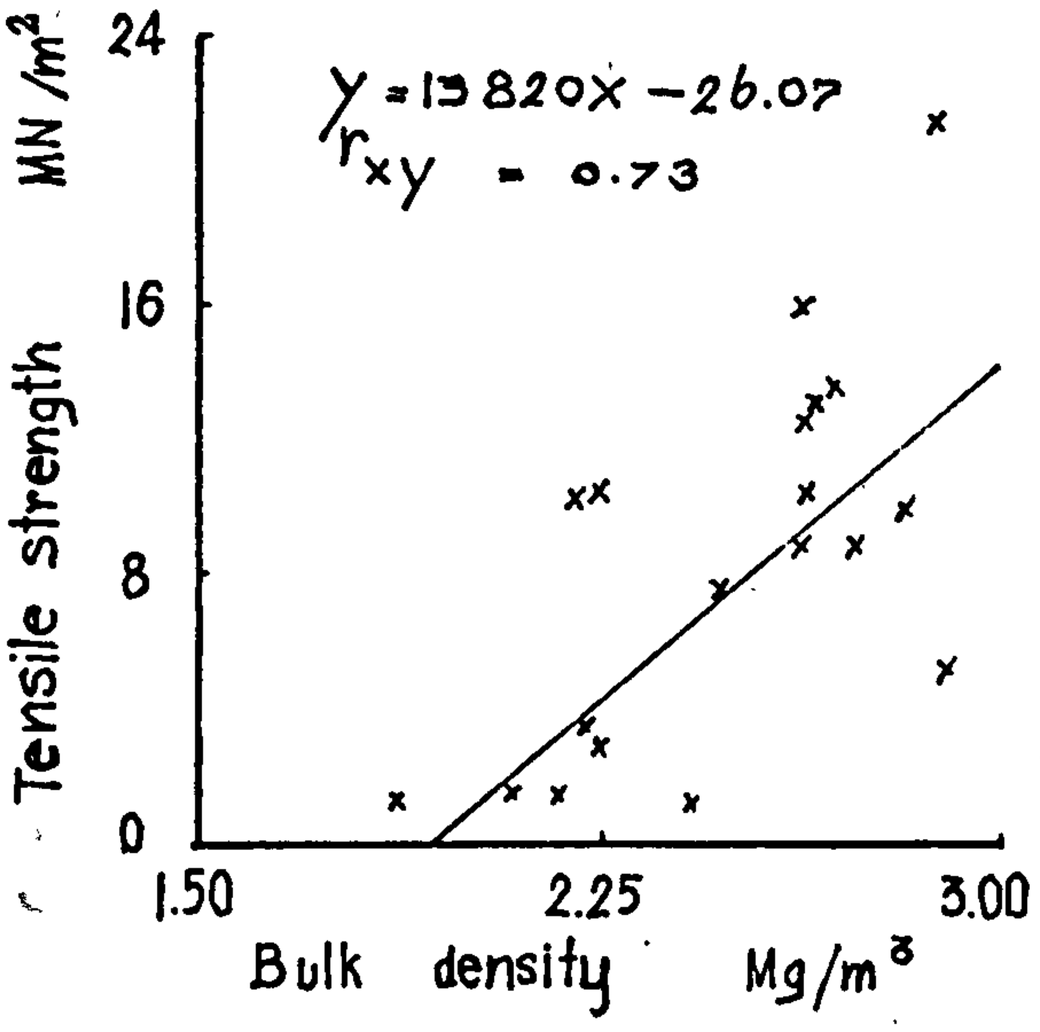
Y = 13.820X − 26.07
r_{xy} = 0.73
Tensile strength MN/m²
24
16
8
0
1.50
2.25
3.00
Bulk density Mg/m³

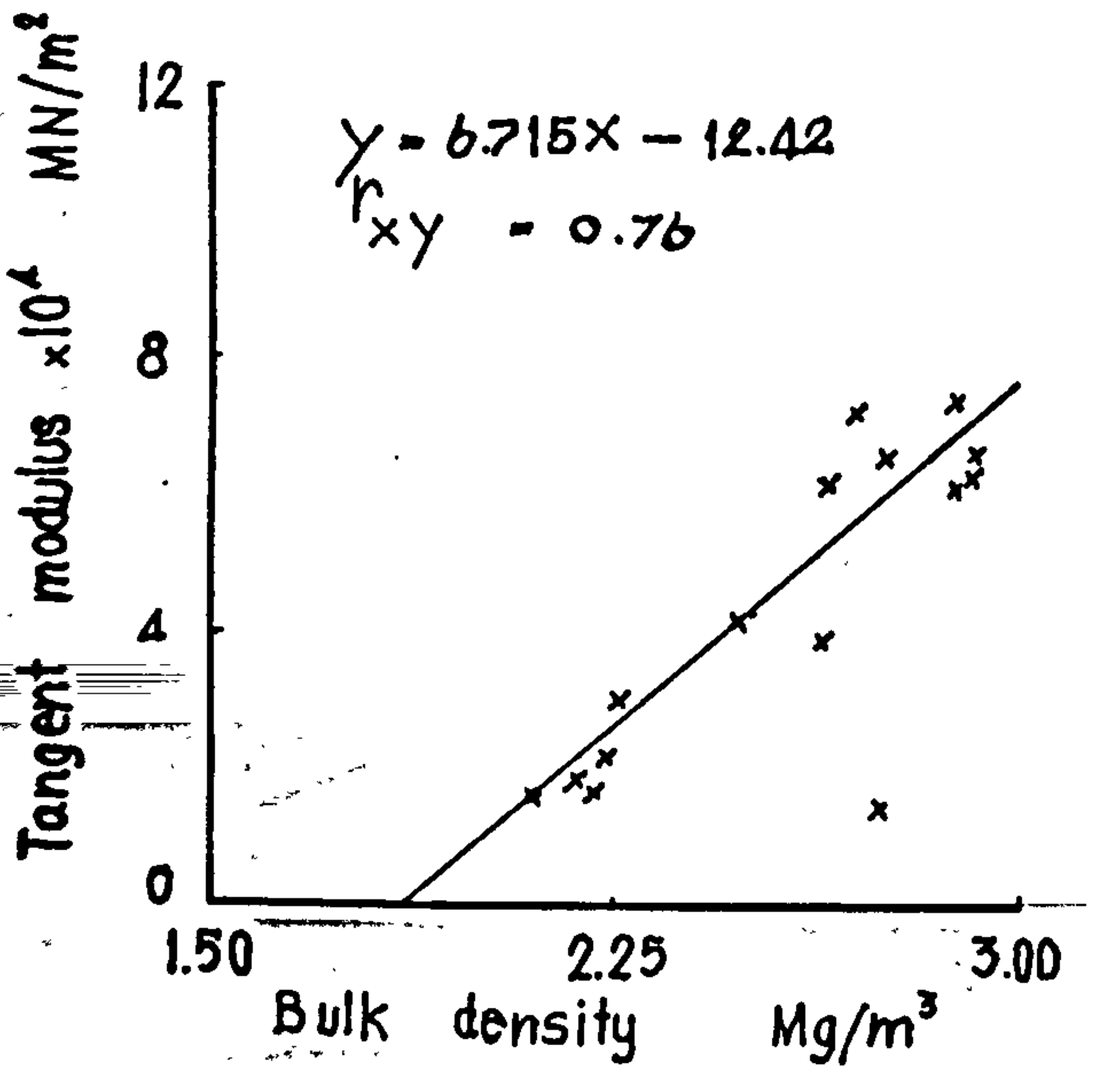
Y = 6.715X − 12.42
r_{xy} = 0.76
Tangent modulus ×10⁴ MN/m²
12
8
4
0
1.50
2.25
3.00
Bulk density Mg/m³

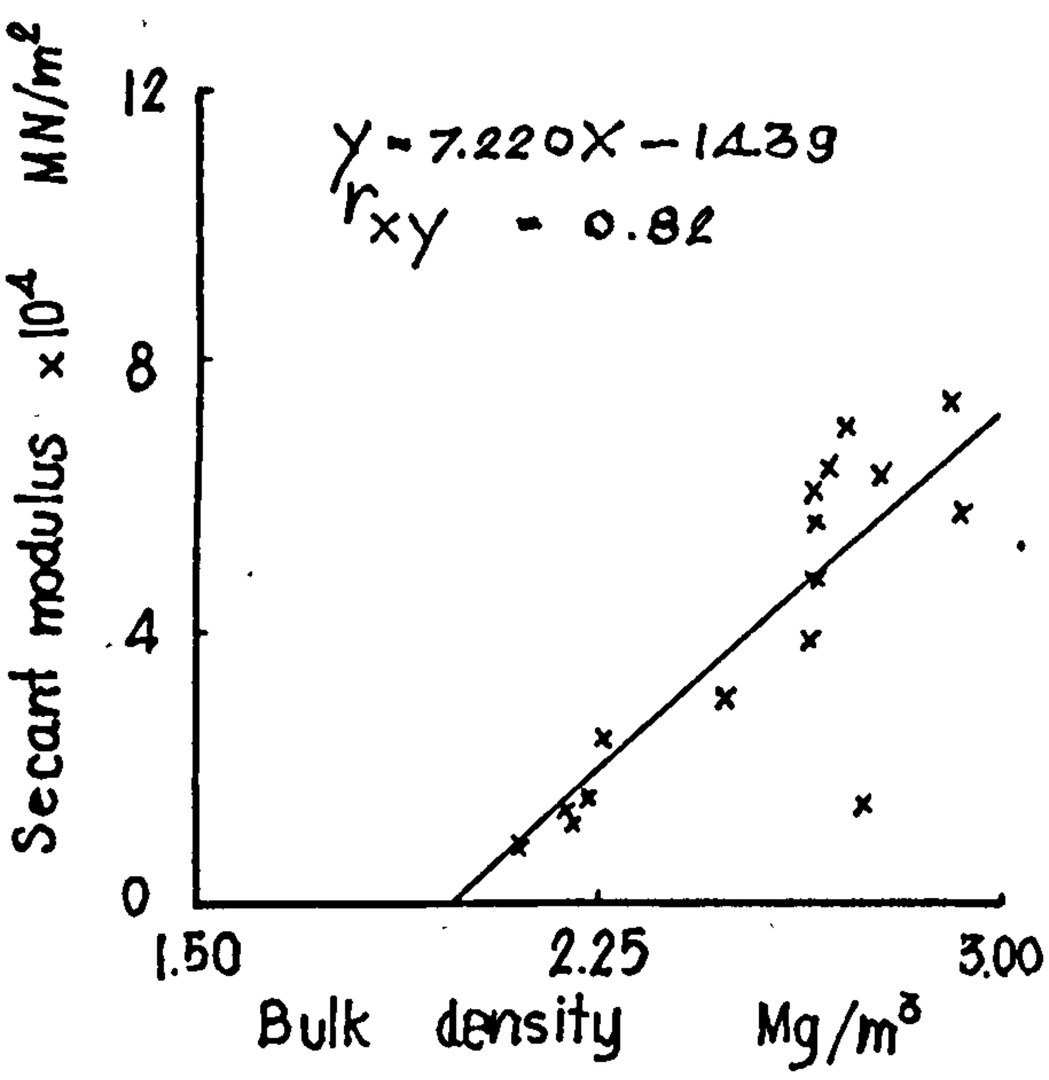
Y = 7.220X − 14.39
r_{xy} = 0.82
Secant modulus ×10⁴ MN/m²
12
8
4
0
1.50
2.25
3.00
Bulk density Mg/m³

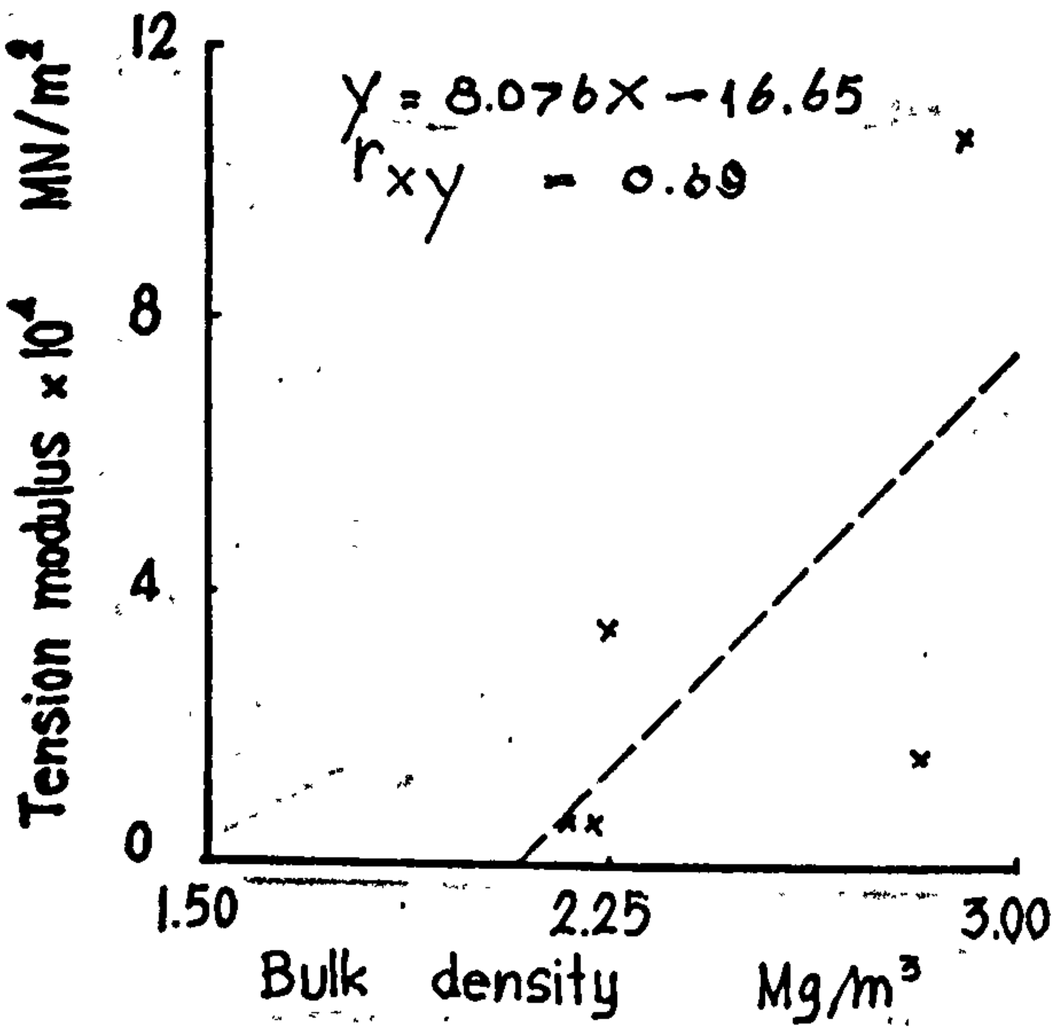
Y = 8.076X − 16.65
r_{xy} = 0.69
Tension modulus ×10⁴ MN/m²
12
8
4
0
1.50
2.25
3.00
Bulk density Mg/m³

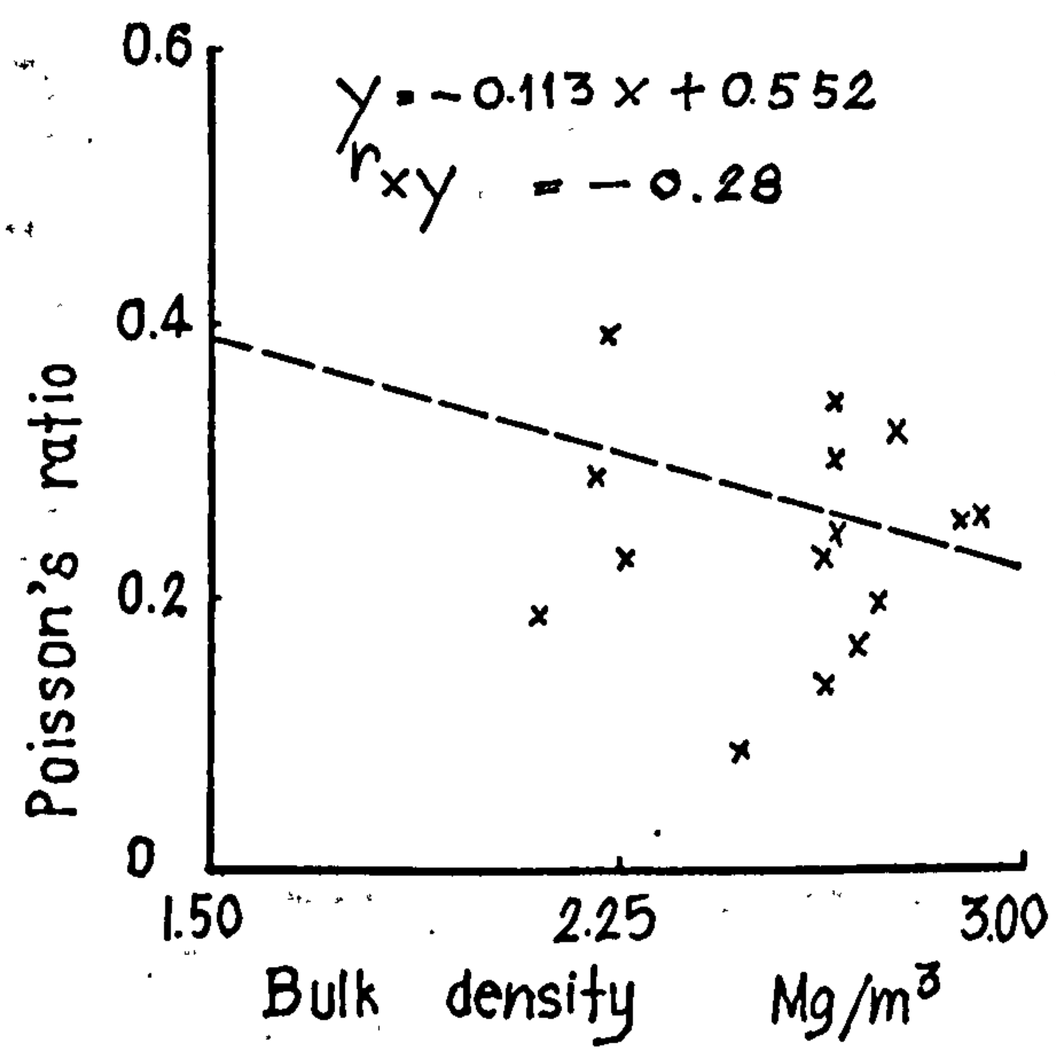
Y = −0.113 x + 0.552
r_{xy} = −0.28
Poisson's ratio
0.6
0.4
0.2
0
1.50
2.25
3.00
Bulk density Mg/m³

Figure 47 (8)

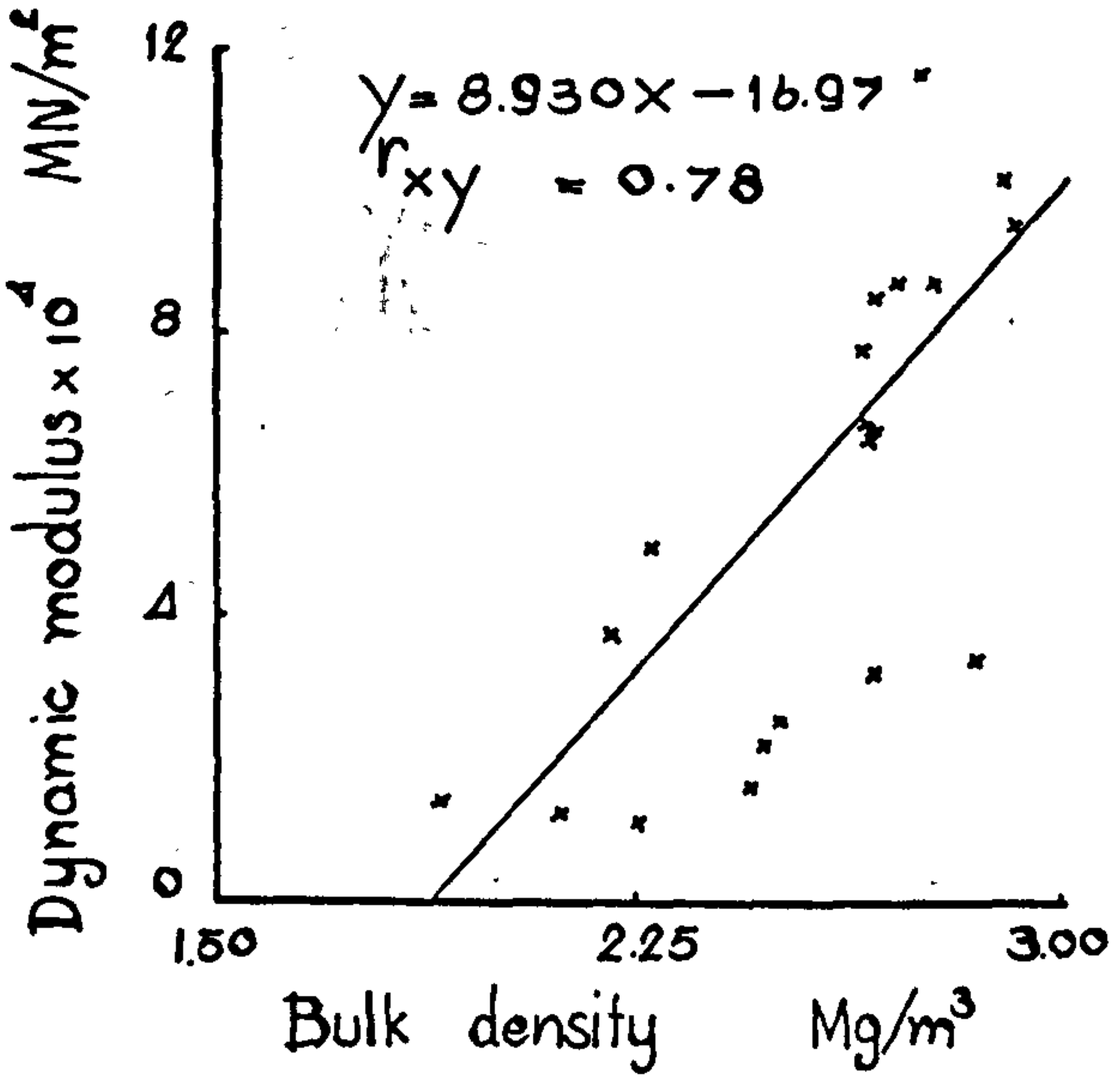
Y = 8.930X − 16.97
r_xy = 0.78
Dynamic modulus × 10⁴ MN/m²
12
8
4
0
1.50
2.25
3.00
Bulk density Mg/m³

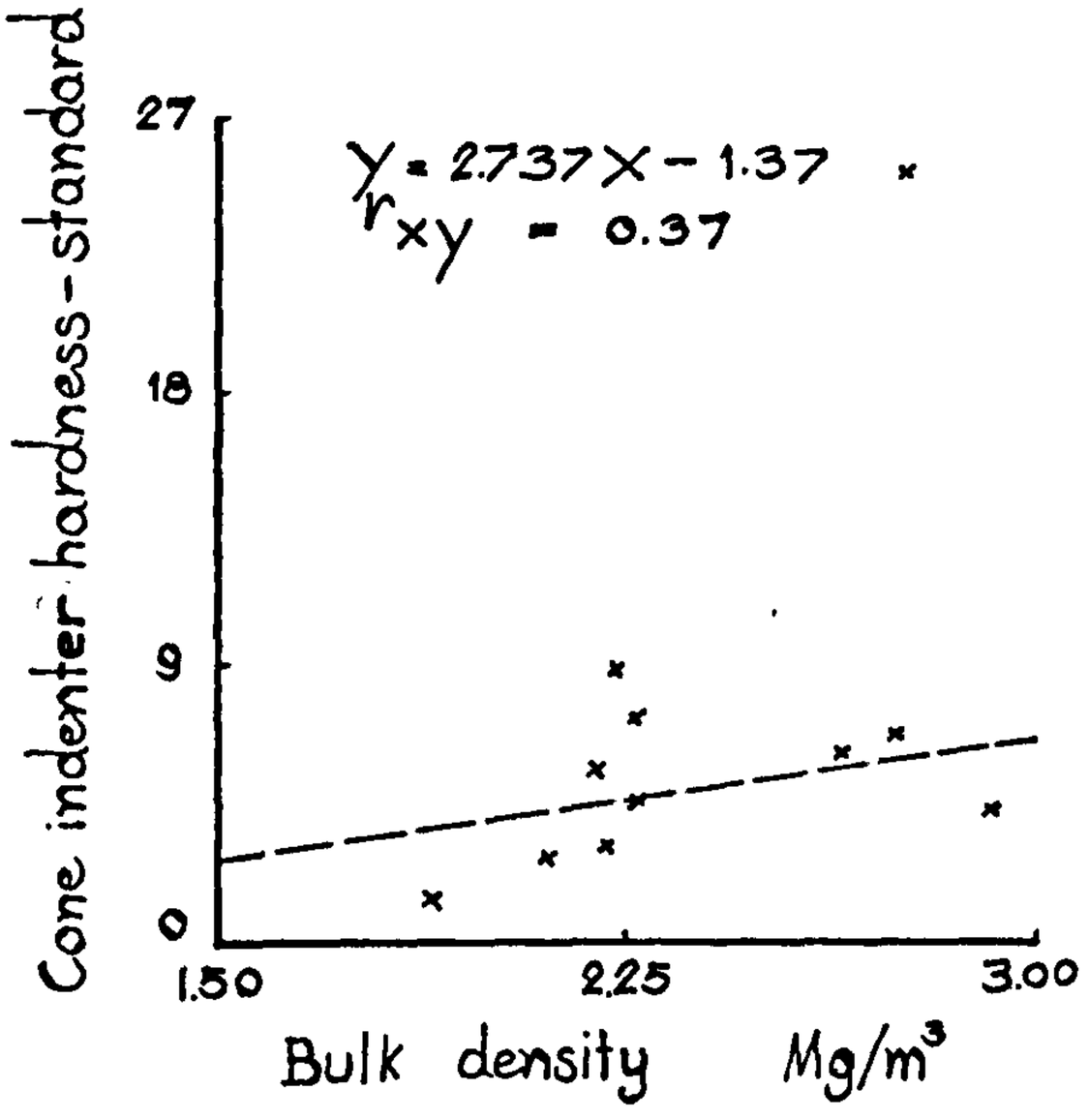
Y = 2.737X − 1.37
r_xy = 0.37
Cone indenter hardness-standard
27
18
9
0
1.50
2.25
3.00
Bulk density Mg/m³

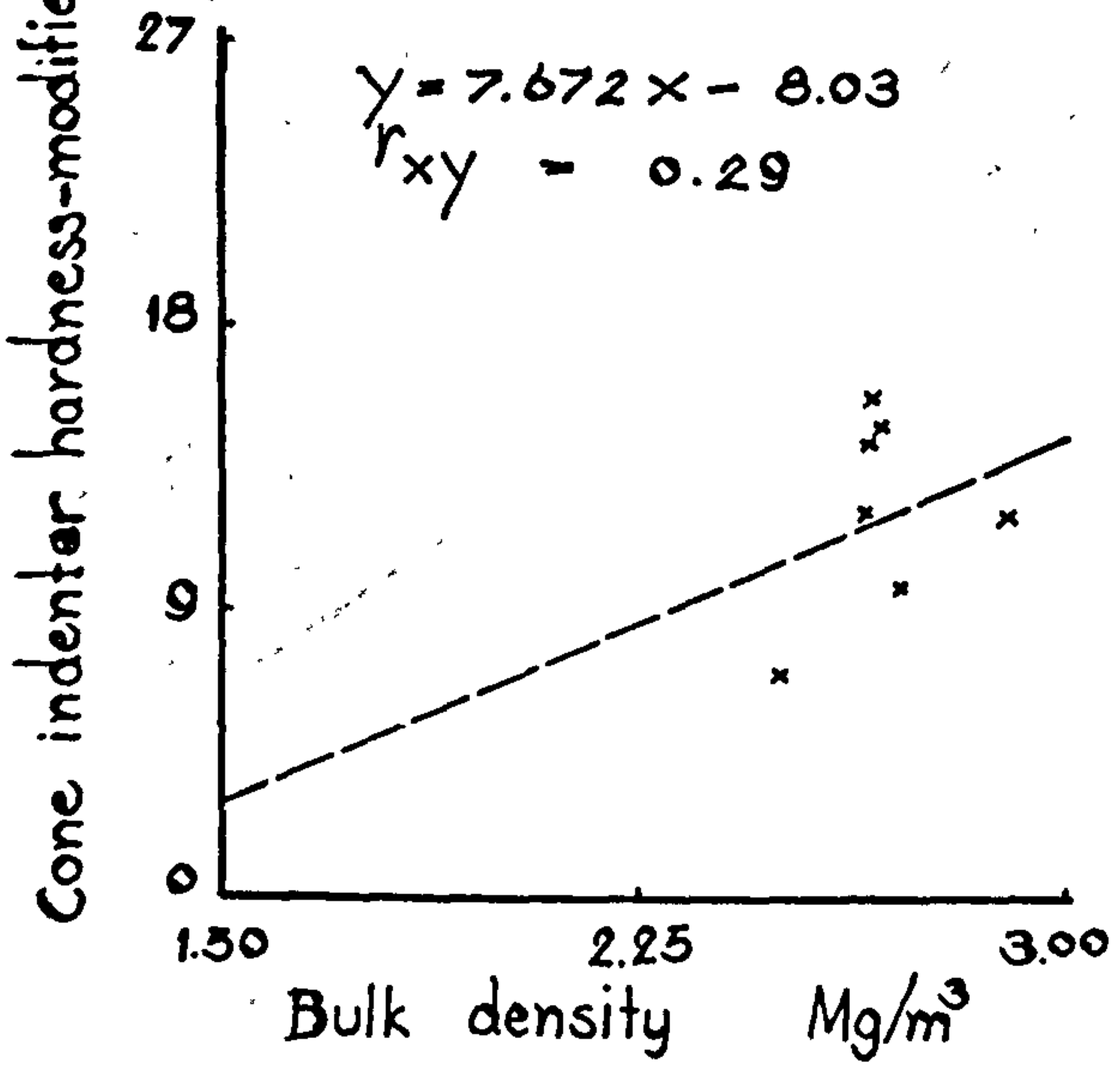
Y = 7.672X − 8.03
r_xy = 0.29
Cone indentar hardness-modified
27
18
9
0
1.50
2.25
3.00
Bulk density Mg/m³

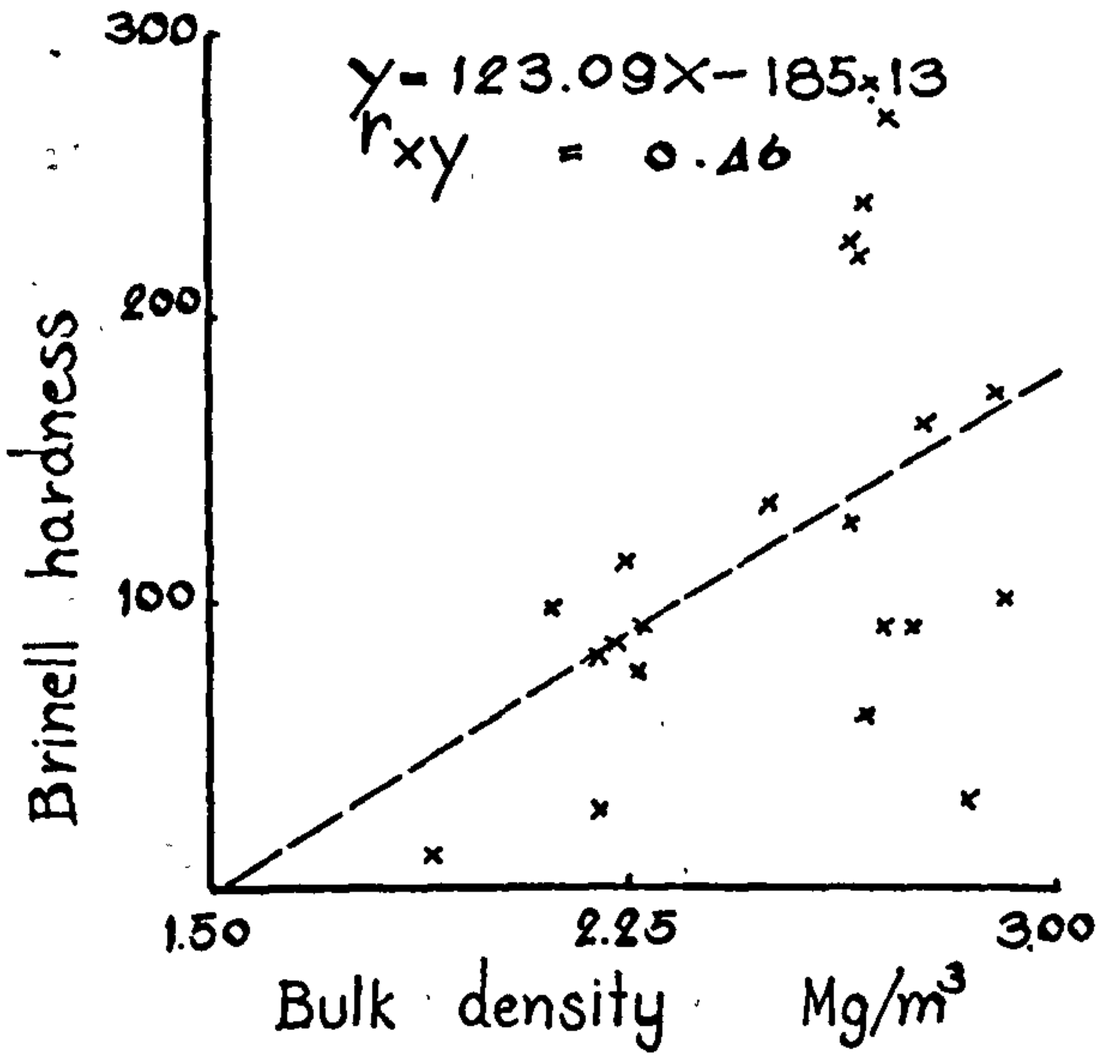
Y = 123.09X − 185.13
r_xy = 0.46
Brinell hardness
300
200
100
1.50
2.25
3.00
Bulk density Mg/m³

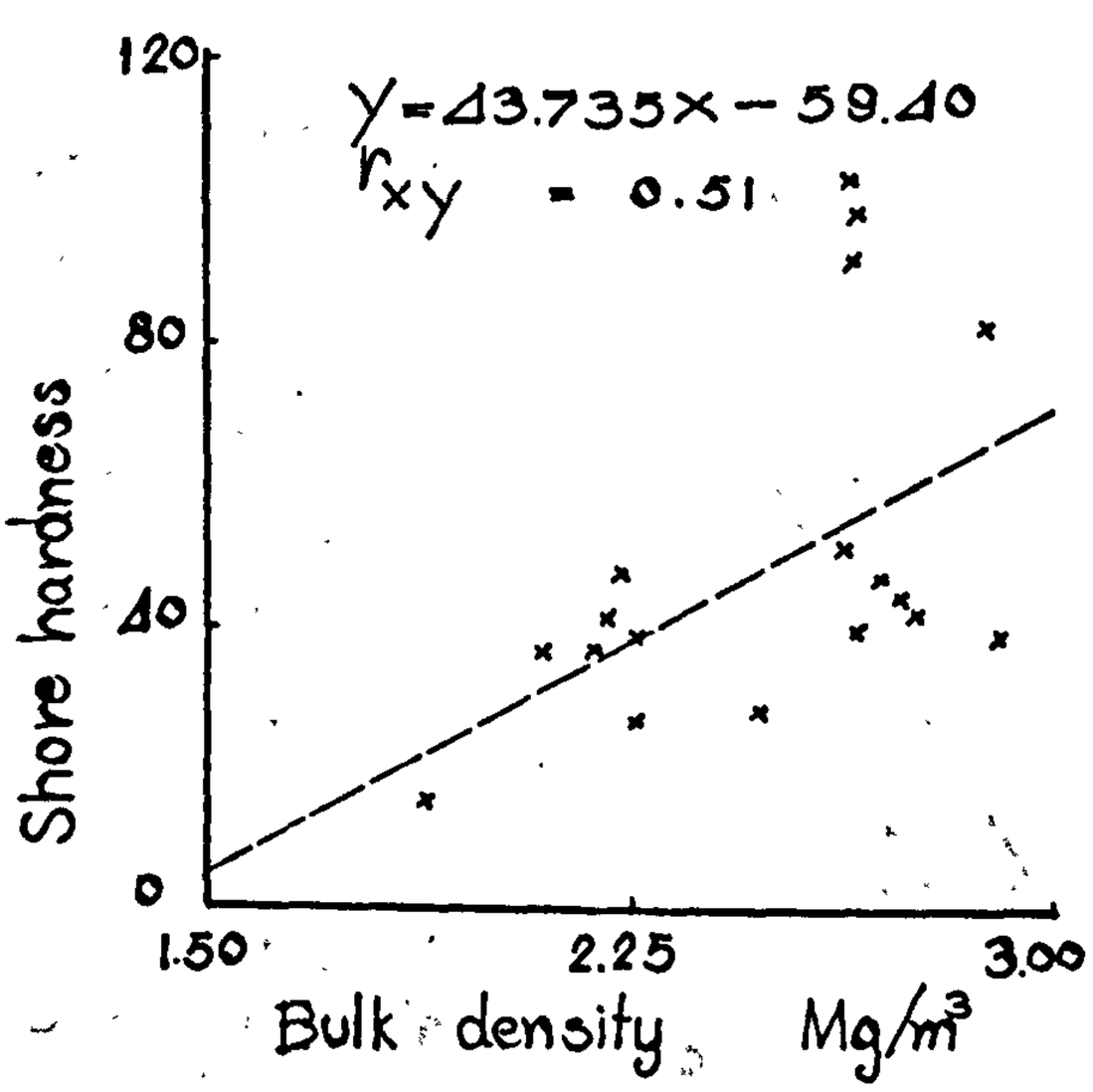
Y = 43.735X − 59.40
r_xy = 0.51
Shore hardness
120
80
40
0
1.50
2.25
3.00
Bulk density Mg/m³

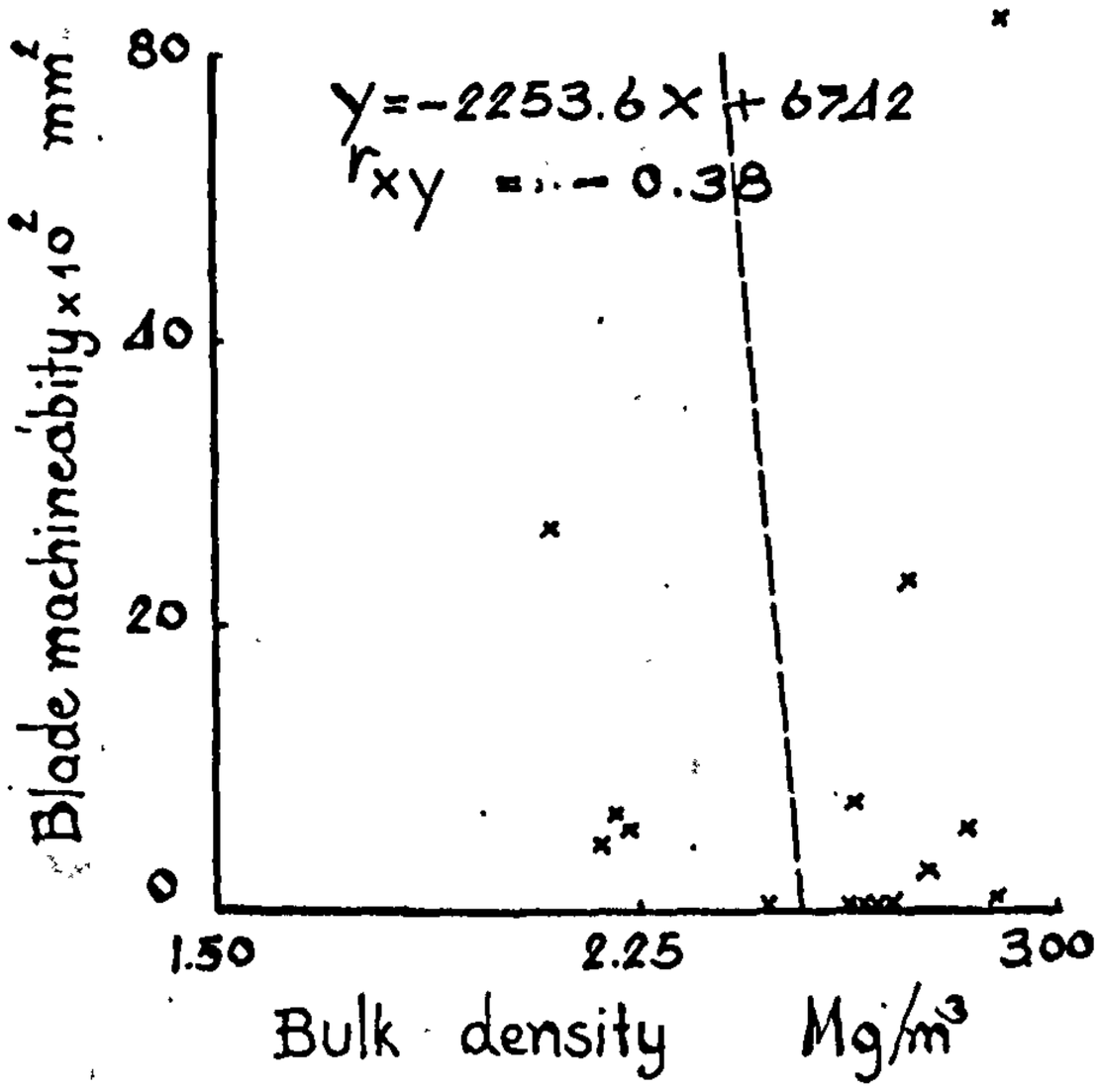
Y = −2253.6X + 6742
r_xy = −0.38
Blade machineability × 10² mm²
80
40
20
0
1.50
2.25
3.00
Bulk density Mg/m³

Figure 47 (9)

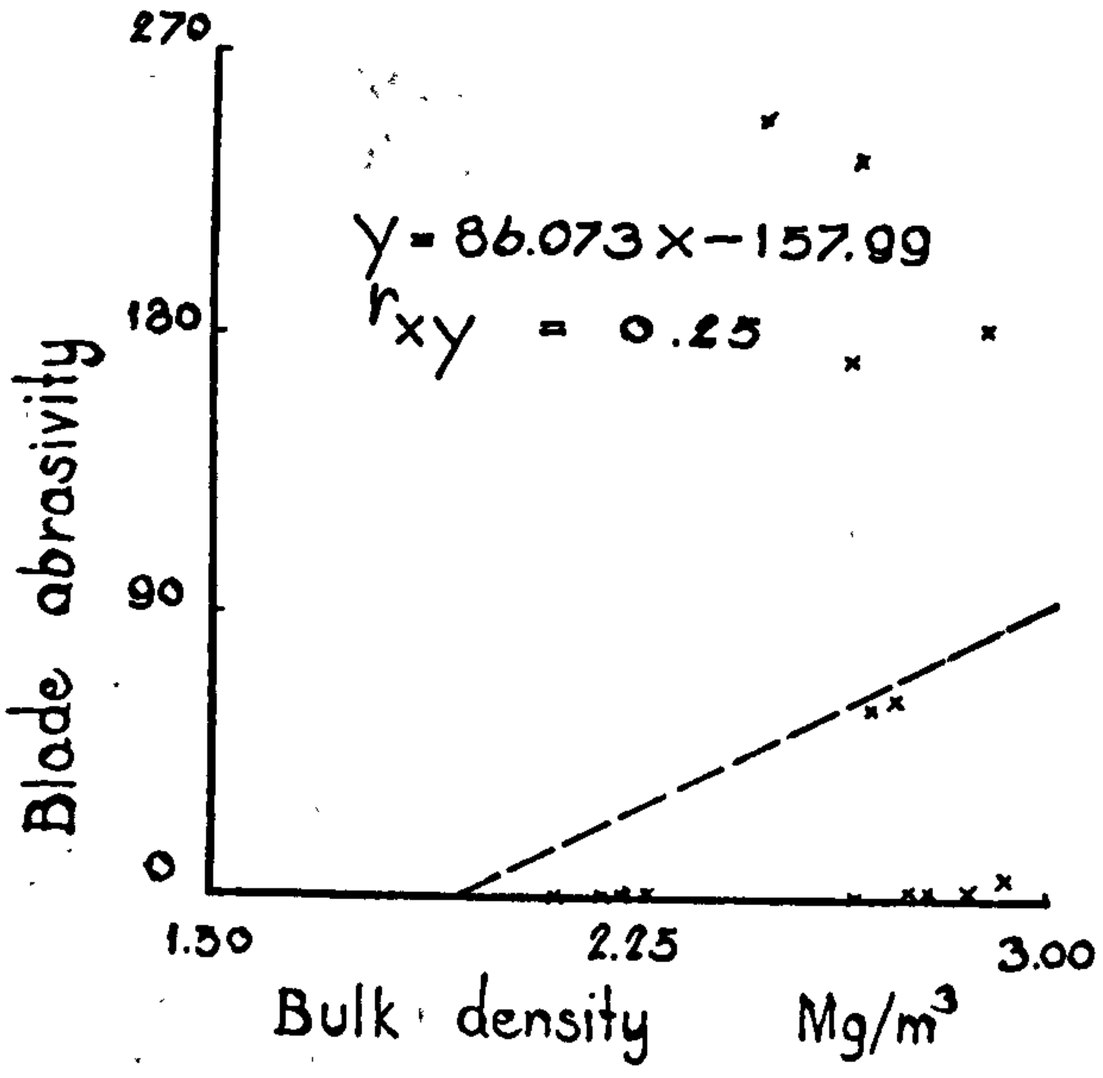
y = 86.073x − 157.99
r_{xy} = 0.25
Blade abrasivity
270
180
90
0
1.50
2.25
3.00
Bulk density Mg/m³

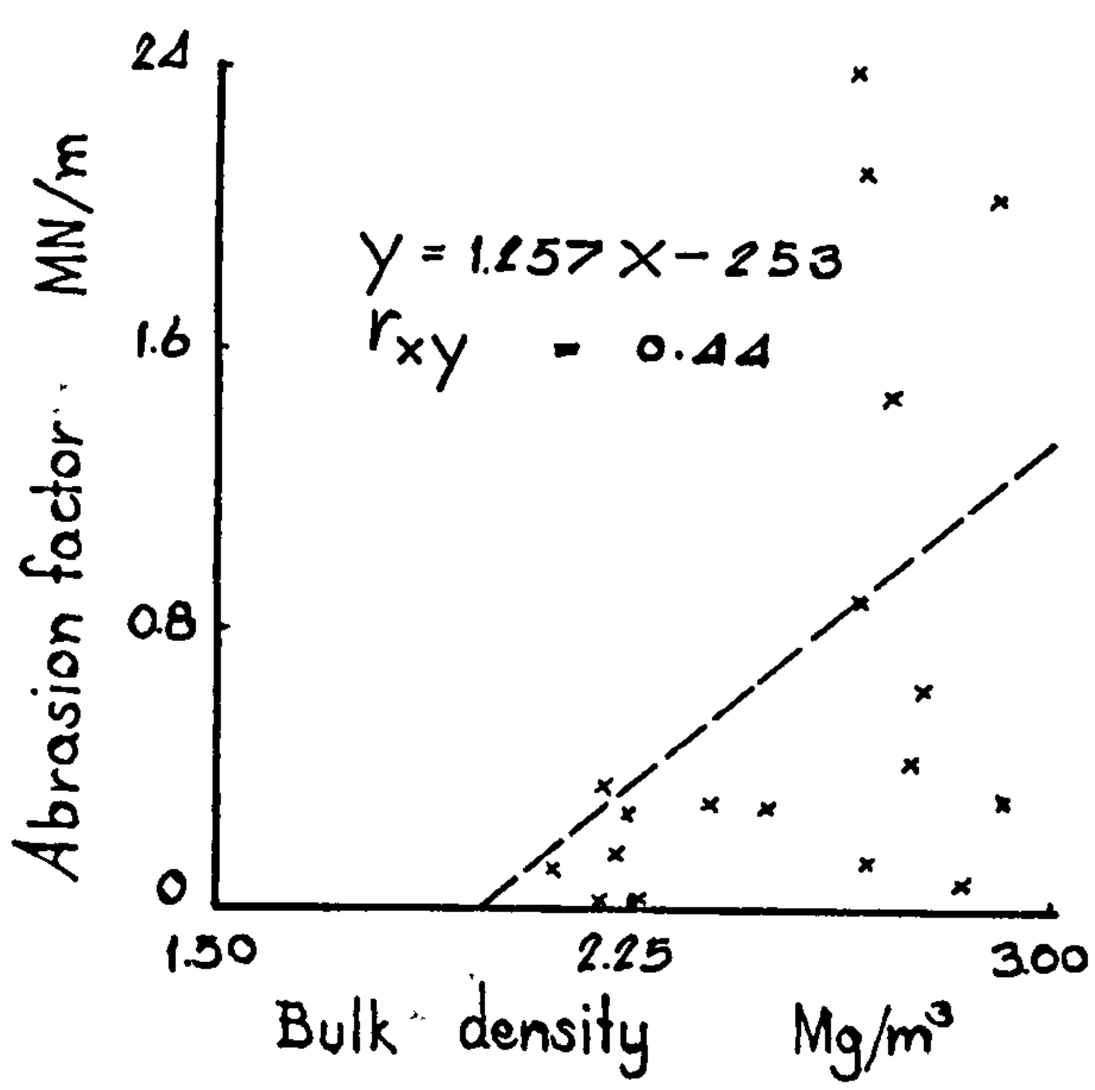
y = 1.257x − 253
r_{xy} = 0.44
Abrasion factor MN/m
2.4
1.6
0.8
0
1.50
2.25
3.00
Bulk density Mg/m³

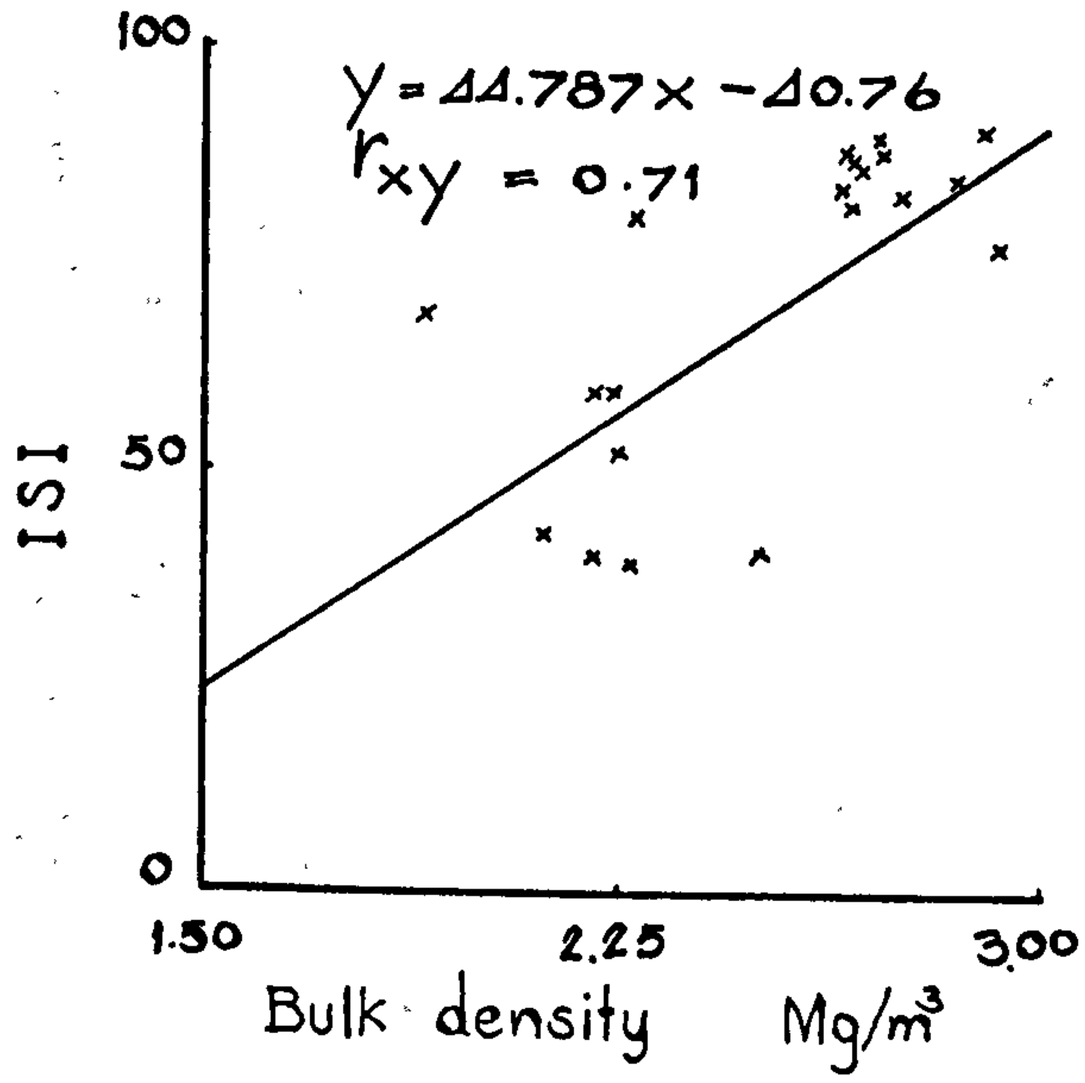
y = 44.787x − 40.76
r_{xy} = 0.71
ISI
100
50
0
1.50
2.25
3.00
Bulk density Mg/m³

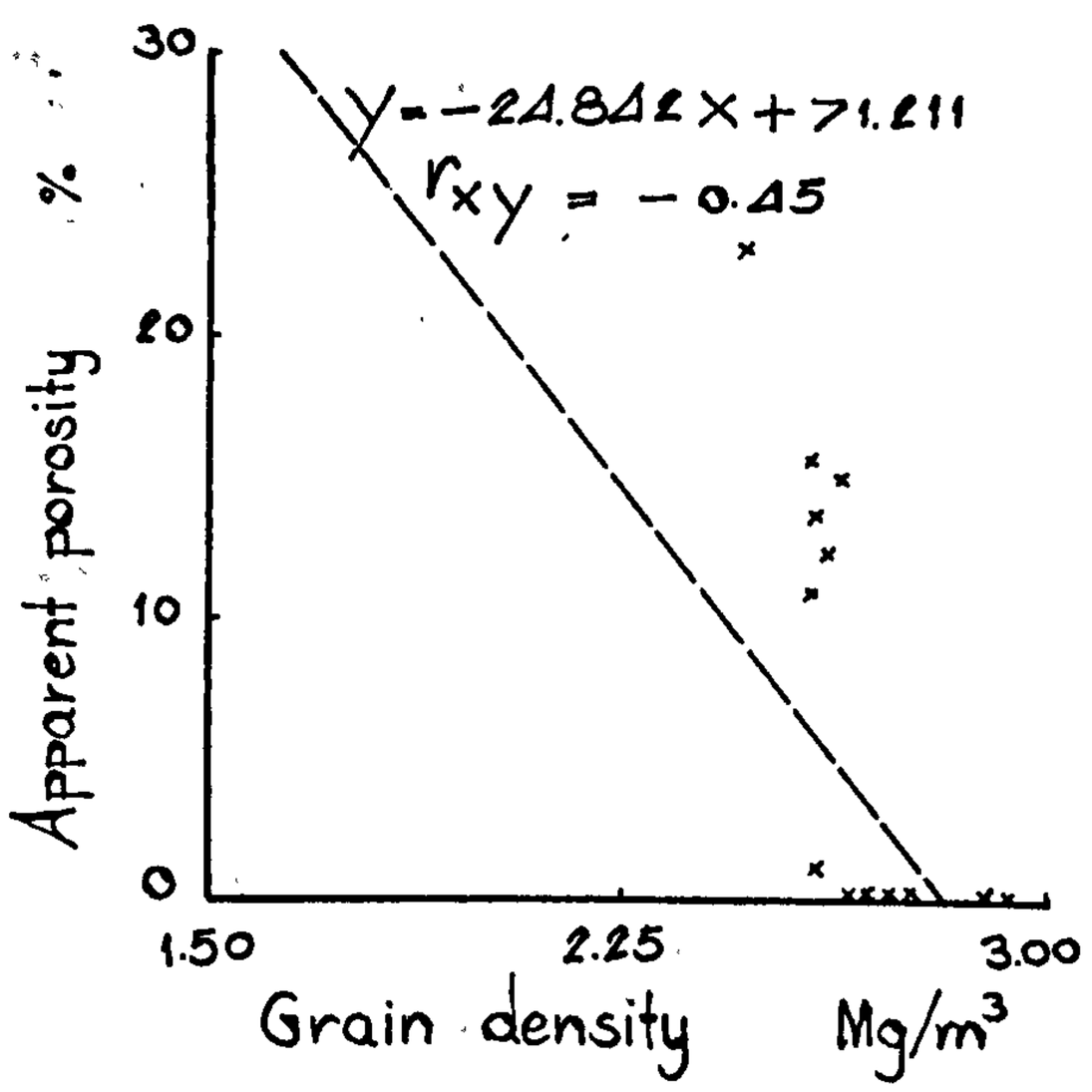
y = −24.842x + 71.211
r_{xy} = −0.45
Apparent porosity %
30
20
10
0
1.50
2.25
3.00
Grain density Mg/m³

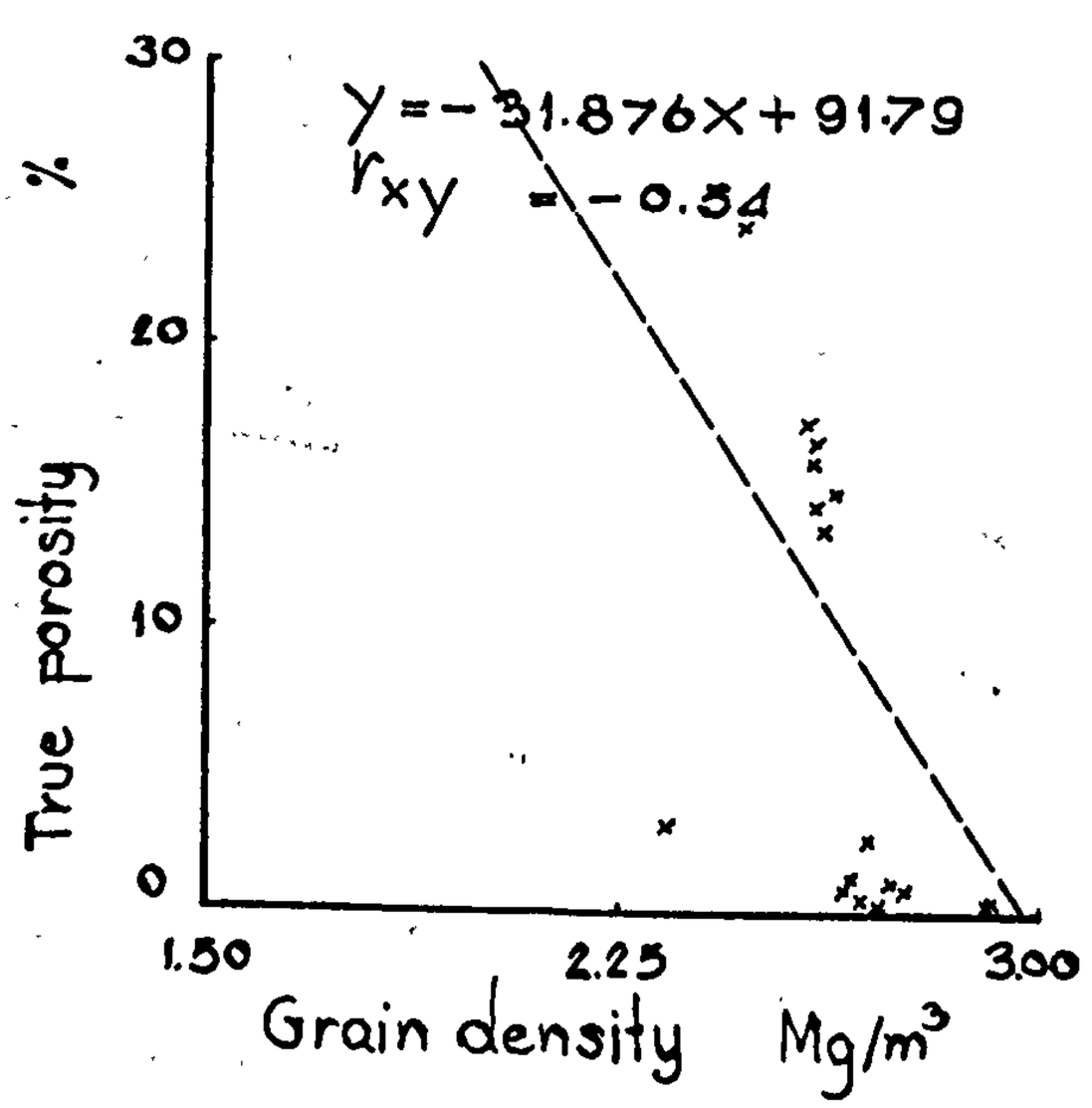
y = −31.876x + 91.79
r_{xy} = −0.54
True porosity %
30
20
10
0
1.50
2.25
3.00
Grain density Mg/m³

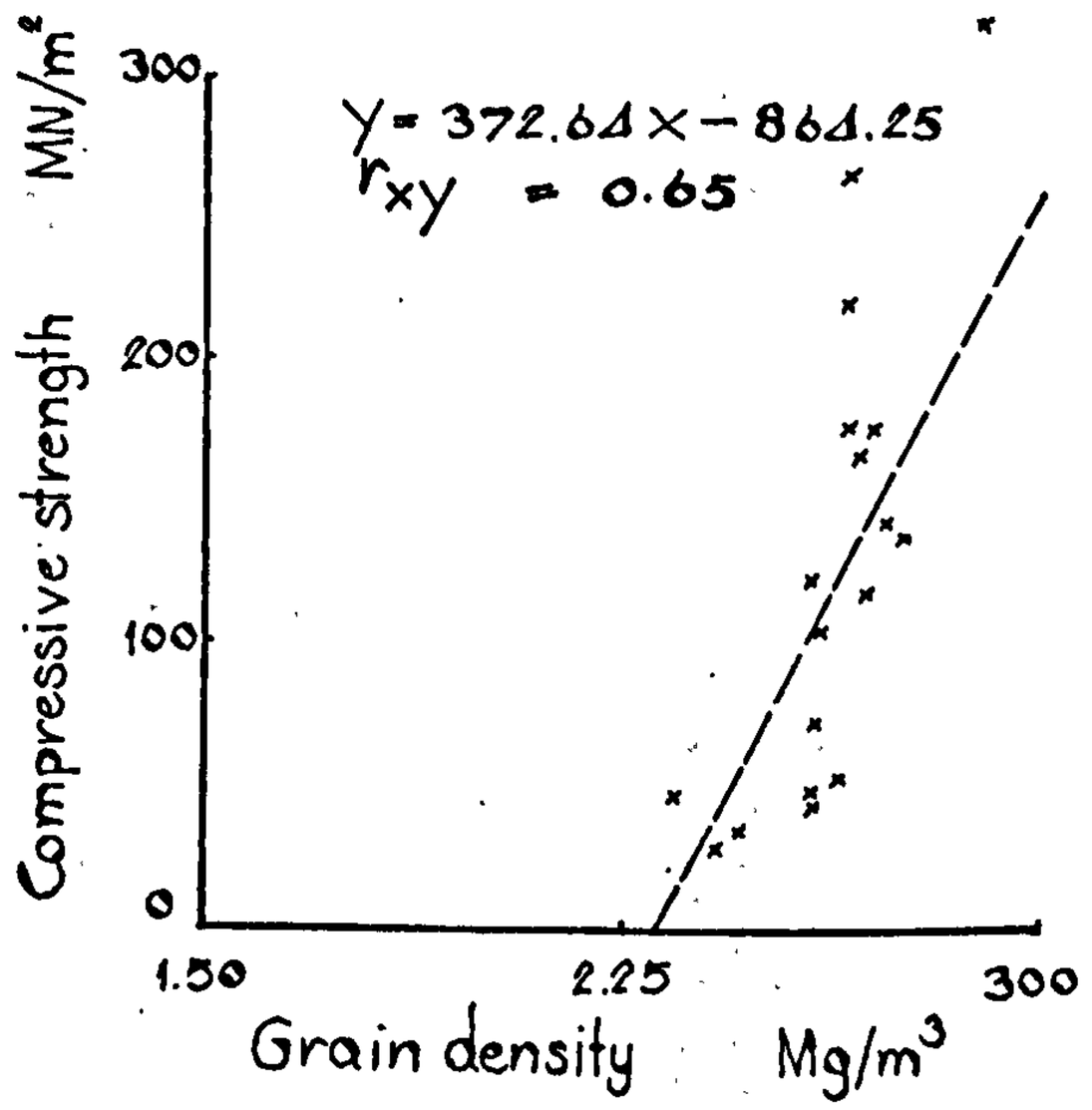
y = 372.64x − 864.25
r_{xy} = 0.65
Compressive strength MN/m²
300
200
100
0
1.50
2.25
300
Grain density Mg/m³

Figure 47 (10)

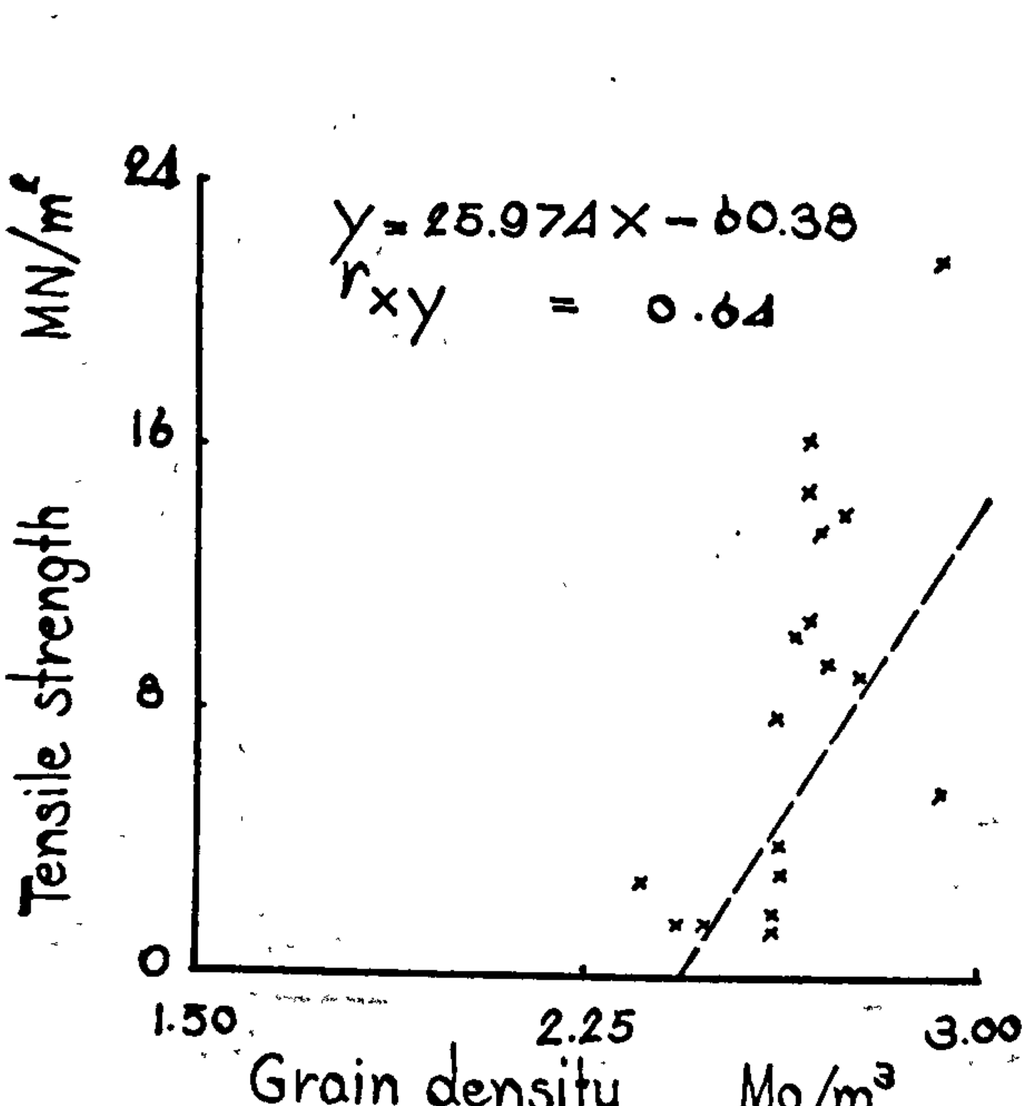
Y = 25.974X − 60.38
r_{xy} = 0.64
Tensile strength MN/m²
24
16
8
0
1.50
2.25
3.00
Grain density Mg/m³

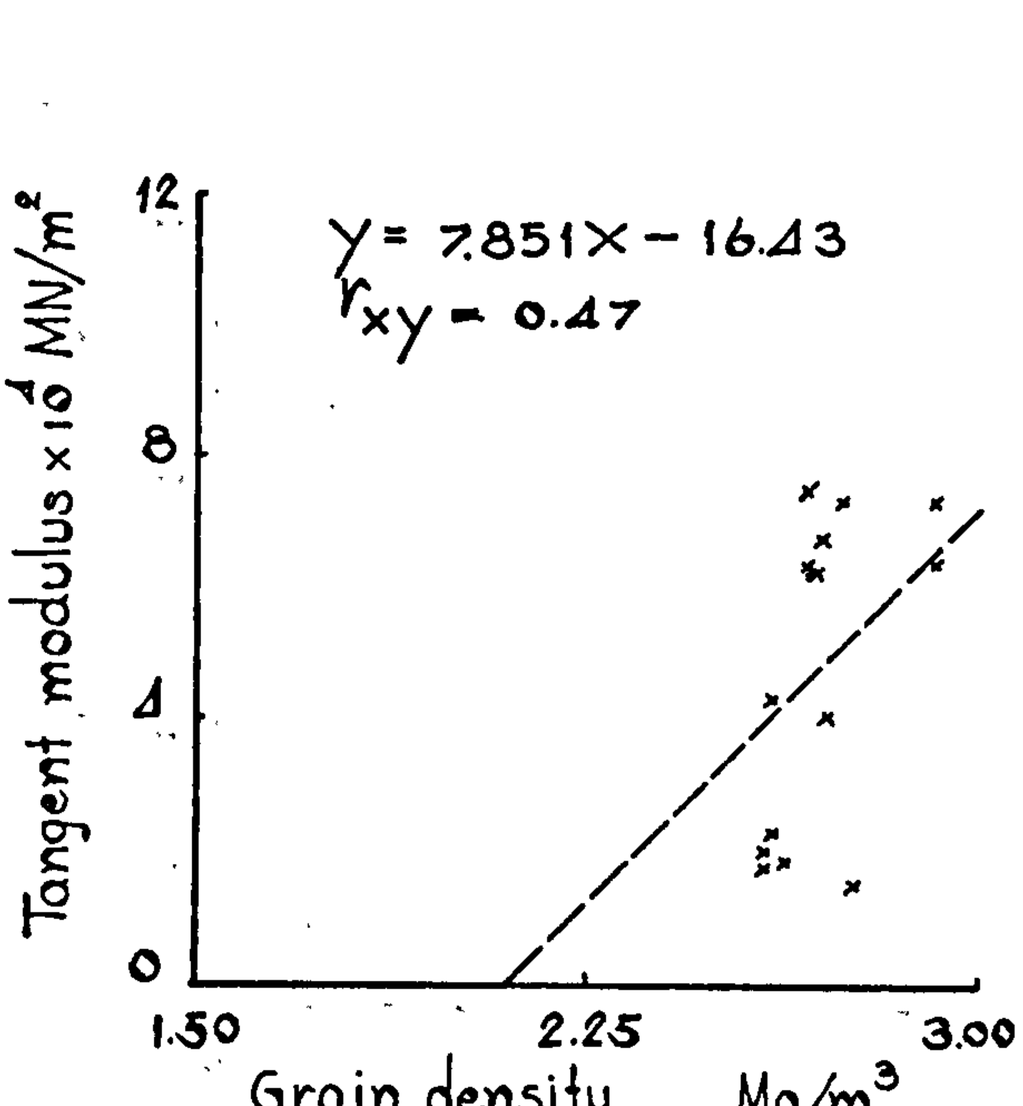
Y = 7.851X − 16.43
r_{xy} = 0.47
Tangent modulus ×10⁴ MN/m²
12
8
4
0
1.50
2.25
3.00
Grain density Mg/m³

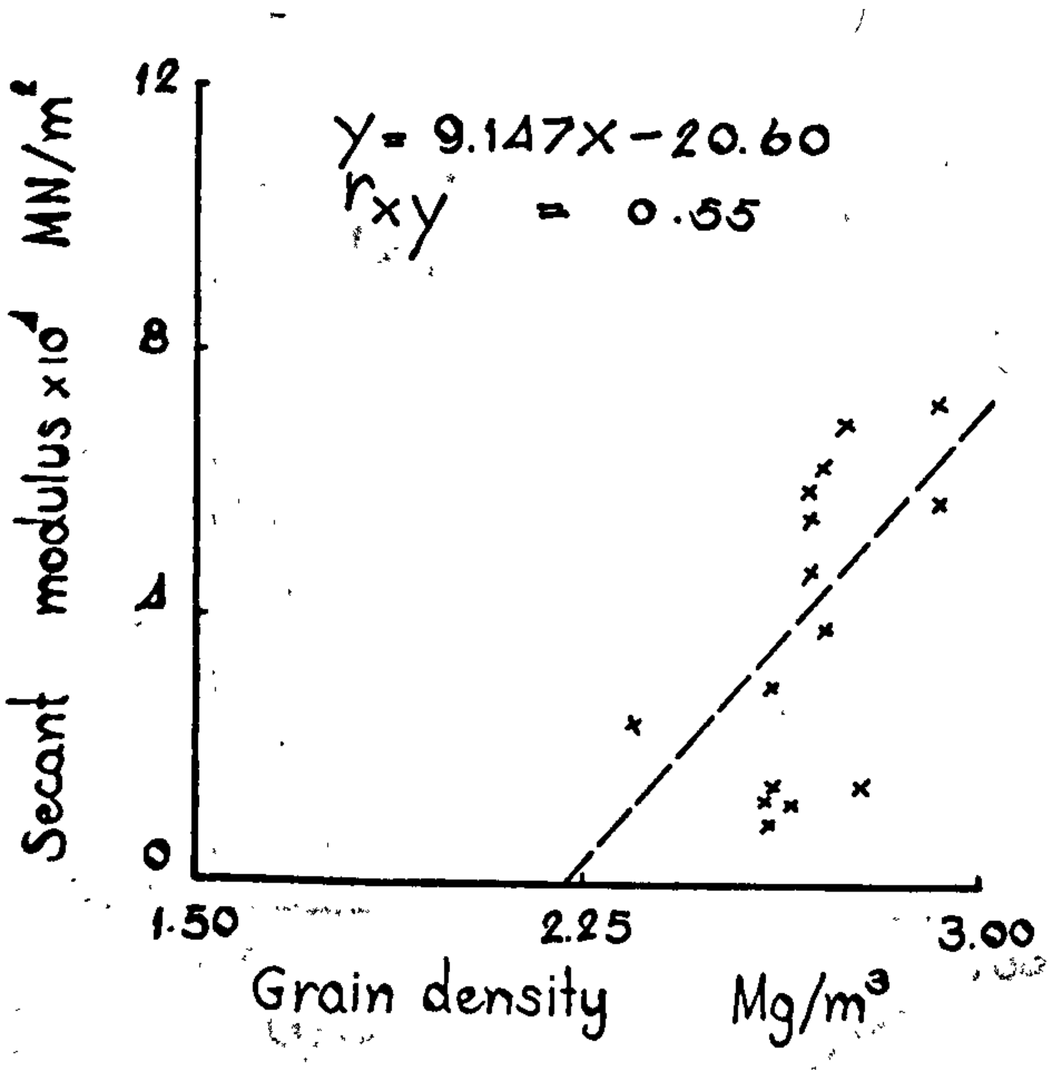
Y = 9.147X − 20.60
r_{xy} = 0.55
Secant modulus ×10⁴ MN/m²
12
8
4
0
1.50
2.25
3.00
Grain density Mg/m³

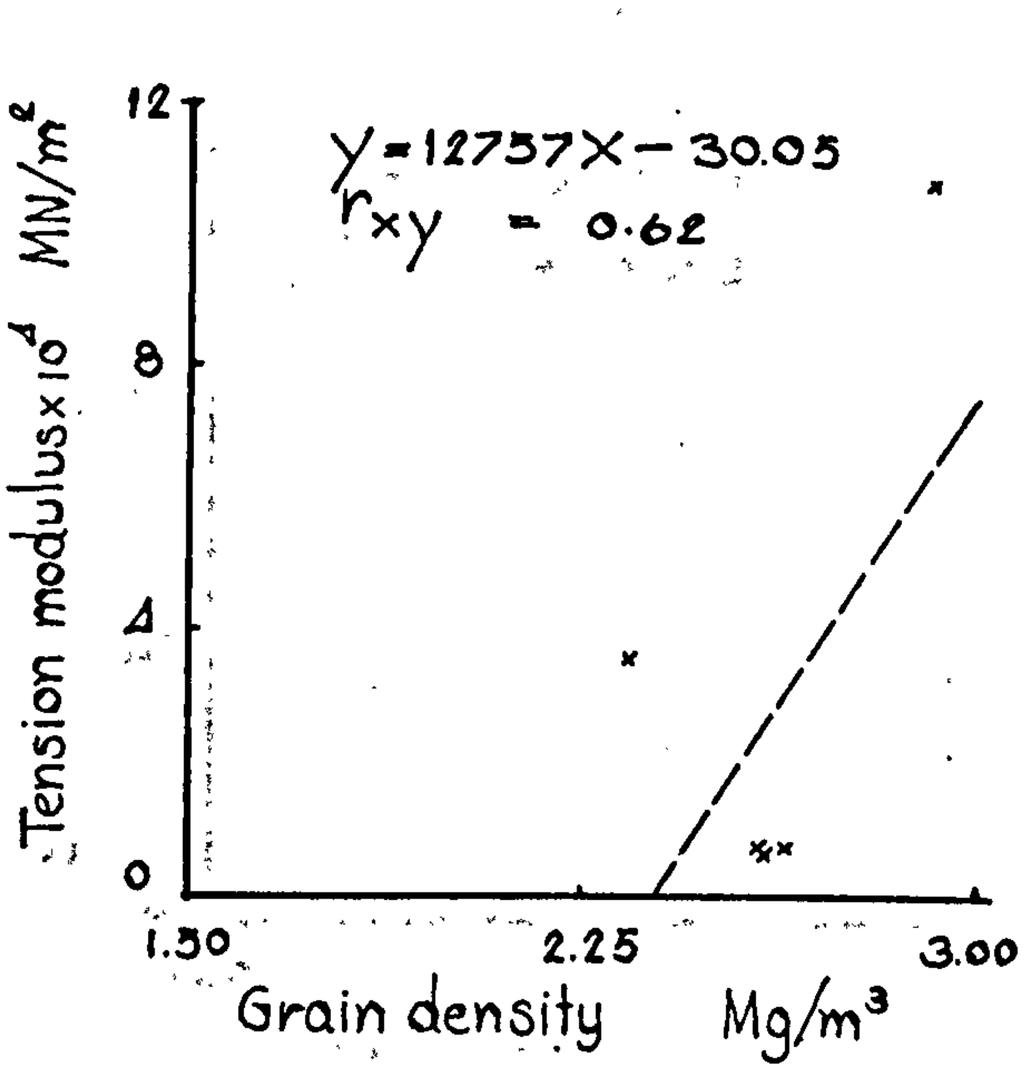
Y = 12757X − 30.05
r_{xy} = 0.62
Tension modulus ×10⁴ MN/m²
12
8
4
0
1.50
2.25
3.00
Grain density Mg/m³

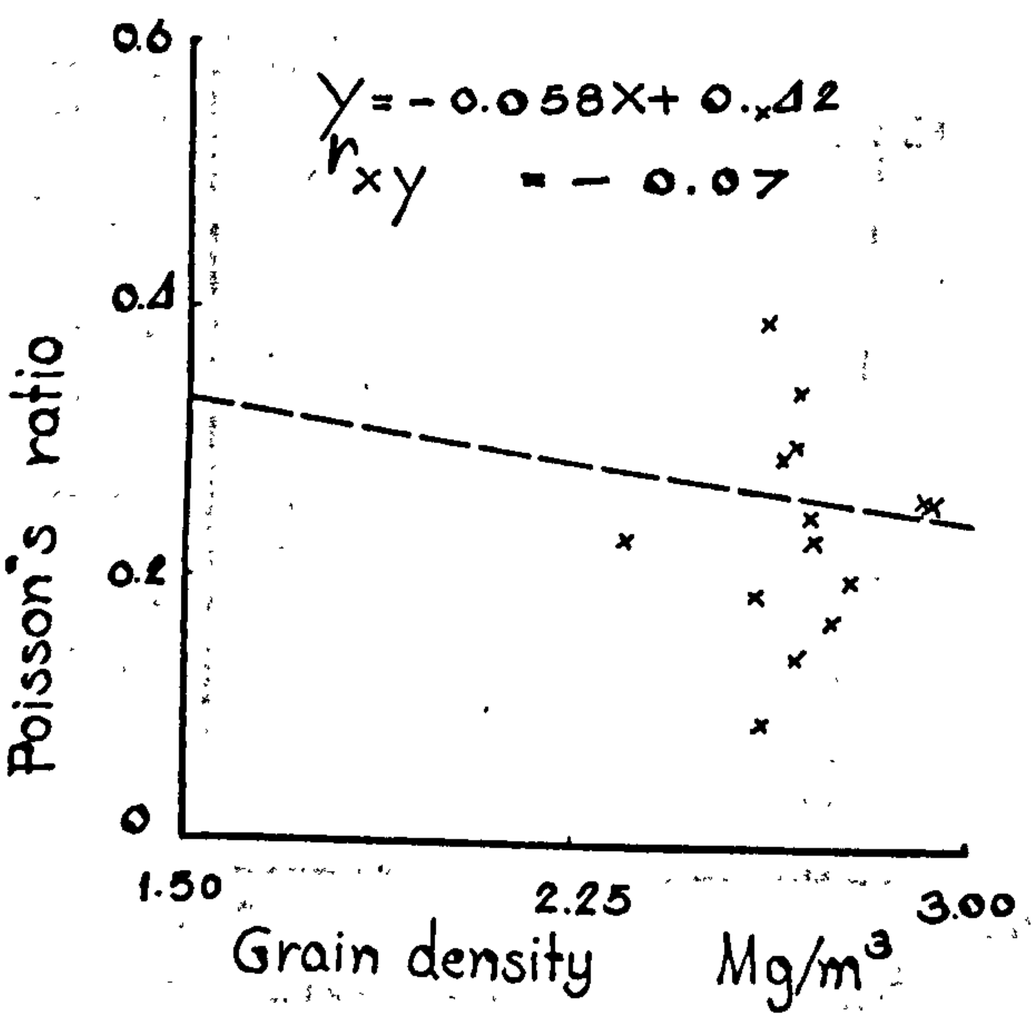
Y = −0.058X + 0.42
r_{xy} = −0.07
Poisson's ratio
0.6
0.4
0.2
0
1.50
2.25
3.00
Grain density Mg/m³

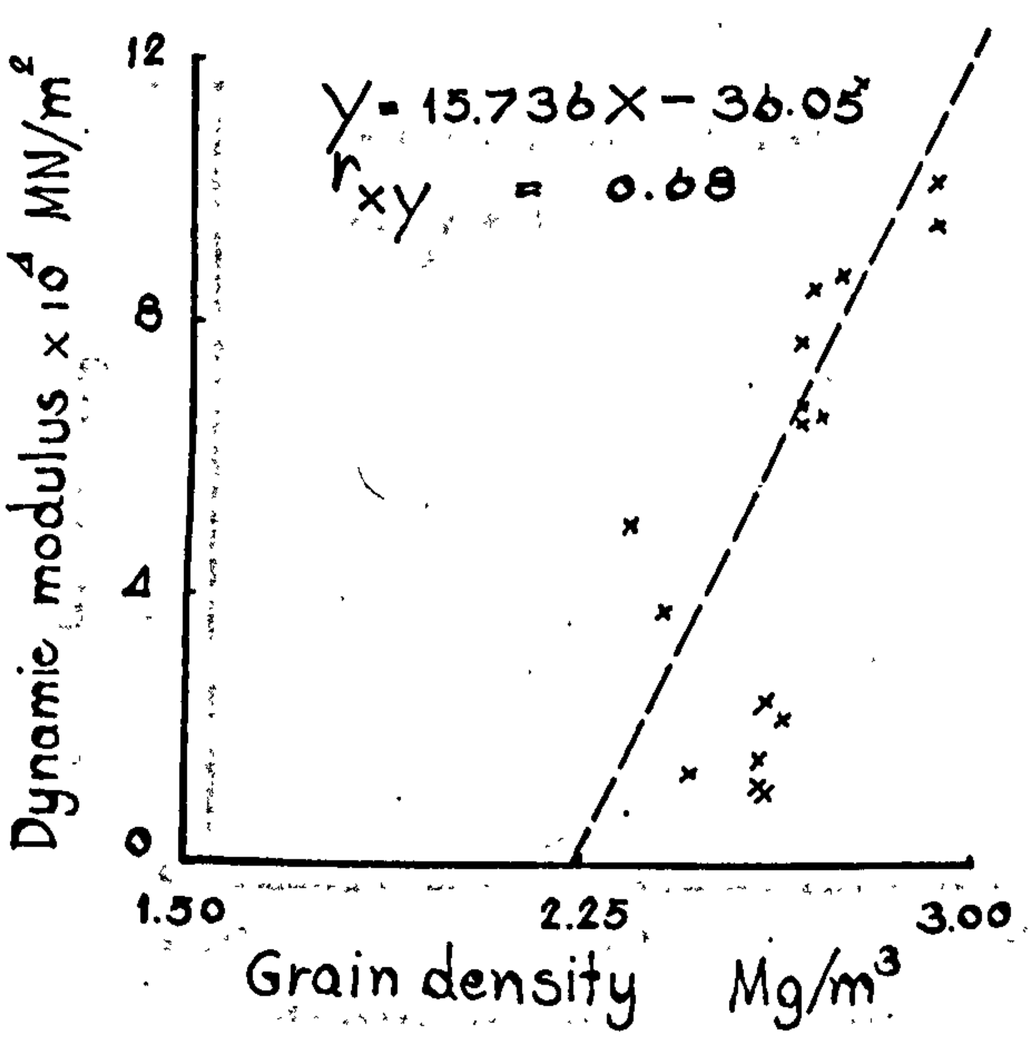
Y = 15.736X − 36.05
r_{xy} = 0.68
Dynamic modulus ×10⁴ MN/m²
12
8
4
0
1.50
2.25
3.00
Grain density Mg/m³

Figure 47 (11).

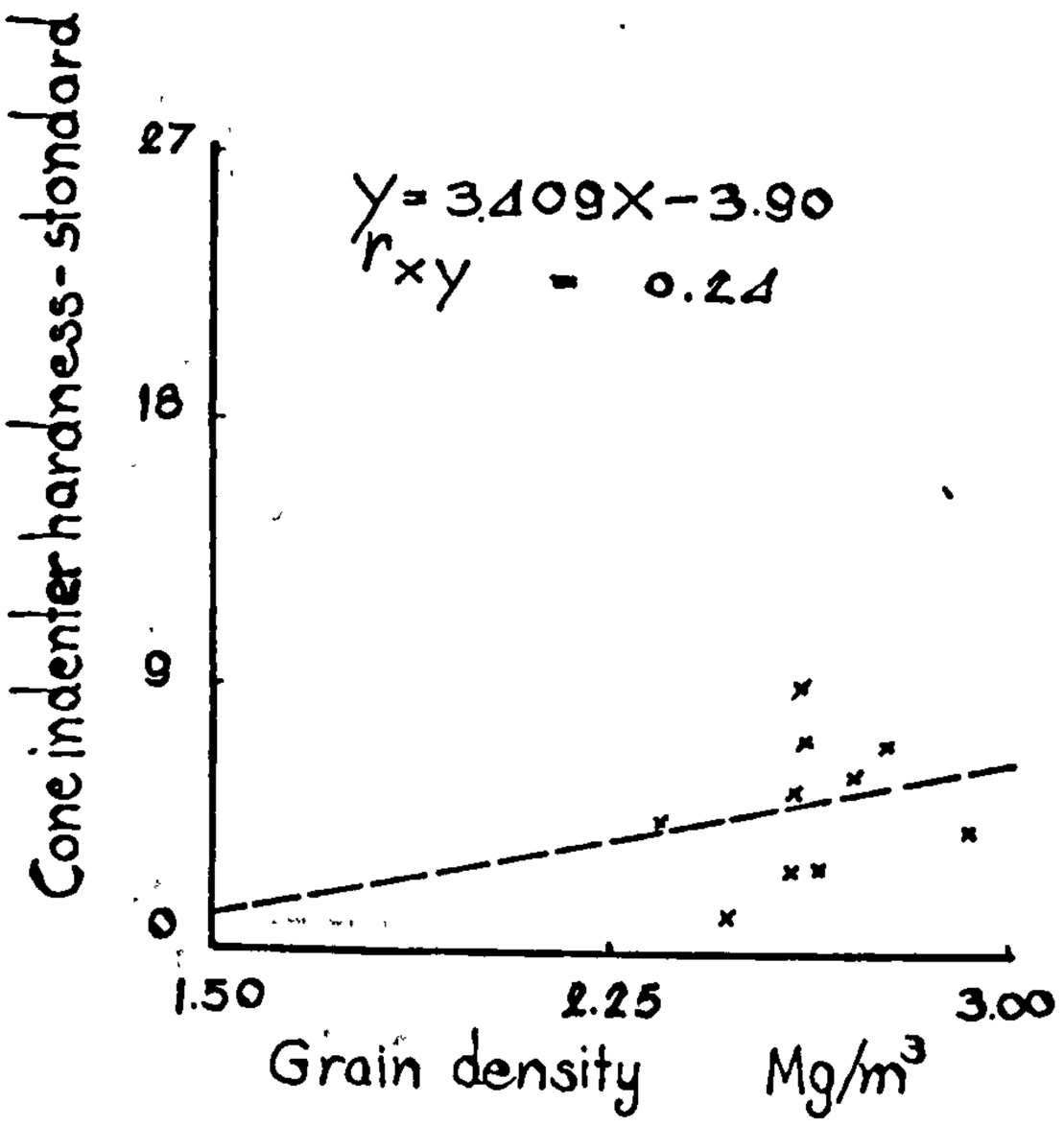
Y= 3.409X-3.90
r_{xy} = 0.24
Cone indenter hardness-standard
27
18
9
0
1.50
2.25
3.00
Grain density Mg/m³

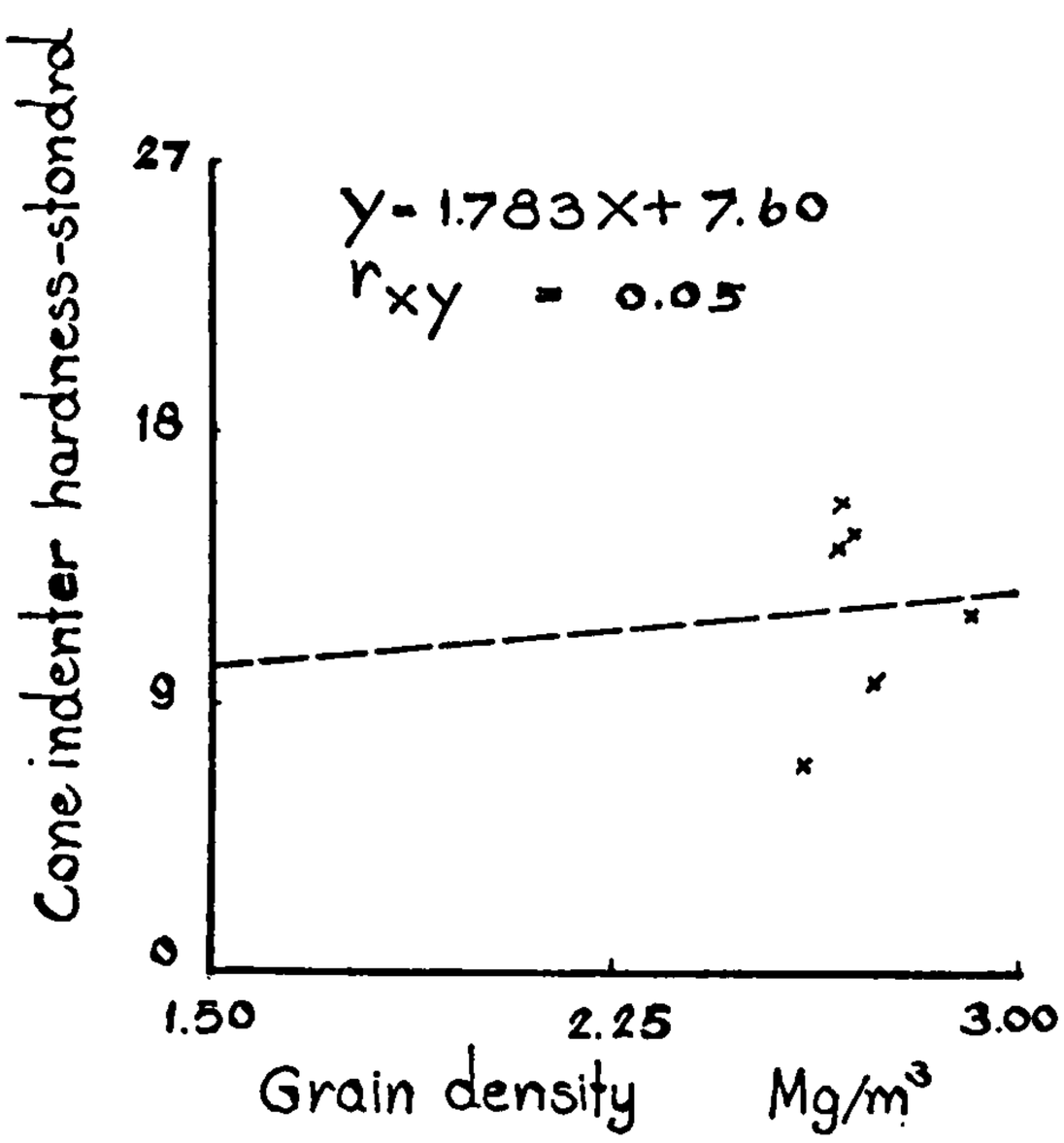
Y= 1.783X+7.60
r_{xy} = 0.05
Cone indenter hardness-standrd
27
18
9
0
1.50
2.25
3.00
Grain density Mg/m³

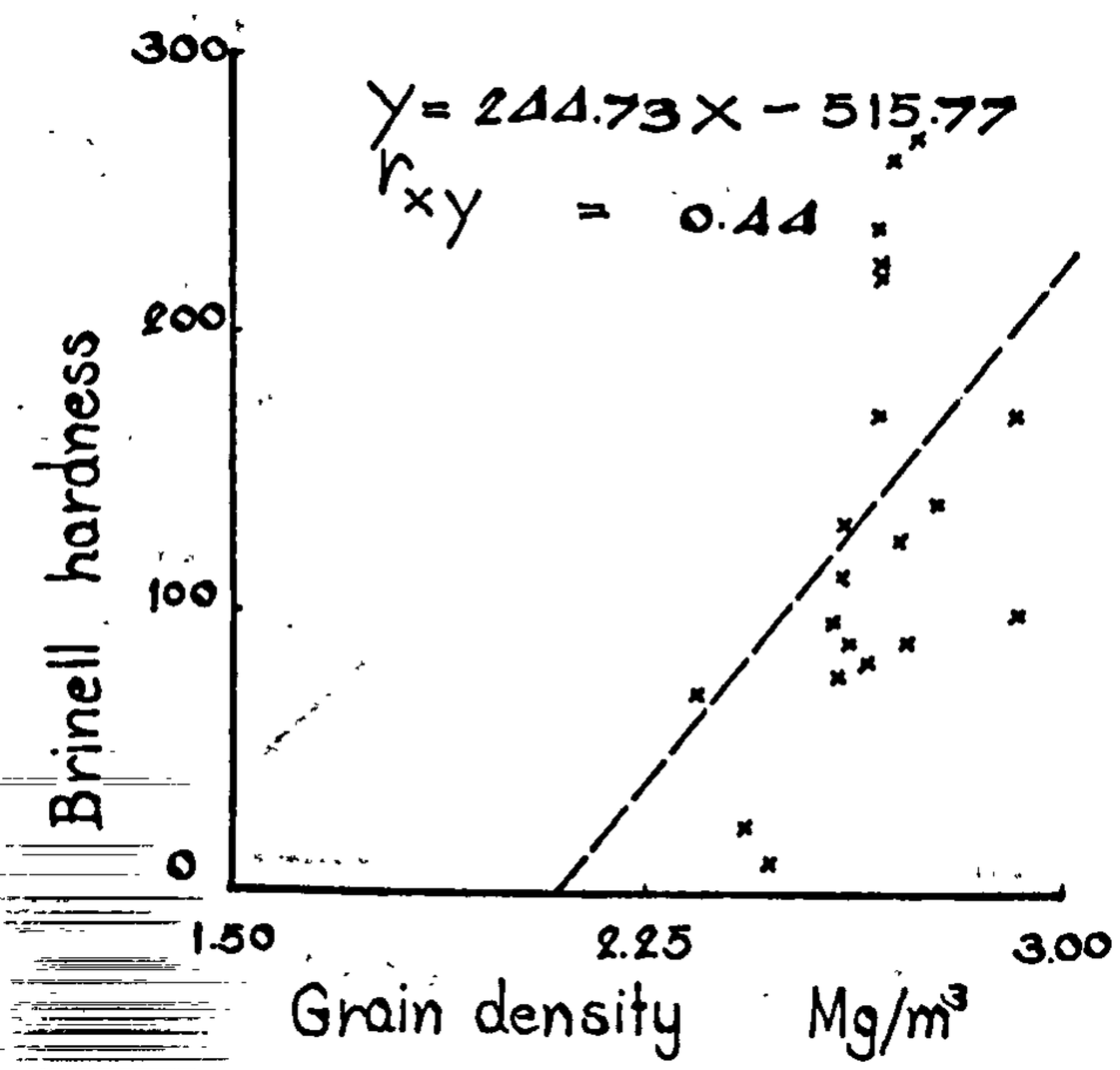
Y= 244.73X - 515.77
r_{xy} = 0.44
Brinell hardness
300
200
100
0
1.50
2.25
3.00
Grain density Mg/m³

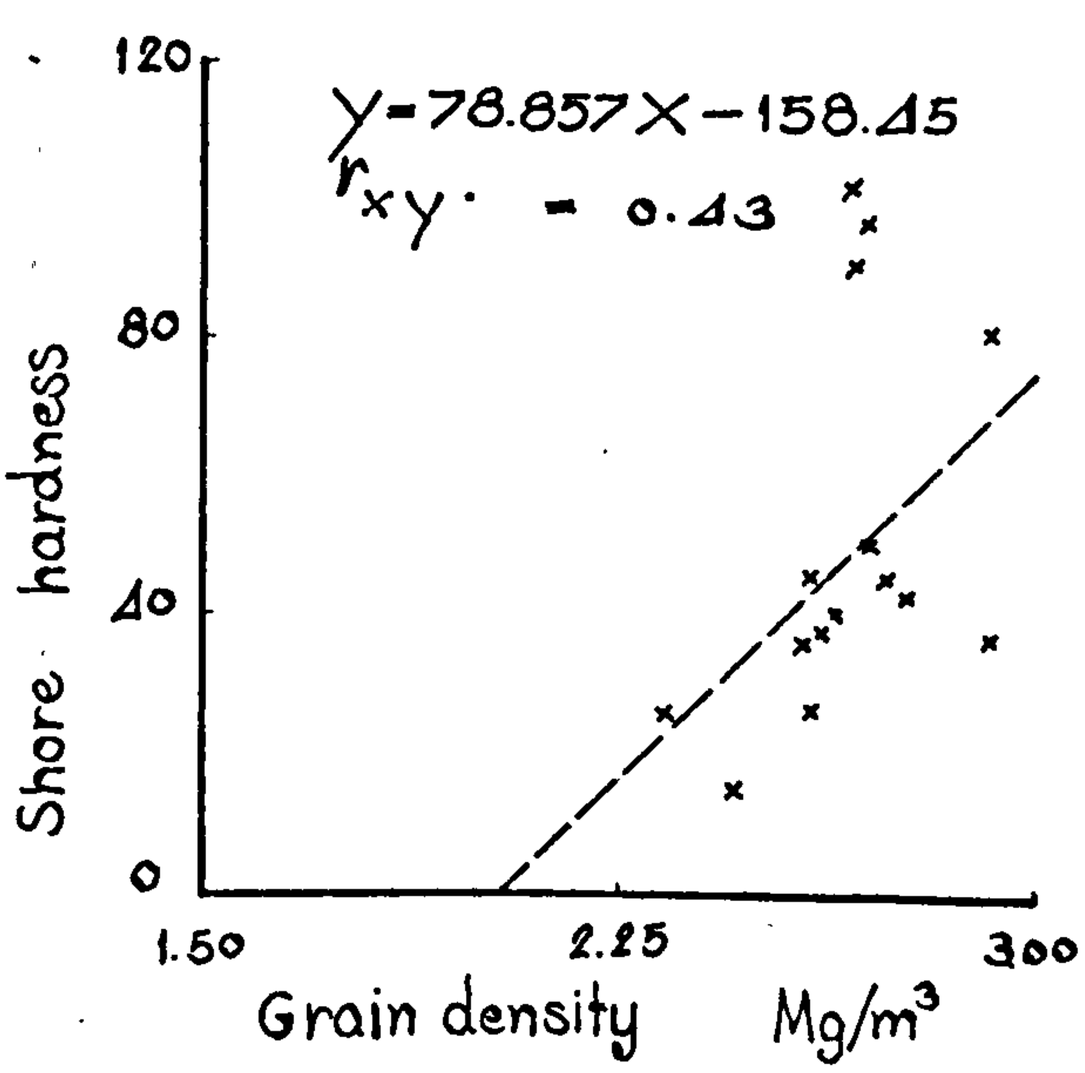
Y= 78.857X - 158.45
r_{xy} = 0.43
Shore hardness
120
80
40
0
1.50
2.25
3.00
Grain density Mg/m³

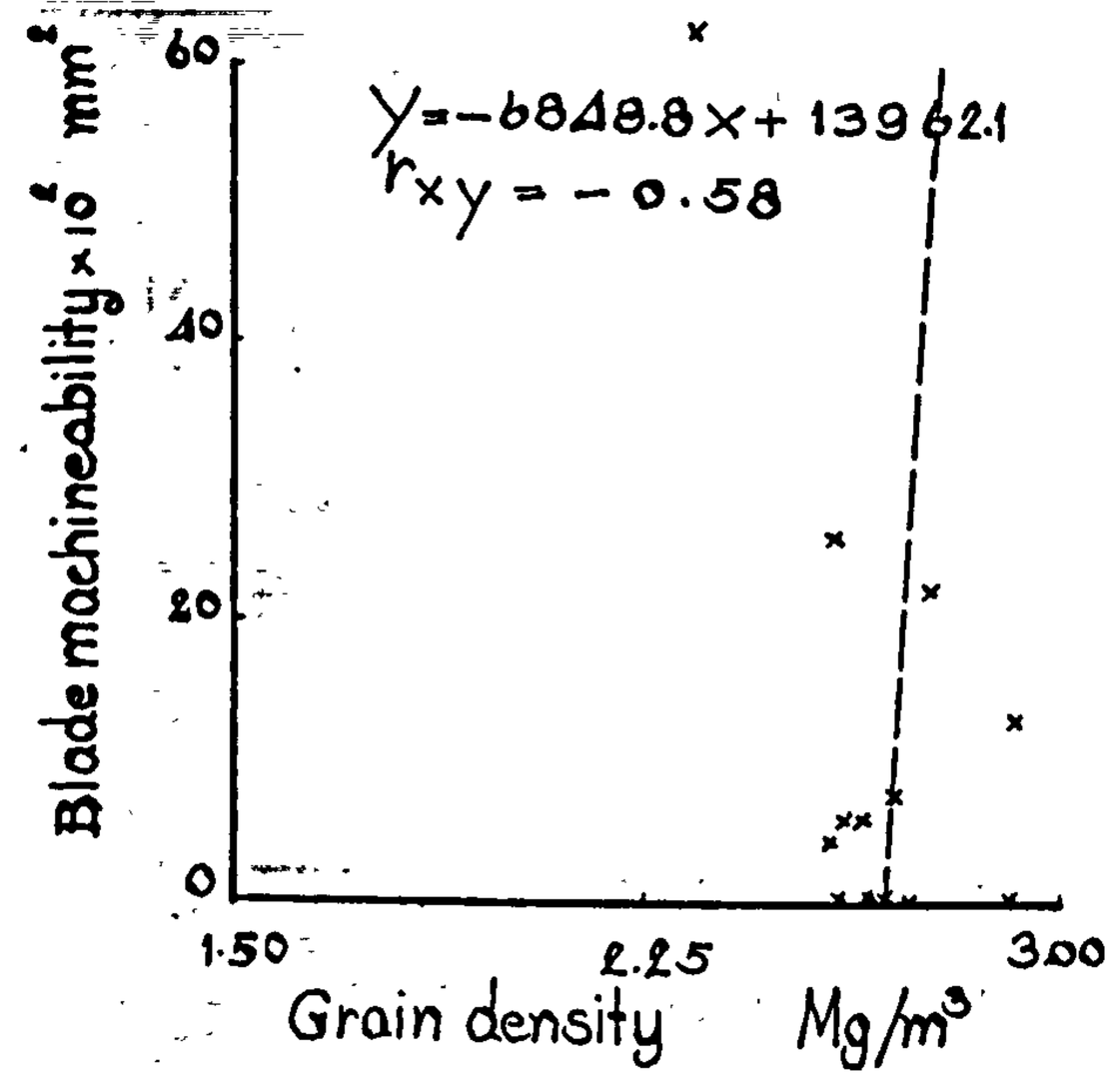
Y= -6848.8X + 13962.1
r_{xy} = - 0.58
Blade machineability x10⁴ mm²
60
40
20
0
1.50
2.25
3.00
Grain density Mg/m³

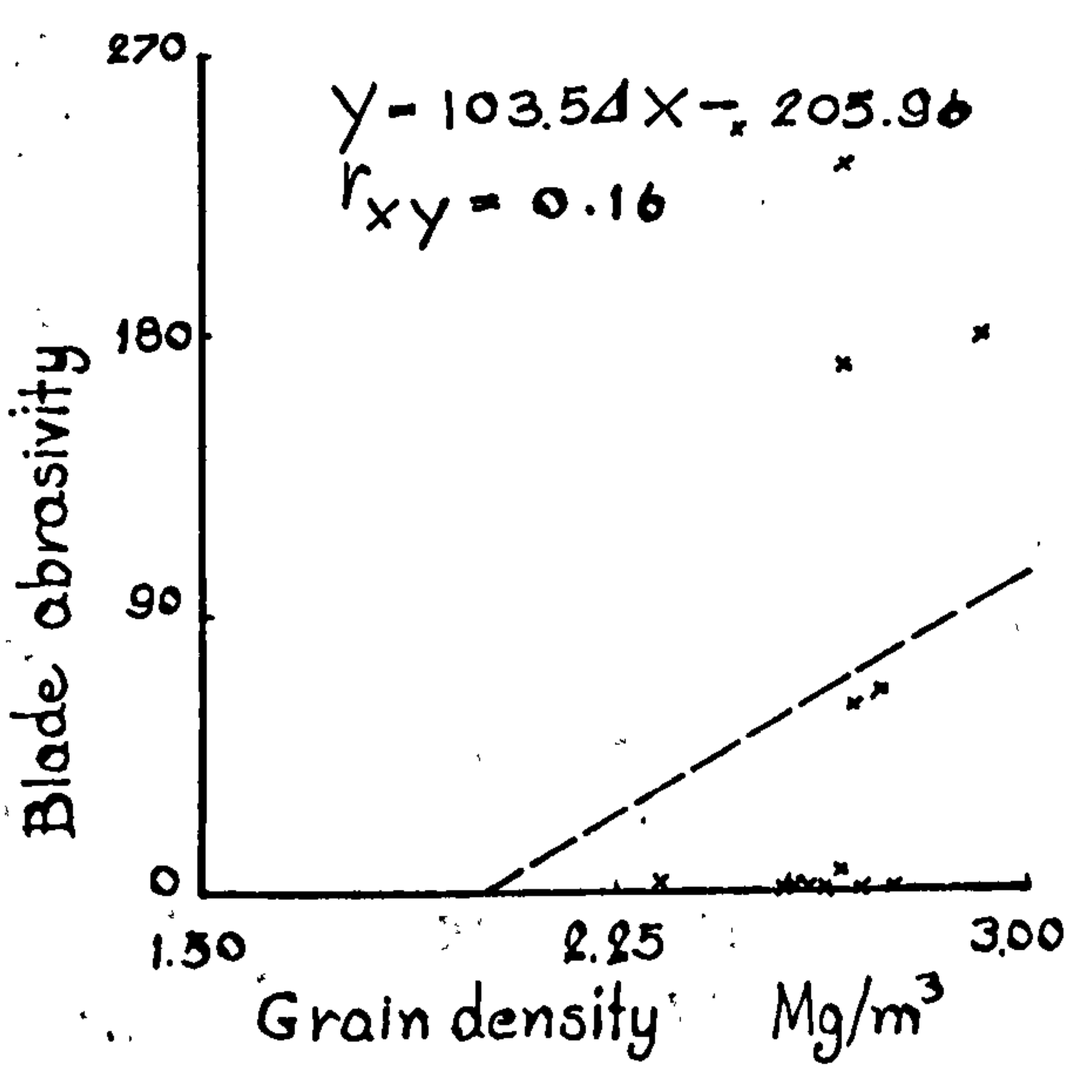
Y= 103.54X - 205.96
r_{xy} = 0.16
Blade abrasivity
270
180
90
0
1.50
2.25
3.00
Grain density Mg/m³

Figure 47 (12)

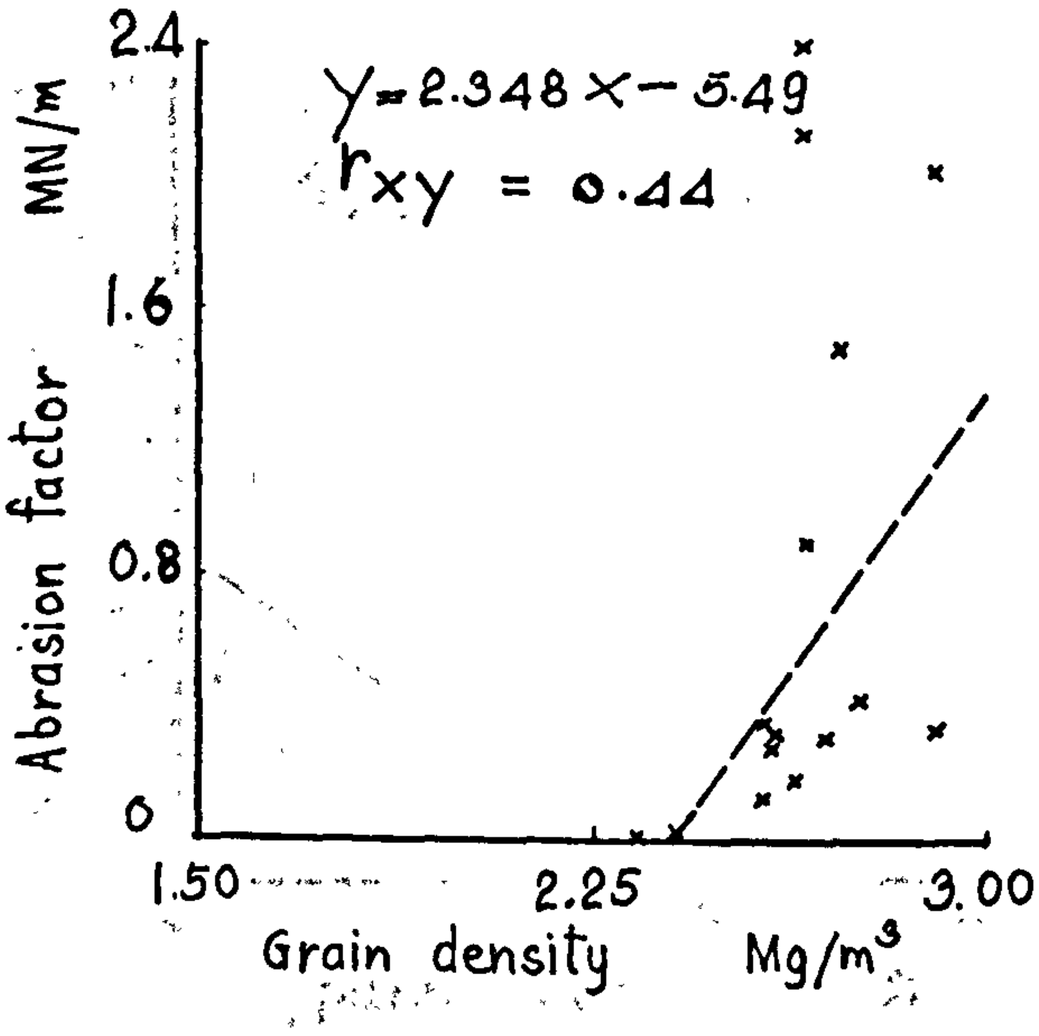
Y=2.348X−5.49
r_{xy} = 0.44
Abrasion factor MN/m
2.4
1.6
0.8
0
1.50
2.25
3.00
Grain density Mg/m³

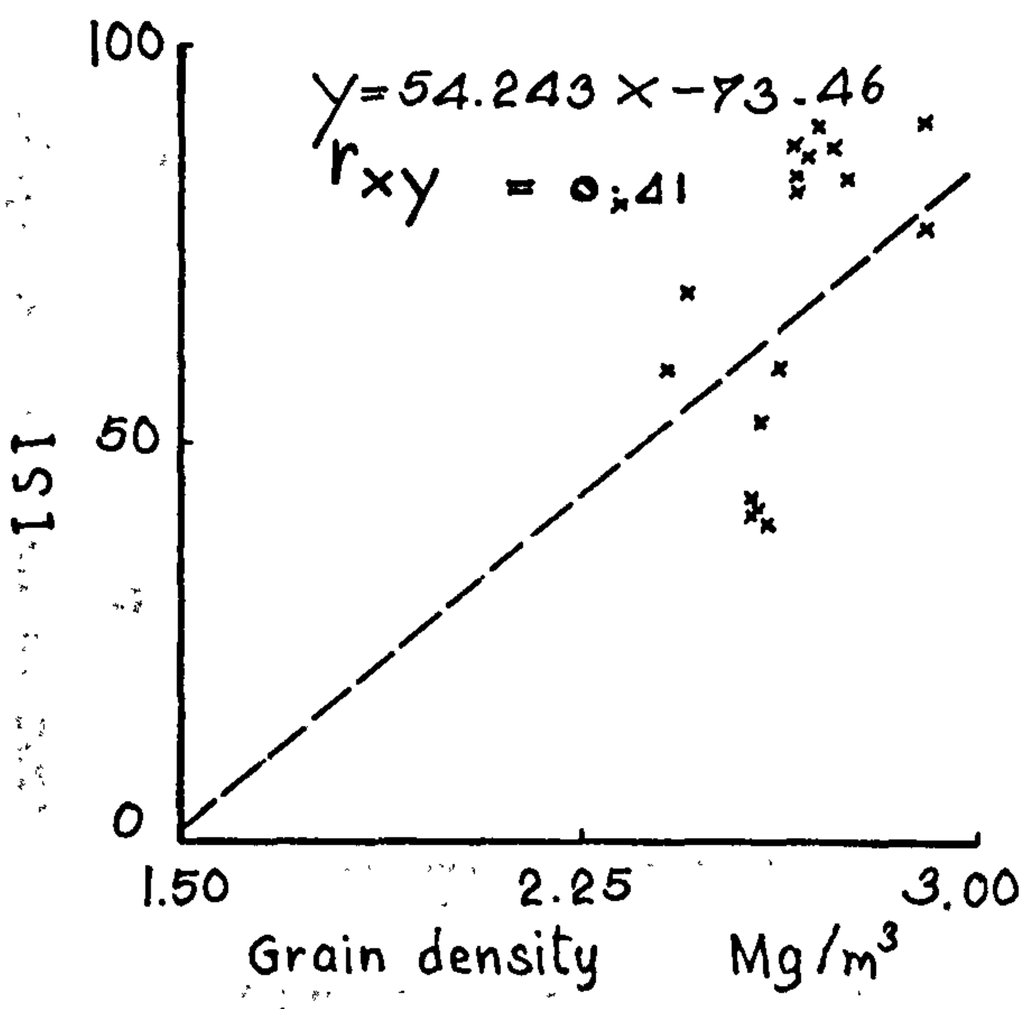
Y=54.243X−73.46
r_{xy} = 0.41
ISI
100
50
0
1.50
2.25
3.00
Grain density Mg/m³

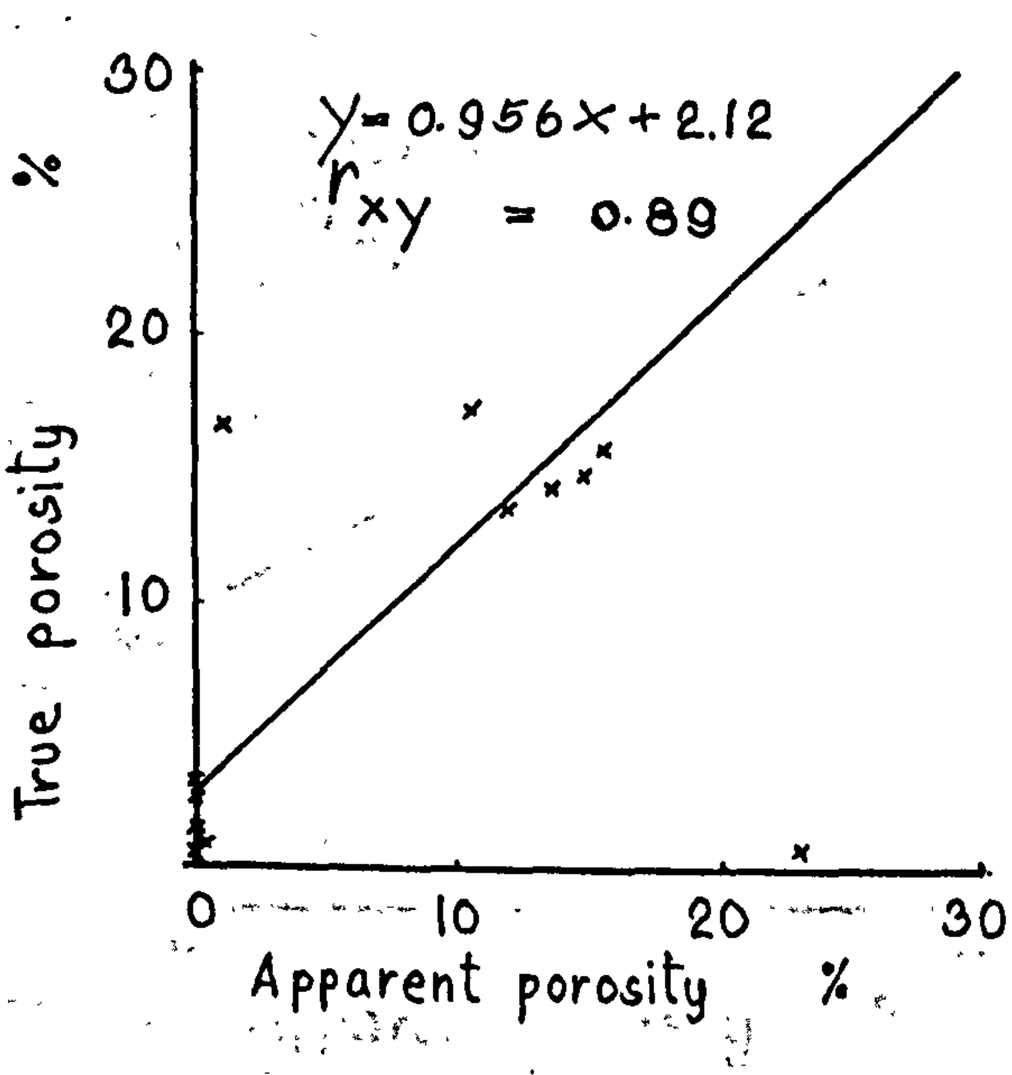
Y=0.956X+2.12
r_{xy} = 0.89
%
30
20
10
True porosity
0
10
20
30
Apparent porosity %

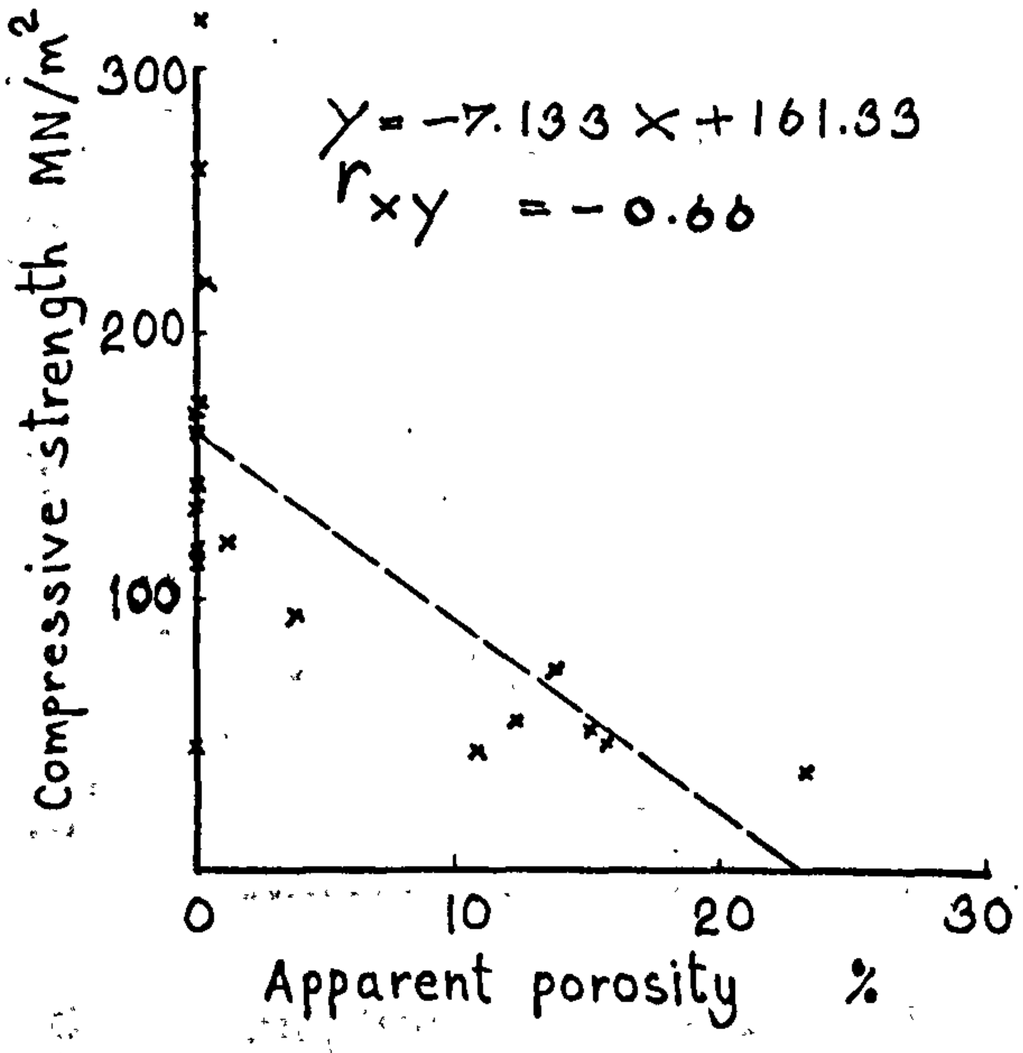
Y=−7.133X+161.33
r_{xy} = −0.66
Compressive strength MN/m²
300
200
100
0
10
20
30
Apparent porosity %

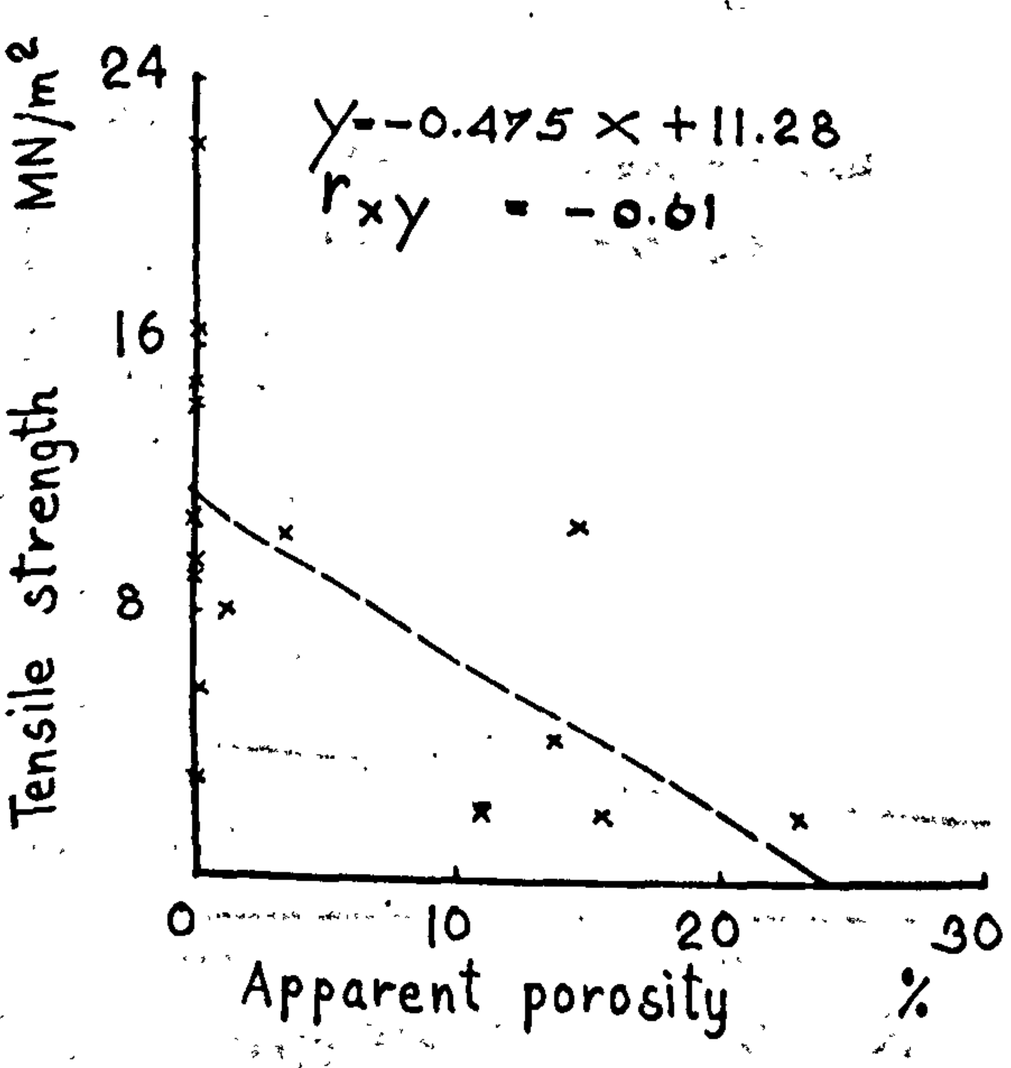
Y=−0.475X+11.28
r_{xy} = −0.61
Tensile strength MN/m²
24
16
8
0
10
20
30
Apparent porosity %

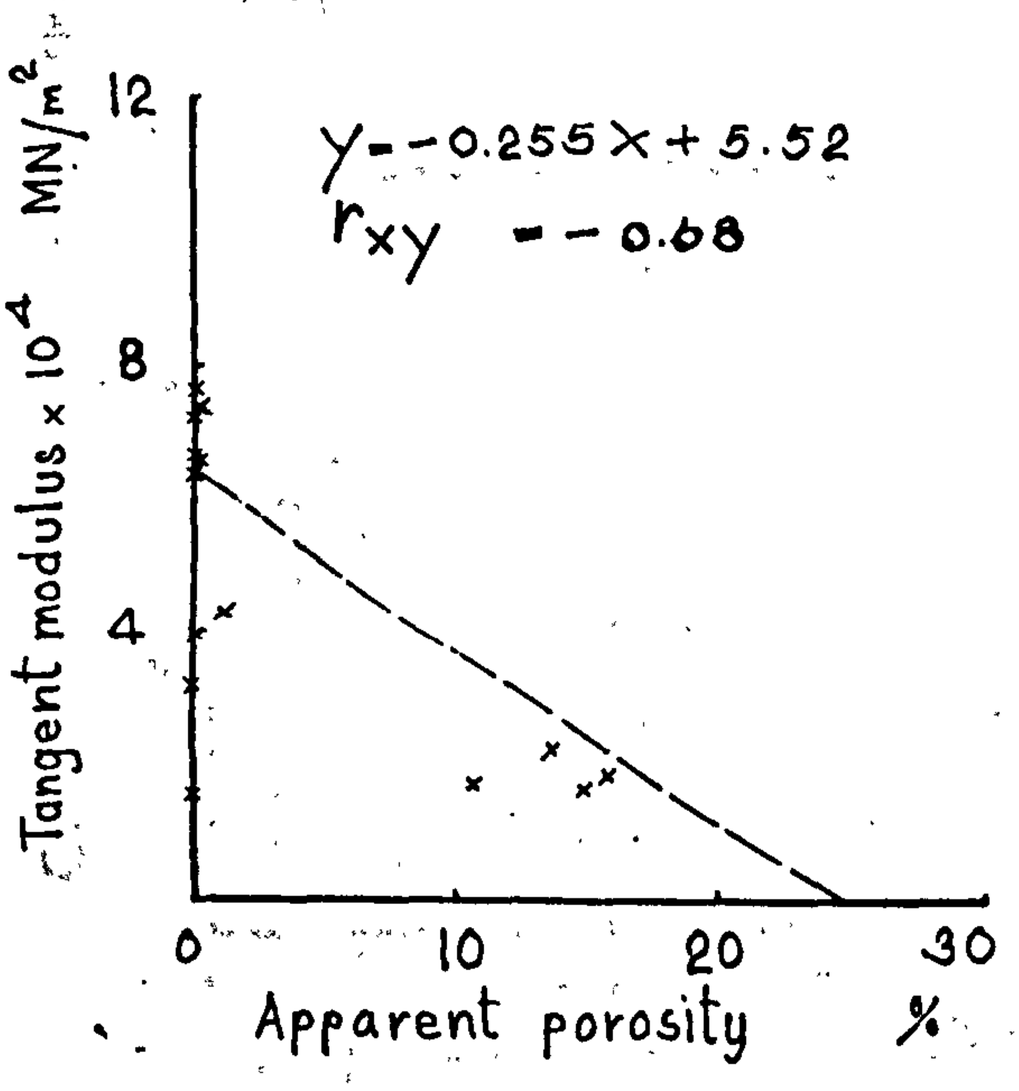
Y=−0.255X+5.52
r_{xy} = −0.68
Tangent modulus × 10⁴ MN/m²
12
8
4
0
10
20
30
Apparent porosity %

Figure 47 (13)

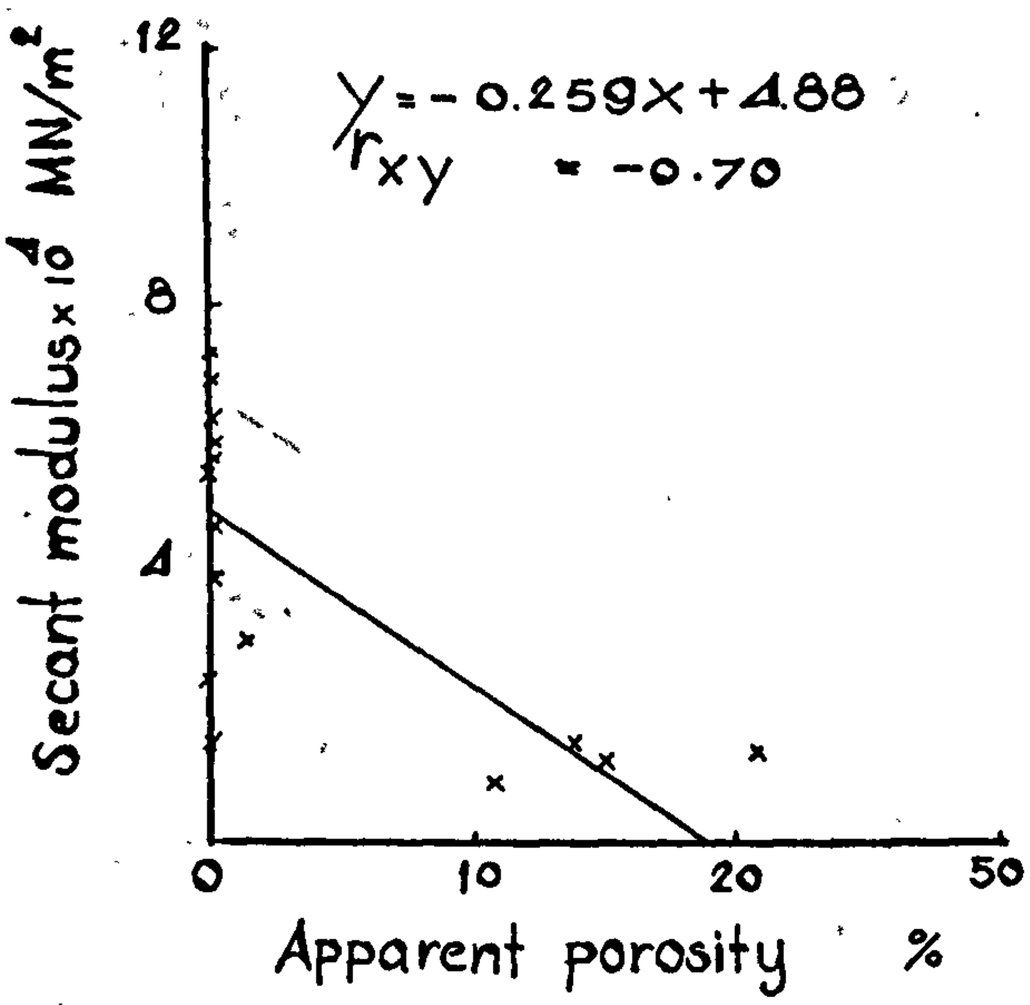
Y = - 0.259X + 4.88
r_xy = -0.70
Secant modulus x 10^4 MN/m^2
12
8
4
0
10
20
50
Apparent porosity %

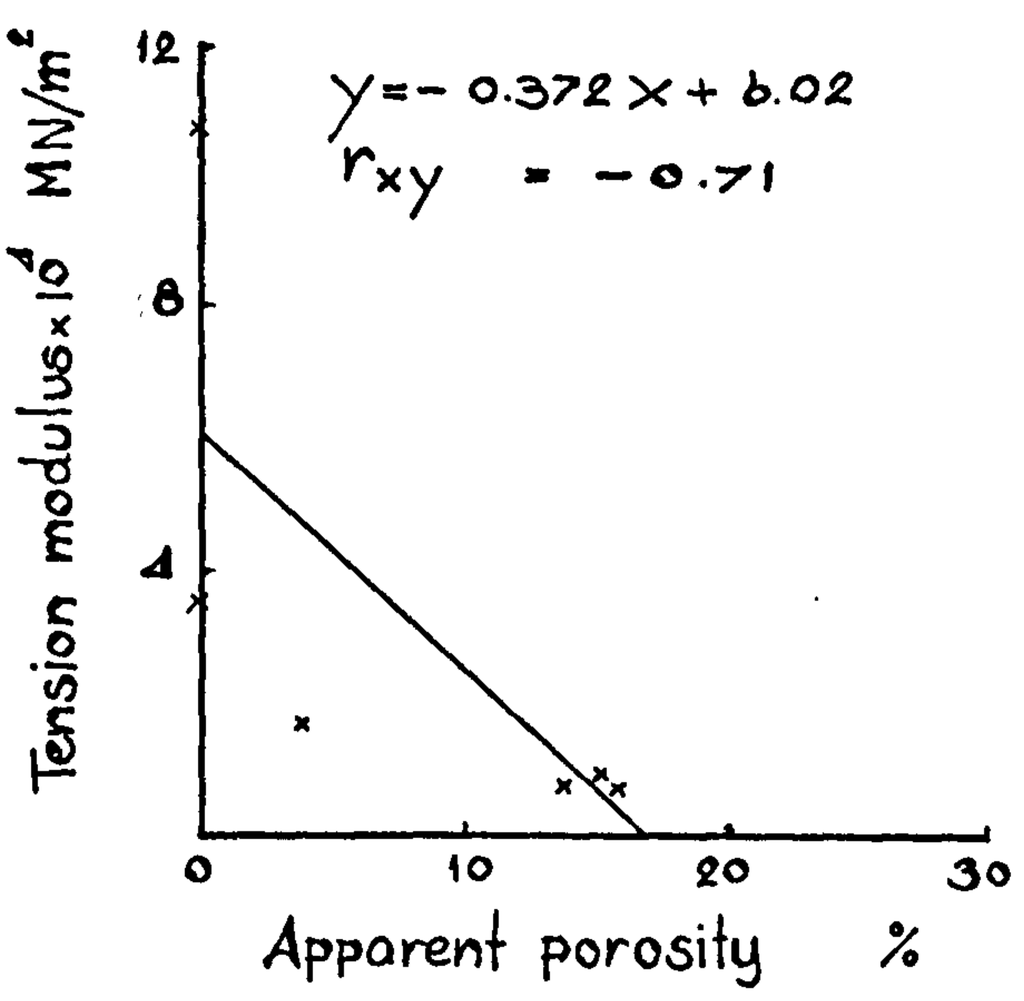
Y = - 0.372X + 6.02
r_xy = - 0.71
Tension modulus x 10^4 MN/m^2
12
8
4
0
10
20
30
Apparent porosity %

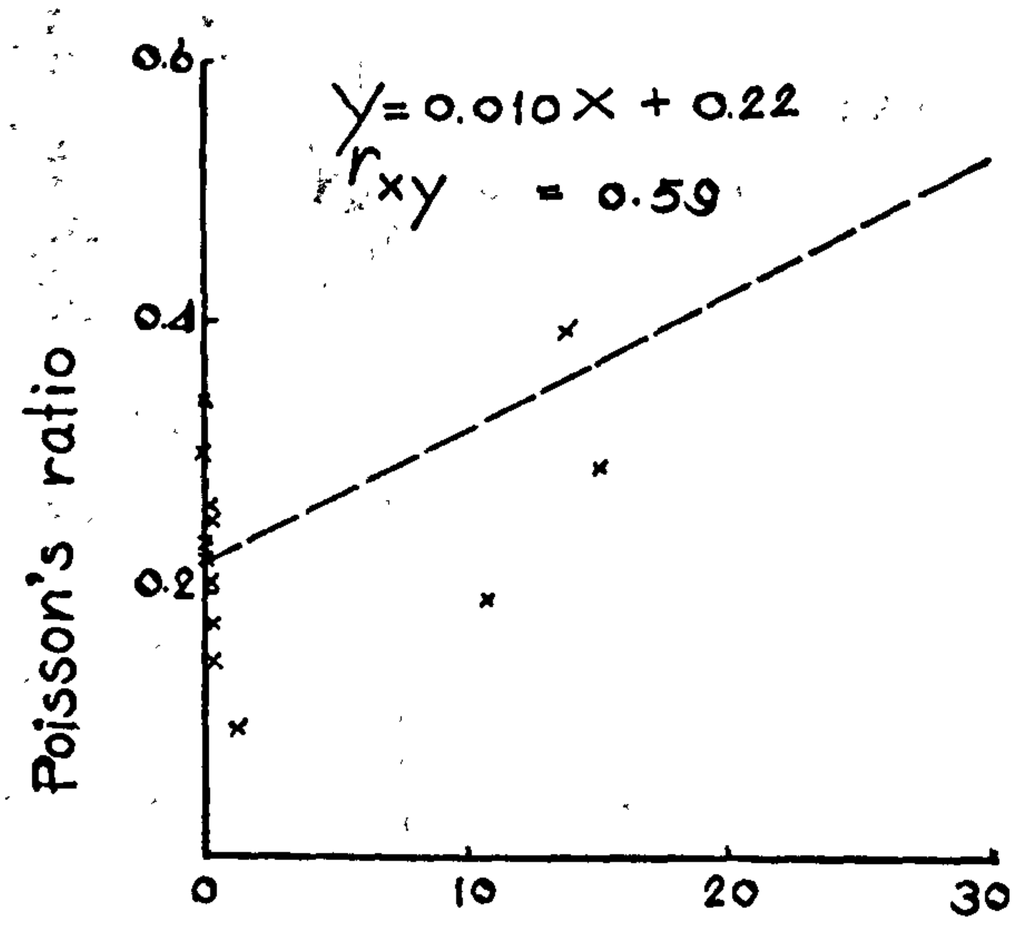
Y = 0.010X + 0.22
r_xy = 0.59
Poisson's ratio
0.6
0.4
0.2
0
10
20
30
Apparent porosity %

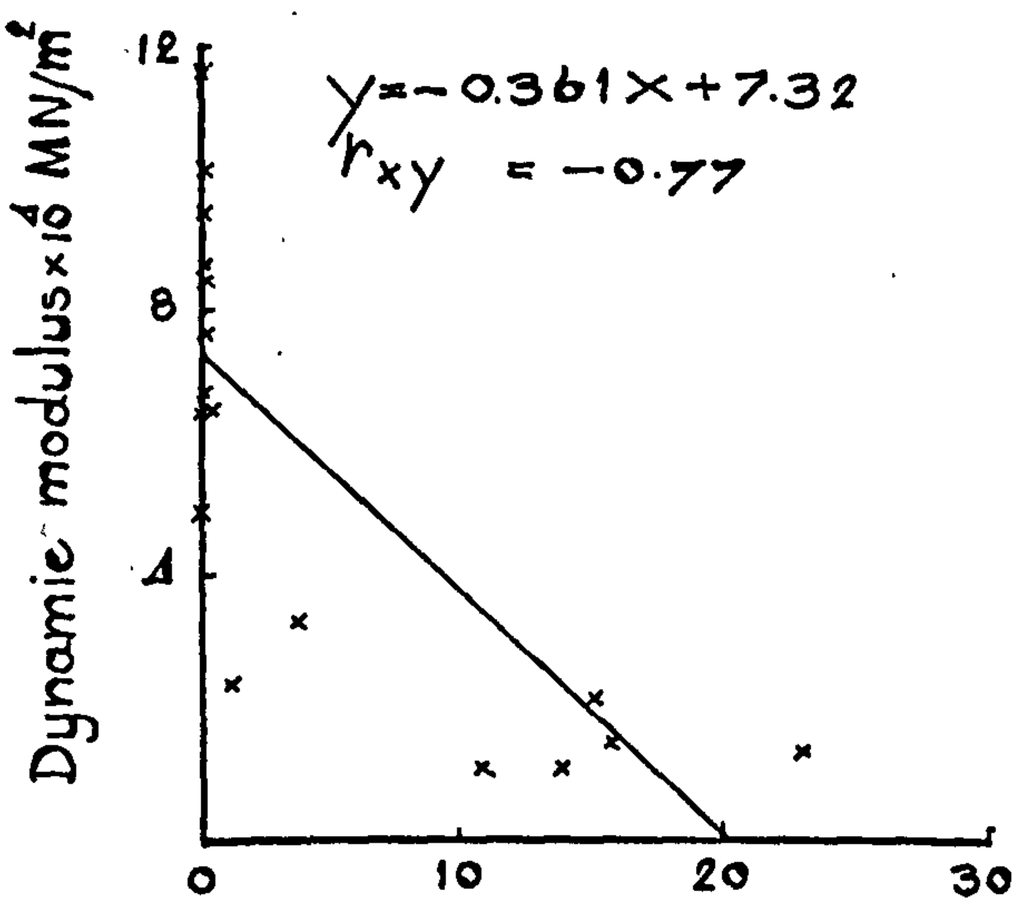
Y = - 0.361X + 7.32
r_xy = - 0.77
Dynamic modulus x 10^4 MN/m^2
12
8
4
0
10
20
30
Apparent porosity %

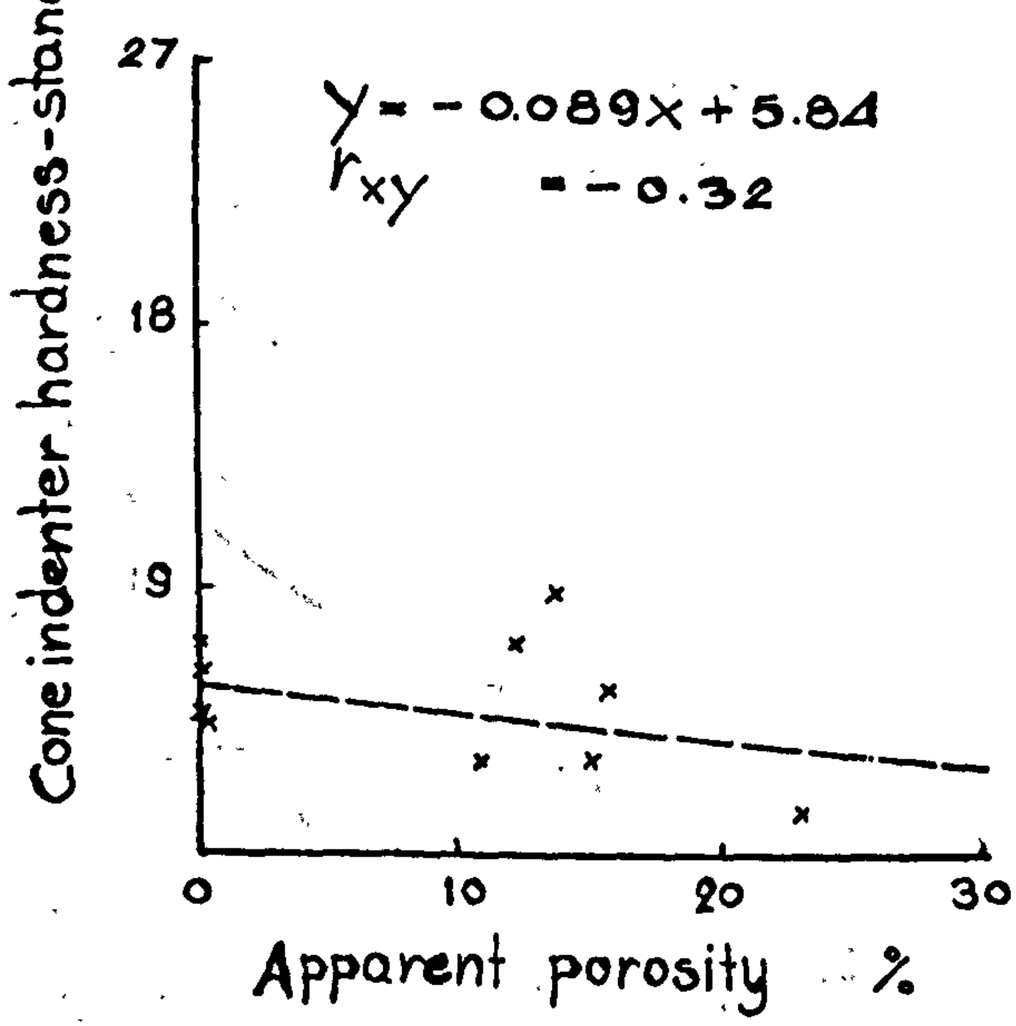
Y = - 0.089X + 5.84
r_xy = - 0.32
Cone indenter hardness-standard
27
18
9
0
10
20
30
Apparent porosity %

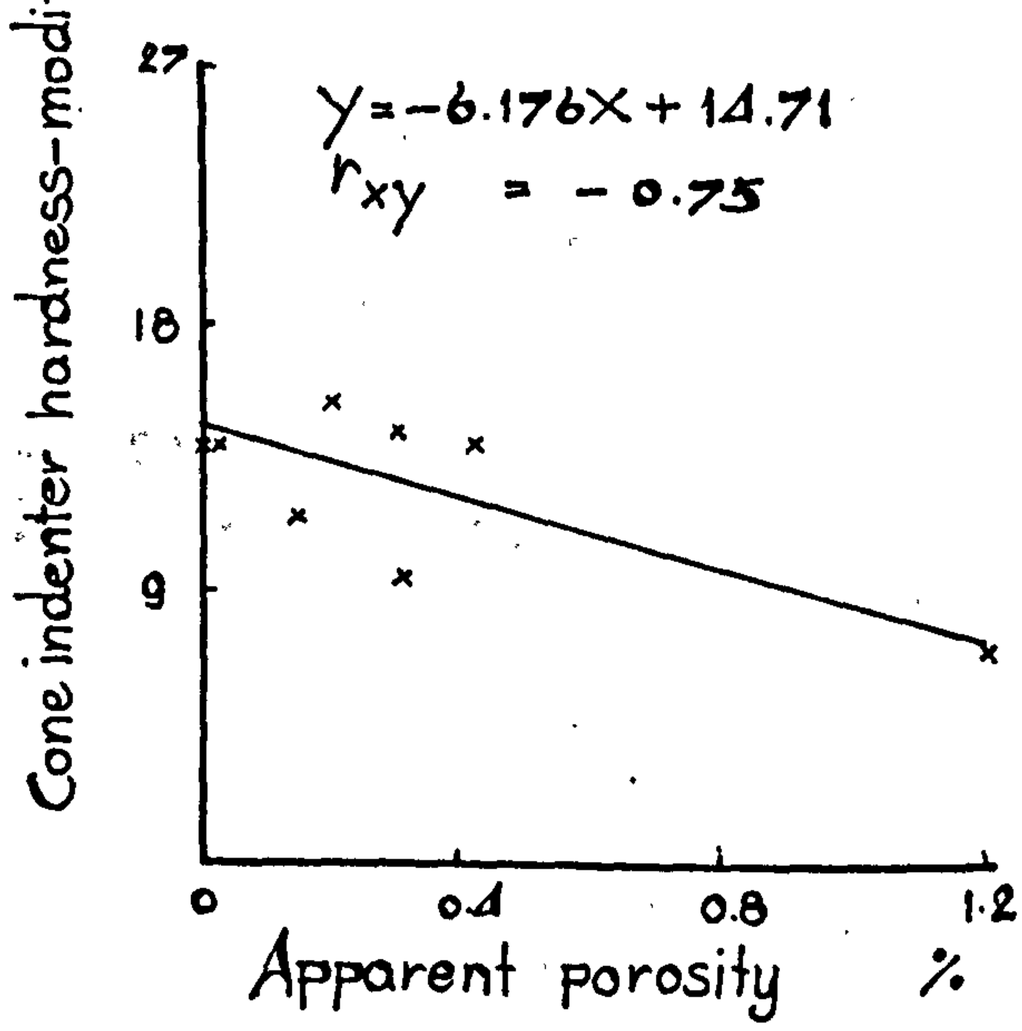
Y = - 6.176X + 14.71
r_xy = - 0.75
Cone indenter hardness-modified
27
18
9
0
0.4
0.8
1.2
Apparent porosity %

Figure 47 (14)

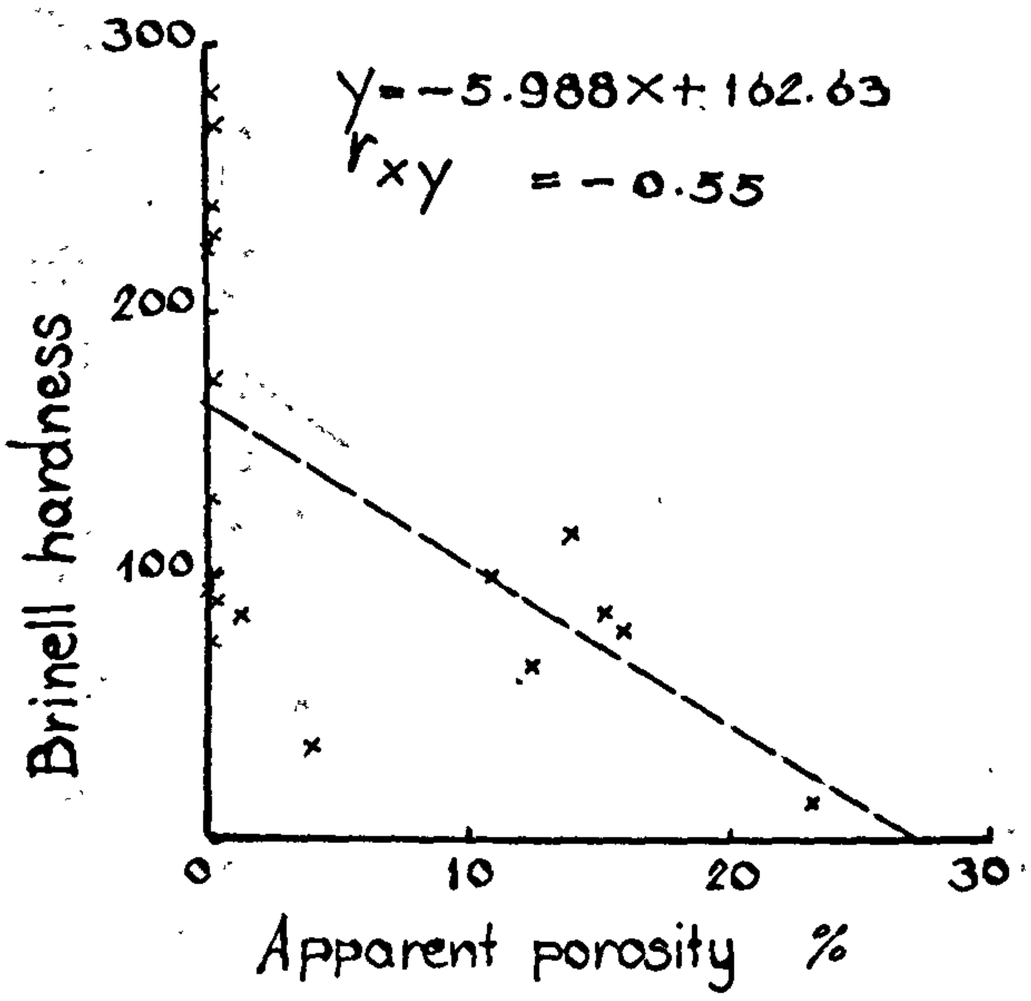
Y=-5.988X+162.63
r_{xy} = -0.55
Brinell hardness
300
200
100
0
10
20
30
Apparent porosity %

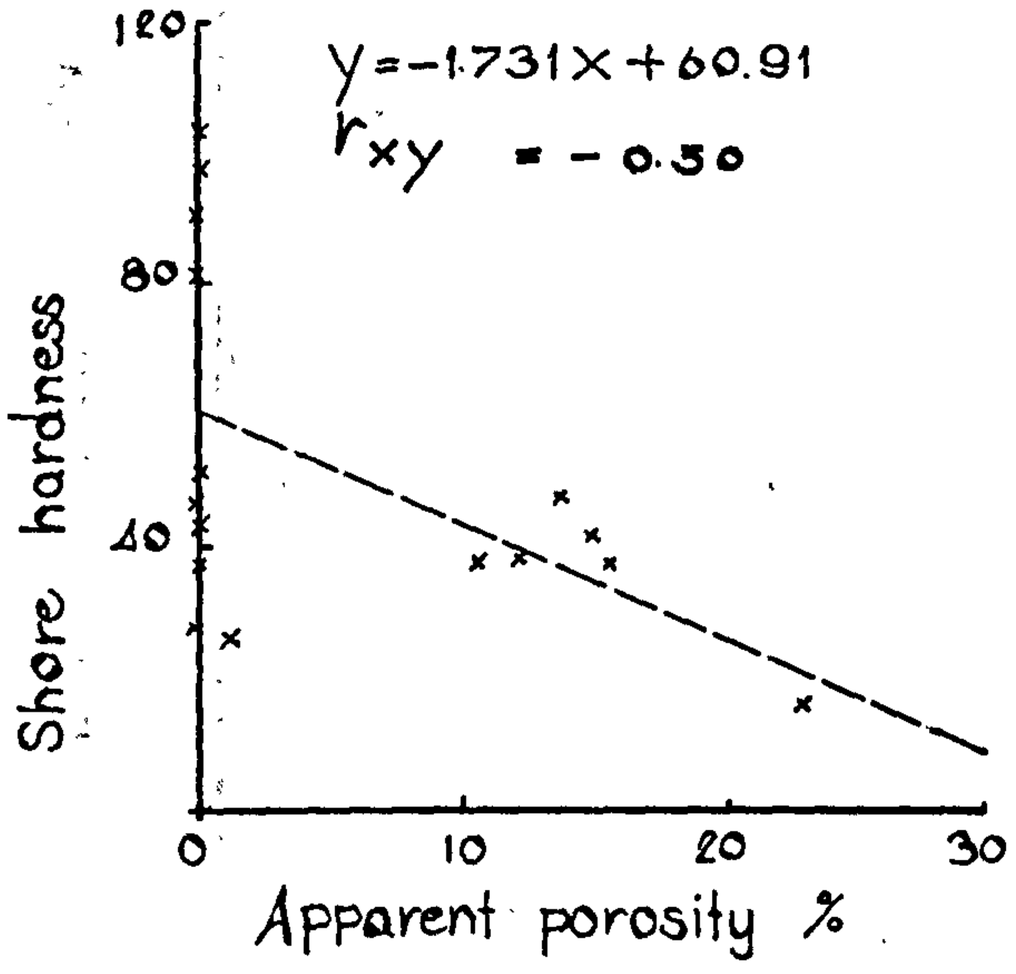
Y=-1.731X+60.91
r_{xy} = -0.50
Shore hardness
120
80
40
0
10
20
30
Apparent porosity %

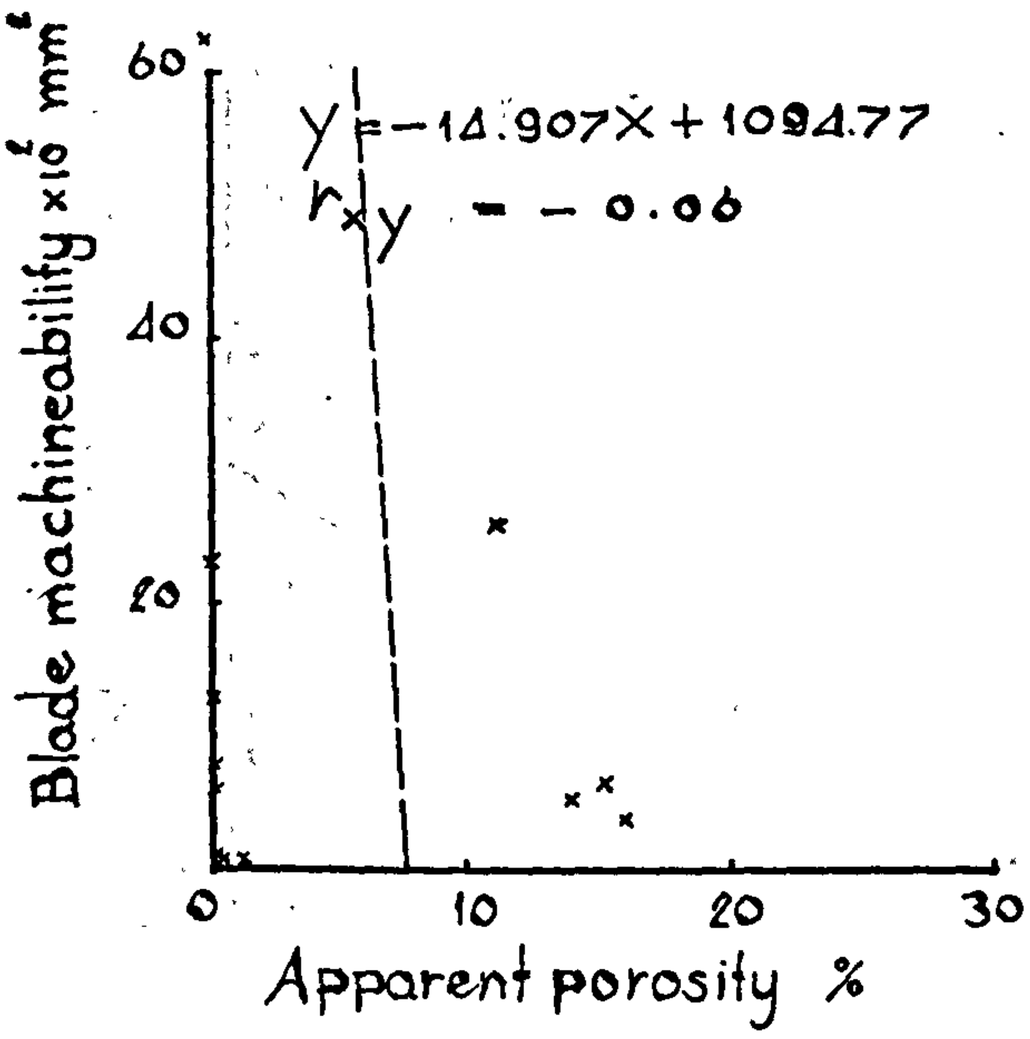
Y=-14.907X+1094.77
r_{xy} = -0.06
Blade machineability $\times 10^2$ mm
60
40
20
0
10
20
30
Apparent porosity %

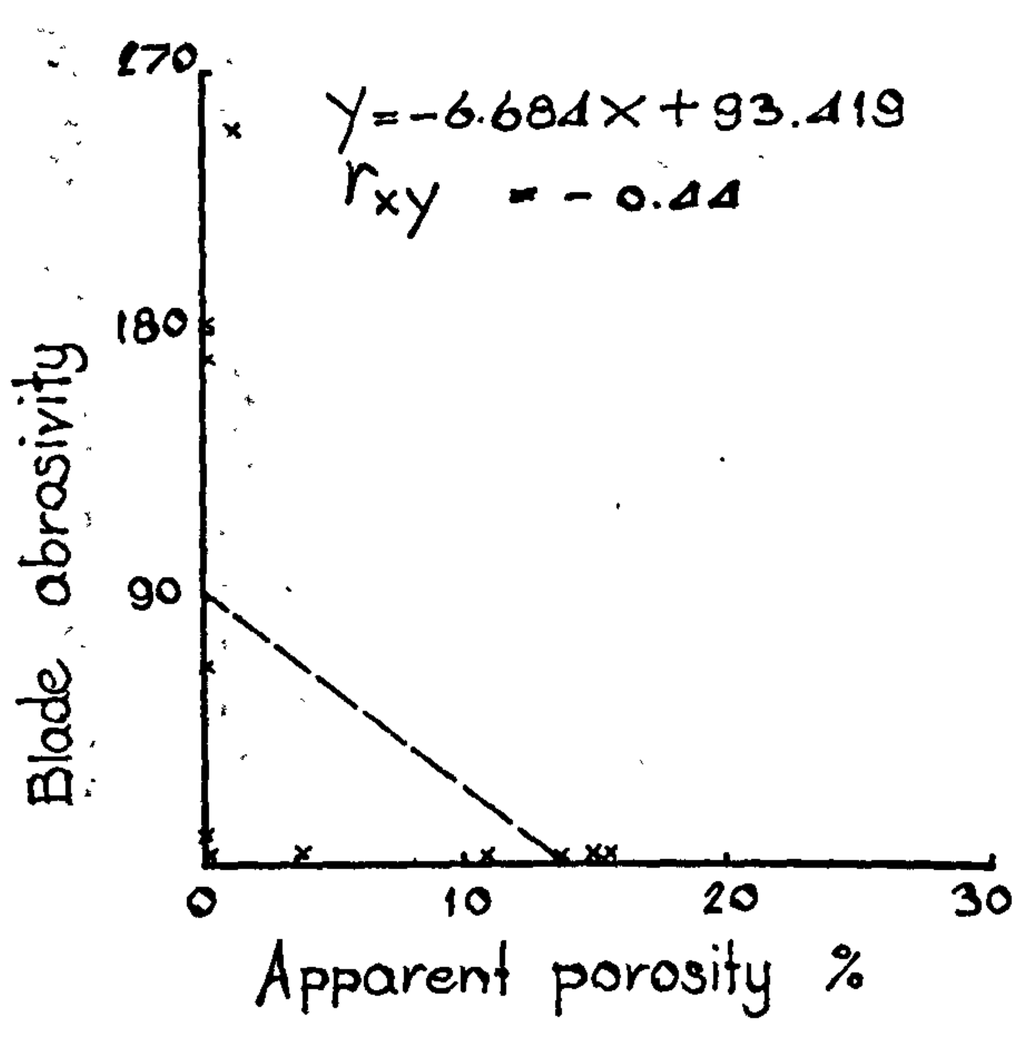
Y=-6.684X+93.419
r_{xy} = -0.44
Blade abrasivity
170
180
90
0
10
20
30
Apparent porosity %

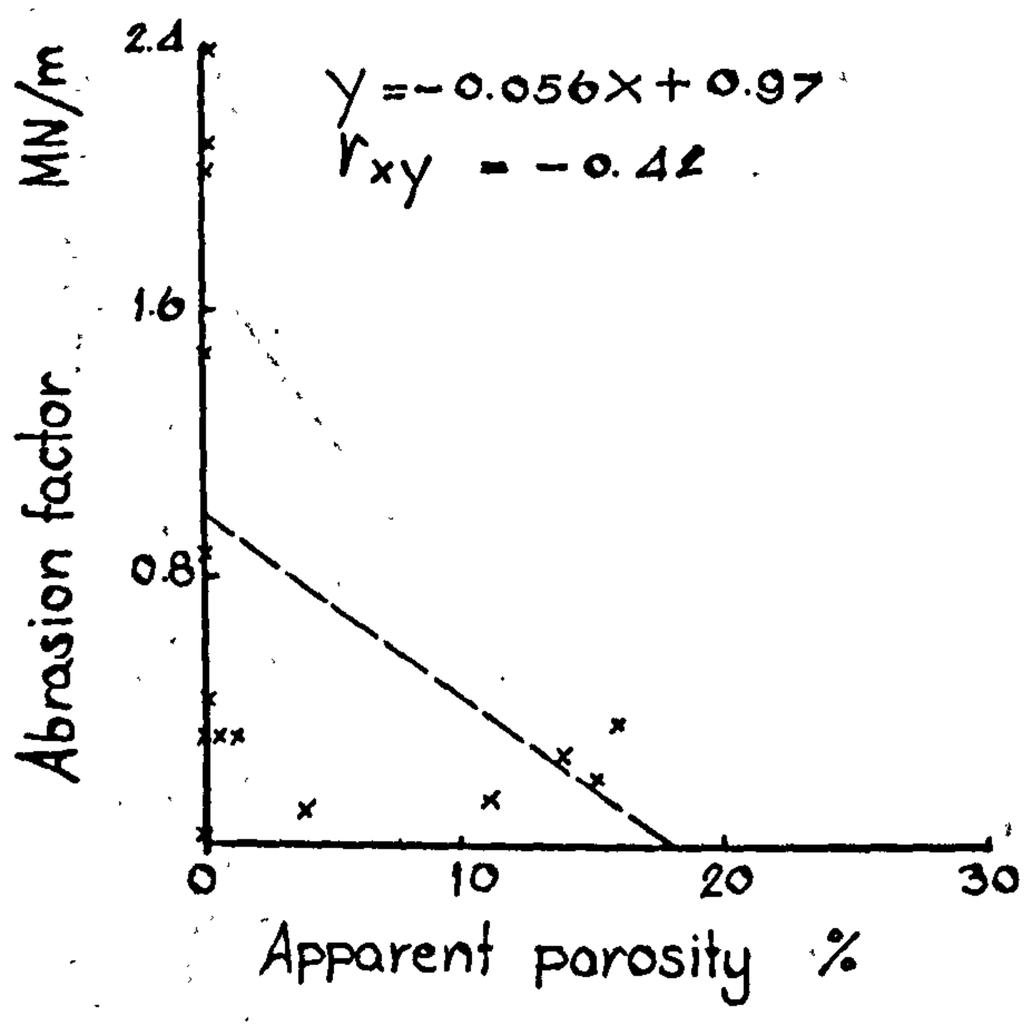
Y=-0.056X+0.97
r_{xy} = -0.42
Abrasion factor MN/m
2.4
1.6
0.8
0
10
20
30
Apparent porosity %

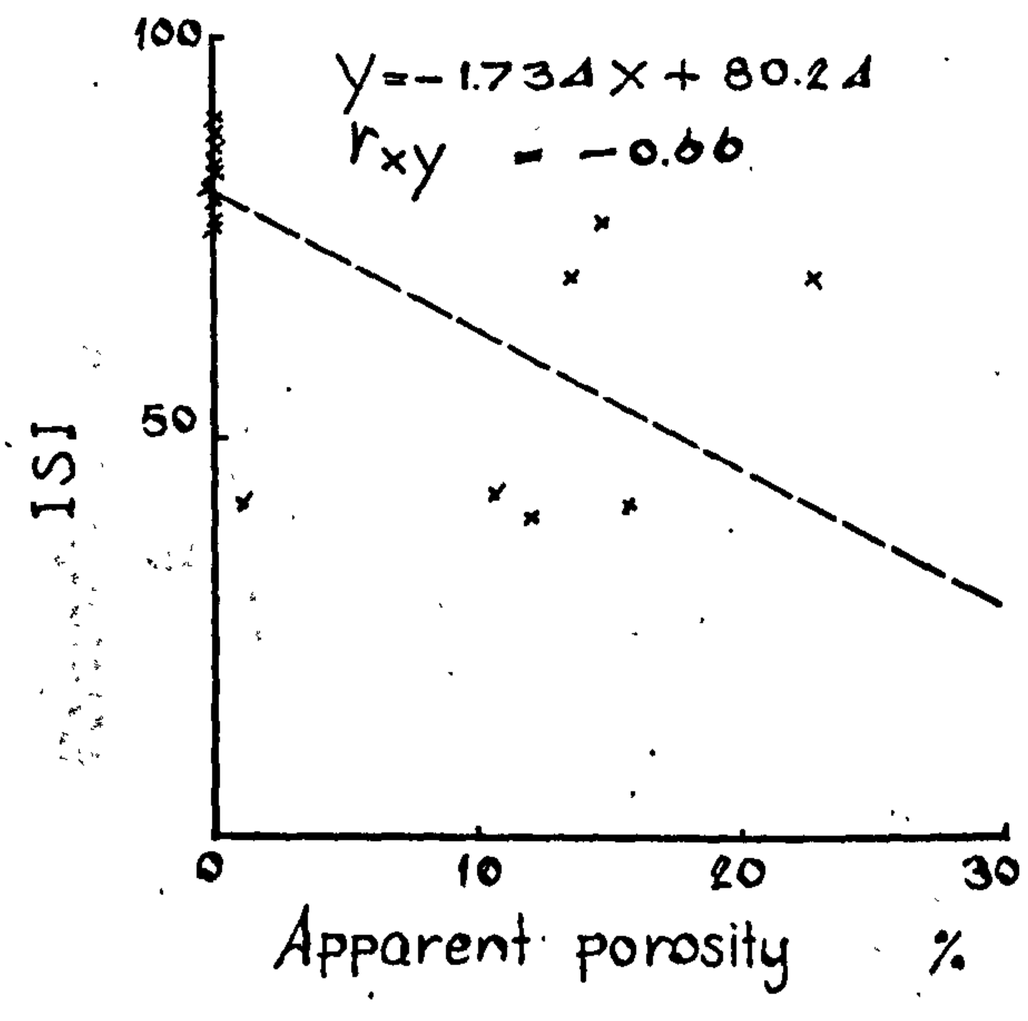
Y=-1.734X+80.24
r_{xy} = -0.66
ISI
100
50
0
10
20
30
Apparent porosity %

Figure 47 (15)

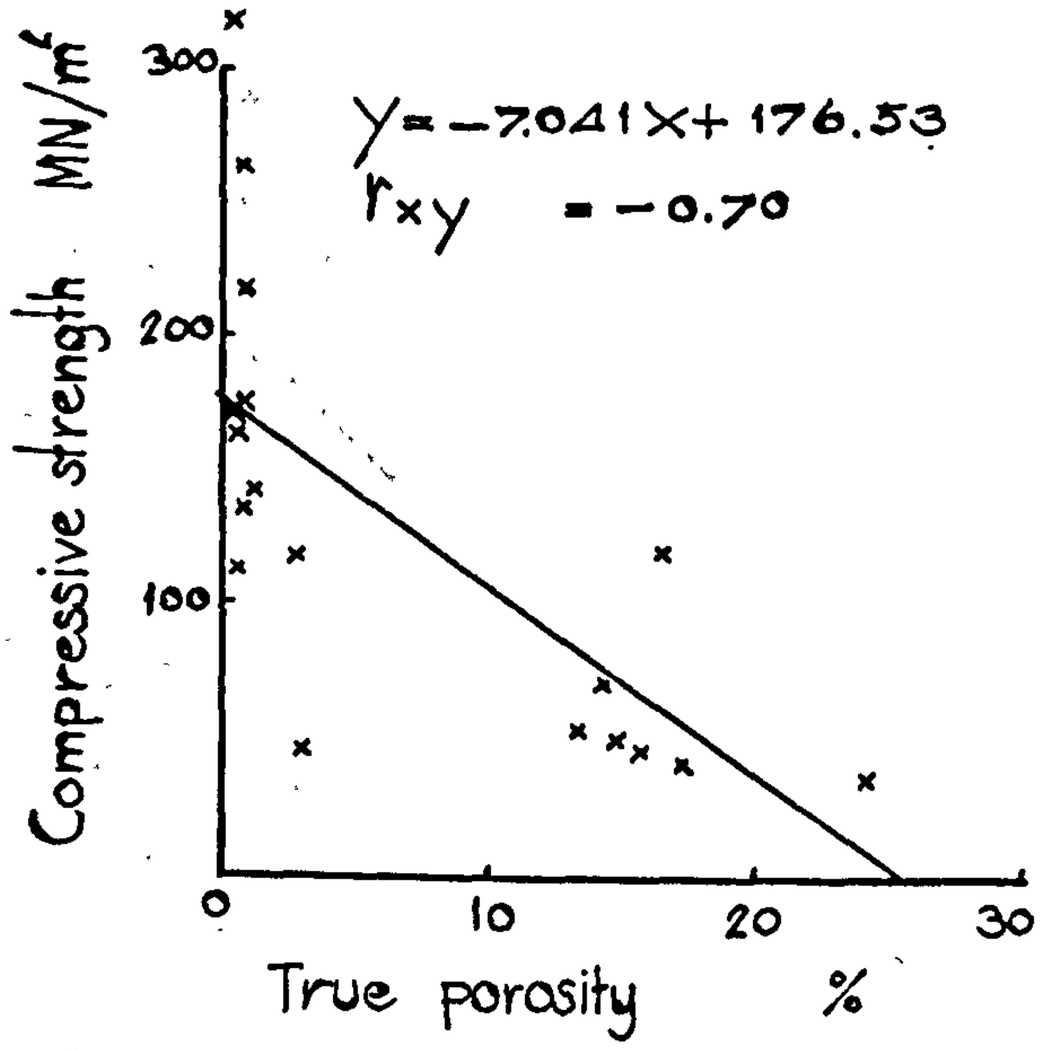
Compressive strength MN/m²
300
200
100
0
10
20
30
True porosity %
Y=-7.041X+176.53
rxy = -0.70

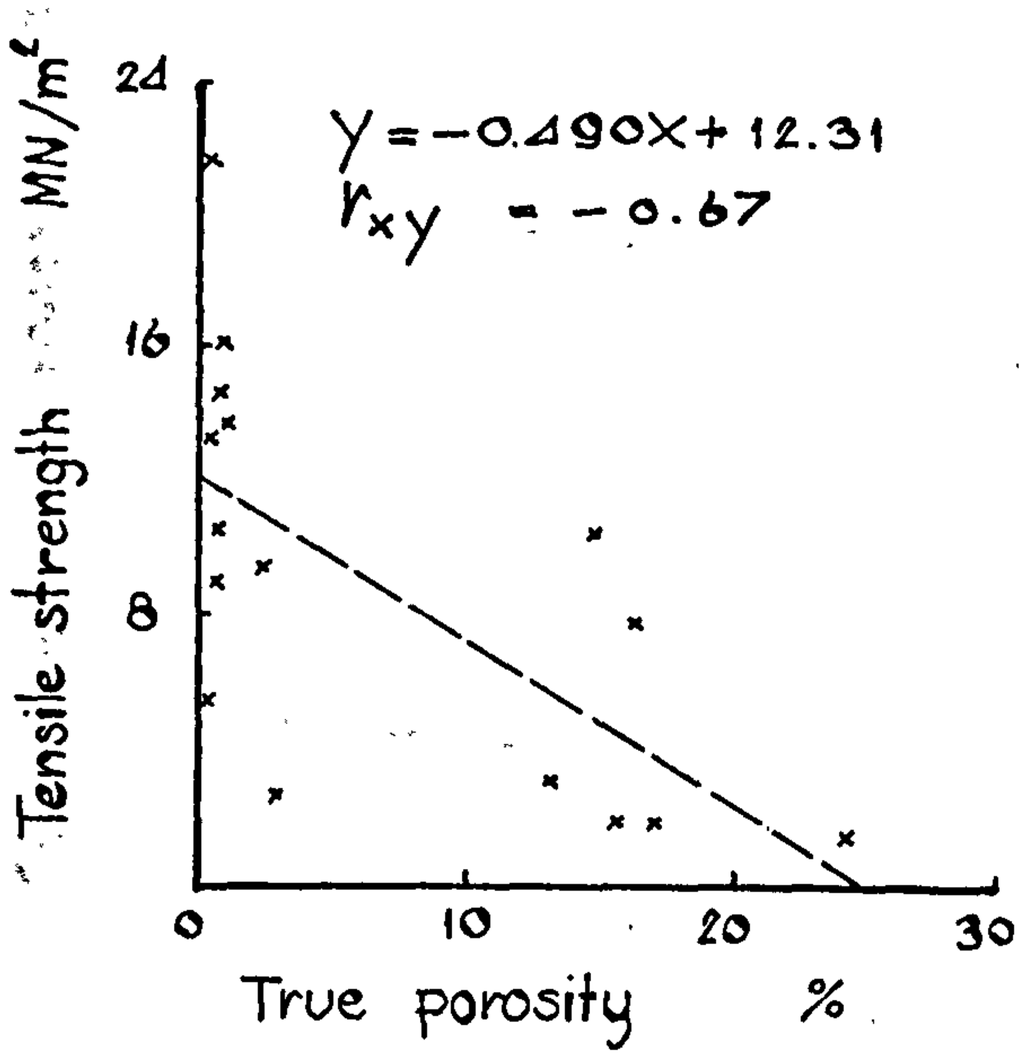
Tensile strength MN/m²
24
16
8
0
10
20
30
True porosity %
Y=-0.490X+12.31
rxy = -0.67

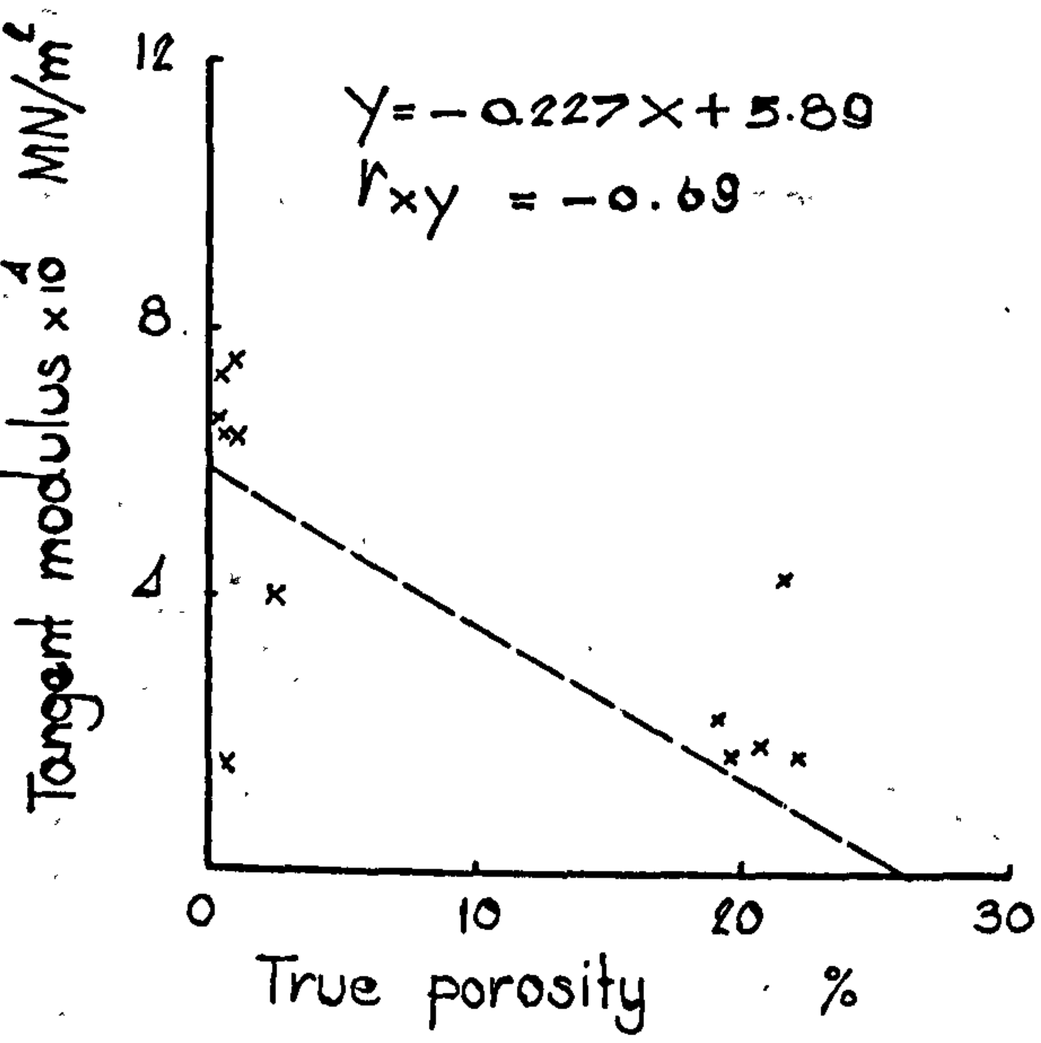
Tangent modulus x10⁴ MN/m²
12
8
4
0
10
20
30
True porosity %
Y=-0.227X+5.89
rxy = -0.69

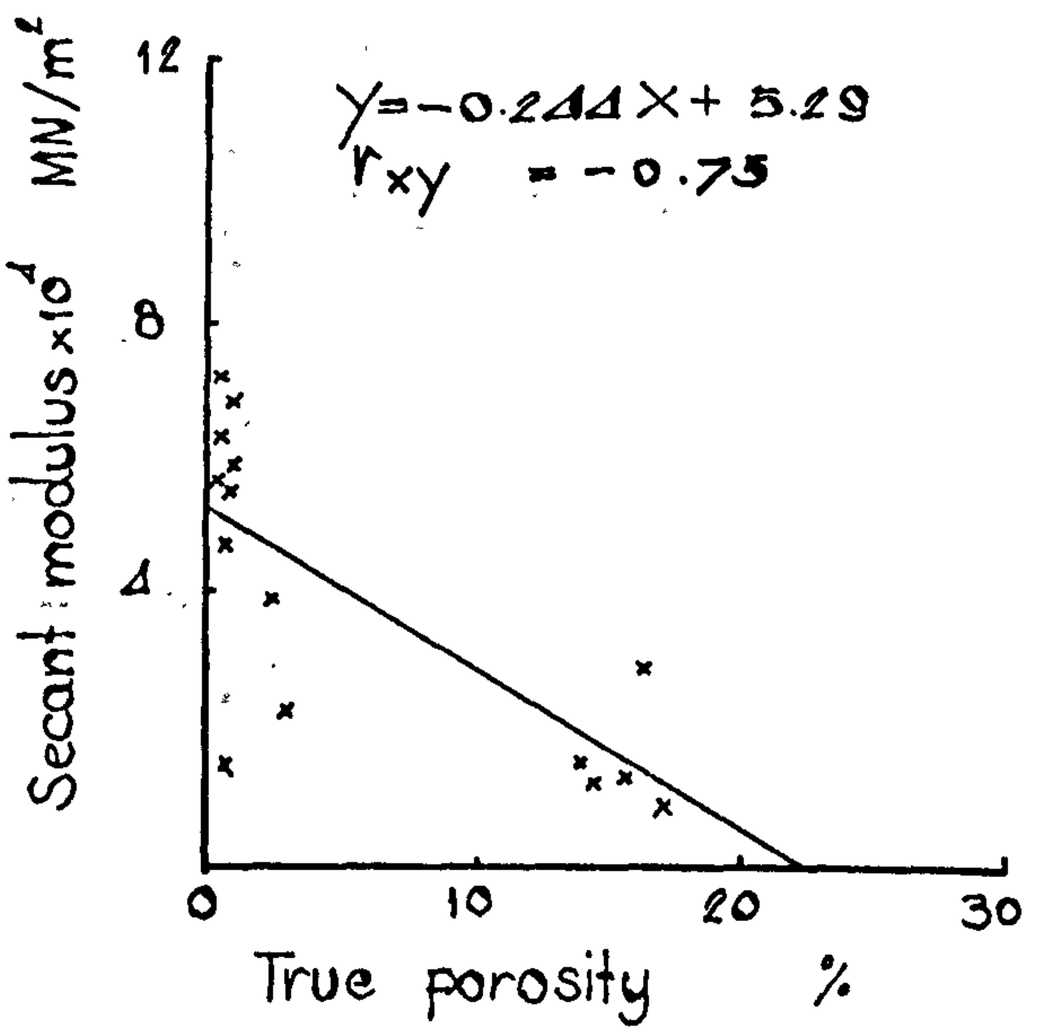
Secant modulus x10⁴ MN/m²
12
8
4
0
10
20
30
True porosity %
Y=-0.244X+5.29
rxy = -0.75

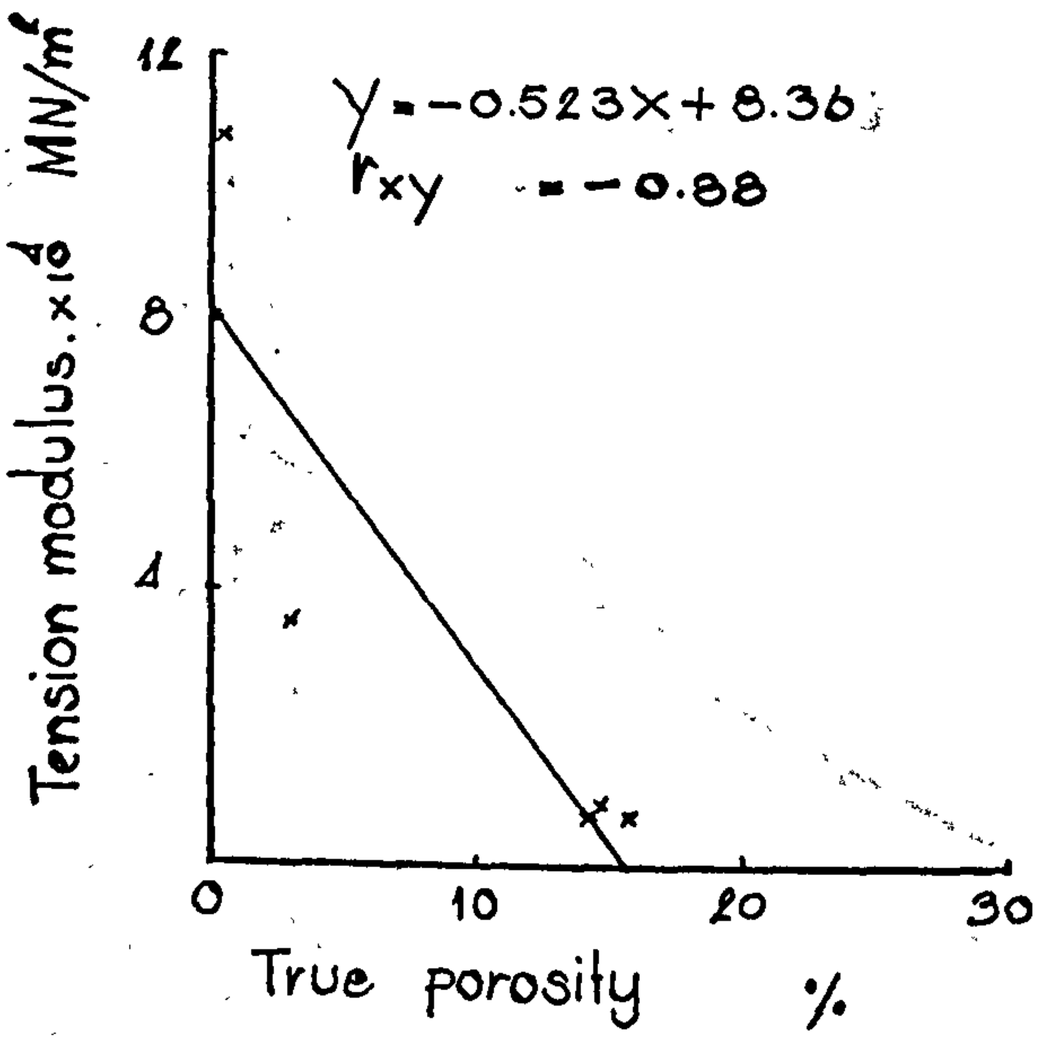
Tension modulus. x10⁴ MN/m²
12
8
4
0
10
20
30
True porosity %
Y=-0.523X+8.36
rxy = -0.88

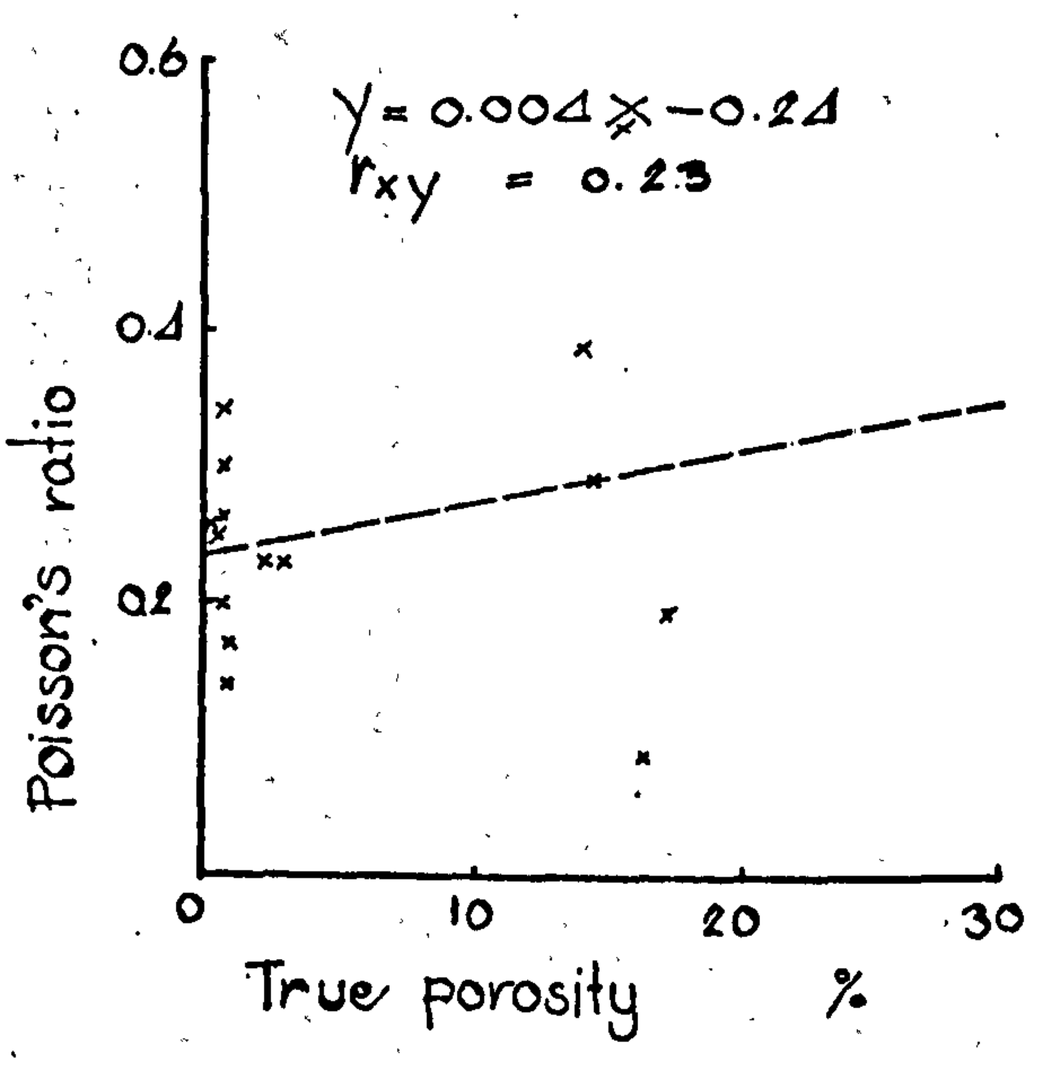
Poisson's ratio
0.6
0.4
0.2
0
10
20
30
True porosity %
Y=0.004X-0.24
rxy = 0.23

Figure 47 (16)

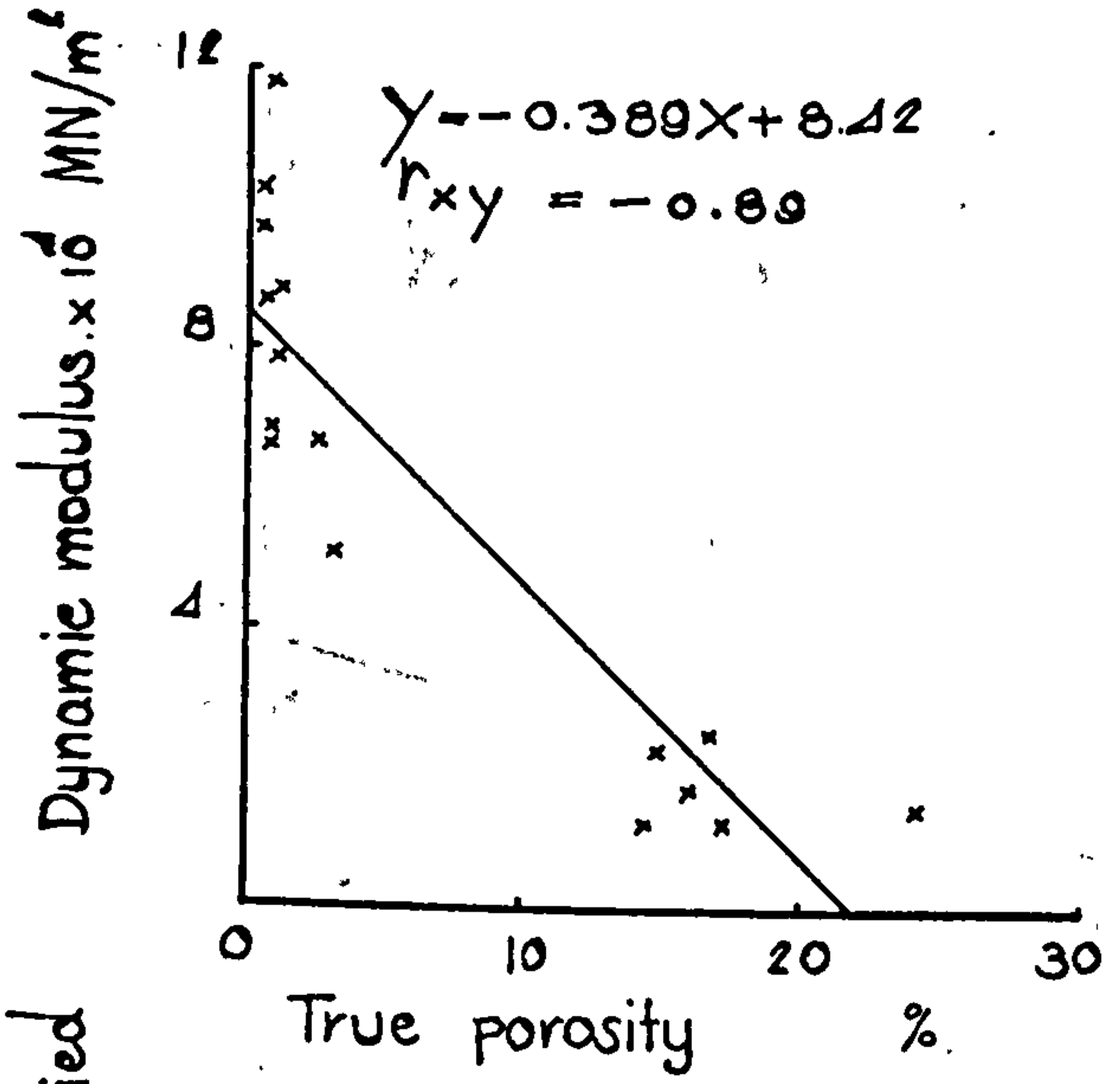
Dynamic modulus.x10⁴ MN/m²
12
8
4
0
10
20
30
True porosity %
Y=-0.389X+8.42
rxy = -0.89

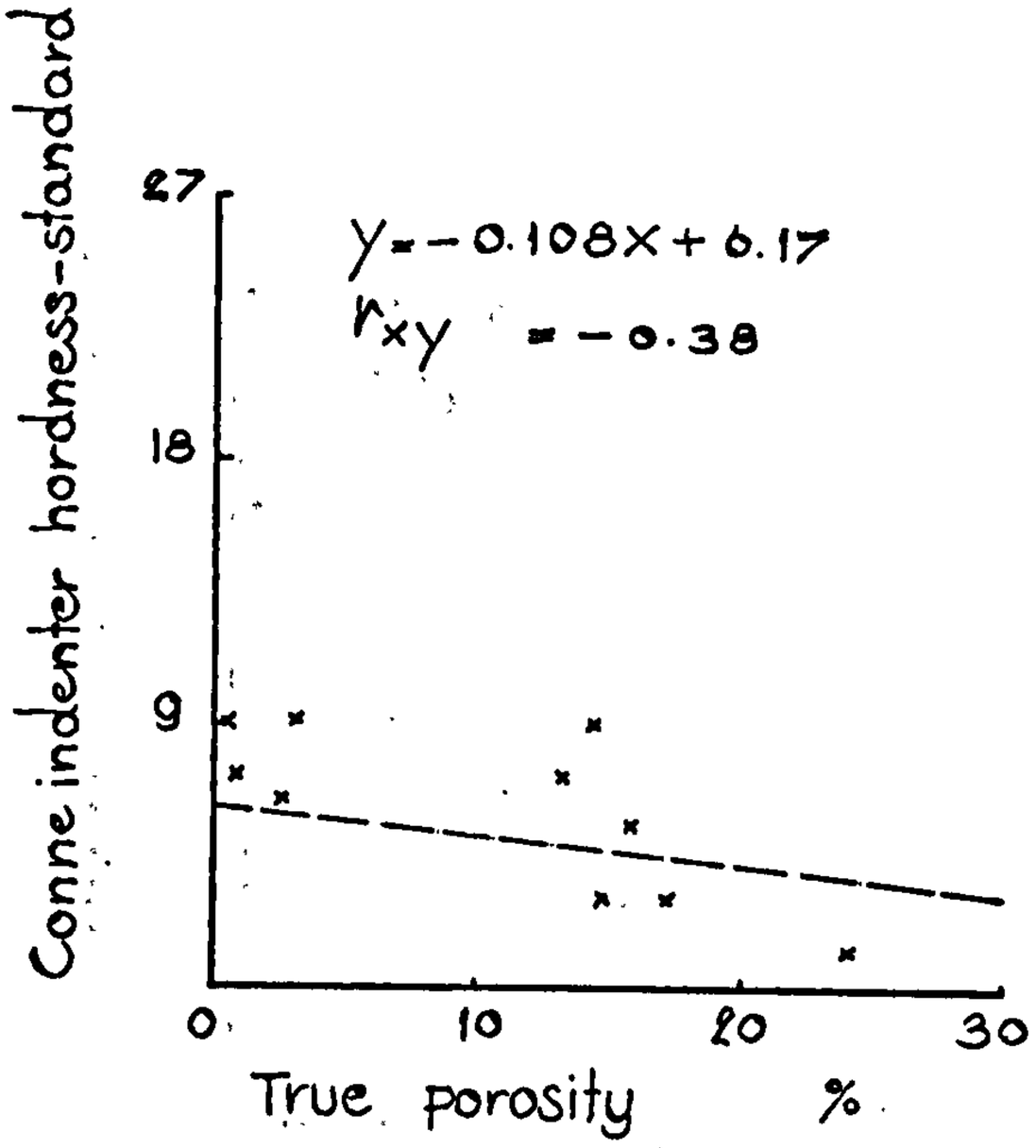
Cone indenter hardness-standard
27
18
9
0
10
20
30
True porosity %
Y=-0.108X+6.17
rxy = -0.38

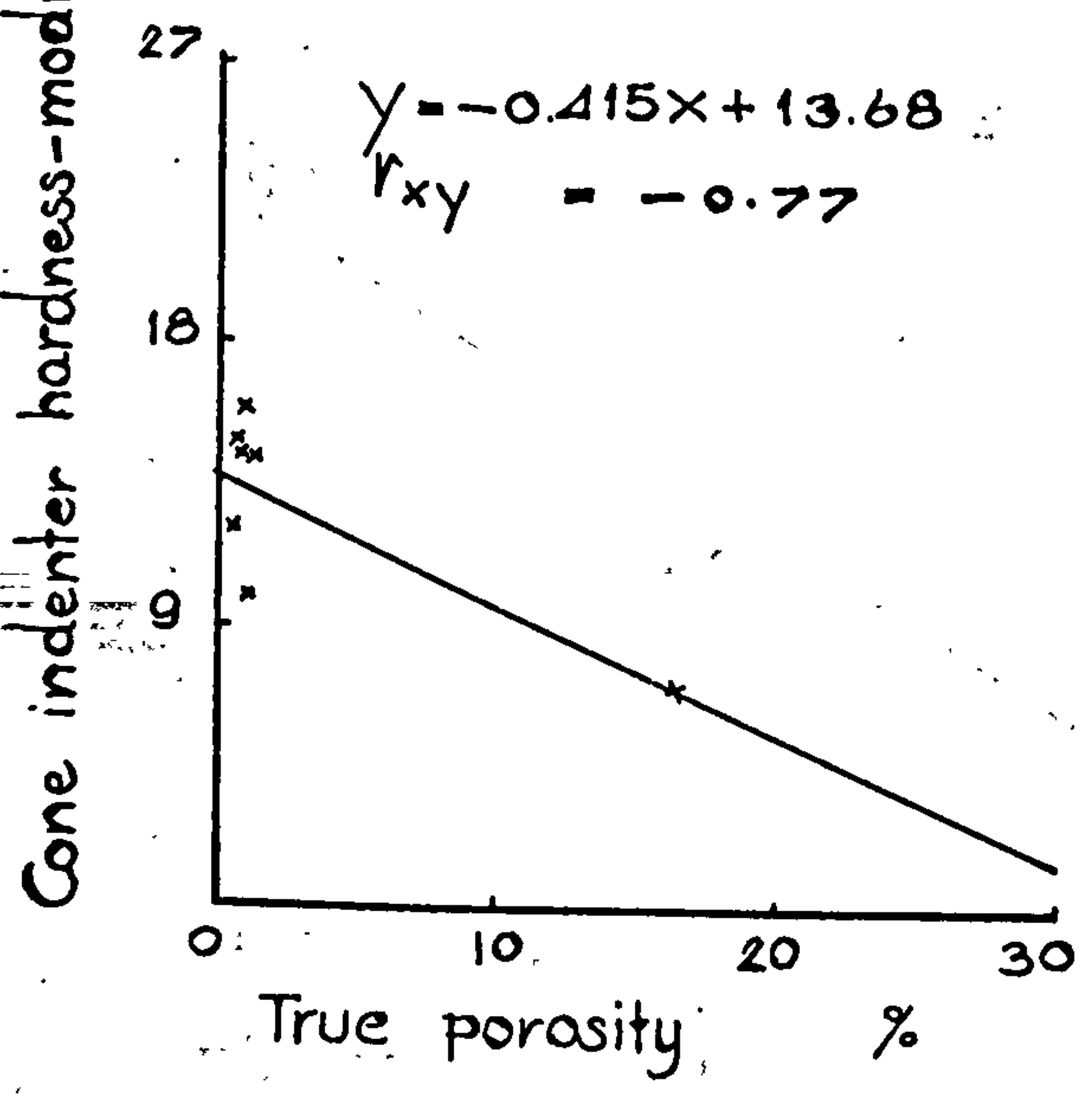
Cone indenter hardness-modified
27
18
9
0
10
20
30
True porosity %
Y=-0.415X+13.68
rxy = -0.77

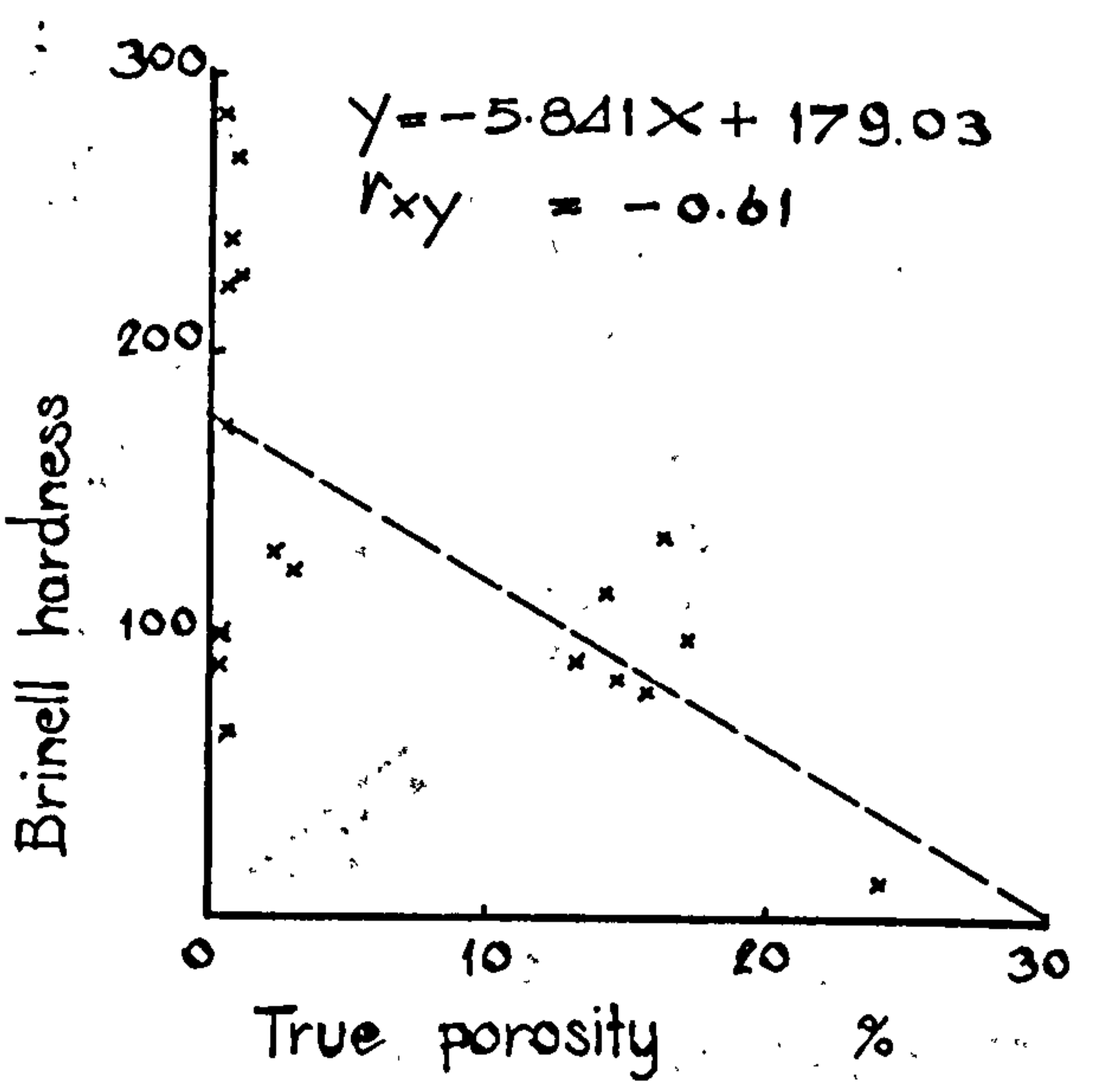
Brinell hardness
300
200
100
0
10
20
30
True porosity %
Y=-5.841X+179.03
rxy = -0.61

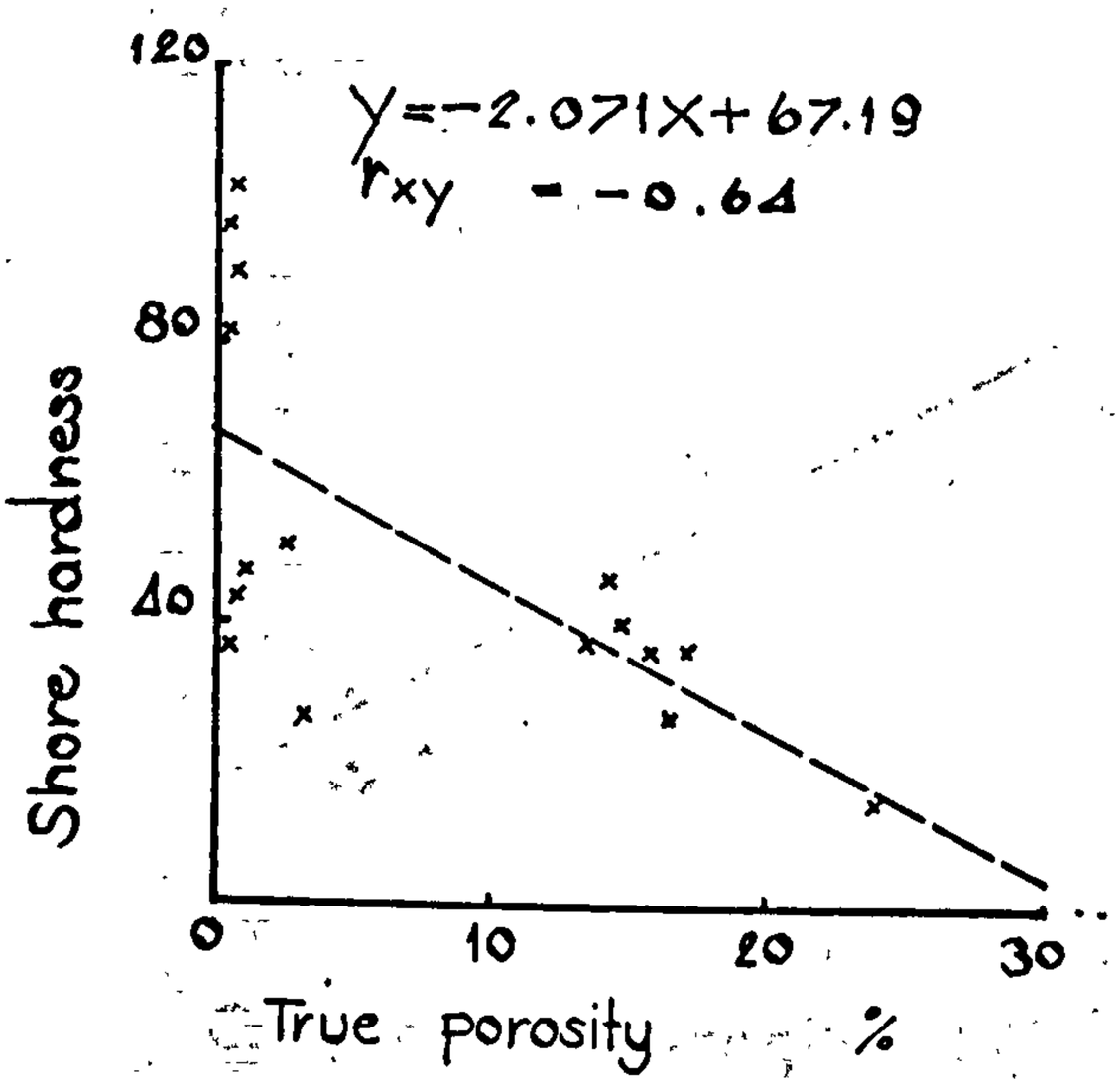
Shore hardness
120
80
40
0
10
20
30
True porosity %
Y=-2.071X+67.19
rxy = -0.64

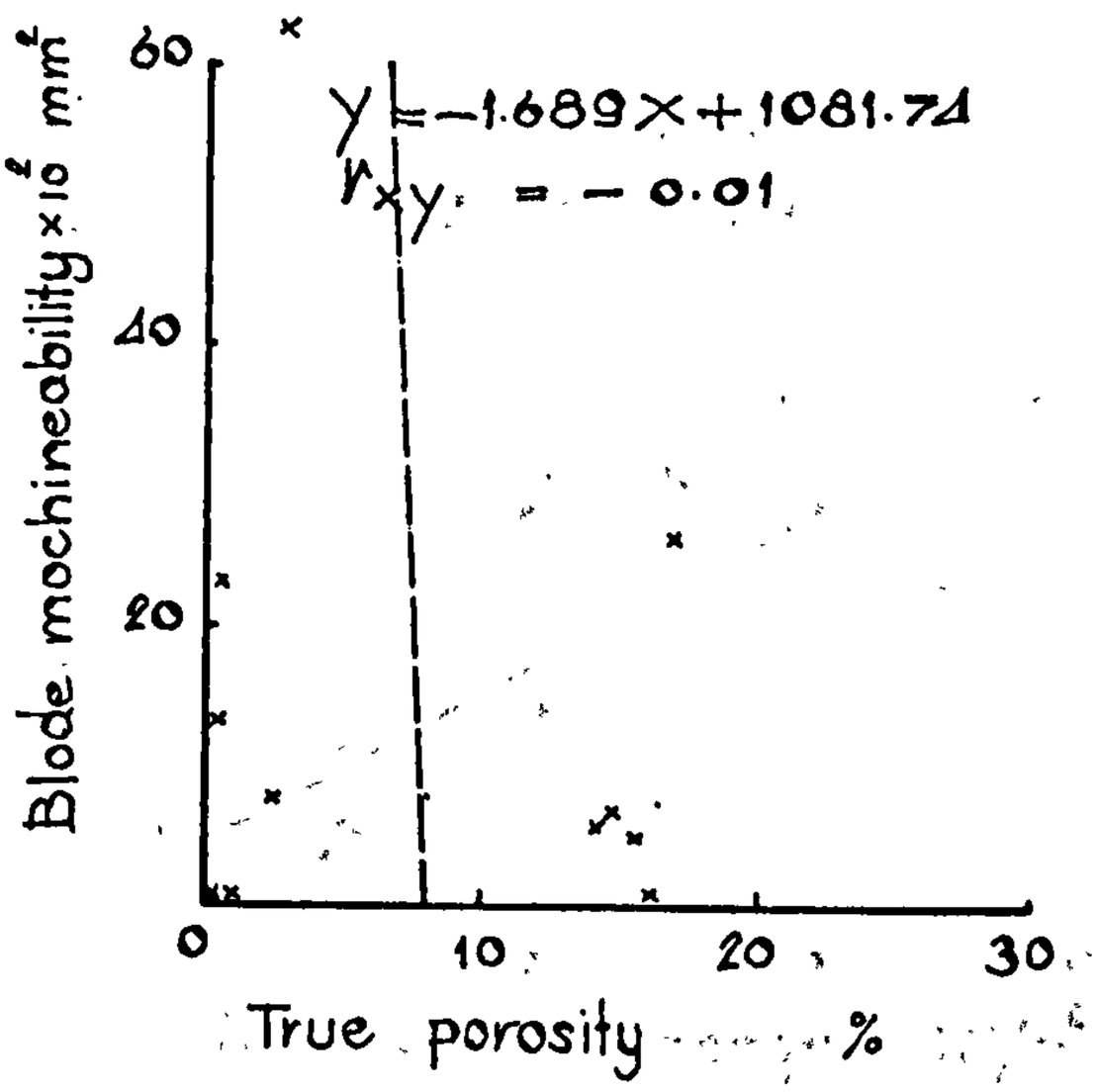
Blade machineability x10⁴ mm²
60
40
20
0
10
20
30
True porosity %
Y=-1.689X+1081.74
rxy = -0.01

Figure 47 (17)

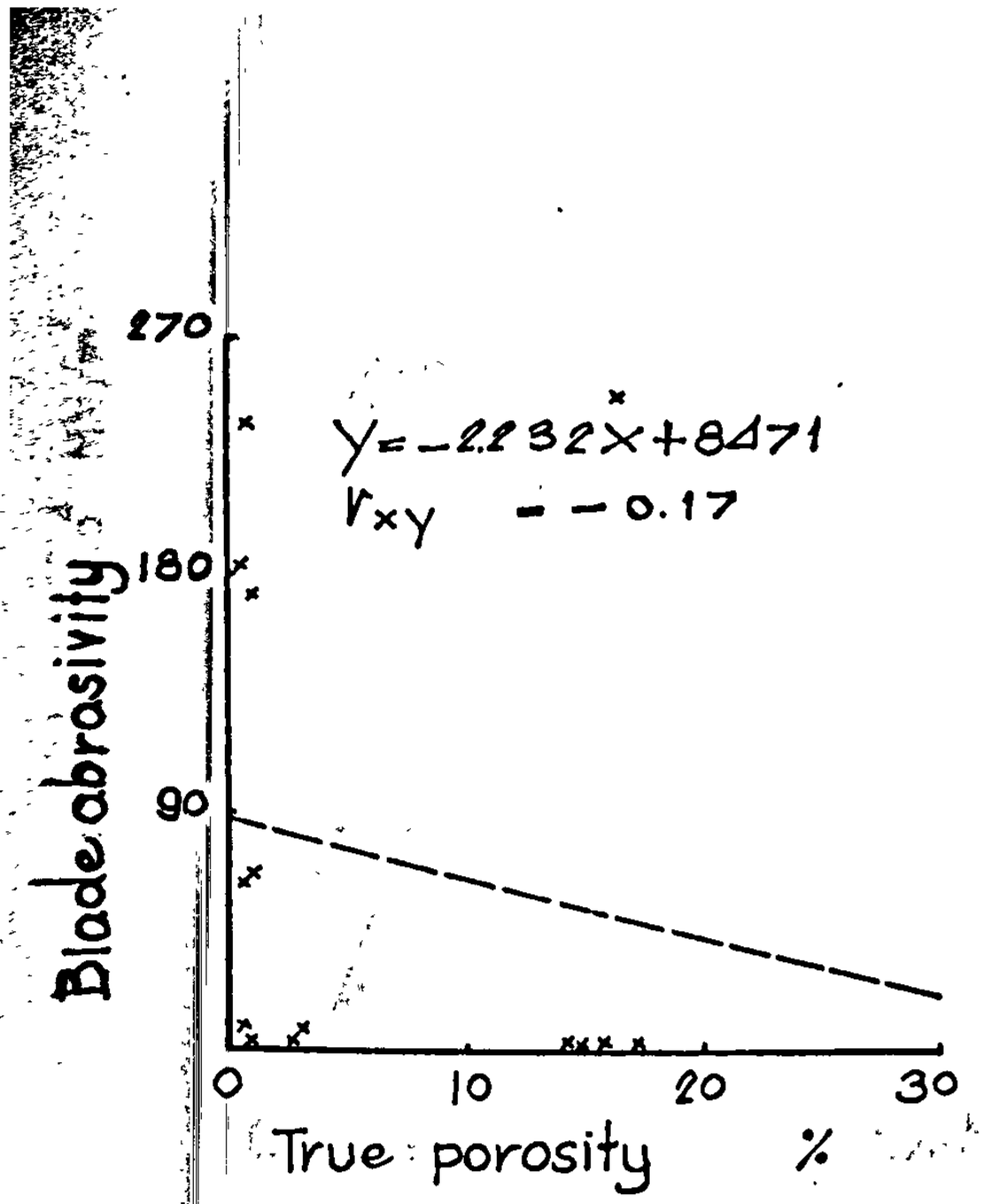
Blade abrasivity
270
180
90
0
10
20
30
True porosity %
Y=-2.232X+84.71
rxy = -0.17

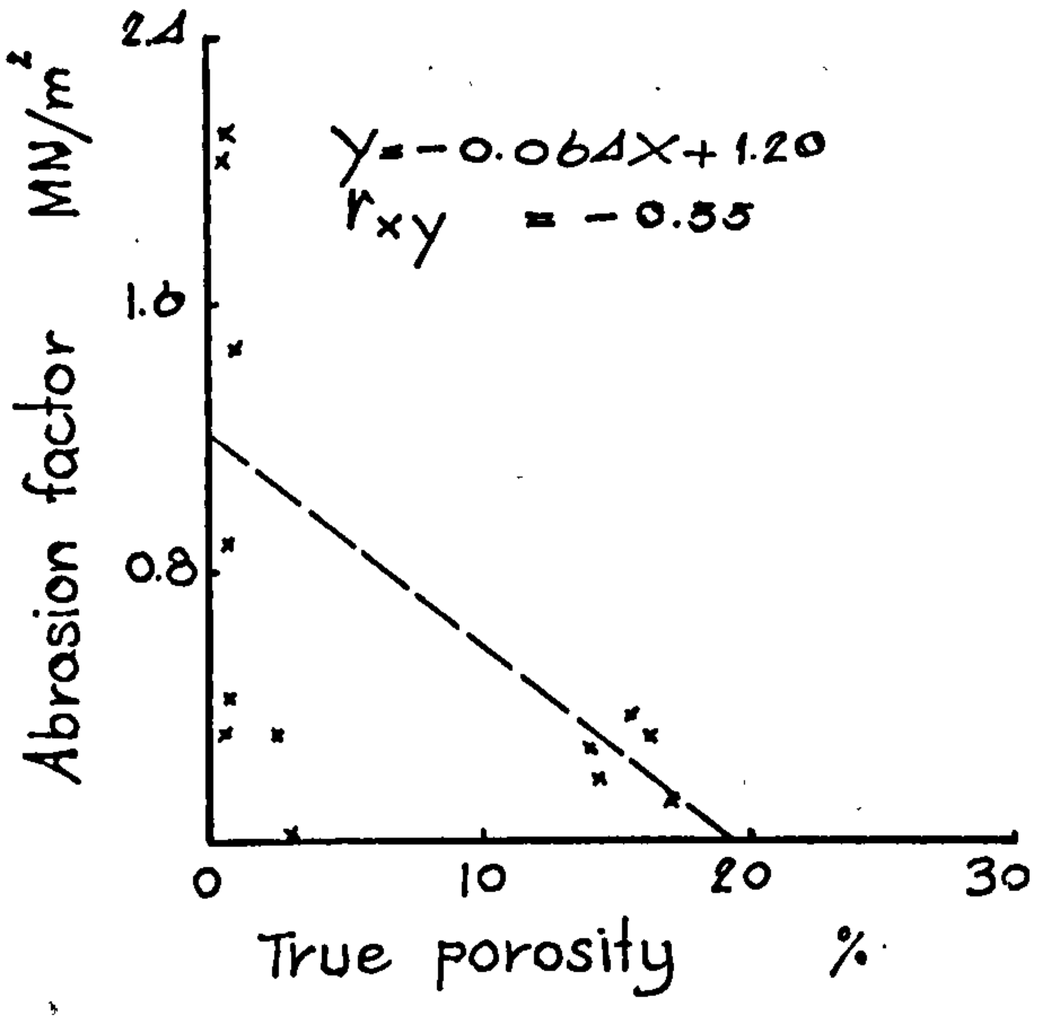
Abrasion factor MN/m²
2.4
1.6
0.8
0
10
20
30
True porosity %
Y=-0.064X+1.20
rxy = -0.55

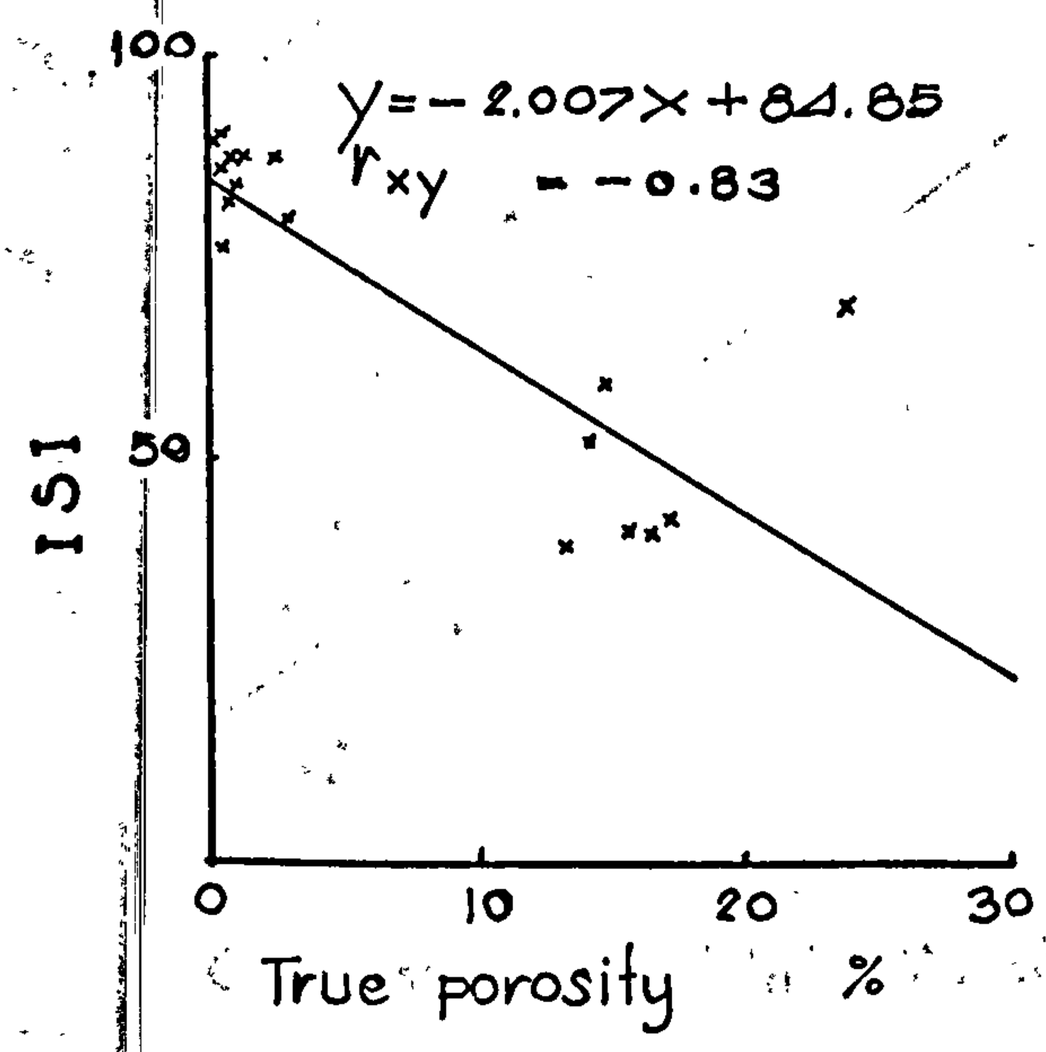
ISI
100
50
0
10
20
30
True porosity %
Y=-2.007X+84.85
rxy = -0.83

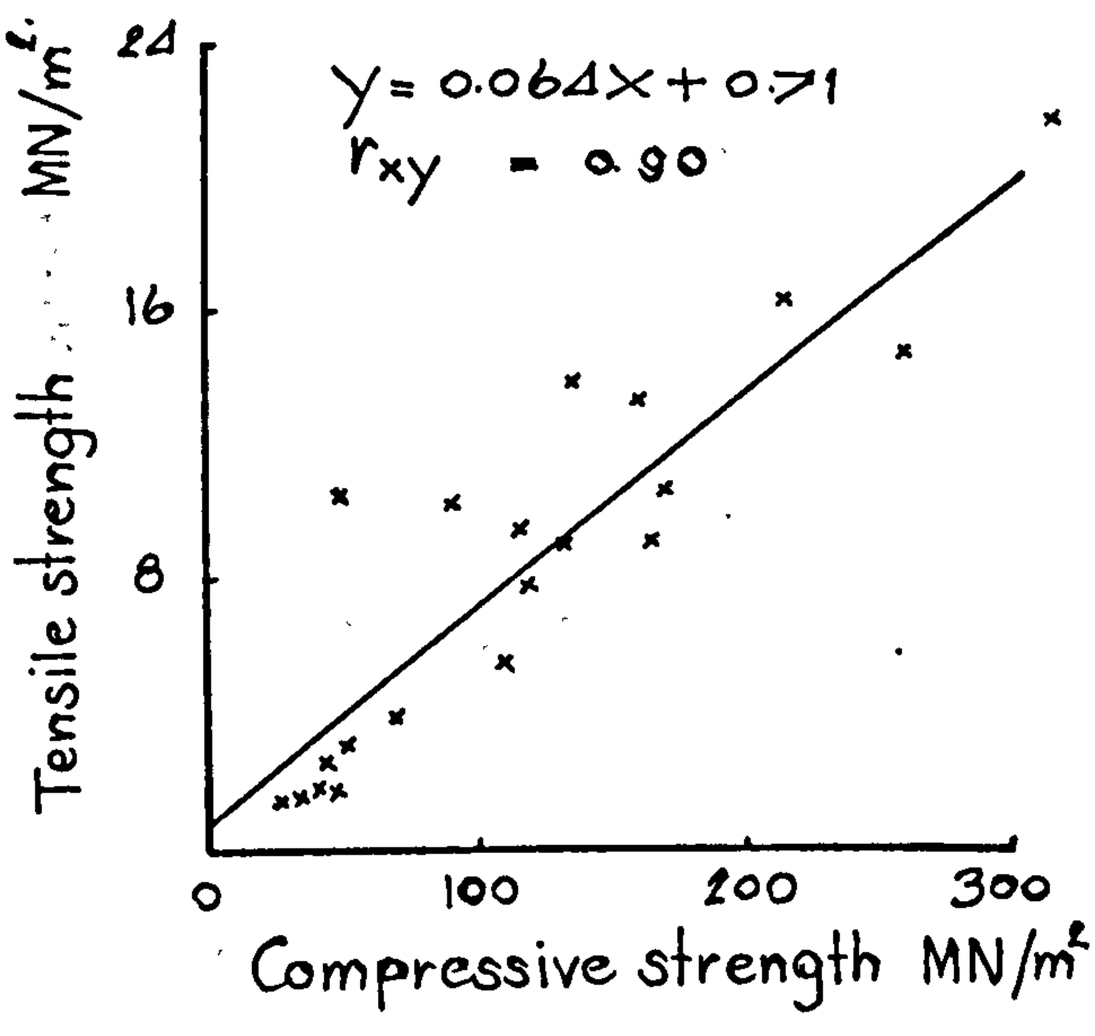
Tensile strength MN/m²
24
16
8
0
100
200
300
Compressive strength MN/m²
Y=0.064X+0.71
rxy = 0.90

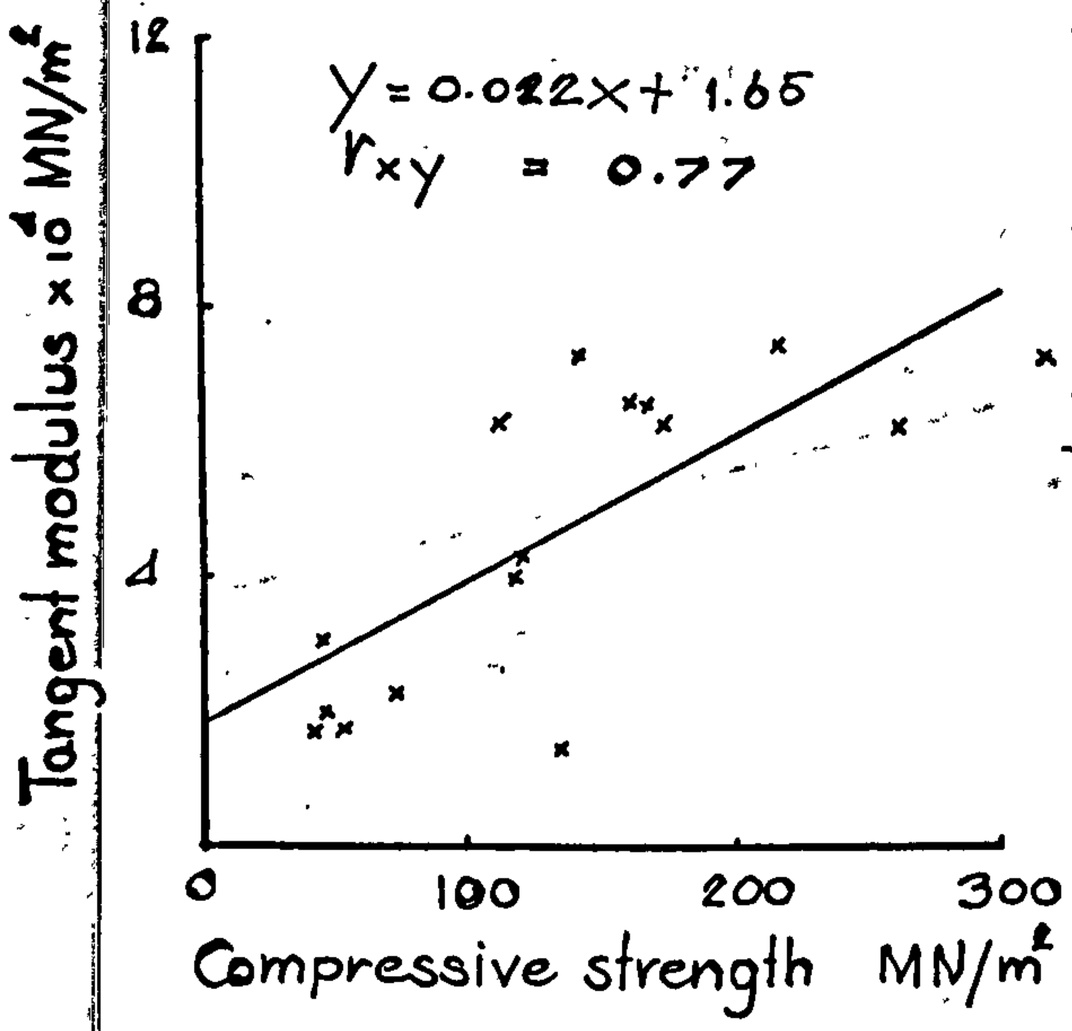
Tangent modulus x10⁴ MN/m²
12
8
4
0
100
200
300
Compressive strength MN/m²
Y=0.022X+1.65
rxy = 0.77

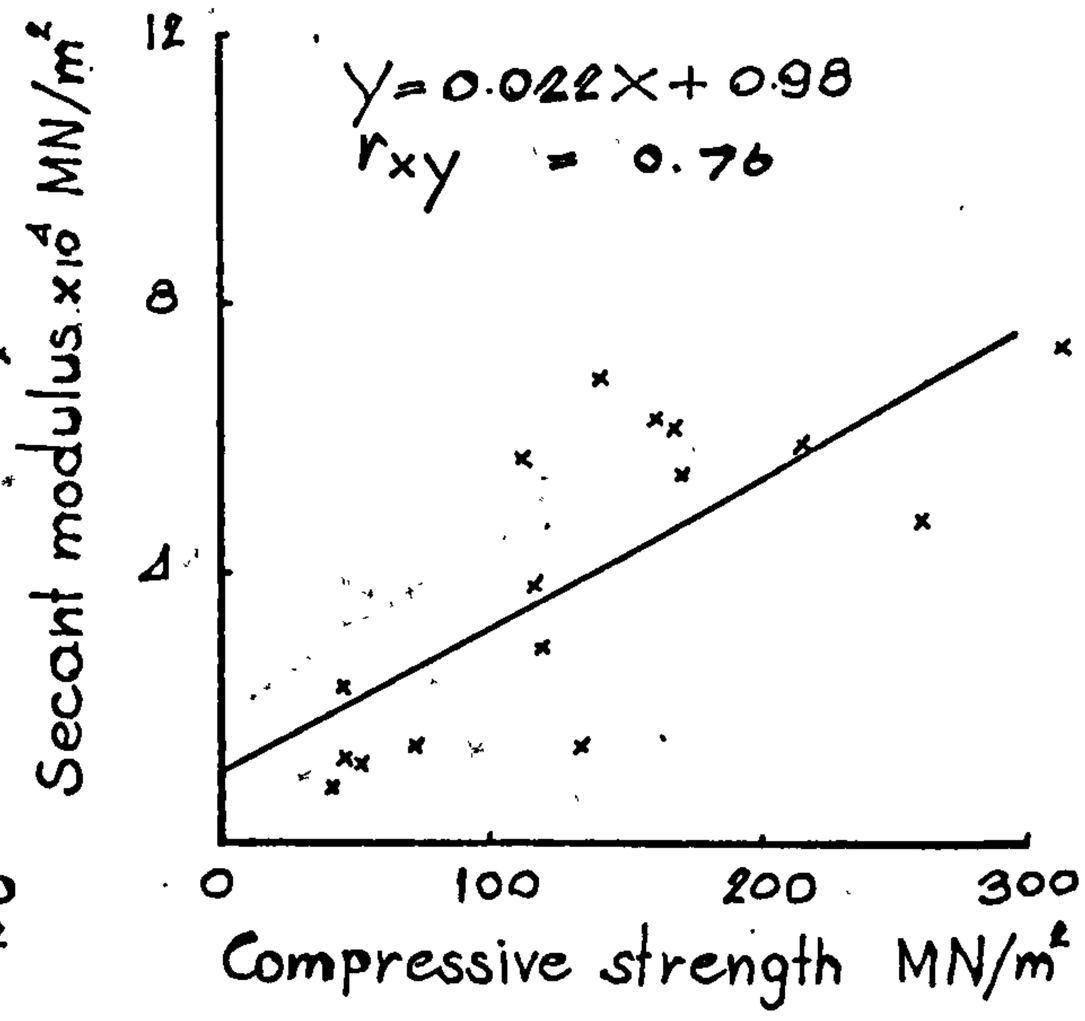
Secant modulus x10⁴ MN/m²
12
8
4
0
100
200
300
Compressive strength MN/m²
Y=0.022X+0.98
rxy = 0.76

Figure 47 (18)

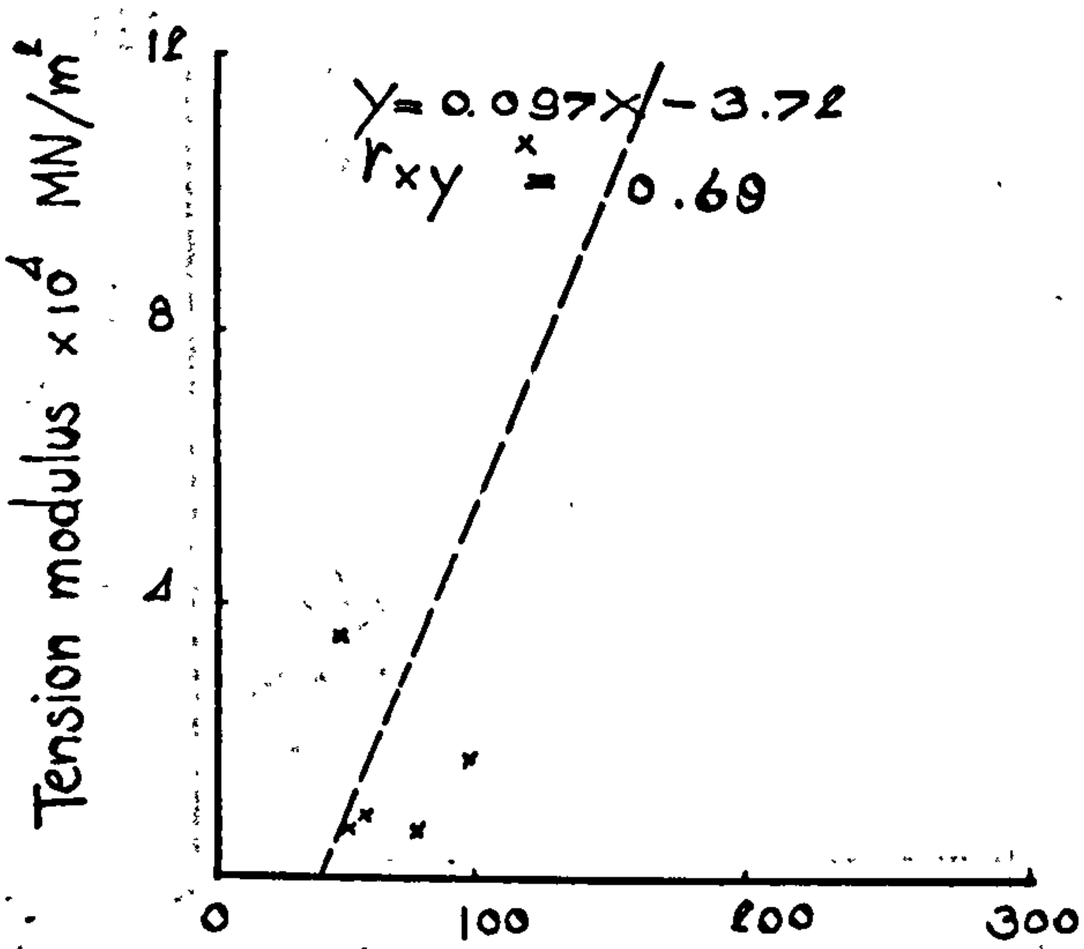
Y = 0.097X - 3.72
r_{xy} = 0.69
Tension modulus ×10⁴ MN/m²
12
8
4
0
100
200
300
Compressive strength MN/m²

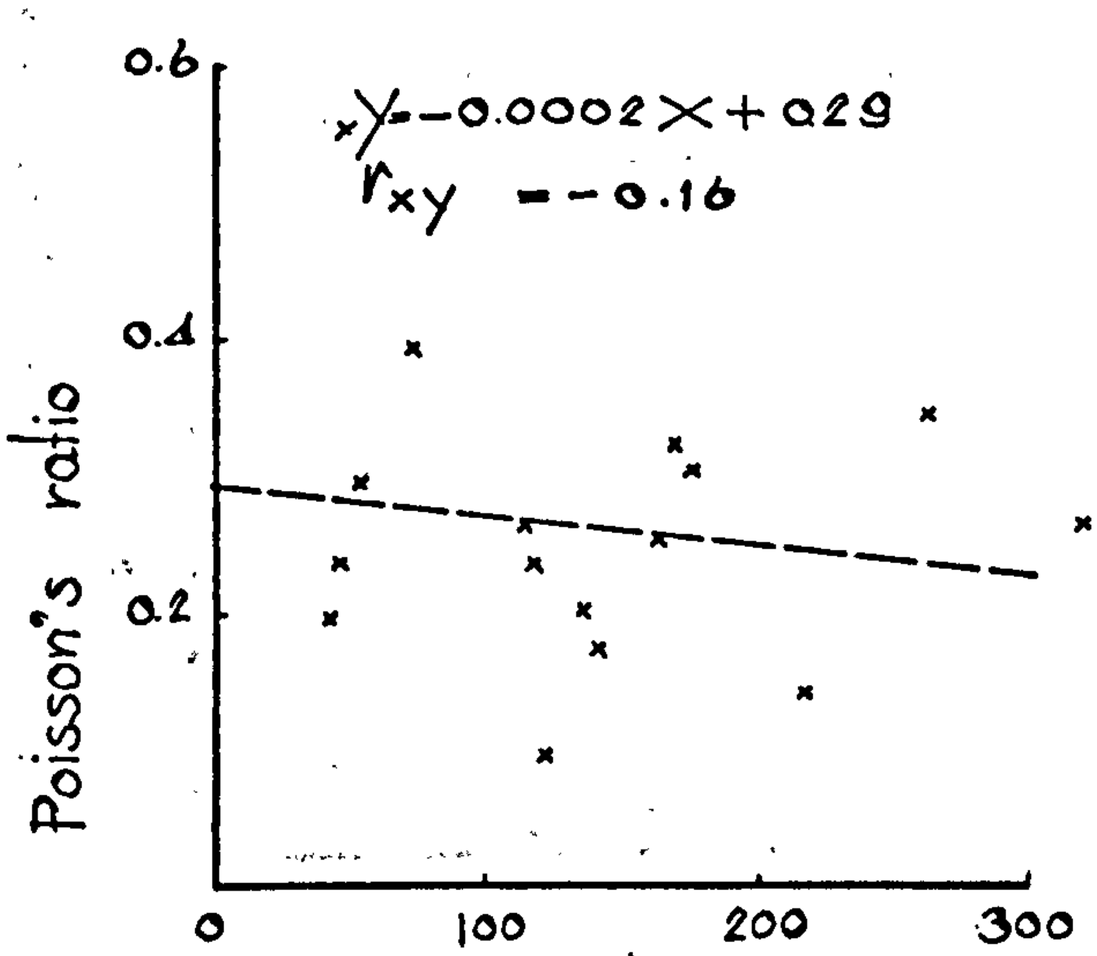
Y = -0.0002X + 029
r_{xy} = -0.16
Poisson's ratio
0.6
0.4
0.2
0
100
200
300
Compressive strength MN/m²

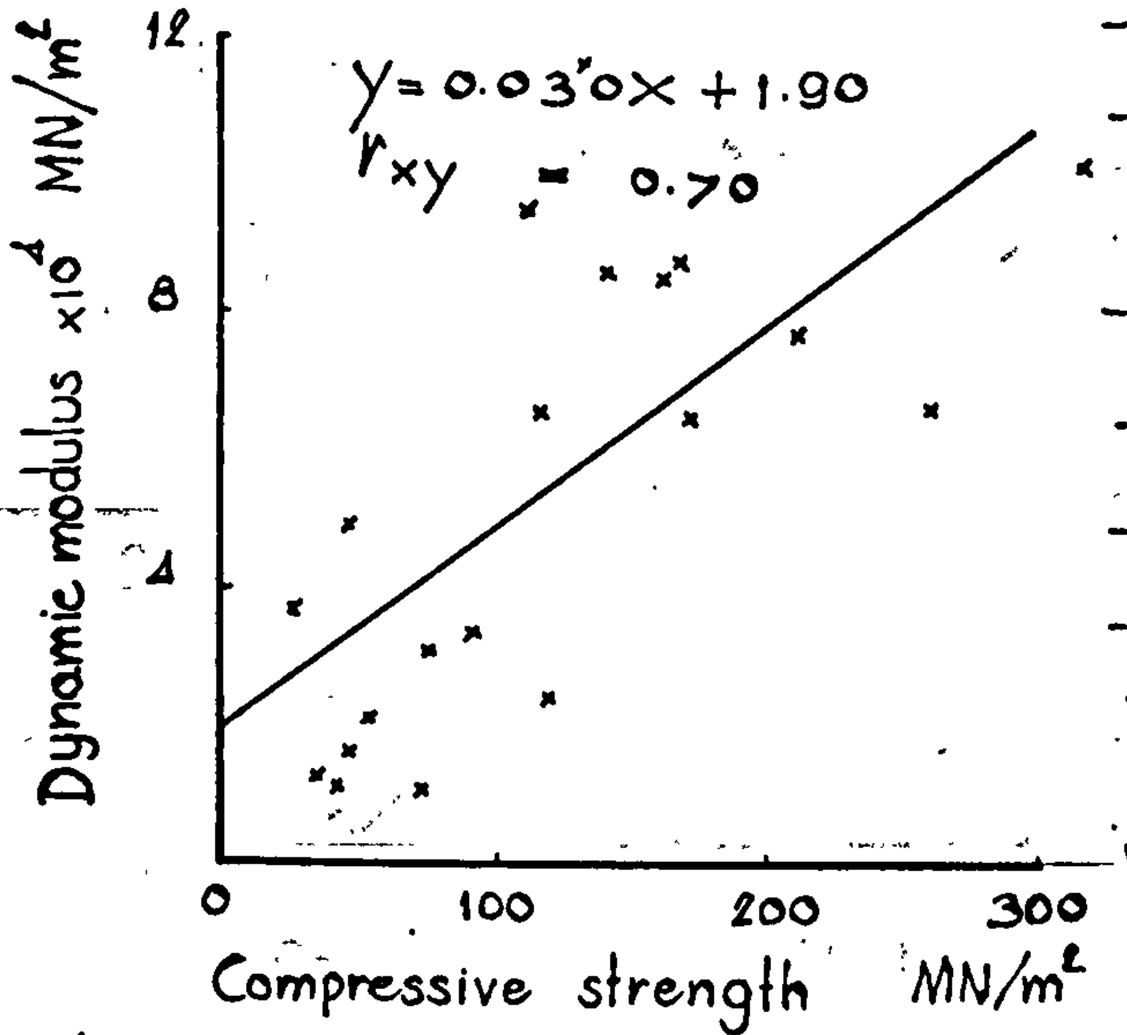
Y = 0.030X + 1.90
r_{xy} = 0.70
Dynamic modulus ×10⁴ MN/m²
12
8
4
0
100
200
300
Compressive strength MN/m²

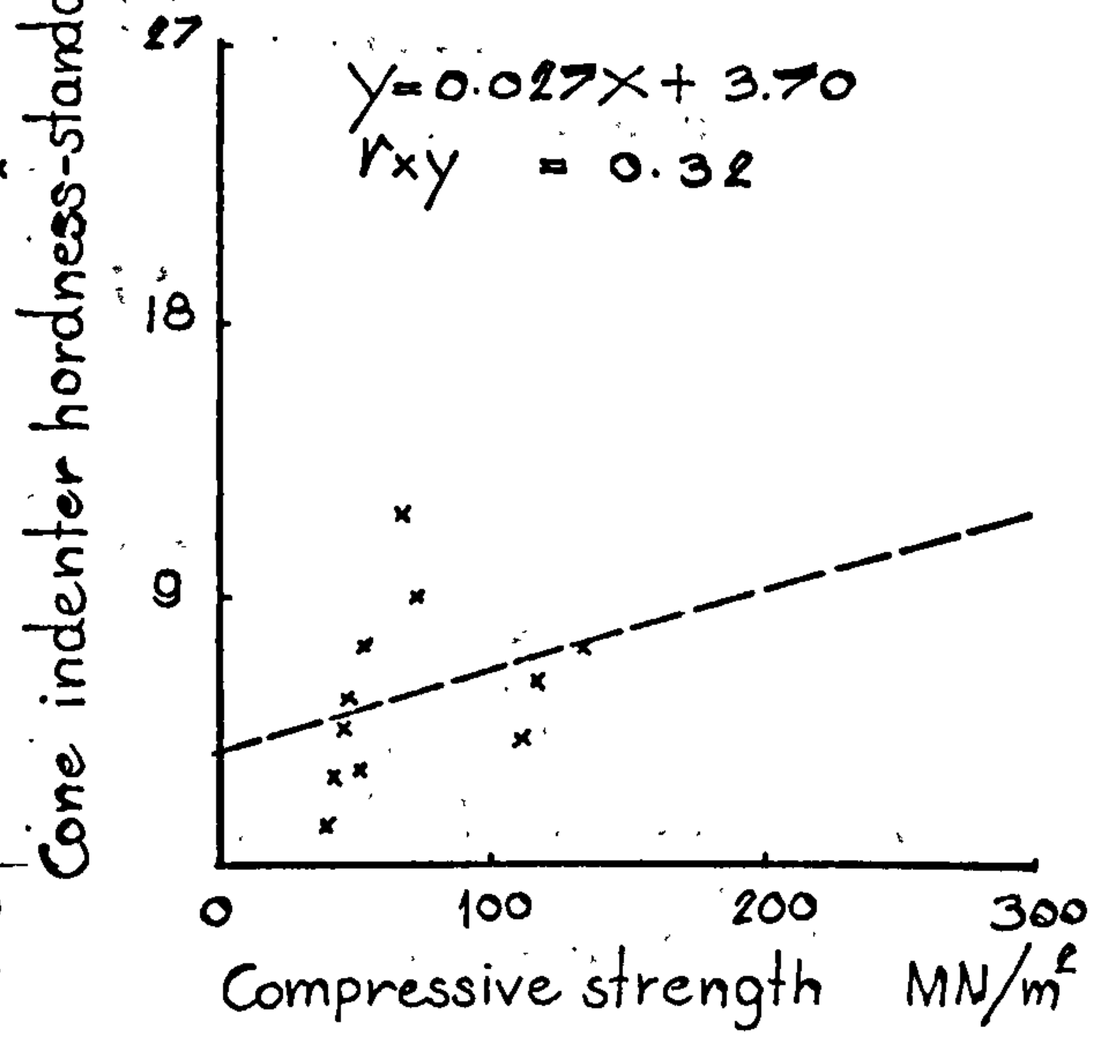
Y = 0.027X + 3.70
r_{xy} = 0.32
Cone indenter hardness-standard
27
18
9
0
100
200
300
Compressive strength MN/m²

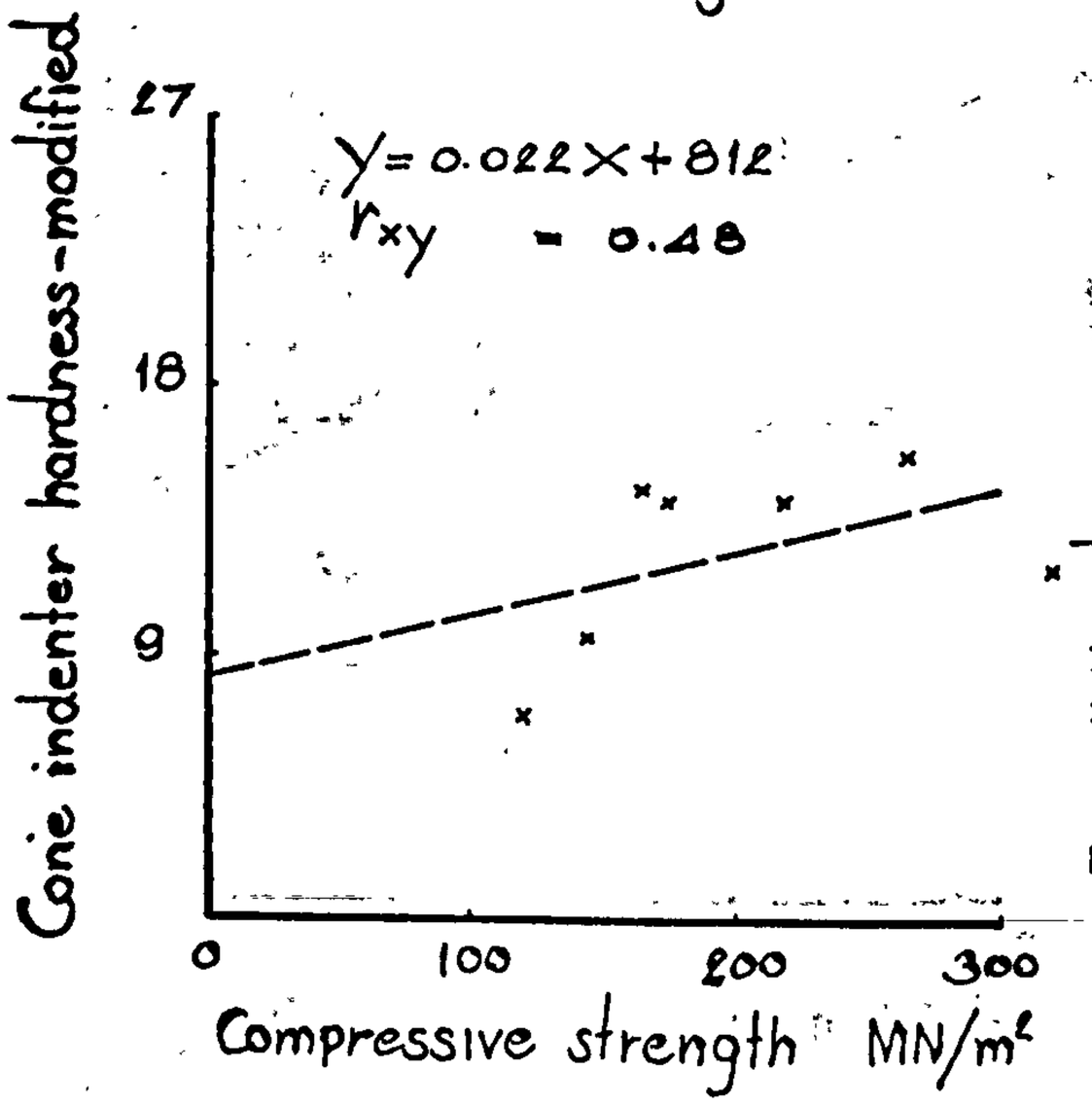
Y = 0.022X + 812
r_{xy} = 0.48
Cone indenter hardness-modified
27
18
9
0
100
200
300
Compressive strength MN/m²

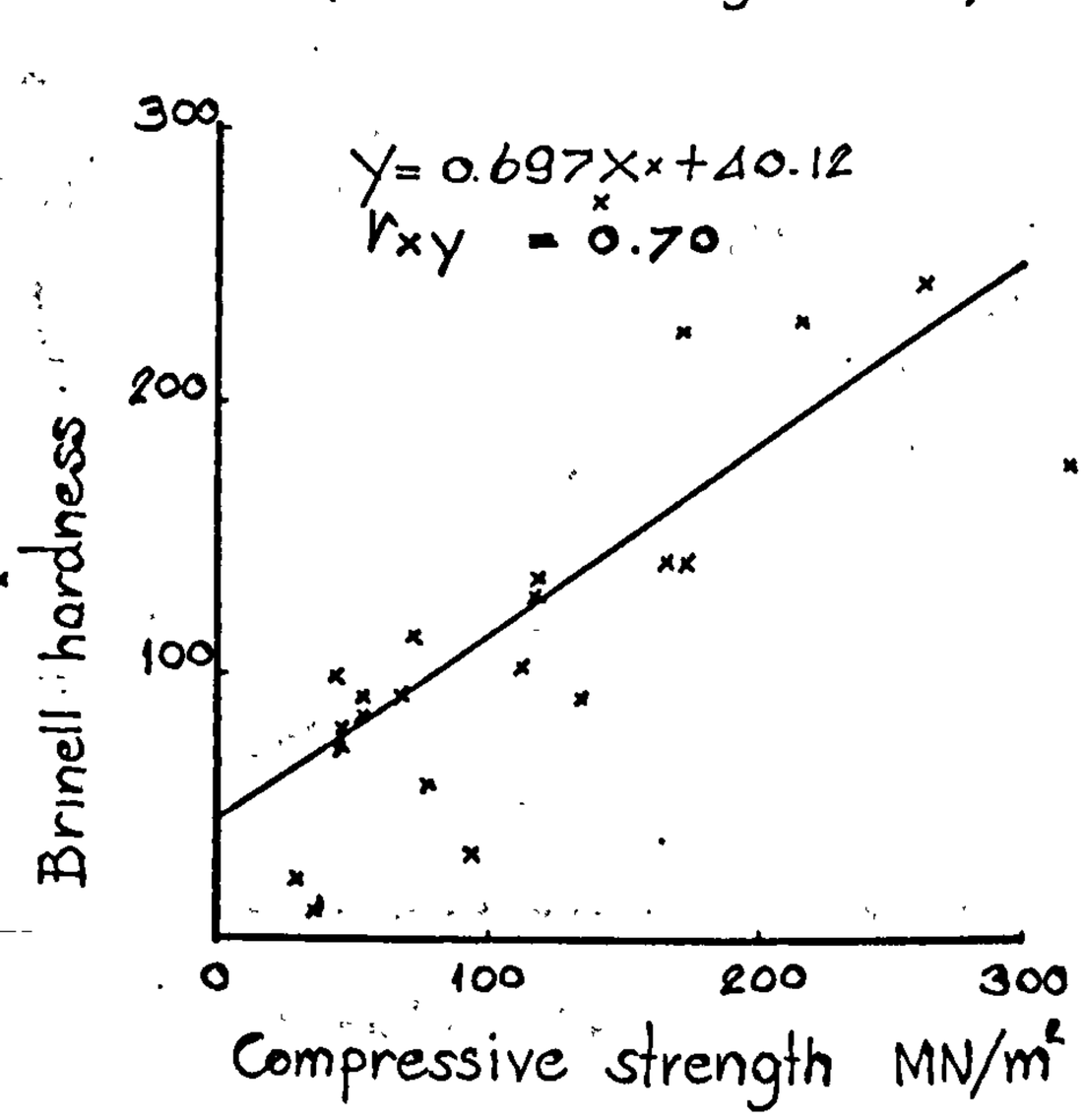
Y = 0.697X + 40.12
r_{xy} = 0.70
Brinell hardness
300
200
100
0
100
200
300
Compressive strength MN/m²

Figure 47 (19)

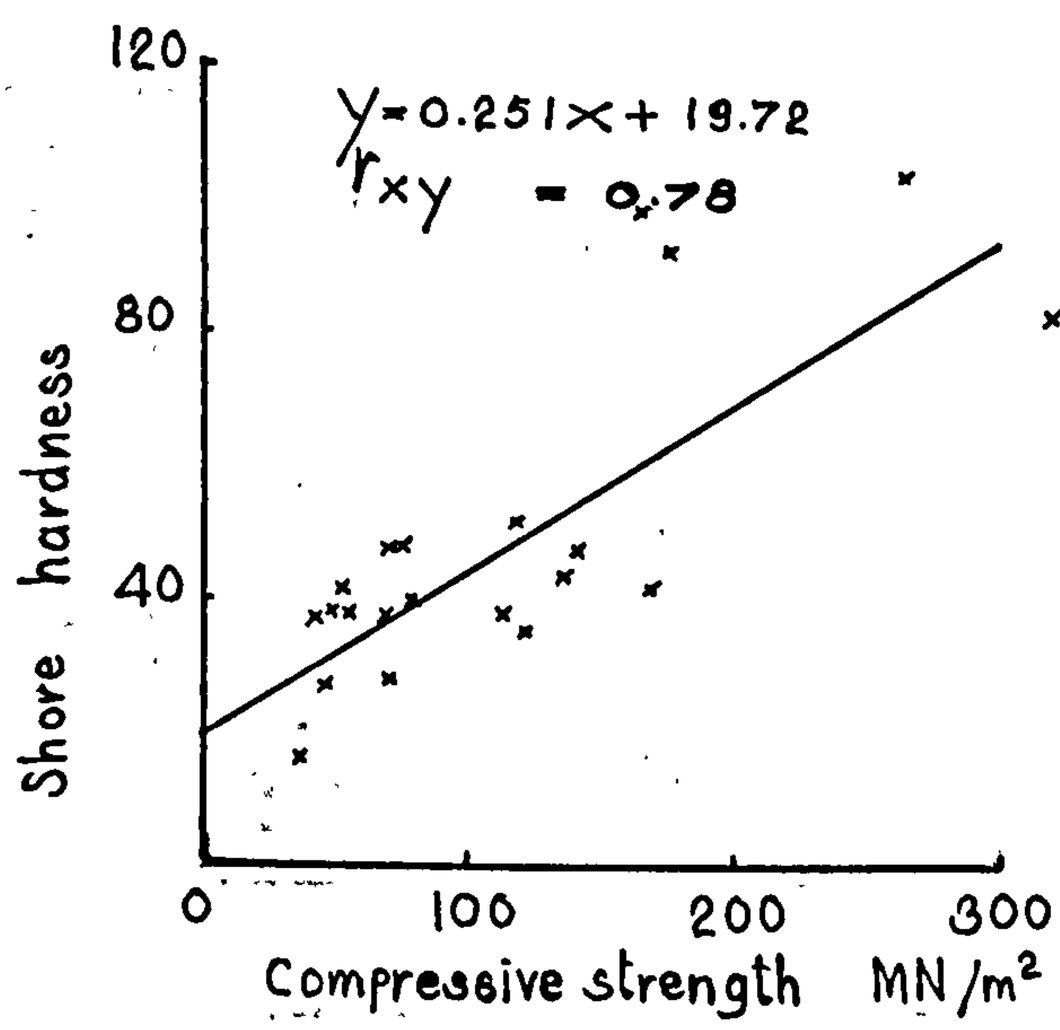
Y=0.251X+19.72
r_{xy} = 0.78
Shore hardness
120
80
40
0
100
200
300
Compressive strength MN/m²

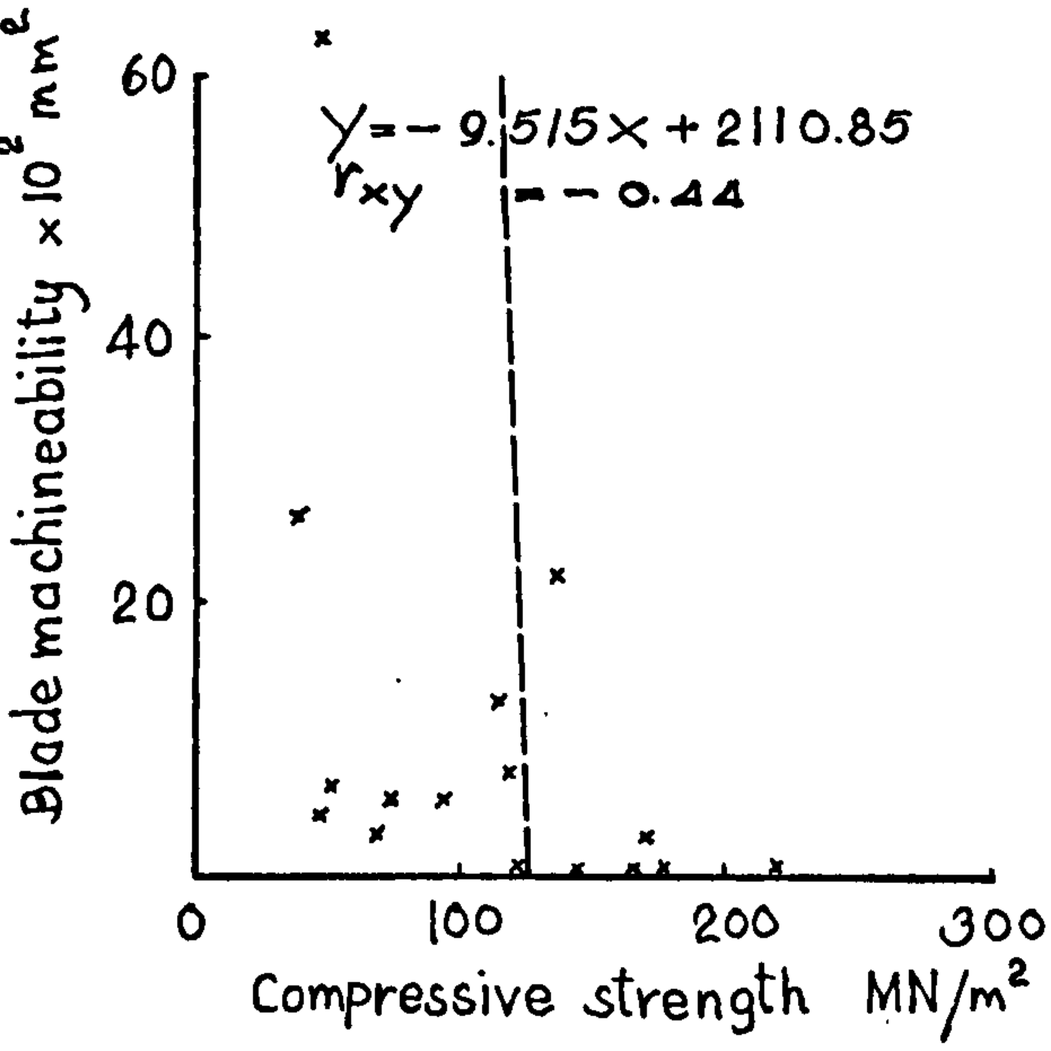
Y=−9.515X+2110.85
r_{xy} = −0.44
Blade machinability ×10² mm²
60
40
20
0
100
200
300
Compressive strength MN/m²

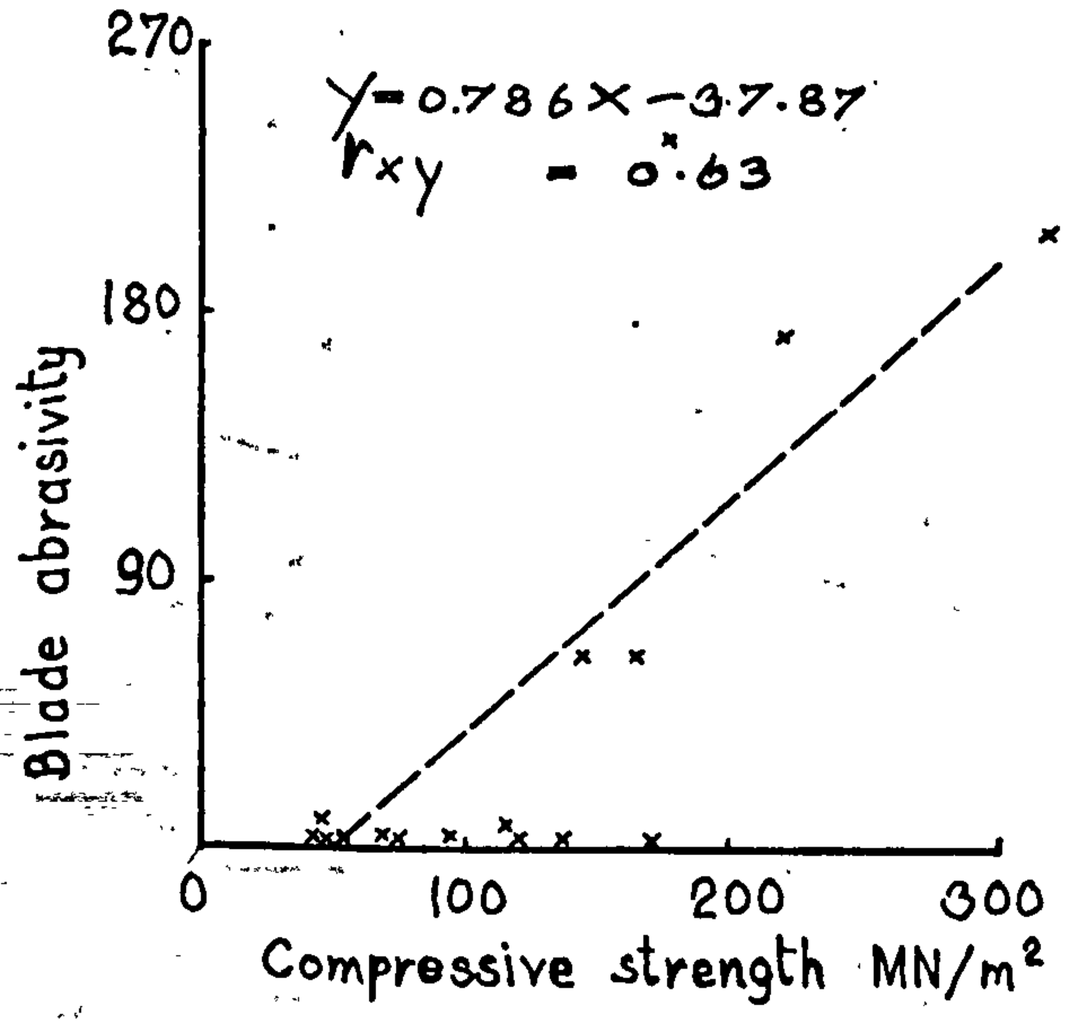
Y=0.786X−37.87
r_{xy} = 0.63
Blade abrasivity
270
180
90
0
100
200
300
Compressive strength MN/m²

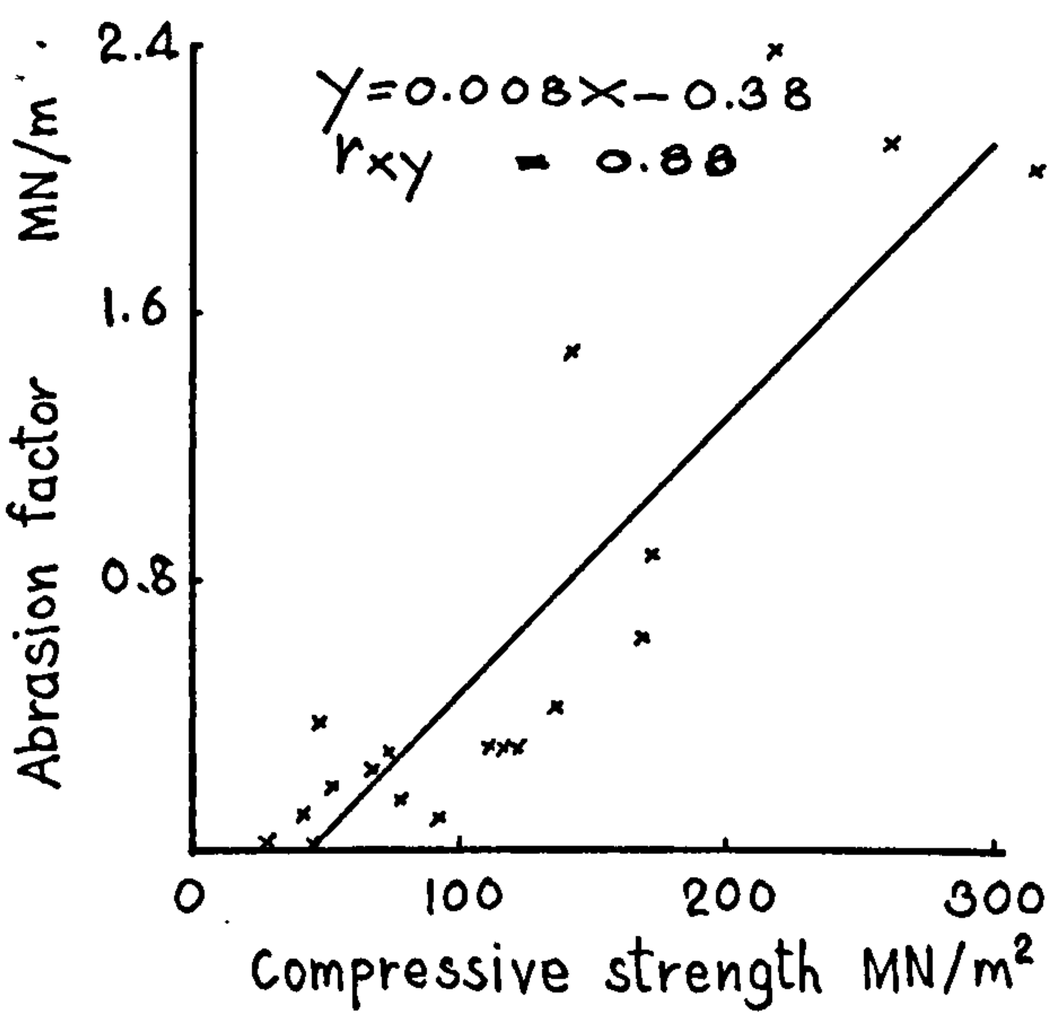
Y=0.008X−0.38
r_{xy} = 0.88
Abrasion factor MN/m
2.4
1.6
0.8
0
100
200
300
Compressive strength MN/m²

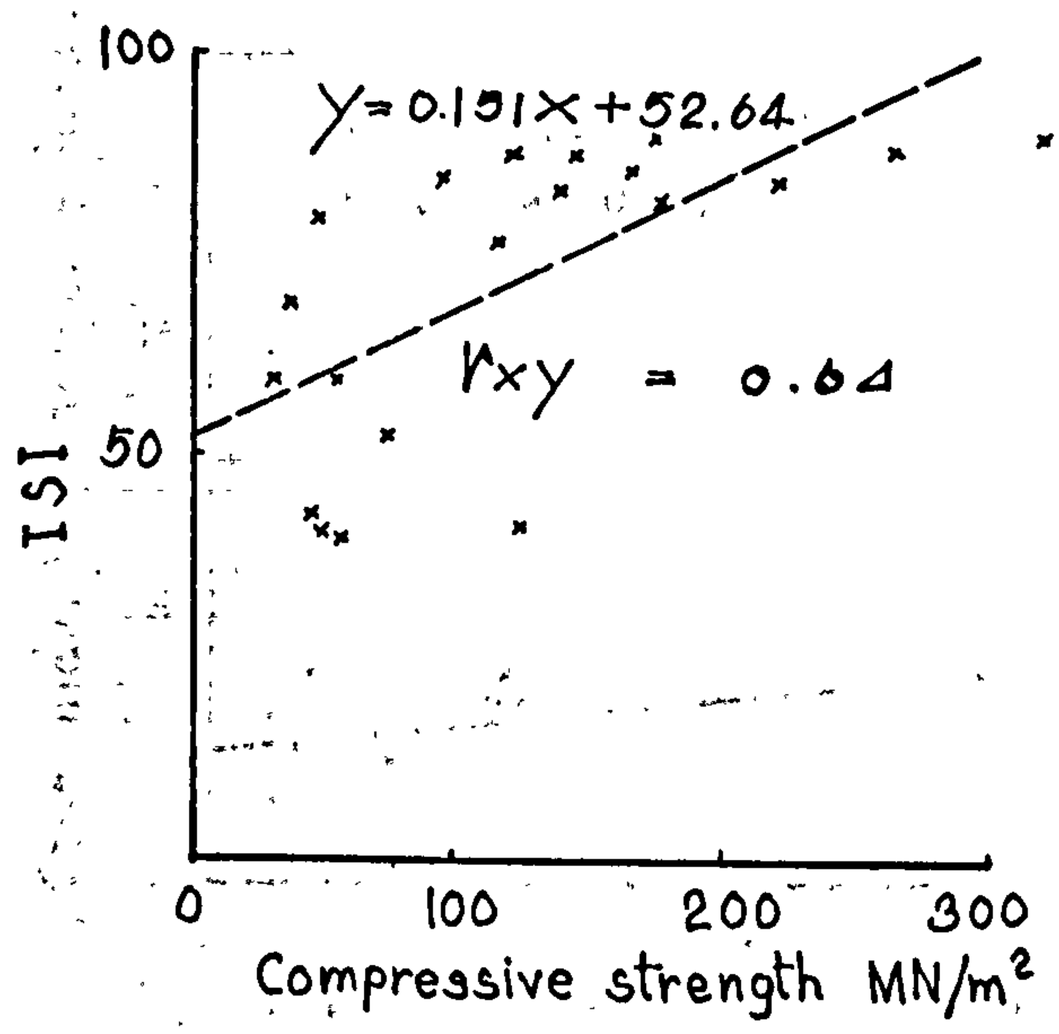
Y=0.191X+52.64
r_{xy} = 0.64
ISI
100
50
0
100
200
300
Compressive strength MN/m²

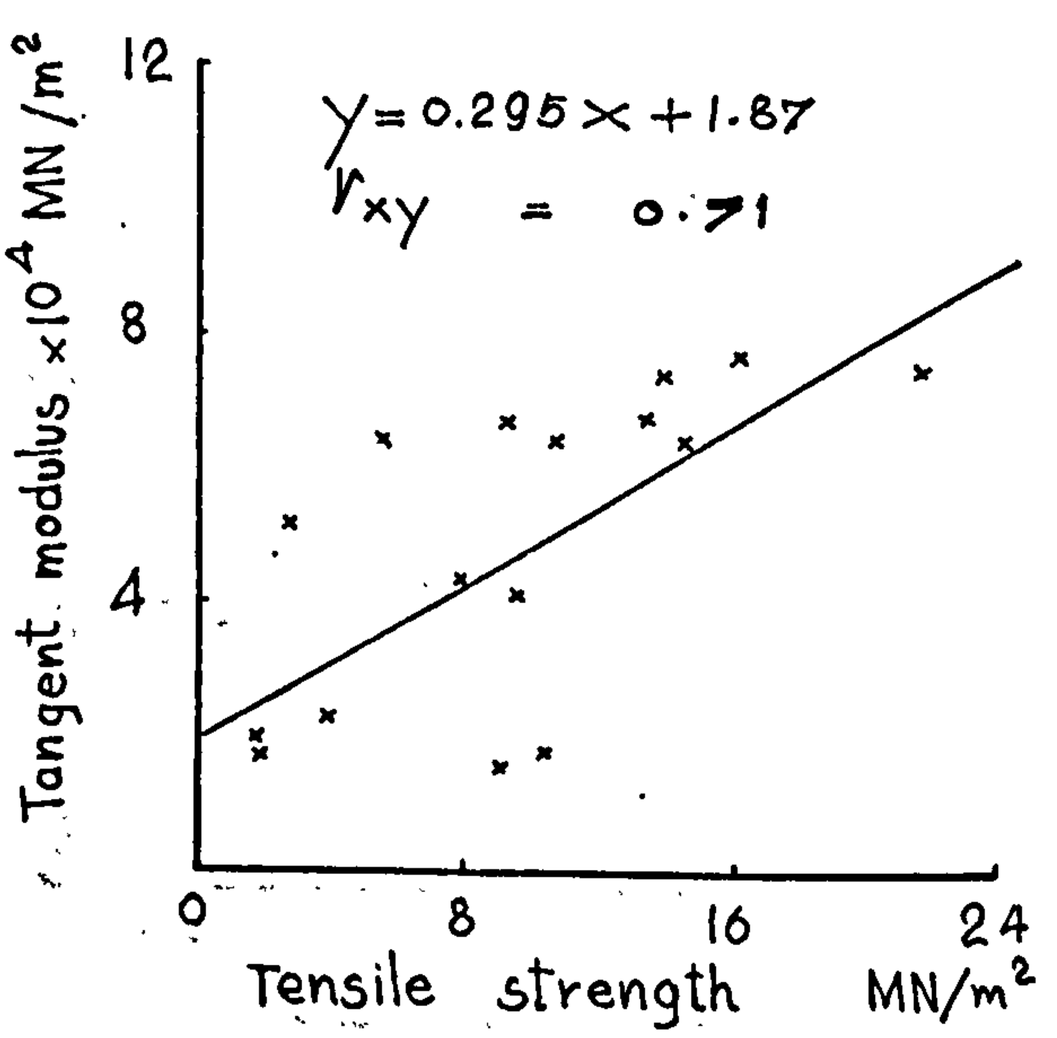
Y=0.295X+1.87
r_{xy} = 0.71
Tangent modulus ×10⁴ MN/m²
12
8
4
0
8
16
24
Tensile strength MN/m²

Figure 47 (20)

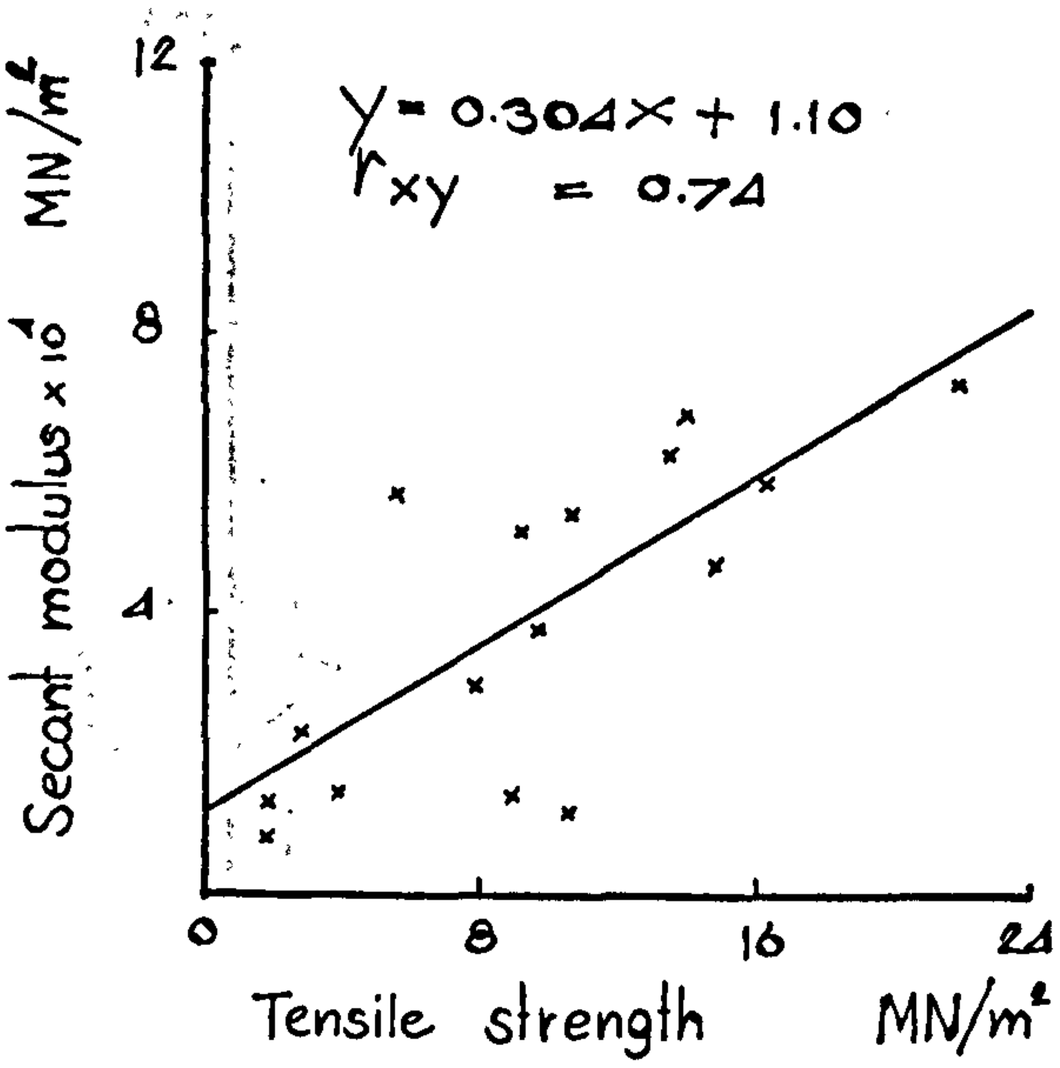
Y = 0.304X + 1.10
r_{xy} = 0.74
Secant modulus x 10^4 MN/m²
12
8
4
0
8
16
24
Tensile strength MN/m²

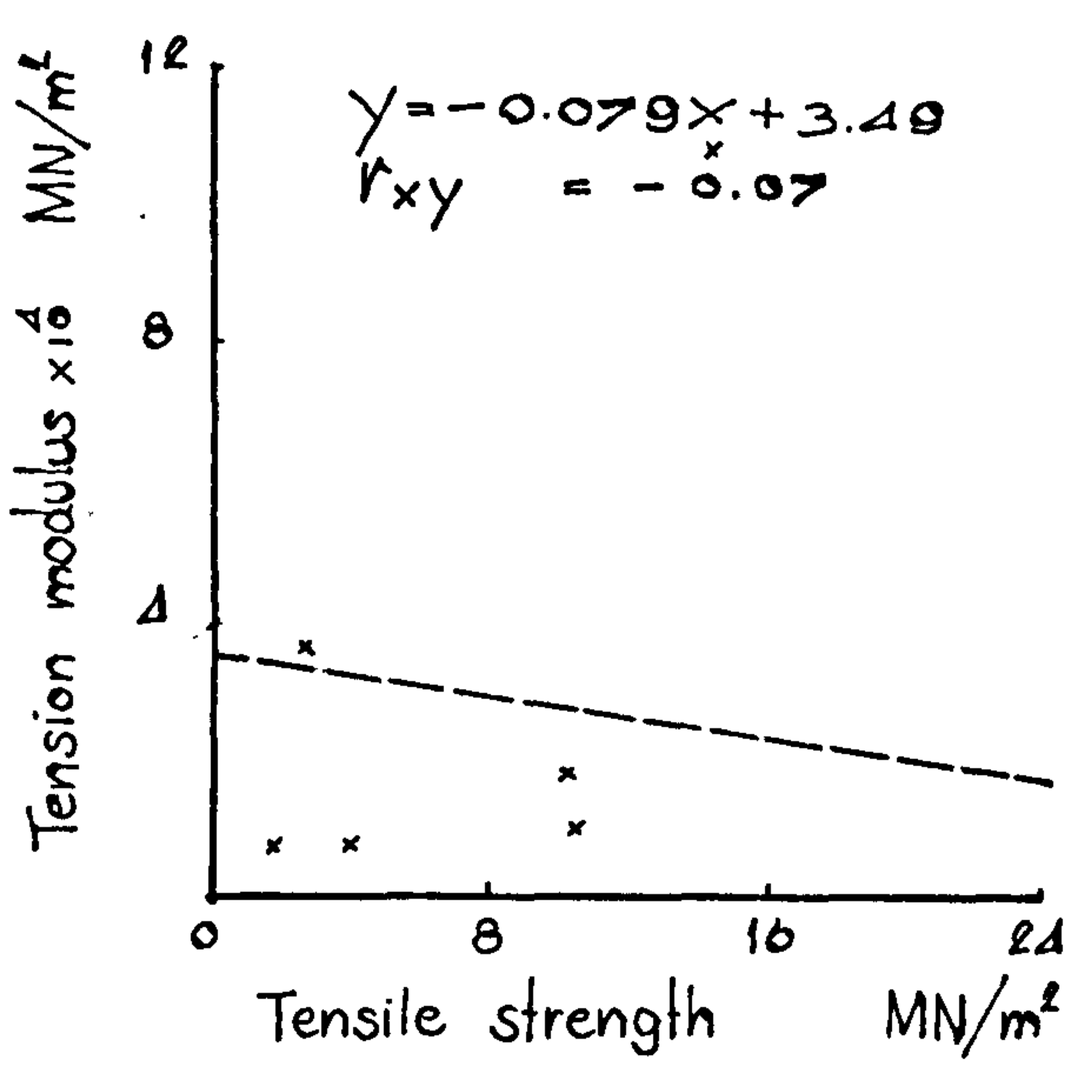
Y = −0.079X + 3.49
r_{xy} = −0.07
Tension modulus x 10^4 MN/m²
12
8
4
0
8
16
24
Tensile strength MN/m²

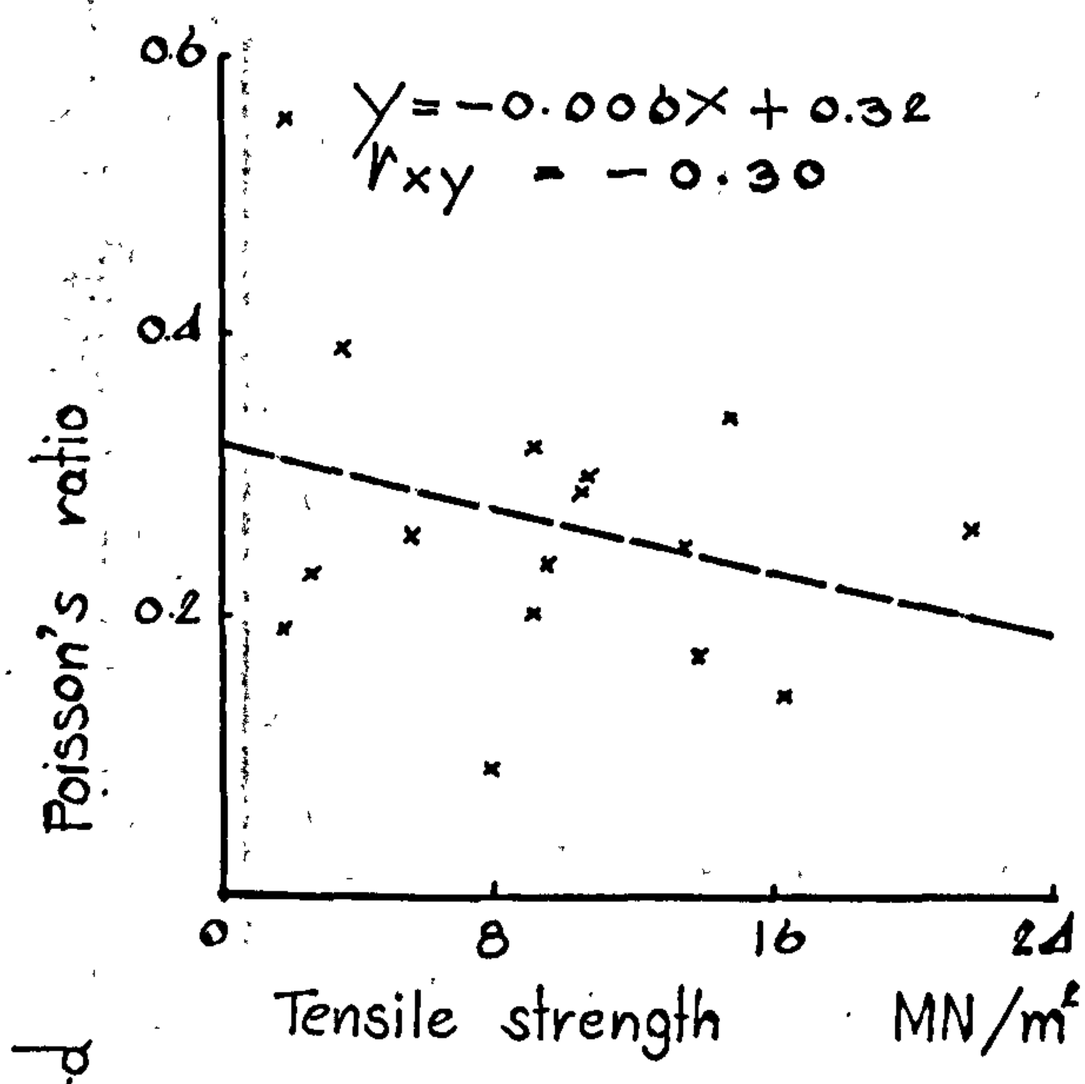
Y = −0.006X + 0.32
r_{xy} = −0.30
Poisson's ratio
0.6
0.4
0.2
0
8
16
24
Tensile strength MN/m²

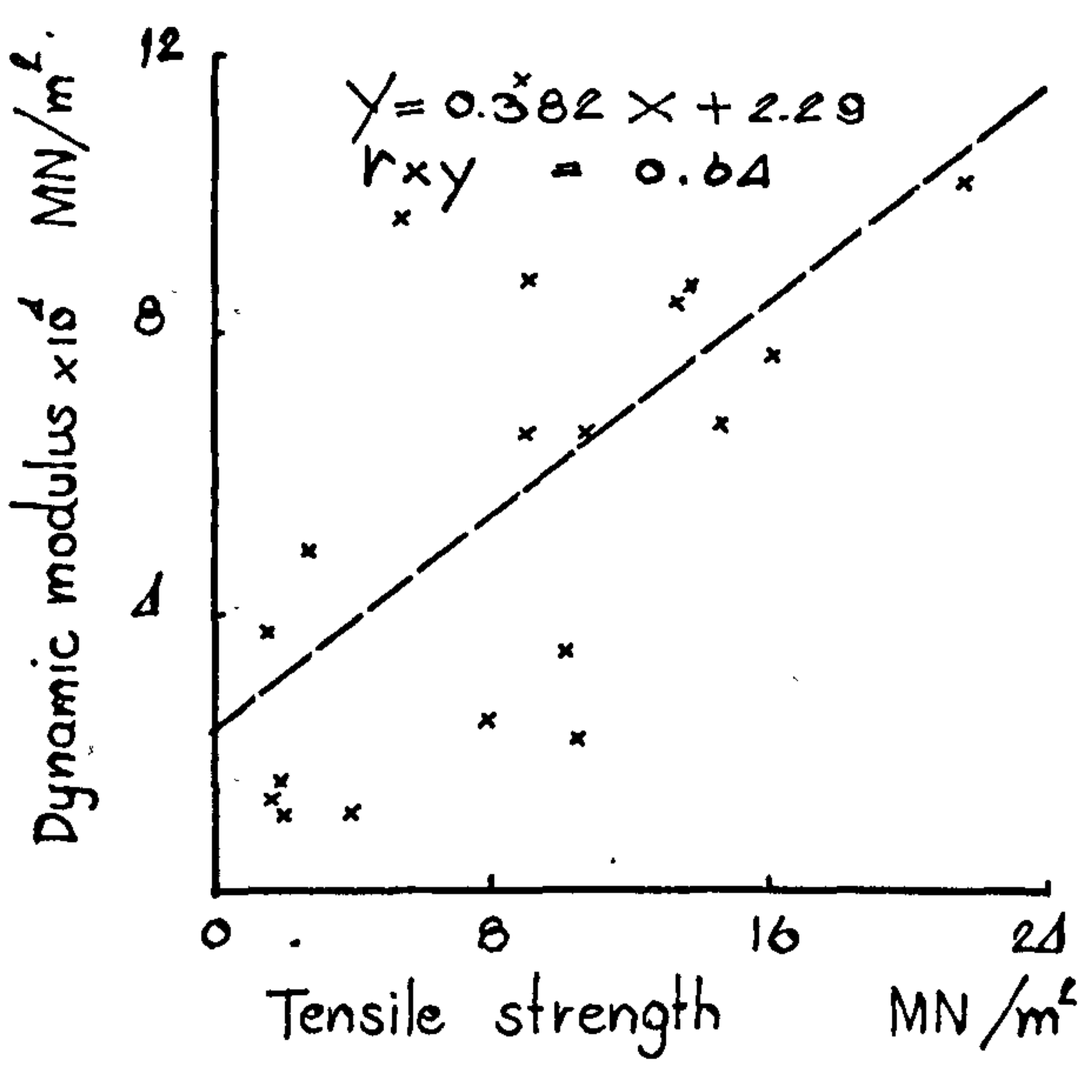
Y = 0.382X + 2.29
r_{xy} = 0.64
Dynamic modulus x 10^4 MN/m²
12
8
4
0
8
16
24
Tensile strength MN/m²

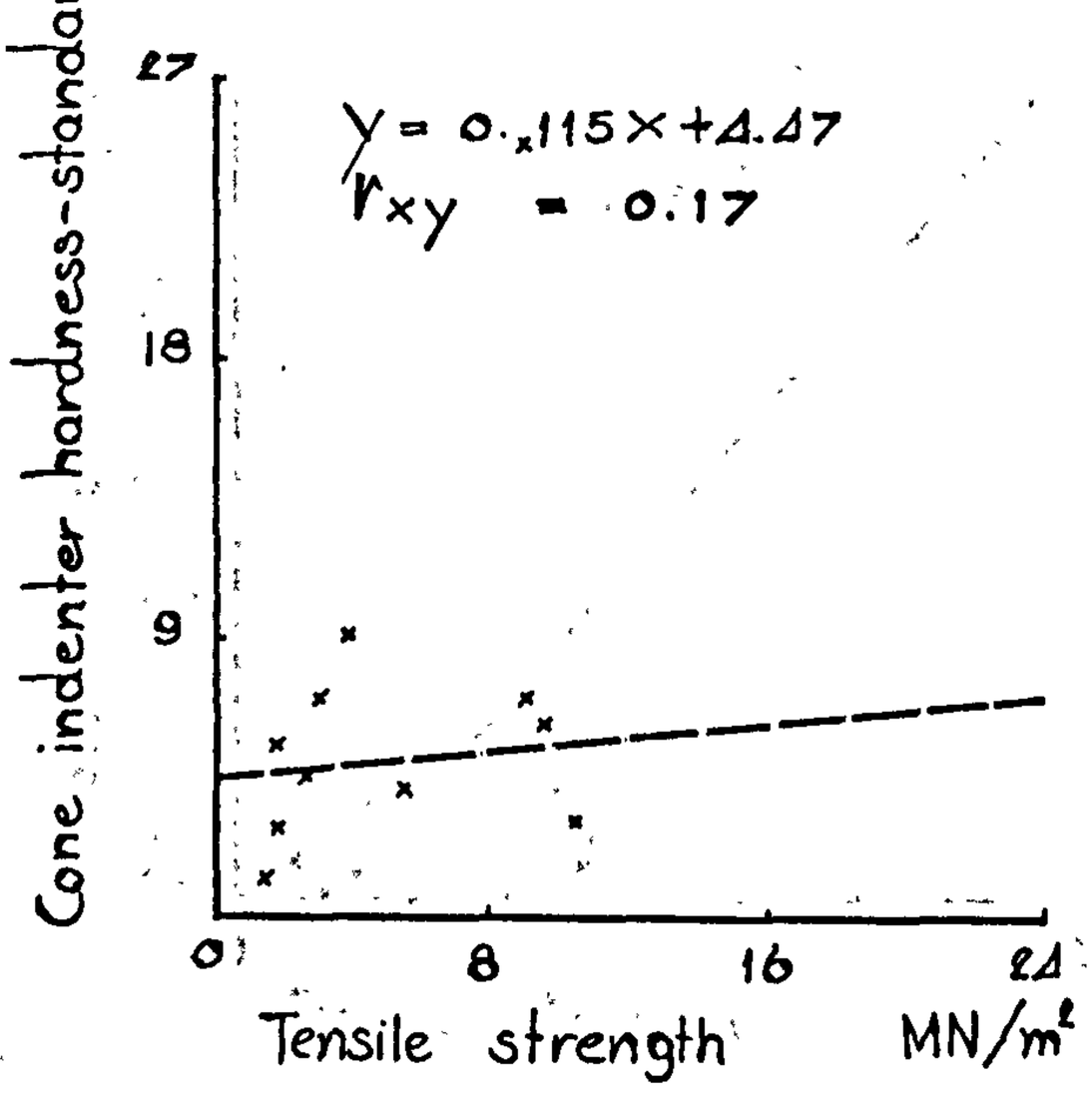
Y = 0.115X + 4.47
r_{xy} = 0.17
Cone indenter hardness-standard
27
18
9
0
8
16
24
Tensile strength MN/m²

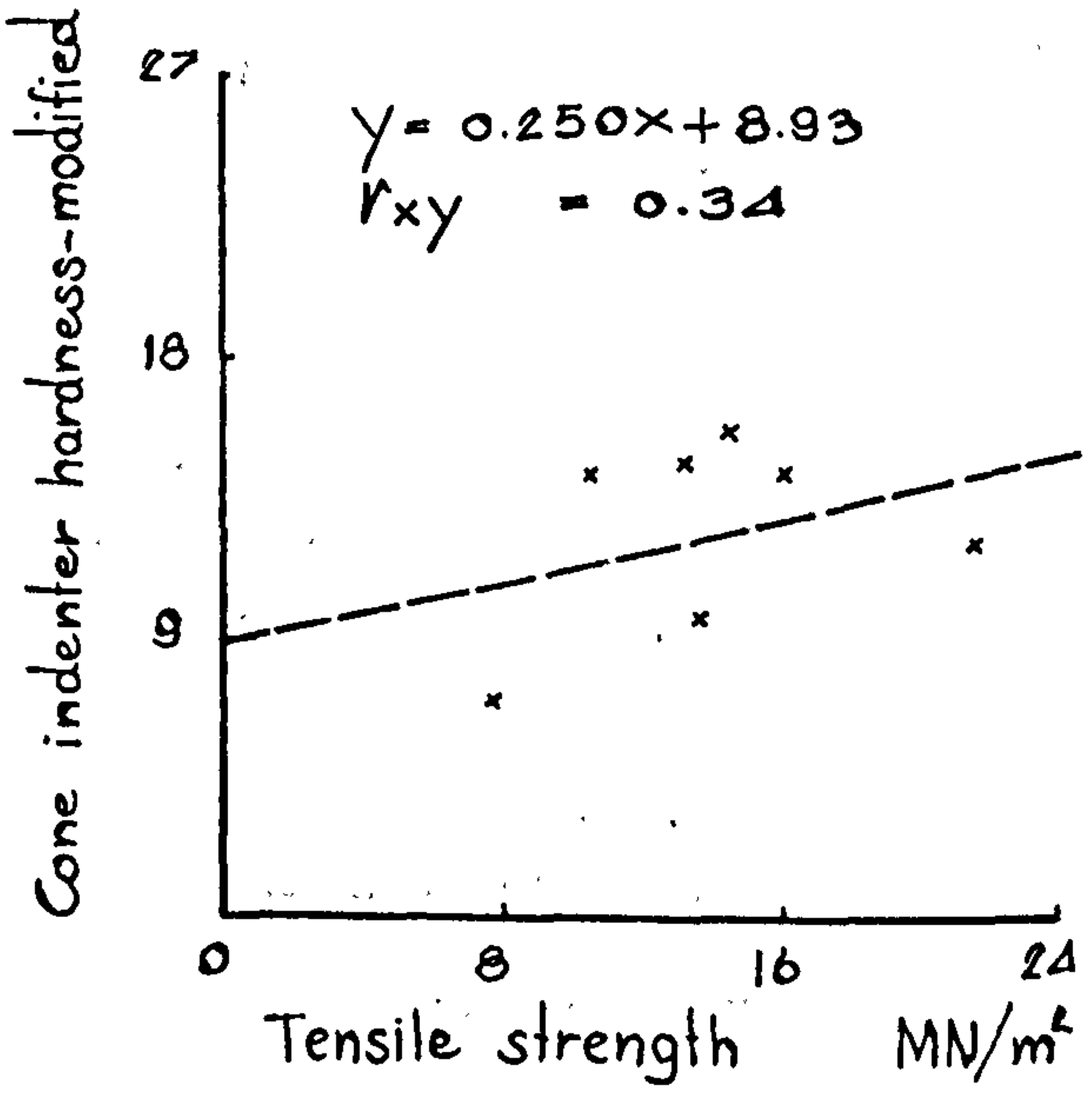
Y = 0.250X + 8.93
r_{xy} = 0.34
Cone indenter hardness-modified
27
18
9
0
8
16
24
Tensile strength MN/m²

Figure 47 (21)

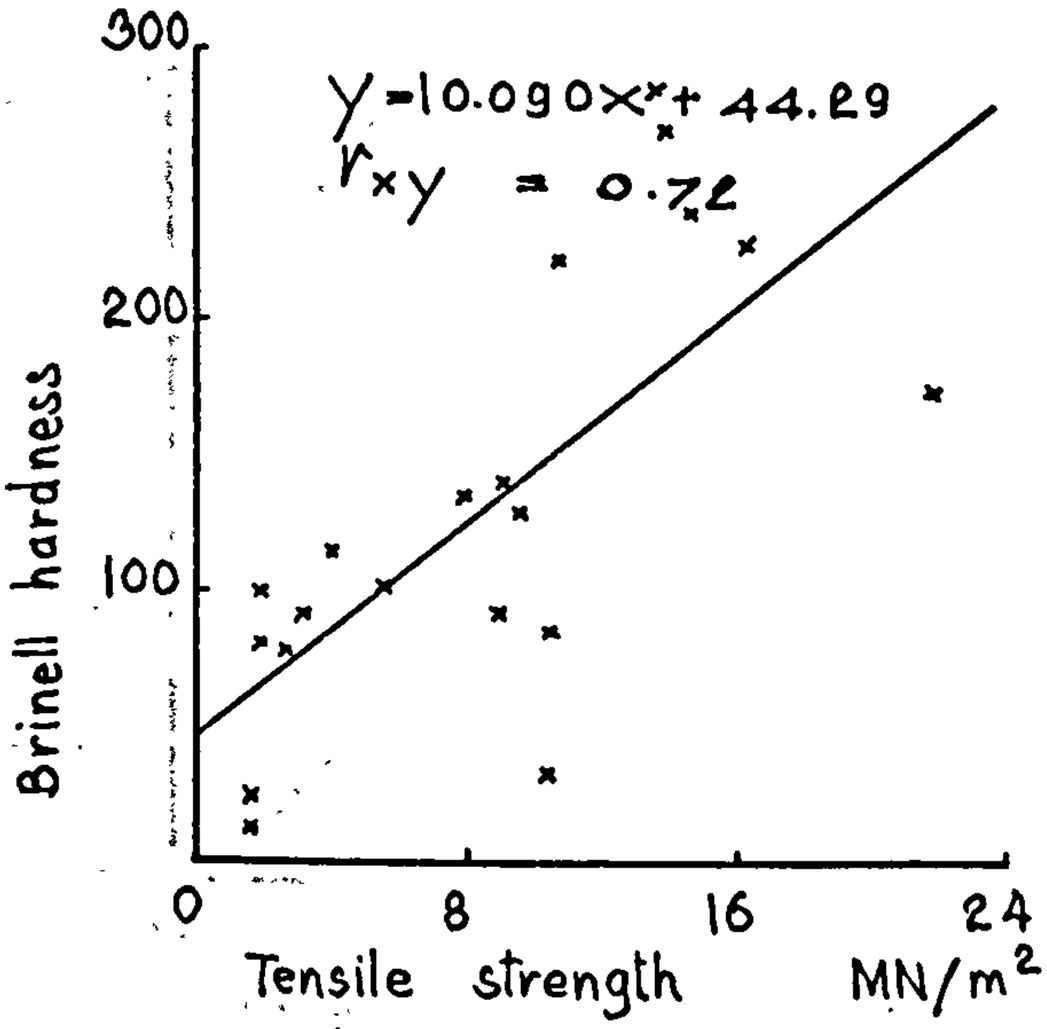
Y=10.090X+44.29
rxy = 0.72
300
200
100
0
8
16
24
Brinell hardness
Tensile strength MN/m²

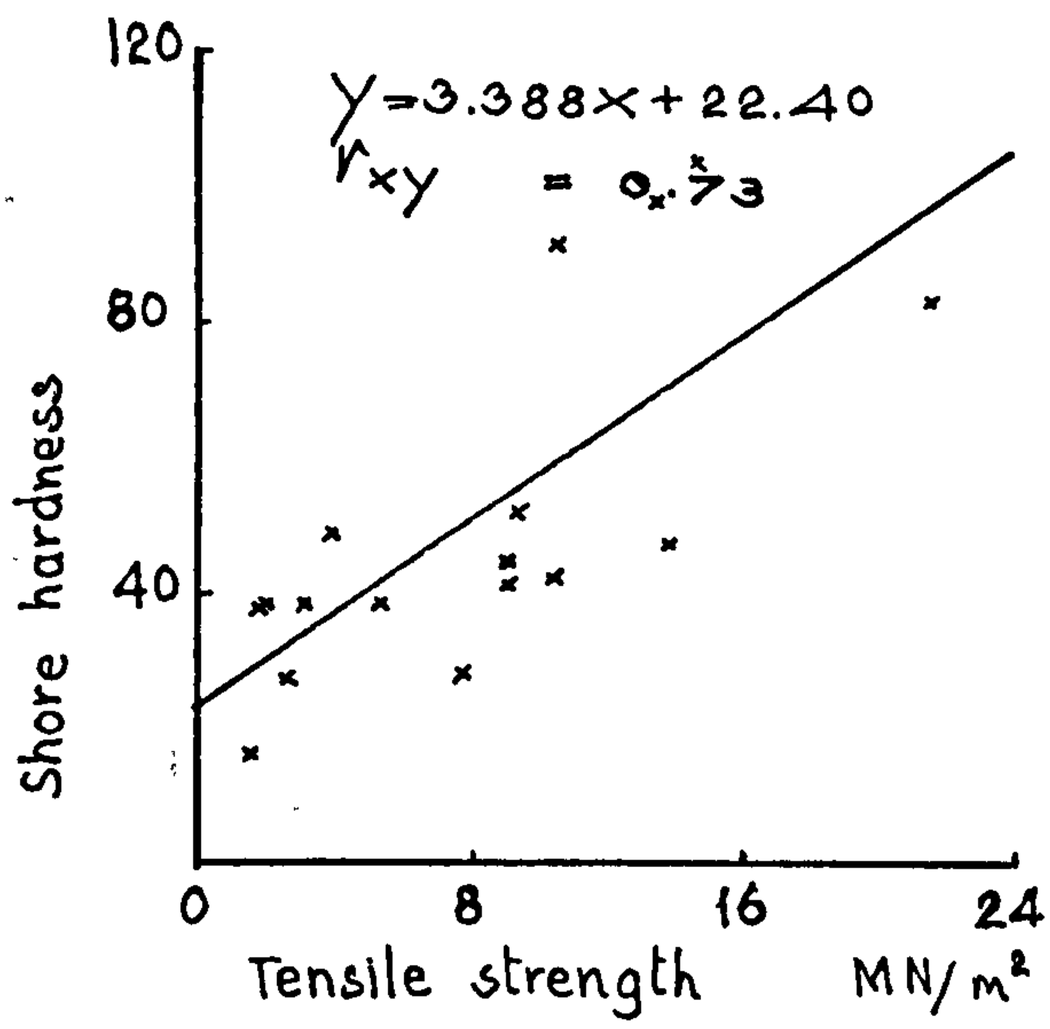
Y=3.388X+22.40
rxy = 0.73
120
80
40
0
8
16
24
Shore hardness
Tensile strength MN/m²

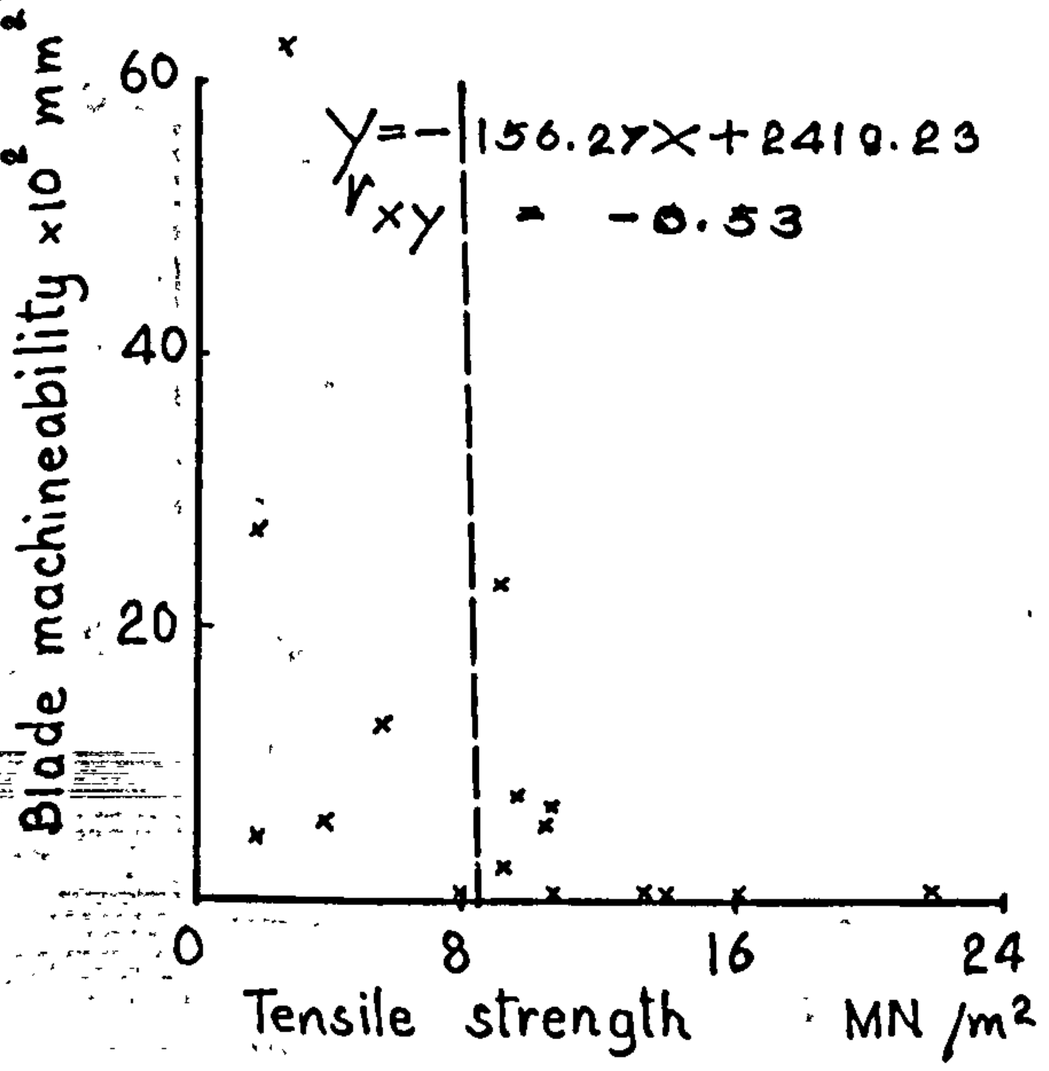
Y=-156.27X+2419.23
rxy = -0.53
60
40
20
0
8
16
24
Blade machineability x10² mm²
Tensile strength MN/m²

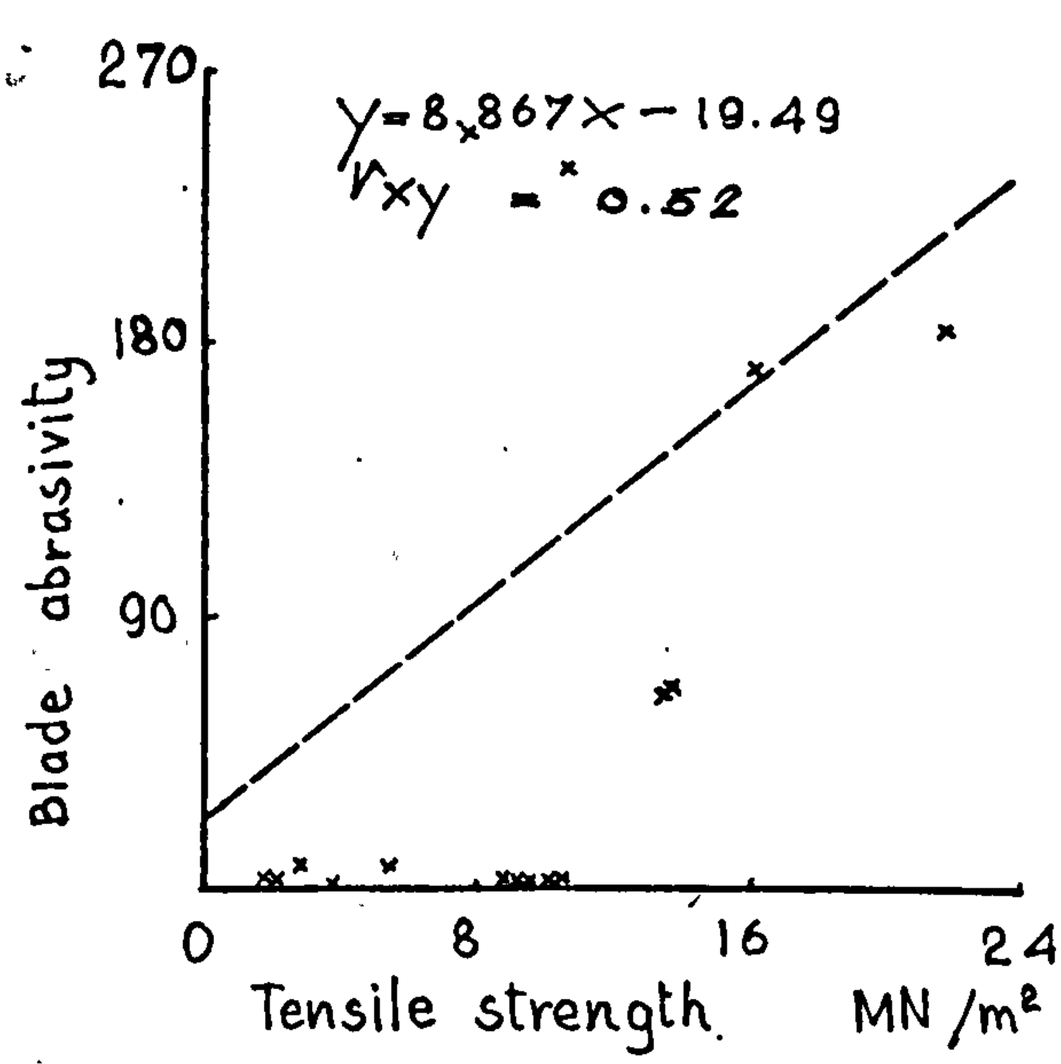
Y=8.867X-19.49
rxy = 0.52
270
180
90
0
8
16
24
Blade abrasivity
Tensile strength MN/m²

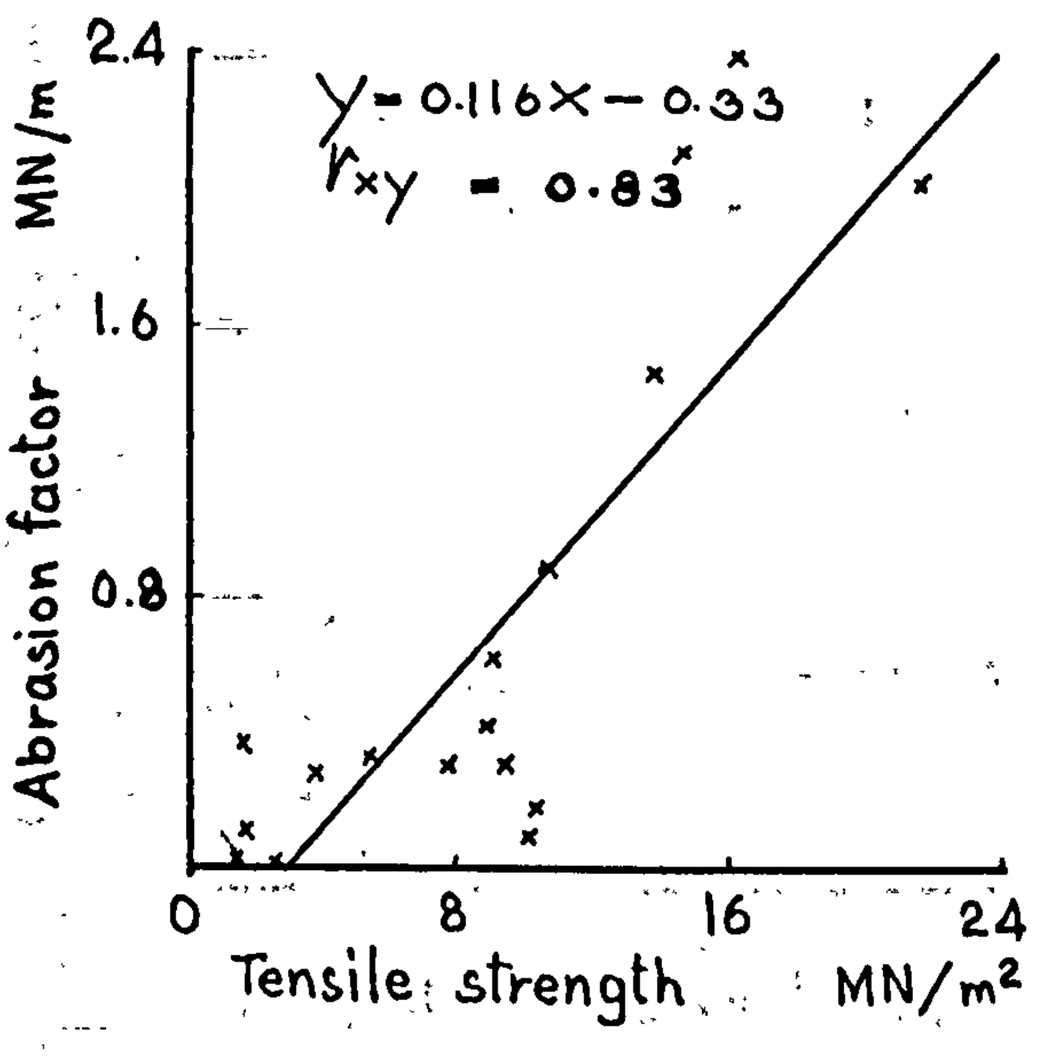
Y=0.116X-0.33
rxy = 0.83
2.4
1.6
0.8
0
8
16
24
Abrasion factor MN/m
Tensile strength MN/m²

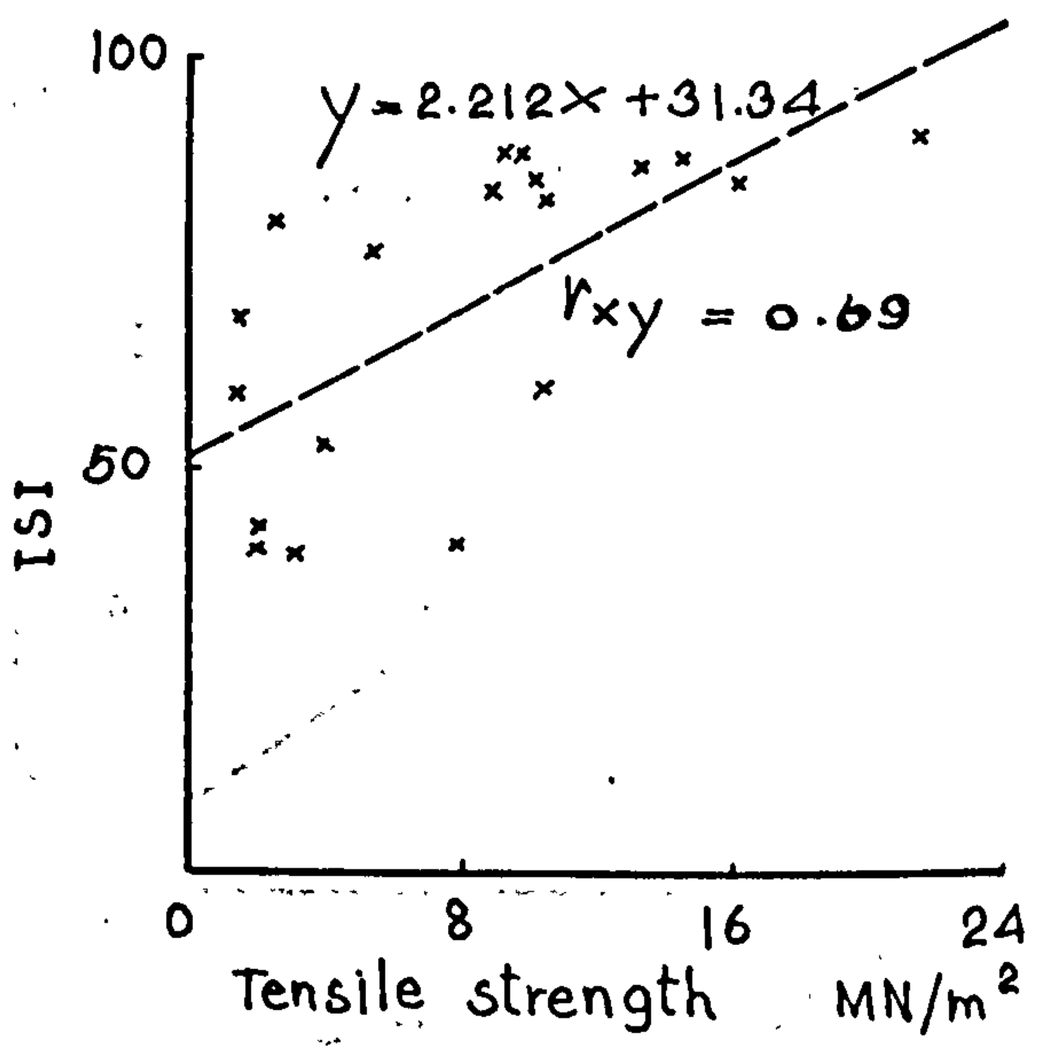
Y=2.212X+31.34
rxy = 0.69
100
50
0
8
16
24
ISI
Tensile strength MN/m²

Figure 47 (22)

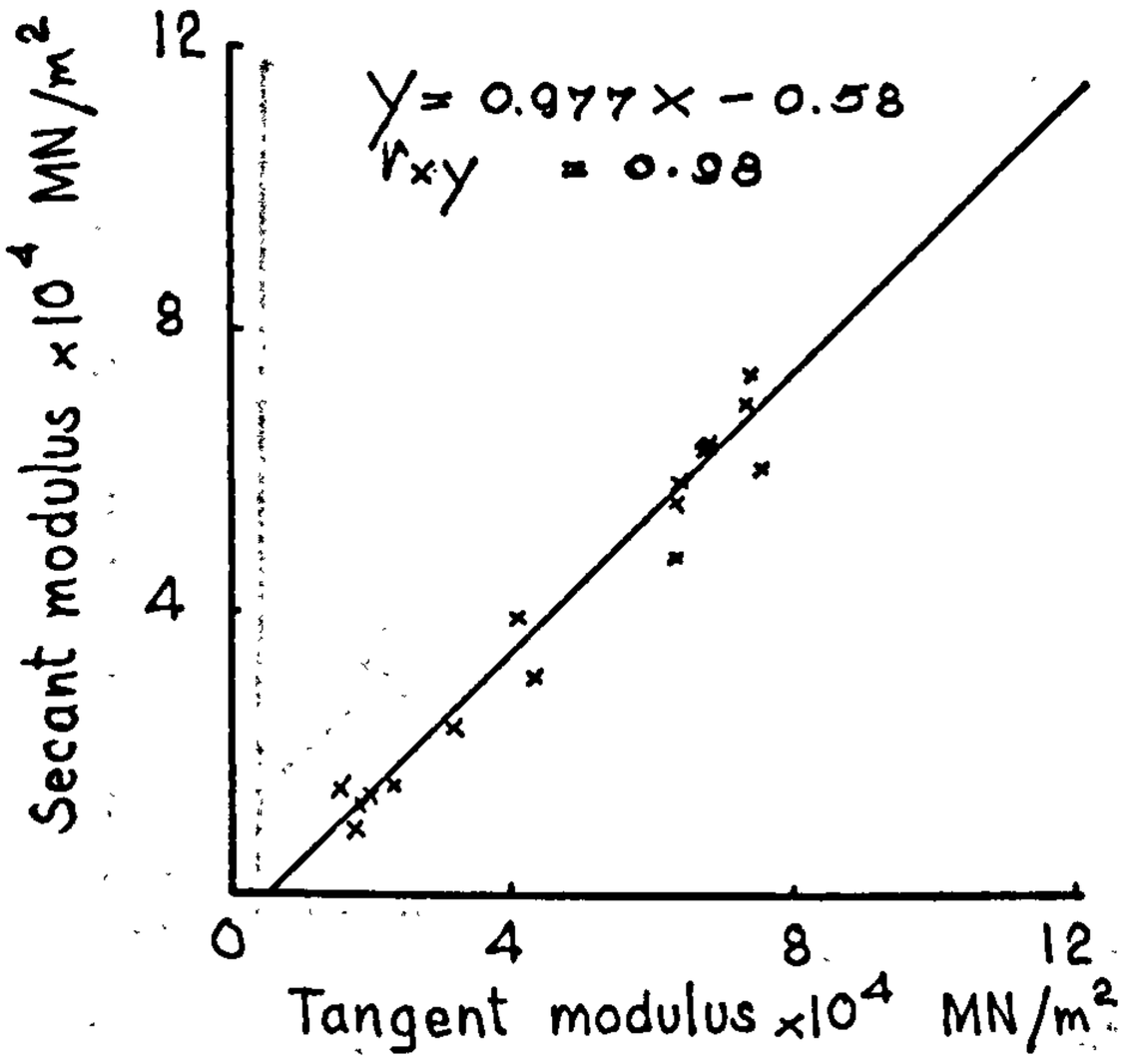
Y = 0.977X − 0.58
r_xy = 0.98
Secant modulus ×10⁴ MN/m²
Tangent modulus ×10⁴ MN/m²
0
4
8
12

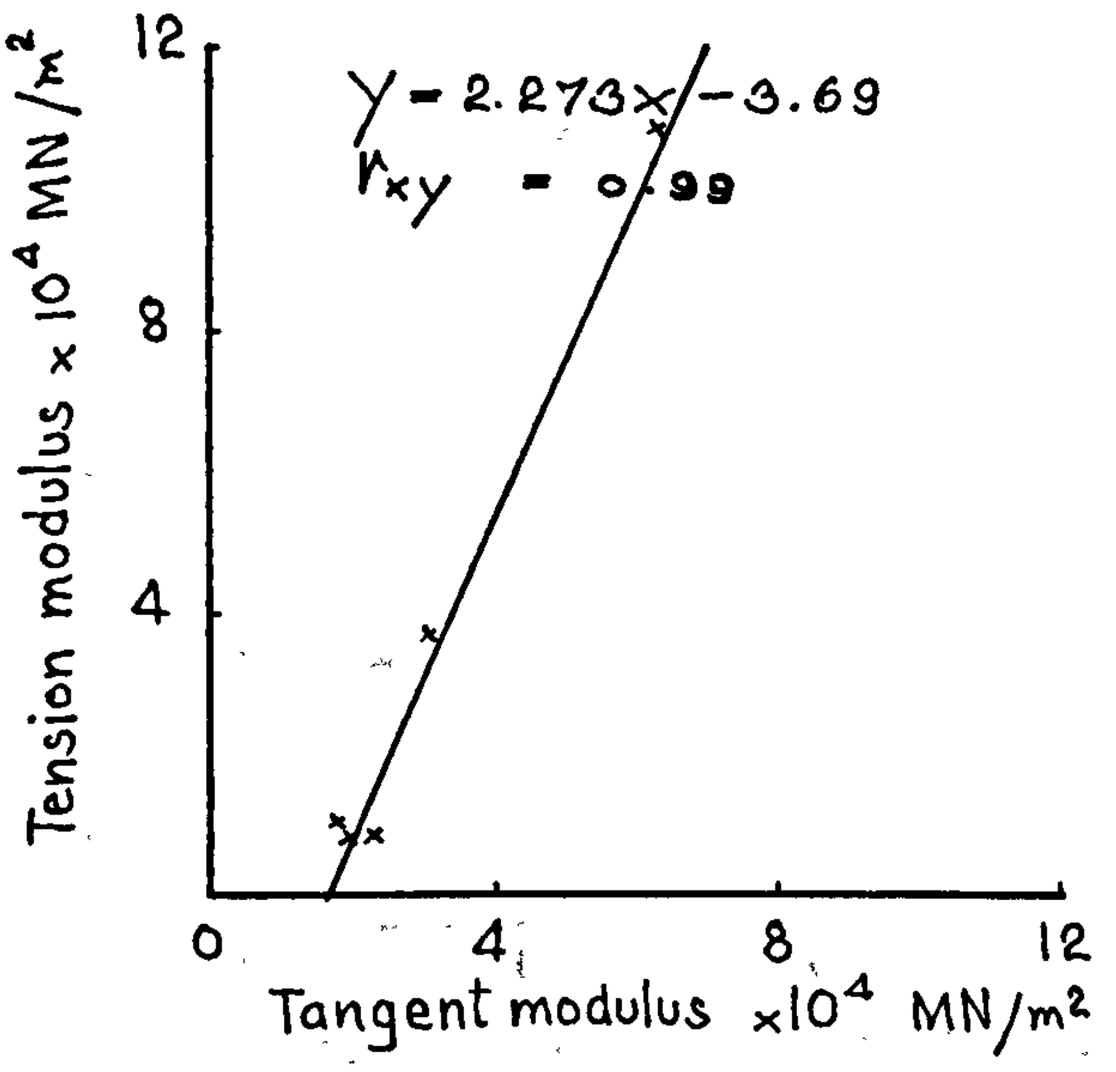
Y = 2.273X − 3.69
r_xy = 0.99
Tension modulus ×10⁴ MN/m²
Tangent modulus ×10⁴ MN/m²
0
4
8
12

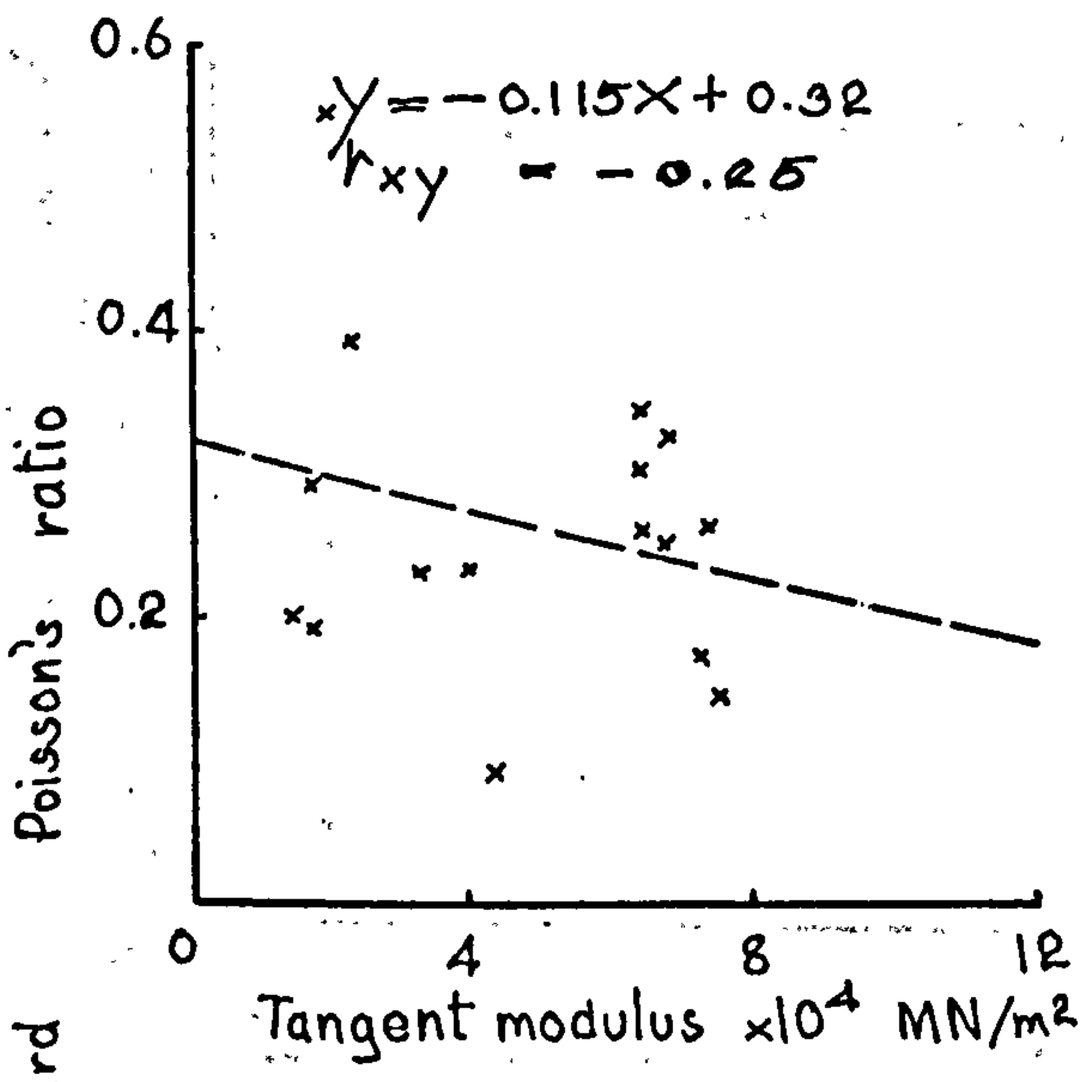
Y = −0.115X + 0.32
r_xy = −0.25
Poisson's ratio
Tangent modulus ×10⁴ MN/m²
0.6
0.4
0.2
0
4
8
12

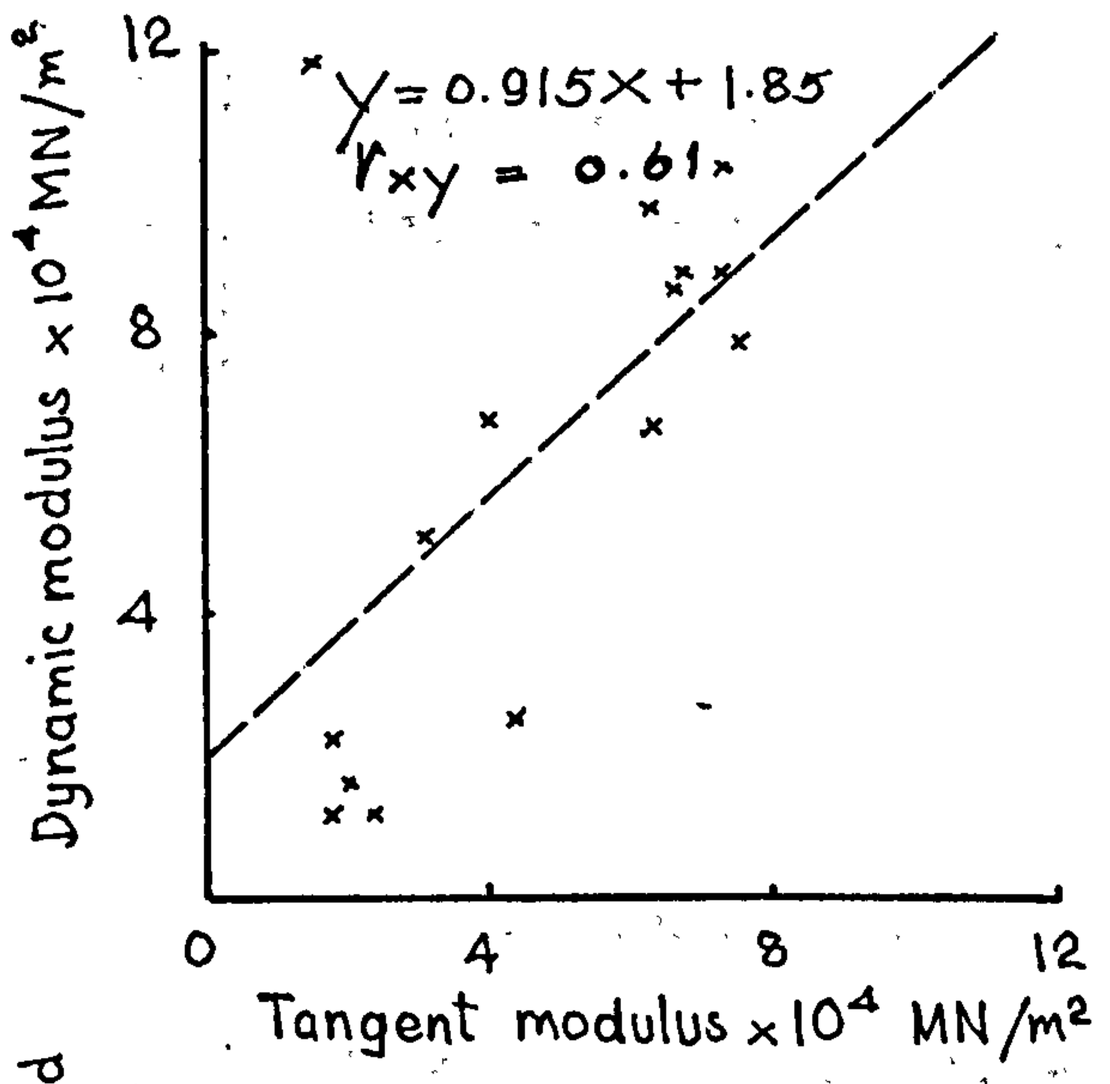
Y = 0.915X + 1.85
r_xy = 0.61
Dynamic modulus ×10⁴ MN/m²
Tangent modulus ×10⁴ MN/m²
12
8
4
0
4
8
12

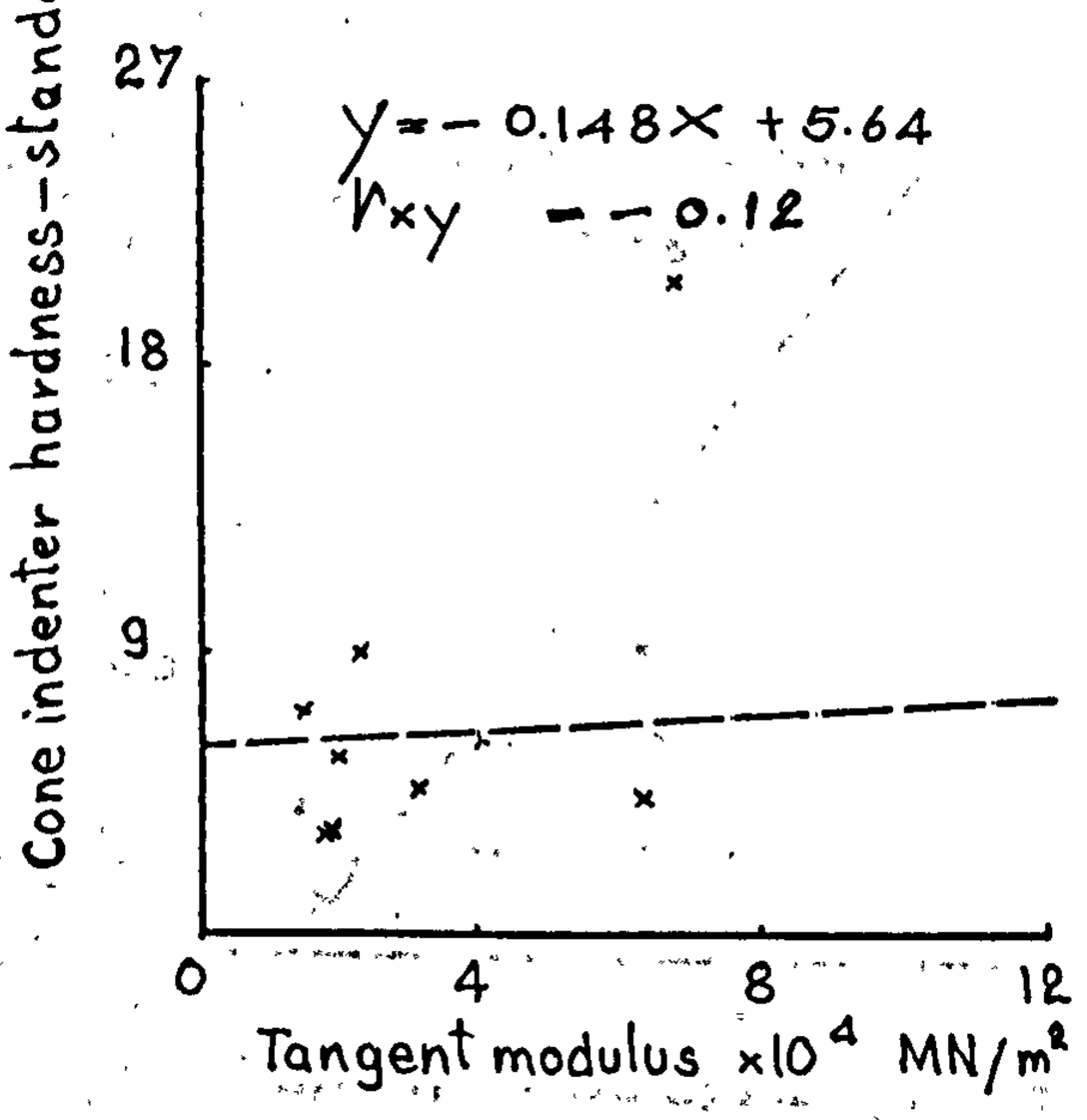
Y = −0.148X + 5.64
r_xy = −0.12
Cone indenter hardness – standard
Tangent modulus ×10⁴ MN/m²
27
18
9
0
4
8
12

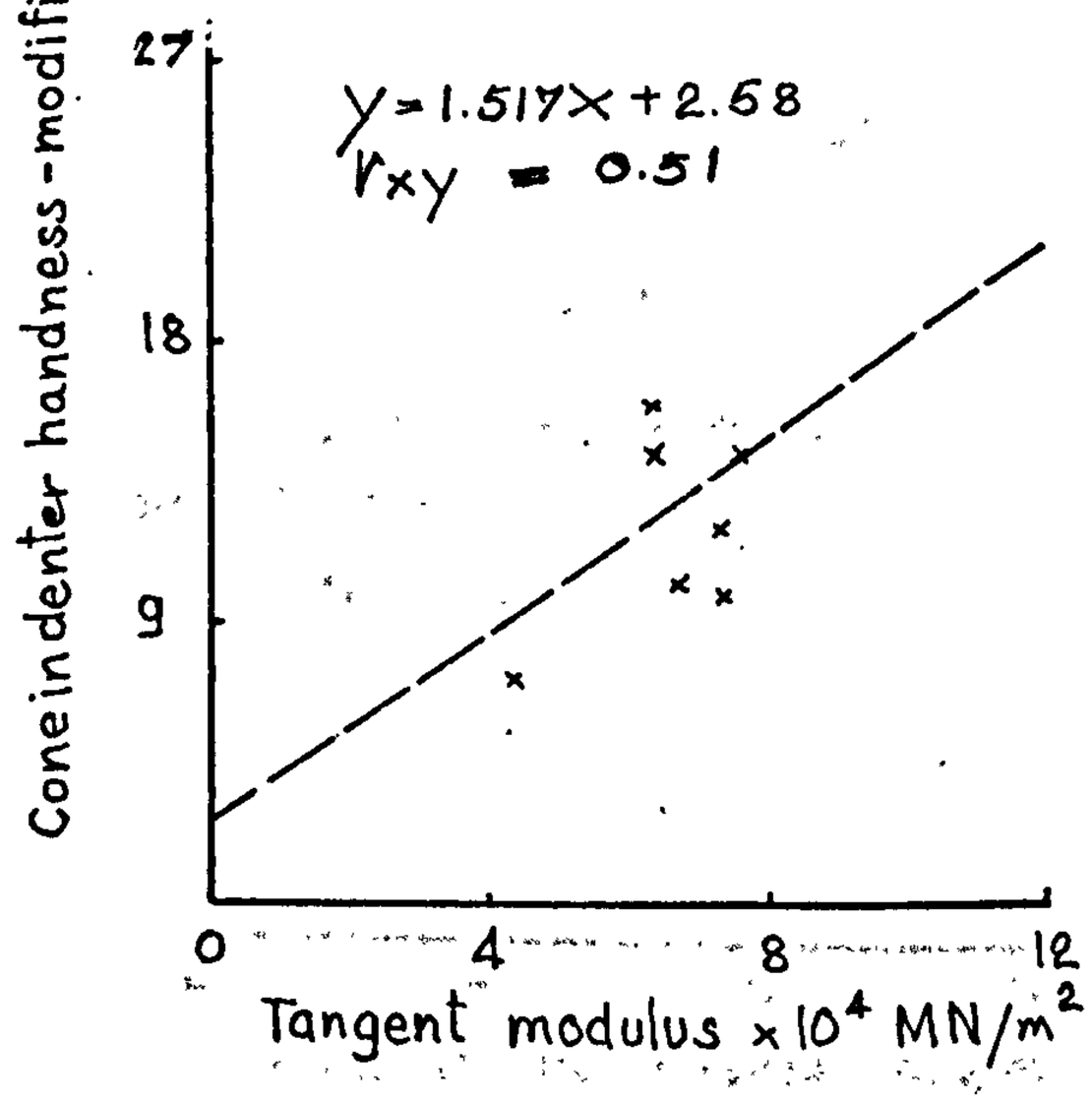
Y = 1.517X + 2.58
r_xy = 0.51
Cone indenter hardness – modified
Tangent modulus ×10⁴ MN/m²
27
18
9
0
4
8
12

Figure 47 (23)

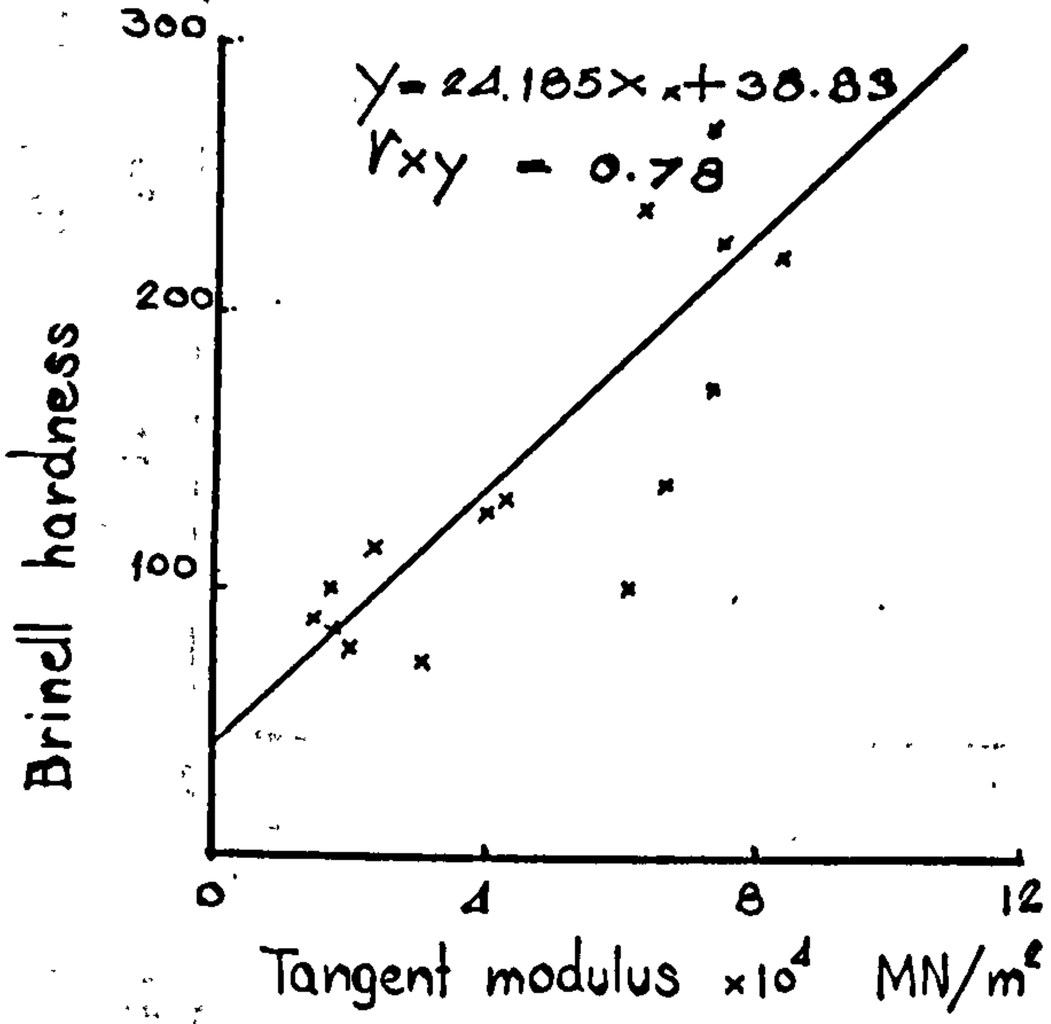
Y = 24.185X + 38.83
rxy = 0.78
Brinell hardness
300
200
100
0
4
8
12
Tangent modulus ×10⁴ MN/m²

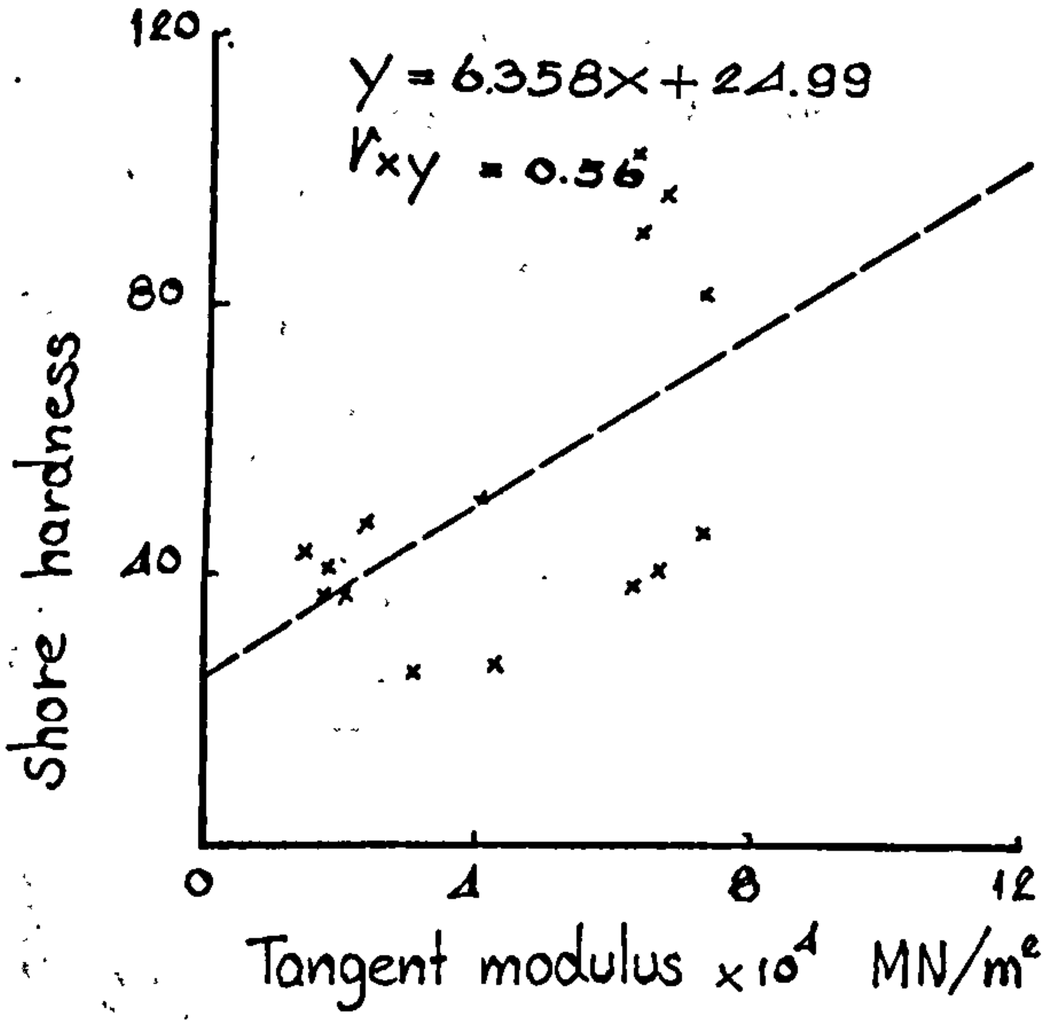
Y = 6.358X + 24.99
rxy = 0.56
Shore hardness
120
80
40
0
4
8
12
Tangent modulus ×10⁴ MN/m²

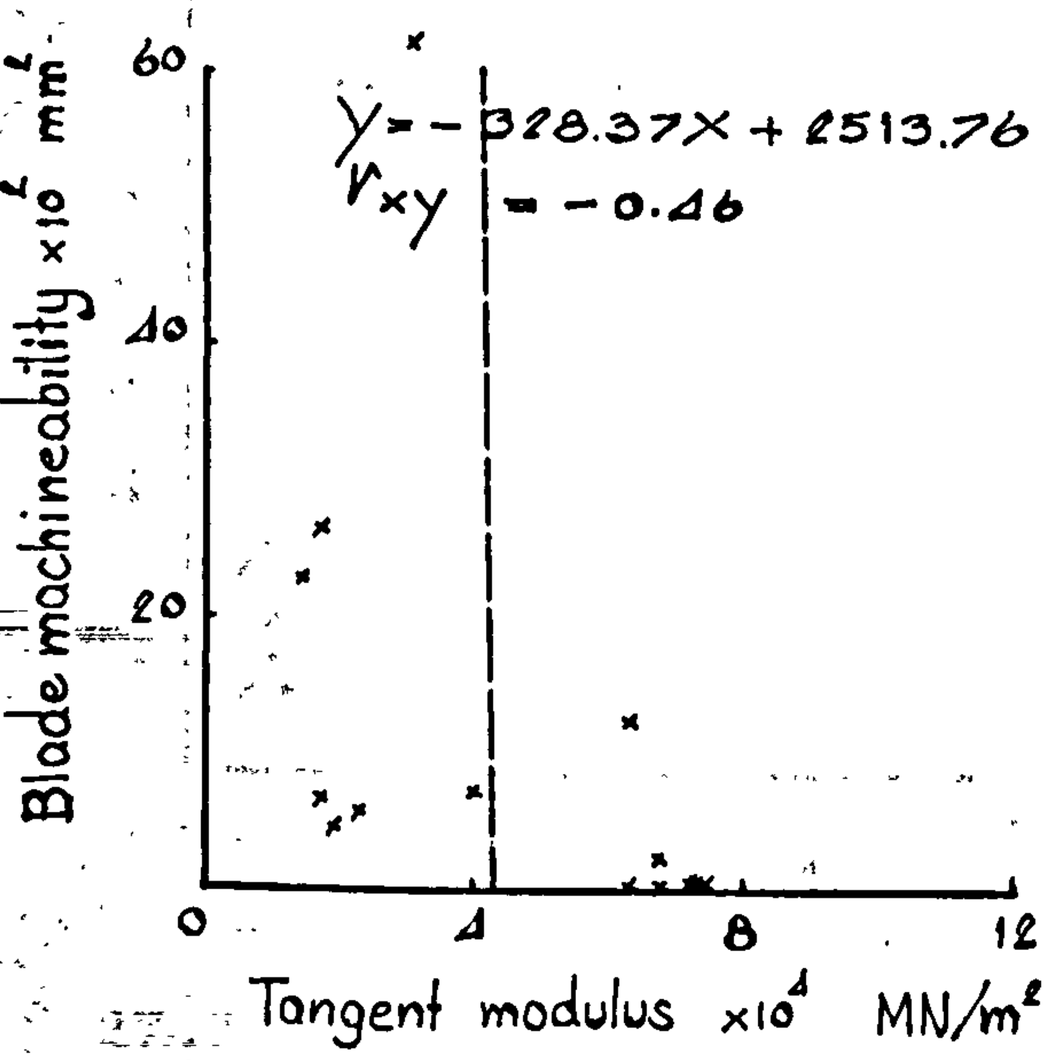
Y = -328.37X + 2513.76
rxy = -0.46
Blade machineability ×10² mm²
60
40
20
0
4
8
12
Tangent modulus ×10⁴ MN/m²

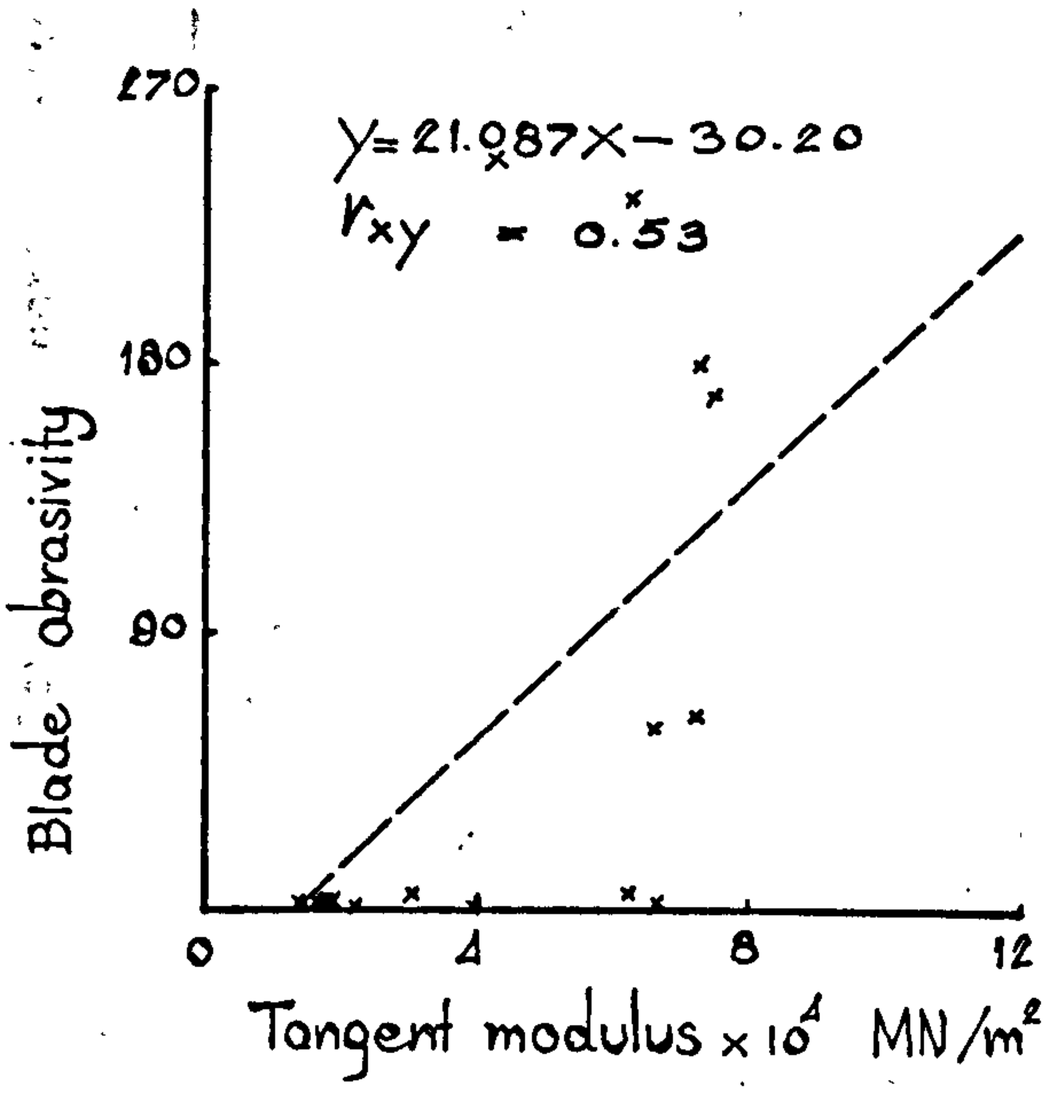
Y = 21.087X − 30.20
rxy = 0.53
Blade abrasivity
270
180
90
0
4
8
12
Tangent modulus ×10⁴ MN/m²

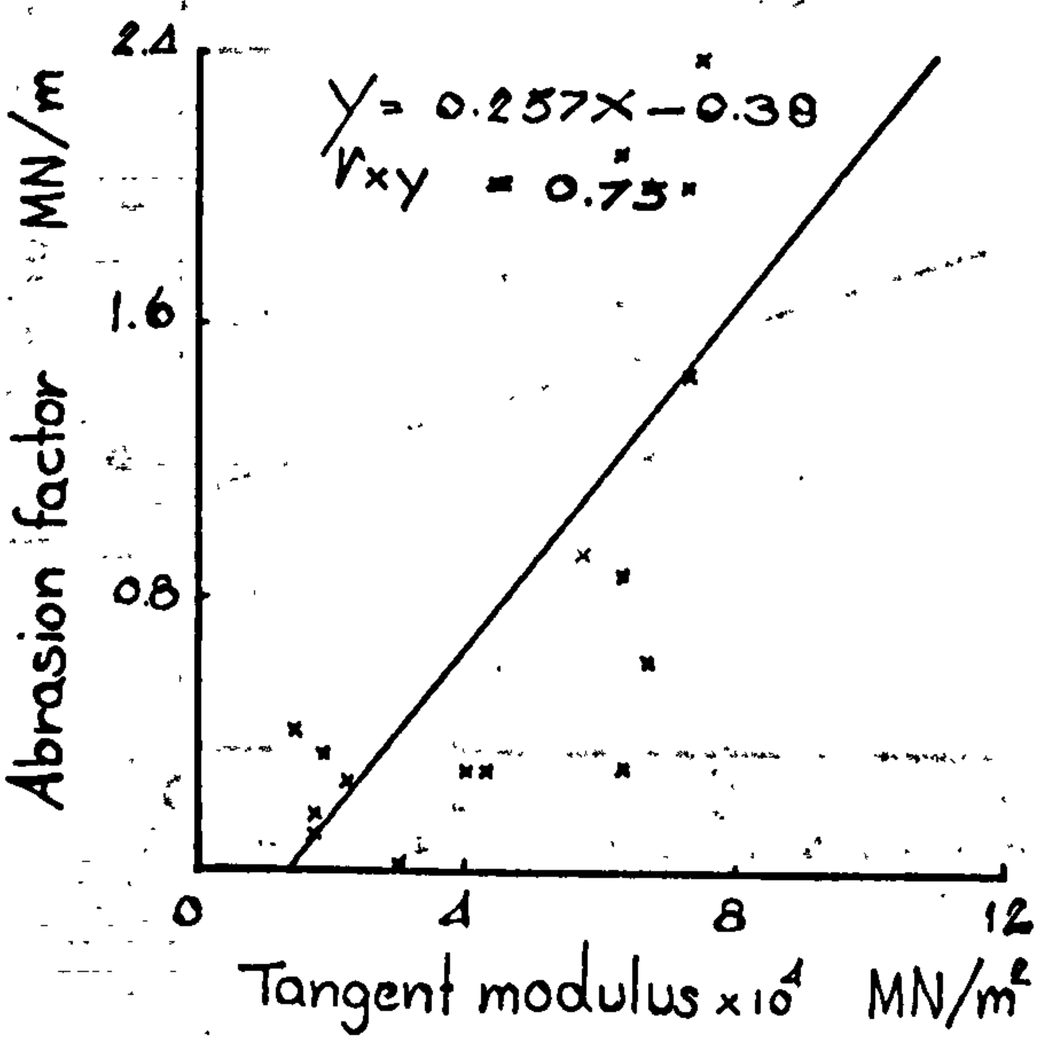
Y = 0.257X − 0.38
rxy = 0.75
Abrasion factor MN/m
2.4
1.6
0.8
0
4
8
12
Tangent modulus ×10⁴ MN/m²

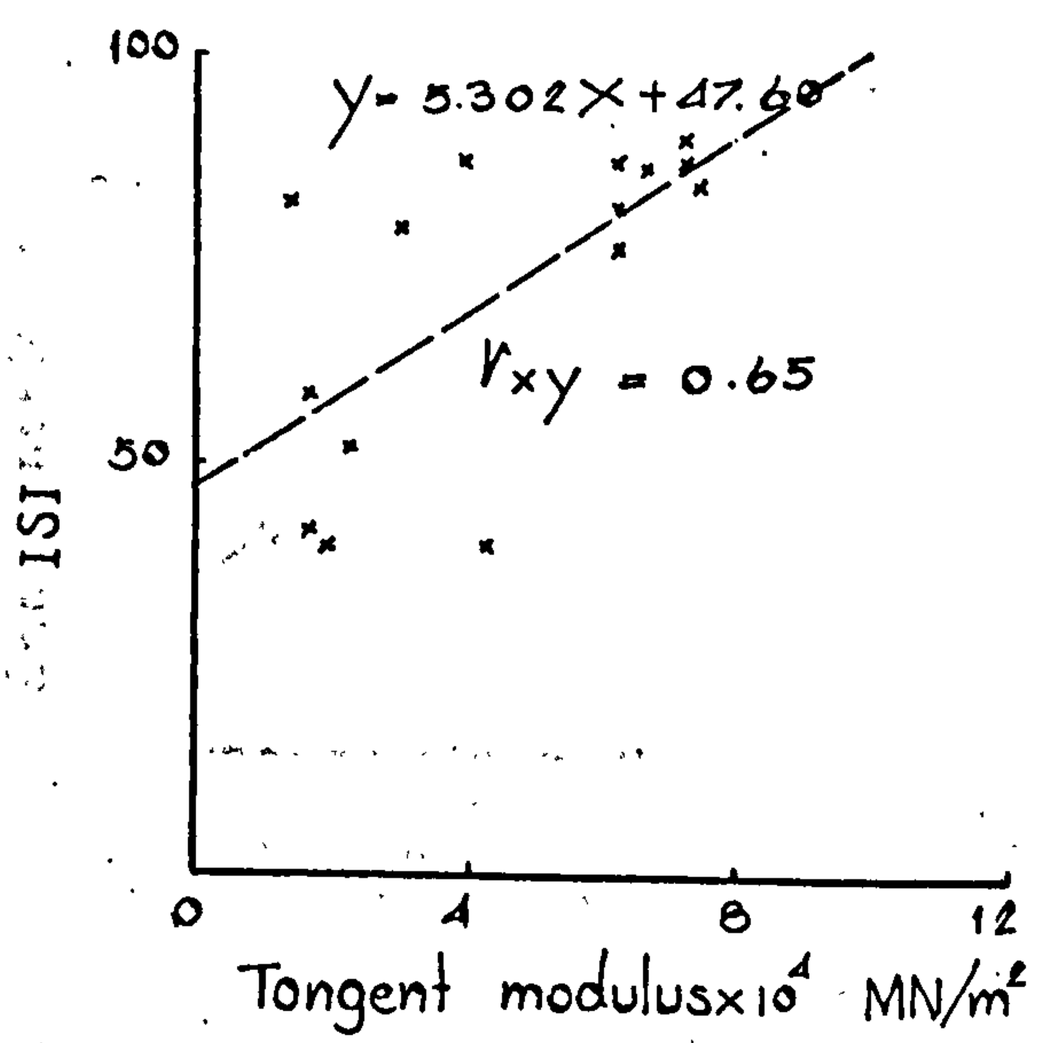
Y = 5.302X + 47.60
rxy = 0.65
ISI
100
50
0
4
8
12
Tangent modulus ×10⁴ MN/m²

Figure 47 (24)

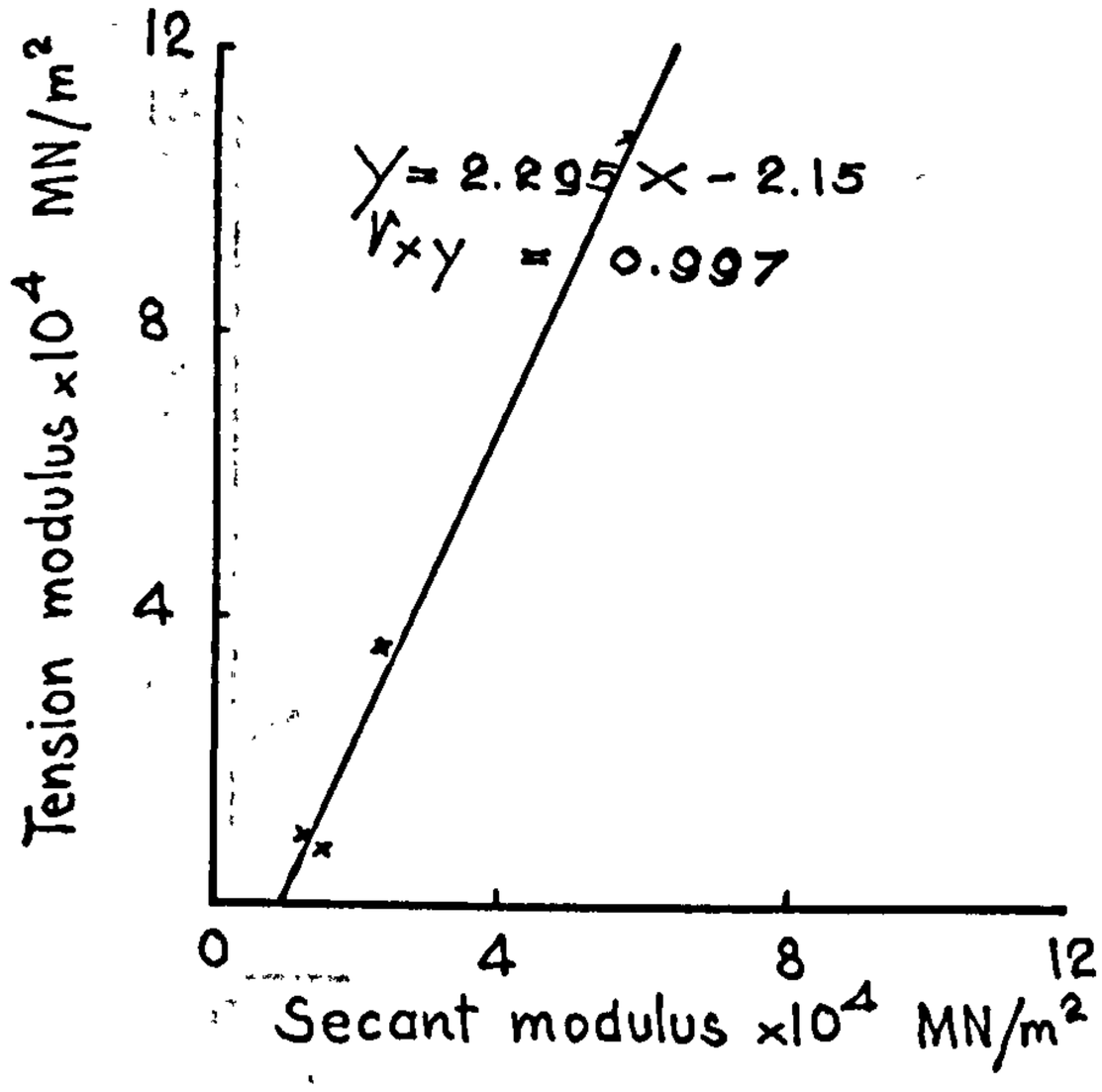
Y = 2.295X - 2.15
r_xy = 0.997
Tension modulus x10^4 MN/m^2
Secant modulus x10^4 MN/m^2
0
4
8
12

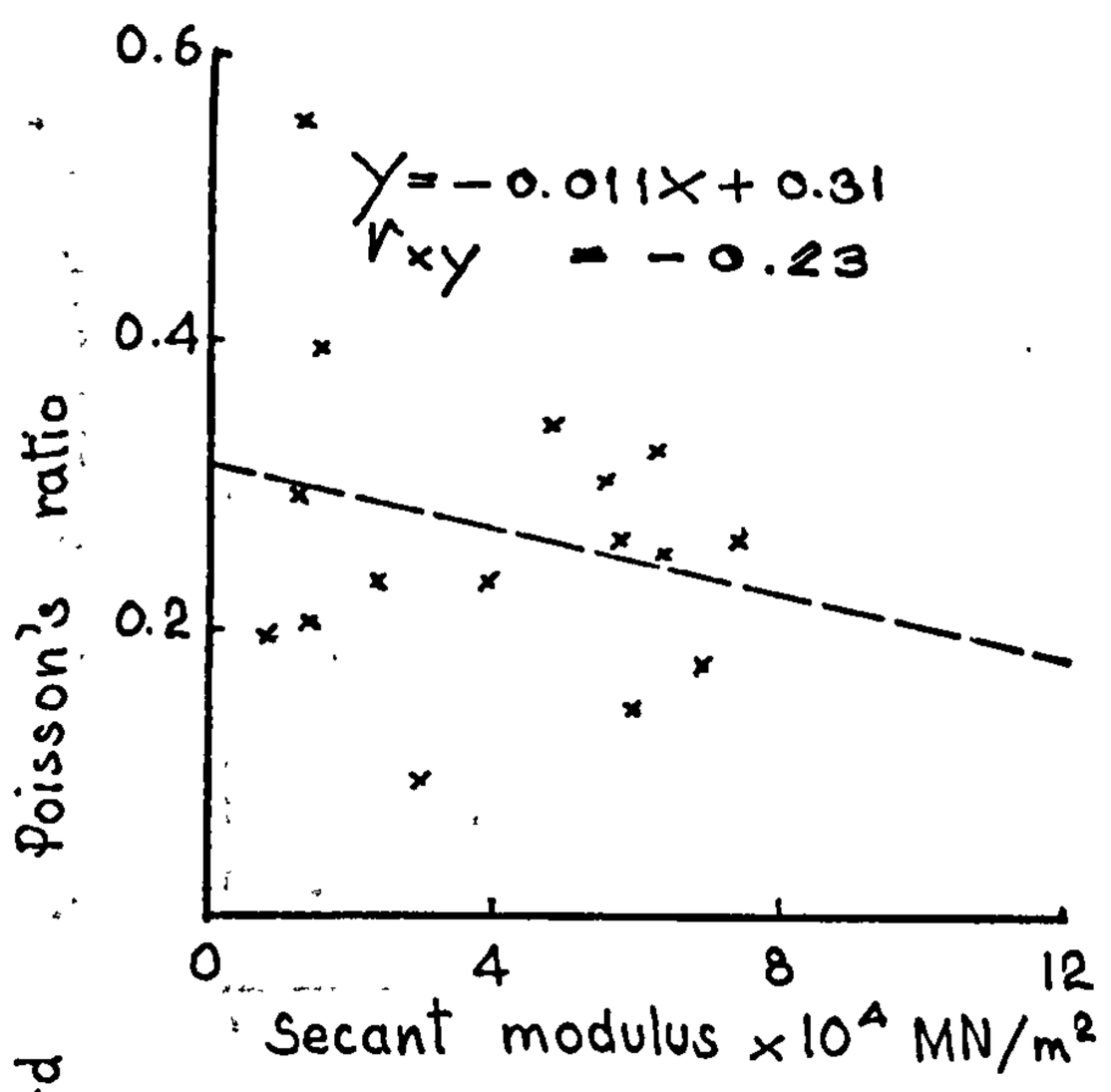
Y = -0.011X + 0.31
r_xy = -0.23
Poisson's ratio
Secant modulus x10^4 MN/m^2
0.6
0.4
0.2
0
4
8
12

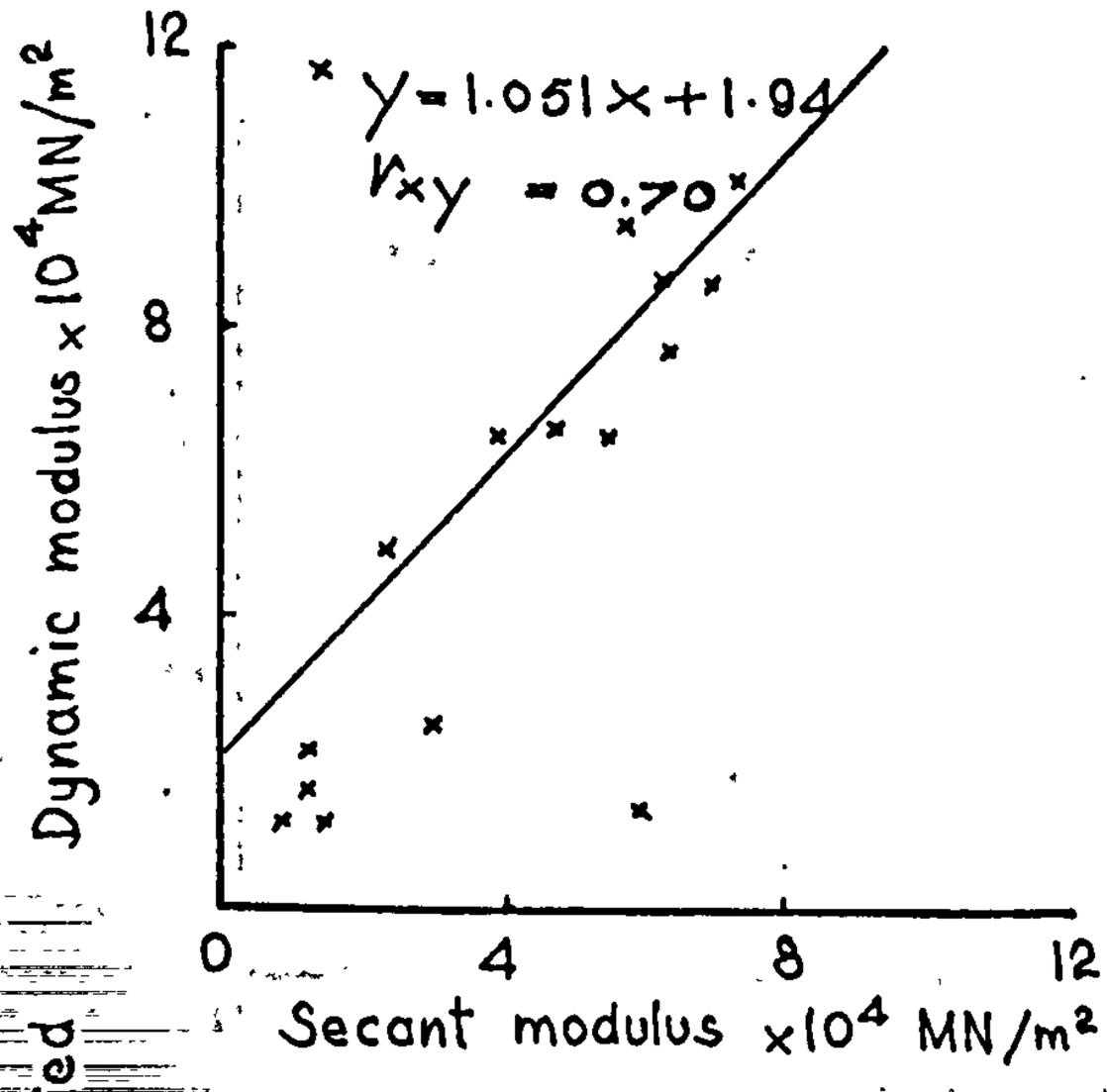
Y = 1.051X + 1.94
r_xy = 0.70
Dynamic modulus x10^4 MN/m^2
Secant modulus x10^4 MN/m^2
12
8
4
0
4
8
12

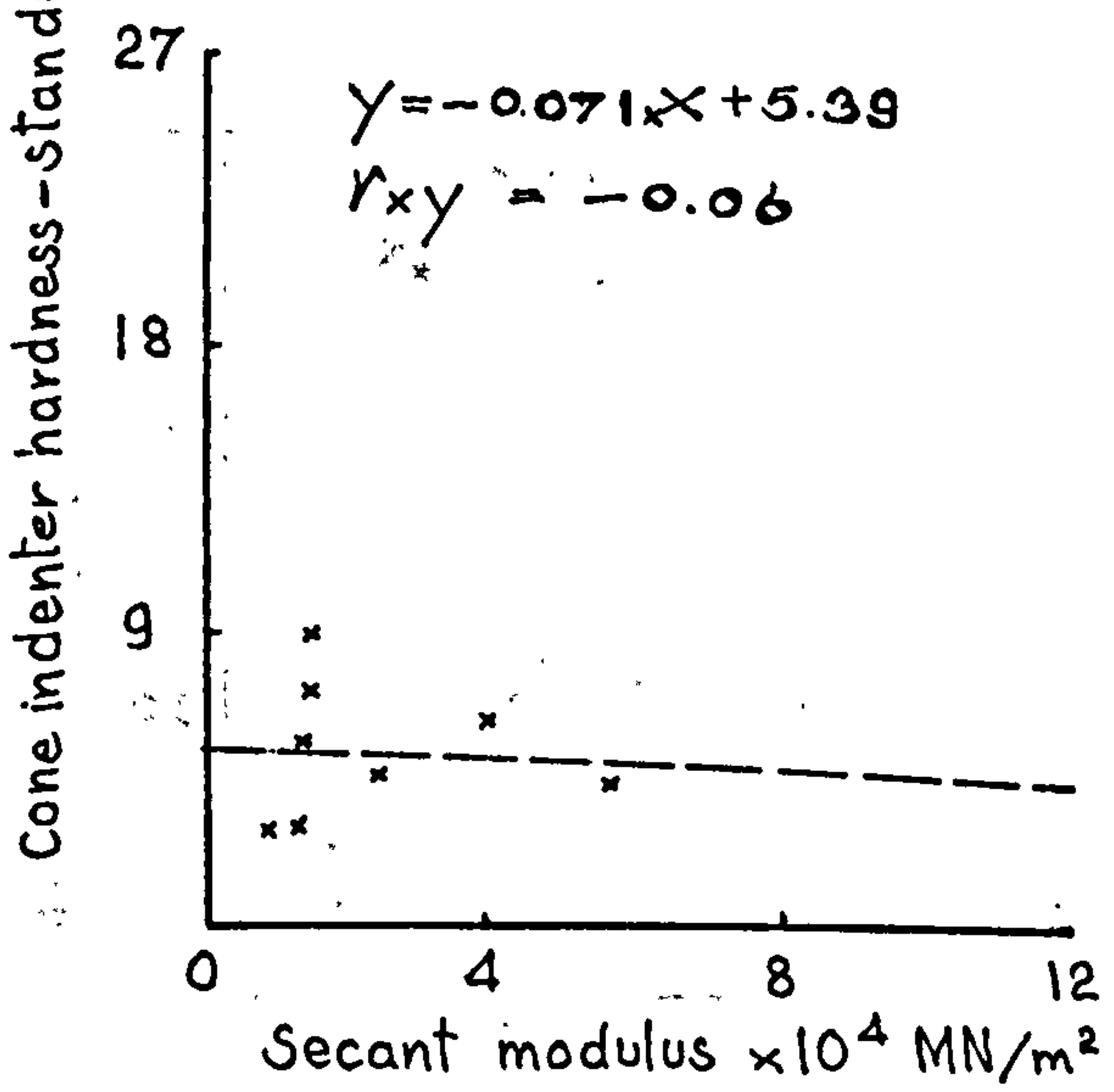
Y = -0.071X + 5.39
r_xy = -0.06
Cone indenter hardness-standard
Secant modulus x10^4 MN/m^2
27
18
9
0
4
8
12

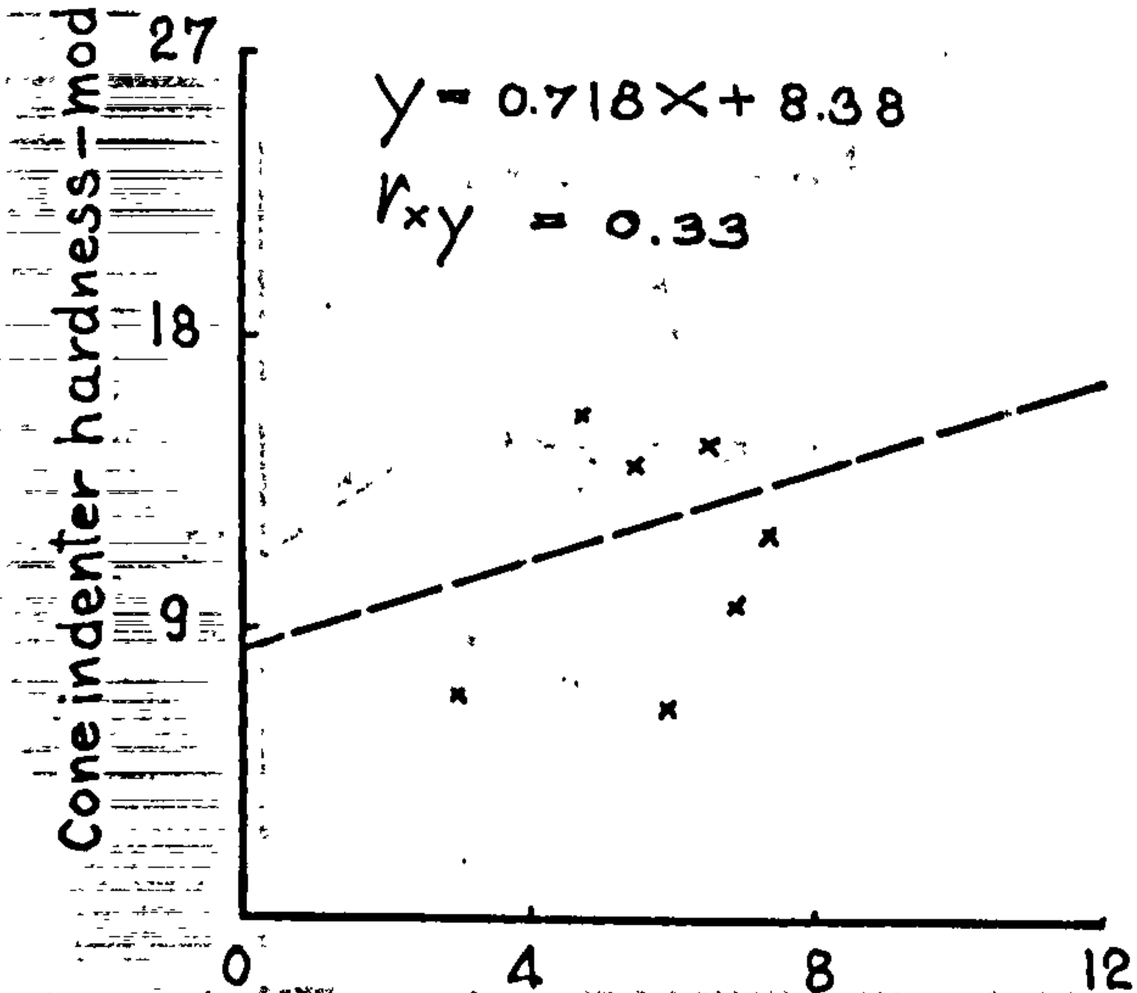
Y = 0.718X + 8.38
r_xy = 0.33
Cone indenter hardness-modified
Secant modulus x10^4 MN/m^2
27
18
9
0
4
8
12

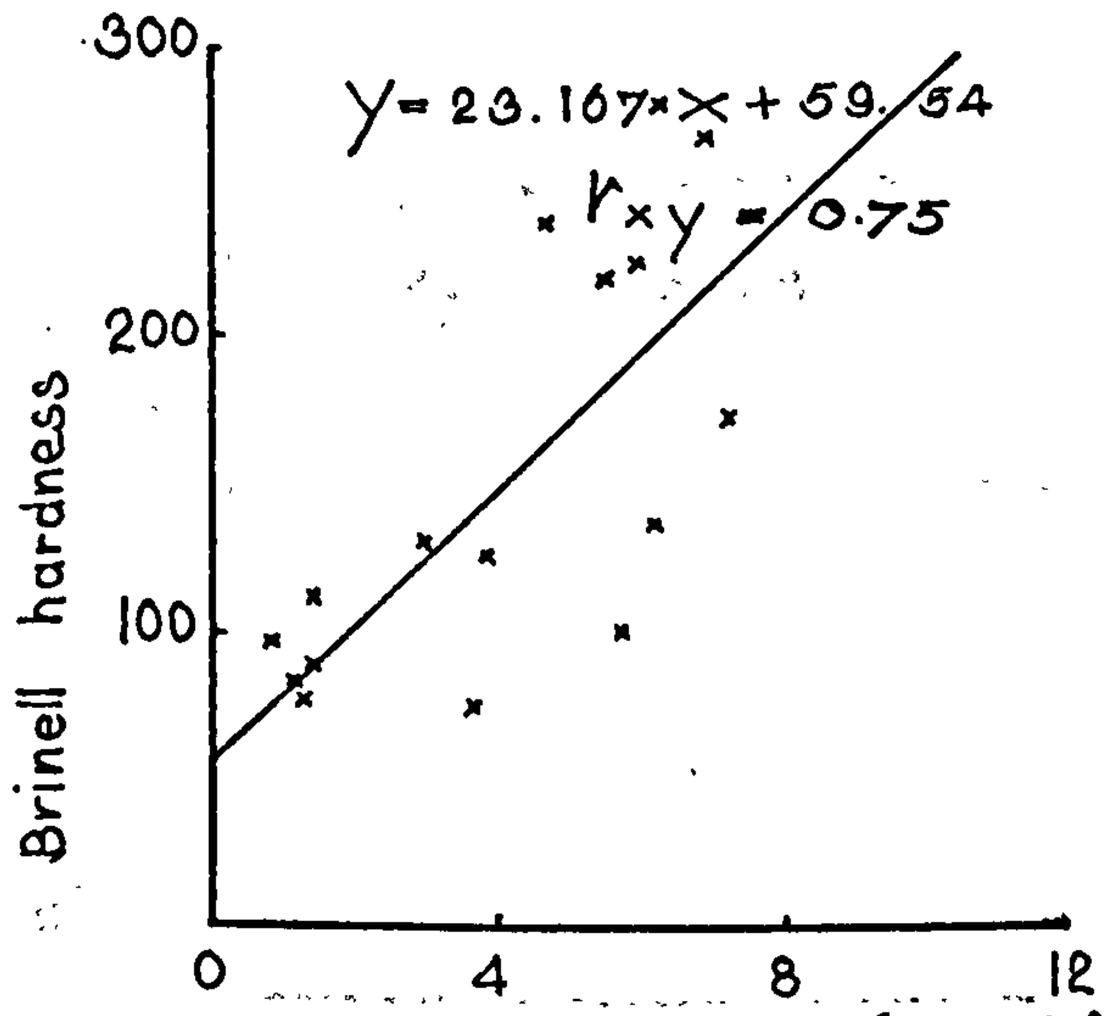
Y = 23.167X + 59.54
r_xy = 0.75
Brinell hardness
Secant modulus x10^4 MN/m^2
300
200
100
0
4
8
12

Figure 47 (25)

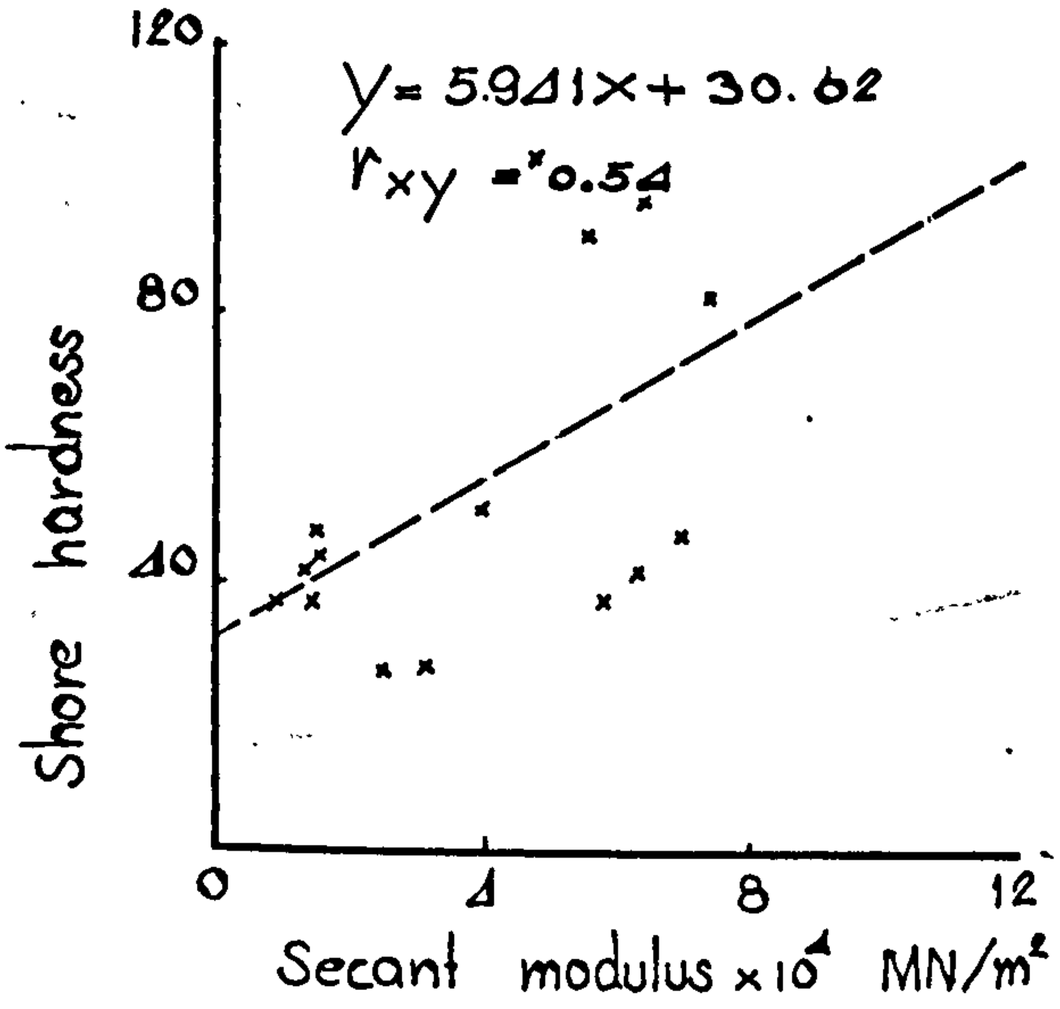
y = 5.941x + 30.62
rxy = 0.54
Shore hardness
120
80
40
0
4
8
12
Secant modulus x 10⁴ MN/m²

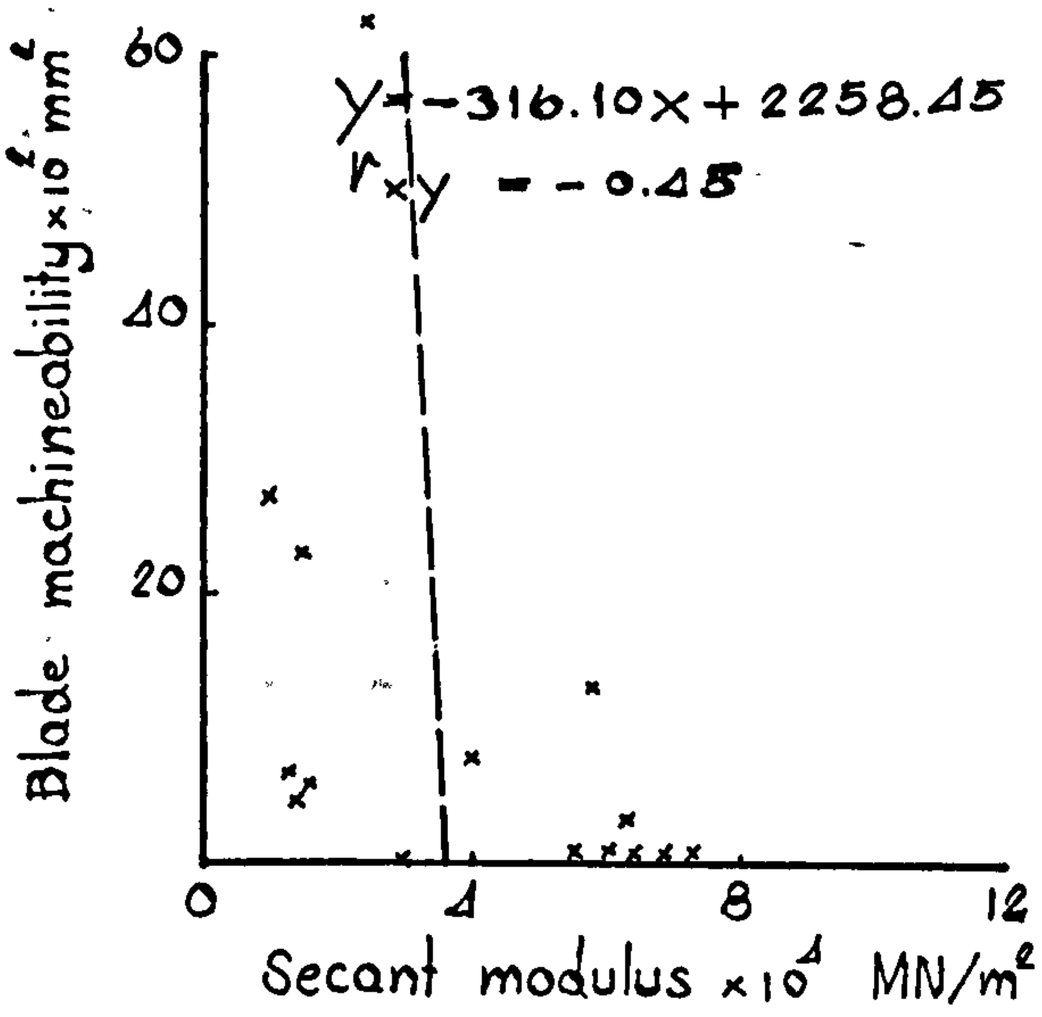
y = -316.10x + 2258.45
rxy = -0.45
Blade machineability x 10⁴ mm²
60
40
20
0
4
8
12
Secant modulus x 10⁴ MN/m²

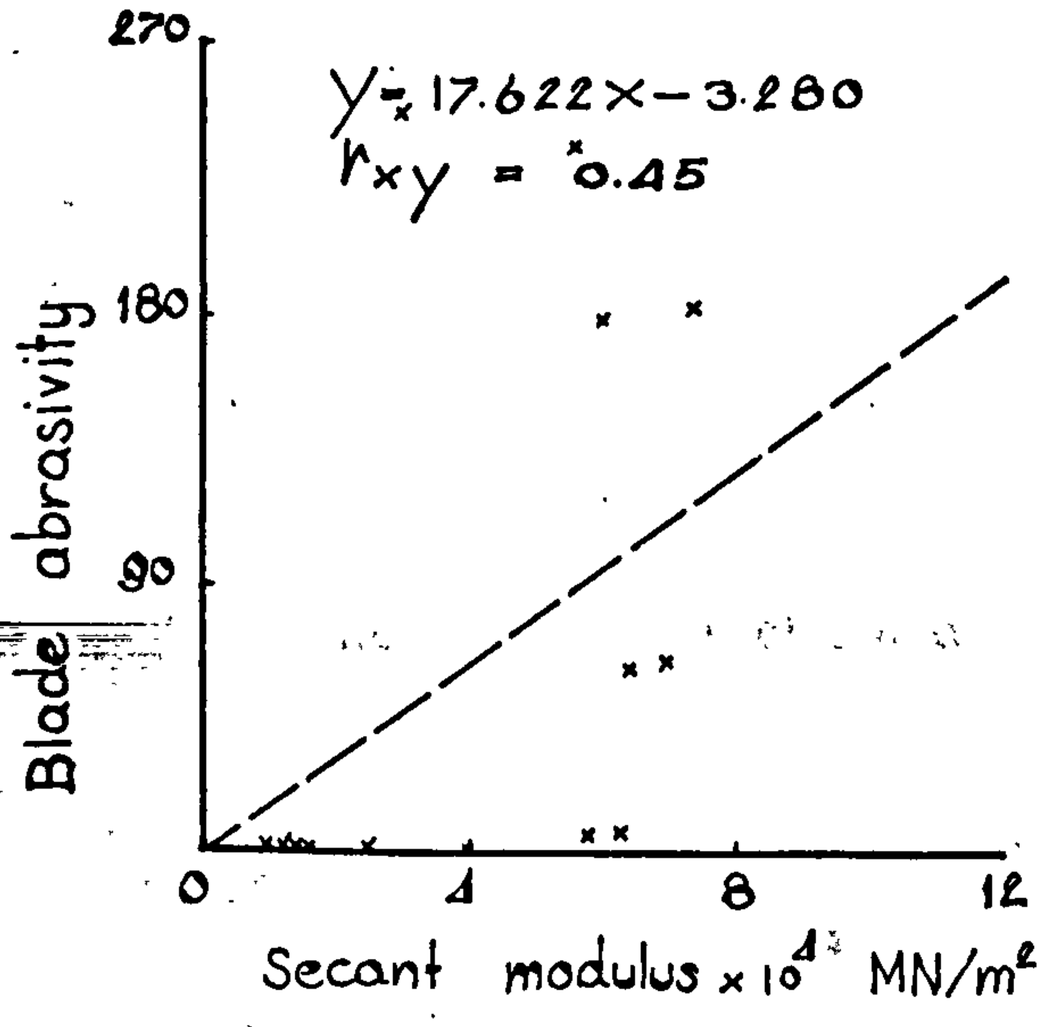
y = 17.622x - 3.280
rxy = 0.45
Blade abrasivity
270
180
90
0
4
8
12
Secant modulus x 10⁴ MN/m²

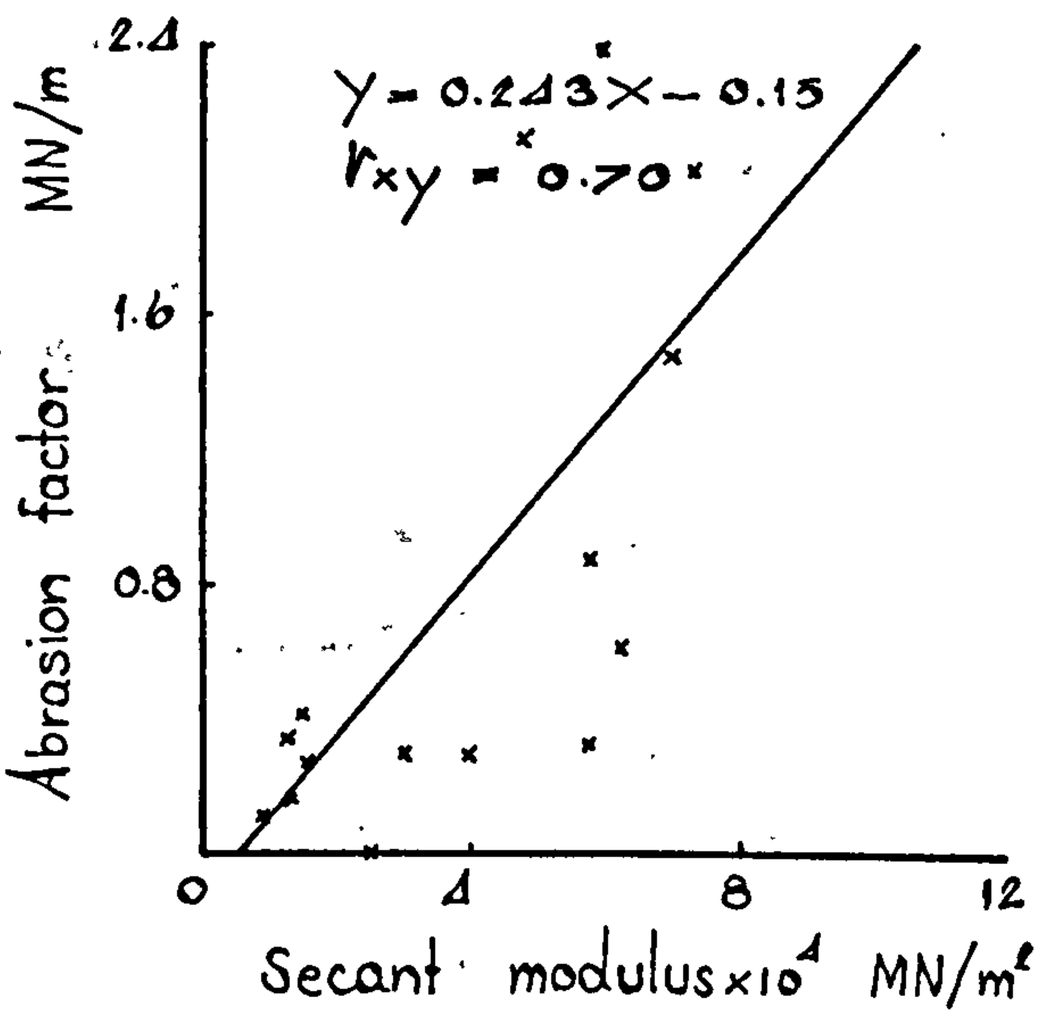
y = 0.243x - 0.15
rxy = 0.70
Abrasion factor MN/m
2.4
1.6
0.8
0
4
8
12
Secant modulus x 10⁴ MN/m²

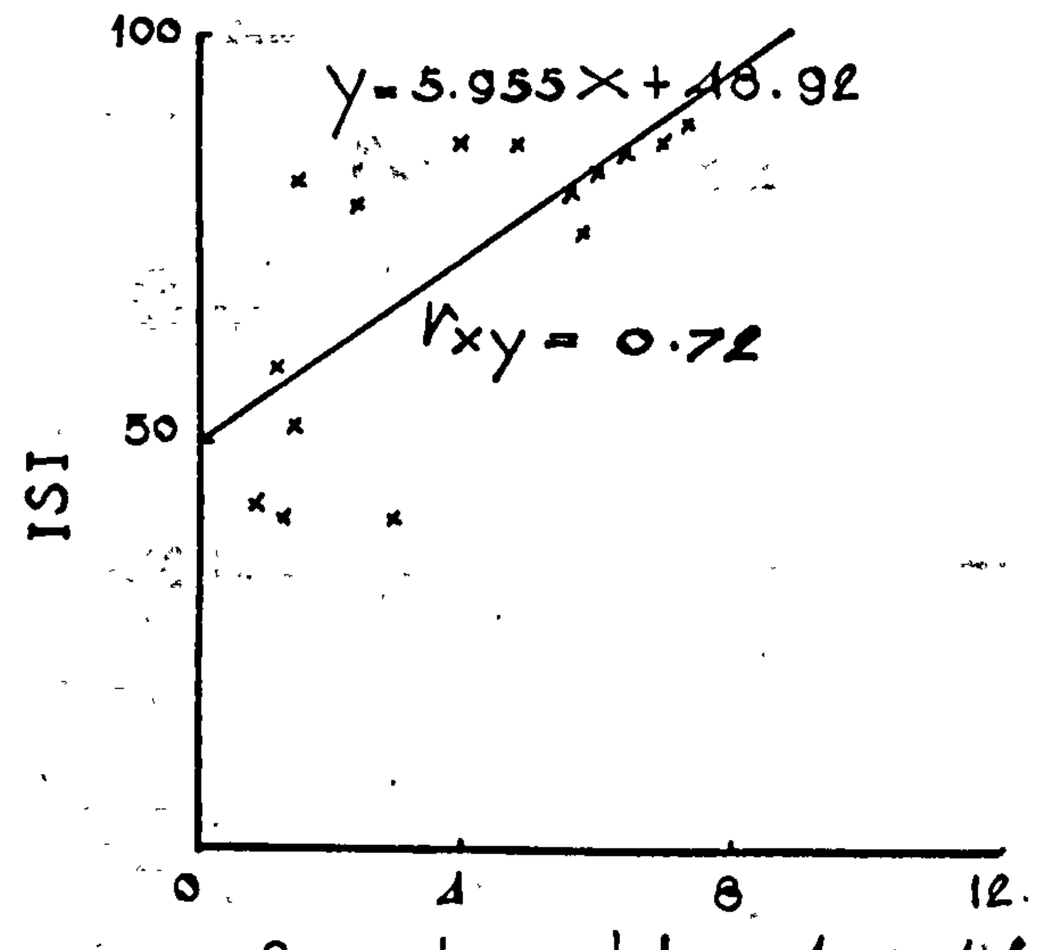
y = 5.955x + 18.92
rxy = 0.72
ISI
100
50
0
4
8
12
Secant modulus x 10⁴ MN/m²

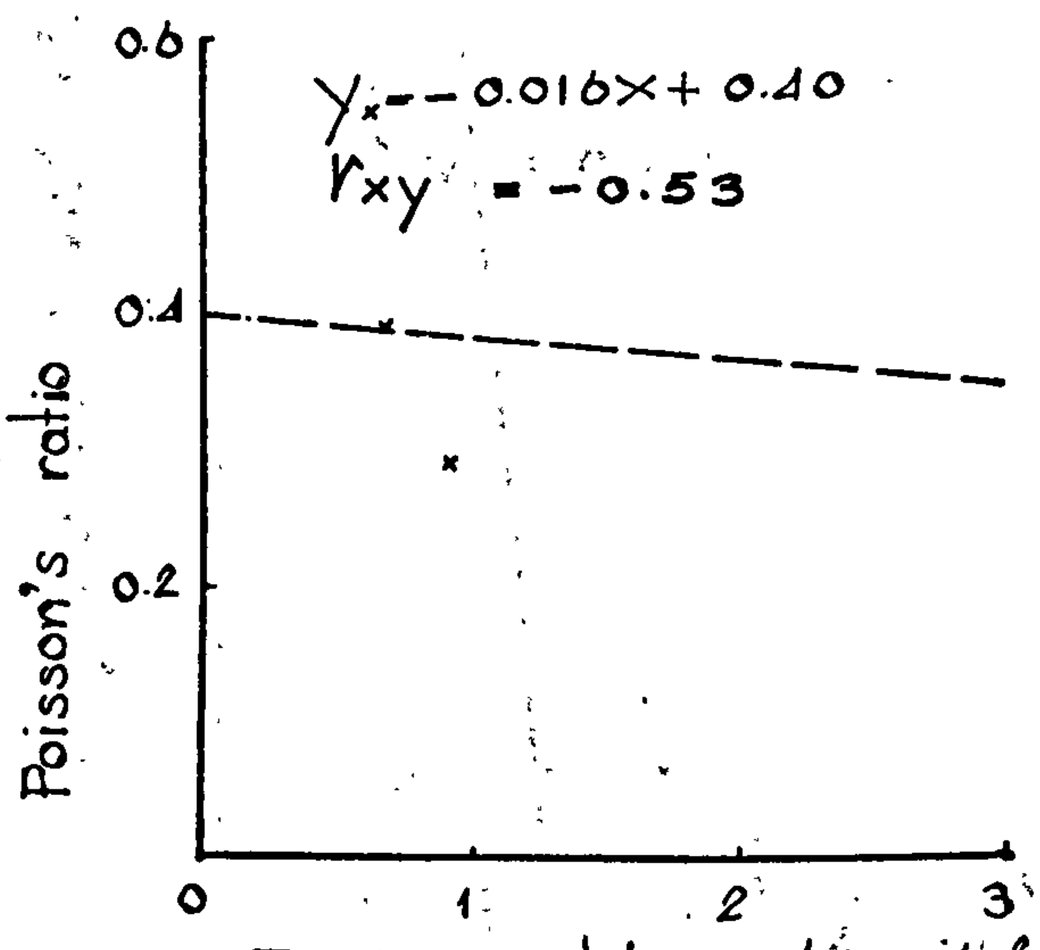
y = -0.016x + 0.40
rxy = -0.53
Poisson's ratio
0.6
0.4
0.2
0
1
2
3
Tension modulus x 10⁴ MN/m².

Figure 47 (26)

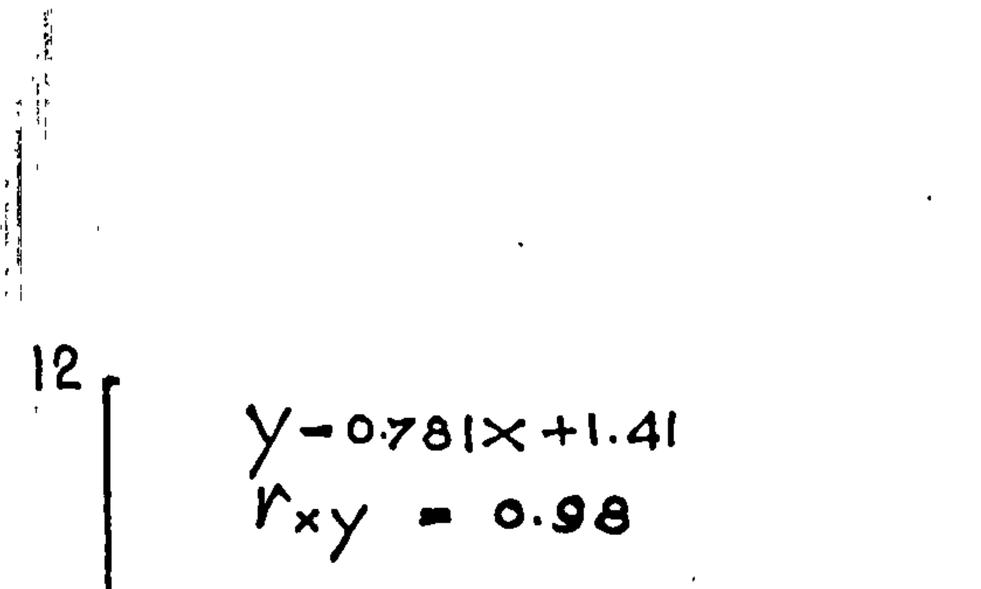
Dynamic modulus ×10⁴ MN/m²
12
8
4
0
1
2
3
Tension modulus ×10⁴ MN/m²
y = 0.781x + 1.41
r_xy = 0.98

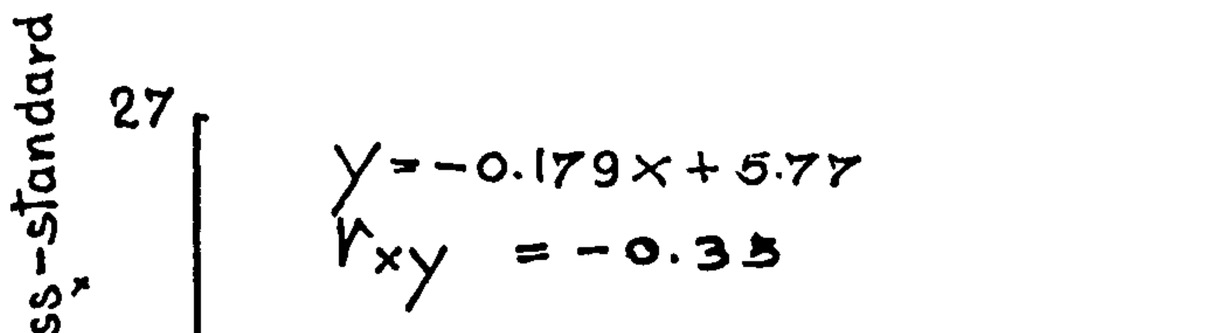
Cone indenter hardness-standard
27
18
9
0
1
2
3
Tension modulus ×10⁴ MN/m²
y = -0.179x + 5.77
r_xy = -0.35

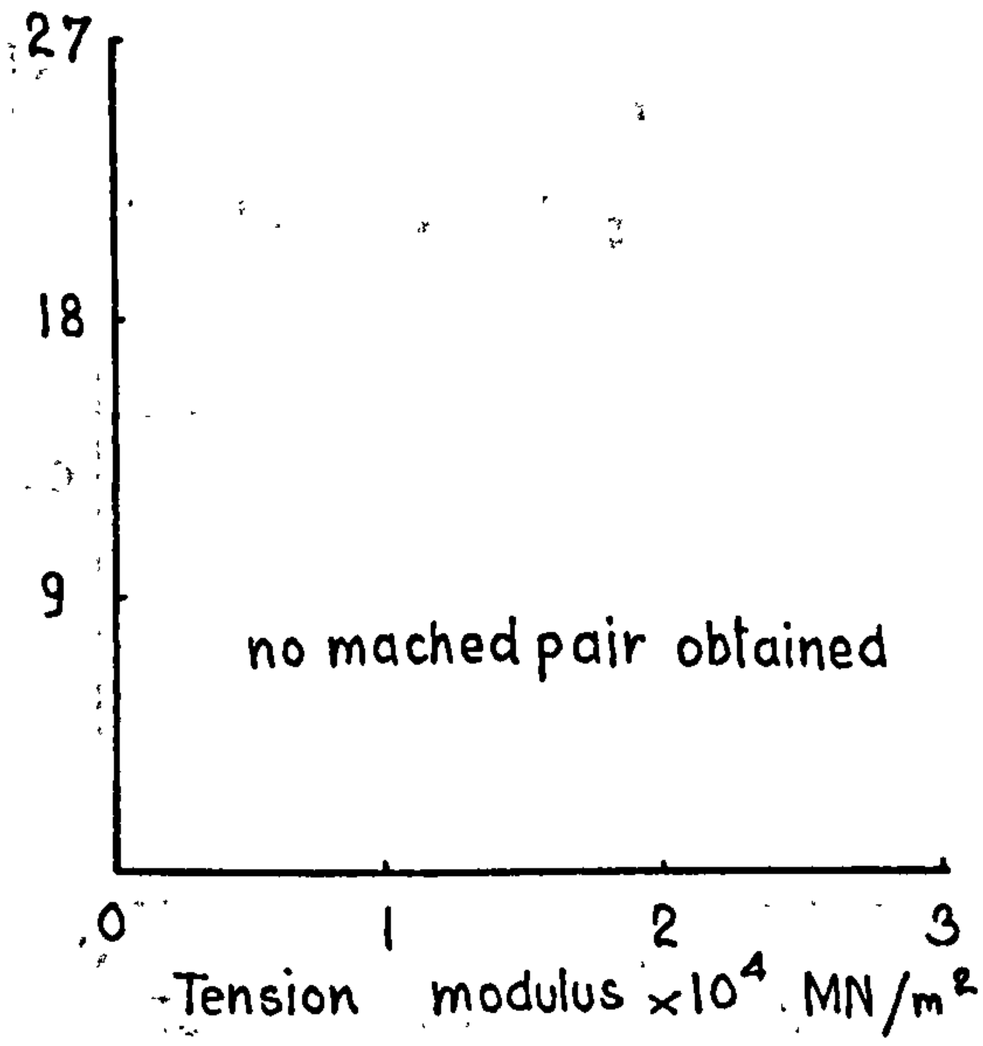
Cone indenter hardness-modified
27
18
9
0
1
2
3
Tension modulus ×10⁴ MN/m²
no machined pair obtained

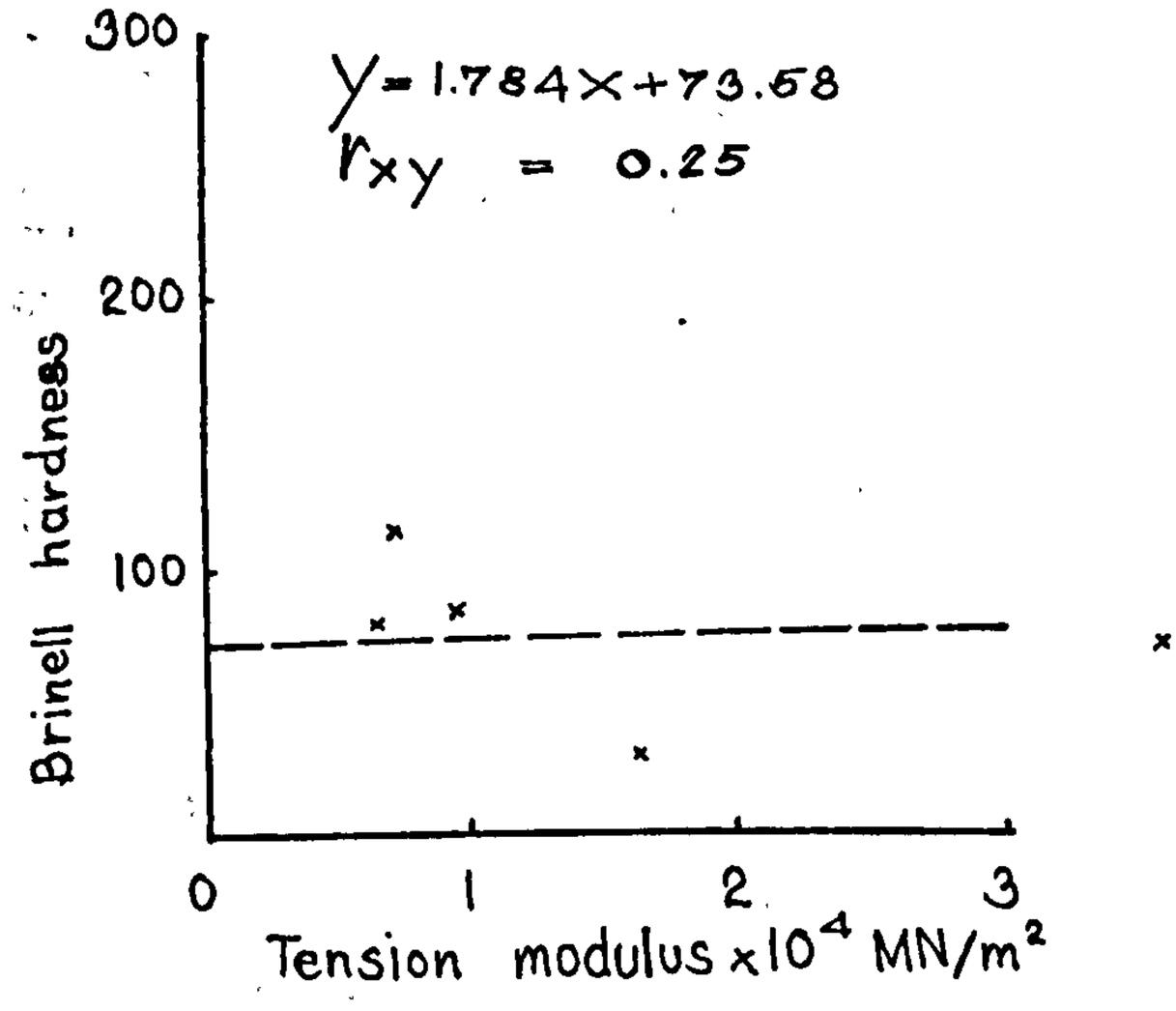
Brinell hardness
300
200
100
0
1
2
3
Tension modulus ×10⁴ MN/m²
y = 1.784x + 73.58
r_xy = 0.25

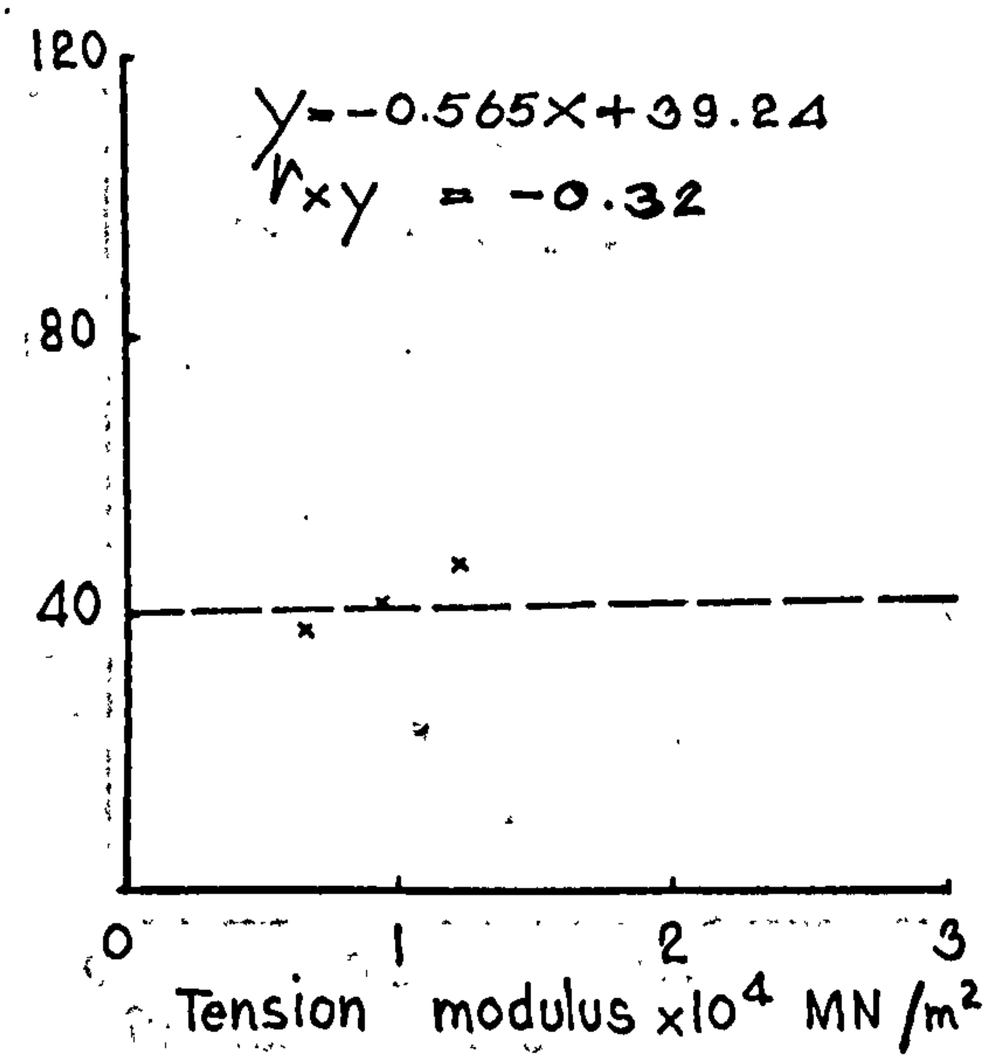
Shore hardness
120
80
40
0
1
2
3
Tension modulus ×10⁴ MN/m²
y = -0.565x + 39.24
r_xy = -0.32

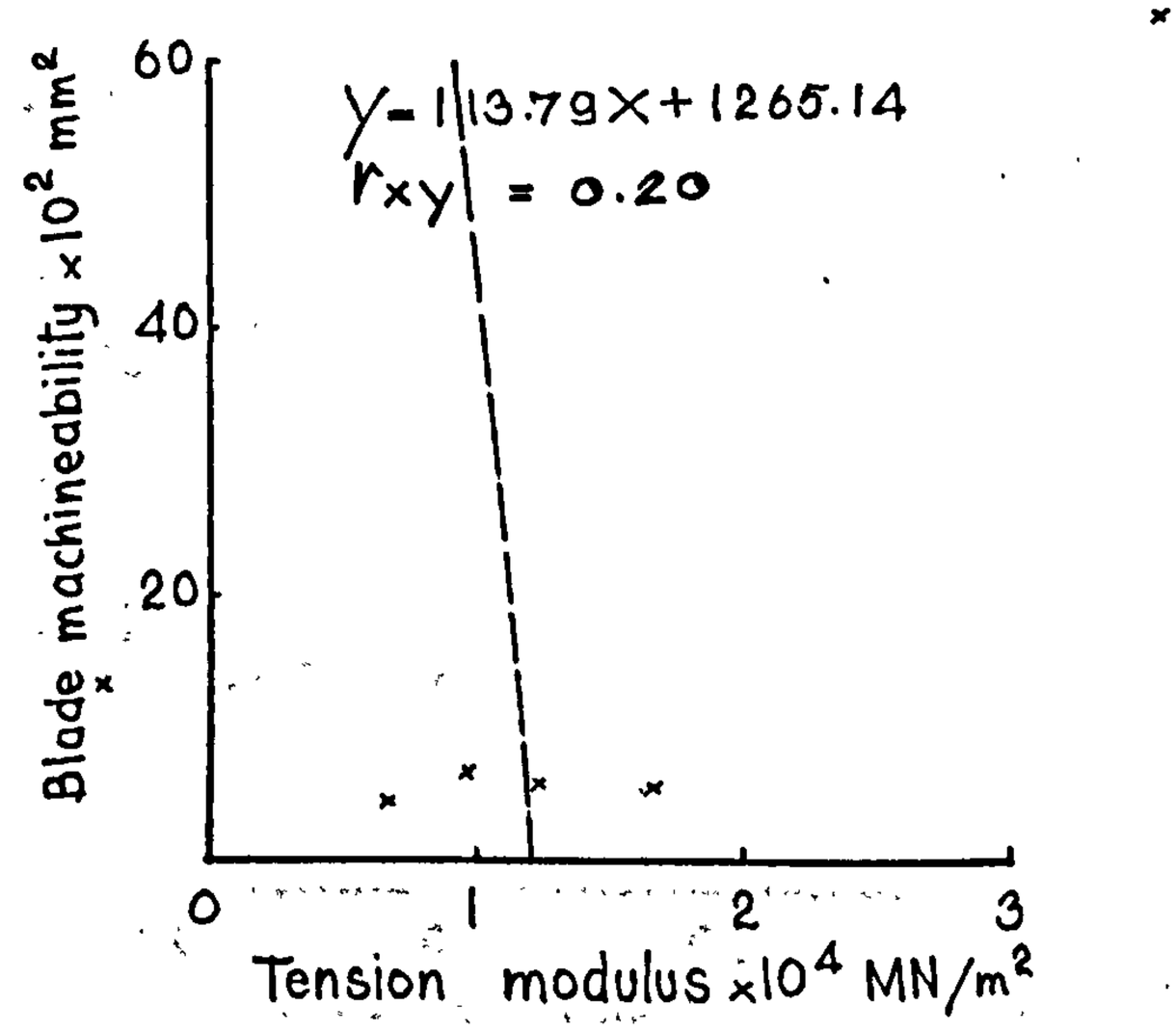
Blade machineability ×10² mm²
60
40
20
0
1
2
3
Tension modulus ×10⁴ MN/m²
y = 113.79x + 1265.14
r_xy = 0.20

Figure 47 (27)

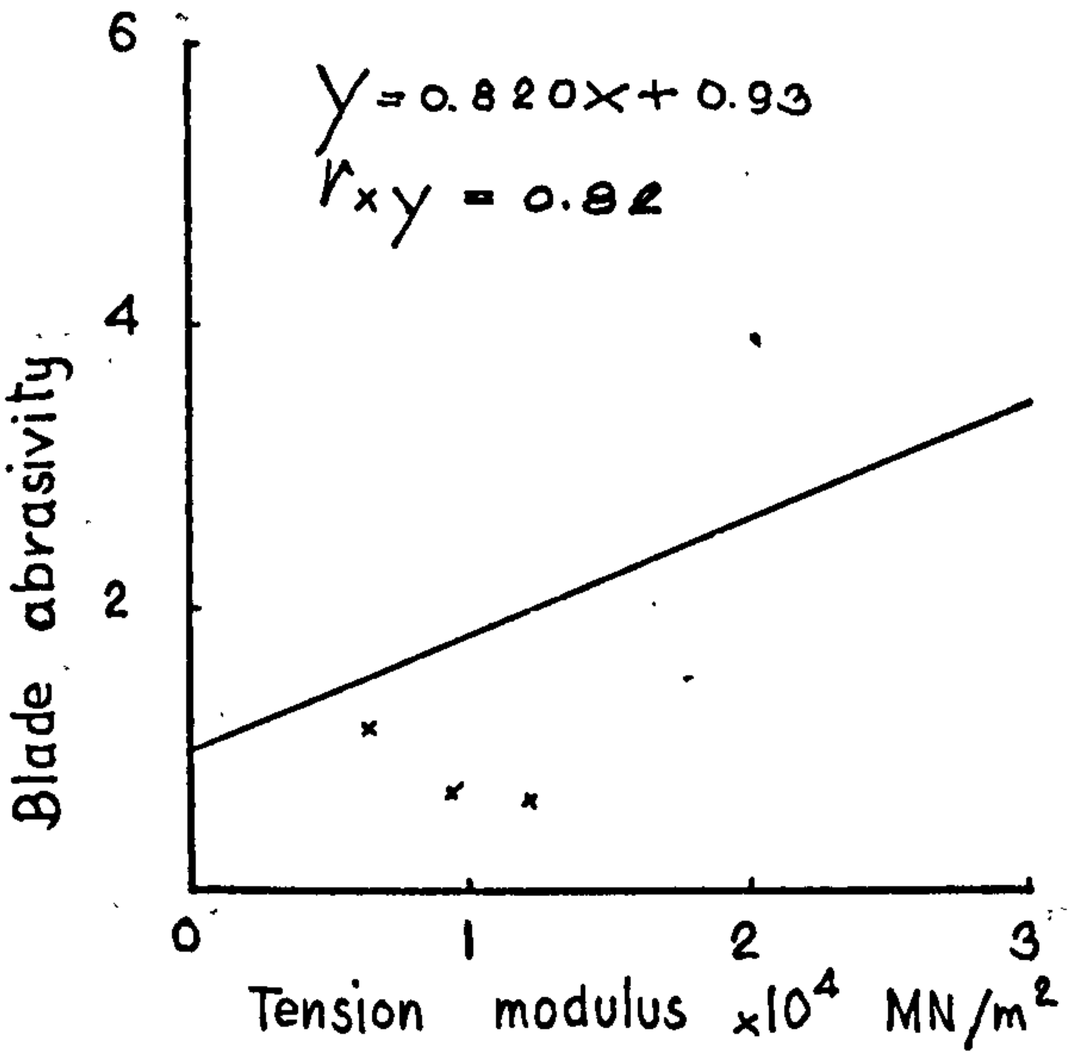
Y = 0.820X + 0.93
r_{xy} = 0.82
Blade abrasivity
6
4
2
0
1
2
3
Tension modulus ×10⁴ MN/m²

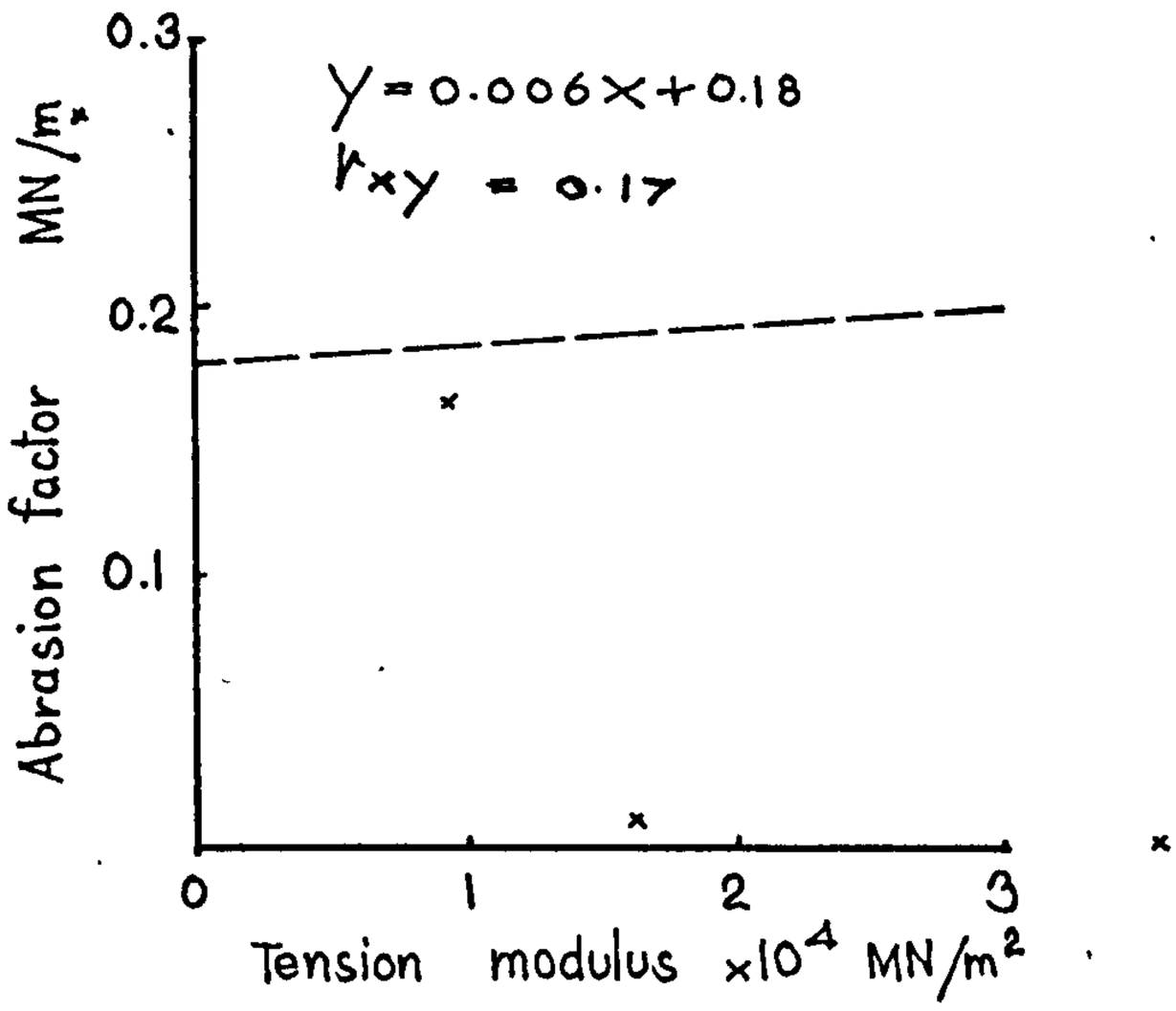
Y = 0.006X + 0.18
r_{xy} = 0.17
Abrasion factor MN/m²
0.3
0.2
0.1
0
1
2
3
Tension modulus ×10⁴ MN/m²

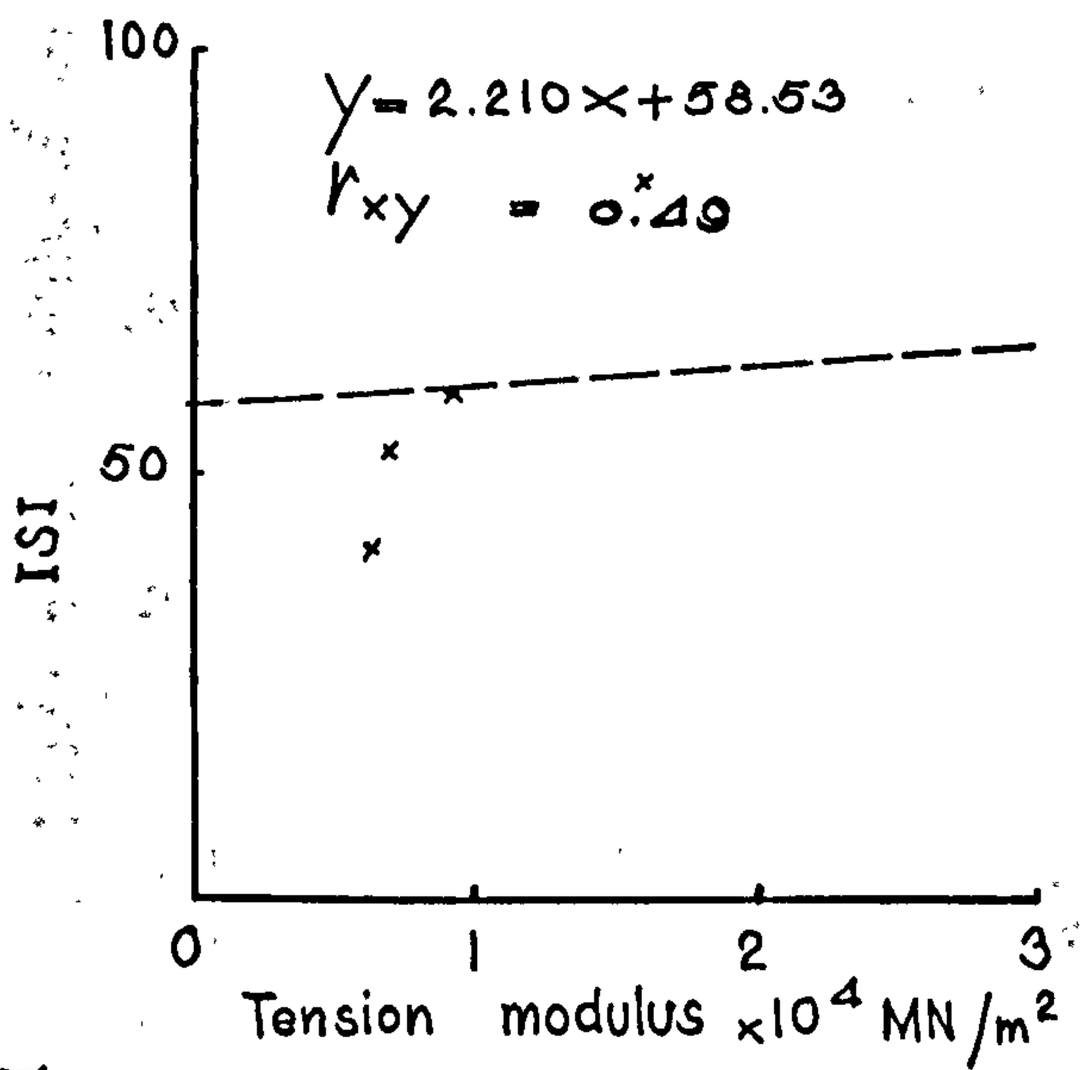
Y = 2.210X + 58.53
r_{xy} = 0.49
ISI
100
50
0
1
2
3
Tension modulus ×10⁴ MN/m²

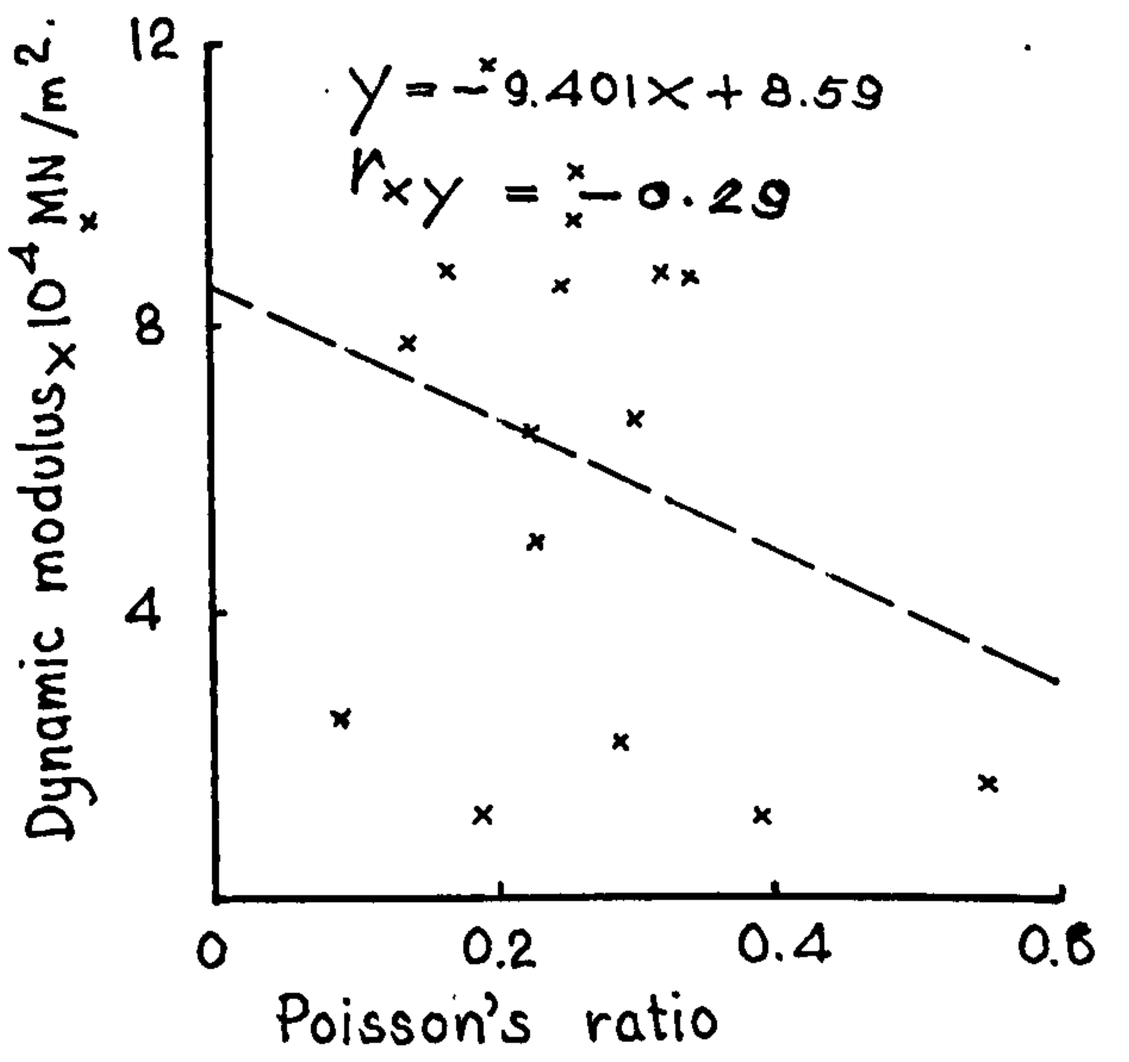
Y = −9.401X + 8.59
r_{xy} = −0.29
Dynamic modulus ×10⁴ MN/m²
12
8
4
0
0.2
0.4
0.6
Poisson's ratio

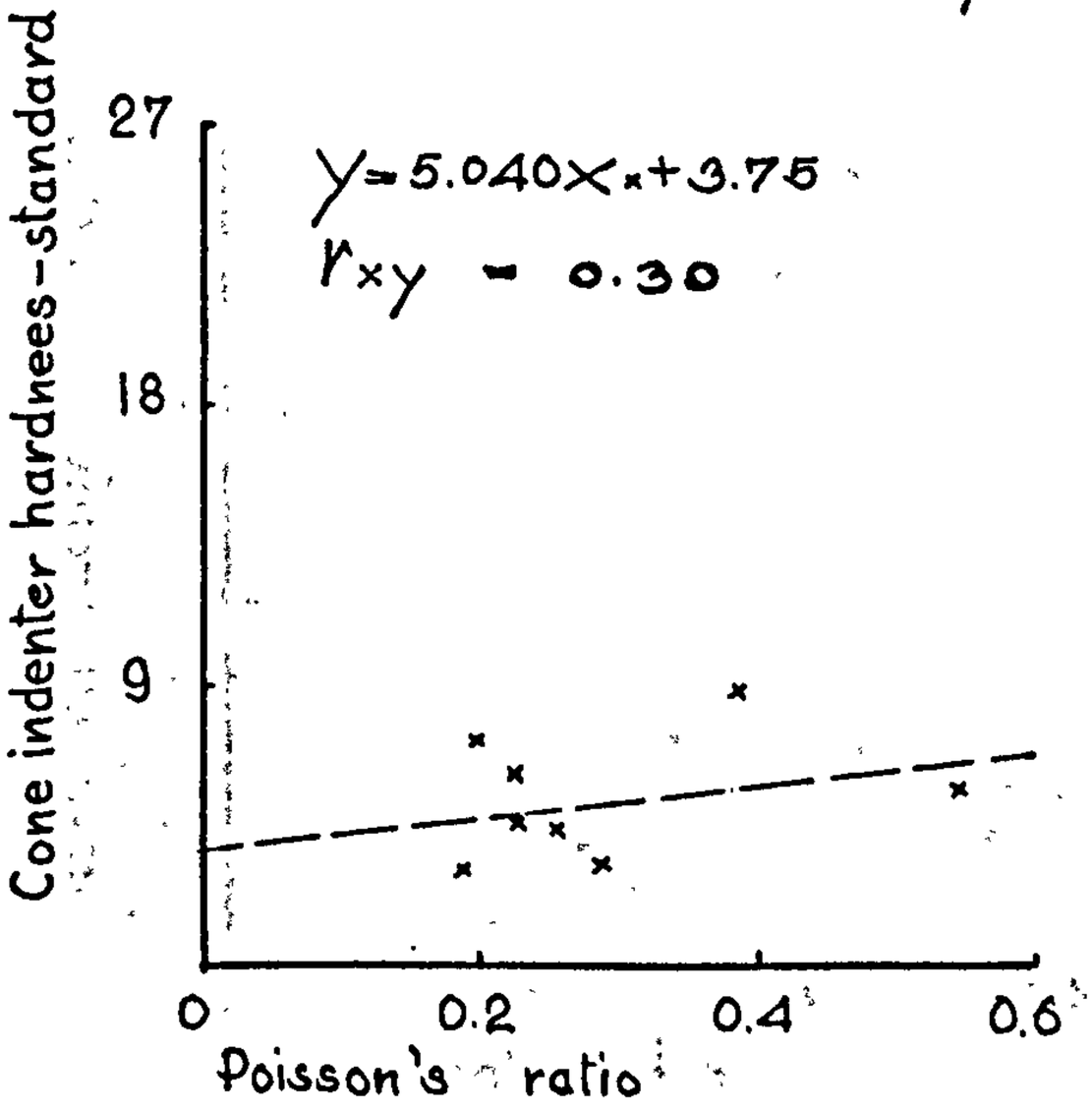
Y = 5.040X + 3.75
r_{xy} = 0.30
Cone indenter hardnees-standard
27
18
9
0
0.2
0.4
0.6
Poisson's ratio

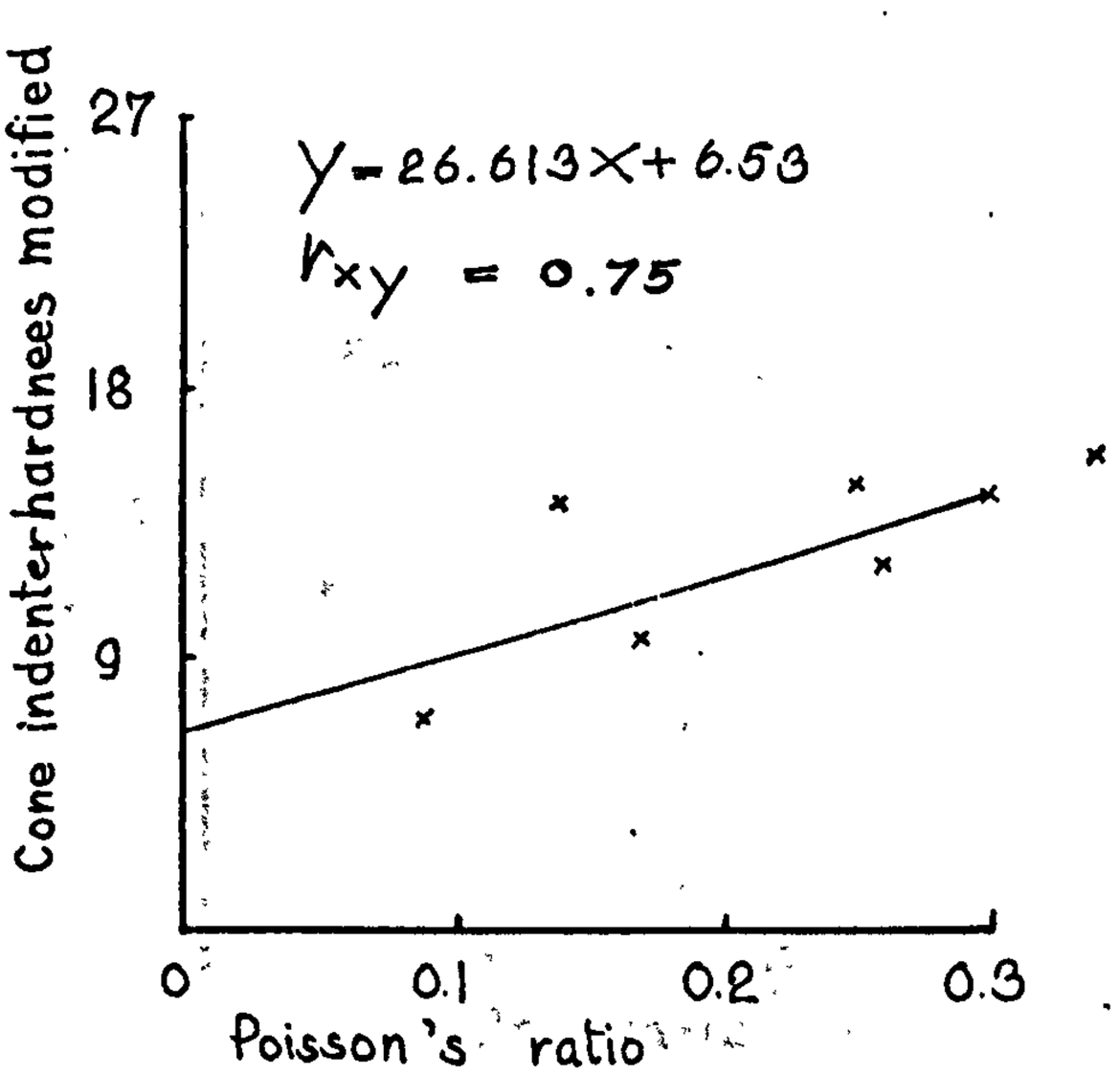
Y = 26.613X + 6.53
r_{xy} = 0.75
Cone indenter hardnees modified
27
18
9
0
0.1
0.2
0.3
Poisson's ratio

Figure 47 (28)

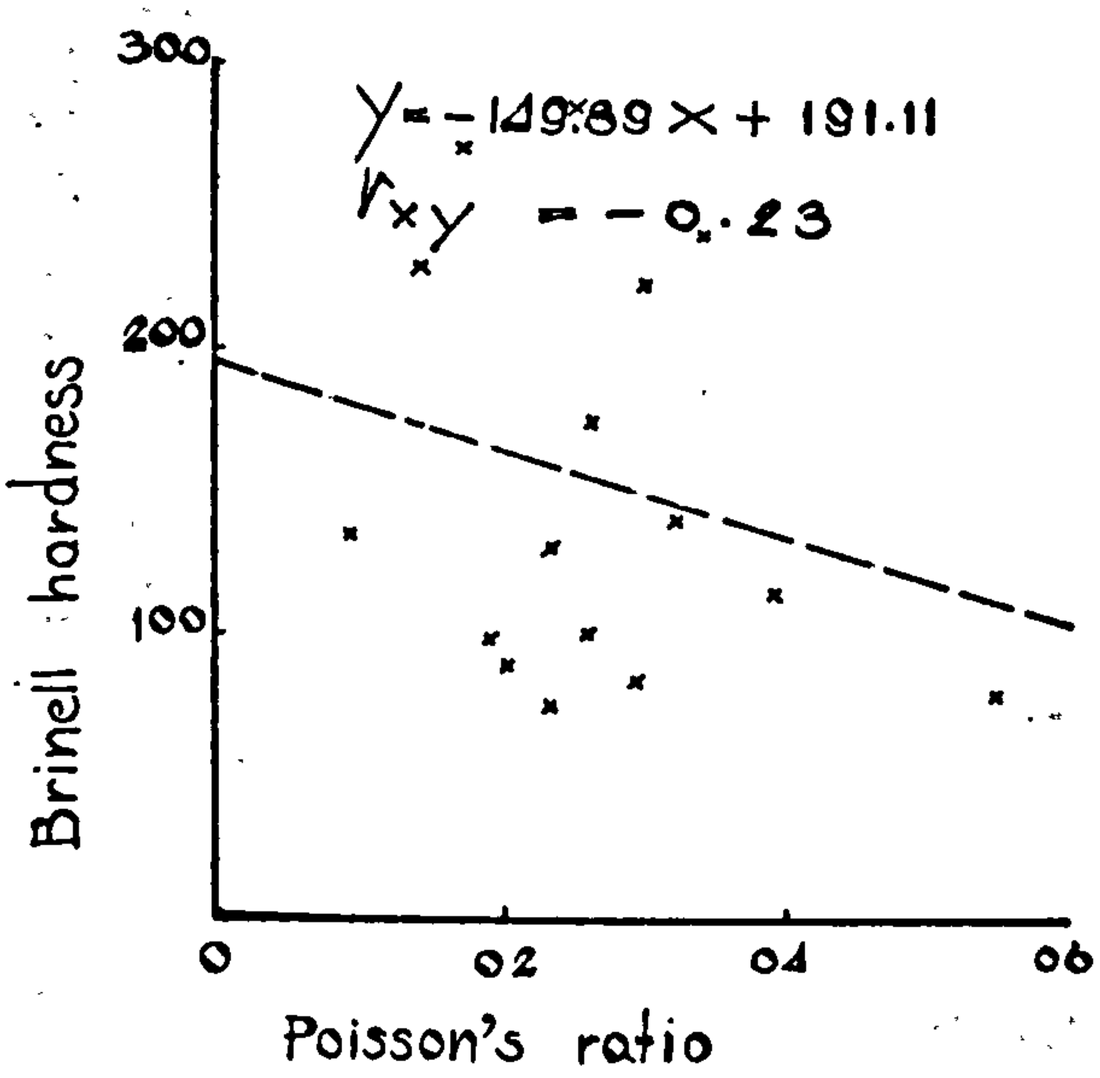
Y = -149.89 X + 191.11
rxy = -0.23
300
200
100
0
0.2
0.4
0.6
Brinell hardness
Poisson's ratio

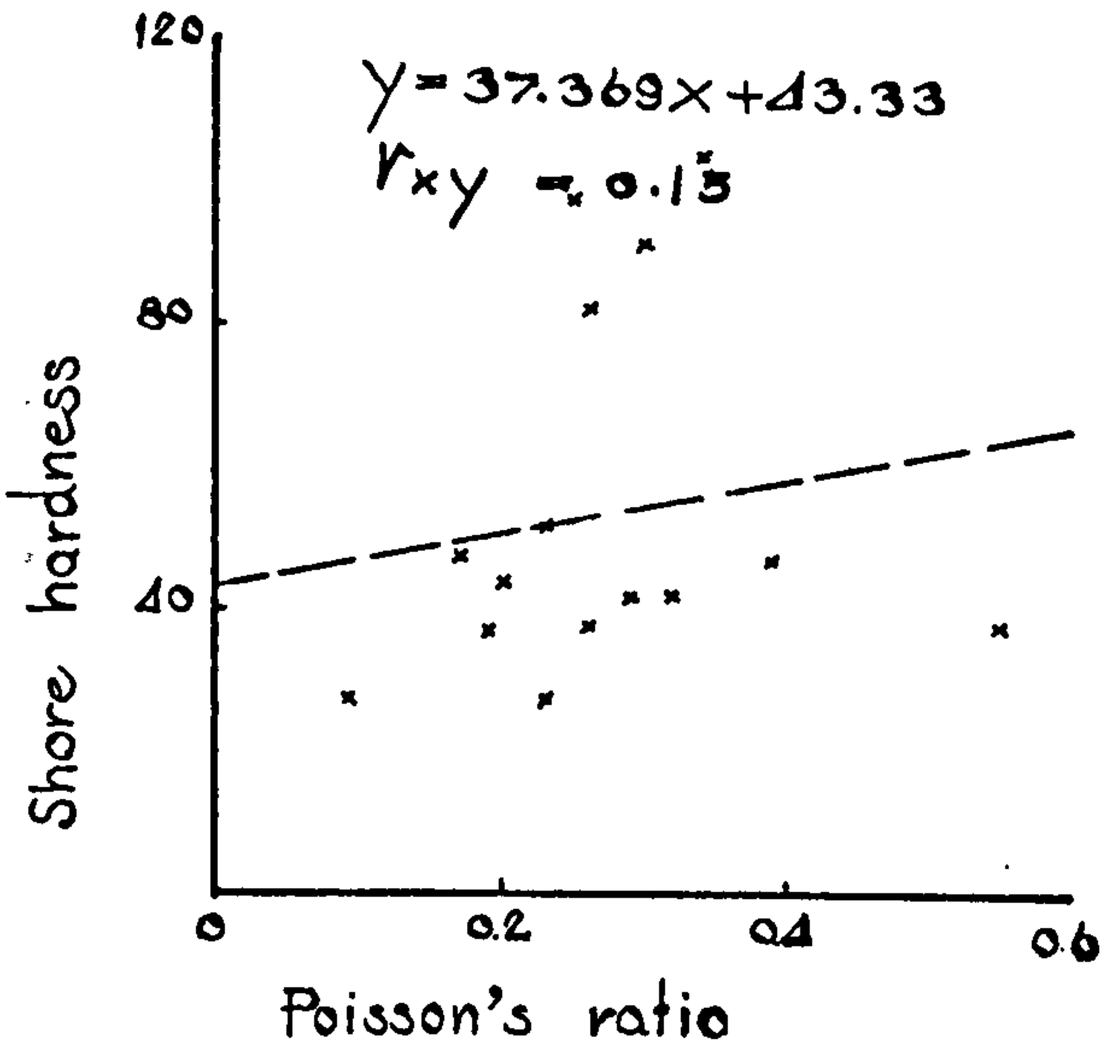
Y = 37.369 X + 43.33
rxy = 0.13
120
80
40
0
0.2
0.4
0.6
Shore hardness
Poisson's ratio

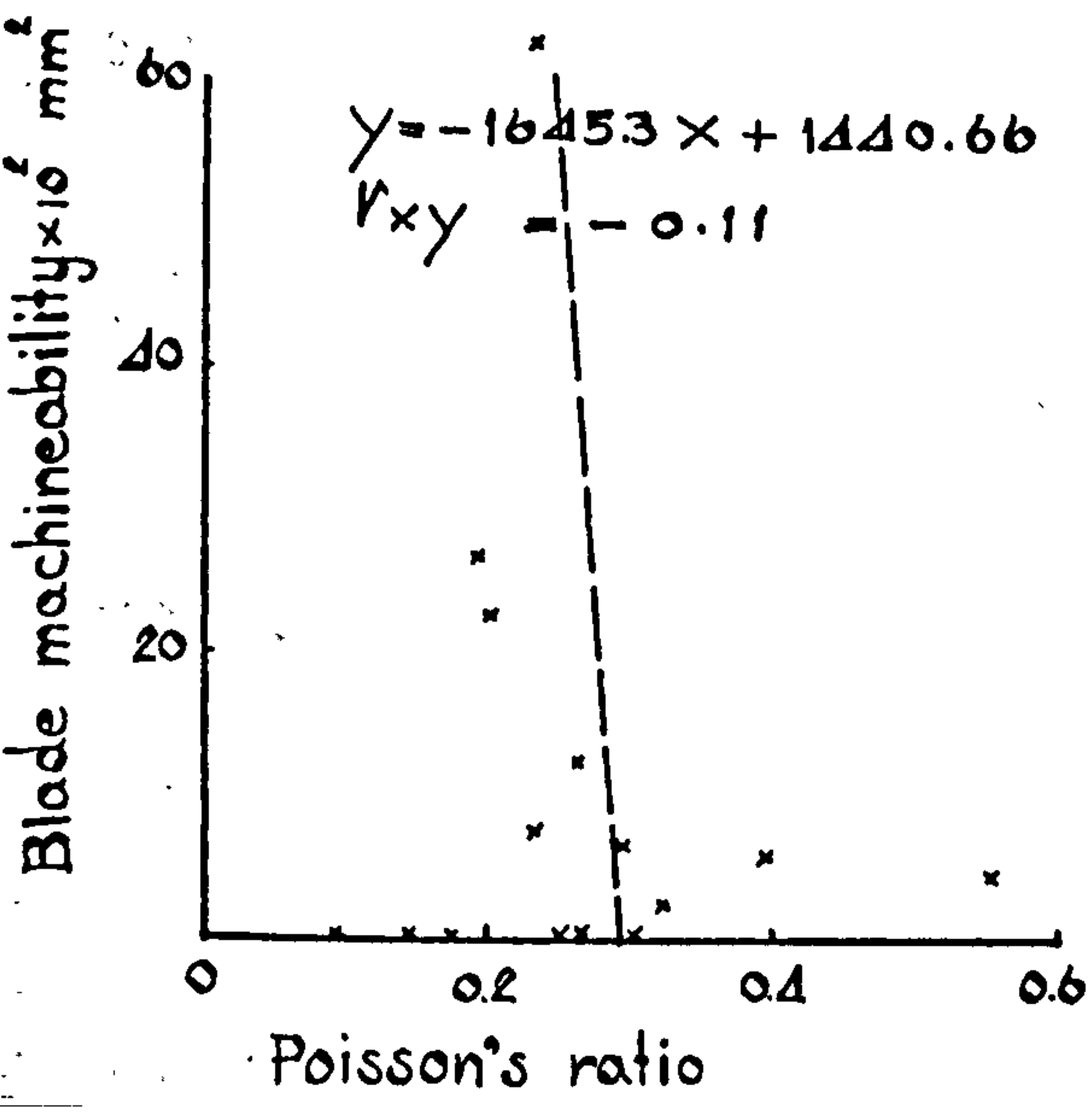
Y = -164.53 X + 1440.66
rxy = -0.11
60
40
20
0
0.2
0.4
0.6
Blade machineability x10⁴ mm²
Poisson's ratio

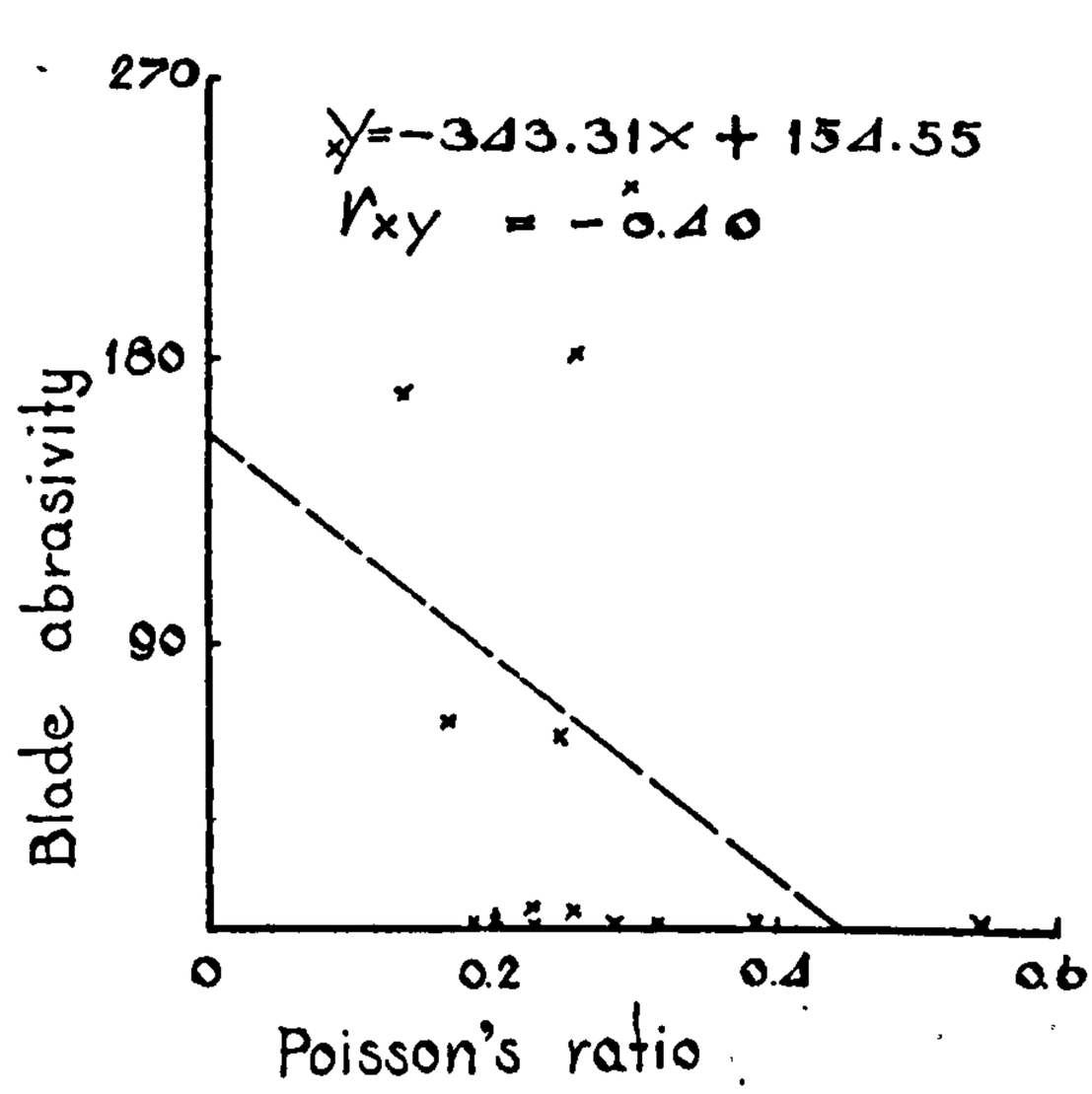
Y = -343.31 X + 154.55
rxy = -0.40
270
180
90
0
0.2
0.4
0.6
Blade abrasivity
Poisson's ratio

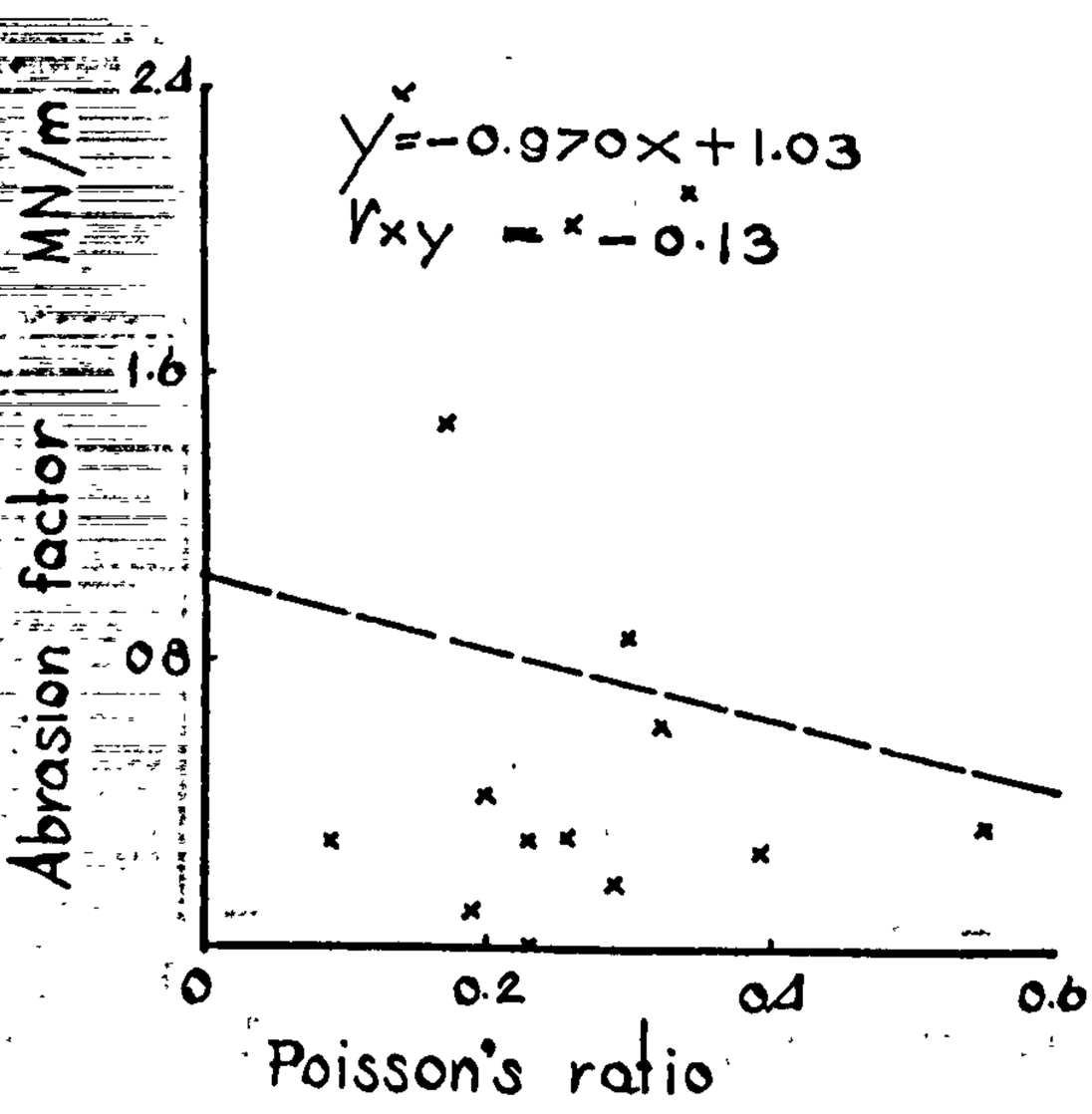
Y = -0.970 X + 1.03
rxy = -0.13
2.4
1.6
0.8
0
0.2
0.4
0.6
Abrasion factor MN/m
Poisson's ratio

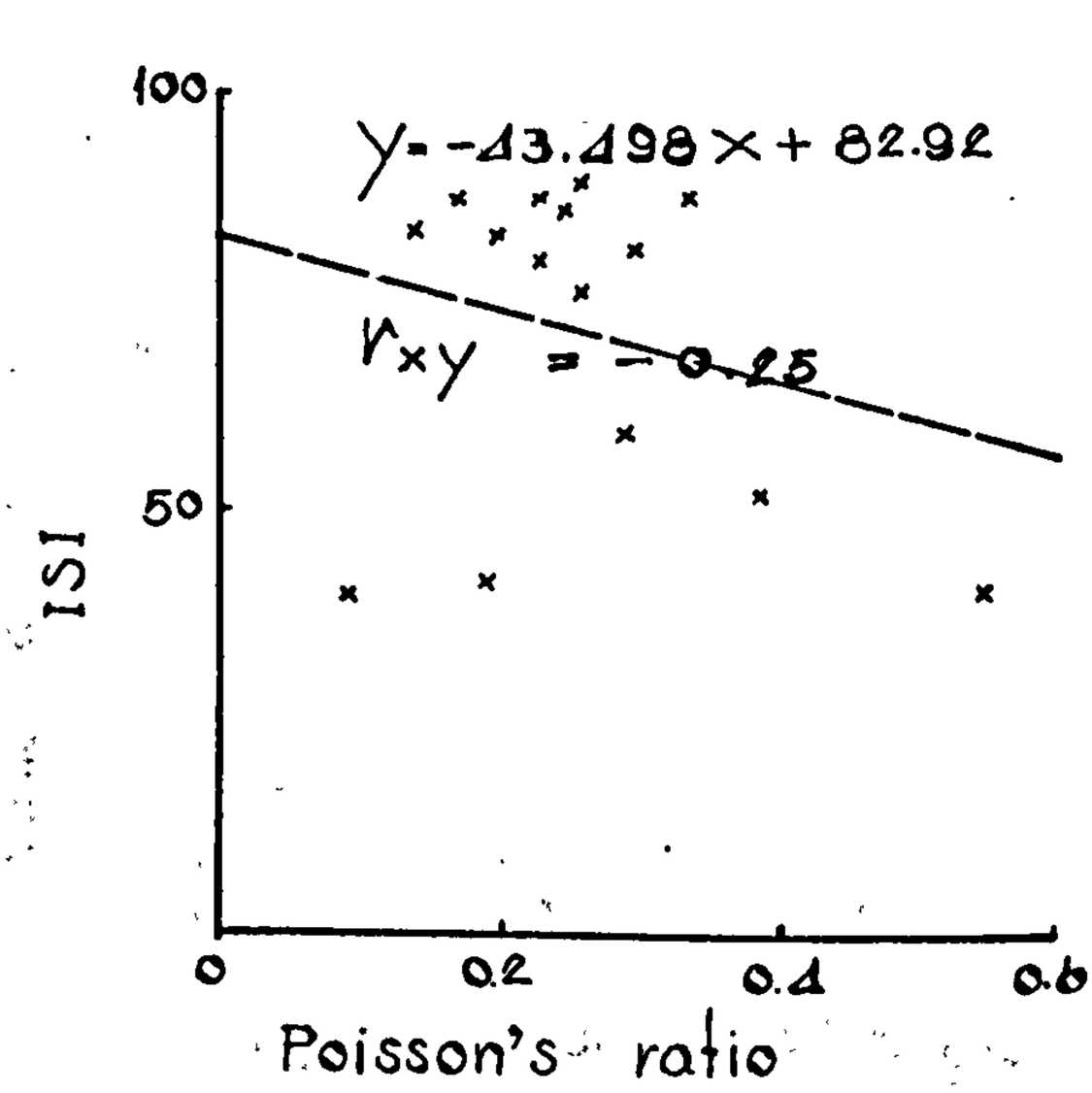
Y = -43.498 X + 82.92
rxy = -0.25
100
50
0
0.2
0.4
0.6
ISI
Poisson's ratio

Figure 47 (29)

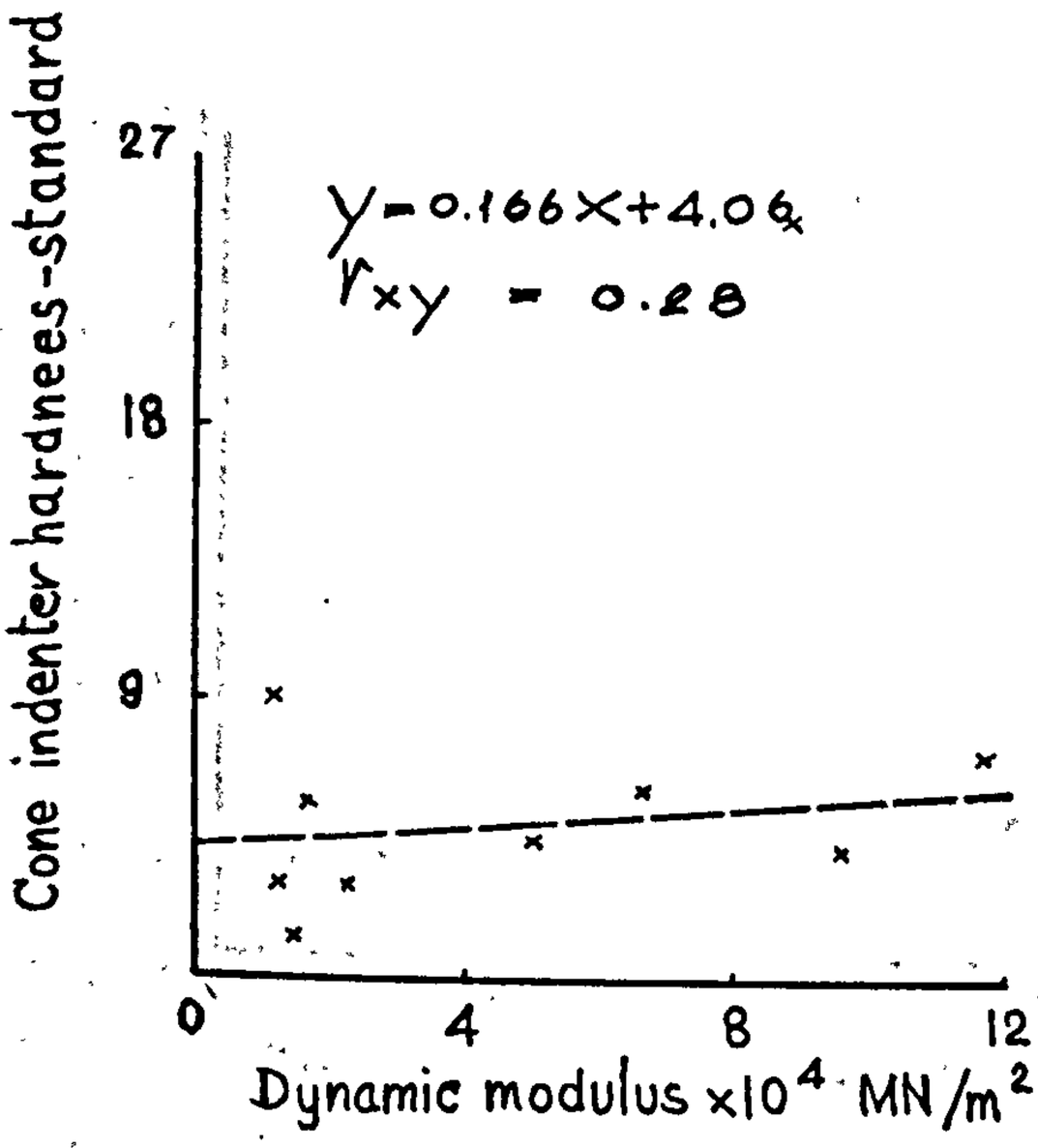
Cone indenter hardnees-standard
27
18
9
0
4
8
12
Dynamic modulus ×10⁴ MN/m²
Y = 0.166X + 4.06
rxy = 0.28

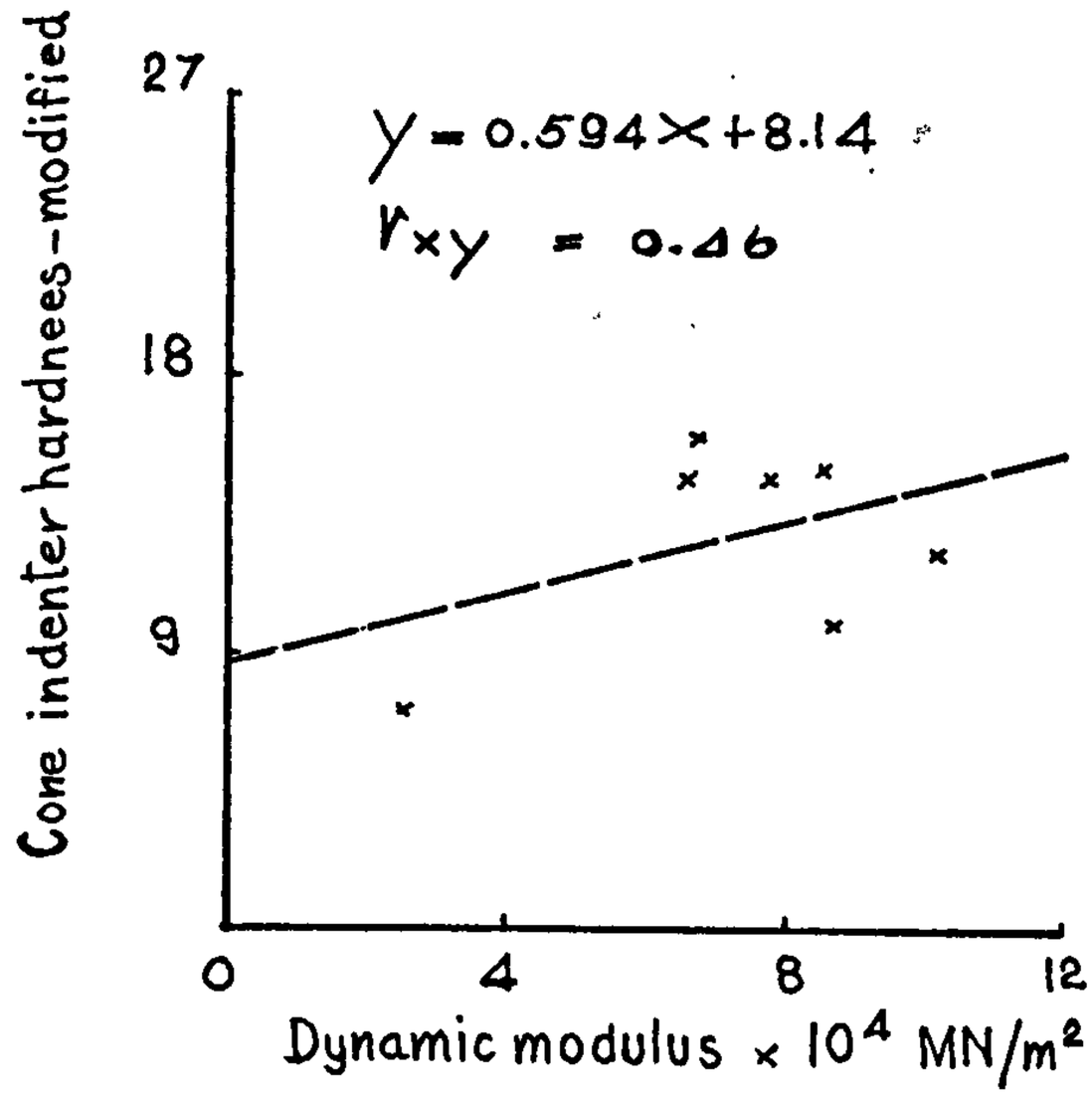
Cone indenter hardnees-modified
27
18
9
0
4
8
12
Dynamic modulus × 10⁴ MN/m²
Y = 0.594X + 8.14
rxy = 0.46

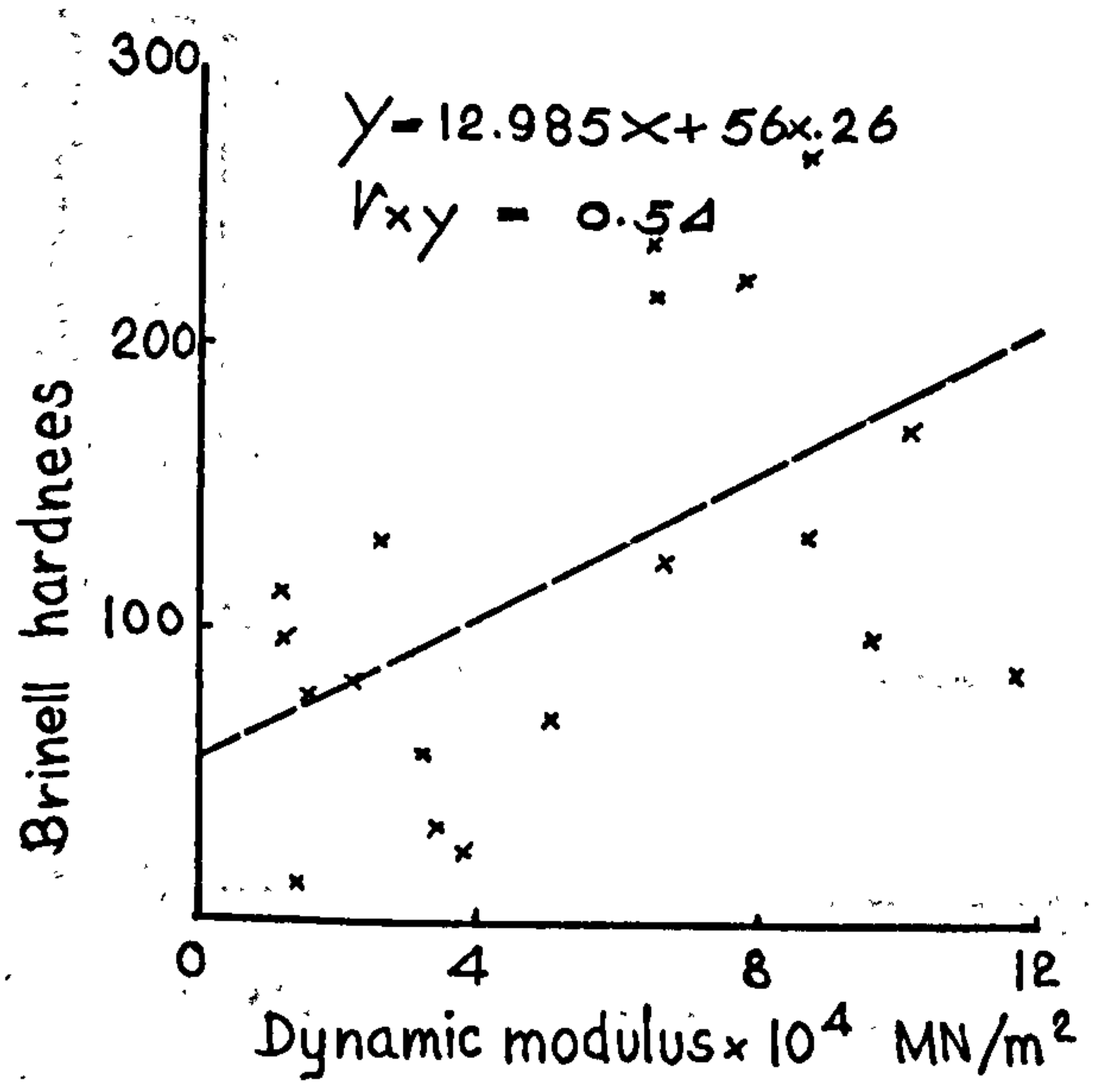
Brinell hardnees
300
200
100
0
4
8
12
Dynamic modulus × 10⁴ MN/m²
Y = 12.985X + 56x.26
rxy = 0.54

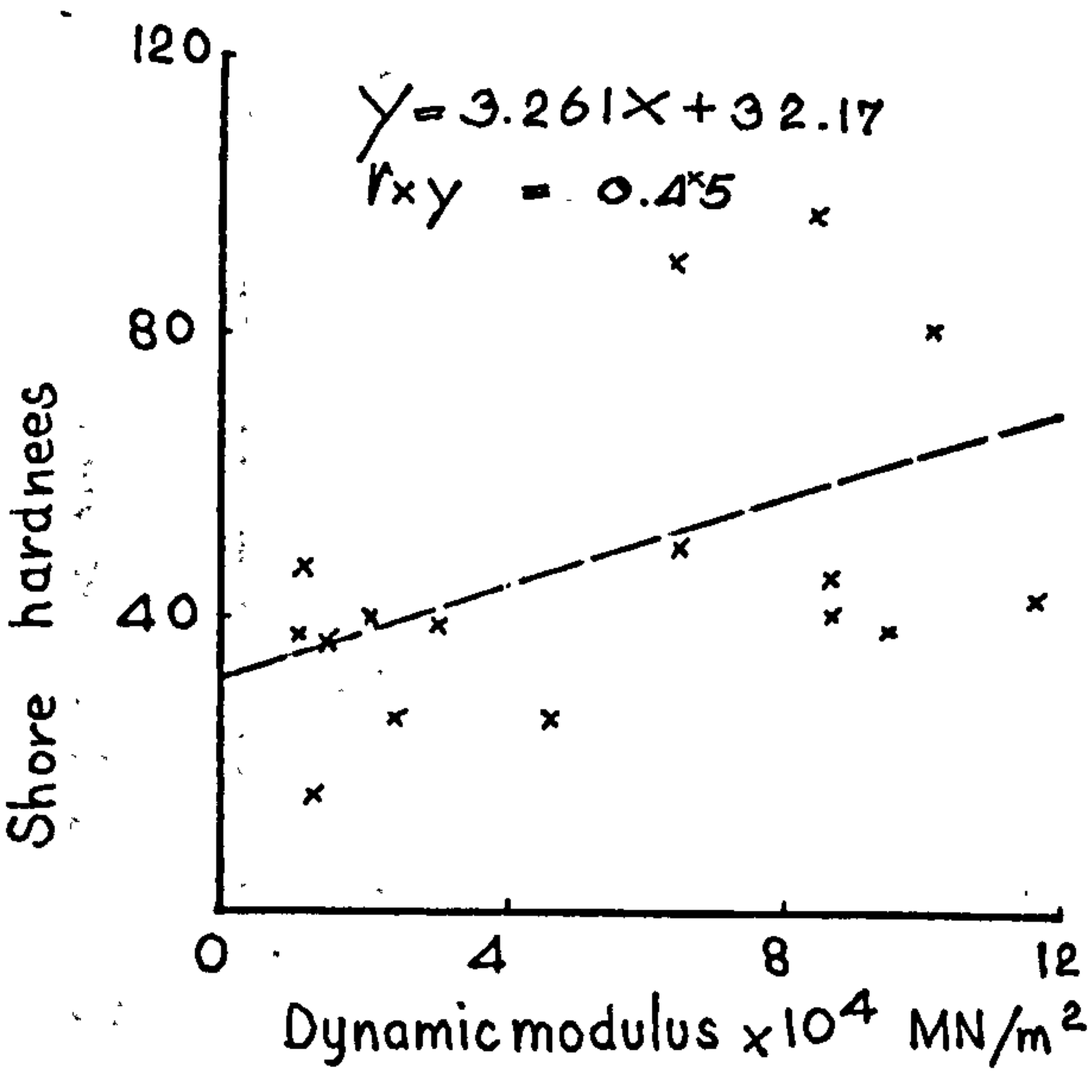
Shore hardnees
120
80
40
0
4
8
12
Dynamic modulus ×10⁴ MN/m²
Y = 3.261X + 32.17
rxy = 0.45

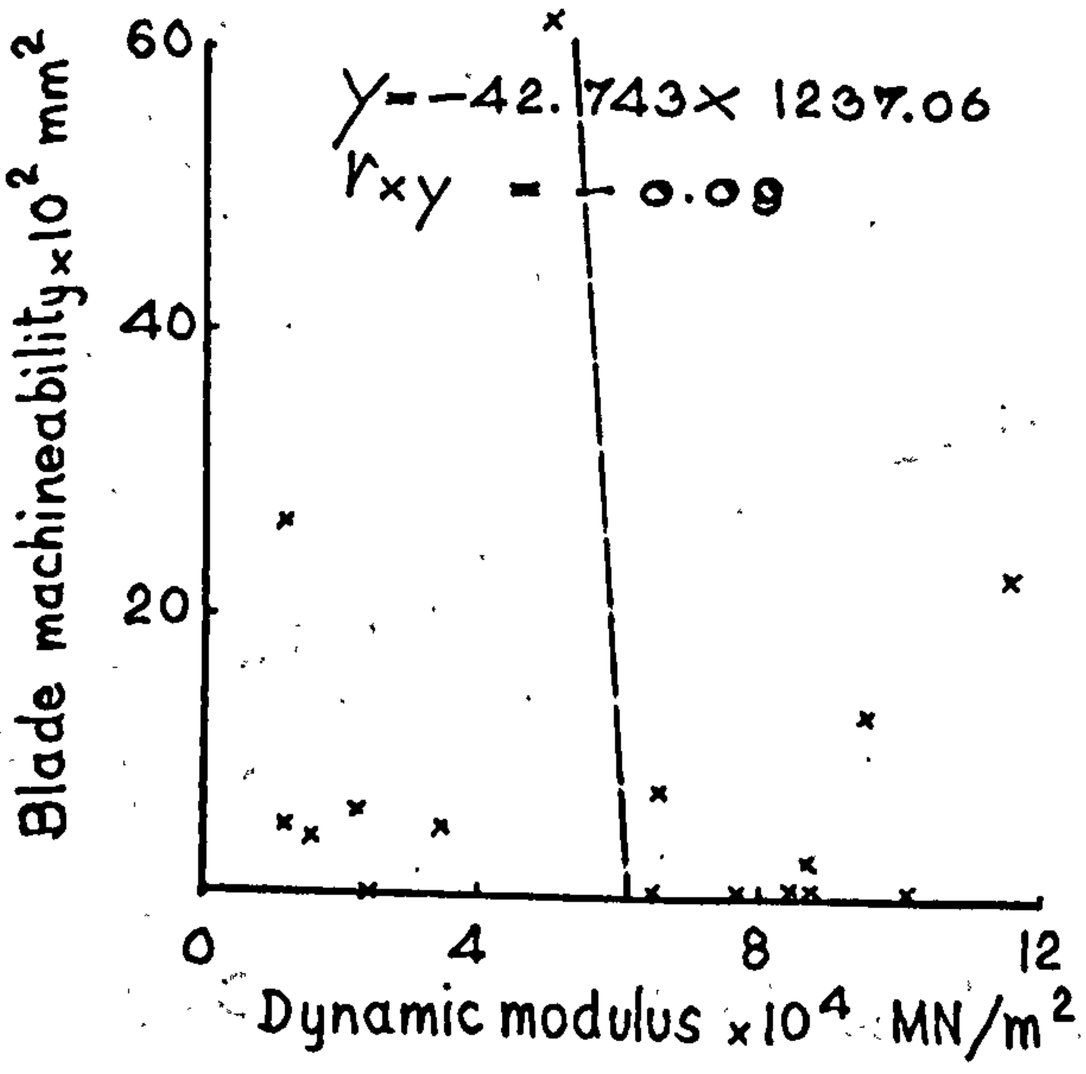
Blade machineability×10² mm²
60
40
20
0
4
8
12
Dynamic modulus ×10⁴ MN/m²
Y = −42.743X 1237.06
rxy = − 0.09

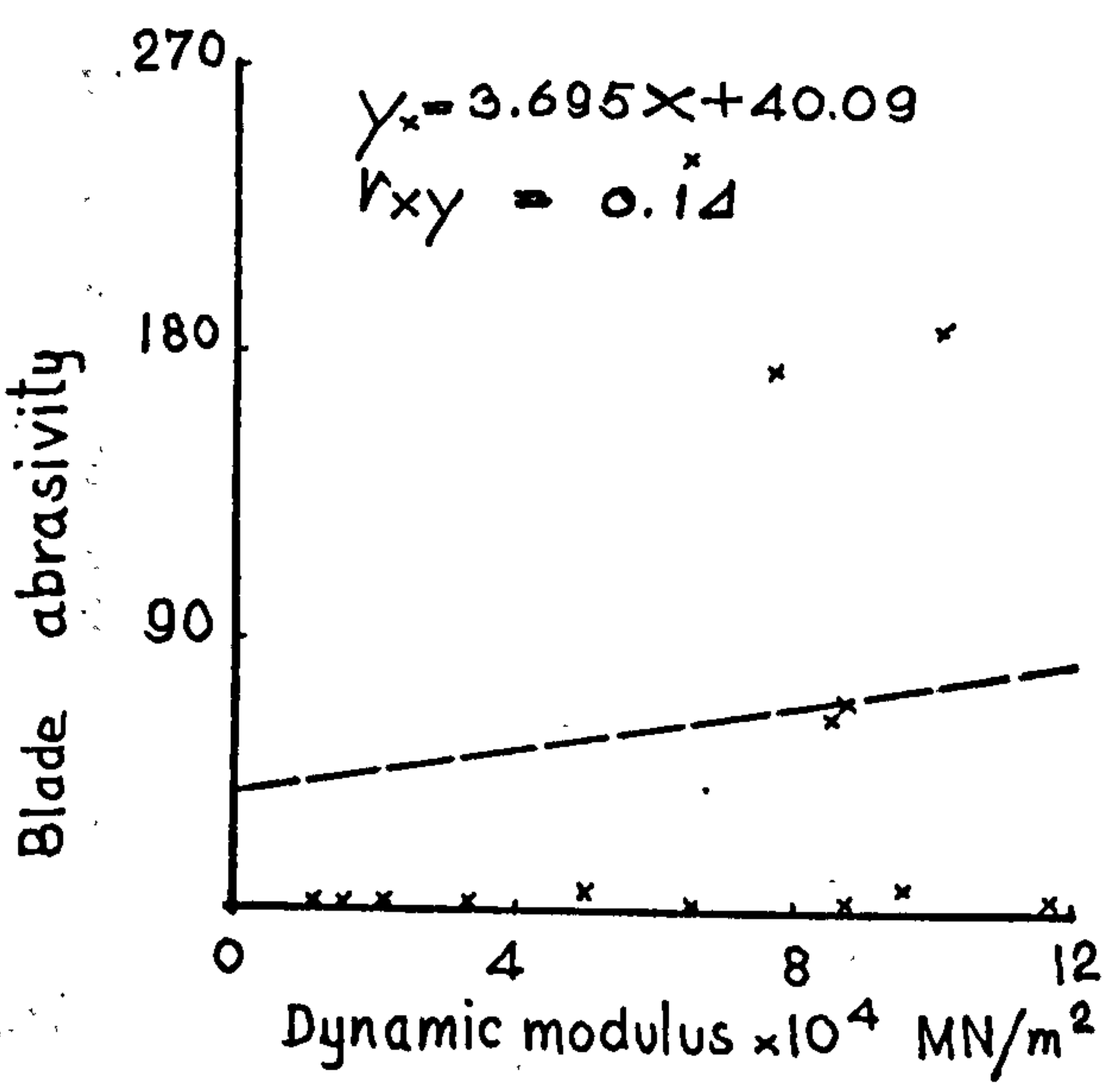
Blade abrasivity
270
180
90
0
4
8
12
Dynamic modulus ×10⁴ MN/m²
Y = 3.695X + 40.09
rxy = 0.14

Figure · 47 (30)

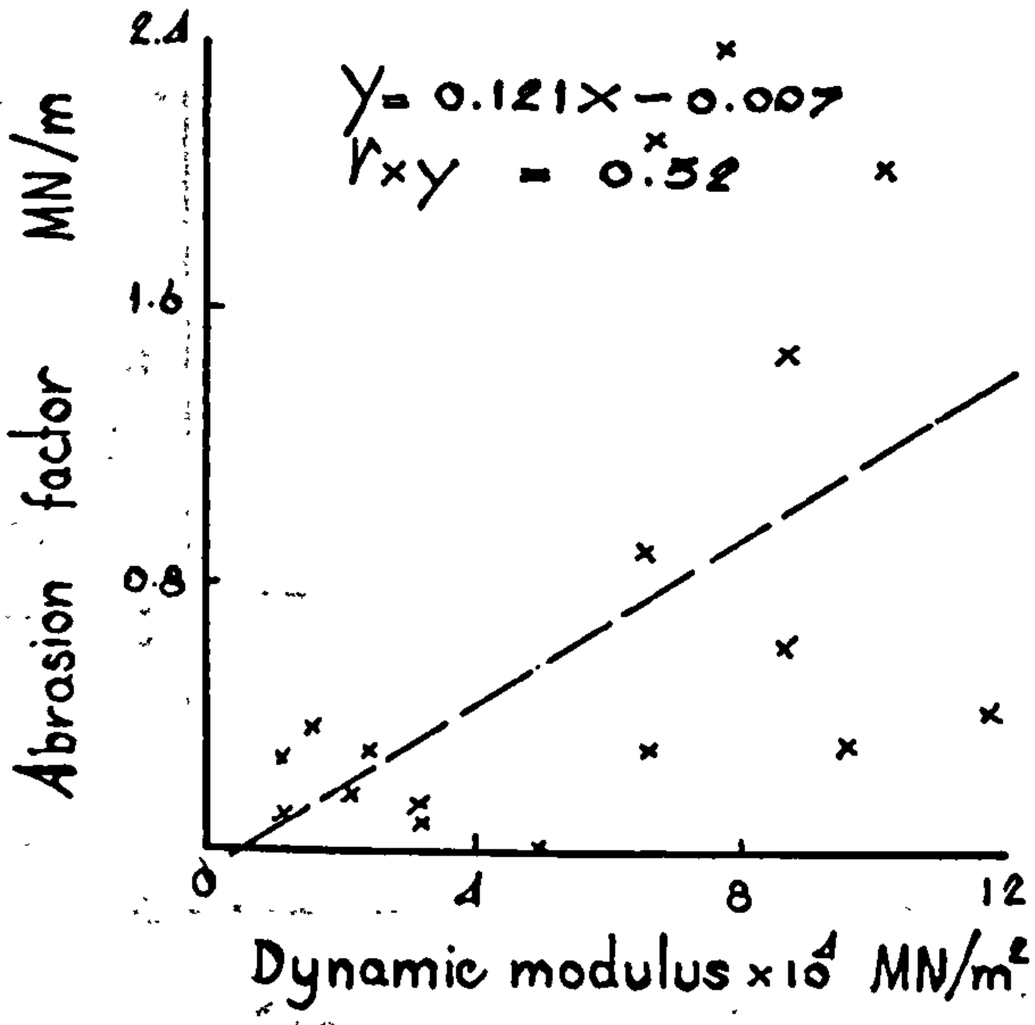
Y= 0.121X − 0.007
rxy = 0.52
Abrasion factor MN/m
2.4
1.6
0.8
0
4
8
12
Dynamic modulus x 10⁴ MN/m²

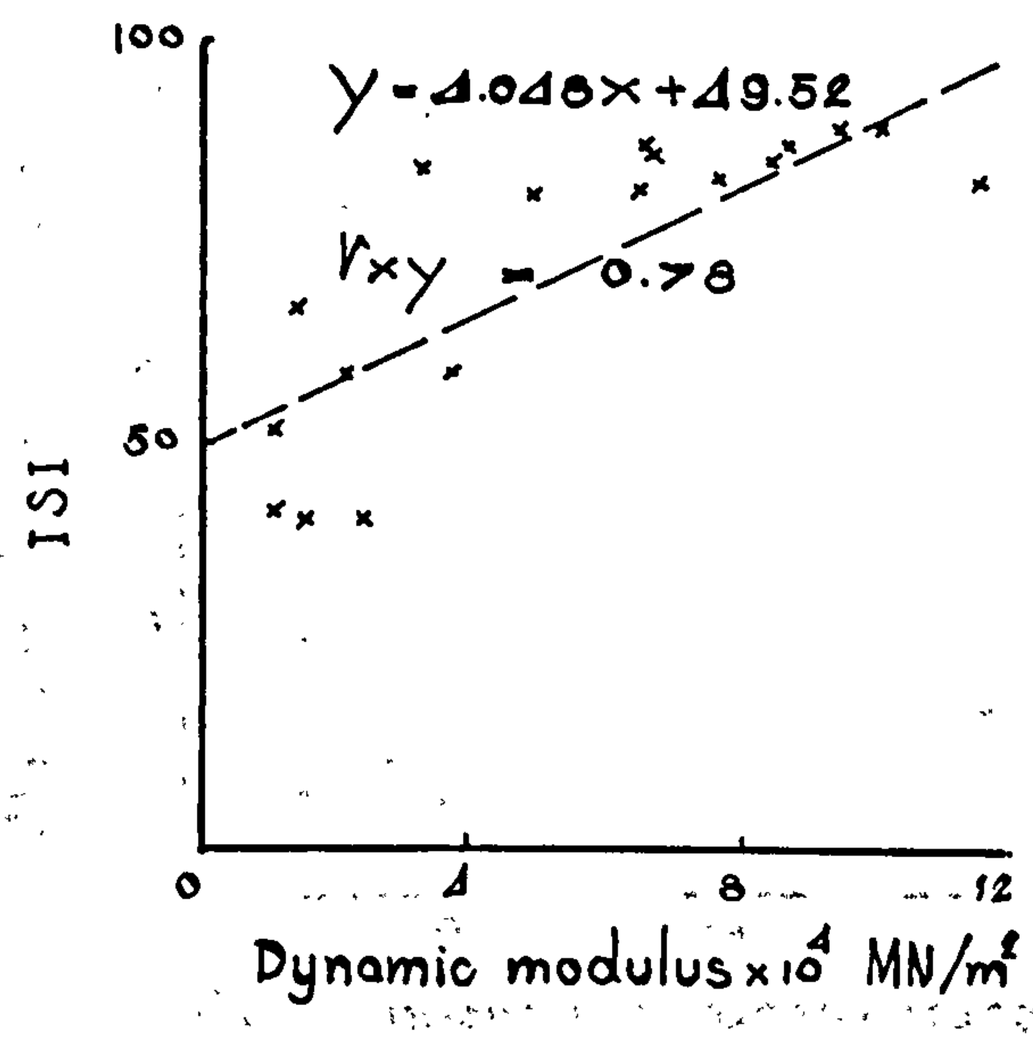
Y = 4.048X + 49.52
rxy = 0.78
ISI
100
50
0
4
8
12
Dynamic modulus x 10⁴ MN/m²

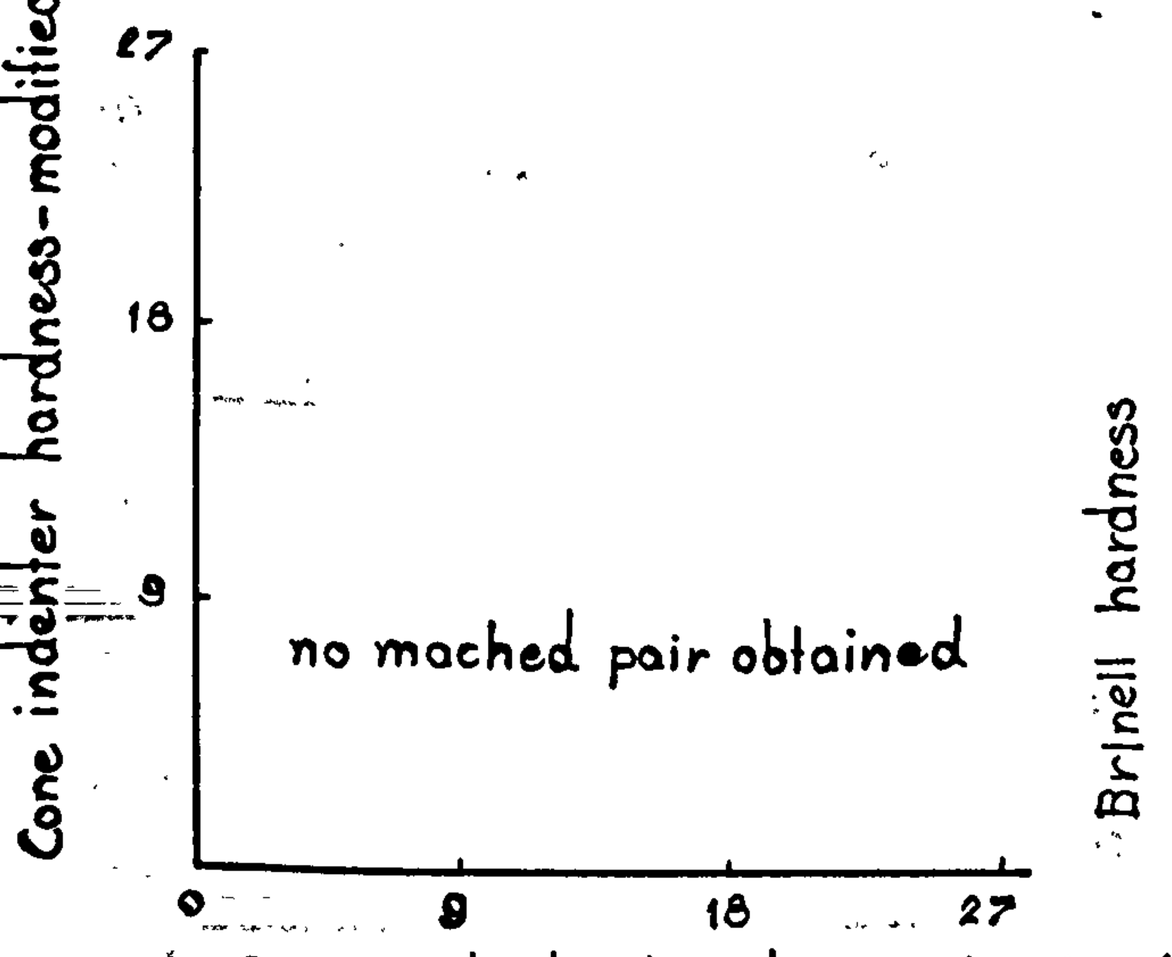
Cone indenter hardness-modified
27
18
9
no mached pair obtained
0
9
18
27
Cone indenter hardness-standard

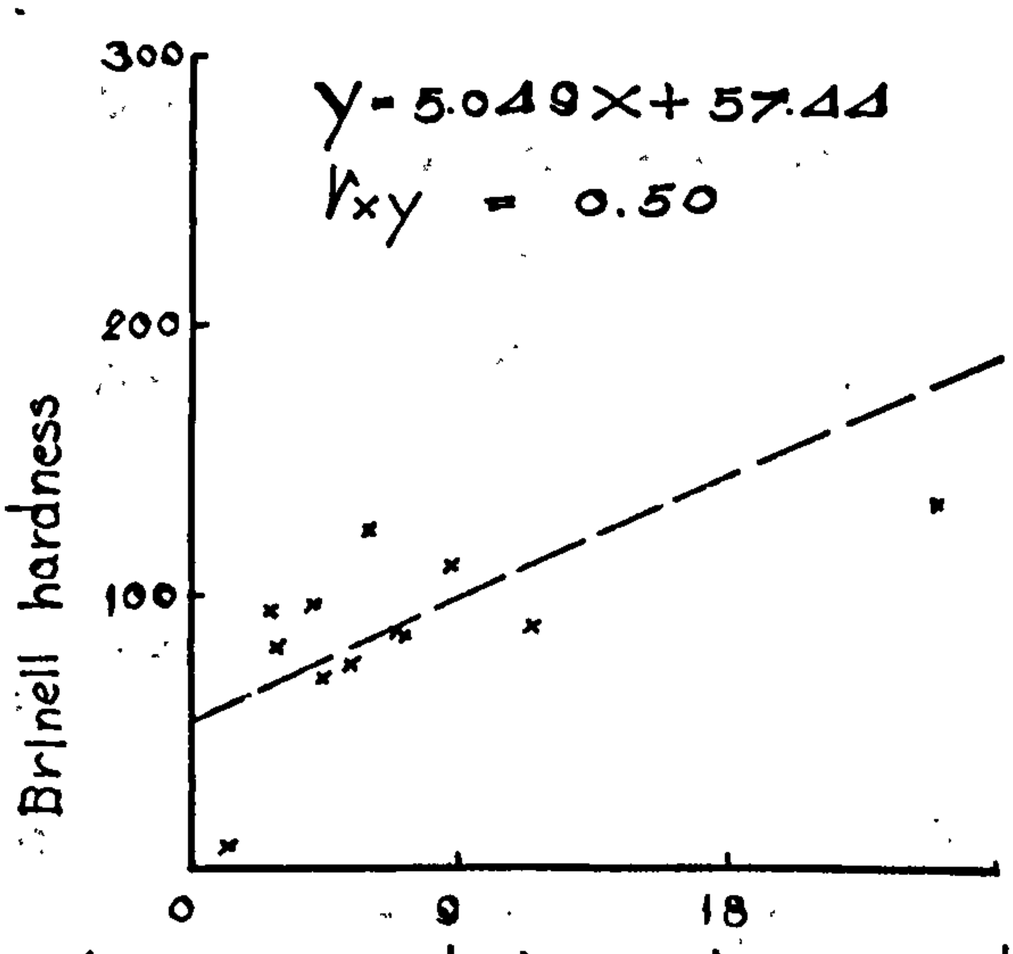
Y = 5.049X + 57.44
rxy = 0.50
Brinell hardness
300
200
100
0
9
18
Cone indenter hardness-standard

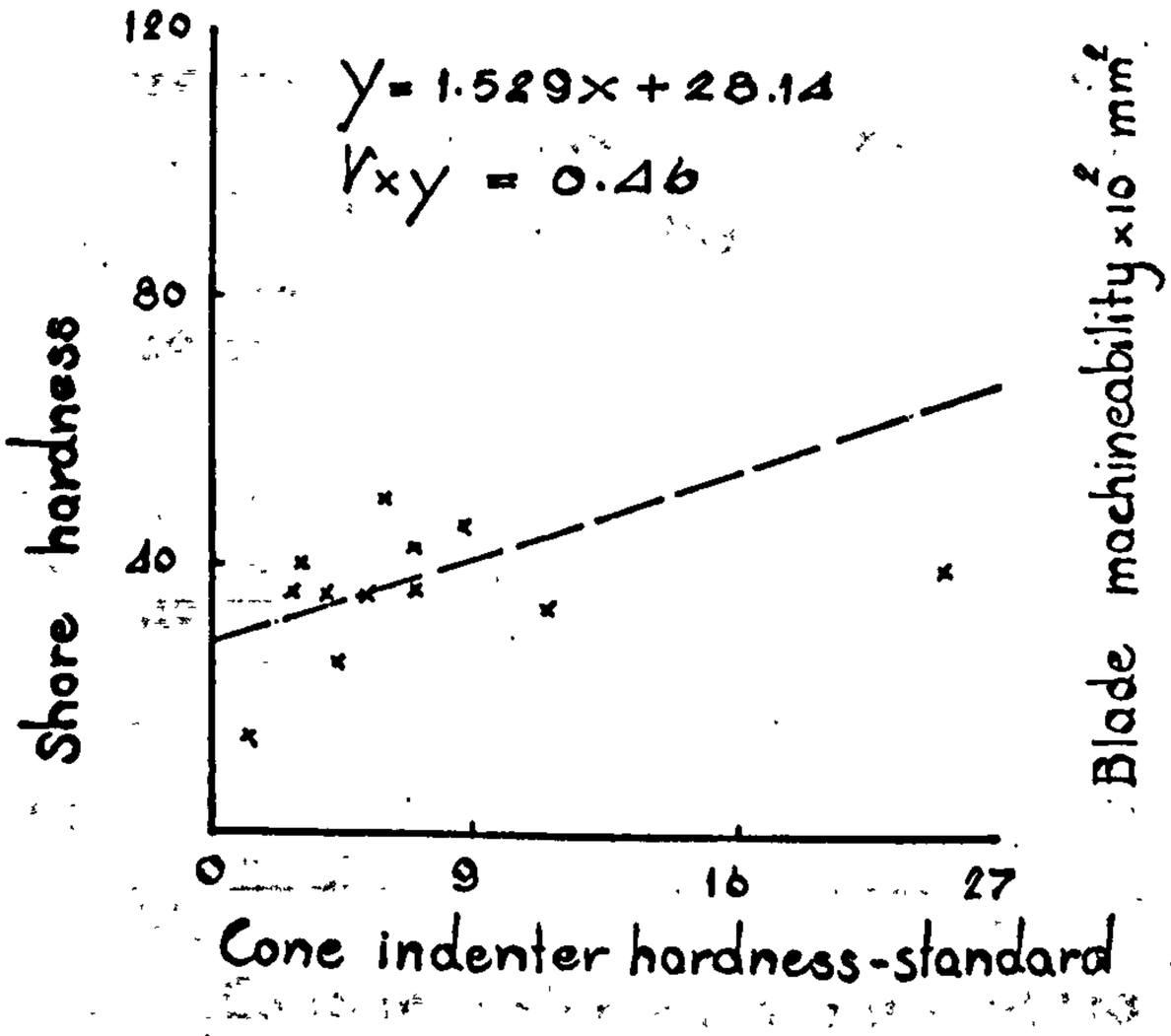
Y = 1.529X + 28.14
rxy = 0.46
Shore hardness
120
80
40
0
9
16
27
Cone indenter hardness-standard

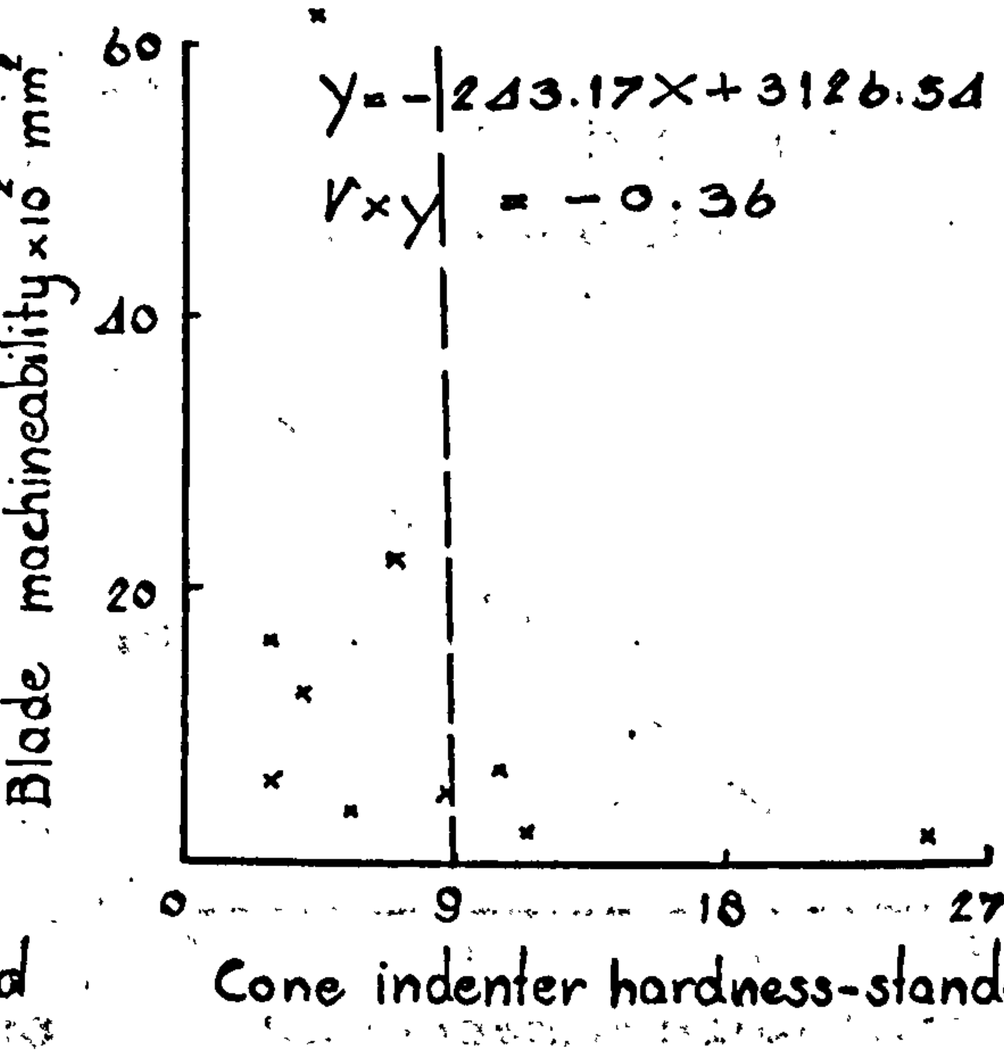
Y = −243.17X + 3126.54
rxy = −0.36
Blade machineability x 10² mm²
60
40
20
0
9
18
27
Cone indenter hardness-standard

Figure 47(31)

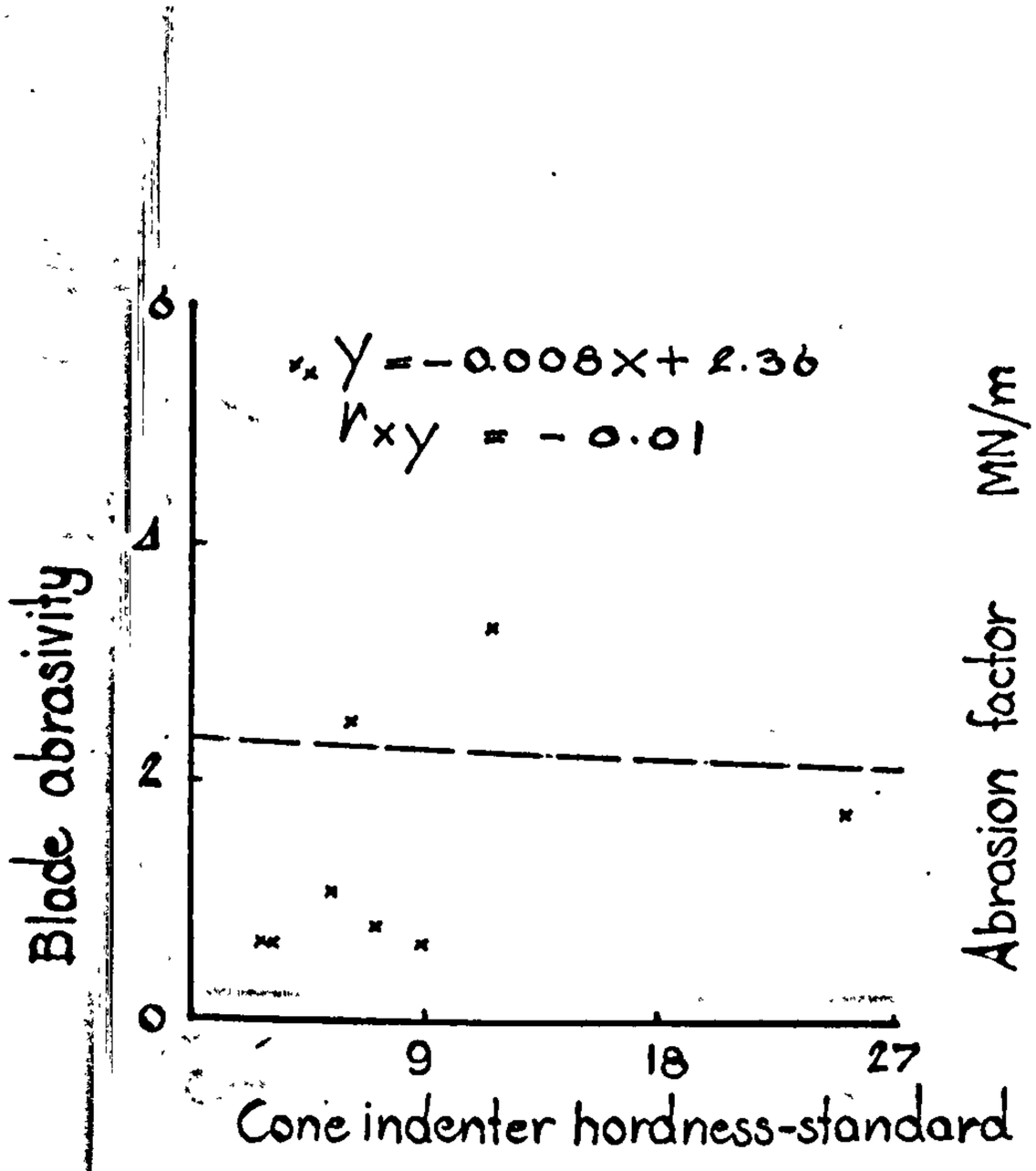
Y = -0.008X + 2.36
rxy = -0.01
Blade abrasivity
6
4
2
0
9
18
27
Cone indenter hardness-standard

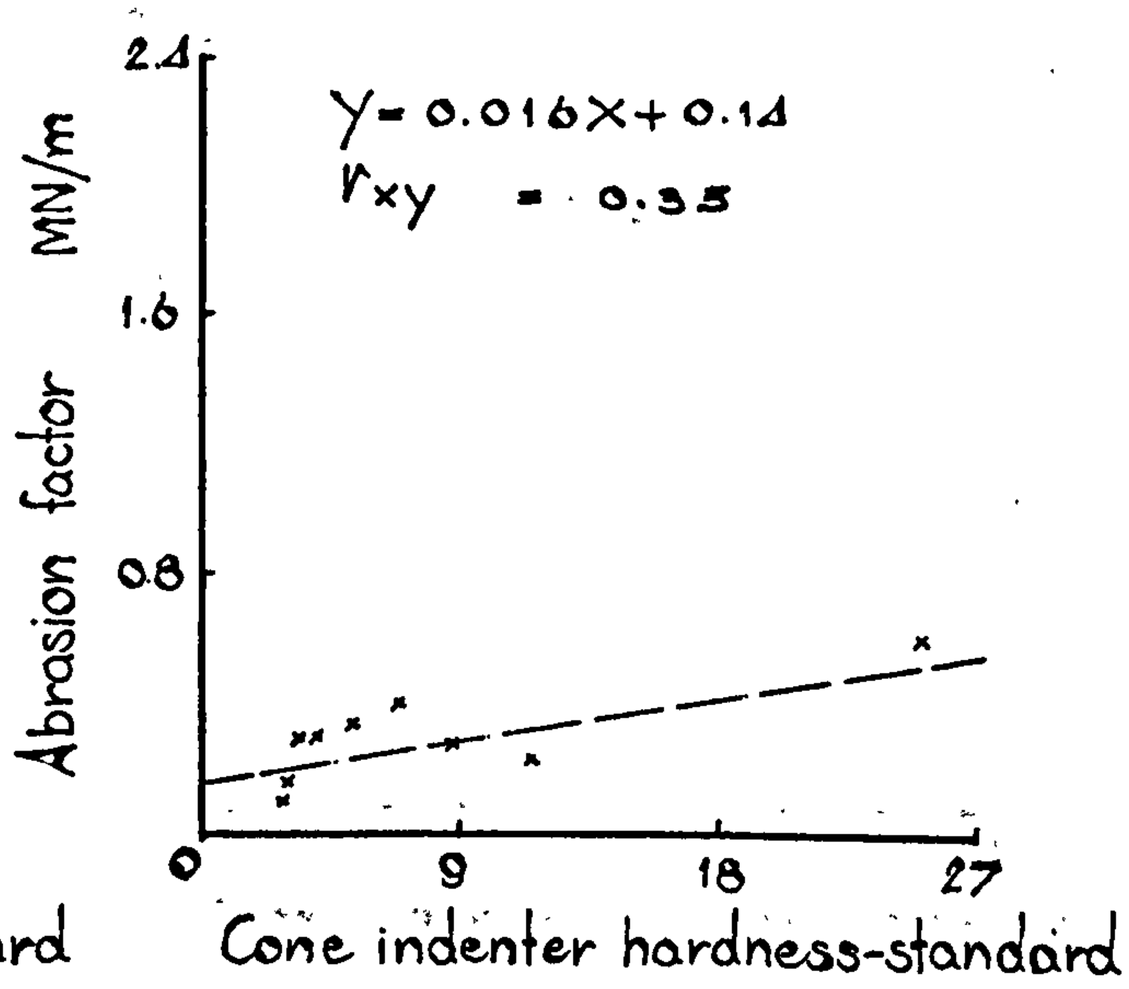
Y = 0.016X + 0.14
rxy = 0.35
Abrasion factor MN/m
2.4
1.6
0.8
0
9
18
27
Cone indenter hardness-standard

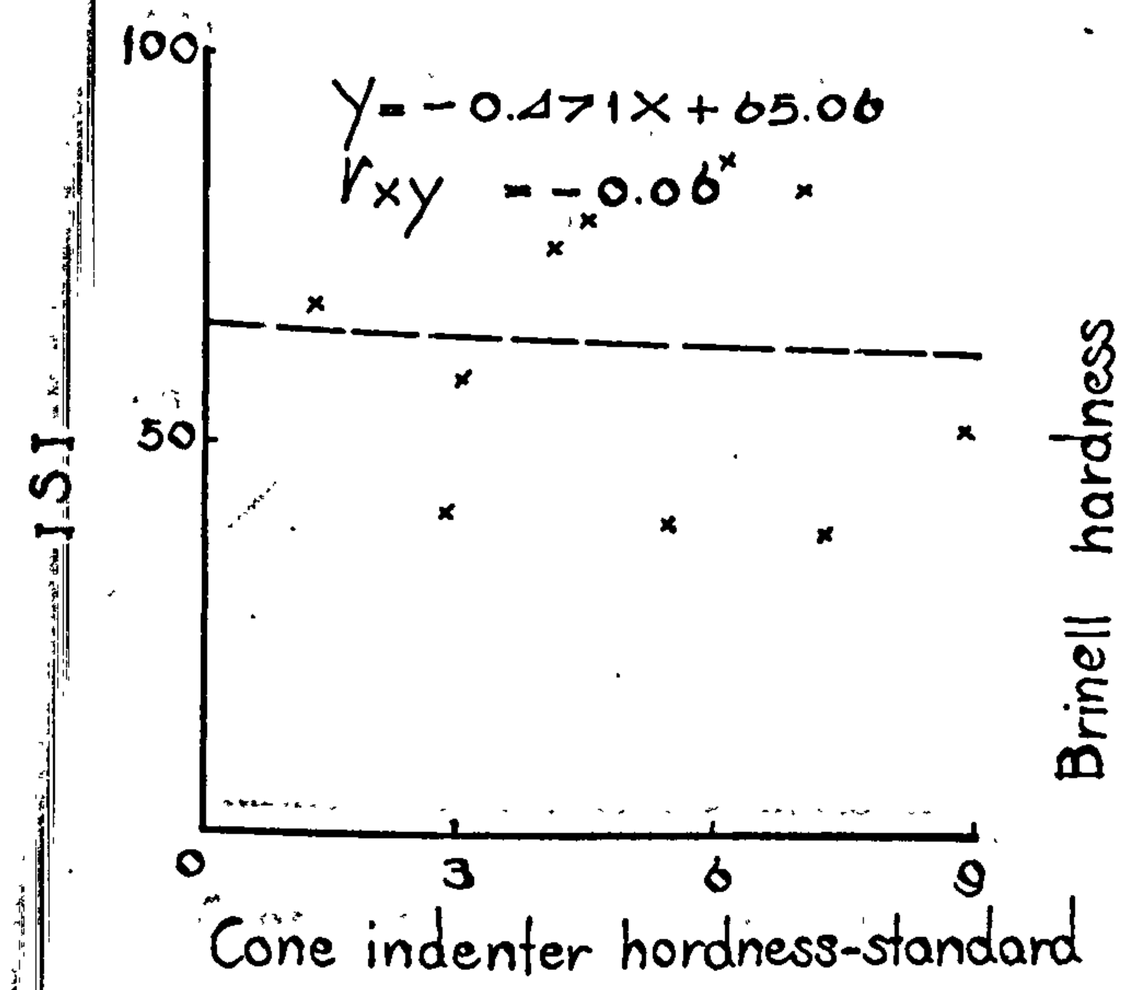
Y = -0.471X + 65.06
rxy = -0.06
ISI
100
50
0
3
6
9
Cone indenter hardness-standard

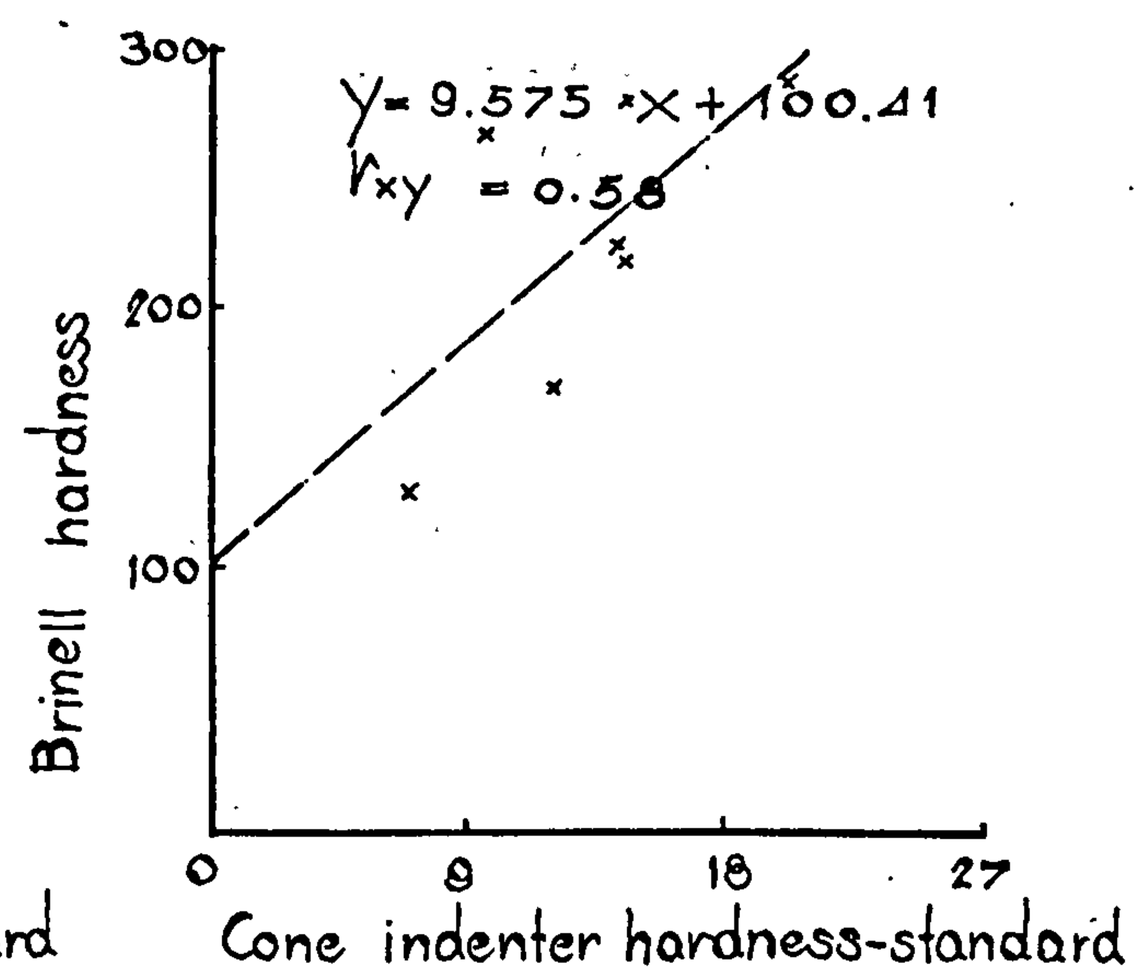
Y = 9.575X + 100.41
rxy = 0.58
Brinell hardness
300
200
100
0
9
18
27
Cone indenter hardness-standard

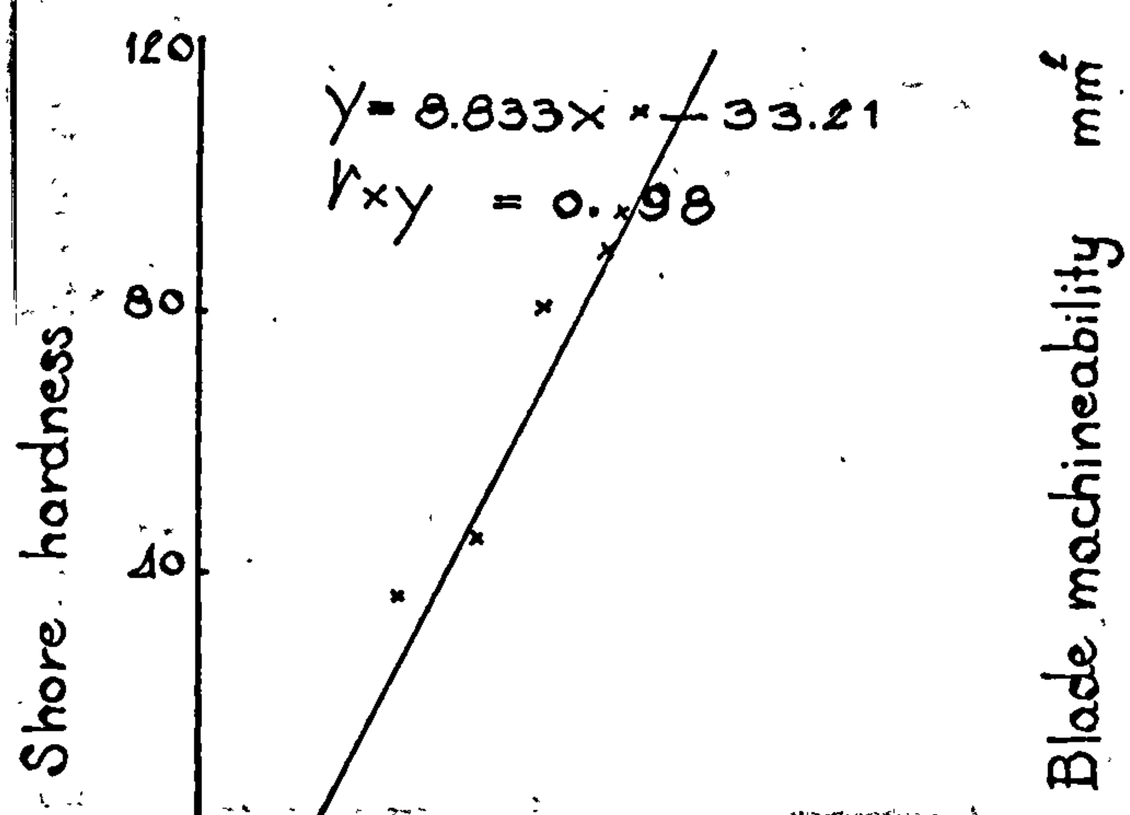
Y = 8.833X + 33.21
rxy = 0.98
Shore hardness
120
80
40
0
9
18
27
Cone indenter hardness-modified

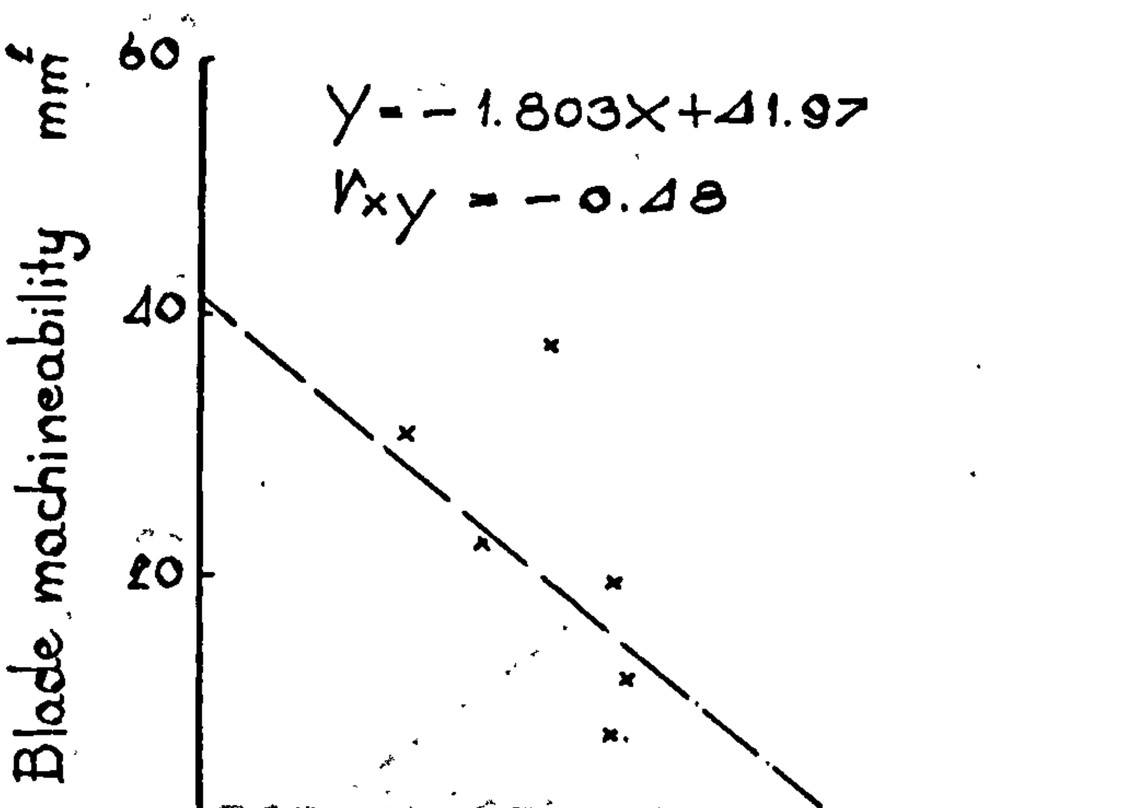
Y = -1.803X + 41.97
rxy = -0.48
Blade machineability mm²
60
40
20
0
9
18
27
Cone indenter hardness-modified

Figure 47 (32)

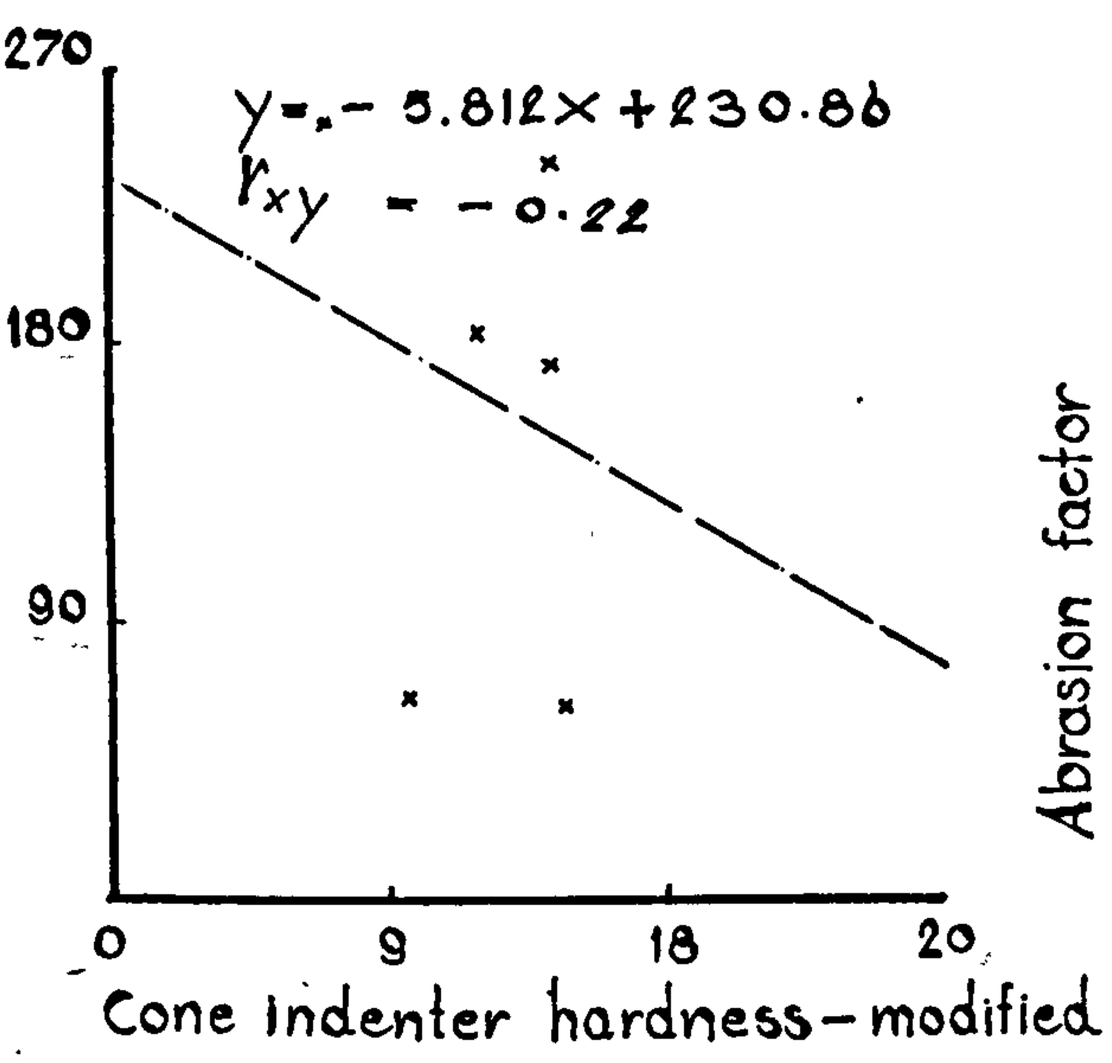
Y = - 5.812X + 230.86
r_{xy} = - 0.22
Blade abrasivity — MN/m
270
180
90
0
9
18
20
Cone indenter hardness - modified

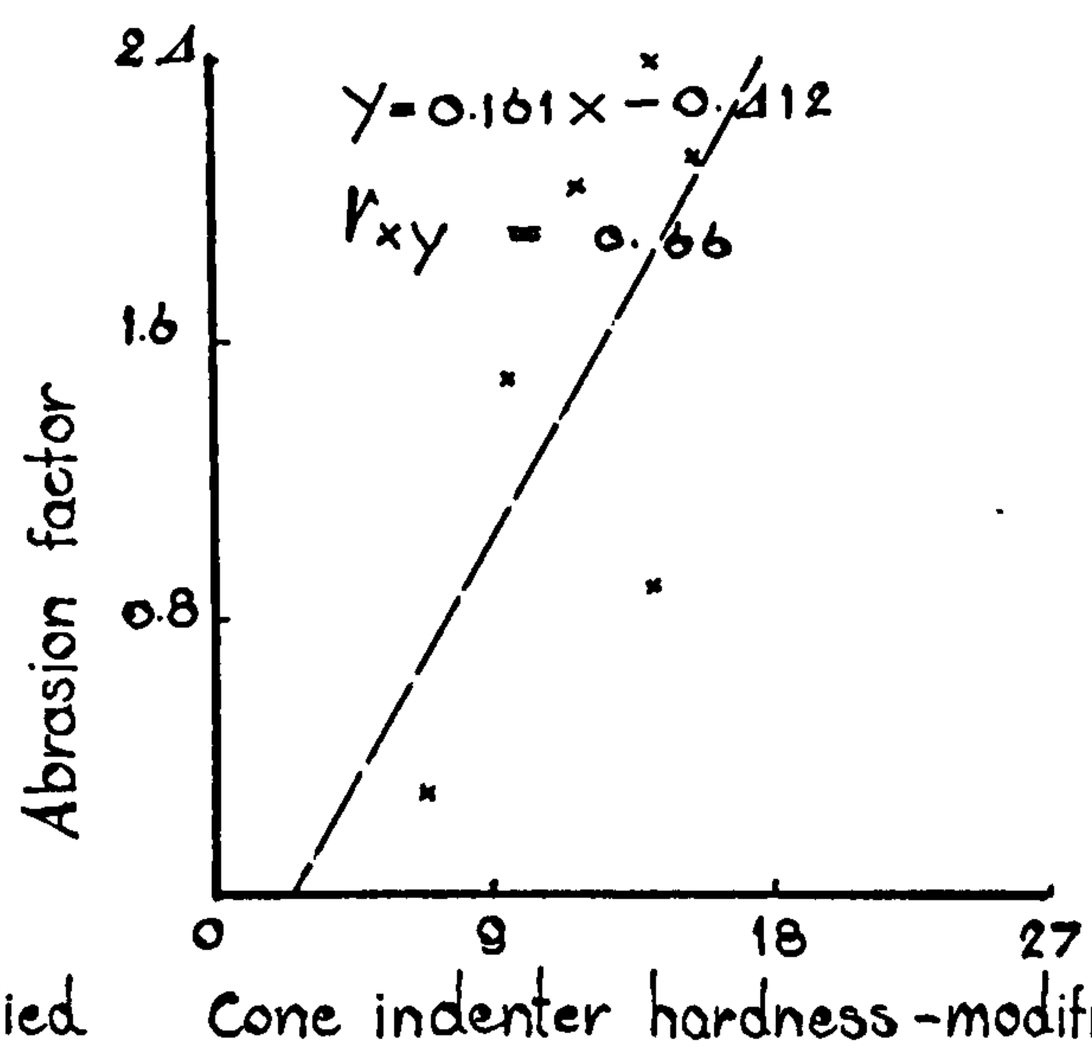
Y = 0.161X - 0.412
r_{xy} = 0.66
Abrasion factor
2.4
1.6
0.8
0
9
18
27
Cone indenter hardness - modified

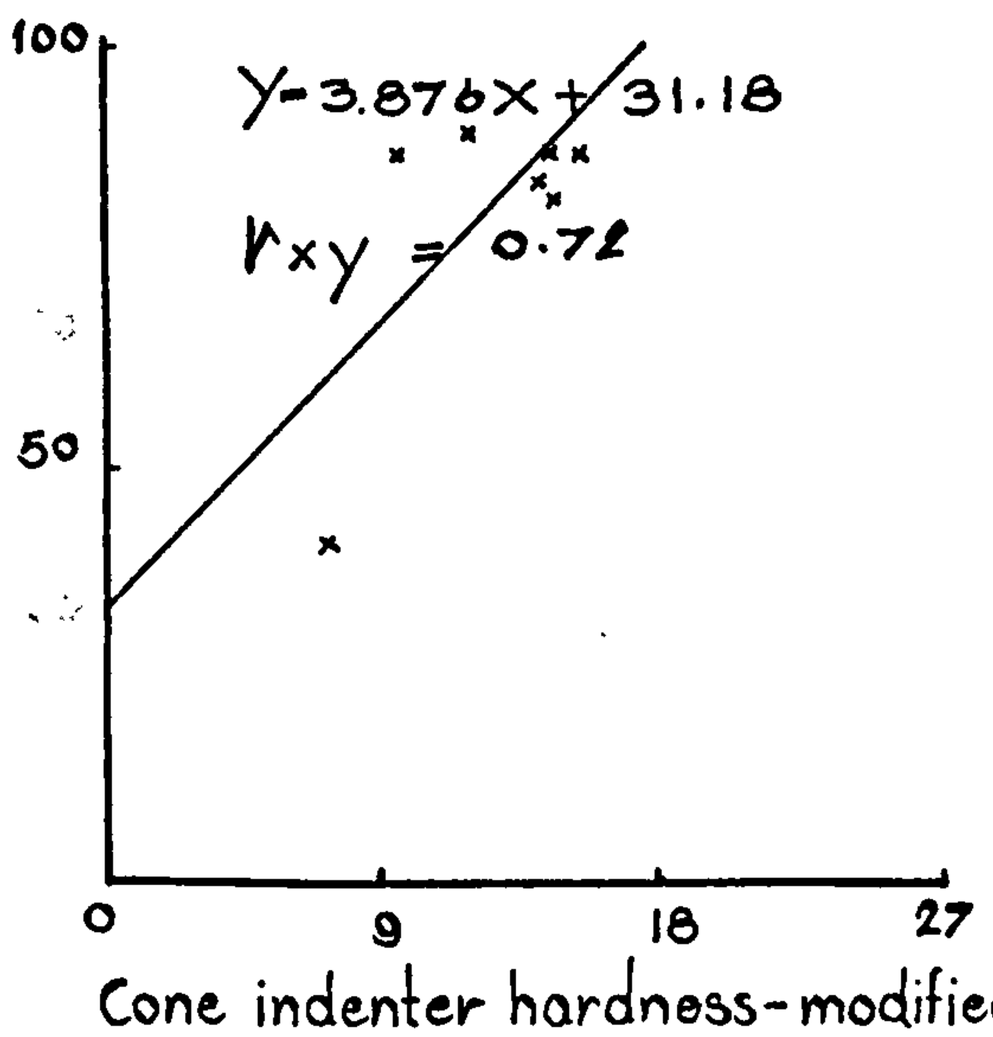
Y = 3.876X + 31.18
r_{xy} = 0.72
ISI
100
50
0
9
18
27
Cone indenter hardness - modified

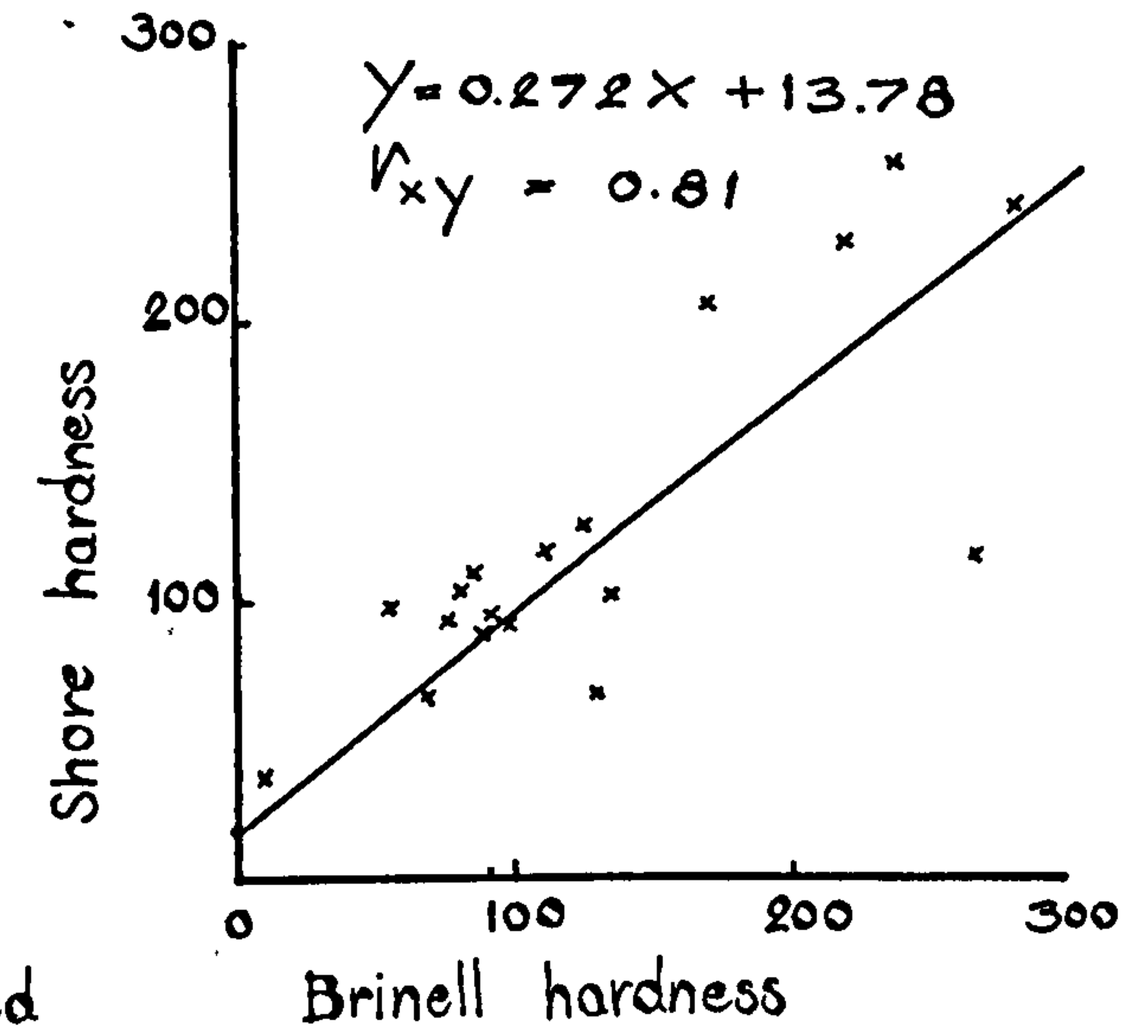
Y = 0.272X + 13.78
r_{xy} = 0.81
Shore hardness
300
200
100
0
100
200
300
Brinell hardness

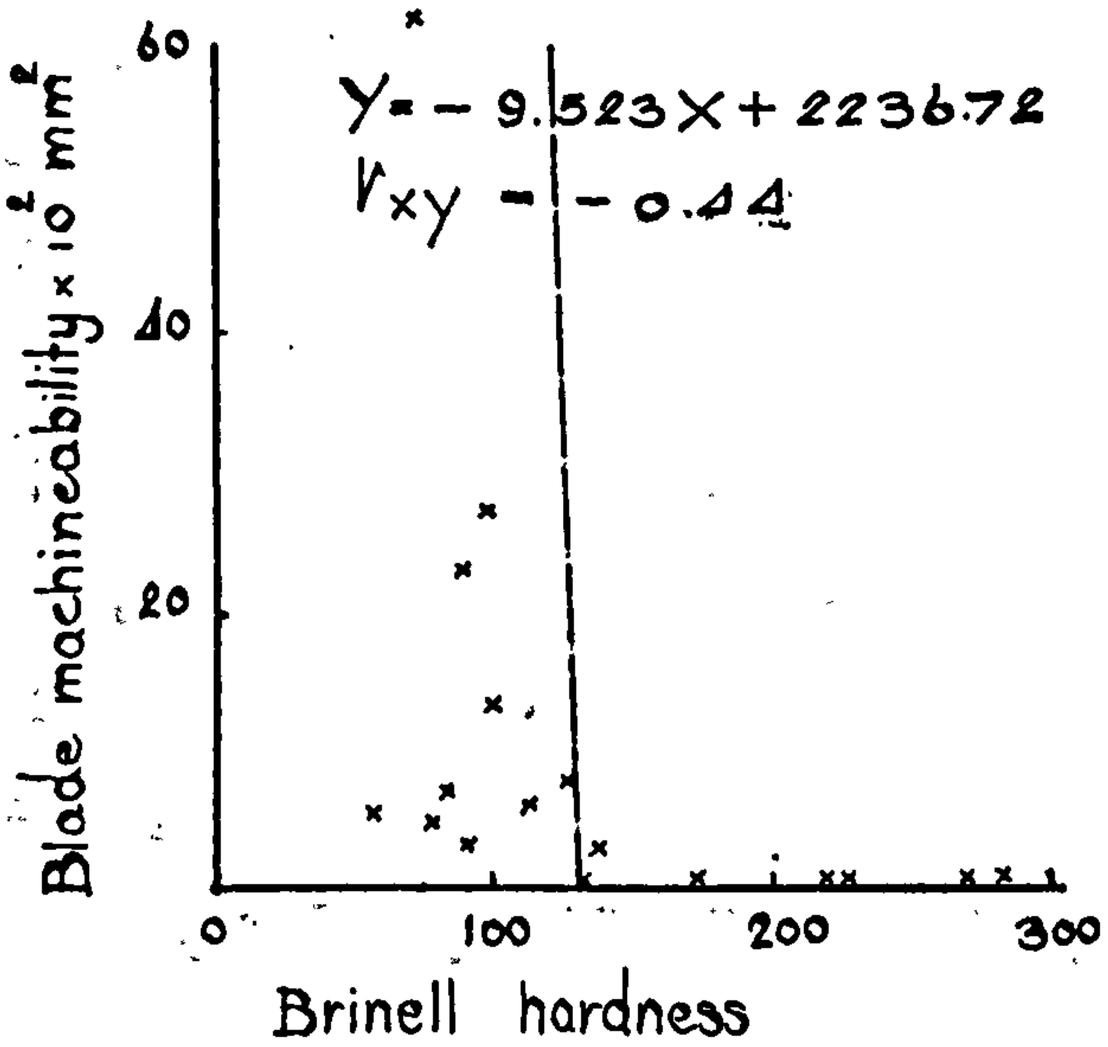
Y = - 9.523X + 2236.72
r_{xy} = - 0.44
Blade machineability x 10 mm²
60
40
20
0
100
200
300
Brinell hardness

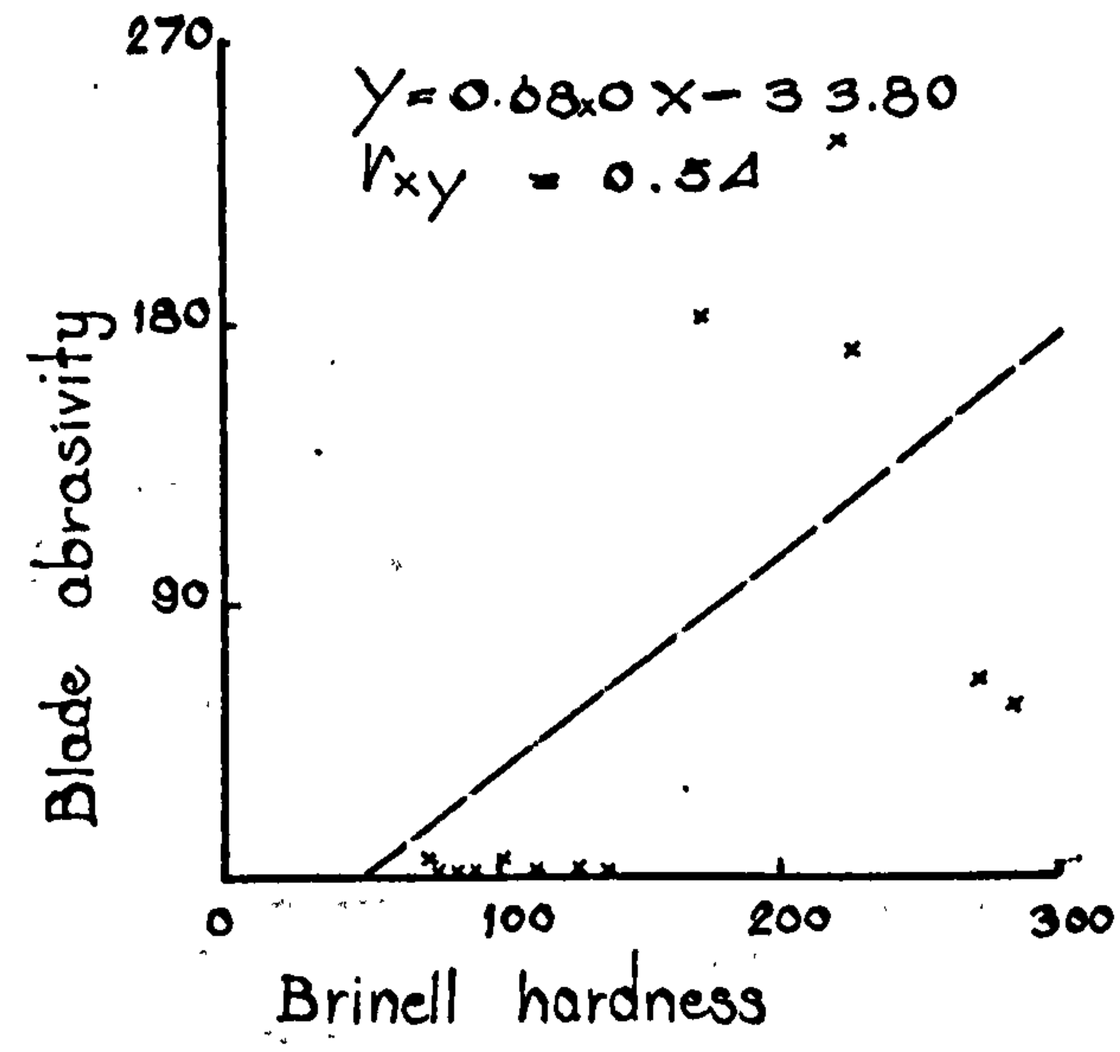
Y = 0.680X - 33.80
r_{xy} = 0.54
Blade abrasivity
270
180
90
0
100
200
300
Brinell hardness

Figure 47 (33)

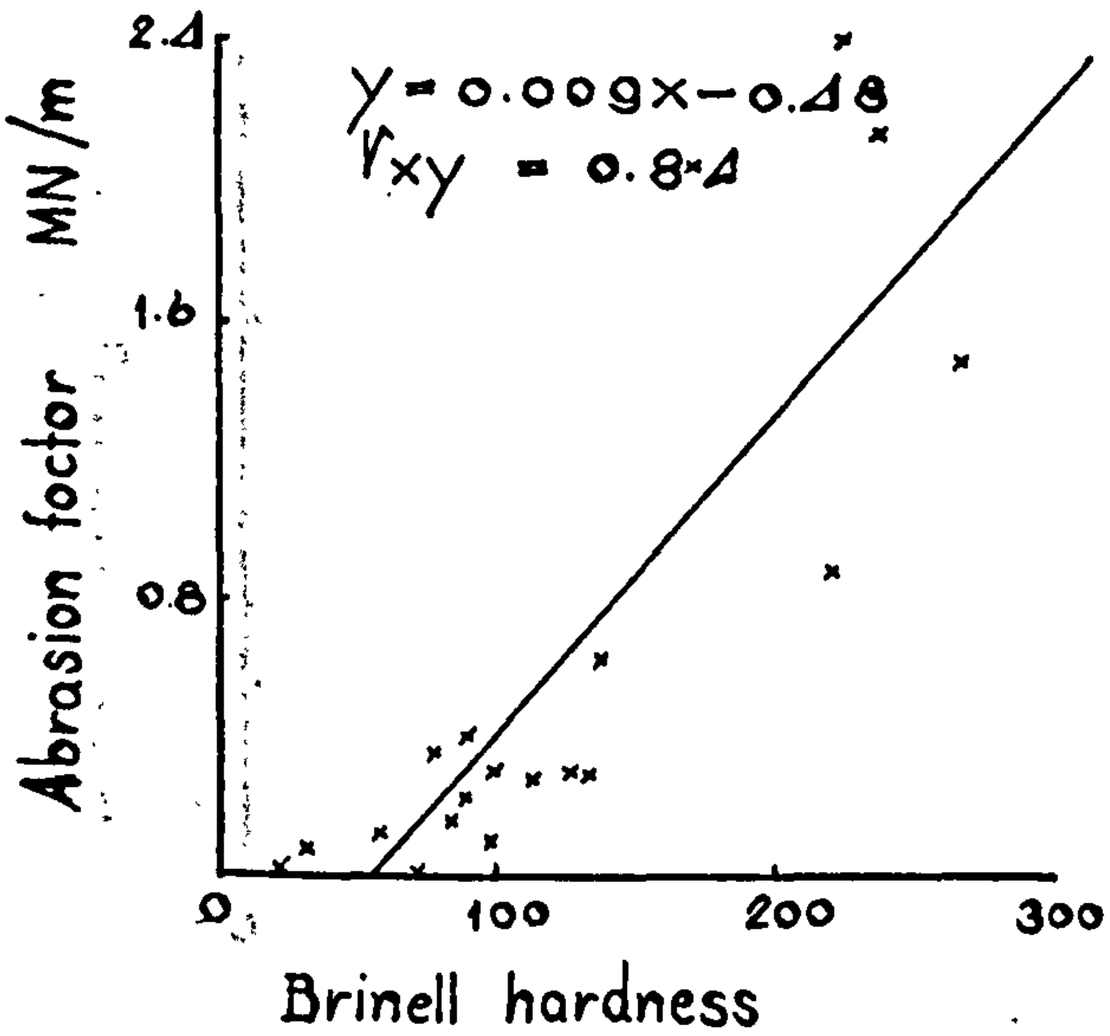
Y = 0.009X − 0.48
r_{xy} = 0.84
Abrasion factor MN/m
2.4
1.6
0.8
0
100
200
300
Brinell hardness

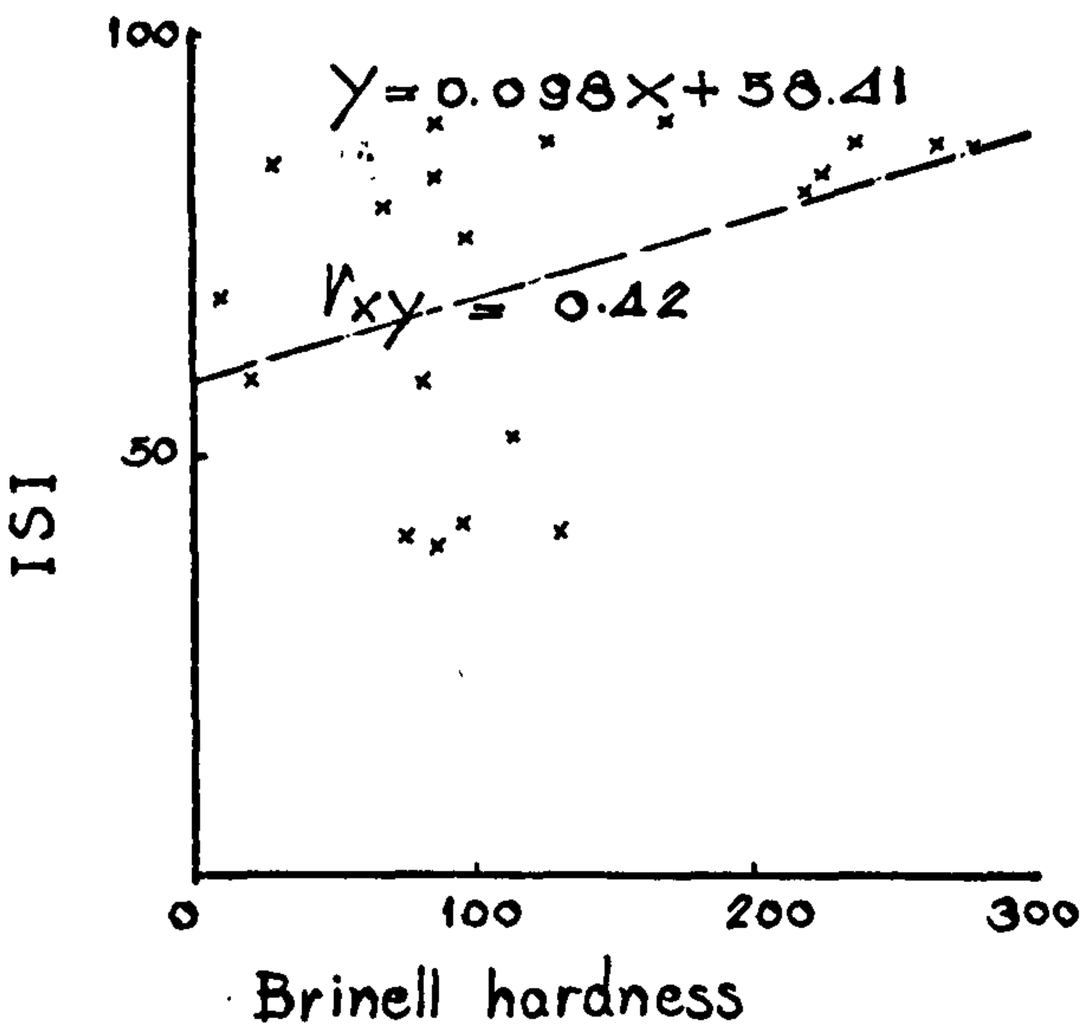
Y = 0.098X + 58.41
r_{xy} = 0.42
ISI
100
50
0
100
200
300
Brinell hardness

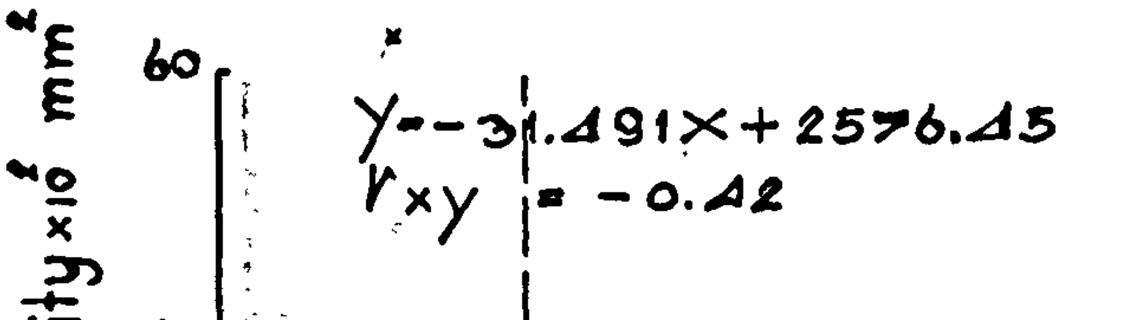
Y = −31.491X + 2576.45
r_{xy} = −0.42
Blade machineability $x10^4$ mm^2
60
40
20
0
40
80
120
Shore hardness

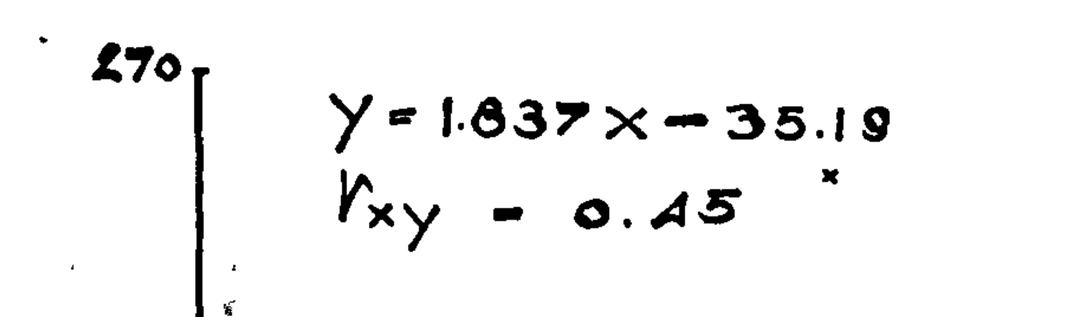
Y = 1.837X − 35.19
r_{xy} = 0.45
Blade abrasivity
270
180
90
0
40
80
120
Shore hardness

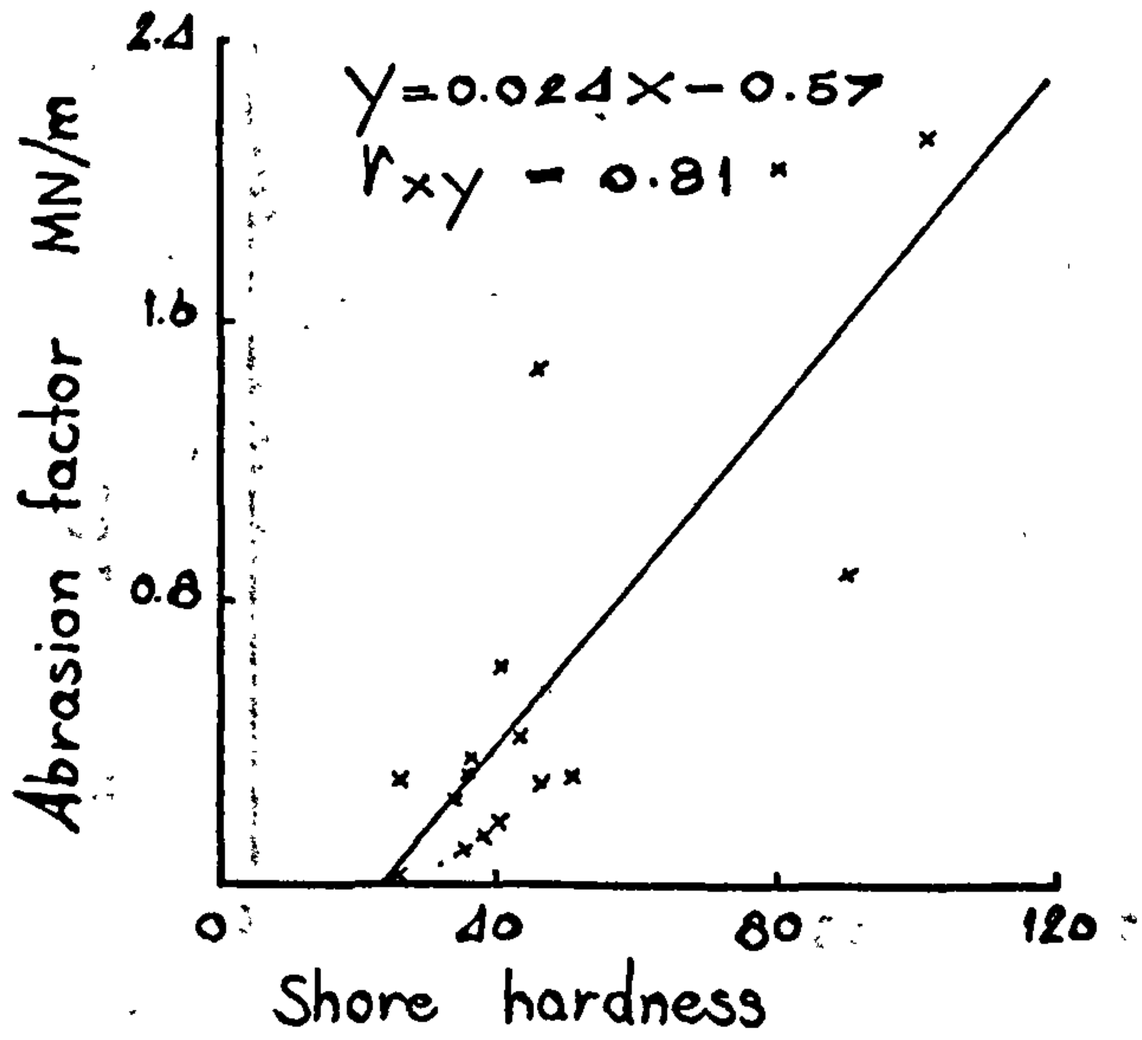
Y = 0.024X − 0.57
r_{xy} = 0.81
Abrasion factor MN/m
2.4
1.6
0.8
0
40
80
120
Shore hardness

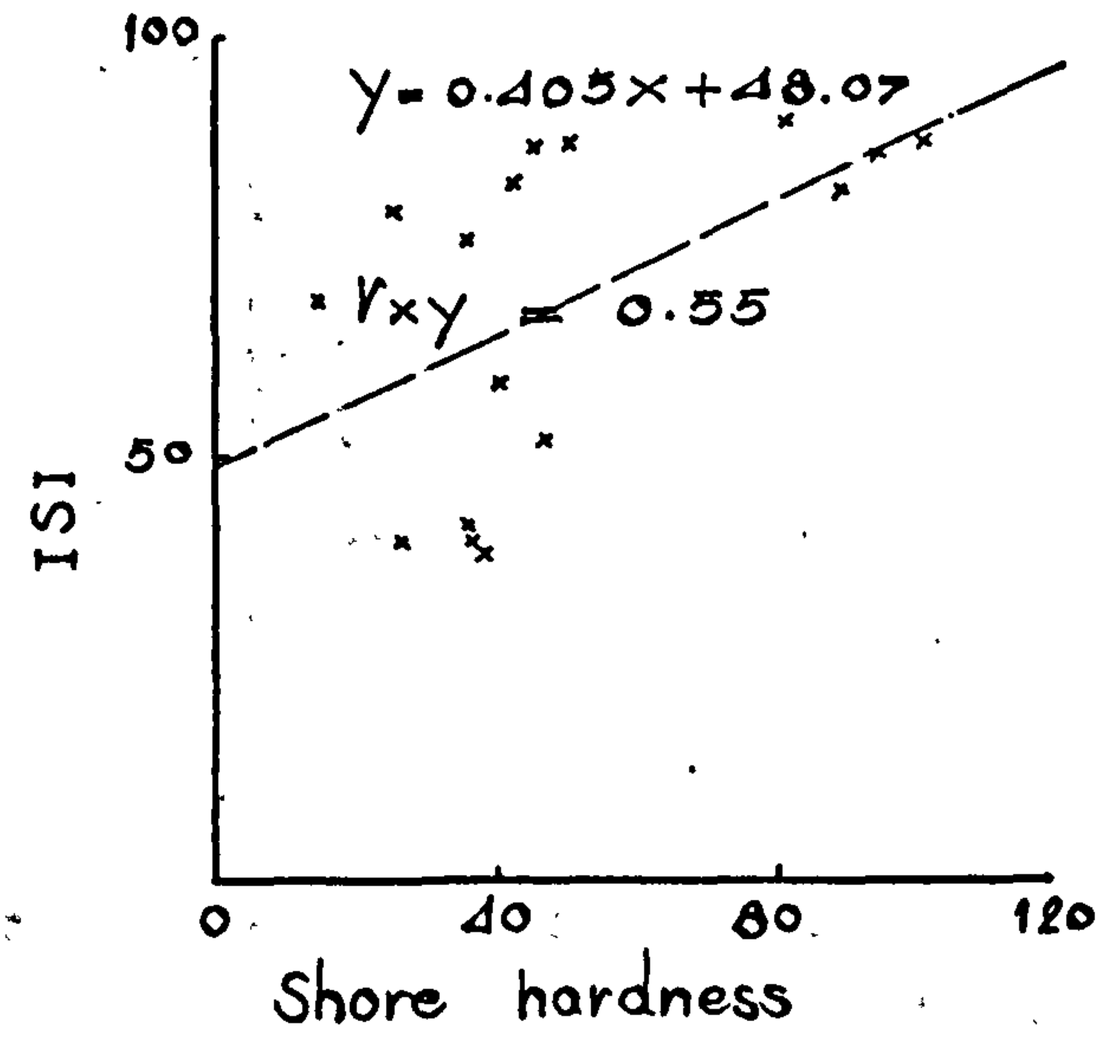
Y = 0.405X + 48.07
r_{xy} = 0.55
ISI
100
50
0
40
80
120
Shore hardness

Figure 17 (34)

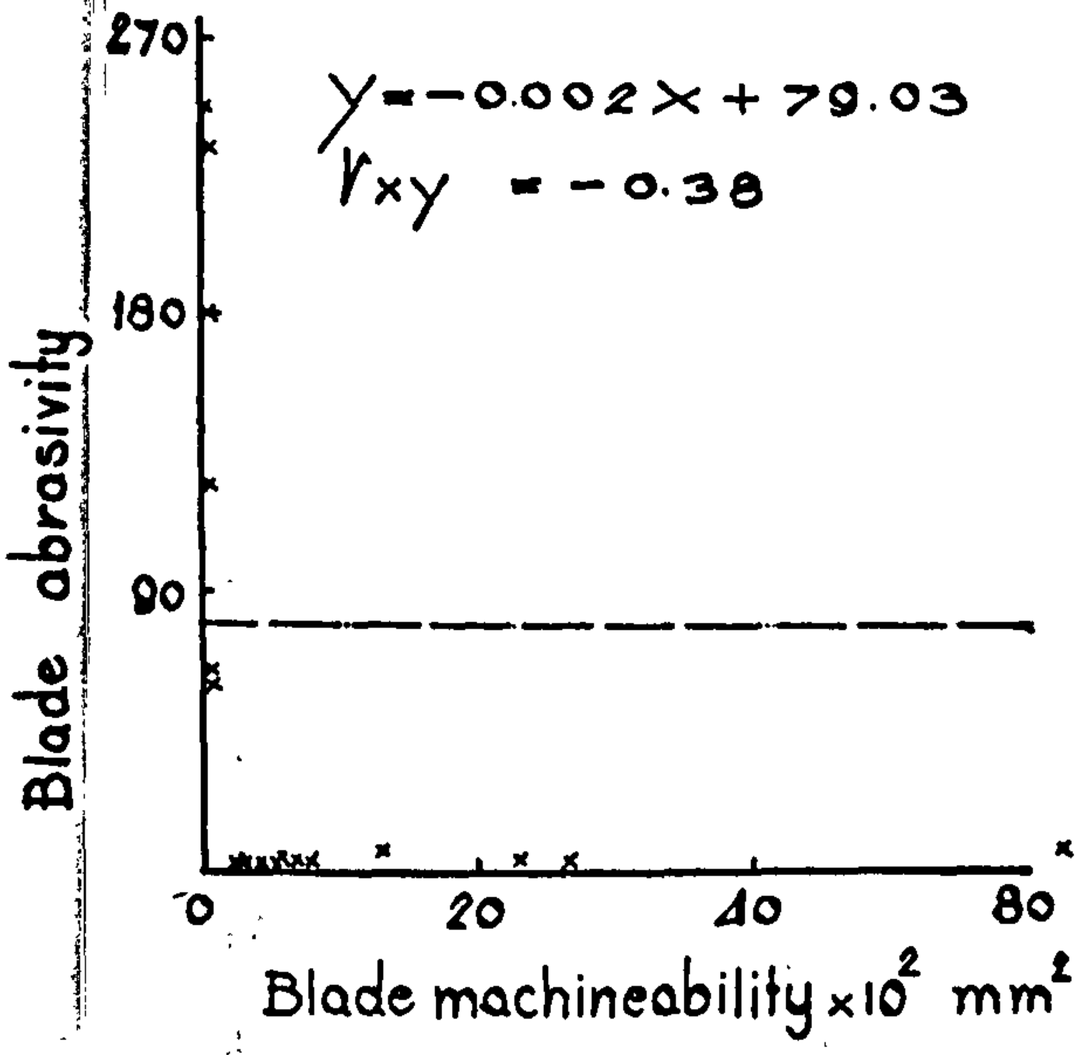
Y=-0.002X+79.03
rxy = -0.38
270
180
90
0
20
40
80
Blade abrasivity
Blade machineability x10² mm²

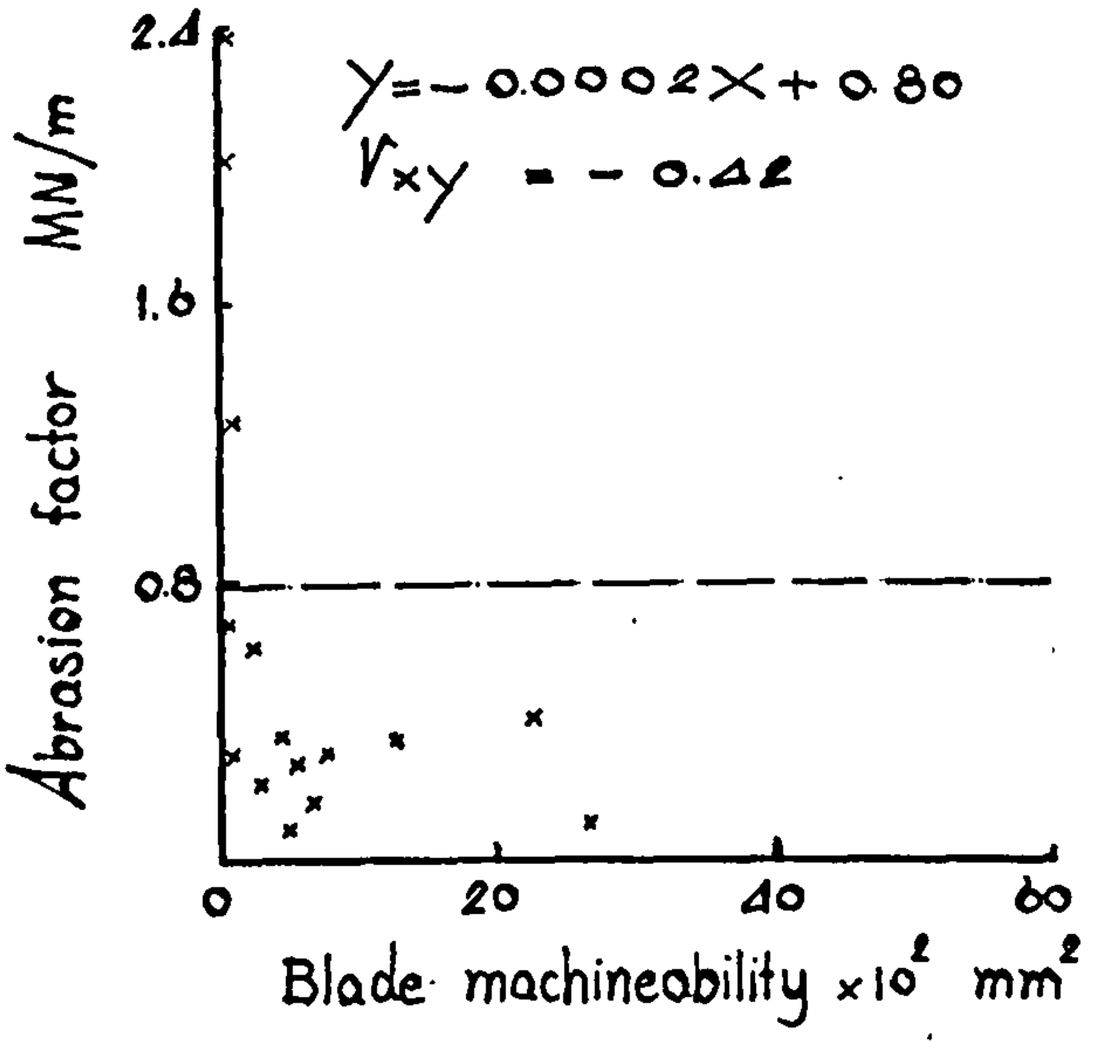
Y=-0.0002X+0.80
rxy = -0.42
2.4
1.6
0.8
0
20
40
60
Abrasion factor MN/m
Blade machineability x10² mm²

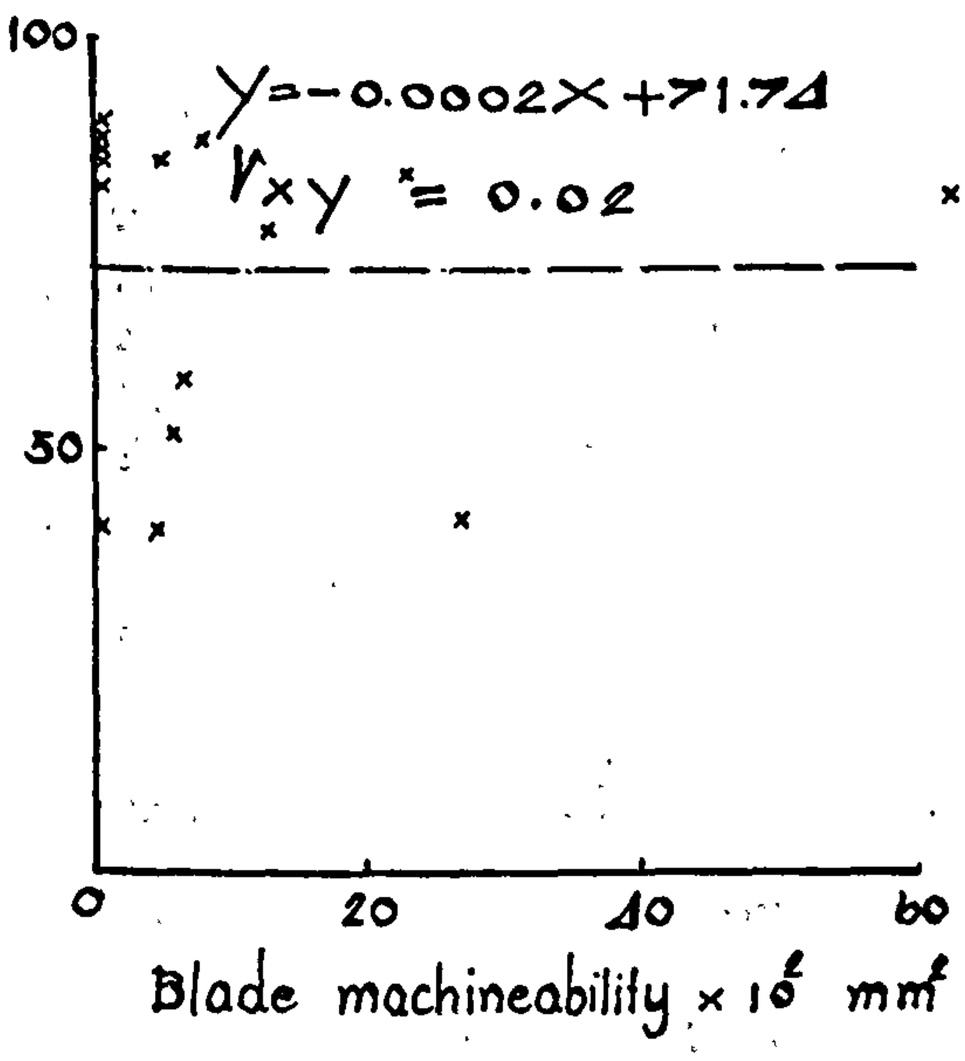
Y=-0.0002X+71.74
rxy = 0.02
100
50
0
20
40
60
ISI
Blade machineability x 10² mm²

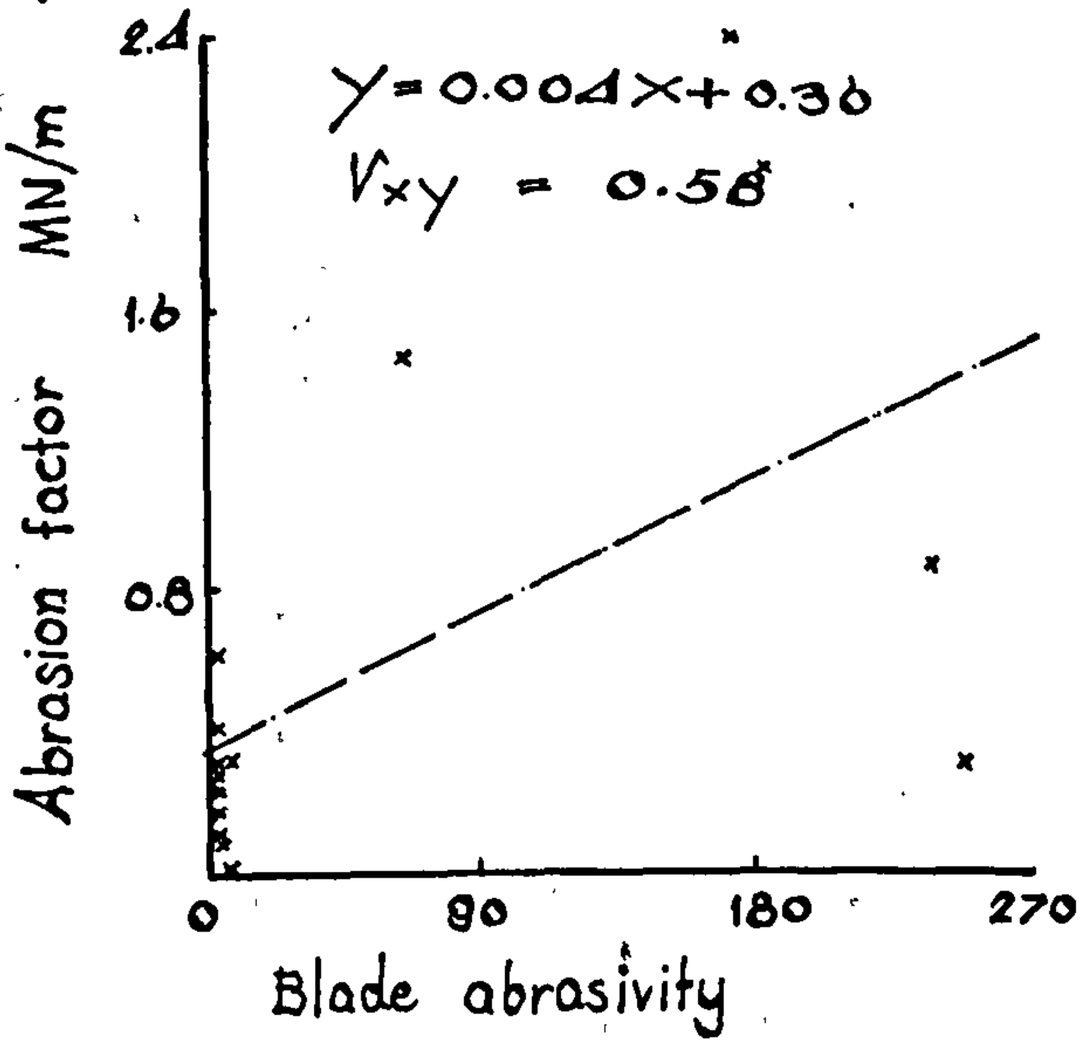
Y=0.0004X+0.36
rxy = 0.58
2.4
1.6
0.8
0
90
180
270
Abrasion factor MN/m
Blade abrasivity

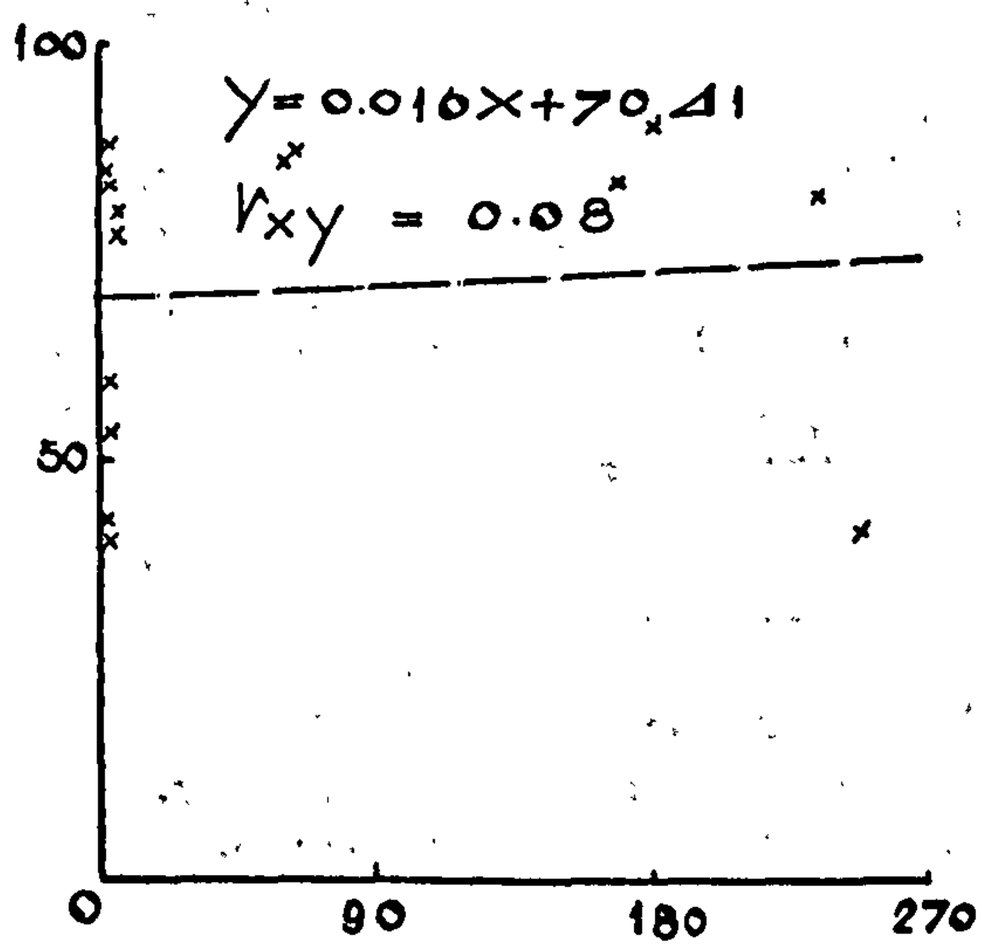
Y=0.016X+70.41
rxy = 0.08
100
50
0
20
40
60
ISI
Blade machineability x 10² mm²

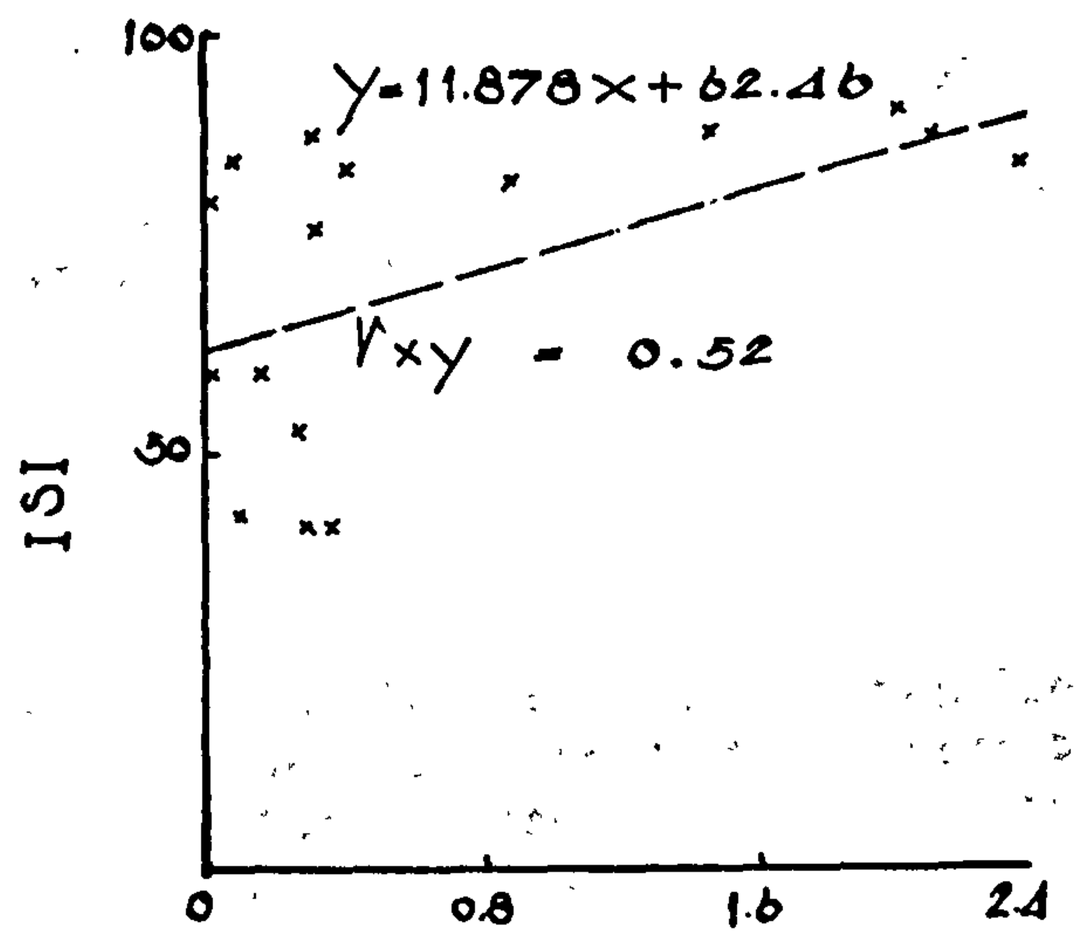
Y=11.878X+62.46
rxy = 0.52
100
50
0
90
180
270
ISI
Blade abrasivity

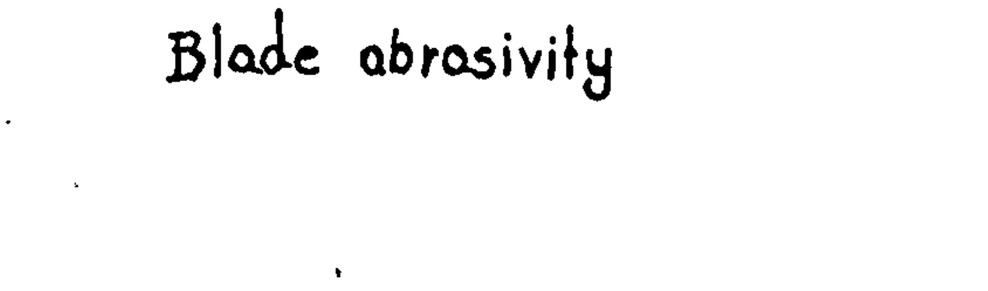
100
50
0
90
180
270
ISI
Blade abrasivity

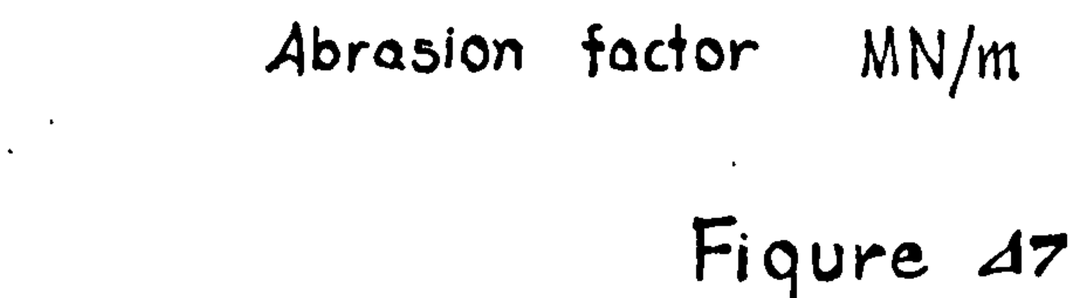
100
50
0
0.8
1.6
2.4
ISI
Abrasion factor MN/m

Figure 47 (35)

Taking $0.70 \leq |r_{xy}| \leq 1.00$ to be accepted as a highly significant statistical correlation, the main conclusions for the linear correlation analysis conducted on the rock properties determined are summarised as follows:-

1. Petrographic analysis - Rock hardness was the only property measured that was found to give a highly significant linear correlation with quartz grain size, whilst quartz content related significantly to porosity, tensile strength, modulus of elasticity, dynamic modulus and impact strength.

The significant relationships between quartz grain size, quartz content and rock hardness are to be expected, as there is a greater probability in a rock containing a high percentage of large grained quartz giving a higher average hardness value, compared with the rock containing a small percentage of quartz in the form of fine grains.

The relation between quartz grain size and quartz content and other properties must be only qualitative since not only the quartz grain size or quartz content affects the said properties but also other factors such as the influence of the bonding matrix.

2. It is well known that rock density varies with the type of mineral constituents and is also inversely related to porosity. In this work the statistical analysis shows that the bulk density relates well with rock strength, modulus of elasticity, dynamic modulus and impact strength index. This is thought to be due to the heavy mineral constituents combining with a strong bonding matrix to form a rock that is able to withstand higher levels of stress and deformation than a rock formed from lower density.mineral.

3. Porosity is one of the major factors affecting rock strength and other properties, such as modulus of elasticity.

4. Compessive strength relates well with indirect tensile strength, having a regression equation of:-

Tensile strength = 0.064 Compressive strength + 0.71
with correlation coefficient = 0.90 at the significance level of 0.01.

Compressive strength also relates well with modulus of elasticity, dynamic modulus and rock hardness.

5. One of the properties influencing the power required by the cutterhead of a boring machine is the tensile strength of the rock. The cutting tool can be assumed to be a wedge which penetrates the rock asymetrically. Evans' (52) has derived the following equation for the peak cutting force (Fc) for this situation.

$$Fc = \frac{2twd \sin \frac{1}{2}(\frac{\pi}{2} - \alpha)}{1 - \sin \frac{1}{2}(\frac{\pi}{2} - \alpha)}$$

where t = tensile strength, α = tool rake angle
d = depth of cut.

The linear relation between compressive strength and tensile strength was found to be highly significant, so that it is theoretically possible to obtain estimates of the cutting force and specific energy for a given cutting situation from the compressive strength. In practice the

errors introduced by the assumptions made at each stage in the calculation could lead to meaningless predictions.

6. The modulus of elasticity and tangent modulus were computed for samples loaded in cyclic compression, whilst only the secant modulus was obtained for samples loaded in tension. This is referred to as the tension modulus.

It was found that the relation between tangent modulus and secant modulus is very good:-

Secant modulus = 0.977 Tangent modulus - 0.58

with r_{xy} = 0.98 having a significance level of 0.01, which is highly significant.

Statistical treatment does show that tangent modulus along with secant modulus relate well with tension modulus, having r_{xy} = 0.99. However it is considered that the number of matched pairs is too small to be accepted.

7. The results from the three types of hardness test do not show any highly significant relationship exists between any other rock properties other than intrinsic abrasivity.

8. For the blade abrasivity test there is no significant relation between this property and any other.

9. It is recognised that high quartz content rock is abrasive, however the intrinsic abrasivity does not relate well to quartz content.

10. Impact strength index correlated well with some of the other properties measured. Poisson's ratio, Cone indenter hardness and blade abrasivity were found to be exceptions.

The correlation coefficient with the corresponding significant level are shown in Table 17A, and the significant level of b in Table 17B.

Linear regression equations have been calculated for the data available, though more information is required before an acceptable degree of confidence can be associated with some of the relationships derived. There is a need for the standard testing procedures to be conducted on carefully selected rock types so that the whole spectrum of rock materials is adequately represented. Future analysis should concentrate on the use of multiple curvilinear regression techniques and subdivision of rock types into discrete categories, such as sandstones, mudstones, etc.

Quartz content is believed to be the major factor determining the abrasivity of rock, however other factors such as grain shape, grain size distribution and the properties of the bonding matrix are also of prime important. The petrographic description should give an idea of the abrasivity of the rock.

Sandstone, is a good example of this. When the sandstone is composed of subangular grains set in a secondary quartz matrix it will be more abrasive than the sandstone which contains nearly the same percentage of quartz, with rounded to subrounded grains and no secondary quartz matrix.

It is also believed that homogeneous sandstone with large grains causes more severe abrasion than the homogeneous sandstone with small grains.

Density and porosity relate well with the other properties. The rock with a relatively large amount of pore space would tend to be weaker than the low porosity rocks.

It is well known that tunnelling machines using drag tools can be employed in non-abrasive formation with compressive strength values lower than 100 MN/m^2. In the next chapter, compressive strength, tensile strength, modulus of elasticity and Poisson's ratio are included in the test matrix to provide information for structural purposes and machine selection.

Rock hardness is recognised to be an important factor in determining the ease with which a tunnelling machine can bore a tunnel.

Abrasivity of rock is an important factor that affects the economical aspects of a tunnelling project and provides a useful idea of the deterioration rate of the picks on the machine.

Impact strength index provides a useful guide for designing a muck disposal system and describes the ease with which the rock is broken down.

It has been decided to include the following tests along with the standard cutting tests on core specimens to provide information on rocks encountered along the line of two proposed tunnelling projects and to provide the choice of tunnelling procedure. These tests are:-

1. Petrographic analysis
2. Bulk density test
3. Porosity test (bulk and true)
4. Compressive strength test
5. "Disc" Tensile strength test
6. Young's modulus test
7. Hardness test (Shore and Cone indenter)
8. Blade "Hacksaw" machineability test
9. Impact strength index test

These methods of testing which would be used for assessing rock cutability are summarised to indicate their spheres of usefulness in Table 18.

Table 18 Summary of Methods Used to Assess Rock Cutability

Method	Lab. Test	Effectiveness	Rock Classification	Remarks
Core Cutting	Yes	Very Good	Specific Energy	Results very reliable. To optimise cutting efficiency a great deal of research must be carried out.
Abrasion Test	Yes	Good	Abrasivity	A good method for assessing abrasivity on a long term basis. Further research is still required,
Compressive Strength	Yes	Good	Strength	Expensive and often unreliable.
Tensile Strength	Yes	Good	Strength	Expensive and often unreliable.
Cone Indenter	Yes	Reasonable	Strength via Hardness	Easy statistical approach.Regular inspection of cone is essential.
Shore Scleroscope	Yes	Reasonable	Strength via Hardness	Easy statistical approach.
Schmidt Rebound Hammer	No	-	Strength via Resilience	Moderate cost field instrument.
Hacksaw Machineability	Yes	Reasonable	Abrasivity and Machineability	Many more rocks must be tested and the results statistically analysed to predict cutability with confidence.
Impact Strength Index	Yes	Doubtful	Strength	Further research is still required.

Chapter 8

Site Investigation

In the previous chapters the technique of rock property testing and the inter-relation between these properties have been described, However these properties of rock alone do not fully explained the main interest in the rock cutting mechanics. The rock cutability can only be obtained by performing the rock cutting test which could be block cutting or core cutting, in the laboratory depending on the availability of rock samples. This test gives information from which the type of tunnelling machine can be selected.

In the proposed tunnelling programme, it is recognised the many different rock types are to be encountered in a tunnel drive. These are rarely of a homogeneous nature and therefore it is desirable to assess in-situ rock. The ideal situation is to assess rocks obtained from a horizontal borehole which follows the line for the proposed tunnel. This however, is seldom possible owing to the economic commitment of such a scheme. A more practical solution is to use a series of vertical boreholes which intersect the proposed tunnel line at predetermined points.

The quantity of test results required depends on the lateral variation of the strata along the tunnel line. Machineability and abrasivity tests should be performed for each strong or abrasive stratum which may occupy a certain length of a tunnel drivage. The number of tests should increase with thickness of stratum to provide variability within a given stratum.

This chapter contains information on the machineability and abrasivity of strata from two proposed tunnel projects namely the Tyne-Tees aqueduct tunnel and the Tyneside Rapid Transit tunnels.

The aim of this series of tests is to provide a basis for the choice of tunnelling procedure, especially if any tunnel boring maching selected to ensure that feasible plant, will be employed for the conditions anticipated.

8.1 Core testing methods

Methods for determining the cutability of rock have been developed at the University's Department of Mining Engineering as part of the research programme in rock cutting mechanics. In the design and development of these techniques, the argument is used that for a test procedure to be meaningful, it should resemble the general mode of action of tunnelling machine cutting tools. Attention must be given also to the abrasivity of the rock material and an assessment made of the rate at which cutting tools are likely to wear.

The core cutting test involves undertaking cutting tests on core samples, using a 12.7 mm wide chisel tool made of Tungsten Carbide (3½ μ grain size 10 % Cobalt). The tool has a front rake angle of -5° and a back clearance angle of 5°.

The tool cuts a slot nominally 5 mm deep axially along the peripheral surface of the core specimen. The cutting force Fc and normal

force Fn generated on the tool during cutting are continuously integrated and recorded. The cutting rig and instrumentation system was described in section 3.3.

Figuro 48 shows a schematic arrangement, the core sample is held firmly in a vice having concave jaws. After taking the first cut, the core sample is rotated through 90°and a repeat test undertaken. Thereafter, 2 further cutting tests are undertaken on the same core, giving four test replications.

The cutting and normal forces and their integrated values are recorded on U.V. chart. These recordings require detailed analysis, Under the action of cutting tools, rock behaves in a brittle fashion and this gives rise to cutting force characteristics, which may be typified as shown in Figure 49. As the tool proceeds through the rock, the force fluctuates in a saw-tooth pattern with a rapid succession of peak forces, each of which is associated with the breakage of chip or fragment of rock. The average size of these peak forces is an important cutting parameter, known as Mean Peak Cutting Force (Fc). The normal force, tending to push the tool out of the rock, fluctuates in similar fashion and this gives rise to a second important parameter Mean Peak Normal Force (Fn).

The area under the cutting force recording (shown cross-hatched in Figure 49), is a direct measure of the energy expended in cutting the rock and if the weight or volume of rock can be calculated. This provides the most important and meaningful parameter of rock cutability, referred to as Specific Energy. This is normally quoted in Megajoules per cubic metre (MJ/m^3) numerically the same as Joules per cubic centimetre (J/cm^3). In older literatures, it is often quoted in imperial units as $ft.lbs/ft^3$ or $in.lbs/in^3$. Specific energy, defined as the energy required to excavate unit volume of rock, is a most useful parameter since it can readily be translated into cutting power requirements to excavate rock at a specific rate. Specific energy is not a unique quantity for a rock material and is affected by several cutting tool and machine design parameters. For example, by changing the geometry of a cutting tool, the forces, and thereby energy, required to cut the same volume of rock are altered. This shows that machine design also influences the ease with which the rock can be excavated.

It is for this reason that the core cutting test has been standardised using a fixed tool shape, at a standard depth of cut, cutting speed and using a constant grade of Tungsten Carbide (Figure 50). This provides values of specific energy which can be used for a direct comparison of rock types, but which can also be adjusted to take account of the type of tool and method of attack to be employed by the proposed machine.

The test procedure closely resembles the cutting action of machines which use drag picks. Many hard rock full face boring machines in fact use free rolling cutters, such as discs. The precise action of such tools is difficult to simulate on a small scale, particularly for use on small core samples. Since all mechanical cutting systems rely on the penetration of a wedge into the rock surface, the drag pick test can be taken as a measure of cutability representative of the common mechanical cutting systems. The variation in performance levels of the different types of cutter in a given rock. Relationships between the performances of the different types of cutter in the same rock have been investigated by

Arrangement for core cutting test

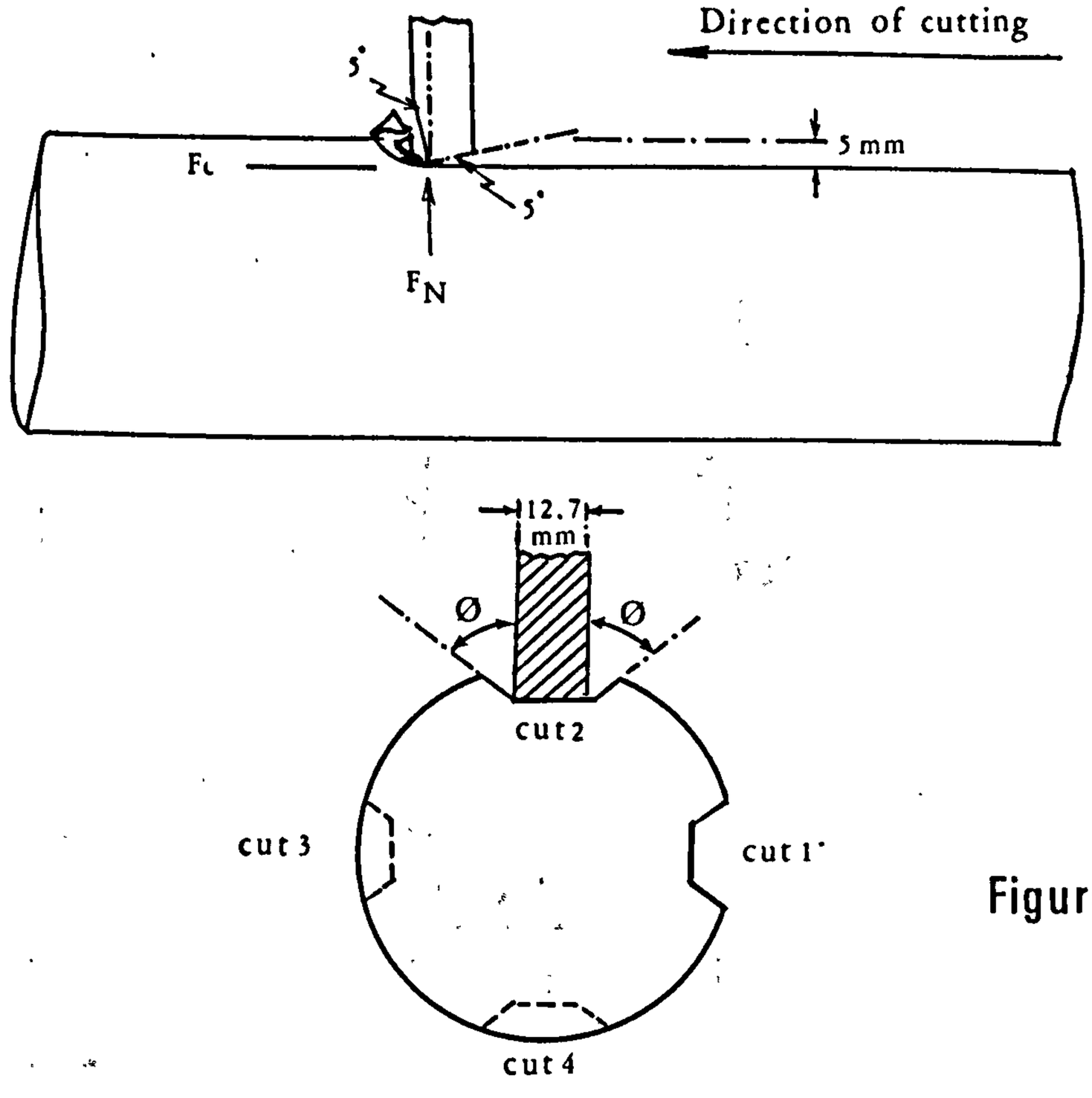

Figure 48

Cutting force diagram

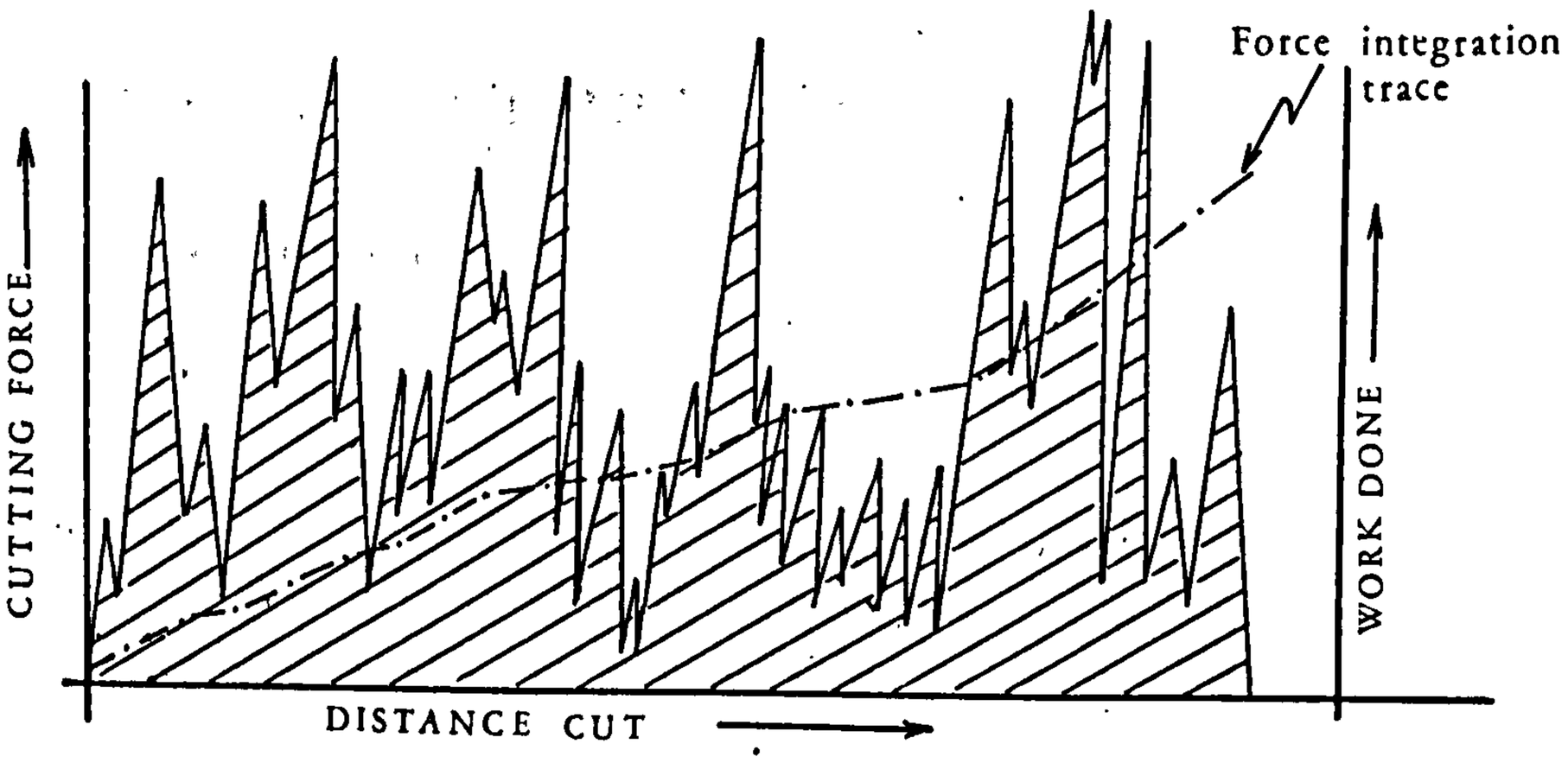

Figure 49

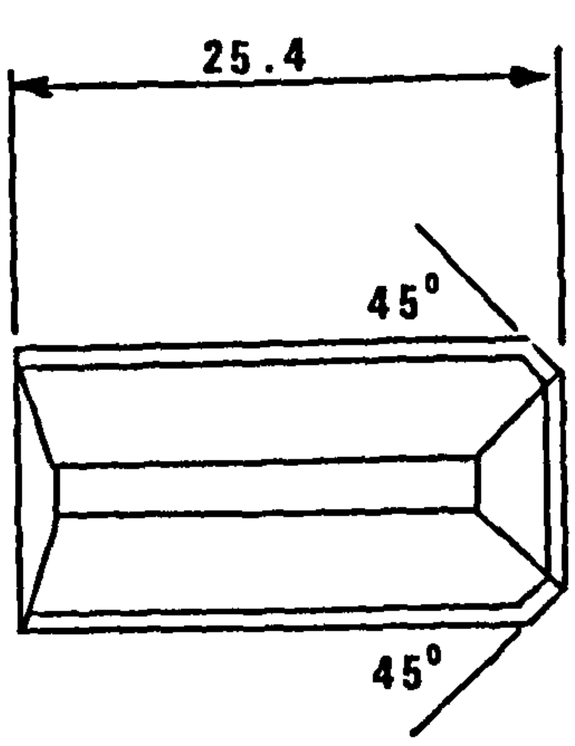

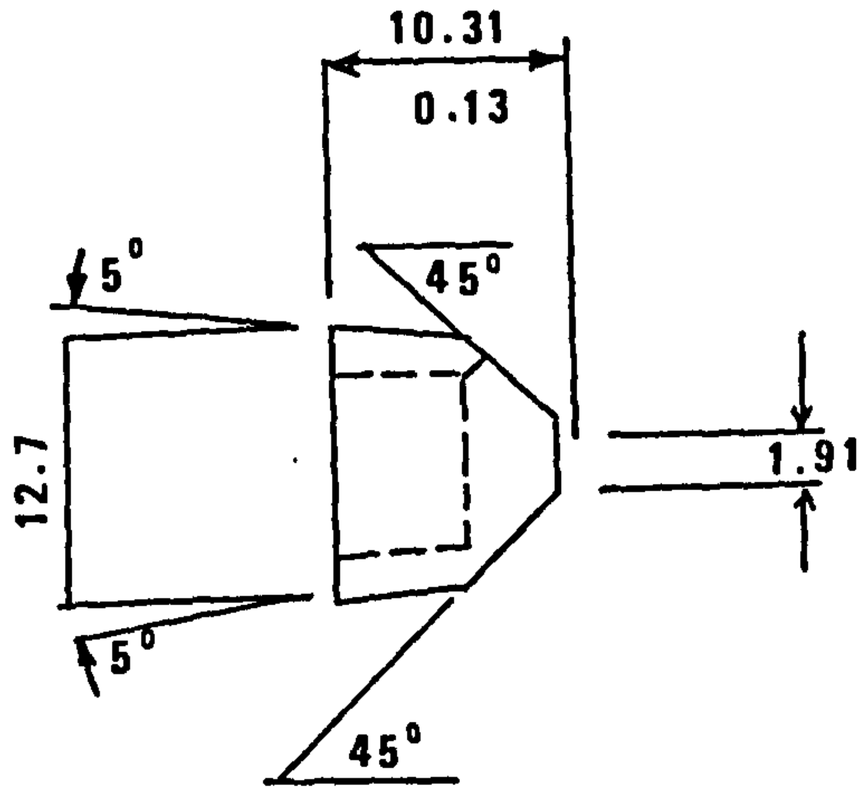

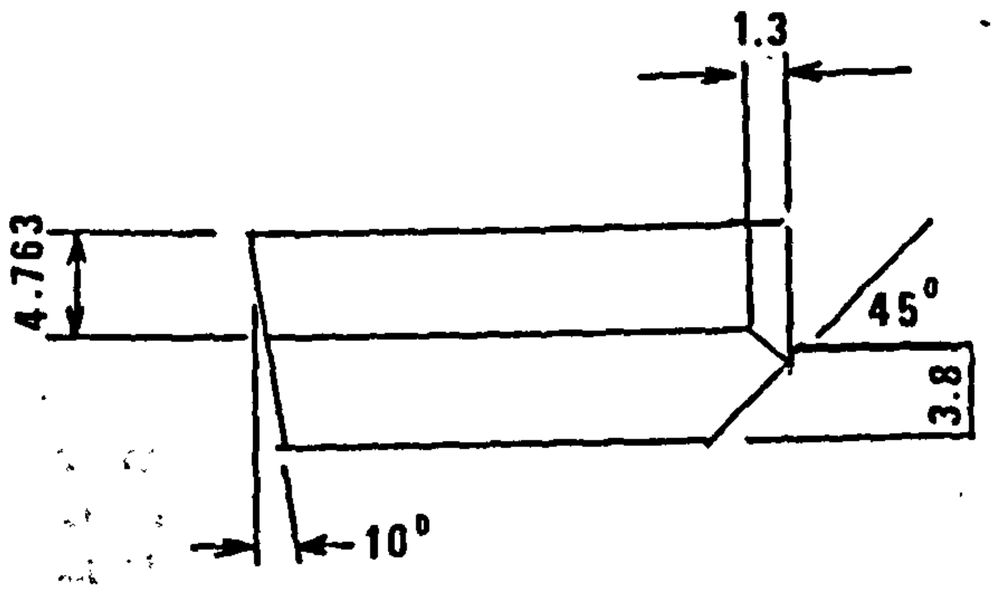

All dimensions in mm

Tip for use with standard shank type 2

5° effective rake angle

Figure 50

several researchers in this field.

Three additional quantities are evaluated from the same cutting tests.

1. Coarseness index - A measure of the size distribution of the rock debris produced during cutting. It is a non-dimensional number, being the sum of cumulative weight percentages of each size fraction into which the sample has been graded. Its range depends only on the number of size fractions taken, providing the cumulating procedure begins with the largest fraction and progressively adding the weight percentages of the smaller fractions. The value of C.I. is arbitrary and must be related to the size of the sieves used. Sieve sizes must, therefore, be selected to suit the size range of the debris. An example of coarseness index and its derivation will clarify the definition.

Size fraction	Wt. (gm)	Wt.%	Cum.Wt. %
+ 25 mm	0	0	0
-25 mm + 8 mm	15	30.0	30.0
- 8 mm + 8 mesh	22	44.0	74.0
- 8 mesh + 30 mesh	8	16.0	90.0
-30 mesh +120 mesh	4	8.0	98.0
-120 mesh	1	2.0	100.0
	50	100.0	= 392.0 = C.I.

In this case, the coarseness index (C.I.) is 392. Note that the maximum possible value of the 6 size fraction is 600, corresponding to all material being larger than 25 mm. Similarly, the minimum value must be 100, corresponding to all material being - 120 mesh.

This parameter provides a useful guide on the relative size distribution of rock debris influencing a muck disposal system.

2. Cutting tool wear - A pristine tool is used for each series of four tests on a core. The wear on the tool is measured by accurately weighting of the carbide lost during the test and is expressed as milligrams lost per metre of linear cutting (tool wear is a function of distance cut by the tool, rather than the volume of rock cut).

3. Breakout angle - The groove produced in the rock due to cutting has a larger cross-sectional area than the area swept by the cutting tool. The rock breaks out on each flank of the tool such that the sides of the grooves are inclined to the vertical. The angle of the breakout (θ in Figure 48) has an important bearing on the spacing of cutting tools on a machine. If the breakout angle is small then it is probable that cutting tools on a tunnelling machine will need to be set very close together and this will result in the need for a large number of cutters completely to excavate the rock face. If breakout angle is large, then the cutters can be widely spaced and thereby the total power to excavate a rock face may not be as great as indicated by specific energy alone.

Abrasive wear is the other quantity to be evaluated using a lathe, in which the undersized core remaining after completing the core grooving

tests is rotated between centres. A tungsten Carbide tool, having the same specification described above, is fed longitudinally along the core surface, taking a small, but continuous, cut of approximately 25 metres in length.

Abrasive wear is a function of both tool material and rock mineralogy and is the gradual erosion of the substance of the tool due to the hardness of mineral constituents in the rock. Therefore it is necessary to adopt a standard material for all test work. Because of its common and increasing use in rock excavation, Tungsten Carbide provides a very convenient standard. The hardness of Tungsten Carbide is, however a variable according to its recipe and quality of production. A medium grade of Carbide was selected, having a nominal grain size of 3½μ and 10% Cobalt content.

Carbide wear rate was assessed by weighing the tip to an accuracy of 0.1 mg at intervals during the test and relating this to the distance cut.

8.2 Associated rock properties

Associated rock properties, which are suitable for cored samples, are also evaluated to provide a reasonably description of rock. These properties are:-

1. Compressive strength
2. "Disc" tensile strength
3. Shear strength
4. Young's modulus (tangent modulus)
5. Schmidt rebound number
6. Wet bulk density
7. Shore hardness
8. Cone indenter hardness
9. Impact strength index
10. Blade (Hacksaw) machineability
11. Dry bulk density
12. Grain density
13. Apparent porosity
14. True porosity.

8.3 Test results

Core specimens have been coded according to the system established by the Consulting Engineers, Messrs.Babtie, Shaw & Morton in the case of Tyne-Tees aqueduct tunnel, and by Messrs. Mott,Hay and Anderson in the case of Tyneside Rapid tunnels.The systen are used throughout the site investigation work.

The results of experiments, however, are presented as a series of tables which shows all values for each major stratum irrespective of location in the line of the tunnels.

Symbols and dimensions for the cutting test results in the tables are:-

Fc	= Mean cutting force (KN)
F$\dot{c}$	= Mean peak cutting force (KN)
Fn	= Mean normal force (KN)
F$\dot{n}$	= Mean peak normal force (KN)
S.E.	= Cutting Specific Energy (MJ/m^3)
	= Cutting Specific Energy (J/g)
C.I.	= Coarseness index of rock debris (dimensionless)
θ	= Rock breakout angle (°)
Cutting wear	= Carbide loss during core slotting test (mg/m)
Abrasive wear	= Carbide loss during long term wear test (mg/m)
Yield	= Weight of rock removed (kg/m).

8.4 Interpretation of cutability results

Tests carried out on core specimens have produced measures of cutting energy, tool forces and wear for each of the major stratum along the proposed tunnel line.

Specific energy provides the most reliable guide of rock cutability and the relative ease with which the various rock materials can be excavated by machine can be assessed by direct comparison of this parameter. Cutting and abrasive wear values also provide a basis for comparing the relative rates at which cutting tools are likely to deteriorate during the excavation process.

Some general indication of the energy or power levels required by a machine can be derived from the test results. Compared with the energy involved in boring a rock face by machine. The cutting procedure used in the test work is an efficient operation. The efficiency of cutting rock by machine is dominated by the type of cutting tools used (i.e., picks, discs, roller cutters, etc.) and also very much influenced by several design and operation variables (e.g. tool size and spacing, axial thrust, speed of head rotation, etc.).

Generally, machine which employ drag picks as the principal cutting element have a high cutting efficiency. This efficiency varies from one machine to the other, but as a category or class of machine the drag pick type breaks more rock per unit input power than any other type of commercially available machine. However, the cutting tools are more vulnerable to and sensitive to wear and breakage. Cutting with blunt or broken tools reduces cutting efficiency dramatically and this type of machine rapidly becomes ineffective in strong and abrasive rock materials. It is therefore, restricted in application to the weaker, non-abrasive rock of up to approximately 100 MN/m^2.

Boring machines using disc cutters, roller cutters or button cutters are much less mechanical efficient than drag pick machines, but in stronger and more abrasive rocks they are much more effective. This machine is less sensitive to variations in rock hardness and its cutting tools are less exposed to the problems of abrasion and damage. Efficiency is low, but effectiveness in strong ground is comparatively high. This type of machine is, however, invariably deployed in full face attack under the constraint of a high axial thrust and this can make a severe demand on mechanical reliability when excavating a face which exposes is significant proportions more than one rock type. If one part of the face, for example, consists of strong rock and another is of a significantly weaker rock then this could lead to excessively imbalanced forces

on the cutting head. This is a situation where machine steering and control could be a problem, coupled with the attendant risk of main bearing collapse.

Drag pick machines could be expected to require a Specific Energy of between 1.5 and 3 times the values obtained from the cutting tests, allow for severe wear.

Disc and other rotary cutter machines will require a Specific Energy of between about 6 and 9 times the values obtained from the cutting tests.

The machine power requirement is clearly related to the rate of excavation and as a basis for comparison, it is assumed that the proposed tunnel has a nominal bore size of 3.5 m and the required rate of boring is 1 meter per hour. This is equivalent to an excavation rate of 9.63 m^3/hr or $26.73 \times 10^{-4} m^3/sec$.

For a cutting Specific Energy of, say 20 MJ/m^3, then the power required to excavate at the above rate = $(20 \times 10^6) \times (26.73 \times 10^{-4})$ Watts
= 53.47 KW
= 72 H.P.

1. Using a drag pick type machine= 100 - 200 H.P.
2. Using a disc-rotary cutter type machine = 400 - 600 H.P.

For a drivage rate of 1 m/hr in a 3.5 m diameter tunnel, therefore, the following factors may be applied to provide a rough guide to machine power requirements for boring in a given rock type of known standard Specific Energy values:-

1. Drag pick type machine H.P. = (5-10) x S.E. in MJ/m^3
2. Disc/rotary cutter type machine H.P. = (20 - 30) x S.E. in MJ/m^3

The range of power requirement for a given machine type appears to be high, but it is impossible to give a more precise indication without reference to details of machine design. The breakout angle of the rock (θ) measured during the cutting test work gives a general indication of the way in which the rock is likely to fracture under the action of cutting tools. A large breakout angle usually means that cutting tools in array can be disposed relatively far apart, so that the total munber of tools on a machine cutting head is reduced, often leading to a saving in both power and consumption of tools. For example, for a fixed depth of cut or penetration into the face, rock having a breakout angle of 75° can be excavated by tools whose separation is twice that required when the rock has a breakout angle of 60°.

In general and all else being equal, the number of cutting tools(N) required to excavate a rock face decreases as the breakout angle increases, roughly as follows:-

$$\frac{N_1}{N_2} = \frac{\tan^{-1}{}_1}{\tan^{-1}{}_2}$$

So, in two rock materials of otherwise similar cutting and abrasive characteristics, the one showing the higher breakout angle is likely to be the better cutting proposition where arrays of tools are to be used. Conversely, the forces on individual tools will be higher with the larger breakout angle, size the greater amount of breakout means a larger rock yield per tool. If, therefore, the Specific Energy is the same, it follows that the forces on the tool must be correspondingly higher.

The cutting force generated by a drag pick is directly proportional to the width of the tool and to its depth of cut, so that the values of mean and mean peak cutting force for drag picks can be interpreted for different sizes of tools operating at different depth of cut.

The normal force values provide an indication of the axial or crowding thrust required to cause the tool to penetrate the rock face and maintain the required depth of cut. Again, the normal force values are directly proportional to tool width and depth of cut.

For disc/rotary cutters, the axial thrust component per tool can be estimated as approximately 20 times the Fn values for drag picks.

Table 19 gives measured values of Specific Energy using drag picks for similar shape and size to those used in the test programme, when cutting in a range of other rock materials. It is important to note that compressive strength, although showing a general tendency to increase with Specific Energy, does indicate several significant departures from this generality. The Specific Energy for Gypsum provides a good example. Gypsum is non-abrasive and according to compressive strength a weak rock at 30-50 MN/m^2, it is a difficult rock to cut according to S.E. values recorded from cutting tests in the laboratory. In fact, several given machines employing drag picks have been used to excavate this rock and although each machine has performed differently, in general rates of extraction have been low and certainly much less than anticipated on the basis of compressive strength. Gypsum has, therefore, been found to be a difficult rock to excavate by machine according to both practical experience and laboratory cutting tests.

Table 19 Specific Energy Values for a Selection of other Rock Materials

Rock type	Location	Cutting S.E. range (MJ/m^3)	Compressive strength (MN/m^2)
Lower chalk	Hertfordshire	1-2	32-38*
Weak coal	Cwmtillery Garw	1-3	7-20*
Mudstone	Gran Sasso	2-3	30-32*
Strong coal	Barnsley Hards	3-5	60-70*
Sandstone	Scotswood	6-8	40-50
Sandstone	Darley Dale	8-12	85-95
Sandstone	Hunterston	8-12	65-70*
Limestone	Hinkley Point	12-18	110-150*
Sandstone	Pennant	15-25	140-160
Anhydrite	Whitehaven	20-25	100-120
Quartzite	Stilfontein	24-32	110-170
Gypsum	Sherburn	30-35	30-50*
Quartzite	Doornfontein	35-50	160-200
Whinstone	Northumberland	45-60	300-320

(* Rock materials in which commercial tunnelling or bulk excavation machines have been employed)

The Hinkley Point limestone has been quite successfully excavated by the Greenside - McAlpine single drum machine in a shallow tunnel of approximately 3.5 m diameter. Drivage rates of between 3 and 5 metres per shift were regularly achieved.

The same machine was used in the Hunterston sandstone to drive a similar tunnel. This operation was not successful and the machine was withdrawn due to the excessive wear on tools and machine components resulting from the highly abrasive nature of the rock.

8.5 Tyne - Tees aqueduct tunnel

It is more common to convey large quantities of water over long distances with the excessive demand on local water sources within large conurbations. Teeside is one such conurbation where the industrial and consumer water requirements will exceed the local supply within the next few years. The Northumbrian River Authority is building the £ 27 million Kielder reservoir to supply the Teeside area with some 200 million gallons of water per day. The Tyne - Tees aqueduct will link the Tees, Wear and Tyne with the Kielder reservoir. The proposed aqueduct will be 25 miles long of which 21 miles will be tunnel under the Northern Penines (Figure 51). It is proposed to install regulators at the Derwent and Wear.

Twenty eight rock samples which range stratigraphically from the Upper Carboniferous Limestone through the Millstone Grit Series to the Lower Coal Measures, a sample of dolerite has also been selected. These samples have been obtained from the Northumbrian River Authority's exploratory boreholes which have been drilled as part of the preliminary site investigation for the proposed Tyne - Tees water tunnel.

The details in physical, mineralogical and mechanical strength properties of cored rock samples recovered from a spread of boreholes along the approximate route of the proposed Tyne - Tees aqueduct tunnel are reported by the Robertson Research laboratories (95).

The objective of this test work is to define the mechanical cutting characteristics of the various rocks and thereby, provide data in decisions concerning the potential of tunnel boring machines as a means of primary excavation.

8.5.1 General geology

The tunnel lines will traverse a sequence of sedimentary rocks ranging from Upper Carboniferous Limestone through the Millstone Grit Series to the Lower Coal Measures.

The Lower Coal Measure will only be encountered in the Graymare Hill tunnel section. They are made up of an interbedded sequence of shales, mudstones and sandstones. The tunnel will pass through the base of the sequence which is predominately sandstone. The bed of most significance is Letch House Sandstone, which accounts for approximately 50% of the drivage medium. The base of the Lower Coal Measures is taken as the Ganister clay coal.

The Millstone Grit Series includes all strata between the Ganister clay coal and the base of the Great limestone. They will be traversed in the Airy Holm - Derwent, Derwent - Wear (full sequence) and Wear - Tees tunnel sections. The sequence is similar to the Lower Coal Measures being made up of shales, mudstones and sandstones. Limestones are present, these being more predominant at the base of the sequence. The Airy Holm-Derwent tunnel is contained with one stratum the Airy Holm sandstone

(First Grit), this is predominantly moderate to thick bedded, medium to coarse - grained sandstone of "grit - type" facies.

The Carboniferous Limestone Series accounts for all the strata below the great limestone which will be encountered in the Derwent - Wear and Wear - Tees tunnel sections. The sequence is again similar to the overlying Millstone Grit Series, although they have much more distinctive cyclothems.

Igneous rocks may be encountered in the Wear - Tees section where the tunnel line approaches the estimated upper boundary of the Little Whin Sill and where it passes through the vertical or near vertical Hett and Cleveland dykes. The sill and dykes are composed of a very hard, blue - grey, fine grained dolerite. The Derwent - Wear and Wear - Tees tunnels pass through the outer margins of the Northern Penines Orefield and there are several recorded mineral veins. The minerals associated with these veins are galena, sphalerite, quartz, fluorspar and calcite.

The general structure of the rocks throughout the four tunnels is comparatively simple, The beds are horizontal, gently undulating or very gentle inclined (unlikely to exceed 5°) except near some faults where steepening of dips may occur.

8.5.2 Summary of cutability and associated data

The following tables show all relevant cutting and associated data collated according to rock type. This provides some indication of the variability likely to be encountered within a given stratum.

Supplementary data, such as shore hardness, Impact strength index, is included only to supplement the main cutting data. One or more of these parameters may be recognised by a contractor or machine manufacturer as relevant to past experiences with machines in ground assessed using such bases.

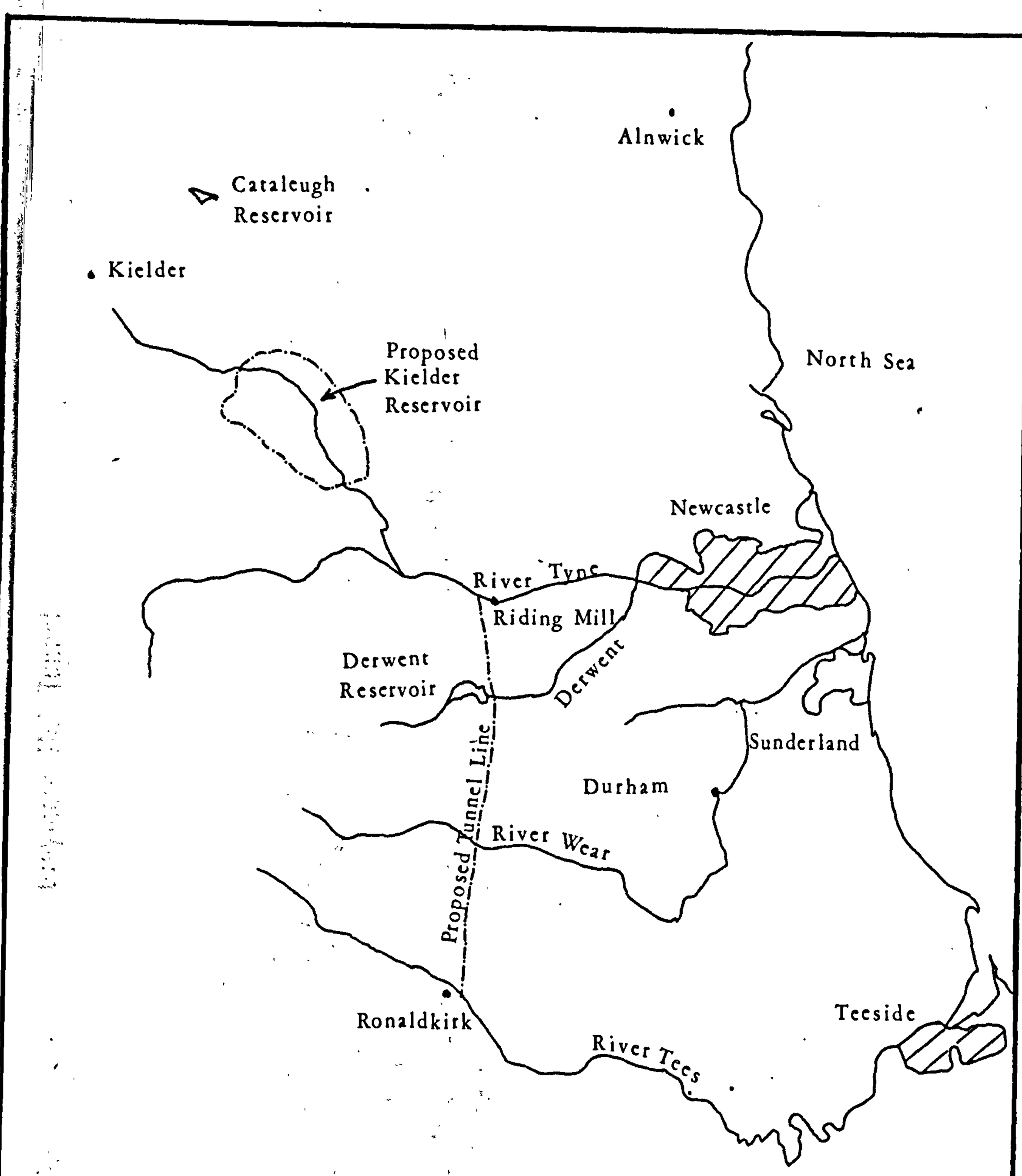

Scale : 10 miles to 1 inch

Figure 51

Greymare Hill Tunnel

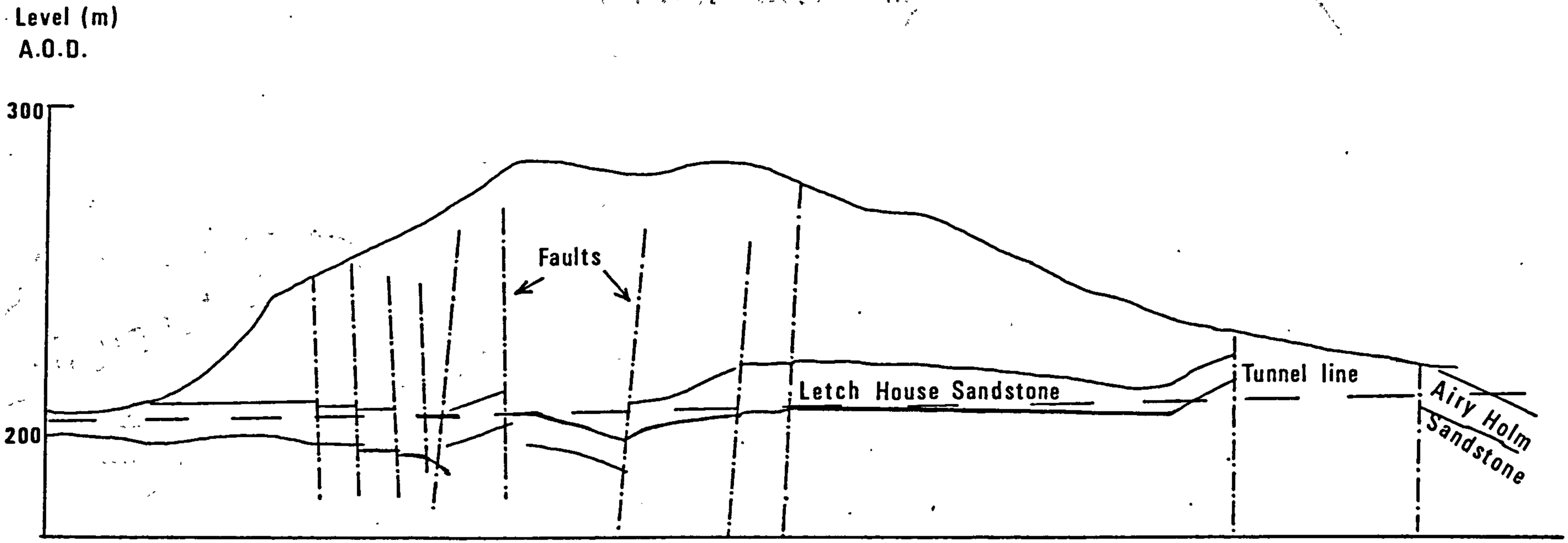

Figure 52

Airy Holm — Derwent Tunnel

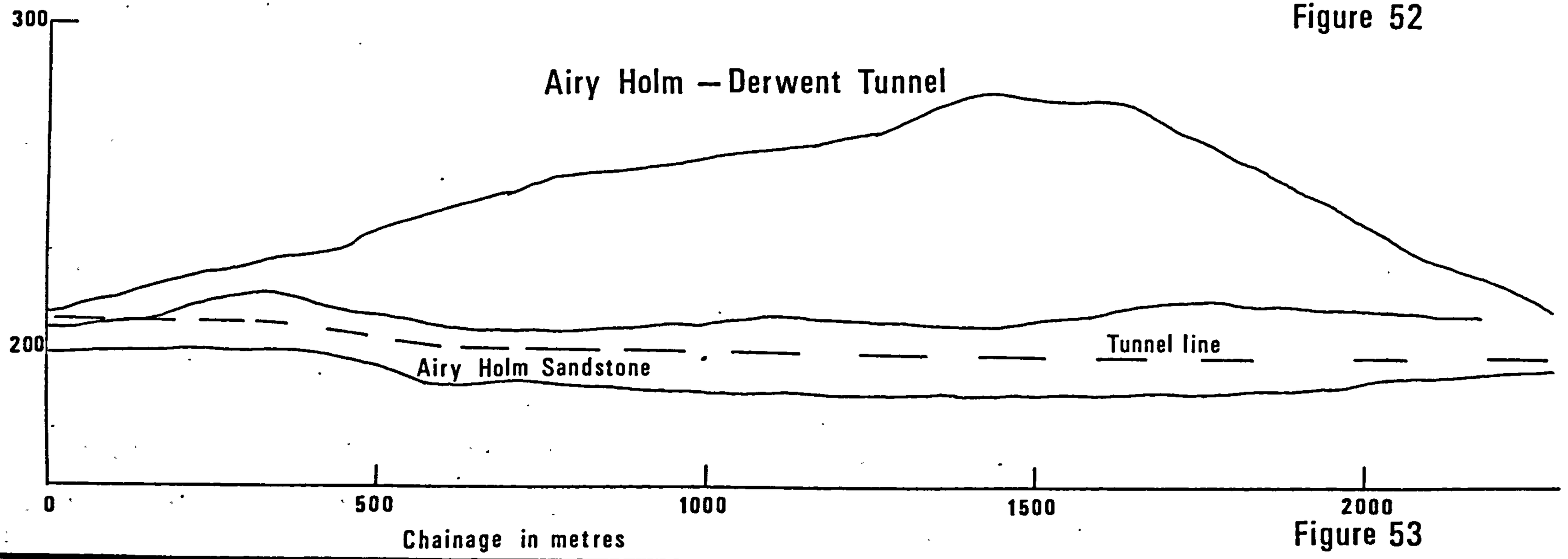

Figure 53

Level (m)
A.O.D.

Derwent – Wear Tunnel

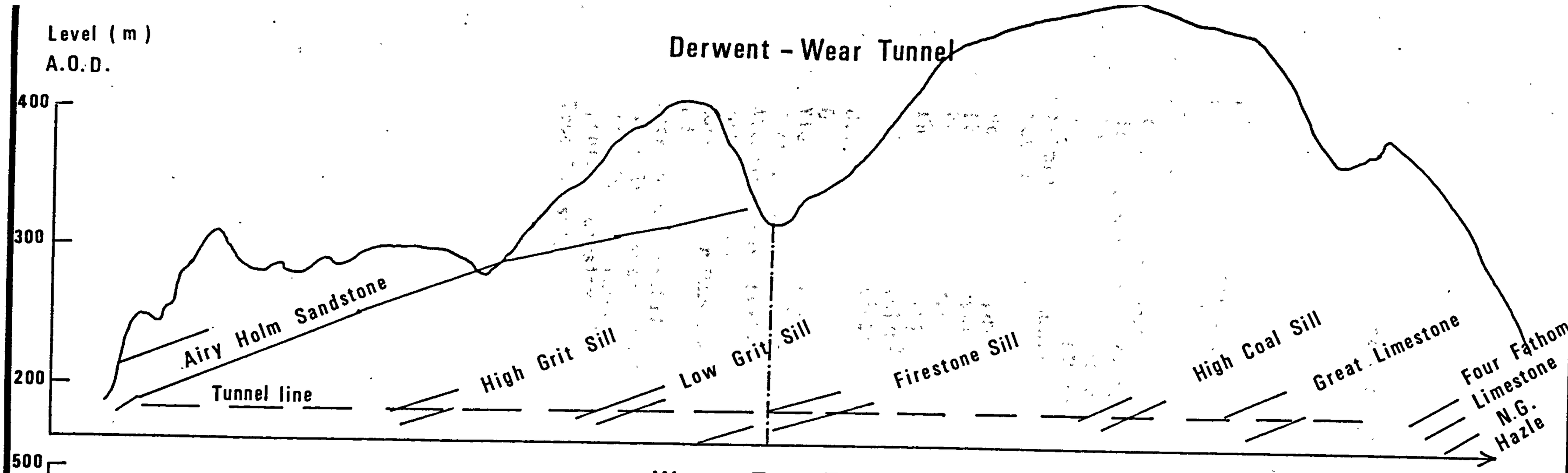

Figure 54

Wear – Tees Tunnel

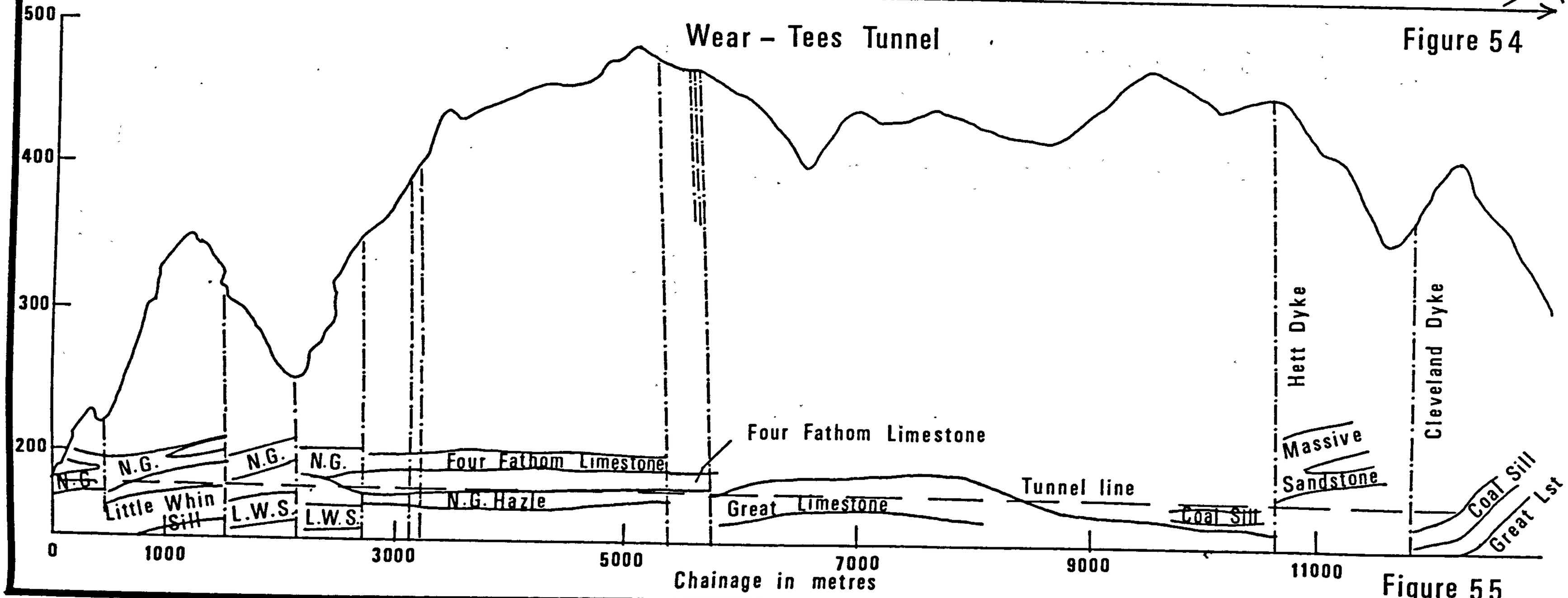

Figure 55

Table 20 Summary of Cutability & Associated Data for The Great Limestone

Parameter	Borehole Code			
	DWG/10	WTB/12A	WT4/10	WT6/10A
Quartz Content (%)	0.50	0	0	0
Compressive Strength (MN/m^2)	91.60	147.40	133.40	192.90
Tensile Strength (MN/m^2)	10.00	10.10	6.40	9.70
Shear Strength (MN/m^2)	21.50	23.30	18.00	30.60
Young's Modulus (GN/m^2)	50.70	43.20	62.30	65.70
Schmidt Rebound Number	58	55	56	55
Wet Bulk Density	2699	2746	2682	2705
Fc (kN)	1.73	1.87	1.96	1.89
F'c (kN)	4.15	4.76	4.53	4.96
Fn (kN)	2.29	2.40	2.17	2.67
F'n (kN)	4.21	4.42	3.71	4.94
S.E. (MJ/m^3)	24.10	23.11	28.11	22.35
(J/g)	9.34	9.03	10.89	8.94
C.I.	436	428	428	444
B	74	74	70	74
Yield (Kg/m)	0.388	0.385	0.341	0.376
Cutting Wear (mg/m)	1.61	1.06	0.78	0.81
Abrasive Wear (mg/m)	0.06	0.05	0.07	0.08
Shore Hardness	41	35	38	39
Cone Indenter Hardness	4.9*	4.4*	6.3*	3.9*
I.S.I	78	76	86	82
Hacksaw Machineability	6.00	9.00	6.00	-
Dry Bulk Density (g/cc)	2.58	2.56	2.58	2.50
Grain Density (g/cc)	2.71	2.71	2.71	2.72
Apparent Porosity (%)	0	0	0	0.80
True Porosity (%)	4.90	5.50	4.70	8.20

Table 21 Summary of Cutability & Associated Data

for The

Four Fathom Limestone

Parameter		Borehole Code	
		DWF/7	WT2/7
Quartz Content (%)		0	0
Compressive Strength (MN/m^2)		144.00	134.00
Tensile Strength (MN/m^2)		7.90	8.60
Shear Strength (MN/m^2)		28.00	23.00
Young's Modulus (GN/m^2)		56.60	48.00
Schmidt Rebound Number		54	53
Wet Bulk Density (kg/m^3)		2607	2637
Fc	(KN)	1.94	1.90
Fc'	(KN)	4.48	4.44
Fn	(KN)	2.18	1.92
Fn'	(KN)	3.95	3.52
S.E.	(MJ/m^3)	32.30	25.80
	(J/G)	12.77	10.71
C.I.		414	417
θ		70	72
Yield	(mg/m)	0.334	0.338
Cutting Wear	(mg/m)	1.3	0.74
Abrasive Wear	(mg/m)	0.06	0.05
Shore Hardness		35	37
Cone Indenter Hardness		11.90	4.40
I.S.I.		83	82
Hacksaw Machineability		7.70	8.30
Dry Bulk Density	(g/cc)	2.53	2.41
Grain Density	(g/cc)	2.67	2.70
Apparent Porosity	(%)	3.40	0.00
True Porosity	(%)	5.30	10.50

Table 22 Summary of Cutability & Associated Data

for The

Low Grit Sill & Firestone

Parameter	Low Grit Sill		Firestone Sill
	DWD/8	WT7B/5	DWE/6
Quartz Content (%)	85	88	82
Compressive Strength (MN/m^2)	74.40	145.50	150.00
Tensile Strength (MN/m^2)	5.20	7.20	10.30
Shear Strength (MN/m^2)	11.50	20.00	22.00
Young's Modulus (GN/m^2)	22.50	38.90	44.80
Schmidt Rebound Number	52	54	60
Wet Bulk Density (kg/m^3)	2568	2499	2622
Fc (kN)	1.42	2.22	2.22
Fc' (kN)	3.67	5.12	6.16
Fn (kN)	1.05	2.50	1.97
Fn' (kN)	2.06	4.41	3.94
S.E. (MJ/m^3)	21.09	30.25	28.22
(J/G)	8.50	12.30	11.16
C.I.	394	412	401
θ	64	70	70
Yield (Kg/m)	0.284	0.325	0.334
Cutting Wear (mg/m)	1.57	1.89	1.82
Abrasive Wear (mg/m)	0.58	0.37	-
Shore Hardness	19	47	44
Cone Indenter Hardness	4.20	7.60	4.80*
I.S.I	73	84	74
Hacksaw Machineability	3.20	0.80	0.70
Dry Bulk Density (g/cc)	2.48	2.46	2.53
Grain Density (g/cc)	2.75	2.67	2.64
Apparent Porosity (%)	13.20	3.10	3.22
True Porosity (%)	-	7.90	5.70

Table 23 Summary of Cutability & Associated Data for The Coal Sill Sandstone

Parameter	Borehole Code		
	WT4/7	WT6/7A Dry Test	WT6/7A Saturated Test
Quartz Content (%)	93	79	79
Compressive Strength (MN/m^2)	122.70	-	158.30
Tensile Strength (MN/m^2)	6.20	-	11.10
Shear Strength (MN/m^2)	18.00	-	24.00
Young's Modulus (GN/m^2)	33.10	-	50.10
Schmidt Rebound Number	54	59	58
Wet Bulk Density (kg/m^3)	2499	-	2560
Fc (kN)	1.88	1.86	1.83
F_c' (kN)	5.15	4.40	4.97
F_n (kN)	1.75	2.16	2.15
F_h' (kN)	3.42	4.21	3.89
S.E. (MJ/m^3)	23.80	21.70	23.80
(J/G)	9.96	9.27	9.30
C.I.	426	413	416
$\beta°$	67	69	64
Yield (Kg/m)	0.292	0.301	0.268
Cutting Wear (mg/m)	2.70	2.32	2.21
Abrasive Wear (mg/m)	-	2.68	1.81
Shore Hardness	38	55	42
Cone Indenter Hardness	3.50*	7.60	4.40*
I.S.I.	85	78	-
Hacksaw Machineability	2.10	0.30	0.40
Bulk Density (g/cc)	2.39	2.34	2.34
Grain Density (g/cc)	2.60	2.61	-
Apparent Porosity (%)	5.10	4.10	4.28
True Porosity (%)	8.30	10.40	-

Table 24 Summary of Cutability & Associated Data for The Nattrass Gill Hazle

Parameter		Borehole Code	
		DWF/8	WT2/12
Quartz Content	(%)	89.50	62.00
Compressive Strength	(MN/m^2)	156.00	52.50
Tensile Strength	(MN/m^2)	7.30	5.80
Shear Strength	(MN/m^2)	18.50	20.50
Young's Modulus	(GN/m^2)	39.80	16.50
Schmidt Rebound Number		59	58
Wet Bulk Density	(kg/m^2)	2525	2577
Fc	(kN)	2.09	3.26
Fc'	(kN)	4.73	6.63
Fn	(kN)	2.15	3.92
Fn'	(kN)	4.14	6.20
S.E.	(MJ/m^3)	26.41	52.61
	(J/g)	11.10	22.78
C.I.		407	399
θ		71	66
Yield	(Kg/m)	0.324	0.276
Cutting Wear	(mg/m)	4.61	8.87
Abrasive Wear	(mg/m)	4.86	-
Shore Hardness		47	52
Cone Indenter Hardness		6.00*	11.60*
I.S.I.		82	85
Hacksaw Machineability		0.40	0.50
Dry Bulk Density	(g/cc)	2.38	2.31
Grain Density	(g/cc)	2.59	2.62
Apparent Porosity	(%)	4.13	3.03
True Porosity	(%)	8.11	11.85

Table 25 Summary of Cutability & Associated Data

for The

First Grit

Parameter	Borehole Code			
	AD1/6 Dry Test	AD1/6 Sat.Test	DWB/2 Dry Test	DWB/2 Sat.Test
Quartz Content (%)	77	77	68	68
Compressive Strength (MN/m^2)		58.30		36.50
Tensile Strength (MN/m^2)		4.20		2.50
Shear Strength (MN/m^2)		8.00		9.50
Young's Modulus (GN/m^2)		18.70		9.30
Schmidt Rebound Number	52	41	37	37
Wet Bulk Density		2434		2490
Fc (kN)	1.37	0.94	1.25	0.89
F'c (kN)	3.17	2.64	3.24	2.33
Fn (kN)	1.02	0.58	0.91	0.59
F'n (kN)	1.92	1.57	1.84	1.27
S.E. (MJ/m^3)	18.46	11.42	14.44	11.08
(J/g)	8.75	4.69	6.88	4.45
C.I.	366	363	389	362
θ	65	58	62	65
Yield (Kg/m)	0.247	0.232	0.252	0.260
Cutting Wear (mg/m)	1.95	2.44	1.84	2.86
Abrasive Wear (mg/m)	1.50	-	-	-
Shore Hardness	28	30	27	24
Cone Indenter Hardness	2.30	2.90	4.60	3.50
I.S.I	66	-	68	67
Hacksaw Machineability	1.70	2.70	2.80	2.60
Bulk Density (g/cc)	2.11	2.24	2.10	2.22
Grain Density (g/cc)	2.59	-	2.57	-
Apparent Porosity (%)	10.30	8.90	6.70	6.25
True Porosity (%)	18.40	-	10.40	-

Table 26 Summary of Cutability & Associated Data for The Letch House Sandstone

Parameter		Borehole Code	
		TA1/8/9	TA2/7
Quartz Content	(%)	-	62
Compressive Strength	(MN/m^2)	45.70	50.40
Tensile Strength	(MN/m^2)	-	3.30
Shear Strength	(MN/m^2)	-	7.50
Young's Modulus	(GN/m^2)	-	12.50
Schmidt Rebound Number		44	51
Wet Bulk Density	(kg/m^3)	2453	2498
Fc	(kN)	1.34	1.27
Fc'	(kN)	3.00	3.25
Fn	(kN)	0.91	0.80
Fn'	(kN)	1.90	1.83
S.E.	(MJ/m^3)	16.52	17.56
	(J/g)	6.74	7.64
C.I.		391	400
θ		62	75
Yield	(Kg/m)	0.266	0.361
Cutting Wear	(mg/m)	1.89	1.93
Abrasive Wear	(mg/m)	0.67	0.79
Cone Indenter Hardness		5.00	4.20
I.S.I		-	81
Hacksaw Machineability		3.20	2.50
Dry Bulk Density	(g/cc)	2.41	2.30
Grain Density	(g/cc)	2.60	2.58
Apparent Porosity	(%)	5.10	
True Porosity	(%)	7.50	10.80

Table 27 Summary of Cutability & Associated Data for The High Grit Sill, High Coal Sill, White Hazle, Massive Sandstone and Dolerite

Parameter		High Grit Sill	High Coal Sill	White Hazle	Massive S/stone	Dolerite
		DWD/2	DWG/3	WTB/8	WTC/1A	WT1A/11
Quartz Content	(%)	81	99	59	80	-
Compressive Strength	(MN/m^2)	72.30	117.10	72.00	84.20	314.00
Tensile Strength	(MN/m^2)	4.60	8.90	8.70	6.70	21.30
Shear Strength	(MN/m^2)	11.50	17.50	20.00	14.30	50.00
Young's Modulus	(GN/m^2)	21.40	38.80	18.70	31.20	80.60
Schmidt Rebound Number		51				
Wet Bulk Density	(kg/m^3)	2595	2502	2478	2519	2971
Fc	(kN)	1.57	1.79	1.63	2.22	2.58
F_c'	(kN)	4.15	4.24	4.52	4.67	6.54
Fn	(kN)	1.30	1.73	1.54	1.99	3.22
F_n'	(kN)	2.52	3.21	3.25	3.35	5.71
S.E.	(MJ/m^3)	20.07	22.10	20.85	32.67	38.90
	(J/g)	8.54	11.05	8.87	13.45	13.46
C.I.		408	407	409	408	418
θ°		66	70	71	68	73
Yield	(Kg/m)	0.281	0.264	0.320	0.305	0.420
Cutting Wear	(mg/m)	2.80	2.04	1.58	1.74	1.70
Abrasive Wear	(mg/m)	1.09	1.46	-	1.97	0.27
Shore Hardness		38	36	43	42	54
Cone Indenter Hardness		2.90	7.10	11.40	10.00	27.80*
I.S.I.		80	61	91	77	81
Hacksaw Machineability		1.30	0.50	1.50	0.60	0.40
Dry Bulk Density	(g/cc)	2.35	2.00	2.35	2.43	2.89
Grain Density	(g/cc)	2.60	2.59	2.60	2.60	2.96
Apparent Porosity	(%)	2.90	4.30	4.90	4.50	0.00
True Porosity	(%)	9.80	22.90	9.70	6.90	13.10

Table 28 Summary of Cutability & Associtated Data for The Mudstone

Both core specimens broke up during the first core cutting test making calculation and measurement of certain parameters impossible.

Parameter		Borehole Code	
		DWG/9A	DWE/2
Quartz Content (%)		5	-
Compressive Strength	(MN/m^2)	41.40	32.20
Tensile Strength	(MN/m^2)	-	6.70
Shear Strength	(MN/m^2)	8.00	9.00
Young's Modulus	(GN/m^2)	9.00	10.80
Bulk Density	(kg/m^3)	2579	2522
Fc	(kN)	0.91	1.37
Fc'	(kN)	3.18	3.82
Fn	(kN)	0.22	0.39
Fn'	(kN)	0.79	1.43
θ		79	72
Cutting Wear (mg/m)		1.00	-

8.5.3 Discussion of test results related to tunnel drivage by machine

The results obtained from the cutability and associated test work make it possible to select the type of tunnelling machine and predict the machine performance for each of the principal stratum. The prediction, however, could not be made with any high degree of confidence due to the relatively few specimens tested (less than 30) to represent a rock material over long lengths of drivage (about 25 miles) and also due to the exclusion of the 'in-situ' effect of the stratum. It is well recognised that the confining pressure of rock increase about 1 MN/m^2 per 45 m depth (1 psi/1 ft depth).

The results of the cutability and associated test work have been interpreted for each of the principal stratum in turn, beginning at the Tyne and moving progressively to the Tees. Two machine types have been considered and an assessment made of their potential in each rock type. Drag pick machines always show a higher theoretical potential than the disc/roller cutter machines, but this has been moderated according to the strength of the rock and particularly where tool wear is likely to be a problem. Those machines which use drag picks as the principal cutting element are classed together as Type A. Full face boring machines which use discs, toothed roller cutters, button cutters or combinations of these are referred to collectively as Type B.

Excavation potential is rated as m^3/hour per 100 machine H.P. and is thereby independent of tunnel size.

Table 30 - 33 relate to the four principal tunnel sections,thus:-
Table 30 - Greymare Hill tunnel
Table 31 - Airy Holm - Derwent tunnel
Table 32 - Derwent - Wear tunnel
Table 33 - Wear - Tees tunnel.

Each is a synopsis of cutability assessment and includes specific comment on machine application.

The recommendations on machine applicability detailed in Tables 30 - 33 are summarised in Table 29 the assessment of probable performance is based on four standards:-

1. Applicable - a high expectation of successful application. Degree of success, rate of drivage, etc; will vary according to individual machine design.
2. Probably Applicable - some machine designs within the type specified might be at risk. This standard includes those Type B machines which may have stability problems, when excavating a mixed face.
3. Significant Failure Risk - possible for machine to excavate rock, but likely to be difficult to maintain standards for anything more than short intervals. Rapid loss of penetration due to tool damage. Frequent tool changes. Some risk of component failure from high wear and tear and overstressing. Machine stability also a significant risk factor.
4. Not Recommended - little expectation of success.

Table 29 Summary of Machine Application Assessment

Tunnel:	Greymare Hill		Airy Holm-Derwent		Derwent - Wear		Wear - Tees	
Total Length of Drive:-	1890 m	100 %	1990 m	100 %	13280 m	100 %	14400 m	100 %
MACHINE TYPE A								
1) Applicable	0	0	0	0	1630 m	12.3 %	0	0
2) Probably Applicable	0	0	0	0	3400 m	25.6 %	0	0
3) Significant Failure Risk	1890 m	100 %	1990 m	100 %	2030 m	15.3 %	950 m	6.6 %
4) Not Recommended	0	0	0	0	6220 m	46.8 %	13450m	93.4 %
MACHING TYPE B								
1) Applicable	0	0	0	0	6930 m	52.2 %	3640 m	25.3 %
2) Probably Applicable	1890 m	100%	1990 m	100 %	4530 m	34.1 %	5710 m	39.7 %
3) Significant Failure Risk	0	0	0	0	1820 m	13.7 %	2220 m	15.4 %
4) Not Recommended	0	0	0	0	0	0	2830 m	19.6 %

Table 30 Greymare Hill Tunnel Rock Cutability Assessment

Chainage (m) From	Chainage (m) To	Dist. (m)	Stratum	Relevant Test Specimen	Test Result Ref. Table No.	Estimated Excavation Rate m^3/h per 100 H.P. Machine Type A	Estimated Excavation Rate m^3/h per 100 H.P. Machine Type B	Remarks
150	530	380	Letch House Sandstone	TA1/8/9 TA2/7	26	5.3-10.5	1.8-2.7	High cutting and abrasive wear. Most Type A machines very doubtful.
1530	1485	955	Letch House Sandstone with Coal Measures & faulting	-	-	-	-	Possible machine problems with faulting and mixed beds.Risk of methane and potential ignitions from cutting tools should not be ignore.
1485	1750	265	Letch House Sandstone	TA1/8/9 TA2/7	26	5.3-10.5	1.8-2.7	High cutting and abrasive wear. Most Type A machines very doubtful (see 1 above).
1570	2040	290	Coal Measures mainly Sandstone	-	-	-	-	Predominantly Sandstone in coal measures. Risk of methane ignitions should be assessed.

Table 31 Airy Holm-Derwent Tunnel Rock Cutability Assessment

	Chainage (m)		Dist. (m)	Stratum	Relevant Test Specimen	Test Result Ref. Table No.	Estimated Excavation Rate m^3/h per 100 H.P.		Remarks
	From	To					Machine Type A	Machine Type B	
1	220	2210	1990	Airy Holm Sandstone First Grit	AD1/6 (see also DWB/2)	25	4.8-9.7	1.6-2.4	Similar to Letch House Sandstone - slightly more difficult since abrasivity tends to be higher. Most Type A machines would experience difficulty in this section. The continuous face of sandstone would favour the Type B machine, but tool wear would still be high.

Table 32 Derwent-Wear Tunnel Rock Cutability Assessment

	Chainage (m)		Dist. (m)	Stratum	Relovant Test Specimen	Test Result Ref; Table No.	Estimated Excavation Rate m^3/h per 100 H.P.		Remarks
	From	To					Machine Type A	Machine Type B	
1	0	1800	1800	Mixed beds of sandstone, shale & thin limestone	-	-	-	-	Possibility of vein at 1680 m. -high risk of hard minerals particularly pure quartz.
2	1800	2840	1040	Mudstone	DWC/9A	28	-	-	Weak rock non-abrasive,within capability of both Type A and Type B machines.
3	2840	3110	270	Interface of Mudstone and High Grit Sill	DWC/9A DWD/2	28 27			Large strength & cutability contrast between Mudstone & High Grit Sill creates high risk of machine Type B instability. Machine Type A applied as selecting miner could be potentially more useful over this length although tool wear would be high.
4	3110	3430	320	High Grit Sill	DWD/2	27	4.5-8.9	1.5-2.2	High cutting & abrasive wear. More difficult than First Grit & Letch House Sandstone; Type A Machine not recommended.
5	3430	3710	280	Interface of mixed shaley beds with High Grit Sill	-	-	-	-	Large strength and cutability contrast between shaley beds and High Grit Sill (see 3 above).
6	3710	4500	790	Shale inter-bedded with Sandstone and Limestone	-	-	-	-	0.25m thick Quartzite exposed in face for 200m advance; high abrasive & impact wear. Type A machine not recommended, possible instability with Type B machine.

Table 32 (continued)

	Chainage (m)		Dist (m)	Stratum	Relevant Test Specimen	Test Result Ref. Table No	Estimated Excavation Rate m^3/h per 100 H.P.		Remarks
	From	To					Machine Type A	Machine Type B	
7	4500	4710	210	Interface of mixed shaley beds with Low Grit Sill	-	-	-	-	Large strength & cutability contrast between shaley beds & Lower Grit Sill (see 3 and 5 above). Possibility of vein in this section (see 1 above).
8	4710	5520	810	Low Grit Sill	DWD/8	22	4.2-85	1.4-2.1	Very similar in strength & cutting characteristics to the High Grit Sill being only marginally stronger Although cutting & abrasive wear is slightly lower it is still very significant & precludes the use of most Type A machines (see 4).
9	5520	5860	340	Interface of Low Grit Sill and Mudstone	-	-	-	-	Large strength and cutability contrast between Mudstone & Low Grit (see 3, 5 and 7 above).
10	5860	6240	380	Mudstone	DWE/2	28	-	-	See 2 above.
11	6240	6450	210	Mudstone with calcareous Sandstone and Shale	-	-	-	-	No serious cutting problems anticipated in this section.
12	6450	6570	120	Firestone Sill	DWE/6	22	3.2-6.3	1.1-1.6	Very strong, abrasive & difficult to cut. Type A machine not recommended. Some Type B machines could experience difficulties.
13	6570	6800	230	Interface of Firestone Sill with Shales, Sandstone and Limestone	-	-	-	-	Large strength and cutability contrast between very strong Firestone Sill and much weaker shales, etc, (see 9 above).

Table 32 (Continued)

	Chainage (m)		Dist. (m)	Stratum	Relevant Test Specimen	Test Result Ref. Table No	Estimated Excavation Rate m^3/h per 100 H.P.		Remarks
	From	To					Machine Type A	Machine Type B	
14	6800	9100	2300	Rythmic sequences of limestone, Sandstone and Shale	-	-	-	-	Apart from abrasive nature of sandstones and regular strata interfaces, and possibly Quartz associated with mineral vein, no serious nachine cutting problem is anticipated on the evidence available.
15	9100	9670	570	Interface of White Hazle, High Coal Sill, Low Coal Sill with other Sandstone bands	DWG/3 (also WTB/8)	27	4.1-8.1	1.3-2.0	High cutting & abrasive wear. Contrasts of rock strength & cutability across interfaces, probably not severe. Type A machine not recommended; suggestions of coalification indicates possible methane risk.
16	9670	10120	450	Interface of Low Coal Sill with other Sandstones & Shales					Probably similar to preceding sequence (see 15 above) with inclusion of thin Mudstones giving high interface contrasts.
17	10120	10300	180	Interface of Great Limestone with Shale beds & possibly Sandstone	-	-	-	-	High abrasion & cutting wear where Sandstone is exposed. Type A machines not recommended. Strength & cutability contrasts across interfaces, probably not excessive but difference in fracture patterns of Sandstone & Limestone could lead to instability on machine Type B.
18	10300	11150	850	Great Limestone	DWG/10	20	3.7-7.4	1.2-1.9	Low abrasivity, but relatively high impact wear. Type A machine not recommended. Type B machine applicable but rock increases in strength southwards.

Table 32 (continued)

	Chainage (m) From	Chainage (m) To	Dist. (m)	Stratum	Relevant Test Specimen	Test Result Ref. Table No.	Estimated Excavation Rate m^3/h per 100 H.P. Machine Type A	Estimated Excavation Rate m^3/h per 100 H.P. Machine Type B	Remarks
19	11150	11320	170	Interface of Great Limestone & Sandstone	-	-	-	-	As 17 above.
20	11320	12190	870	Interfaces of Sandstone Limestones & Marine Bands Possibly 2 veins.	-	-	-	-	As 17 above. Type B machine instability risk not so high here. Mineral veins high risk of quartz.
21	12190	12350	160	Interface of Four Fathom Limestone and Sandstone					As 17 above.
22	12350	12700	350	Four Fathom Limestone	DWF/7	21	2.8-5.5	0.9-1.4	Very low abrasivity but significant impact wear. Type A machine not recommended. Type B machine should be applicable.
23	12700	12910	210	Interface of Four Fathom Limestone and Nattrass Gill Hazle	-	-	-	-	As 17 above.
24	12910	13280	370	Nattrass Gill Hazle	DWF/8	24	3.4-6.8	1.1-1.7	Excessively high abrasivity & cutting wear. Type A machine not recommended. Type B machine will experience difficulty & will require frequent cutter changes.

Table 33 Wear - Tees Tunnel Rock Cutability Assessment

	Chainage (m) From	Chainage (m) To	Dist. (m)	Stratum	Relevant Test Specimen	Test Result Ref. Table No.	Estimated Excavation Rate m3/h per 100 H.P. Machine Type A	Estimated Excavation Rate m3/h per 100 H.P. Machine Type B	Remarks
1	0	750	750	Nattrass Gill Hazle	WT2/12 (also DWF/8)	24	1.7-3.4	0.6-0.9	Prohibitively high cutting wear and abrasivity due to secondary quartz matrix. Type A machine is not recommended. Type B machine has high failure risk (n.b.misleadingly.low compressive strength of WT/12).
2	750	900	150	Interface of Nattrass Gill Hazle & thin bands of Mudstone, Sandstone and Siltstone.	-	-	-	-	Excessive abrasion & cutter wear where N.G. Hazle is exposed. Type A machine not recommended. Type B machine has high failure risk.
3	900	2400	1500	Interfaces of Mudstone, Sandstone and Limestone and possibility of Dolerite.	-	-	-	-	Strong sandstone and siltstone bands, probably highly abrasive. type A machine not recommended. Type B machine prone to instability. Possibility of Dolerite exposure in invert, so high risk of Type B machine failure. Faulting in this section.
4	2400	2600	200	Interface of Nattrass Gill Hazle & thin bands of Mudstone, Sandstone and Silstone.	-	-	-	-	As 2 above.
5	2600	2700	100	Nattrass Gill Hazle	WT2/12 (also DWF/8	24	1.7-3.4	0.6-0.3	As 1 above.

Table 33 (continued)

	Chainage (m) From	Chainage (m) To	Dist. (m)	Stratum	Relevant Test Specimen	Test Result Ref. Table No.	Estimated Excavation Rate m^3/h per 100 H.P. Machine Type A	Estimated Excavation Rate m^3/h per 100 H.P. Machine Type B	Remarks
6	2700	3700	1000	Interfaces of Limestone, Seat Earth and Siltstone	-	-	-	-	High strength and cutability contrasts across interfaces. Type A machine not recommended. Type B machine should accommodate contrast since strong rock is Limestone.
7	3700	5330	1630	Interface of Siltstones with Nattrass Gill Hazle	WT2/12 (also DWF/8)	24	1.7-3.4	0.6-0.3	Prohibitively high cutting wear and abrasivity. Type A machine not recommended Type B machine has high failure risk.
8	5330	5660	330	Four Fathom Limestone	WT2/7	21	3.5-6.9	1.2-1.7	Low abrasivity, significant impact wear Type A machine not recommended. Type B machine should be applicable.
9	5660	6080	420	Interfaces of Sandstone, Siltstones & Mudstones.	-	-	-	-	Sandstone exposures relatively weak, but possibly high abrasive and cutting wear. Interface contrasts probably not sufficiently high to cause instability of machine Type B.
10	6080	6210	130	Interface of Sandstones, Shales and Mudstones with Great Limestone	-	-	-	-	High strength contrasts across interfaces. Possible instability of Type B machine.
11	6210	8210	2000	Great Limestone	WT4/10 WTB/12A	20	3.2-6.4	1.1-1.6	Low abrasivity, significant impact wear Type A machine not recommended. Type B machine should be applicable.
12	8210	8400	190	Limestone of Great Limestone with Sandstone.	-	-	-	-	As 10 above.

Table 33 (continued)

	Chainage (m)		Dist. (m)	Stratum	Relevant Test Specimen	Test Result Ref. Table No.	Estimated Excavation Rate m^3/h per 100 H.P.		Remarks
	From	To					Machine Type A	Machine Type B	
13	8400	10650	2250	Interface of Sandstones, Shales and Mudstones.	WT4/7	23	3.8-7.5	1.3-1.9	Strong and highly abrasive Sandstones, Type A machine not recommended. High contrast across interfaces-possible instability of Type B machine.
14	10650	10660	10	Hett Dyke.	WT1A/11	27	2.3-4.6	0.8-1.2	Modest abrasivity, high impact wear, but not prohibitibe. Use of certain type of Type B machine not impossible.
15	10660	12680	2020	Interfaces of rythmic sequences of Limestones, Sandstones and shales. Intrusion of Cleveland Dyke.	-	-	-	-	Thin beds showing interface strength contrasts with highly abrasive Sandstones suggests Type B machine instability. Type A machine not recommended. Cleveland Dyke weaker than Hett Dyke, maybe possible to use Type B machine.
16	12680	12800	120	Coal Sill Sandstone.	WT6/7A	23	3.8-7.5	1.3-1.9	High cutting and abrasive wear. Type A machine not recommended. Type B machine will require frequent tool changes.
17	12800	12900	100	Interfaces of Sandstone, Mudstone and Limestone.	-	-	-	-	Sandstone exposures relatively weak, but possibly high abrasive. Interface contrasts probably not sufficiently high to cause instability of machine Type B.
18	12900	13100	200	Great Limestone.	WT6/10A	20	4.0-8.0	1.3-2.0	Low abrasivity but significant impact wear. Type A machine not recommended. Type B machine should be applicable.
19	13100	13690	590	Rapid succession of Sandstone, Limestone, Nattrass Gill Hazle & Six Fathom Hazle.	-	-	-	-	Type A machine not recommended. Nattrass Gill Hazle might prevent use of Type B machine (see WT/23 & DWF/8).

Table 33 (continued)

	Chainage (m)		Dist. (m)	Statum	Relevant Test Specimen	Test Result Ref. Table No.	Estimated Excavation Rate m^3/h per 100 H.P.		Remarks
	From	To					Machine Type A	Machine Type B	
20	13690	13800	110	Sandstone (Lunedale Fault Belt)	-	-	-	-	Medium strength Sandstones - Possibles high abrasion & cutting wear. Type B machine should be applicable. Faulting may promote block type failure of rock.
21	13800	14400	600	Low Grit Sill	WT7B/5	22	3.0-5.9	1.0-1.5	Strong & abrasive Sandstone. Type B machine applicable with frequent tool changes. Some risk of instability due to reported inclusions of Shale bands in stratum.

8.6 Tyneside Rapid Transit tunnels

The rapid urbanization of the worlds population and the consequential development of large conurbations is creating a demand for commuter travel which is greater than can be accomodated by the conventional surface transport systems. Many authorities are contemplating the construction of underground railway systems to ease traffic congestion in urban areas.

Tyneside, with a population of approximately 1 million concentrated in a relatively small area is attemping to rationalise its urban transport system. The several large independent transport authoritise covering the area have merged into a new single authority, the Tyneside Passenger Executive (PTE), which is now responsible for the whole range of commuter and local passenger traffic.

The PTE has recently introduced a new plan for Tyneside which embraces much of what already exists and includes an underground railway system linking the main railway terminal with key points in and around the city centre and tying in with the local railway routes.

The scheme is at its early stages of development and details of tunnel sizes, routes, depth and so on will to some extent be determined by the preliminary site investigation which is currently being undertaken.

The absence of detailed geological sections showing the proposed tunnel lines makes it impossible to produce a synopsis of cutability assessment and machine application as in section 8.5.3. The following general review is based entirely on the machine prospects within the broad geological description.

Because of the short intricate drivages associated with rapid transit systems there is no practical application of machine type B which would employ a full face attack. Also there are some disadvantages of full face attack in this situation:-

1. The scheme would allow multiple drivages to be made simultaneously and the expensive and relatively inflexible full face borer is almost certain to be uneconomic, when several machines in short drivages are required.

2. The full face borer produces only circular tunnel section of a fixed size which makes the machine redundant, where changes in tunnel diameter or shape of excavation are required.

3. The tunnelling scheme is likely to require curves having a smaller radius than can readily be produced by conventional full face boring machines.

Table 34 Summary of Cutability and Associated Data for The Massive Sandstones

Parameter	Borehole Code and Depth (m)				
	S8 5.90-6.20	S8 9.10-9.40	S9 12.60-12.95	S9 13.80-14.30	S10 12.50-13.00
Quartz content %	76	76	74	76	78
Compressive Strength (MN/m^2)	44.6	37.7	43.8	43.3	39.0
Tensile Strength (MN/m^2)	3.5	3.4	2.9	3.1	2.2
Young's Modulus (GN/m^2)	7.0	7.7	9.8	9.9	10.1
Dry Bulk Density (g/cc)	2.15	2.18	2.14	2.15	2.16
Grain Density (g/cc)	2.59	2.59	2.57	2.57	2.61
Apparent Porosity (%)	12.8	12.6	14.2	11.9	12.2
True Porosity (%)	17.1	15.6	16.7	16.5	17.1
Fc (KN)	0.97	1.01	1.10	1.15	1.05
Fc' (KN)	2.54	2.54	2.76	2.96	2.66
Fn (KN)	0.49	0.55	0.68	0.71	0.63
Fn' (KN)	1.34	1.28	1.60	1.64	1.59
S.E. (MJ/m^3)	8.24	10.30	11.71	12.27	12.46
(J/g)	3.83	4.72	5.47	5.71	5.77
C.I	423	396	381	387	360
θ	68°	67°	67°	63°	62°
Yield (Kg/m)	0.27	0.27	0.26	0.24	0.24
Cutting Wear (mg/m)	2.61	1.52	1.07	1.57	1.63
Abrasive Wear (mg/m)	0.40	0.69	0.68	0.69	1.04
Shore Hardness	23.6	20.9	24.7	28.1	22.1
Cone Indenter Hardness	2.6	2.5	3.3	2.4	2.9
I.S.I	68	73	60	61	48
Hacksaw Machineability	-	-	-	5.2	7.1

Table 35 Summary of Cutability and Associated Data for The Sandstones with Dark Micaceous carbonaceous Siltstone Bands

Parameter	Borehole Code and Depth (m)				
	S1 13.25-13.45	S1 14.25-14.50	S1 15.30-15.60	S2 17.60-17.90	S2 18.55-18.80
Quartz content %	82	84	86	80	80
Compressive strength (MN/m^2)	80.2	74.2	82.9	75.5	98.9
Tensile strength (MN/m^2)	6.2	4.5	6.0	5.4	5.6
Youngs Modulus (GN/m^2)	9.9	14.4	12.8	9.9	14.8
Dry Bulk Density (g/cc)	2.25	2.36	2.35	2.33	2.31
Grain Density (g/cc)	2.61	2.61	2.57	2.64	2.60
Apparent Porosity (%)	5.7	6.9	7.2	4.8	7.7
True Porosity (%)	13.8	9.7	8.8	11.5	11.3
Fc (KN)	1.33	1.36	0.99	1.41	1.29
F_c' (KN)	3.74	3.53	2.95	4.00	3.62
Fn (KN)	0.63	0.78	0.54	0.77	0.68
F_n' (KN)	1.76	1.87	1.53	1.92	2.16
S.E (MJ/m^3)	10.74	12.70	9.56	13.83	11.73
(J/g)	4.77	5.38	4.07	5.94	5.08
C.I	404	421	434	412	433
θ°	75°	65°	72°	69°	66°
Yield (Kg/m)	0.35	0.28	0.33	0.30	0.28
Cutting Wear (mg/m)	2.76	2.12	1.08	1.40	2.09
Abrasive Wear (mg/m)	-	0.24	0.18	0.13	0.29
Shore Hardness	29.5	31.9	32.9	26.8	35.7
Cone Indenter Hardness	2.7	2.8	3.7	2.6	3.5
I.S.I	78	80	82	80	83
Hacksaw Machineability	-	-	-	-	-

Table 36 Summary of Cutability and Associated Data for The Sandstone with Micaceous Carbonaceous Silstone Bands

Parameter	Borehole Code and Depth (m)				
	S8 18.20-18.50	S8 19.50-19.80	S8 25.90-26.10	S9 17.25-17.55	S9 22.20-22.40
Quartz content %	70	76	76	84	75
Compressive Strength (MN/m^2)	82.1	70.8	85.8	50.7	-
Tensile strength (MN/m^2)	5.9	7.4	-	3.5	-
Youngs Modulus (GN/m^2)	9.8	10.6	10.0	9.6	-
Dry Bulk Density (g/cc)	2.29	2.19	2.31	2.23	2.39
Grain Density (g/cc)	2.62	2.64	2.87	2.60	2.60
Apparent Porosity (%)	7.4	7.8	4.5	10.9	3.0
True Porosity (%)	12.8	17.0	19.5	14.3	8.3
Fc (KN)	1.29	1.46	2.12	1.10	0.81
F_c^1 (KN)	3.55	4.27	5.13	2.74	2.54
Fn (KN)	0.77	0.82	1.09	0.59	0.39
F_n^1 (KN)	1.87	2.15	2.25	1.42	1.34
S.E. (MJ/m^3)	11.63	14.66	14.15	11.12	4.94
(J/g)	5.08	6.70	6.13	4.99	2.07
C.I.	431	413	466	401	443
θ°	69	68	69	67	77
Yield (Kg/m)	0.29	0.27	0.30	0.27	0.41
Cutting Wear (mg/m)	1.53	1.40	-	0.98	-
Abrasive Wear (mg/m)	0.14	0.14	-	0.39	-
Shore Hardness	29.6	31.6	33.4	28.1	20.9
Cone Indenter Hardness	3.8	2.6	2.2	2.5	1.6
I.S.I.	79	81	84	76	79
Hacksaw Machineability	-	-	-	-	-

Table 37 Summary of Cutability and Associated Data for The Carbonaceous Seatearth Sandstones

Parameter	Borehole Code and Depth (m)	
	S4 13.35-13.65	S5 11.50-11.85
Quartz content %	60	60
Compressive strength (MN/m^2)	56.2	52.5
Tensile Strength (MN/m^2)	4.7	3.1
Youngs Modulus (GN/m^2)	5.9	6.1
Dry Bulk Density (g/cc)	2.33	2.28
Grain Density (g/cc)	2.57	2.58
Apparent Porosity (%)	7.5	8.4
True Porosity (%)	9.5	11.8
Fc (KN)	1.15	0.77
$F_c^!$ (KN)	3.16	2.32
Fn (KN)	0.50	0.39
$F_n^!$ (KN)	1.55	1.05
S.E. (MJ/m^3)	10.58	7.02
(J/g)	4.54	3.08
C.I.	420	422
$\theta°$	70	75
Yield (kg/m)	0.31	0.36
Cutting Wear (mg/m)	1.47	1.46
Abrasive Wear (mg/m)	-	-
Shore Hardness	30.2	25.1
Cone Indenter Hardness	2.9	2.2
I.S.I.	77	77.
Hacksaw Machineability	-	-

Table 38 Summary of Cutability and Associated Data for The Calcareous Rocks

Parameter	Borehole Code and Depth (m)		
	S3 17.20-17.40	S5 13.50-13.95	S8 17.15-17.35
Quartz content %	19	33	38
Compressive strength (MN/m2)	187.5	187.5	118.3
Tensile Strength (MN/m^2)	15.6	14.8	7.0
Youngs Modulus (GN/m^2)	22.7	29.3	18.8
Dry Bulk Density (g/cc)	2.49	2.62	2.47
Grain Density (g/cc)	2.75	2.75	2.73
Apparent Porosity %	1.4	1.5	3.7
True Porosity %	9.4	4.6	9.6
Fc (KN)	1.43	1.78	1.90
Fc' (KN)	4.75	5.27	5.10
Fn (KN)	1.59	1.68	1.62
Fn' (KN)	3.48	3.69	3.19
S.E. (MJ/m^2)	11.22	23.09	20.50
(J/g)	4.51	8.81	8.30
C.I.	464	433	436
θ°	79°	68°	69°
Yield (kg/m)	0.48	0.33	0.32
Cutting Wear (mg/m)	1.76	1.44	1.32
Abrasive Wear (mg/m)	0.04	0.09	0.06
Shore Hardness	41.1	37.3	32.9
Cone Indenter Hardness	7.1	3.8	3.0
I.S.I	91	91	87
Hacksaw Machineability	-	1.4	2.7

Table 39 Summary of Cutability and Associated Data for The Seatearth Mudstones

Parameter	Borehole Code and Depth (m)			
	S3 24.40-24.60	S8 25.5-25.75	S9 20.70-21.00	S10 22.50-22.85
Quartz content %	-	-	-	-
Compressive strength (MN/m^2)	-	-	-	-
Tensile Strength (MN/m^2)	5.9	4.9	-	3.6
Youngs Modulus (GN/m^2)	-	-	-	-
Dry Bulk Density(g/cc)	2.50	2.47	2.71	2.45
Grain Density (g/cc)	2.64	2.65	2.71	2.64
Apparent Porosity %	4.4	8.5	7.84	5.8
True Porosity %	5.2	-	-	7.0
Fc (KN)	1.40	1.12	1.33	1.46
Fc' (KN)	4.03	3.47	3.60	4.10
Fn (KN)	0.46	0.55	0.65	0.72
Fn' (KN)	1.66	1.50	1.59	1.83
S.E. (MJ/m^3)	8.46	8.20	13.09	15.32
(J/g)	3.38	3.32	4.83	6.25
C.I.	430	444	414	396
$\theta°$	82°	73°	81°	69°
Yield (kg/m)	0.60	0.36	0.60	0.32
Cutting Wear (mg/m)	-	0.55	1.24	0.91
Abrasive Wear (mg/m)	-	-	-	-
Shore Hardness	26.5	24.9	23.6	27.0
Cone Indenter Hardness	1.9	1.7	1.4	1.7
I.S.I	81	80	81	80
Hacksaw Machineability	-	-	-	-

Table 40 Summary of Cutability and Associated Data

for The

Silty Mudstones

Parameter	Borehole Code and Depth (m)				
	S1 29.15-29.35	S2 23.60-33.90	S3 14.95-15.10	S3 19.75-19.90	S3 26.35-26.50
Quartz content %	-	-	-	-	-
Compressive strength (MN/m^2)	-	-	-	-	-
Tensile Strength (MN/m^2)	4.9	6.3	5.9	6.1	6.8
Youngs Modulus (GN/m^2)	-	-	-	-	-
Dry Bulk Density(g/cc)	2.55	2.50	2.39	2.44	2.55
Grain Density (g/cc)	2.65	2.66	2.64	2.75	2.67
Apparent Porosity %	4.4	4.3	4.3	2.8	5.1
True Porosity %	-	6.2	9.4	11.2	-
Fc (KN)	1.20	1.86	1.62	1.34	1.51
F'c (KN)	3.81	4.77	4.399	3.67	4.02
Fn (KN)	0.50	1.03	0.60	0.50	0.79
F'n (KN)	1.32	2.15	2.07	2.53	2.95
S.E.(MJ/m^3)	7.11	22.41	21.31	7.51	9.42
(J/g)	2.79	8.96	8.92	3.08	3.70
C.I.	451	381	408	443	448
θ	79°	69°	64°	77°	82°
Yield (kg/m)	0.49	0.32	0.27	0.42	0.62
Cutting Wear (mg/m)	1.65	2.10	1.16	1.54	-
Abrasive Wear (mg/m)	-	-	-	-	-
Shore Hardness	25.3	32.8	30.7	27.7	27.9
Cone Indenter Hardness	1.5	2.2	2.2	1.4	1.9
I.S.I.	78	78	77	78	79
Hacksaw Machineability	-	-	-	-	-

8.6.1 General review of machining prospects

8.6.1.A Massive sandstone

The computed values of specific energy for this stratum vary between 8-13 MJ/m^3. A general comparison of this rock type, in terms of specific energy and compressive strength, can be made with Hunterston sandstone in which a commercial tunnelling machine of type A has been employed. Using this comparison it can be seen that it is well within the capability of machine type A to excavate this rock type.

However the abrasive wear tests indicate high values of abrasive wear and there will be a significant risk of machine failure in this stratum due to excessive tool consumption. The values of cutting wear are general slightly lower than the other sandstones tested. This is probably due to the homogeneity of this rock type and its lack of strength conditions which does not give rise to severe impact condition during cutting.

8.6.1.B Sandstone with dark siltstone band

This is very broad geological description and embraces a wide range of sandstone within the sequence. There is, however, a very small variation in the values of computed specific energy, the general range being between 11 and 15 MJ/m^3. These values indicate that these rocks, should be excavate with ease by a machine of type A. Direct interpretation of compressive strength as a measure of cutability could be misleading in this rock type, the variation being nearly 100 %.

As in section 8.6.1.A. there will be a significant risk of failure due to excessive tool wear. The heterogeneity of this strata, however, generally appears to increase the cutting wear and reduce the abrasive wear slightly.

8.6.1.C Carbonaceous Seatearth sandstones

The two samples tested were obtained from different boreholes but their similarlity (from visual inspection) indicates that they are from the same stratum. Specific energy values show that the stratum can be excavated by employing a machine type A. The values for cutting wear are still significant. It was not possible to perform any abrasive wear tests due to the presence of thin stringers of carbonaceous material along which the core tends to crack.

8.6.1.D Calcareous rocks (sandy limestone)

This is very broad geological description of the rocks in table 38. They have been tabulated to show the effect of percentage of calcite present (approximately 100-quartz content) on the rate of wear. It can be seen from the same table that a large calcite percentage reduces the abrasive wear, although there is still a risk of impact wear.

Specific energy values show large variation within this section (S.E. varies between 11 and 23 MJ/m^3). Machine type A is restricted in application to relatively weak rocks and is not recommended for use where the strata approaches the high value of specific energy listed above (samples S5, 13.50 - 17.40 has a high value of compressive strength in relation to its specific energy.

8.6.1.E Seatearth mudstone

Machine type A should operate successfully in this strata. Specific energy values are all within the capabilities of the machine and the values of cutting wear are low (no abrasion tests possible).

8.6.1.F Silty mudstones

There is a significant risk of failure in this strata when employing a type A machine. The values of specific energy often being high, as well as the relatively high values of cutting wear.

8.7 Discussion of the cutting results

At University of Newcastle upon Tyne (81) experiments have been carried out to determine the number of replications of cutting tests to detect a certain percentage change in the mean values of specific energy. It was found that to have confidence in detecting a 10 % change in mean, which is acceptable for the nature of test, four replications were required. Therefore throughout the cutting test programme, four replicates were usually obtained for each rock and so the values of specific energy can be computed with some confidence. The value of specific energy has surely indicated the cutting characteristics of certain rocks, for example Gypsum and Hinkley Point limestone. It has therefore, been used to assess the machining prospects in the Tyne-Tees and Tyneside Rapid Transit tunnels.

A computer programme for linear regression was also employed to find the best straight line relationship between one of the associated rock properties and specific energy. The programme also indicate the level of significance of the relationship and its reliability.

8.7.1 Shore hardness against specific energy

Figure 56 shows a linear relationship between Shore hardness and specific energy, with a correlation coefficient (r_{xy}) of 0.76 and significance level of 0.001:-

Specific energy = 0.82 Shore hardness - 9.06

The computed value of Shore hardness is the mean value of 20 Tests performed on each sample. From the test results it is shown again that the standard deviations for the sandstones is high and it is low for the limestones and mudstones.

SHORE HARDNESS V SPECIFIC ENERGY

$Y = 0.82X - 9.06$

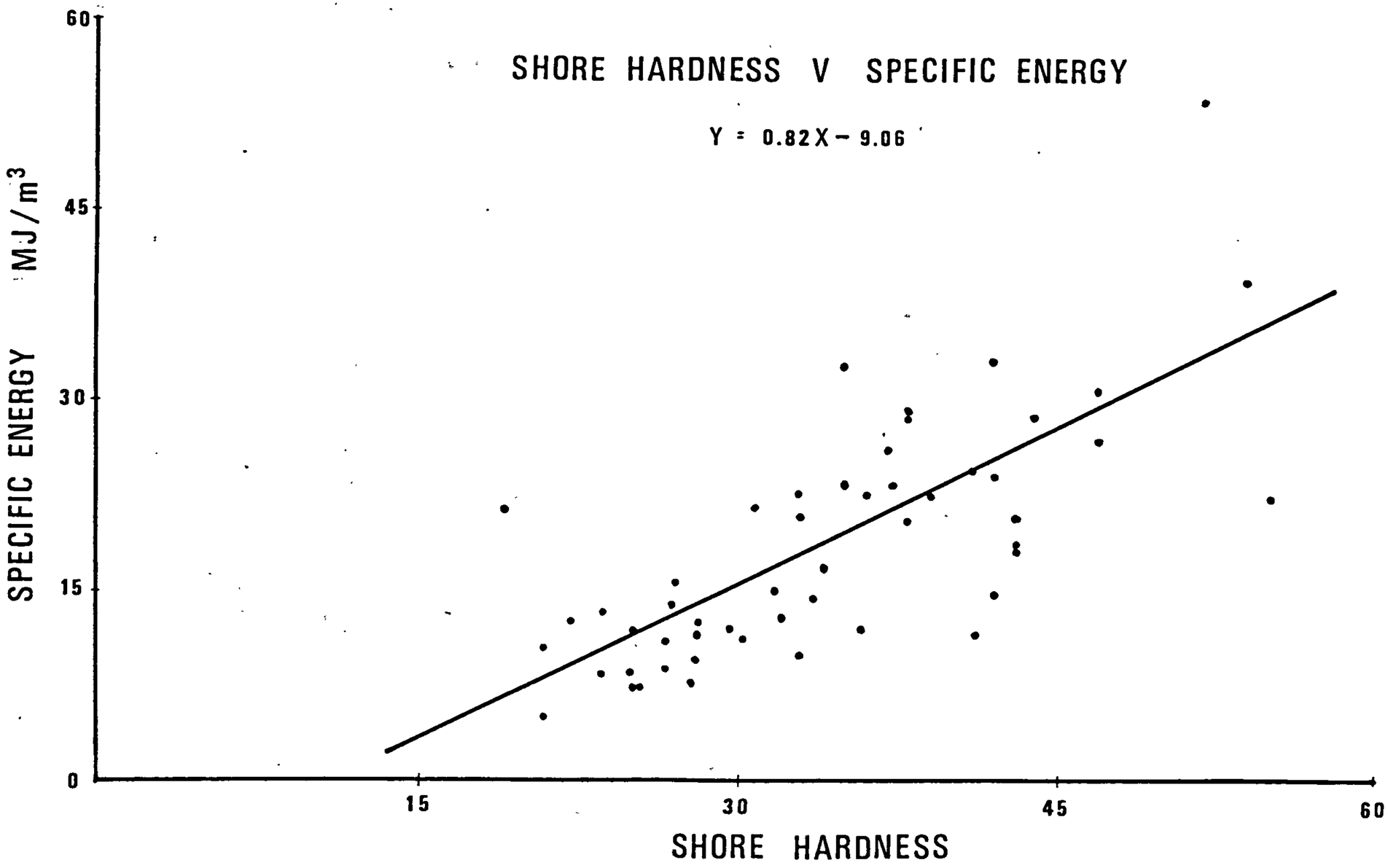

FIGURE 56

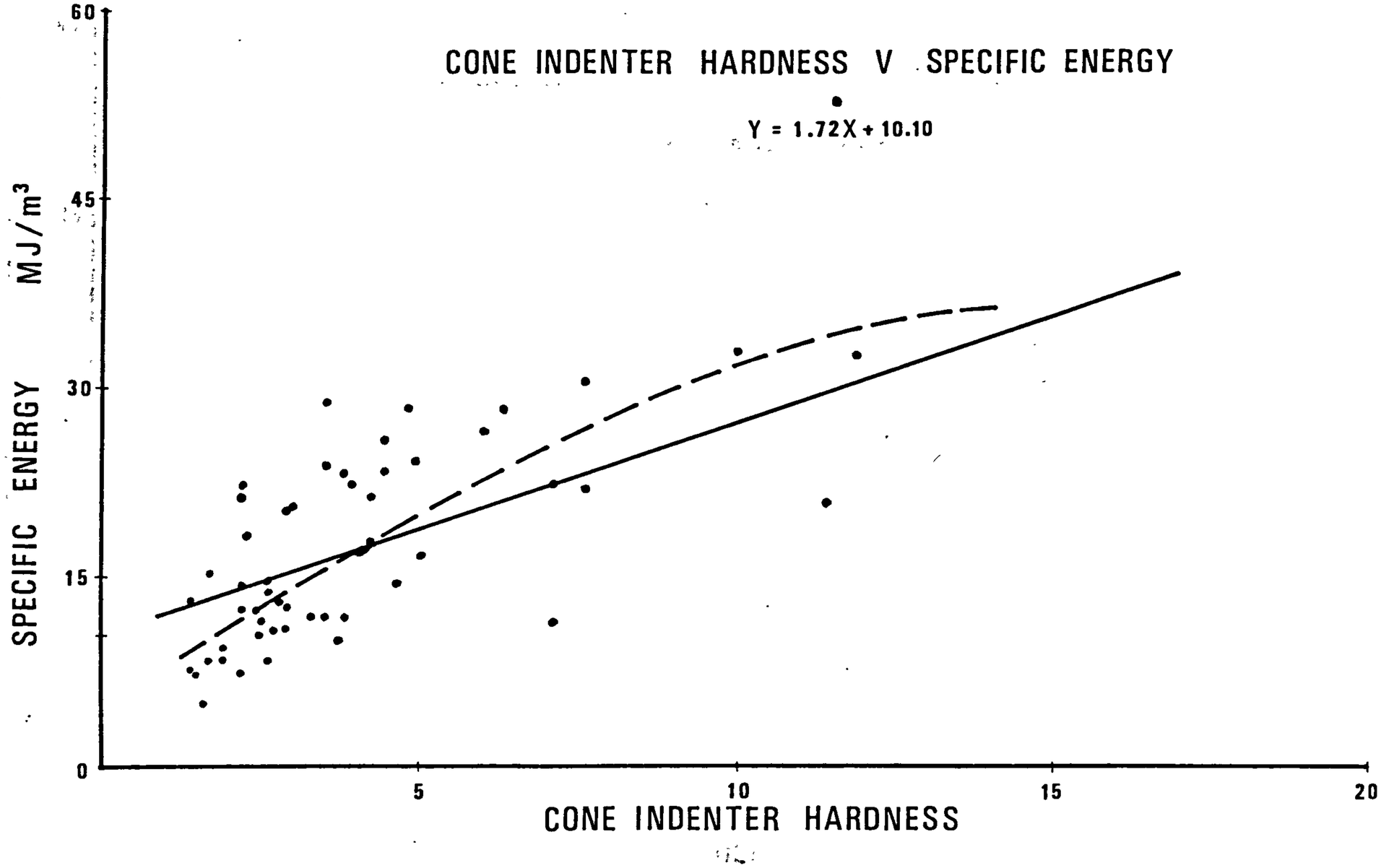
CONE INDENTER HARDNESS V SPECIFIC ENERGY
Y = 1.72X + 10.10
SPECIFIC ENERGY MJ/m3
60
45
30
15
0
5
10
15
20
CONE INDENTER HARDNESS

FIGURE 57

REBOUND NUMBER V SPECIFIC ENERGY

$Y = 0.92X - 23.98$

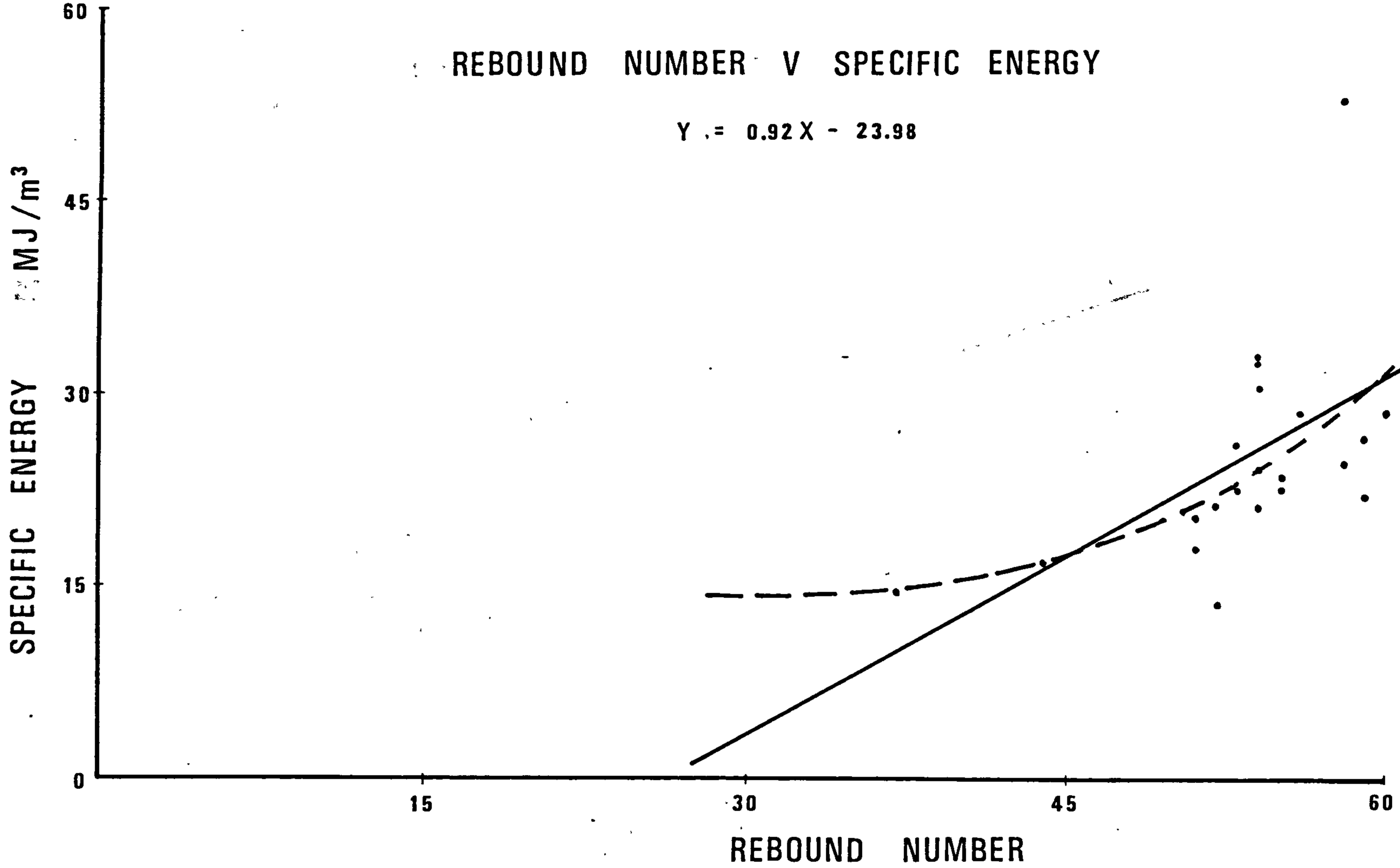

FIGURE 58

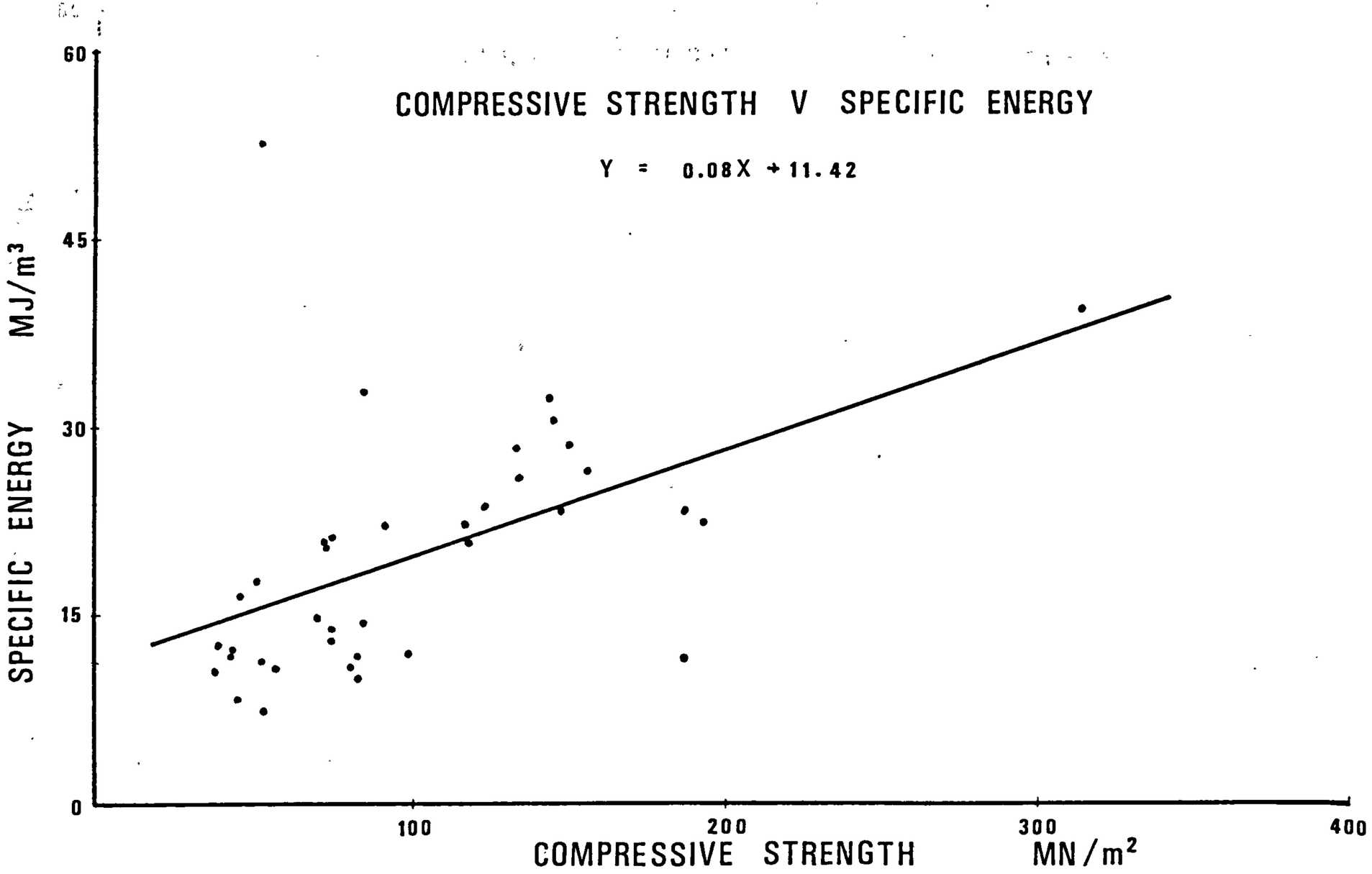
COMPRESSIVE STRENGTH V SPECIFIC ENERGY
Y = 0.08X + 11.42
SPECIFIC ENERGY MJ/m3
60
45
30
15
0
100
200
300
400
COMPRESSIVE STRENGTH MN/m2

FIGURE 59

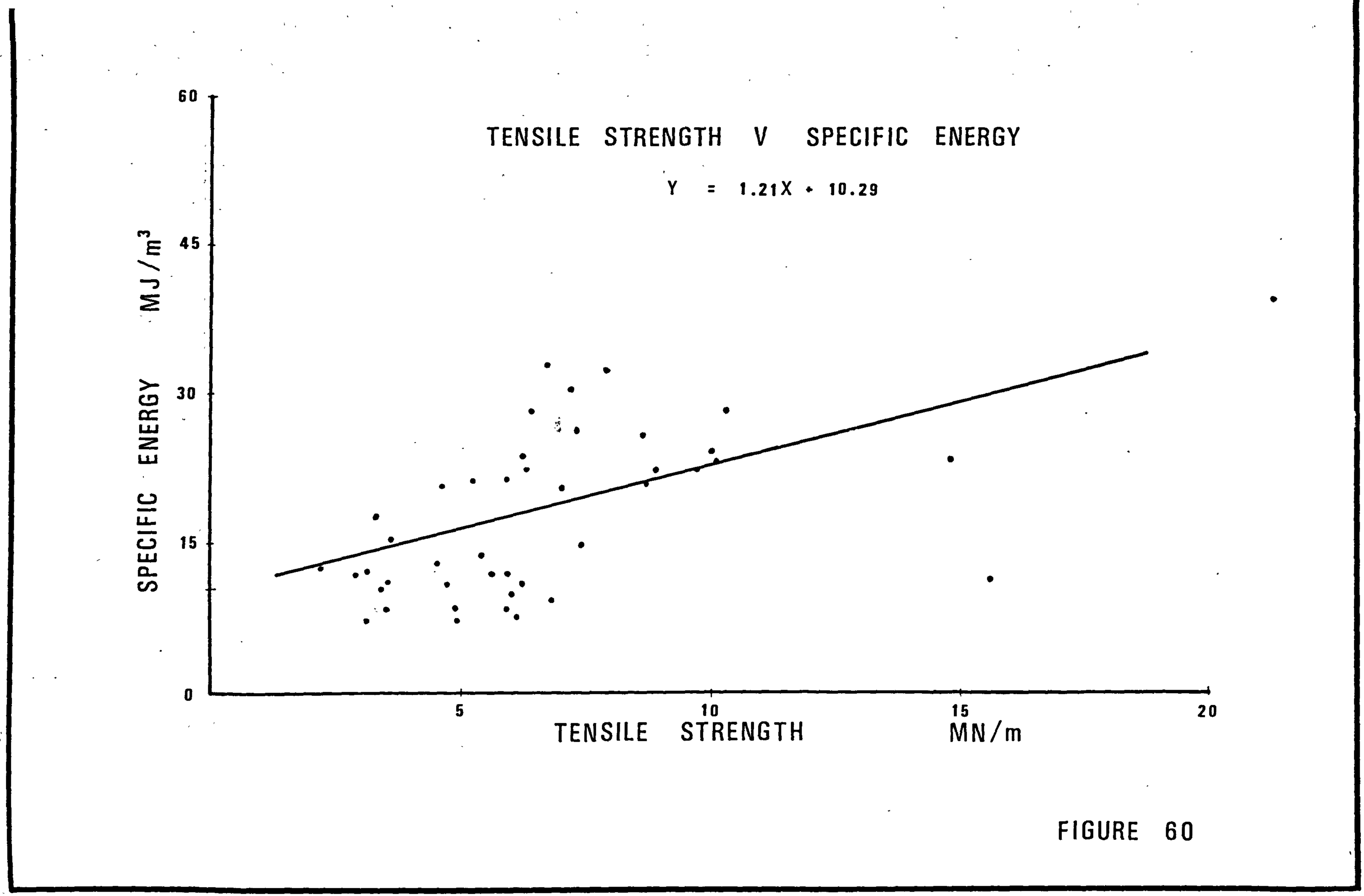
TENSILE STRENGTH V SPECIFIC ENERGY
Y = 1.21X + 10.29
SPECIFIC ENERGY MJ/m³
60
45
30
15
0
5
10
15
20
TENSILE STRENGTH MN/m

FIGURE 60

YOUNG'S MODULUS V SPECIFIC ENERGY

$Y = 0.32X + 11.23$

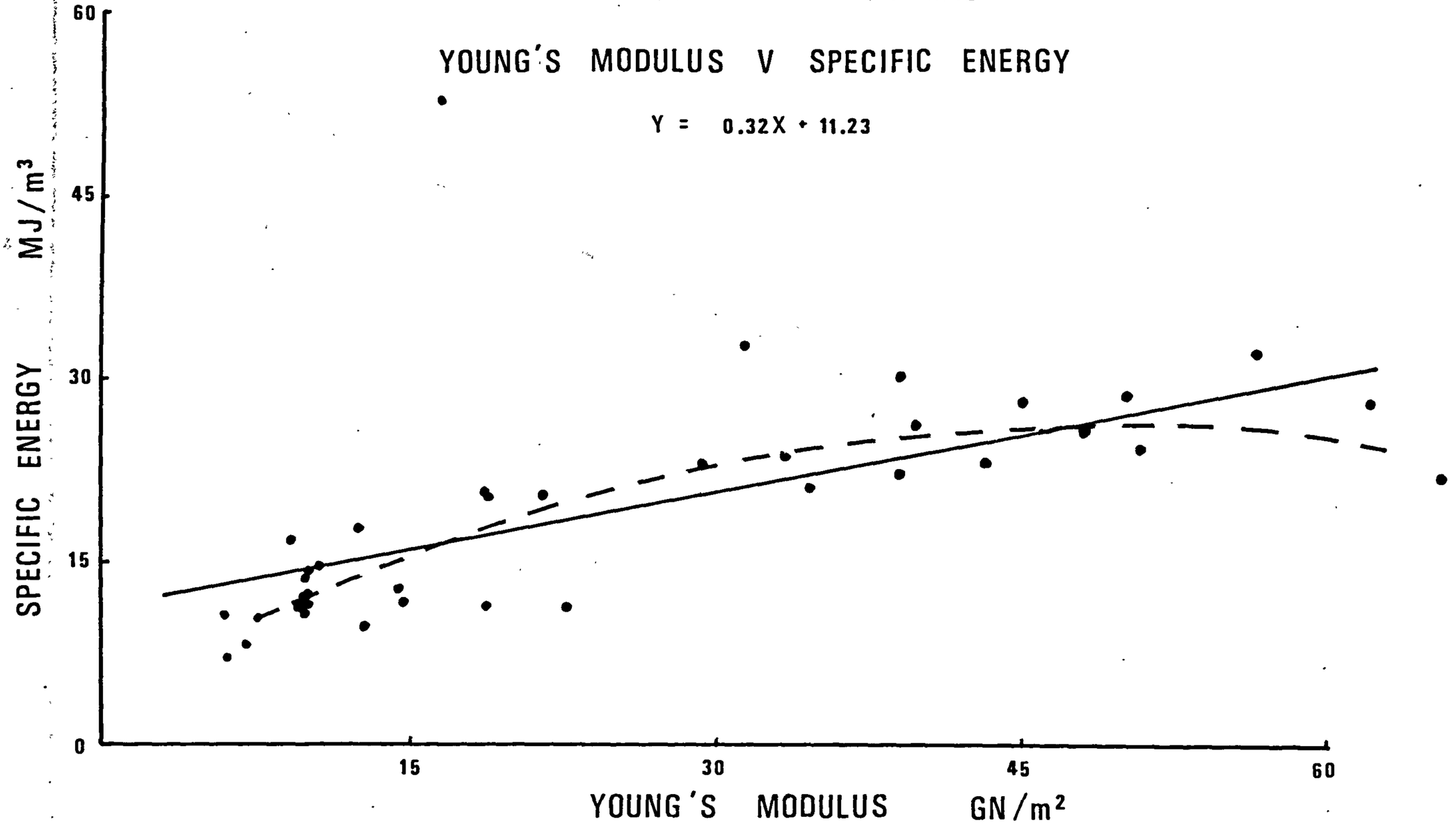

FIGURE 61

Specific energy v Coarseness index

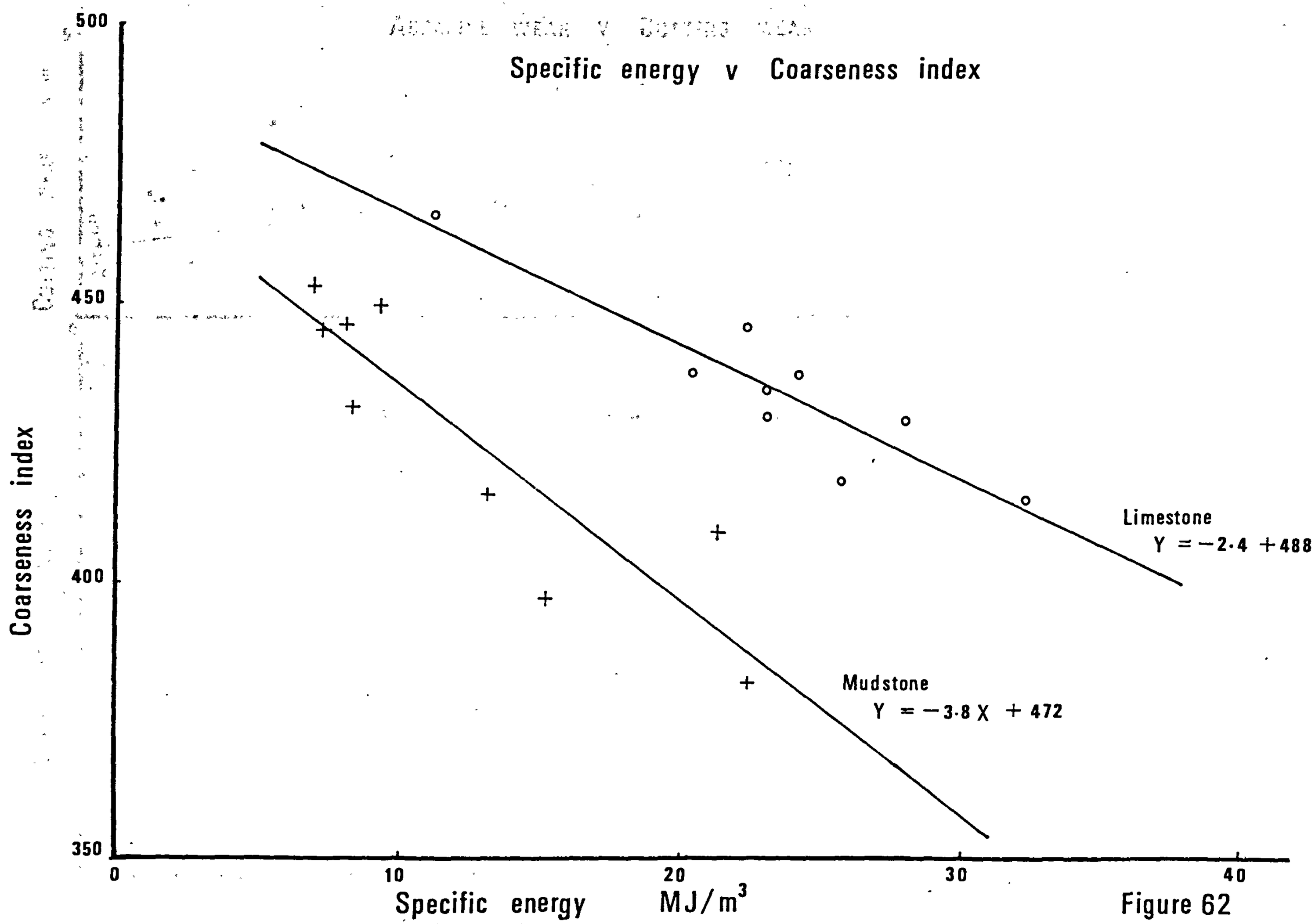

Figure 62

ABRASIVE WEAR V CUTTING WEAR

$Y = 0{\cdot}6X + 1{\cdot}3$

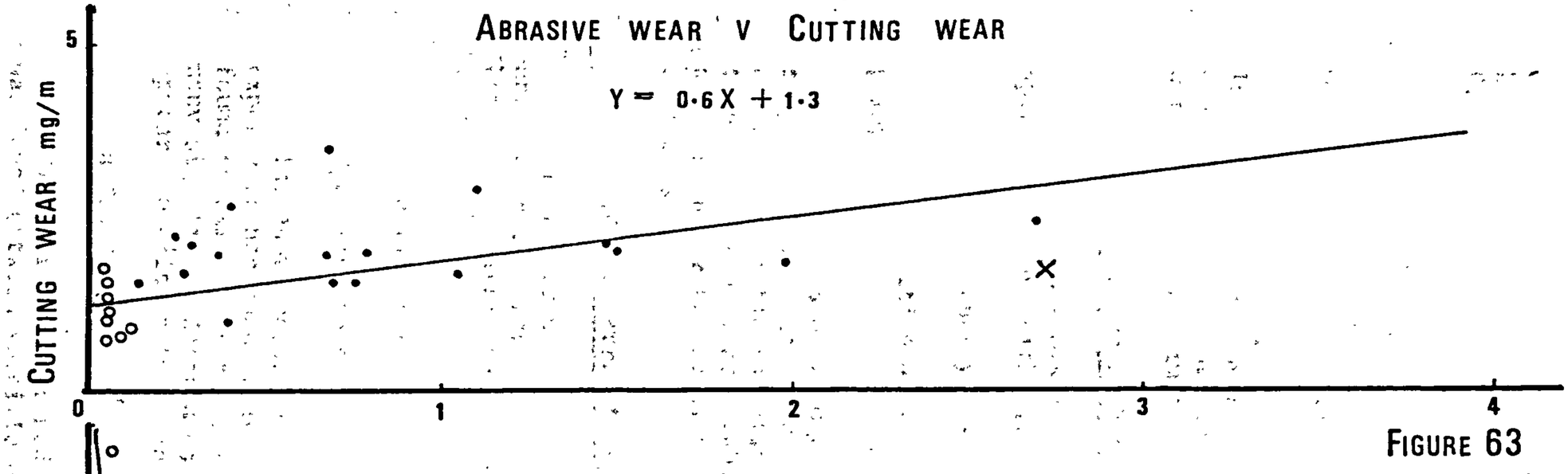

FIGURE 63

ABRASIVE WEAR V MACHINEABILITY INDEX

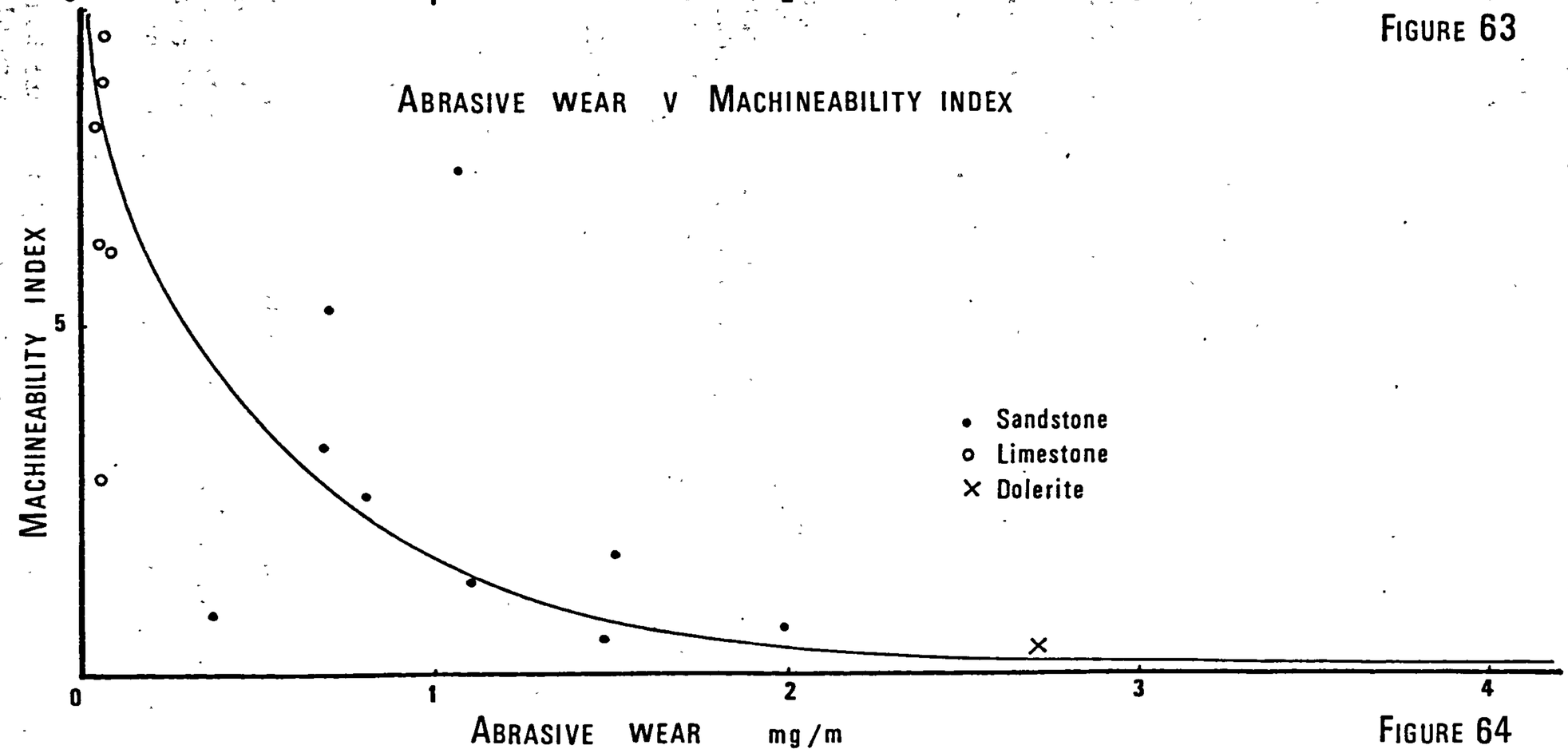

FIGURE 64

8.7.2 Cone indenter hardness against specific energy

Figure 57 shows a linear relationship between Cone indenter hardness and specific energy, with r_{xy} = 0.75 and significance level of 0.001:-

Specific energy = 1.72 Cone indenter hardness + 10.10

It can be seen from the same figure that a curvi-linear regression may provide a curve more suited to the points plotted.

In this case, the computed value of hardness is the mean value of 10 tests performed on each sample. And it was described before the wear flat of the cone was analysed at regular intervals to keep it within the 0.2 mm limit.

8.7.3 Rebound number against specific energy

Figure 58 shows a linear relationship between rebound number and specific energy, with r_{xy} = 0.59 and significance level of 0.01:-

Specific energy = 0.92 Rebound number - 23.98

As in section 8.7.2, a curve is probably suited to the plotted points.

The values of rebound number were obtained by clamping a core sample in a vice and using the Schmidt hammer. The computed rebound number show little variation (generally being 52-60) and their application to assessment of cutability in laboratory is questionable. A possible reason for the small range of values might be the rigid clamping system used.

8.7.4 Rock strength against specific energy

Figures 59 and 60 show relationships between compressive strength and specific energy and between tensile strength and specific energy, both with a significance level of 0.01 and r_{xy} = 0.49 and 0.45 repectively:-

Specific energy = 0.08 Compressive strength + 11.42

Specific energy = 1.21 Tensile strength + 10.29

The above relationships are purely qualitative because practical experience has shown that, although previous correlation (96) have been found to exist between rock strength and machine performance, there are many significant departures from it. A more significant relationship appears to exist between Young's modulus and specific energy (Figure 61).

8.7.5 Specific energy against Coarseness index

By separating the mudstone and limestone samples, a relationship was found between specific energy and coarseness index for each rock type. The equations are as follows:-

Limestone Y = -2.4 X + 488 (significance level of 0.01)
Mudstone Y = -3.8 X + 472 (significance level of 0.01)

where

Y = Coarseness index
X = Specific energy

This indicates that, as the coarseness index decreases, the cutting process is becoming less efficient (Specific energy increasing).

8.7.6 Abrasive wear against Cutting wear

Figure 63 displays a linear relationship between abrasive wear and cutting wear, with a significance level of 0.001:-

Cutting wear = 0.6 Abrasive wear + 1.3

The values obtained for cutting wear are generally higher than those for pure abrasive wear due to impact loading to the tip during the cutting process.

8.7.7 Abrasive wear against Machineability index

Figure 64 shows an exponential relationship between abrasive wear and machineability index (from Hacksaw test). As abrasive wear increases, the machineability index decreases rapidly.

8.8 General geological summary of cutability.

The rock type in which most tests have been performed is sandstone. This is significant when one considers that it is perhaps the most familiar of all rocks. Sandstone is made up of worn fragments derived from the disintegration of some older rock, such as Granite, and mainly consists of grains of quartz together with smaller percentages of micas and feldspars. Although all sandstones are made up of these basic ingredients, there is a great variation in their mechanical properties,

The value of Specific energy for the sandstones shows a general increase as you go down the stratigraphical columm (i.e.,from productive coal measures to the Carboniferous limestone series). This increase could be attributed to several factors:-

1. The environmental conditions during deposition;
2. The cementing materials and their binding qualities;
3. The effect of consolidation by overburden.

The most difficult sandstone to cut on energy basis is Nattrass Gill Hazle, which probably gains its strength from its secondary quartz matrix.

Figures65 - 70 show the progressive loss in weight due to abrasive wear as the distance the cutting tool has travelled is increased. It can be seen from these graphs that the abrasion effect is most pronounced in rocks whose main mineral constituent is Quartz, i.e., sandstone. A comparison between abrasive wear and percentage of Quartz present did not yield any satisfactory relationship. This would suggest

that it is not only the quartz content in a rock which causes abrasive wear. A detailed petrographic study carried out on the samples does indicate the importance of grain shape, grain size and bonding between the grains. The Nattrass Gill Hazle, which was extremely abrasive, was composed of sub-angular grains set in a secondary quartz matrix, while Victoria sandstone and the Low Grit sandstone, with their rounded to sub-rounded grains and no secondary quartz matrix, are less abrasive. An indication that homogeneous sandstone with large grains also cause severe abrasion is apparent from the abrasion wear test carried out in the First Grit sandstone and also in the Massive sandstone.

The limestone samples in section 8.5 are composed almost entirely of fine grained calcite, while those in section 8.6 contain a significant percentage of quartz. The value of specific energy for this rock type again shows a general increase as you descend the stratigraphical column, although the variation is much smaller than in the case of sandstone (general range being between 20 - 30 MJ/m^3). Figure 69 and Figure 70 show the constant non - abrasive nature of the limestones.

The mudstone samples are composed of compacted clay minerals. There is no stratigraphical/specific energy relationship for this rock type and any increase in specific energy is almost solely due to the presence of silt.

Dolerite is an intrusive igneous rock and is basically composed of feldspar and pyroxene minerals. It is an extremely difficult rock to cut on an energy basis, although it is not very abrasive. Metamorphism of the country rock when the Dolerite is in a molten state could lead to strengthening of it and the position of the Dolerite is therefore a very important stratigraphical consideration.

Saturated samples have been tested to determine the influence of moisture content on the cutting characteristics of rock. In a porous rock, saturation greatly reduces the value of specific energy, The values of wear, however, do show a slight increase on the cutting tool. In practice, if a constant flow of water was present, the previous effect would not be found in fact, the wear would probably be reduced with the water acting as a cooling agent.

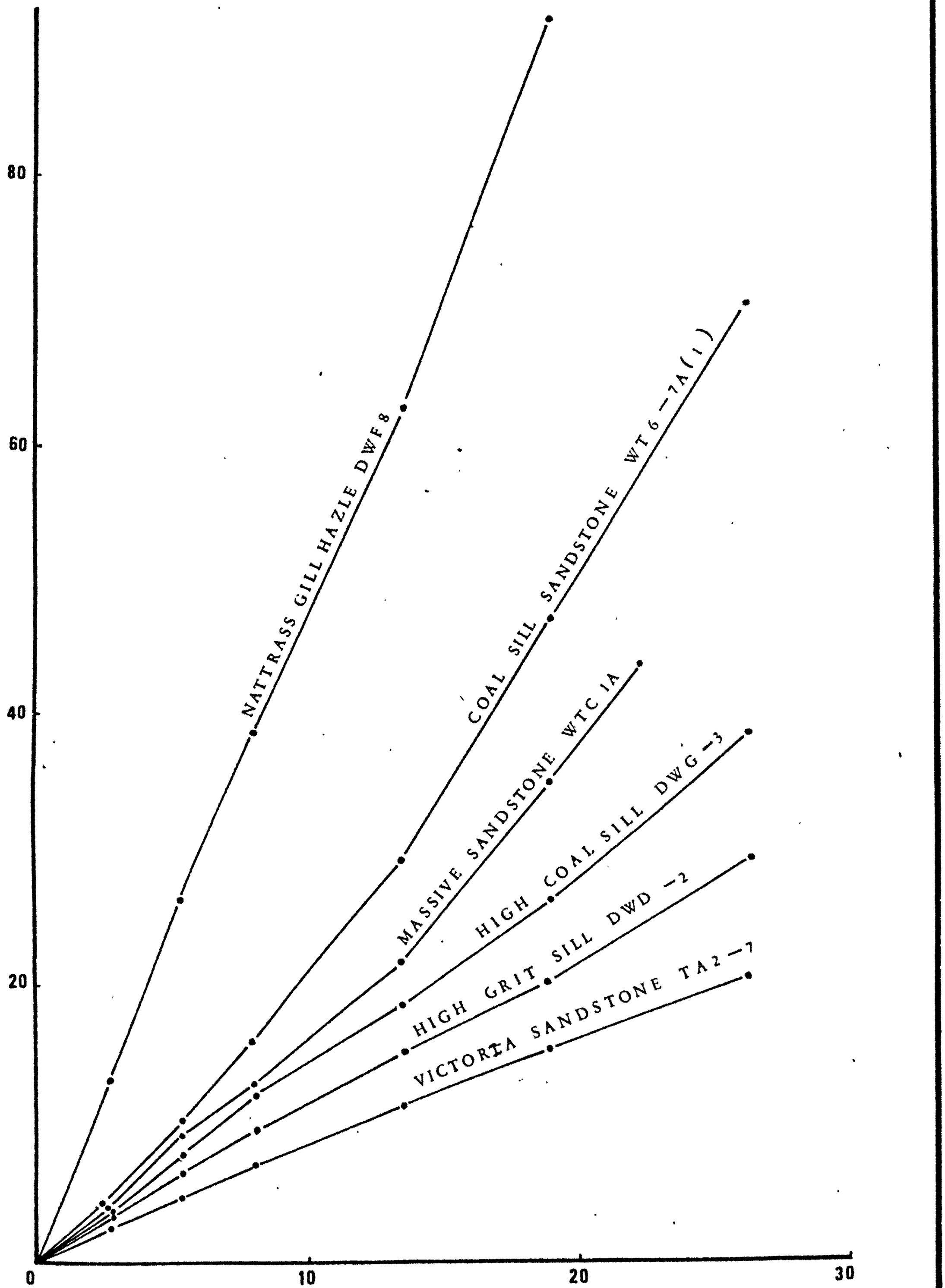
WEIGHT LOSS mg
80
60
40
20
0
10
20
30
NATTRASS GILL HAZLE DWF8
COAL SILL SANDSTONE WT6-7A(1)
MASSIVE SANDSTONE WTC 1A
HIGH COAL SILL DWG-3
HIGH GRIT SILL DWD-2
VICTORIA SANDSTONE TA2-7
DISTANCE CUT m

FIGURE 65

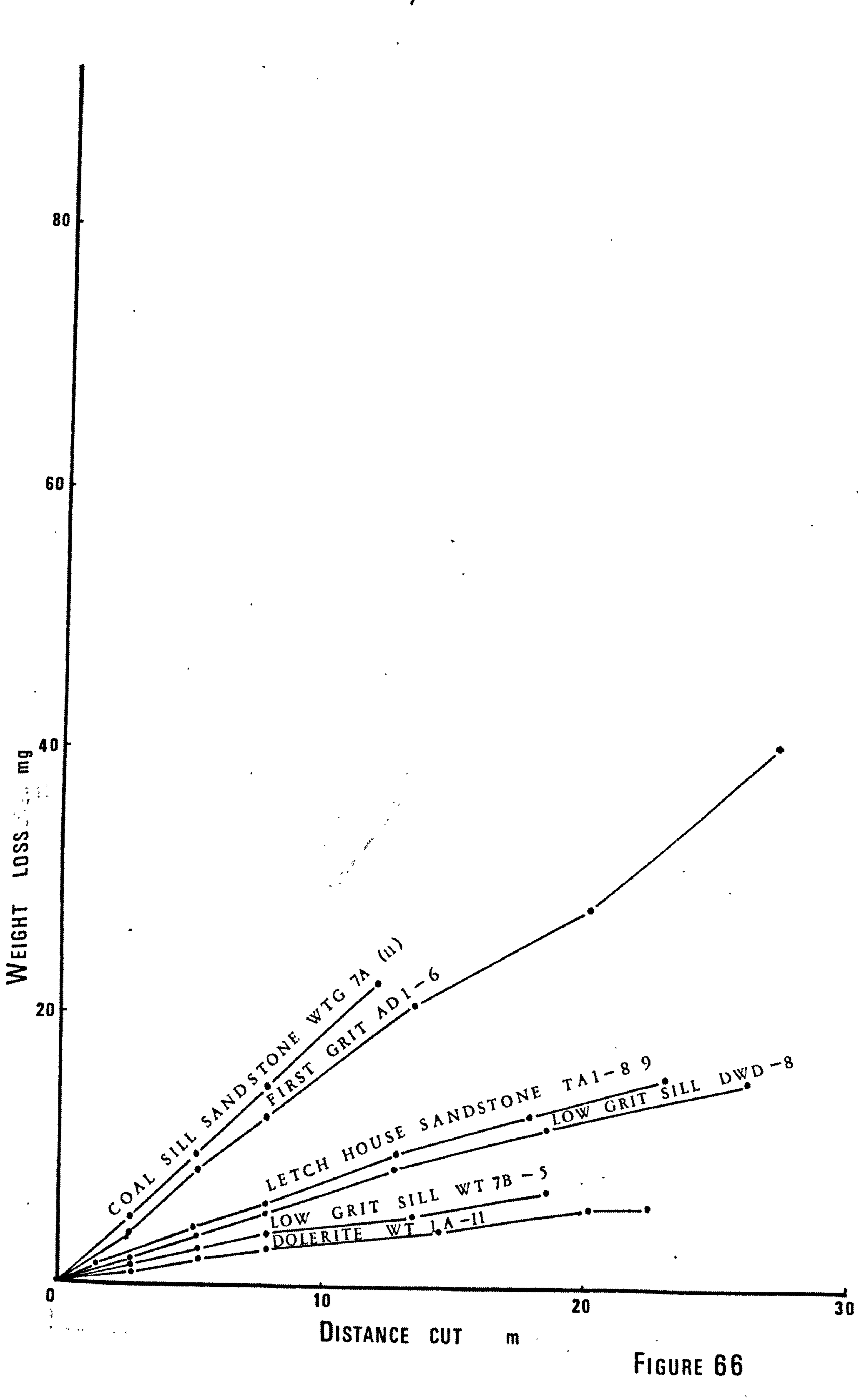
80
60
40
20
0
WEIGHT LOSS mg
COAL SILL SANDSTONE WTG 7A (ii)
FIRST GRIT ADI-6
LETCH HOUSE SANDSTONE TA1-8 9
LOW GRIT SILL DWD-8
LOW GRIT SILL WT 7B-5
DOLERITE WT 1A-11
10
20
30
DISTANCE CUT m

FIGURE 66

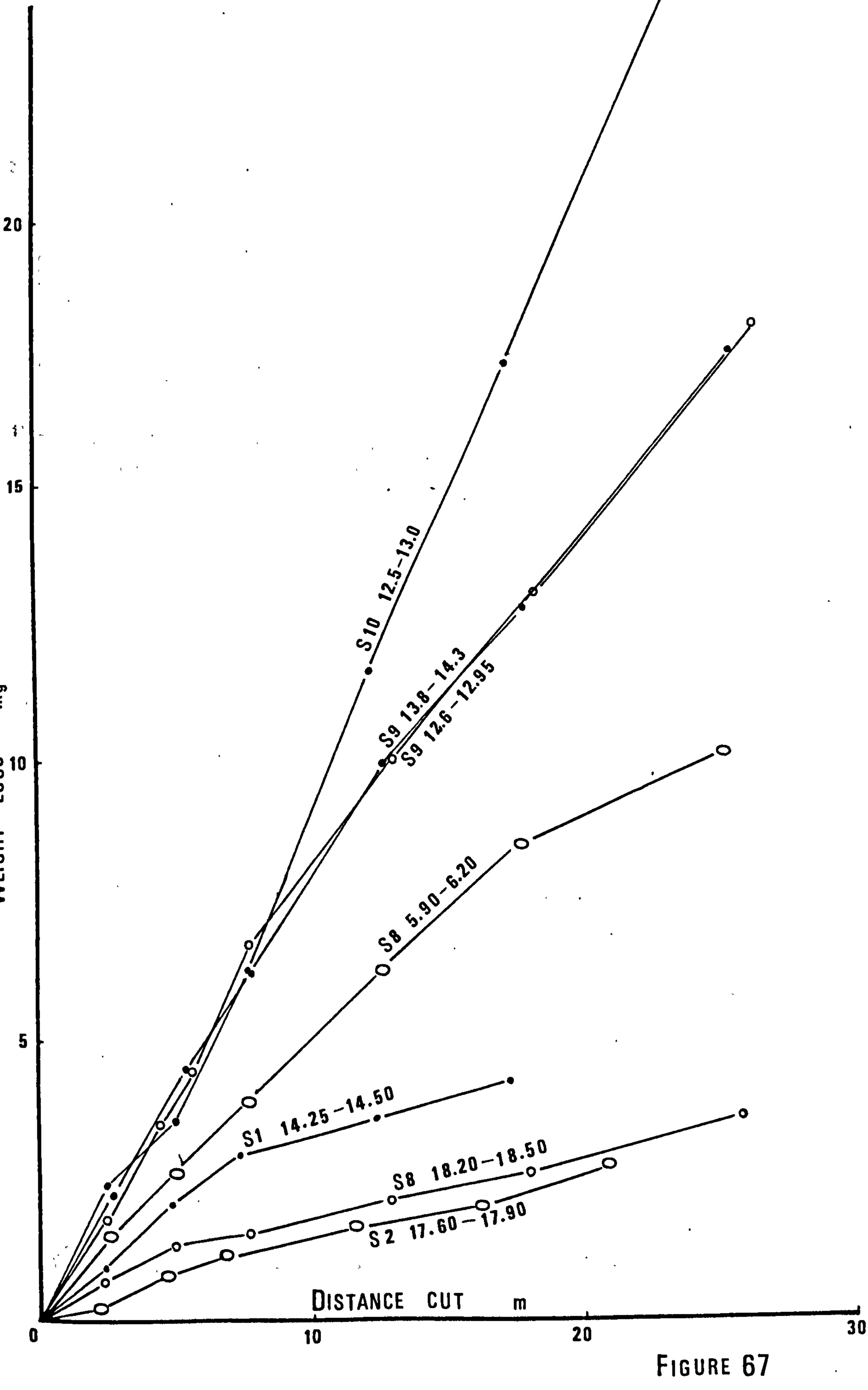
WEIGHT LOSS mg
0
5
10
15
20
DISTANCE CUT m
0
10
20
30
S10
S9 13.8–14.3
S9 12.6–12.95
S8 5.90–6.20
S1 14.25–14.50
S8 18.20–18.50
S2 17.60–17.90
12.5–13.0

FIGURE 67

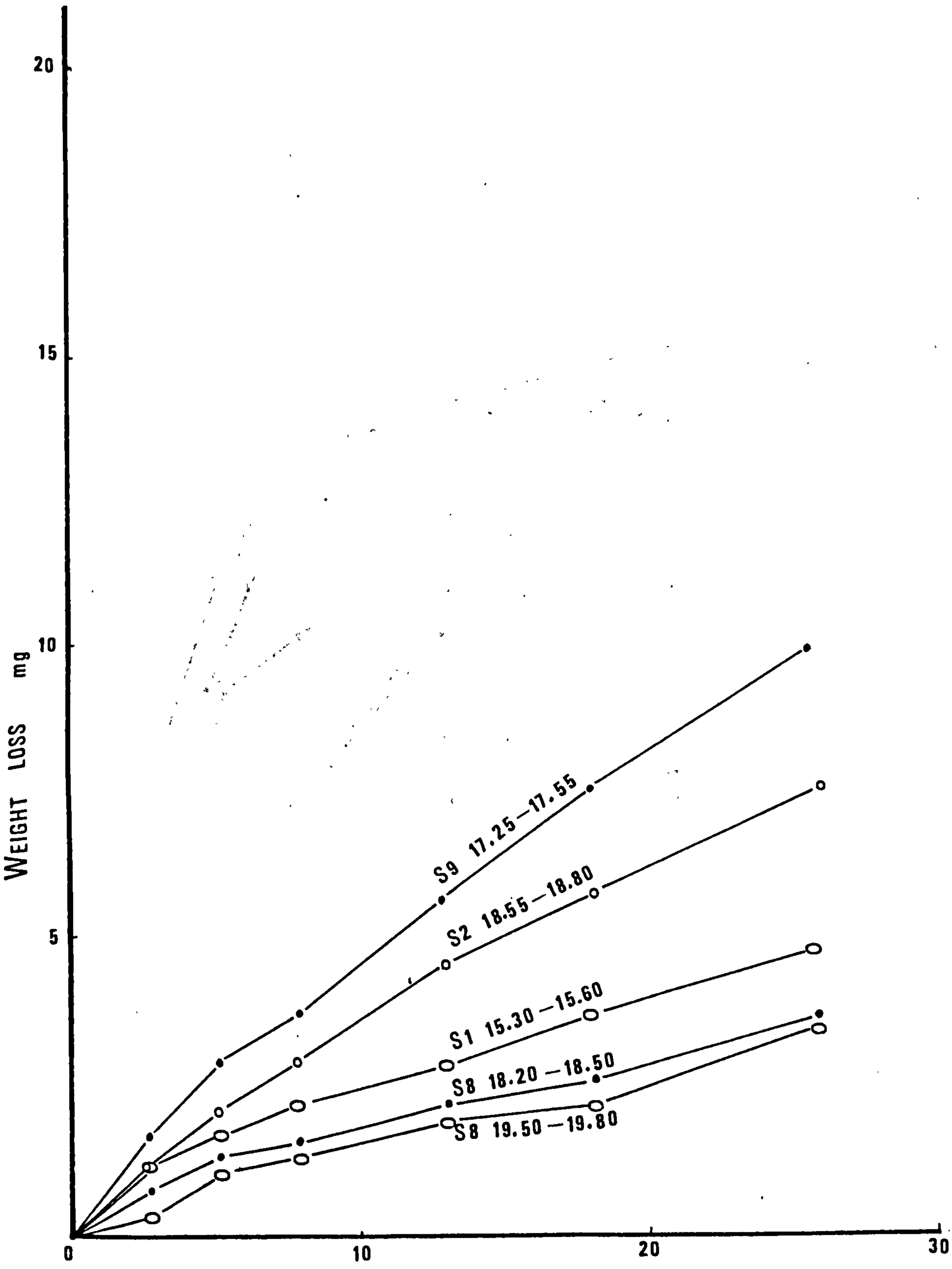
20
15
10
5
0
10
20
30
WEIGHT LOSS mg
DISTANCE CUT m
S9 17.25–17.55
S2 18.55–18.80
S1 15.30–15.60
S8 18.20–18.50
S8 19.50–19.80

FIGURE 68

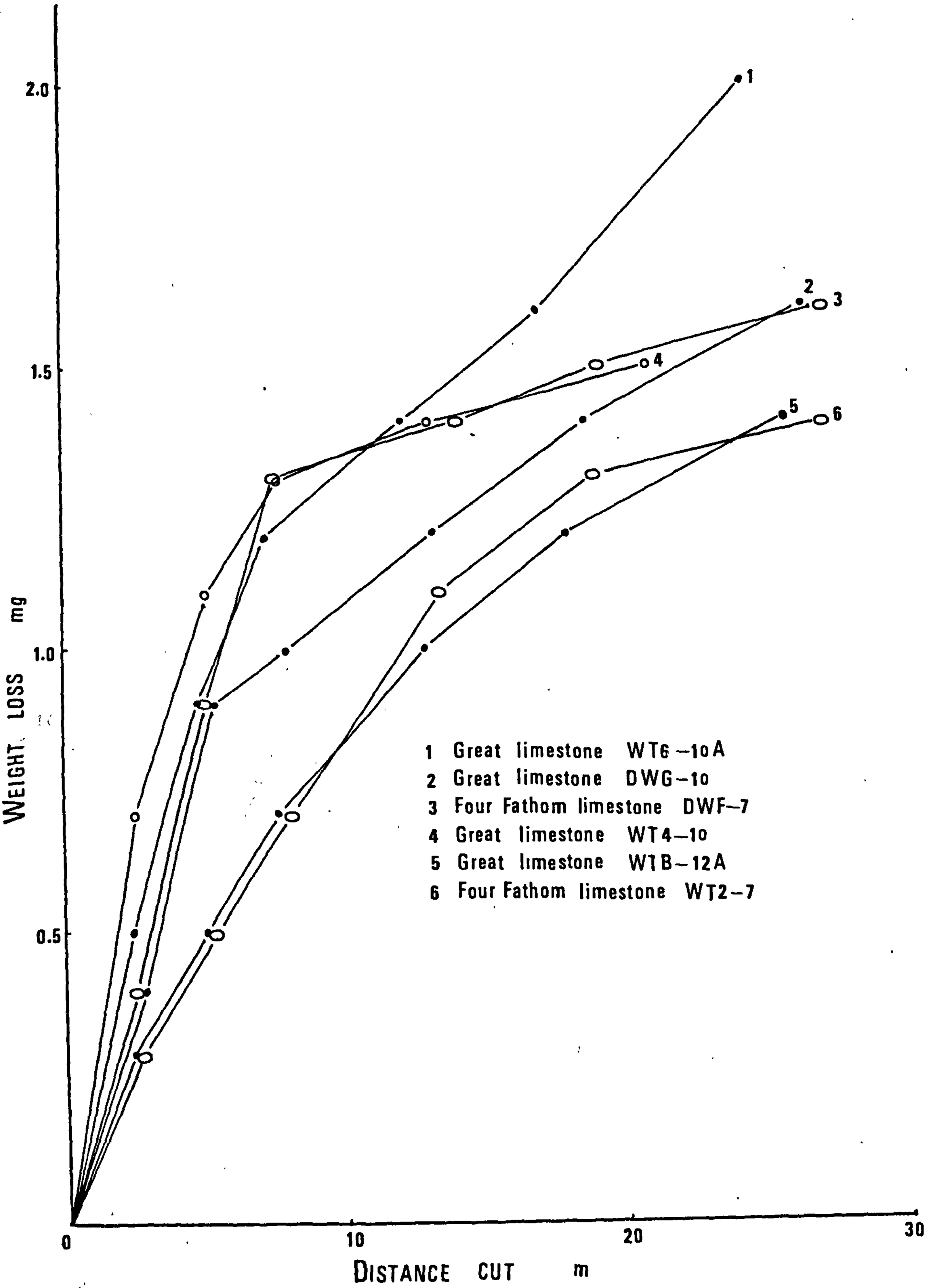
2.0
1.5
1.0
0.5
mg
WEIGHT LOSS
0
10
20
30
DISTANCE CUT m
1
2
3
4
5
6
1 Great limestone WT6–10A
2 Great limestone DWG–10
3 Four Fathom limestone DWF–7
4 Great limestone WT4–10
5 Great limestone WTB–12A
6 Four Fathom limestone WT2–7

FIGURE 69

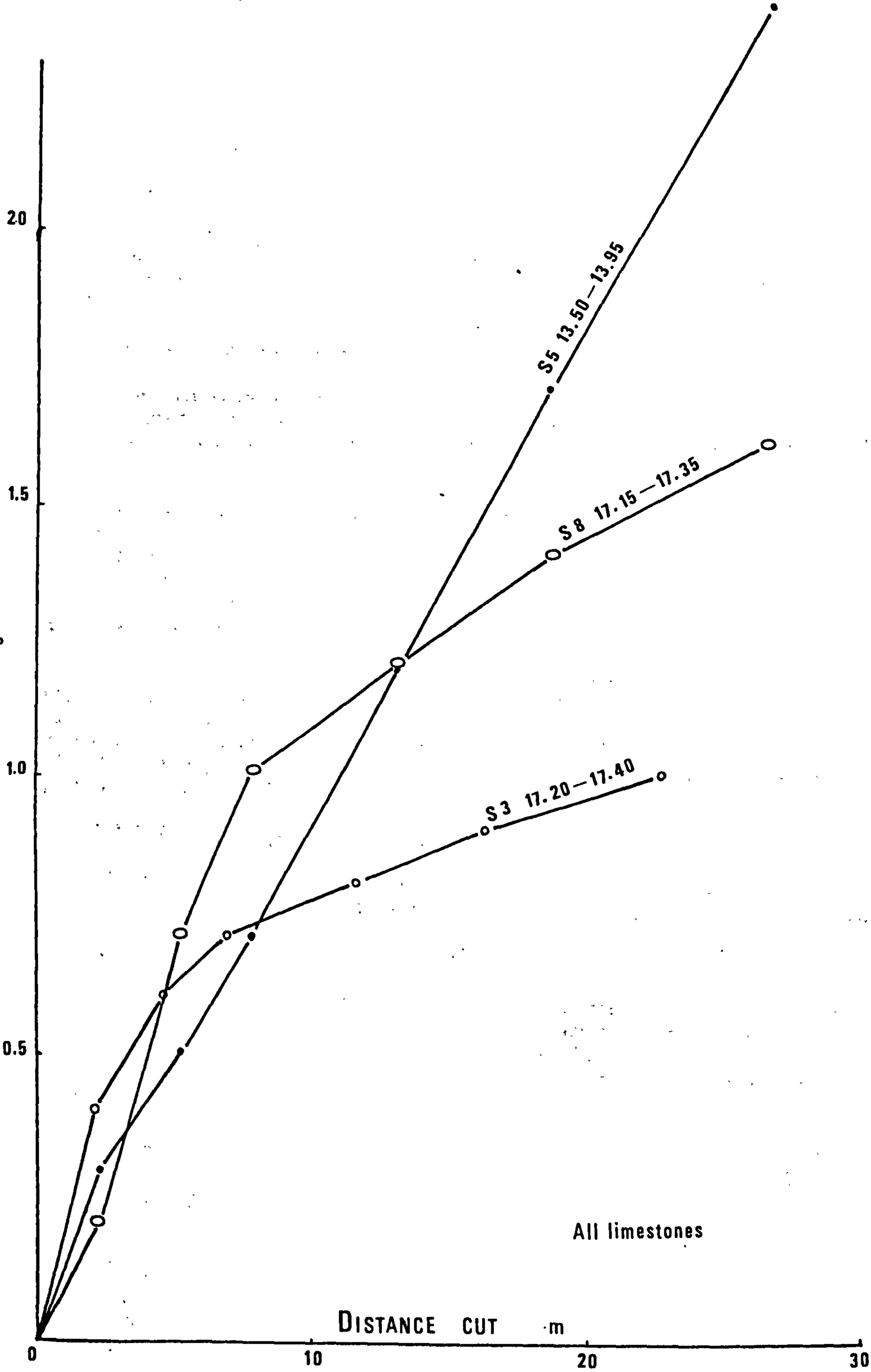
20
1.5
1.0
0.5
0
WEIGHT LOSS mg
S5 13.50—13.95
S8 17.15—17.35
S3 17.20—17.40
10
20
30
DISTANCE CUT m
All limestones

FIGURE 70

Chapter 9

Conclusions and Recommendations

9.1 Conclusions

As individual conclusions for each investigation have been given at the end of the appropriate sections, only the general conclusions will be considered in this chapter. Recommendations for further work are also included in each section of this chapter.

9.1.1 Petrographic analysis

The analysis provided useful information on the mineral constituents, quartz content, grain shape, grain size distribution, and bonding matrix which enable the estimation of abrasivity of rock with some confidence.

It was found the abrasivity of rock depends on the following variables:-

1) presence of quartz
2) grain size
3) grain shape

and 4) bonding matrix.

For the rock whose main mineral constituent is quartz, i.e.sandstones, the type which is composed of subangular grains set in secondary quartz matrix is more abrasive than the type which is composed of subrounded grains and no secondary quartz matrix. Also there was an indication that homogeneous sandstones with large grain always cause severe abrasion.

9.1.2 Density and porosity test

Standard procedure for density and porosity tests are simple, however tests for grain density and true porosity required further steps of operation and more complex than the bulk density and apparent porosity tests.

It was found that grain density bears no significant relation to other rock properties investigated so far, therefore this property should be omitted from the test matrix. Furthermore the true porosity test required the figure of the grain density during the calculation process, it has to be neglected in succession.

It was also found the inverse relation between porosity and rock strength, meaning that porosity affects strength of rock, as follows:-

compressive strength = -7.133apparent porosity + 161.33
with r_{xy}(correlation coefficient)
= -0.657

tensile strength = -0.475apparent porosity + 11.28
with r_{xy} = -0.612

and impact strength index = -1.734apparent porosity + 80.24
with r_{xy} = -0.662.

9.1.3 Rock strength

In rock strength test the uniaxial compression test and the indirect tension test were the only accepted ones to be included in the test matrix. It was found impossible to apply the direct tension test to hard rocks, whilst specimen preparation was found to be difficult with the bending test. The multi-axial strength tests are complex and too expensive, these tests were therefore neglected.

Both tests were loaded, on the compression machine, at the loading rate of 0.69 MN/m^2/sec (100 psi/sec). Slenderness ratio (L/D) for compression test was kept to be 2:1. Steel platens were used throughout the investigation.

It was found that rock strength are influenced by its internal structure, so sedimentary rocks with a relatively large amount of pore space will tend to be weaker in compression than fine-grained metamorphic or igneous rocks. This is supported by the statistical relationships:-

compressive strength = -7.133apparent porosity + 161.33
tensile strength = -0.475apparent porosity + 11.28

with r_{xy} of -0.657 and -0.612 respectively.

Compressive strength of rock could be used as a guide for selecting the type of tunnelling machine (3) as:-

CS MN/m^2	Hardness	Cutter type	Rock type
40 (max.)	soft	picks, discs, gear rollers	shale, clay
40 - 80	medium	picks, discs, gear rollers	dolomite, sandstone, marble
80 - 170	medium hard	buttons, discs	limestone, gneiss, granite
170 +	hard	button cutters	diorite, quartzite, hornblende.

The important relationships between rock strength and specific energy were found to be:-

compressive strength = 3.00 specific energy + 40.50
and tensile strength = 0.25 specific energy + 3.50

however the above relationships are purely qualitative since practical experience has shown that there are many significant departures from it.

9.1.4 Modulus of elasticity

Both static and dynamic modulii were investigated, using the conventional cycle loading test for static modulus and the longitudinal wave velocity test for dynamic modulus.

Tension modulus was also investigated using the direct tension procedure incorporate with the Huggenberger extensometers, secant modulus was computed.

Secant modulus , tangent modulus, and Poisson's ratio were computed from the third loading cycle at load level of 50 per cent of the compressive strength.

The expense for performing static test is high and it is a time consuming test while the dynamic test is cheaper and quick to carry out.

Some significant inter-relations between these properties were found to be:-

Dependent variable	Independent variable	Slope	Y-intercept	r_{xy}
Secant modulus	Tangent modulus	0.977	-0.58	0.978
Tension modulus	Tangent modulus	2.274	-3.69	0.993
Dynamic modulus	Tangent modulus	0.915	1.85	0.612
Tension modulus	Secant modulus	2.295	-2.15	0.997
Dynamic modulus	Secant modulus	1.051	1.94	0.701
Dynamic modulus	Secant modulus	0.781	1.41	0.980

9.1.5 Hardness test

Four methods of test representing two types of hardness were studied, i.e.:-

indentation hardness - Cone indenter test
- Firthbrown hardometer test

rebound hardness - Shore Scleroscope test
- Schmidt hammer test.

The idea of the indentation hardness test is to measure the resistance of the sample to be indented, while measuring the sample's resilience in the rebound hardness test.

In all hardness tests it is necessary to take a large number of readings and treat the results statistically due to the heterogeneous nature of rocks.

Considering the suitability of the four tests for laboratory use, all tests but the Schmidt hammer test are accepted. The Schmidt hammer is only suitable for field test only. The most suitable instrument for laboratory and field work might be the Cone indenter because of its compactness.

Hard rocks required special application for the Cone indenter test and the Shore hardness test. The first method required a double load level, which is called the modified test, while the latter required a heavier mass, the diamond tipped mass instead of the tungsten carbide tipped mass. This would allow the readings to be within the scale.

In the Firthbrown hardometer test, load level and diameter of the indenter used for a particular rock have to be predetermined depending on rock strength. However the readings on rock specimens were not clear enough, it is necessary to grind the test surface to a flat finish and coat it with a thin film of aluminium paint.

The Schmidt Betonpruf-hammer type N could be used for laboratory testing, if required providing the specimen size is larger than a 200 mm square block.

Using a statistical approach, a linear relationship was found between Specific energy and Shore hardness as:-

Shore hardness = 0.70 Specific energy + 20.60.

9.1.6 Hacksaw machineability test

Rock machineability obtained from this test is the average cumulative area of ten cuts on rock specimen by hacksaw machine using high speed steel blades of 800 VPN as a cutter.

The machineability index of a particular rock can be computed by the equation:-

$$\text{Machineability index} = \frac{\text{Machineability of rock}}{\text{Machineability of gypsum}} \times 100 .$$

Abrasivity of rock can be determined from the graph plotted between cut number and area cut. The tangent of the curve between the first and second cut multiplied by 100 is the abrasivity of a particular rock.

The effectiveness of this test is considered to be reasonable, however many more rocks must be tested in order to analyse the results statistically to get a reliable prediction of rock cutability.

9.1.7 Intrinsic abrasivity test

This test is similar to the Cerchar abrasivity test and is based on a steadily-applied constant force of 7 kg on a rod having a sharp point of 90° cone angle applied against the rock sample. The rock is then displaced by dragging it a distance of 1 cm at low speed. The abrasivity is a function of the diameter of wear flat created on the point of the tool.

It was found impossible to select one type of tool material that could be applied through the whole range of rock materials. Due to this reason, silver steel was used for soft rocks and high speed steel for hard rocks. Fortunately both types of material could be applied to some rocks. The regression equation of the abrasion factor of the two materials were then computed and enable one to construct an arbitrary wear flat scale, which makes it possible to calculate a standard abrasion factor.

The abrasion index of a particular rock can be computed from the equation:-

$$\text{Abrasion index} = \frac{\text{standard abrasion factor of rock} \times 100}{\text{standard abrasion factor of Scottish qtz.}}$$

9.1.8 Impact strength index test

This is a simple test to measure the ease with which a rock can be degraded. Rock with high impact strength index indicates that the rock is difficult to degrade.

Using statistical approach it was found that ISI relates to other properties by:-

Dependent variable	Independent variable	Slope	Y-intercept	r_{xy}
ISI	App. porosity	-1.734	80.24	-0.662
ISI	True porosity	-2.007	84.85	-0.832
ISI	Compressive strength	0.151	52.64	0.643
ISI	Tensile strength	2.212	51.34	0.686

However the test is still unreliable without further investigation.

9.1.9 Core cutting test

The test involves undertaking cutting tests on core sample using a standard tool shape, at a standard depth of cut and cutting speed and using a constant grade of tungsten carbide. The test provides the values of Specific energy which can be used for a direct comparison of rock types, but which also be adjusted to take account of the type of tool and method of attack to be employed by the proposed machine.

Coarseness index which provides a useful guide on the relative size distribution of rock debris influencing a muck disposal system are obtained, in the test, as well as cutting tool wear, and breakout angle which is the important guide on the spacing of cutting tools on machine.

Abrasive wear is the other quantity evaluated, using a lathe, in which the undersized core remaining after completing the core grooving test is rotated between centres. A standard tool is fed longitudinally along the core surface, taking a small cut of some distance.

Specific energy is the most useful parameter since it can be translated into cutting power requirements to excavate rock at a specific rate.

In all, the machine performance at the rate at which cutting tools are likely to wear could be predicted with some confidence by this test.

9.1.10 Site investigation

The test consists of the geological description and the standard core cutting test on the specimens obtained from the preliminary bore-holes along the proposed tunnel lines.

The geological description thus provides information on the type of the major stratum and its constituents.

The standard cutting test provides an information on Specific energy of the rocks enabling one to derive the power levels required by the machine, also provides the relative rates at which cutting tools are likely to deteriorate during the excavation process.

Considering the above informations along with the standard rock property tests, a useful guide for choosing the type of tunnelling

machine, the design and operation variables can be obtained easily.

The tests were used on two tunnelling projects.

It is hoped that this work has prepared the way for more detailed investigations into cutability of selected strata. Once more information is known about successful application on TBM's and thus is related to geological and operational parameters, the mechanised winning of the world's much needed minerals can be undertaken.

9.2 Recommendations

1. Work on standard rock property tests should be continued to provide a sufficient number of rock tested in order to get the precise correlation between the properties.

2. Rock tested, then, should be classified according to the type, for example, granite, limestone, sandstone, quartzite, marble, slate, and etc.. Then the relation of the properties in the class should be investigated.

3. Work on rock cutability should be continued, using core samples as well as block samples of a wider range of rock. When selecting the rocks for further investigations, it would be useful to embrace the strata in which tunnelling experience has been gained. Data would then be available on rocks which have been excavated and those which are likely to be excavated.

4. If either of the two projects under consideration in this thesis employs a tunnelling machine, it would be extremely useful to instrument the machine to provide a precise relationship between field effectiveness and laboratory assessment. The rate of tool consumption in the various strata should also be compared with the values obtained for abrasivity to quantify the abrasive wear parameter.

5. Saturation of test samples was found to increase the efficiency of cutting in porous rock. The effect of saturation should be studied in other rock types. Cutting and abrasive wear tests using water sprays at the rock—tool interface should be carried out to study the effects on wear.

6. The use of linear regression has helped in the evaluation of the various relationships between the different methods of assessment. As has been indicated previously, a curvi-linear regression may yield more precise relationships in certain cases. The application of multi-linear regression analysis should also be investigated.

Appendix 1

Method of Making Thin Section of Rocks and Minerals, and Method of Impregnation of Specimens

For the examination of rocks and minerals under the microscope thin slices or sections are required. A chip of rock is ground perfectly flat on one side, with emery powder or carborundum powder on a glass or metal plate. The grinding is begun with a coarse powder (220), and continued with finer powders (320 and 600) respectively, until a perfectly smooth flat surface is obtained. In transferring the chip from one grinding plate to a finer one, it is necessary to wash the chip free from emery otherwise the grades of grinding powder become mixed on the plates. A glass slip (7.5 x 2.5 cm) is taken and a small amount of Canada balsam, or other transparent fixing material such as Lakeside 70, placed in its centre and heated gently until sufficient turpentine or xylol has been driven off to cause the balsam to become hard and compact when cool. The correct moment to cease heating the balsam is judged by taking up a small quantity on forceps, and, by opening the forceps, causing a bridge or thread of balsam to be formed. If the balsam has been sufficiently heated, this bridge will be hard and brittle when cool. The chip of rock is then placed on the slip with the flattened side in contact with the balsam and glass. By pressing the chip air bubbles are removed from the film of balsam between the chip and glass. When cool, the chip will be firmly cemented to the glass slip. The next operation consists of grinding down the thick chip as in the first process, begining with the coarse and ending with the finest powder. Great care is necessary during the final stages, or the rock will be completely rubbed away. The thickness of the slice can be judged by the polarization colours given by recognizable mineral, such as quartz, and grinding must be continued until this mineral shows its usual polarization colours-for quartz, grey and yellow of the first order, i.e. 0.03 mm thick. After the final grinding, the section is carefully washed and all remaining balsam scraped from around the rock. The slice is then covered with fresh balsam and heated again to a slightly less extent than before. When the balsam is of the right consistency, a very thin sheet of glass - the cover-slip of about 0.17 mm thick - is carefully placed over the rock and pressed down so that no air bubbles are present. Any balsam round the cover-slip is removed by methylated spirit. The result of these operations is what is known as a thin section or a thin slice of the rock or mineral.

Some friable rocks, such as Bunter sandstone, mudstone, and etc., needed to be impregnated before it will be ground into thin slice. The impregnating procedure used here is the impregnation with Bakelite Resin SR 17497 which has the refractive index at 20°C = 1.527. Other impregnating materials can be used provided that they have as low a viscosity as possible under the conditions of impregnation, and should set with a minimum volume of change. When set, the impregnation material should be relatively hard and brittle at room temperature, colourless and isotropic in thin section, with a refractive index as close as possible to that of canada balsam (1.536) the classical mounting medium for thin sections of rock

Impregnating procedure with Bakelite Resin SR 17497

Resin	Bakelite SR 17497
Accelerator	Bakelite Q 17446
Catalyst	Bakelite Q 17447

In general 100 grammes resin is mixed with 2 cc accelerator and 2 cc catalyst and a number of specimens, which have been dried in the oven for 24 hours and already cool at room temperature, immersed in the mixture. The mixture is then placed in dessicator, and air evacuator, for 10 minutes. Pressure is restored and the specimens placed out on the bench. When these specimens are hardened, they will be treated in the usual way.

Appendix 2 Linear Regression Analysis

Pairs of x and y	n	r_{XY}	Significant Level of r		$Y = a + bX$	Significant Level of b			T	S.E. $_{Y.X.}$	R^2_X
			.05	.01		.05	.01	.005			
1,2	25	.47669	*	*	Y = 20.8121 + .083855 X	*	*		2.6006	34.830	.22723
1,3	21	-.13107			Y = 2.56865- .000144 X				-.57630	0.26512	.01718
1,4	18	-.02385			Y = 2.65871 - .0000138 X				-.095426	0.14570	.00056
1,5	18	.12893			Y = 3.35899 + .003263 X				.52007	6.2228	.01662
1,6	17	.03159			Y = 5.85342 + .000915 X				.12243	7.3073	.00099
1,7	22	.14566			Y =112.176 + .04825 X				.65844	77.614	.02122
1,8	19	.14334			Y = 8.00063 + .003364 X				.59716	5.7292	.02055
1,9	16	.24149			Y = 4.14448 + .00224 X				.93113	2.3281	.05832
1,10	16	.17771			Y = 3.59375 + .001647 X				.67567	2.3586	.03158
1,11	6	-.57187			Y = 4.91834 + .012511 X				-1.3942	3.6118	.32703
1,12	16	.27296			Y = 0.23566 + .000118 X				1.0616	0.10760	.07451
1,13	19	-.03178			Y = 5.77628 - .000437 X				-1.13110	3.4206	.00101
1,14	10	.07417			Y = 5.86381 + .001194 X				-.21036	2.8797	.00550
1,15	7	.53421			Y = 10.0039 + .006329 X				1.4131	2.9643	.28538
1,16	22	.64252	*	*	Y = 86.4370 + .207490 X	*	*	*	3.7499	58.604	.41283
1,17	19	.52908	*	*	Y = 35.6147 + .057087 X	*	*		2.5707	22.342	.27992
1,18	17	-.36744			Y =1447.84 -2.4552 X				-1.5301	1514.3	.13501
1,19	17	.37372			Y = 28.9054 + .144080 X				1.5605	87.133	.13967
1,20	19	.36647			Y = 0.413495- .001272 X				1.6240	0.73155	.13430
1,21	19	-.00795			Y = 72.29120 - .006437 X				-.32900	19.899	.00633
2,3	21	.57406	*	*	Y = 2.68069 - .003923 X				-3.0506	0.21897	.32954
2,4	18	-.20942			Y = 2.68578 - .003923 X				-.85669	0.14251	.04381
2,5	18	.74634	*	*	Y = -0.882782+ .119470 X				4.4855	4.1765	.55702
2,6	17	.80324	*	*	Y = -0.09026 + .14535 X				5.2227	4.3548	.64519
2,7	22	-.36893	*		Y =149.582 - .73793 X				-1.7751	72.917	.13611
2,8	19	-.23672			Y = 10.1211 - .034875 X				-1.0046	5.6244	.05604
2,9	16	-.34255			Y = 5.48369 - .020842 X				-1.3634	2.2540	.11734
2,10	16	-.41514	*		Y = 4.96731 - .025234 X				-1.7074	2.1805	.17234
2,11	6	-.75066	*		Y = 6.36292 - .068245 X				-2.2724	2.9088	.56349
2,12	16	-.11446			Y = 0.250381+ .000324 X				.43112	0.11111	.01310
2,13	19	-.57326	*	*	Y = 7.48360 - .051664 X				-2.8847	2.8041	.32863
2,14	10	.22098			Y = 5.36197 + .013751 X				.64087	2.8162	.04883

Appendix 2 (continued)

Pairs of X and Y	n	r_{XY}	Significant Level of r		Y = a + bX	Significant Level of b			T	$S.E_{Y.X.}$	R^2_{XY}
			.05	.01		.05	.01	.005			
2,15	7	-.51342			Y = 14.6017 - .051599 X				-1.3378	3.0091	.26360
2,16	22	.08562			Y =121.158 + .16691 X				.38432	76.199	.00733
2,17	19	-.14303			Y = 52.0136 - .092292 X				-.59587	26.059	.02046
2,18	17	-.33470			Y =1560.77 - 14.290 X				-1.3756	1534.3	.11202
2,19	17	.07550			Y = 50.4530 + .18599 X				.29328	93.672	.00570
2,20	19	-.09203			Y = .704953 - .001860 X				-.38109	0.78291	.00847
2,21	19	-.72358	*	*	Y = 85.4471 - .36760 X	*	*	*	-4.3223	13.779	.52357
3,4	19	.81795	*	*	Y = 1.65242 + .40162 X	*	*	*	5.8622	0.08556	.66904
3,5	19	-.85126	*	*	Y = 57.7903 - 21.024 X	*	*	*	-6.6888	3.9594	.72464
3,6	18	-.88673	*	*	Y = 67.5354 - 24.303 X	*	*	*	-7.7627	3.8480	.78629
3,7	22	.71790	*	*	Y = -362.775 +192.45 X	*	*	*	4.6119	55.588	.51538
3,8	20	.72877	*	*	Y =-26.0719 + 13.820 X	*	*	*	4.4891	4.0260	.52819
3,9	16	.76048	*	*	Y =-12.4152 + 6.7148 X	*	*	*	4.3820	1.5579	.57833
3,10	16	.81847	*	*	Y =-14.3882 + 7.2197 X	*	*	*	5.3302	1.3770	.66989
3,11	6	.68931	*		Y =-16.6500 + 8.0759 X				1.9029	3.1897	.47515
3,12	16	-.27567			Y = .551783 - .11384 X				-1.0703	0.10752	.07599
3,13	20	.78496	*	*	Y =-16.9697 + 8.9304 X	*	*	*	5.3754	2.1507	.6161
3,14	10	.37292			Y = -1.37317 + 2.7365 X				1.1868	2.2869	.13907
3,15	7	.28983			Y = -8.03456 + 7.6718 X				0.67713	3.3560	.08400
3,16	22	.45638	*		Y = -185.132 +123.09 X	*			2.2938	71.484	.20828
3,17	18	.51334	*		Y =-59.3977 + 43.735 X	*			2.3927	22.490	.26352
3,18	16	-.37732			Y = 6742.31 - 2253.6 X				-1.5245	1551.9	.14237
3,19	16	.25145			Y = -157.990 + 86.073 X				.97208	92.959	.06323
3,20	18	.43518	*		Y = -2.53157 + 1.2573 X	*			1.9334	0.7235	.18938
3,21	20	.70536	*	*	Y =-40.7641 + 44.787 X	*	*	*	4.2217	13.757	.49753
4,5	18	-.45395	*		Y = 71.2110 - 24.842 X	*			-2.0379	6.9227	.20607
4,6	18	-.54368	*	*	Y = 91.7942 - 31.876 X	*	*		-2.5911	6.9863	.29559
4,7	19	.65349	*	*	Y = -864.250 +372.64 X	*	*	*	3.5596	64.199	.42705
4,8	18	.63889	*	*	Y =-60.3767 + 25.974 X	*	*	*	3.3219	4.7667	.40818

Appendix 2 (continued)

Pairs of X and Y	n	r_{XY}	Significant Level of r		Y = a + bX	Significant Level of b			T	$S.E_{Y.X}$	R^2_{XY}
			.05	.01		.05	.01	.005			
4,9	15	.47175	*		Y = -16.4346 + 7.8514 X	*			1.9290	2.1379	.22255
4,10	15	.55425	*		Y = -20.6011 + 9.1474 X	*			2.4009	2.0012	.30719
4,11	5	.61674			Y = -30.0500 + 12.757 X				1.3571	3.9405	.38037
4,12	15	- 073943			Y = .415118- .058332X				-.26734	0.11461	.00547
4,13	17	.68269	*	*	Y = -36.0533 + 15.736 X	*	*	*	3.6212	2.6454	.46643
4,14	10	.23551			Y = -3.89758 + 3.4086 X				.68541	2.3954	.05547
4,15	7	.054945			Y = 7.60495 + 1.7832 X				.12305	3.5012	.00302
4,16	19	.44317	*		Y = -515.769 +244.73 X	*			2.0383	73.628	.19640
4,17	16	.42966	*		Y = -518.454 + 78.857 X	*			1.7804	25.040	.18461
4,18	14	-.58020	*		Y = 19362.1 - 6848.8 X	*			-2.4677	1457.8	.33663
4,19	14	.15648			Y = -205.964 +103.54 X				.54882	99.095	.02449
4,20	15	.43713	*		Y = -5.48989 + 2.3481 X				1.7524	0.77379	.19108
4,21	19	410107	*		Y = 73.4607 + 54.243 X	*			1.8543	17.939	.16824
5,6	18	.89189	*	*	Y = 2.11886 + .95556X	*	*	*	7.8885	3.7645	.79547
5,7	19	-.65696	*	*	Y = 161.330 - 7.1332 X	*	*	*	-3.5928	61.770	.43160
5,8	18	-.61204	*	*	Y = 11.2820 - .47506X	*	*	*	-3.0957	4.7085	.37459
5,9	15	-.68356	*	*	Y = 5,52291 - .25500X	*	*	*	-3.3767	1.7697	.46725
5,10	15	-.70085	*	*	Y = 4.83411 - .25927X	*	*	*	-3.5426	1.7150	.49119
5,11	6	-.70827	*		Y = 6.02192 - .37176X				-2.0066	3.1081	.50165
5,12	15	.59105	*	*	Y = .218804+ .010451 X	*	*		2.64619	.09270	.34934
5,13	17	-.76553	*	*	Y = 7.32337 - .36052X	*	*	*	-4.6082	2.3388	.58604
5,14	10	-.31889			Y = 5.83870 - .08885X				-.95163	2.3360	.10169
5,15	7	-.74760	*		Y = 14.7121 - 6.1755 X	*			-2.5170	2.3289	.55891
5,16	19	-.55444	*	*	Y = 162.632 - 5.9876 X	*	*		-2.7469	67.815	.30740
5,17	16	-.50367	*		Y = 60.9099 - 1.7313 X	*			-2.1815	23.956	.25368
5,18	15	-.05538			Y = 1094.77 - 14.907 X				-.20002	1723.6	.00307
5,19	15	-.43670	*		Y = 93.4188 - 6.6837 X				-1.7502	88.313	.19071
5,20	15	-.41820			Y = .972170-.055783 X				-1.6600	0.77772	.17489
5,21	19	-.66237	*	*	Y = 80.2406 - 1.7336 X	*	*	*	-3.6454	14.795	.43873
6,7	18	-.69745	*	*	Y = 176.527 - 7.0407 X	*	*	*	-3.8929	60.219	.48644

Appendix 2 (continued)

Pairs of X and Y	n	r_{XY}	Significant Level of r		Y = a + bX	Significant Level of b			T	$S.E._{Y.X}$	R^2_{XY}
			.05	.01		.05	.01	.005			
6,8	17	-.67119	*	*	Y= 12.3058 - .49027 X	*	*	*	-3.5067	4.5497	.45050
6,9	15	-.69326	*	*	Y= 5.88947 - .22684 X	*	*	*	-3.4683	1.7474	.48061
6,10	15	-.75180	*	*	Y= 5.28629 - .24394 X	*	*	*	-4.1108	1.5854	.56520
6,11	5	-.87543	*		Y= 8.35603 - .52296 X	*			-3.1371	2.4196	.76638
6,12	15	.23478			Y= .237575+ .003641X				0.87085	0.11171	.05512
6,13	16	-.89481	*	*	Y= 8.42480 - .38914 X	*	*	*	-7.4996	1.6586	.80068
6,14	10	-.38108			Y= 6.17342 - .10758 X				-1.1658	2.2787	.14522
6,15	7	-.77051	*		Y= 13.6780 - .41459 X	*			-2.7029	2.2352	.59369
6,16	18	-.60917	*	*	Y= 179.031 - 5.8406 X	*	*	*	-3.0726	2.2352	.59369
6,17	16	-.63563	*	*	Y= 67.1912 - 2.0709 X	*	*	*	-3.0807	21.407	.40403
6,18	14	-.007134			Y= 1081.74 - 1.6889 X				-0.024717	1789.8	.00005
6,19	14	-.16823			Y= 84.7107 - 2.2323 X				-.59119	98.901	.02830
6,20	14	-.55258	*		Y= 1.19589 - .063694X	*			-2.2967	0.72425	.30534
6,21	18	-.83225	*	*	Y= 84.8462 - 2.0067 X	*	*	*	-6.0048	11.127	.69264
7,8	20	.90195	*	*	Y= .70872 + .064907X	*	*	*	8.8613	2.5311	.81351
7,9	16	.76829	*	*	Y= 1.64642 + .022081X	*	*	*	4.4909	1.5257	.59026
7,10	16	.76232	*	*	Y= .98406 + .022081X	*	*	*	4.4073	1.5512	.58113
7,11	6	.68936	*		Y= -3.72422 + .096900X				1.9032	3.1895	.47522
7,12	16	-.16212			Y= .292828- .000217X				-0.61474	0.11037	.02628
7,13	20	.69687	*	*	Y= 1.89606 + .029574X	*	*	*	4.1224	2.4897	.48563
7,14	11	.32202			Y= 3.70019 + .027271X				1.0204	2.9450	.10370
7,15	7	.47706			Y= 8.11757 + .021561X				1.2138	3.0818	.22759
7,16	23	.69720	*	*	Y= 40.1247 + .69710 X	*	*	*	4.4569	56.440	.48609
7,17	19	.77977	*	*	Y= 19.7240 + .25095 X	*	*	*	5.1354	16.078	.60804
7,18	17	-.44071	*		Y= 2110.85 - 9.5151 X	*			-1.9015	1461.6	.19423
7,19	17	.63066	*	*	Y= -37.8707 + .78559 X	*	*	*	3.1473	72.903	.39773
7,20	19	.87901	*	*	Y= -.376406+ .008434X	*	*	*	7,6011	0.37489	.77266
7,21	20	.64316	*	*	Y= 52.6417 + .15093 X	*	*	*	3.5635	14.861	.77266
8,9	16	.71458	*	*	Y= 1.87422 + .29490 X	*	*	*	3.8220	1.6783	.51062
8,10	16	.73701	*	*	Y= 1.10068 + .30386 X	*	*	*	4.0801	1.6199	.54318

Appendix 2 (continued)

Pairs of X and Y	n	r_{XY}	Significant Level of r		$Y = a + bX$	Significant Level of b			T	$S.E._{Y.X.}$	R^2_{XY}
			.05	.01		.05	.01	.005			
8,11	6	-.07494			Y= 3.49215 + .078824 X				-.15032	4.3904	.00562
8,12	16	-.25547			Y= .316936 + .005684 X				-1.1572	0.10686	.08730
8,13	19	.60368	*	*	Y= 2.28979 + .38152 X	*	*	*	3.4042	2.7182	.40536
8,14	10	.17154			Y= 4.46923 + .11534 X				.49249	2.4281	.02943
8,15	7	.34260			Y= 8.93232 + .24966 X				.81543	3.2943	.11737
8,16	20	.71534	*	*	Y= 44.2946 + 10.090 X	*	*	*	4.3432	57.770	.511711
8,17	17	.73045	*	*	Y= 22.3950 + 3.3884 X	*	*	*	4.1423	18.379	.53356
8,18	16	-.52579	*		Y=2419.23 - 156.27 X	*			-2.3128	1425.5	.27646
8,19	16	.52053	*		Y=-19.4850 + 8.8666 X	*			2.2811	82.007	.27095
8,20	17	.82889	*	*	Y= -.325097 + .11553 X	*	*	*	5.7386	0.4575	.68706
8,21	19	.68617	*	*	Y= 51.3381 + 2.2115 X	*	*	*	3.8892	14.132	.47083
9,10	16	.97829	*	*	Y= .582944 + .97732 X	*	*	*	17.664	0.49667	.95705
9,11	5	.99308	*	*	Y= -3.69063 + 2.2739 X	*	*	*	14.650	0.58776	.98621
9,12	16	-.24624			Y= .316687 - .011480 X				-.95063	0.10841	.06063
9,13	16	.61163	*	*	Y= 1.84695 + .91492 X	*	*		2.8904	2.8414	.37372
9,14	8	-.11878			Y= 5.64408 - .14803 X				-.29302	2.2134	.01411
9,15	7	.51249			Y= 2.57914 + 1.5174 X				1.3345	3.0110	.26265
9,16	16	.77877	*	*	Y= 38.8301 + 24.185 X	*	*	*	4.6451	46.738	.60648
9,17	15	.56025	*		Y= 24.9937 + 6.3578 X	*			2.4387	22.151	.31388
9,18	15	-.46375	*		Y=2531.76 - 328.37 X	*			-1.8873	1536.0	.21506
9,19	15	.52609	*		Y= -30.1994 + 21.087 X	*			2.2305	83.464	.27677
9,20	15	.74566	*	*	Y= -.387396+ .25705 X	*	*	*	4.0348	0.55723	.55601
9,21	15	.64946	*	*	Y= 47.6014 + 5.3017 X	*	*	*	3.0795	15.050	.42180
10,11	5	.99723	*	*	Y= -2.15266 + 2.2945 X	*	*	*	23.208	0.37257	.99447
10,12	16	.23017			Y= .305843- .010741 X				-.88499	0.10885	.05298
10,13	16	.70135	*	*	Y= 1.93719 + 1.0507 X	*	*	*	3.6815	2.5594	.49189
10,14	8	-.057598			Y= 5.38604 - .071096 X				-.14132	2.2255	.00332
10,15	7	.32646			Y= 8.38258 + .71767 X				.77231	3.3144	.10658
10,16	16	.74523	*	*	Y= 59.5385 + 23.167 X	*	*	*	4.1817	49.681	.55537
10,17	15	.53835	*		Y= 30.6170 + 5.9405 X	*			2.3033	22.536	.28982
10,18	15	-.45199	*		Y=2258.45 - 316.10 X	*			-1.8270	1546.5	.20430

Appendix 2 (continued)

Pairs of X and Y	n	r_{XY}	Significant Level of r		Y = a + bX	Significant Level of b			T	$S.E_{Y.X.}$	R^2_{XY}
			.05	.01		.05	.01	.005			
10,19	15	.44511	*		Y= -3.28026 + 17.622 X	*			1.7922	87.885	.19812
10,20	15	.69630	*	*	Y= -.150394+ .24305 X	*	*	*	3.4978	0.60024	.48483
10,21	15	.72094	*	*	Y= 48.9167 + 5.9349 X	*	*	*	3.7509	13.716	.51975
11,12	5	-.53179			Y= .396943- .015937X				-1.0876	0.12705	.28280
11,13	6	.98003	*	*	Y= 1.40742 + .78112 X	*	*	*	9.8564	.69784	.96046
11,14	5	-.34814			Y= 5.77358 - .17868 X				-.64323	2.4086	.12120
11,15											
11,16	6	.24630			Y= 73.5814 + 1.7842 X				.50826	30.911	.06067
11,17	5	-.32117			Y= 39.2372 - .56809 X				-.58740	8.3857	.10315
11,18	6	.19566			Y= 1265.14 + 113.79 X				.39903	2511.1	.03828
11,19	6	.81992	*		Y= .926342+ .81992 X	*			2.8645	1.5382	.67227
11,20	6	.17097			Y= .179947+ .006099X				.34705	0.15476	.02923
11,21	6	.49347			Y= 58.5274 + 2.2102 X				1.1347	17.151	.24351
12,13	16	-.29286			Y= 8.58935 - 9.4013 X				-1.1460	3.4331	.08577
12,14	8	.29729			Y= 3.75212 + 5.0398 X				.76269	2.1284	.08838
12,15	7	.75199	*		Y= 6.53421 + 26.613 X	*			2.5509	2.3114	.56549
12,16	16	-.22501			Y= 191.108 - 149.59 X				-.86407	72.595	.05063
12,17	15	.15453			Y= 43.3284 + 37.369 X				.56394	26.421	.02388
12,18	15	-.10815			Y= 1440.66 -1645.3 X				-.39225	1723.5	.01170
12,19	15	-.39865			Y= 154.546 - 343.31 X				-1.5673	90.008	.15892
12,20	15	-.13460			Y= 1.03456 - .97030 X				-.48977	0.82867	.01812
12,21	15	-.25256			Y= 82.9198 - 43.498 X				-.94114	19.151	.06379
13,14	9	.28290			Y= 4.05603 + .16552 X				.78037	2.3877	.08003
13,15	7	.45704			Y= 8.13791 + .59443 X				1.1490	3.1189	.20889
13,16	20	.53793	*	*	Y= 56.2620 + 12.985 X	*	*		2.7073	70.638	.28937
13,17	17	.44786	*		Y= 32.1678 + 3.2611 X	*			1.9400	24.031	.20058
13,18	16	-.093254			Y= 1237.06 - 42.743 X				-.35045	1668.5	.00870
13,19	16	.14065			Y= 40.0856 + 3.6949 X				.58156	95.091	.01978
13,20	18	.51865	*		Y= -.006692+ .12077 X	*			2.4265	0.68708	.26900
13,21	18	.77898	*	*	Y= 49.5151 + 4.0482 X	*	*	*	4.9692	11.557	.60681

Appendix 2 (continued)

Pairs of X and Y	n	r_{XY}	Significant Level of r		$Y = a + bX$	Significant Level of b			T	$S.E._{Y.X.}$	R^2_{XY}
			.05	.01		.05	.01	.005			
14,15											
14,16	11	.50417	*		Y= 57.4405 + 5.0490 X				1.7514	26.904	.25419
14,17	11	.45949			Y= 58.1407 + 1.5289 X				1.5520	9.1932	.21113
14,18	9	-.36457			Y=3126.54 - 243.17 X				-1.0358	1896.3	.13 91
14,19	9	-.011713			Y= 2.36458 - .0084583X				-.03099	2.2046	.00014
14,20	9	.35130			Y= .144802+ .015872 X				.99273	0.12915	.12341
14,21	10	-.058604			Y= 65.0600 - .47069 X				-.16604	19.762	.00343
15,16	7	.58003			Y= 100.408 + 9.5746 X				1.5922	47.150	.33643
15,17	6	.58003	*	*	Y= -33.2070 + 8.8329 X	*	*	*	10.951	6.1395	.96772
15,18	6	-.47838			Y= 41.9708 - 1.8029 X				-1.0895	11.644	.22885
15,19	6	-.22351			Y= 230.861 - 5.8120 X				-.45863	89.169	.04996
15,20	6	.66247			Y= -.412128+ .16064 X				1.7687	0.67757	.43887
15,21	7	.71660	*		Y= 31.1812 + 3.8756 X	*			2.2974	13.227	.51352
16,17	19	.80805	*	*	Y= 13.7793 + .27187 X	*	*	*	5.6555	15.129	.65294
16,18	17	-.43864	*		Y=2236.72 - 9.5229 X	*			-1.8904	1463.2	.19241
16,19	17	.54265	*	*	Y= 33.8006 + .67971 X	*			2.5021	78.906	.29447
16,20	19	.83628	*	*	Y= -.476344+ .009031 X	*	*	*	6.2887	0.43110	.69936
16,21	20	.41807	*		Y= 58.4116 + .097573 X	*			1.9526	17.630	.17478
17,18	15	-.42364	*		Y=2576.45 - 31.491 X				-1.6863	1560.4	.17947
17,19	15	.45081	*		Y= -35.1917 + 1.8368 X	*			1.8209	84.283	.20323
17,20	16	.81323	*	*	Y= -.572736+ .024179 X	*	*	*	5.2288	0.4041	.66134
17,21	16	.54861	*		Y= 48.0742 + .40506 X	*			2.4552	17.118	.30091
18,19	17	-.37724			Y= 79.0254 - .002176 X				-1.5776	86.999	.14231
18,20	16	-.41891	*		Y= .804028- .000186 X				-1.7262	0.67282	.17549
18,21	15	-.021582			Y= 71.7428 - .000245 X				--.077832	19.663	.00047
19,20	16	.58151	*	*	Y= .359150+ .0044315X	*	*		2.6745	0.60280	.33815
19,21	15	.081337			Y= 70.4141 + .016296 X				.29424	19.602	.00661
20,21	16	.52138	*		Y= 62.4613 + 11.878 X	*			2.2861	16.452	.27184

References

1 Nasiatka, T.M. "Tunnelling Technology. Its Past and Present" U.S. Department of Interior, Bureau of Mines, 1968.

2 Hirschfeld, R.C. "Hard Rock Tunnelling Investigation" Massachusetts Institute of Technology, (Prepared for the U.S. Department of Commerce), October 1965.

3 Muirhead, I.R. & Glossop, L.G. "Hard Rock Tunnelling Machines" Transaction Institute of Mining & Metallurgy, Volume 77, January 1968, p. A1-A21.

4 Allington, A.V. "The Machining of Rock Materials" Ph.D. Thesis, University of Newcastle upon Tyne, September 1969.

5 Robbins Bulletin.

6 Nicholson, W.E. "Big Bits Drill Big, Part 1" World Mining, Volume 20, Number 10, September 1967.

7 Ingersoll-Rand Bulletin Number 16001.

8 Jarva Tunnelling Machines & Cutters Bulletin.

9 Western Construction, August 1972.

10 Dresser Industry Incorporation Bulletin 205/8-71/10M.

11 Wirth Tunnelling Machine Bulletin.

12 "Full Section Tunnelling Machine for Hard Rock" Demag Bulletin.

13 Peake, C.V. "Development of an Experimental Ripping Machine" Transaction Institute of Mining Engineer, Volume 119, Part 2.

14 Shuttleworth, P. "Ripping Machine Development at Bretby" Paper Presented to King's College Mining Society, March 1963.

15 "Ripping Machine for Coal Mines" The Engineer, October 1961.

16 Anderson Mavor Leaflet 826b.

17 Eickhoff Leaflet D-Nr 2037 8 71 20.

18		"Tunnelling at Hinkley Point Power Station" Mining Engineering, Volume 5, January 1969.
19		"Tunnelling Through Hard Limestone" Mining Journal, 271, December 1968.
20		"Tunnelling Machines Maintain Good Progress on Victoria Line Excavation" Civil Engineering, May 1966.
21	Pirrie, N.D.	"Hinkley Tunnels Prove Economics of Machine for Short Distance Tunnels" Distributed by Sir Robert McAlpine & Sons Limited.
22	Phillips, M.	"The Tunnel under the Bridge" Engineering, October 1970.
23	Lyons, A.C. & Scofield, J.	"Great Charles Street Road Tunnel" Tunnels and Tunnelling, Volume 1, May-June 1969.
24	Cottrin, A.	"Greenside - McAlpine Machines on the Severn-Wye Cable Tunnel Project" Construction News, July 22, 1971.
25	Morse, W.	"Greenside - McAlpine Tunneller" Contractors' Plant Review, June 1969.
26		"Applications of McAlpine Tunnelling Machines" Paper Distributed by Sir Robert McAlpine & Sons Limited, August 1971.
27	Geller, L.B.	"Research in Improved Methods of Rock Breakage" T.I.M.M., Volume 76, 1967, p A105-A124.
28	Huck, P.J. & Singh, M.M.	"Rock Breakage by High Speed Water Jets" Report to Office of High Speed Ground Transportation, U.S. Department of Transportation, 1970.
29	Singh, M.M.	"Rock Breakage by Pellet Impact" Report to Office of High Speed Ground Transportation, U.S. Department of Transportation, 1970.
30	Greggson, V.G., Jr. & Singh, M.M.	"Rock Breakage by Light - Gas Gun Projetiles" I.I.T. Research Institute, Report Number D 6000-06, January 1969.
31	Maurer, W.C.	"Novel Drilling Techniques" Pergamon Press, 1968.
32	Maurer, W.C.	"Novel Drilling Techniques" Proceeding 8th Symposium Rock Mechanics, Minnesota, 1966.

33 Crow, S.C. "Jet Tunnelling Machines" Tunnels and Tunnelling, Volume 7, March-April 1975.

34 Crow, S.C. "A Theory of Hydraulic Rock Cutting" International Journal Rock Mechanics & Mining Society, Volume 10, 1973.

35 Hoshino, K., Nagano, T. & Tsuchishima, H. "Rock Cutting and Breaking Using High Speed Water Jets together with TBM Cutters" First International Symposium on Jet Cutting Technology, British Hydromechanics Research Association, Carnfield, Bedford, England, 1972.

36 Nagano, T., Hoshino, K. & Narita, Y. "The Development of a Water Jet Drilling Machine" Second International Symposium on Jet Cutting Technology, British Hydromechanics Research Association, Carnfield, Bedford, England, 1974.

37 Shapir, Y.I. "Research in Forced-Flame Drilling in the Altyn-Topkan and Krivorozh Quarries" Proceeding of the All-Union Research Institute for Drilling Technology, USSR., Number 10, Moscow, 1963.

38 Adams, W.M. "Nuclear Reactor Apparatus for Earth Penetration" U.S. Patent Number 3155194, 1965.

39 Anon, "Laser May be Hard Rock Tunneller" Engineering News Record, Volume 177, 1956.

40 Ward, E.J., Lucke, W.M., & Carstens, J.P. "U.S. Research to Reduce Tunnelling Costs" Tunnels and Tunnelling, Volume 2, July-August 1970.

41 McGee, E. "New Down-Hole Tool" Oil and Gas Journal, Volume 54, August 1955.

42 "Split Second Tubing Cutter" Oil Forum, September 1955.

43 Robbins, R.J. "Economic Factors in Tunnel Boring" TUNCON 70, University of Witwatersrand, South Africa.

44 Schwartzkopf, P. & Kieffer, R. "Cemented Carbides" Macmillan, 1960.

45 Doeg, H.H. "Cemented Hard Metals" Journal of the South African Institue of Mining & Metallurgy, July 1960.

46	Lardner, E.	In Discussion of Reference 45.
47	Cook et al	"Rock Cutting and Its Potentialities as a New Method of Mining" Journal of the South African Institute of Mining & Metallurgy, May 1968.
48	Osburn, H.J.	"Some Considerations of the Metallurgy of Rock Cutting Tools" M.Sc. Dissertation, University of Newcastle upon Tyne, September 1968.
49	Pearson, R.	"Wear and Its Effects in the Cutting of South African Quartzite" B.Sc. Thesis, University of Newcastle upon Tyne, September 1970.
50	Rae, D.	S.M.R.E. Report Number 223, 1964.
51	Latin, A.	"Studies of Wear and Fracture of Cemented Carbide as Used in Coal Mining Tools" M.R.E. Report Number 2025.
52	Evans, I. & Pomeroy, C.D.	"Strength, Fracture and Workability of Coal" Pergamon, 1966.
53	Johnson, S.N. & Morgan, W.T.A.	"A Laboratory Study of Abrasive Wear in Cutting Tools: The Cutting Performance of Tungsten Carbide and Other Tool Materials as Wear Progress" M.R.D.E. Report Number 1, October 1969.
54	Brodbeck, H.W.	"Successful Application of the Habegger Tunnelling Machine to Hard Rock" English Translation of a German Paper.
55	Lauber, E.	"The Present State of Development of the Swiss Wohlmeyer Tunnelling Machine" English Translation from Glukauf, 1969.
56	Gurland, J.	"Microstructural Aspects of the Strength and Hardness of Cemented Tungsten Carbide" B.I.S.R.A. & I.S.I. Conference, April 1970.
57	Osburn, H.J.	"Wear of Rock Cutting Tools" Powder Metallurgy, Volume 12, Number 24, 1969.
58	Knudsen, F.P.	Journal of the American Ceramic Society, 1959.
59	Kenny, P.	"An Assessment of Tools Tipped with Materials Containing Boron Nitride" M.R.E. Report Number 238, December 1967.

60 Rispin, A.
"An Investigation into the Application of Linear Cutting Tools to the Machining of Strong and Abrasive Rock Material"
Ph.D. Thesis, University of Newcastle upon Tyne, September 1970.

61 Humphries, J.H.
"Some Considerations of the Metallurgy of Rock Cutting Tool Materials with Special Reference to Abrasive Wear"
M.Sc. Dissertation, University of Newcastle upon Tyne, September 1971.

62 Dalziel, J.A. & Davies, E.
"Initiation of Cracks in Coal Specimens by Blunted Wedges"
The Engineer, Number 217, January 1964.

63 Evans, I.
"A Theory of the Basic Mechanics of Coal Ploughing"
International Symposium of Mining Research, Volume 2, Pergamon, 1962.

64 Evans, I.
"The Forces Required to Cut Coal with Blunted Wedges"
International Journal of Rock Mechanics Mining Society , Volume 2, Pergamon, 1965.

65 O' Dogherty, M.J.
"A Laboratory Examination of the Effect of Rake Angle and Back Clearance Angle of Cutter Pick Performance in Barnsley Hards"
N.C.B./M.R.E. Report Number 2217, 1962.

66 Robinson, D.J. & Pomeroy, C.D.
"Laboratory Tests with Picks of Different Profile"
N.C.B./M.R.E. Report Number 2244, 1963.

67 Dalziel, J.A.
"The Effect on the Performance of a Cutter Pick of Ridging the Rake and Clearance Face"
N.C.B./M.R.E. Report Number 2291, 1965.

68 Barker, J.S.
"A Laboratory Investigation of Rock Cutting Using Large Picks"
International Journal of Rock Mechanics & Mining Society, Volume 1, Pergamon, 1964.

69 Roxborough, F.F.
"Rock Cutting Research for the Design and Operation of Tunnelling Machines"
Tunnels and Tunnelling, Volume 1, September-October 1969.

70 Shepherd, R. & O'Dogherty, M.J.
"A Study of Forces Acting on a Model Star Wheel Cutter"
N.C.B./M.R.E. Report Number 2099.

71 Teale, R.
"Studies in Rock Working:III, Preliminary Experiments with Roller Cutters"
N.C.B./M.R.E. Report Number 2194.

72 Dalziel, J.A. "A Laboratory Examination of Disc Cutters for Rock Cutting" N.C.B./M.R.E. Report Number 2354.

73 Bruce, W.E. & Morrel, R.J. "Principle of Rock Cutting Applied to Mechanical Boring Machines" U.S.B.M. Report of Investigation Number 7410.

74 Shepherd, R. & Price, W.J. "Roller Bit Penetration Experiments in Concretes" N.C.B./M.R.E. Report Number 2095.

75 Obert, L., Windes, S.L. & Duvall, W.I. "Standardized Tests for Determining the Physical Property of Mine Rock" U.S.B.M. Report of Investigation Number 3891, August 1946.

76 Mazanti, B.B. & Sowers, G.F. "Laboratory Testing of Rock Strength" Testing Techniques for Rock Mechanics, ASTM, STP 402, American Society Testing Materials, 1966.

77 Gaye, F. "Method of Assessing Rock Cutability" N.C.B./ C.E.E. Report Number 65(1), December 1964.

78 White, C.G. "A Rock Drillability Index" Quarterly Colorado School of Mines, Volume 64, April 1969.

79 Schimazek, J. & Knatz, H. "The Effect of Rock Structure on the Cutting Speed and Tool Wear of a Tunnel Boring Machine" Gluckauf, Volume 106, March 1970.

80 Obert, L. & Duvall, W.I. "Rock Mechanics and the Design of Structures in Rock" John Wiley & Sons, 1966.

81 Fowell, R.J. "Assessing the Machineability of Rocks" Tunnels and Tunnelling, Volume 2, July-August 1970.

82 Hansen, H. Kielland, A. Nielsen, K.E.C. & Thaulow, S. "Compressive Strength of Concrete-Cube or Cylinder" Bulletin Reunion International Laboratory Essais Rech. Materials Construction, Volume 17, 1962.

83 Low, J.R. "The Relation of Microstructure to Brittle Fracture, in Relation to Microstructure" National Metal Congress Exposition, 35th, Cleveland, Ohio, 1963.

84 Hardy, H.R.
"Standard Procedures for the Determination of the Physical Properties of Mine Rock under Short Period Uniaxial Compression"
Mines Branch, Department of Mines Technical Survey, Ottawa Technical Bulletin, 1959.

85 Coates, D.F. & Gyenge, M.
"Plate-Load Testing on Rock for Deformation. in: Testing Techniques for Rock Mechanics"
American Society Testing Materials Specification Technical Publication, 1966.

86 Hobbs, D.W.
"Rock Compressive Strength"
Colliery Engineering, July 1964.

87 Mogi, K.
"Some Precise Measurements of Fracture Strength of Rock under Uniform Compressive Stress"
Rock Mechanics & Engineering Geology, 1966.

88 Chakravarty, P.K.
"Application of the Photoelastic Technique to the Problem of Rock Mechanics"
Ph.D. Thesis, Sheffield University, 1963.

89 Fish, B.G. & Others
"Studies in Rotary Drilling IX, The Abrasive Wear Effect"
M.R.E. Report Number 2115, November 1958.

90 Greenland, B.J.
"Rock Mechanics"
Colliery Guardian, Volume 203, September 1961.

91 Belagons, P. et al.
"Determination de la Nocivite des Roches vis des Piest-Test de Durete et d'Abrasavite Cerchar"
6th January 1964.

92 Protodyakonov, M.M., Jr.
"mechanical Properties and Drillability of Rocks"
Proceeding of the 5th Symposium Rock Mechanics, Minnesota, 1963.

93 Hawkes, I.
"Modulii Measurements on Rock Cores"
First Proceeding Congress International Society Rock Mechanics, Lisbon.

94 Garret, H.E.
"Statistics in Psychology and Education"
Longmans, Green and Company.

95
"Report on Tyne-Tees Aqeduct Tunnel"
Robertson Laboratory, 1972.

96 Teale, R.
"The concept of Specific Energy in Rock Drilling"
International Journal Rock Mechanics & Mining Society, Volume 2, Oxford Pergamon Press, 1965.